

POLITECNICO DI TORINO

Corso di Laurea Magistrale in Automotive Engineering

Tesi di Laurea Magistrale

Design and manufacturing of a formula student car gear-box



Relatore

Prof. Andrea Tonoli

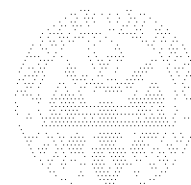
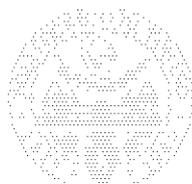
.....

Candidato

Daniele Bonatti

.....

A.A. 2017/18



Thanksgiving.

Turin, November 14th 2018.

Outcome of the work presented by actual text represents a milestone in my job career and in my personal life. Such thesis encloses my first work as engineer and my last as student. Due to importance and difficulty of such work, It's dutiful for me write some words to be grateful to all people who sustained and believed in me during the hard path to gain this place.

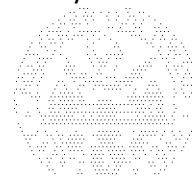
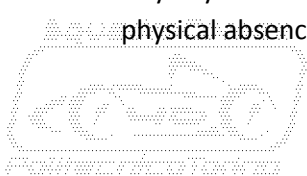
First of this large group is Laura, tender girlfriend and mate of life. She shared several years with me, bearing my lack of time, my tiredness and my absences due to work or to study. Anytime she have been able to transmit me enthusiasm and serenity without exhibit jealousy for cars which have been in fact my real girlfriends.

Clearly, showing my gratitude, I must to take into account my parents, Giovanni and Giovanna. They always accepted and motivated my ambitions peacefully, with no fear that my path could take me far from them. Both have been always enthusiast of motor racing disciplines, instilling in me the most sincere passion for races which I wonder could be my job for a long time. Moreover, I must be grateful to Pierdelfino and Giuliana, further couple of parents met in the middle of Piedmont Alps. They hosted me in their cozy house, taking care of my person, just after a serious surgery. Time spent in their company with Laura and Dario, have been fundamental to recover a good mental and physical condition, giving me the occasion to write scrupulously the following text.

Can't forget to mention Alessandra, more a sister than a cousin, the person with which I spent best moments of my childhood and youth. To her a sincere wish to achieve all targets, following her dreams with her great motivation. Then, It's necessary to take into account a real "elder sister", Raffaella (Zia). She and her strong nature have always pushed me through my targets, overcoming bad moments and difficulties with serenity and great liveliness. To her I wish an happy new life in Bologna, with the enjoyable company of Matteo and Giovanni.

A big grateful goes to my entire family, cousins, aunts and uncles who always make me perceive importance and pride of what i was doing. In particular, Tony and Luca, must be considered "guilty" for the memorable days in Imola, seven years ago. That was the weekend in which I definitively fell in love for racings and consequently took decisions about my future path.

An affectionate though must be addressed to Luigi, Piera, Rino and Anna, beloved grandparents who unfortunately cannot physically take part to the achievement of my graduation. They are mainly responsible for my education and my fair childhood. Luigi, in particular, spent many good time talking me about his amazing working experiences in the middle of tooling machines and secret proects. My passion and my sensitivity for fine mechanics derives from these themes heard in early ages. While contribution of Rino was make me seat behind the steering wheel for the first time. He risked his health several times letting me drive his car, kidding me by appointing surnames of legendary Alfa Romeo racing drivers. Anyway I can be pretty sure that grandparents are able to be proud of my achievements, despite their physical absence.



Another special thank must be addressed to all people from Madrignano, in particular “guys”: Tiziano, Mirko, Manuel, Stefano and Luca. I’m lucky to have enjoyed their friendship and their company, transmitting me warmth and simplicity of the small country land where I growth.

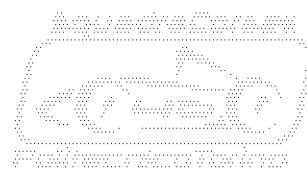
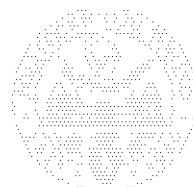
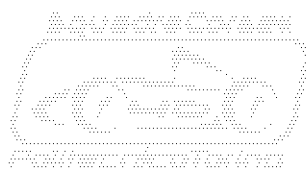
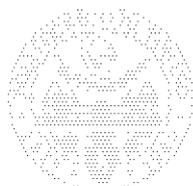
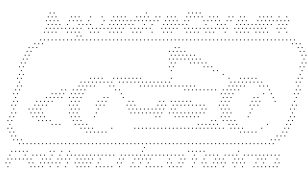
Chapter of thanksgiving must be closed spending some grateful words for Squadra Corse PoliTo team. Such institution, which for many students have been a real family, gave me the possibility to grow gaining so many technical knowledge precious in my present and in my future. By human point of view, team gave me faith and enthusiasm which are at the base of this work. Particular thanks to head of team, Professor Andrea Tonoli, which is the supervisor of this thesis but he’s skilled engineer and teacher first of all.

I must be proud of time shared with so many magnificent people, passing through good experiences but through difficult situations also. It may be restrictive give thanks to every team mate and risk may be forget someone due to several long years full of experiences. By virtue of that, following text is rich of pictures which portrait team in different events and seasons. I’m pretty sure that names of large majority of characters will be lost in several decades, but not proud, enthusiasm and tiredness on their faces, those will endure forever on pictures. To any of this guys I address my gratitude and wish a future rich of success and happiness.

Daniele



Picture 0-1: Posing on S.C.12e in Autodromo Riccardo Paletti, Formula SAE Italy, Varano de’ Melegari 2012.



[IT.] Ringraziamenti

Torino, 14 Novembre 2018.

Il frutto dell'attività descritta dal testo attuale rappresenta una pietra miliare nella mia carriera lavorativa e nella mia vita personale. La presente tesi costituisce contemporaneamente il mio primo lavoro in veste di ingegnere e l'ultimo in veste di studente. Proprio a causa dell'importanza e della difficoltà racchiuse in questa attività, trovo doveroso scrivere un pensiero per ringraziare tutte le persone che mi hanno sostenuto e hanno creduto in me durante il duro cammino per arrivare fin qui.

4

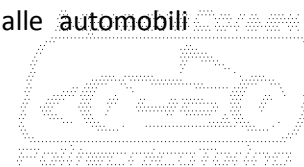
In testa al nutrito gruppo di persone c'è Laura, affettuosa fidanzata e compagna di vita. Laura ha condiviso con me diversi anni di vita, sopportando di buon grado la mia mancanza di tempo, la mia stanchezza e le ripetute assenze imputabili allo studio o al lavoro. In ogni momento è stata capace di trasmettermi entusiasmo e serenità senza manifestare gelosia verso le automobili che, per lungo tempo, sono state le sue più dure rivali in amore.

Chiaramente, scrivendo i miei ringraziamenti, è doveroso citare i miei genitori, Giovanni e Giovanna. Loro hanno sempre accettato e motivato le mie ambizioni con serenità, senza il timore che queste ultime potessero allontanarmi da loro. Entrambi sono sempre stati attratti dalle discipline motoristiche e sono stati capaci di trasmettermi la più sincera passione per le competizioni, che spero possano essere il mio mestiere per lungo tempo ancora. Sempre in tema di genitori, voglio esprimere la mia gratitudine a Pierdelfino e Giuliana, i genitori "d'adozione", che ho incontrato nel cuore delle alpi Piemontesi. Loro mi hanno ospitato nella loro casa accogliente, prendendosi cura di me dopo un doloroso intervento chirurgico. Il tempo passato in loro compagnia, con Laura e Dario, è stato fondamentale per ritrovare una buona condizione fisica e mentale, inoltre è stata una preziosa occasione per completare scrupolosamente il testo che segue.

Procedendo, non posso dimenticare un pensiero per Alessandra, più sorella che cugina, è lei la persona con cui ho passato i momenti migliori dell'infanzia e della giovinezza. Per Alessandra, un sincero augurio di soddisfare le sue ambizioni, seguendo i suoi sogni con la grande motivazione che ha sempre manifestato. Sempre in tema di sorelle, la prossima menzione va a Raffaella (Zia) che è stata per me una "sorella maggiore" a tutti gli effetti. Con il suo carattere forte e autoritario, Raffaella, è sempre riuscita a spingermi verso i miei obiettivi senza mai rinunciare alla serenità e a tanta allegria. Per lei auspico un felice futuro a Bologna, allietato dalla preziosa compagnia di Matteo e Giovanni.

Tanta gratitudine va al resto della mia famiglia, ai cugini, alle zie e agli zii che mi hanno sempre fatto percepire l'importanza e l'orgoglio per quello che stavo facendo. In particolare, voglio ringraziare Tony e Luca, "colpevoli" per quei magnifici giorni passati ad Imola sette anni fa. Fu proprio in quel weekend che mi abbandonai completamente alla passione per le corse e decisi quale sarebbe stata la mia strada per gli anni a seguire.

Un pensiero affezionato va ai nonni, Luigi, Piera, Rino ed Anna che non potranno partecipare fisicamente alla cerimonia di proclamazione. A loro devo essere particolarmente grato per l'educazione ricevuta e per l'ambiente sereno in cui mi hanno cresciuto. Un ricordo particolare va a Luigi il quale, fin dalla tenera età, mi ha intrattenuto raccontandomi le sue avventure lavorative ambientate tra macchine utensili e progetti segreti. A Luigi si deve la passione e la sensibilità che ho maturato, negli anni, verso la cosiddetta meccanica fine. Altrettanto importante è stato il contributo di Rino, il quale mi ha introdotto alle automobili



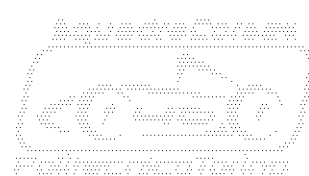
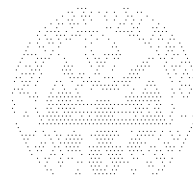
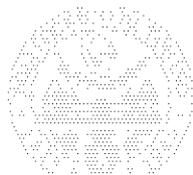
seguendomi scrupolosamente durante le prime guide per la patente. Rino, uomo coraggioso, come mio istruttore di guida ha rischiato tante volte la sua incolumità. A dispetto di ciò, non si è mai spazientito e ha sempre conservato la sua vena scherzosa, apostrofandomi con i cognomi dei leggendari piloti Alfa Romeo. In ogni modo, malgrado manchino da parecchi anni, spero tanto che i cari nonni riescano in qualche modo a seguirmi e a gioire dei traguardi che ho raggiunto e raggiungerò negli anni a venire.

Un altro ringraziamento speciale deve essere dedicato alla gente di Madrignano, in particolare ai “ragazzi”: Tiziano, Mirko, Manuel, Stefano e Luca. Mi considero molto fortunato ad aver goduto da sempre della loro amicizia e della loro compagnia. Ancora oggi riesco ad apprezzare la loro capacità di trasmettermi il calore e la semplicità tipiche del paesello in cui sono cresciuto.

La sezione dei ringraziamenti non può essere terminata senza manifestare la mia gratitudine verso il team Squadra Corse PoliTo. Questa istituzione, che per molti studenti è stata una famiglia vera e propria, mi ha dato la possibilità di crescere, acquisendo conoscenze tecniche preziose per il mio presente e per il mio futuro. Dal punto di vista umano, devo ringraziare il team per la fiducia e per l’entusiasmo che mi ha trasmesso, questi valori sono il fondamento per il lavoro presentato nella tesi in oggetto. Un ringraziamento particolare al vertice del team, il Professor Andrea Tonoli che è relatore di questa tesi ma è soprattutto ingegnere ed insegnante di grande talento.

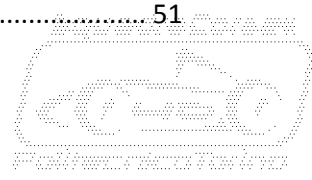
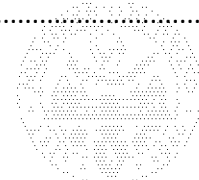
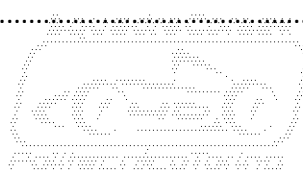
Mi sento di essere orgoglioso per gli anni spesi nel team, al fianco di persone meravigliose. Con queste ho attraversato momenti di grande soddisfazione, ma anche situazioni molto faticose e difficili. Citare uno a uno i compagni di squadra potrebbe rivelarsi limitante e, gli intensi anni trascorsi, potrebbero agevolare l’oblio. Per questo motivo, ho pensato di arricchire il testo con numerose fotografie che ritraggono il team in diversi eventi e stagioni. Sono ragionevolmente sicuro che dimenticherò molti nomi nel giro di pochi decenni, ma l’orgoglio, l’entusiasmo e le fatiche rimarranno impressi nelle fotografie, sui visi dei ragazzi. Verso tutti loro, va la mia gratitudine, la mia ammirazione e un sincero augurio per un futuro ricco di successi e felicità.

Daniele

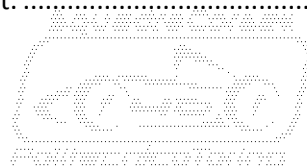


Index

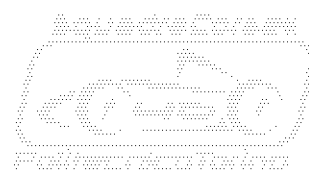
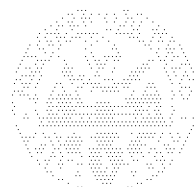
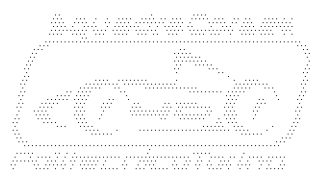
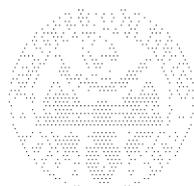
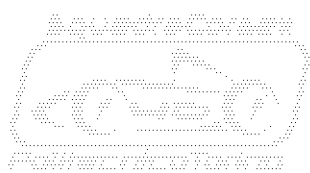
- Summary..... 9
- 1. Introduction..... 11
 - 1.1. What is Formula S.A.E.?..... 11
 - 1.2. Squadra Corse – Polytechnic University of Turin. 19
 - 1.3. S.C.R. and S.C.R. evo. 23
 - 1.4. Design evolution in Squadra Corse transmissions..... 35
 - 1.4.1. S.C.12e. 35
 - 1.4.2. S.C.R. 36
 - 1.4.3. S.C.X.V. 37
 - 1.5. Bench Mark..... 38
 - 1.5.1. D.U.T. Racing, Delft University of Technology, Netherlands. 38
 - 1.5.2. A.M.Z., Eidgenössische Technische Hochschule Zürich, Switzerland. 38
 - 1.5.3. Green Team, Universität Stuttgart, Germany. 39
 - 1.5.4. T.U.G. Racing, Technische Universität Graz, Austria. 39
 - 1.5.5. Ka-Raceing, Karlsruher Institut für Technologie, Germany. 40
 - 1.5.6. DART Racing, Technische Universität Darmstadt, Germany. 41
 - 1.5.7. Racetech, Technische Universität Bergakademie Freiberg, Germany. 42
 - 1.5.8. R.M.I.T. Racing, University of Melbourne, Australia. 42
- 2. Choice of electric motors. 43
 - 2.1. Magneti Marelli Deal. 43
 - 2.2. F.S.A.E. rules and restrictions. 43
 - 2.3. Electric motors and manufacturers. 44
 - 2.4. Different types of electric motors. 46
 - 2.5. Permanent magnet motors. 47
 - 2.6. Comparative chart. 47
 - 2.7. Magneti Marelli TMG small size (MGU012). 48
- 3. Design targets. 50
 - 3.1. Performance. 50
 - 3.2. High efficiency. 50
 - 3.3. Technical evolution..... 50
 - 3.4. High level of integration. 51
 - 3.5. Higher gear ratio..... 51
 - 3.6. Best weight stiffness trade off..... 51



3.7.	Easy and accurate assembly	52
3.8.	Fast maintenance and tuning	53
4.	Design boundaries.....	54
4.1.	Gear ratio calculation.	54
4.2.	Packaging of the vehicle.	62
4.2.1.	Transversal with internal transmission.	65
4.2.2.	Transversal with external transmission.....	66
4.2.3.	Longitudinal.	67
4.3.	Technology of gears.....	68
4.3.1.	Evolution of gears.....	69
4.3.2.	Orthogonal axes.....	70
4.3.2.1.	Worm Screw.	70
4.3.2.2.	Bevel Gears.....	71
4.3.2.3.	Face Gears.	72
4.4.	Distribution of Gear Ratio.....	73
5.	Basics of gears calculation.	76
5.1.	Geometrical and design parameters.....	76
5.2.	Importance of materials and preliminary evaluations.....	77
5.3.	Minimum number of teeth.....	78
5.4.	Module.	79
5.5.	Radial dimensions.....	81
5.6.	Axial Dimension.	83
5.7.	Overlap ratio.....	83
5.8.	Fatigue verification in bend.....	84
5.9.	Static verification on Hertzian contact.....	90
5.10.	Fatigue verification on Hertzian contact.	91
5.11.	Calculations on bevel gears.	98
5.12.	Profile correction factor of gears.	102
6.	Software aided Calculation.	104
6.1.	Collection data and set up of input power.....	105
6.2.	Choice of main parameters on first stage.	112
6.3.	Choice of main parameters on second stage.....	116
6.4.	Choice of material.	118
6.5.	Choice of lubrication and lubricant.....	120



- 6.5.1. Lubrication systems..... 120
- 6.5.2. Operation of lubrication oil..... 123
- 6.5.3. Damages caused by improper lubrication..... 125
- 6.5.4. Selection of lubricant characteristics..... 126
- 6.6. Results of first stage of reduction calculus..... 130
- 6.7. Results of second stage of reduction calculus..... 132
- 7. Design of shafts..... 134
 - 7.1. Forces acting on shafts, driving case..... 135
 - 7.2. Forces acting on shafts, energy recovery case..... 140
 - 7.3. Forces acting on shafts, braking case..... 143
 - 7.4. Shaft 1..... 145
 - 7.5. Shaft 2..... 164
 - 7.6. Shaft 3..... 191
- 8. Bearings..... 198
 - 8.1. Static and fatigue verification..... 198
 - 8.2. Preload..... 202
 - 8.3. Description of Bearings..... 205
- 9. Gear-box case..... 208
 - 9.1. Design concept..... 209
 - 9.2. Interface with motors and chassis..... 212
 - 9.3. Interface with bearings and brakes..... 224
 - 9.4. Oil containment and lubrication..... 231
- 10. Manufacturing..... 236
- 11. Conclusions..... 241
- 12. References..... 242
- Appendix 1..... 243
- Appendix 2..... 249
- Appendix 3..... 256
- Appendix 4..... 257
- Appendix 5..... 258
- Appendix 6..... 259



Summary.

Actual thesis describes the engineering work performed by a small team of designers from Power-Train division of Squadra Corse PoliTo, during the academic year 2012/2013. Members of the team were about five young undergraduate students from Polytechnic University of Turin, applied to courses of Mechanical or Automotive engineering. Task of the group was design and manufacture of power transmission, cooling system of high voltage components and energy accumulator system. All the work was finalized to create an innovative prototype of formula student electric vehicle, S.C.R.

In charge as responsible of the division and graduate in Mechanical engineering at this athenaeum, I have been particularly focused on the mechanical design of power transmission system. By virtue of that, actual thesis represents a detailed report about design and manufacturing activities, finalized to realize the core of the transmission system, the gear-box. Such text is not only a technical report but is intended to be a clear evidence of work performed during almost one year of activity.

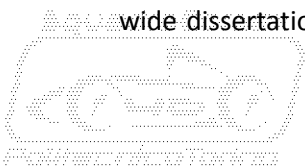
Starting point of the work is a thesis written by me in occasion of bachelor degree: *“Studio di fattibilità su trasmissione a ruote dentate per vettura di formula student”* ([ENG.]: *“Feasibility study about gearwheels transmission on a formula student car”*). Mentioned thesis includes studies about basic packaging performed on formula student car electric power-train. Anyway, core of the work is represented by a study about fundamentals of gears and bearings calculation, combined with applied examples. It’s suitable underline that large majority of such work have been translated in English and integrated in this text.

How It’s possible to appreciate by following chapters, engineering work must begin with a deep study of Formula Student Technical Rules. That’s because first target to achieve is circumscribe potential safety issues and determine where and how boundary of design freedom are applied.

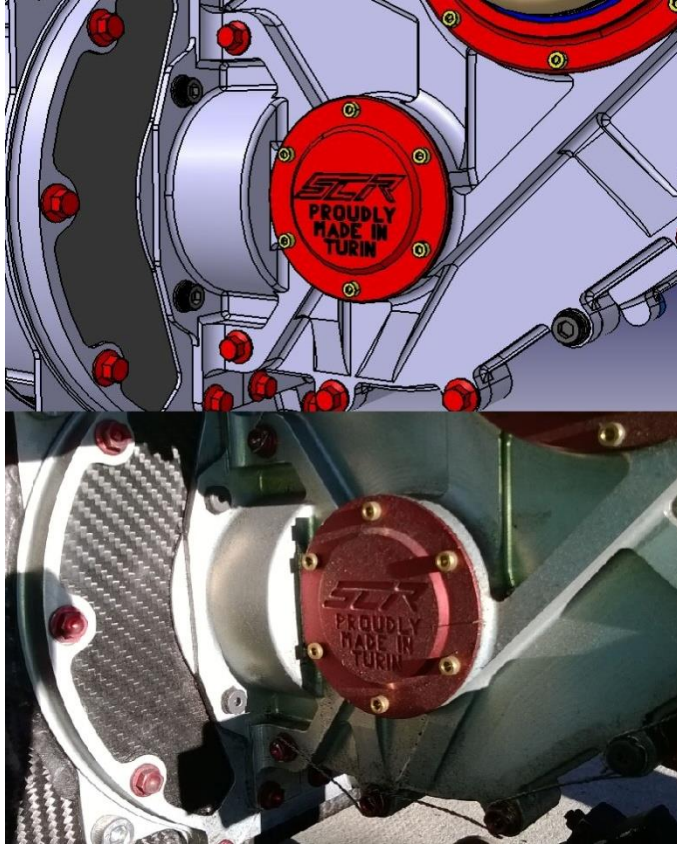
Next step of the job represents an intense and accurate investigation performed on race fields and on the web. Such activity is known as “bench mark” and It’s applied in various fields of work, that’s because allows to save time and resources by warning of total blank sheet design. Main target of this kind of study have been aimed to gather information about transmission solutions adopted by other concurrents. Such work allowed to develop a precise idea about general level of opponent teams and provided precious technical suggestions. Resulting detailed and neat investigation drove the design team to set up a mechanical project at best of owned possibilities.

Once work on analysis of concurrency is concluded, It has been necessary to define general boundaries of gear-box design, deriving from technical aspects. First of all, It has been necessary study motors and their mechanical performances, exploited in accordance with F.S.A.E. rules in theme of power. This study leads to calculation of a total gear ratio more suitable to weight of the car, if compared with previous platform S.C.12e. Then, basic layout and packaging issues of a formula student car have been deeply analyzed. Analysis of technical aspects include an updated evaluation of available gear technology solutions.

Description of work continues with introduction to Kisssoft, the gear calculation software employed by the team during calculus phase. Such phase have been open by a deep analysis of S.C.12e telemetry data, in order to define mechanical inputs of transmission system. Forward in text, It’s possible to notice the detailed set up of gear parameters performed on the software aided calculation. Description of each chosen parameter is coupled with exhaustive technical explanations. In particular, actual topic includes a wide dissertation about evaluated materials and surface treatments aimed to improve performances and



efficiency. In addition, It's possible to notice a wide topic about properties of lubrication oil and lubrication techniques, which affect inputs of gear calculations. Description of work on gear design ends with a detailed summary of calculation outputs regarding geometrical dimensions, safety factors and calculated efficiency.



Picture 0-2: From C.A.D. to trackside testing.

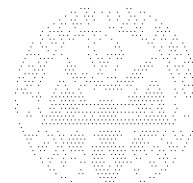
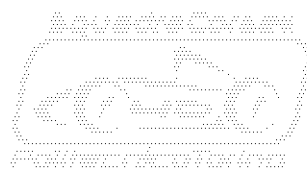
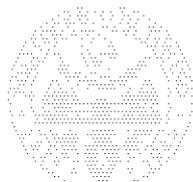
Another step through complete definition of each transmission component, is detailed design of gear-box spinning items, shafts. Such step of the work includes resolution of basic mechanical design issues and description of structural parametric verification performed on each shaft. Most critical components have been verified by point of view of mechanical stress on material and by point of view of displacements evaluated on teeth. Work carries on with focus about choice of bearings. A joint work performed in collaboration with SKF engineering service have been addressed in order to achieve maximum of performance and of reliability from each chosen bearing.

Particular interest can raise by description of structural calculus and weight optimization process performed on gear-box case components. By use of forefront calculation technique, some finite elements models have been processed in order to find the best trade off between weight and stiffness of the

structure. Description about this step of work concludes with explanation of basic mechanical issues faced during design of case. Solutions to shaft alignment issues and lubricant oil containment are deeply explained.

A brief report of activities performed during manufacturing phase follows in the text. It consists on description of manufacturing technologies employed to realize main gear-box components. Like in the case of gear calculus, chosen materials and related surface treatments are described. Topic about manufacturing closes with description of issues and procedures related to gear-box assembly process.

In order to conclude the work in a clear and neat way, main results achieved by project of the power transmission are displayed and discussed in the end of such text. Bibliographic references are then enlisted.



1. Introduction.

How It's possible foresee by the previous abstract, context of this thesis is quite original and unusual. By virtue of that, a deep and scrupulous introduction is necessary in order to achieve a good knowledge of the operative scenario. Purpose of such introduction is help the reader to understand deeply the project and the context in which It has been developed. In this way only It will be possible to appreciate work and sacrifices of involved persons.

1.1. What is Formula S.A.E.?



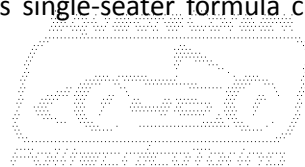
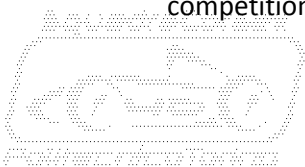
Picture 1.1-1: Formula S.A.E official logo (https://it.wikipedia.org/wiki/Formula_SAE).

Formula S.A.E., known in Europe as Formula Student, born in United States of America in 1981. The name derives from S.A.E., **Society of Automotive Engineers**, the bespoke standard developing organizations which organizes Formula Student competitions. F.S.A.E., by definition, is an **“international car design competition”**, more complex and structured than a common motorsport event.



Picture 1.1-2: Typical example of Formula car, single-seater open wheels (<http://www.tatuus.it>).

The word **“Formula”**, which is present in the definition, refers to the category of vehicles admitted to competitions: basically, open wheels single-seater formula cars, similar to that displayed on Picture



1.1-2. Any car, any team, any driver have to undergo a specific system of rules. Main target of these rules is achievement of the safety. By the way, It's necessary clarify that safety is much more important than entertainment in such a competition. Second target is attenuate the natural discrepancies which are common between different teams. It the specific, actual adopted system is "SAE – 2013 Formula SAE Rules 03-05-2013 revision", Ref.[1].



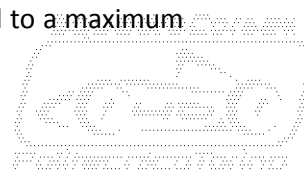
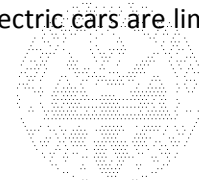
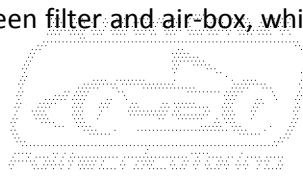
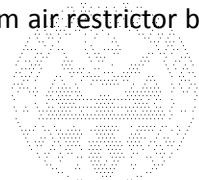
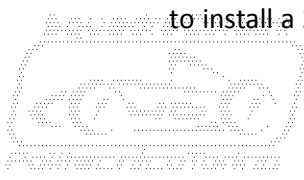
Picture 1.1-3: Group photo of the teams, Formula Student Germany, Hockenheim 2009 (https://it.wikipedia.org/wiki/Formula_SAE).

The second term of European definition is "Student", that's due to the source of competitors, the Universities. More than 400 Athenaeums from all the globe, challenge every year in this real engineering competition. Any athenaeum can deploy one only combustion car, one only electric car or both. Cars are designed, manufactured and managed by staff of universities, organized by teams. The basic requirement to be part of the team is being an undergraduate student, properly enrolled in the athenaeum. This requirement is obviously extended to drivers too.

Differently from main motorsport championships, like Formula1, Moto-GP, World Endurance Championship, Formula Student isn't based on a seasonal ranking. F.S.A.E. is based on different yearly competitions, but any competition is different from others. Official competitions supported by S.A.E. are nine in one year: Formula S.A.E. Virginia, Formula S.A.E. Michigan, Formula S.A.E. California take place in America. I.MECH.E. Formula Student (United Kingdom), Formula Student Germany and formula S.A.E. Italy take place in European summer. Other competitions are Formula S.A.E. Japan, Formula S.A.E. Brazil and Formula S.A.E. Australasia.

However, many other unofficial competitions were organized in last years: Formula Student Austria, Formula Student Hungary, Formula Student Spain, Formula Student Netherlands, Formula North, Formula Student China, Baltic Open and other nice events.

Differently from many motorsport series, there is not a real "Balance of Performance" which is intended to level out the performance of different manufactured cars. No ballast are assigned and there is not a minimum weight to respect. Bounds on aerodynamic wings size is the same for any car. Anyway, maximum power of cars is limited by issues of safety. By Ref.[1], combustion engine cars have to install a 20mm air restrictor between filter and air-box, while electric cars are limited to a maximum



power of 85kW for two-wheels traction and 80 [kW] for four wheels traction cars. Limitations on electric cars are managed electronically, for this reason are much more precise and effective.

Ref.[1] prescribes that any competition undergoes a rigid structure which is respected in order to award the team which performed the best vehicle design. The competition is therefore divided in three main sections, structured to guarantee safety and evaluate the engineering job scrupulously:

- **“Scrutineering” or “Technical Inspections”.**
- **“Static Events”.**
- **“Dynamic Events”.**

During Static Events and Dynamic Events any team can collect precious points that are going to result on the overall competition standing.

During Scrutineering teams cannot collect any point but they can obtain the eligibility to take part to Dynamic events. To explain scrutineering relevance, it’s necessary to remember that cars are prototypes designed and manufactured by students, autonomously. Many of such projects are affected by lack of time or money. In a situation like that, low experience of competitors may cause risks and serious issues of safety.

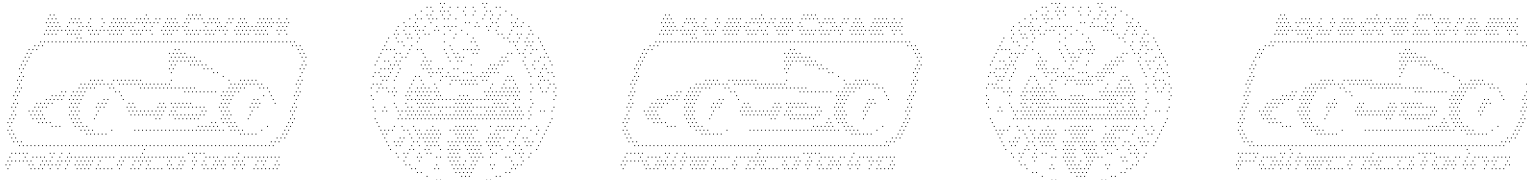
In addition, it’s necessary recall to that safety is the most important driver to respect, in the automotive world. By virtue of that, rigid system of rules described by Ref.[1], affects mainly design and manufacturing choices of teams.

“Scrutineering” is a scrupulous series of checks aimed to ensure the congruity of any vehicle with the so important technical regulations. Stickers are applied on the front end of the car in order to identify which safety test are fulfilled.

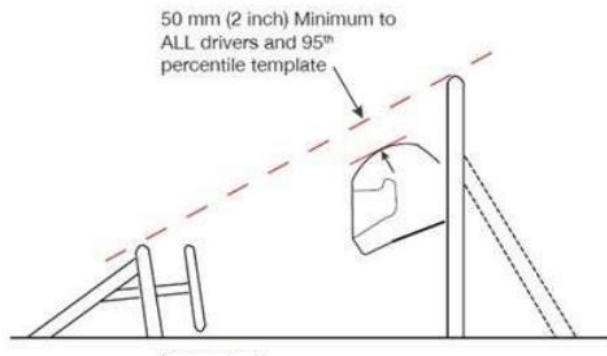


Picture 1.1-4: Application of scrutineering stickers on the nose of SCXV, Formula SAE Italy, Varano 2015 (<https://www.facebook.com/SCPolito/>).

Following are explained safety tests applied to an electric car during the **I.MECH.E. Formula Student** which takes place every year on the magnificent Silverstone Race Track.



- **“Safety”**: is the inspection of safety equipment owned by team. Driving suits, helmets, fire extinguishers, High Voltage gloves and other safety issues are checked in order to verify their congruity with specifications of technical regulations and their validity in the time.

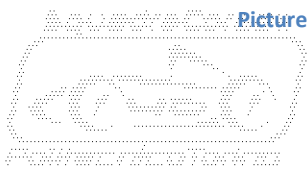


Plot 1.1-1: Minimum clearance between helmet and triangulation of hoops, Ref.[1].

- **“Chassis”**: is a series of tests aimed to ensure that the structures of the frame fulfil the safety requirements of the driver. Minimum volume and opening of cockpit are deeply checked with the help of standard jigs. One of these is called “Percy”, It’s a jig which represents a 95th percentile male. It’s fitted into the car to check if the room of the cockpit is large enough to house the jig with no issues of interference. Anyway, main purpose of Percy is to check that helmet of the driver fall into the triangulation between front hoop and main hoop, with a precise clearance, like is depicted in Plot 1.1-1. Furthermore, chassis test, is the occasion to verify the minimum thickness of safety hoops.
- **“Brake”**: is a short acceleration on a straight line, followed by a strong brake. Test is positively settled if braking system is able to block all the 4 wheels in a maximum range of distance.
- **“Electric”**: is a series of tests performed in order to ensure the safety of the vehicle by the electric point of view. It’s necessary remember that an electric formula student car is moved by an High Voltage tractive system $250\div 600 [V]$. A bad designed or bad manufactured electric loom may cause severe injuries or death in the worst case. For these reasons, all vehicles must be provided by safety features implemented on hardware and software both. Proper operation of any safety feature is accurately checked by scrutineers.



Picture 1.1-5: SC12e during rain test, Formula Student Hungary, Gyor 2012 (<https://www.facebook.com/SCPolyto/>).



- **“Rain”**: is the test displayed by Picture 1.1-5. It’s performed splashing water on the vehicle for a period of time of two minutes. In this time, none of electric devices of the car can show a failure. In particular safety light installed on the top of the main hoop is continuously observed in its operation.
- **“Tech”**: is a series of checks performed to verify the right assembly of car components. In particular, checks are performed to verify the proper assembly of mechanical systems which may cause issues for the safety of the driver. Typical example are suspensions, steering column and pedal-box. Level of detail in verifications is very high and systems are checked in component and fastener. Nuts, for example, needs to exploit self-locking features. Length of bolt have to be proper and in some cases screws must be held by safety wire.



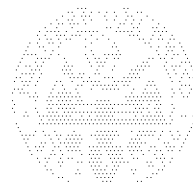
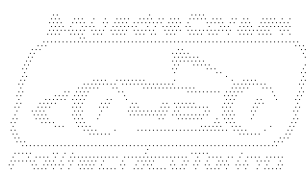
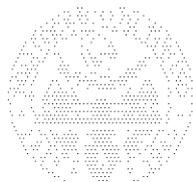
Picture 1.1-6: Scrutineers checking SC12e during the tilt test, Formula Student Hungary, Gyor 2012 (<https://www.facebook.com/SCPolito/>).

- **“Tilt”**: is the test depicted by Picture 1.1-6. Vehicle stands on a tilting platform. During this test, vehicle must not display rollover behaviour due to inclination of the platform. Maximum inclination of the platform is 60°. In addition, vehicle must not display leakage of fluids.

As revealed in advance, vehicles can take part to dynamic events if and only if have completed positively all scrutineering phases. Anyway, participation to static events is not compromised.

Following, next events to take place are **“Static Events”**, unofficially known as **“Statics”**. Statics are structured on three different tests.

- **“Cost Analysis”**: judges have to verify a cost esteem of the car, performed by the members of the team. To alienate all esteems , in order to be compared each others, a standard template have to be followed. Standard template is structured in order to assign an arbitrary cost to materials, solutions and technologies utilized to manufacture the vehicle. Costs of technologies are referred to a large scale production scenario. More precise and more accurate is the esteem, better is the score appointed by judges. Finally the overall cost of the vehicle is evaluated. Cars that can be realized with a low budget on a large scale, are very appreciated and earn precious points in the final rank. Maximum score assigned is 100/1000.





Picture 1.1-7: Jonathan, Claudia and Giuseppe, former members of Squadra Corse, wait to discuss their Business Plan Presentation, Formula SAE Italy, Varano 2012 (<https://www.facebook.com/SCPolito/>).

- **“Business Plan Presentation”**: It’s substantially a huge marketing simulation. Scenario is a case of large scale production in which teams needs to perform strategy to obtain money resources. Resources would be necessary to start the business. Strategies are often based on investigations of the race car market, trying to conciliate the needs of likely customers with business perspectives of investors. This test doesn’t repay marketing and business knowledge only, it repays fantasy and ability persuasion too. Maximum score assigned is 75/1000.



Picture 1.1-8: Carlo, former Squadra Corse member, welcome Evan Short, team leader of track electronic in AMG Mercedes F1 and engineering design judge, Formula SAE Italy, Varano 2012 (<https://www.facebook.com/SCPolito/>).



- **“Engineering Design”**: that’s the most important phase for hopeful race car designers. During a F.S.A.E. event, skilled engineers of motorsport and automotive world became severe judges. Their task is evaluate scrupulously design choices of different teams. Solutions, materials and manufacturing technologies needs to be extensively illustrated by team members to judges. The target for every team member is demonstrate of doing the better choice compared to resources of the team and of the athenaeum. The main feature of this test is the debate that rising designers need to withstand against older and experienced engineers from all the most important companies of the world. Maximum score assigned is 150/1000.

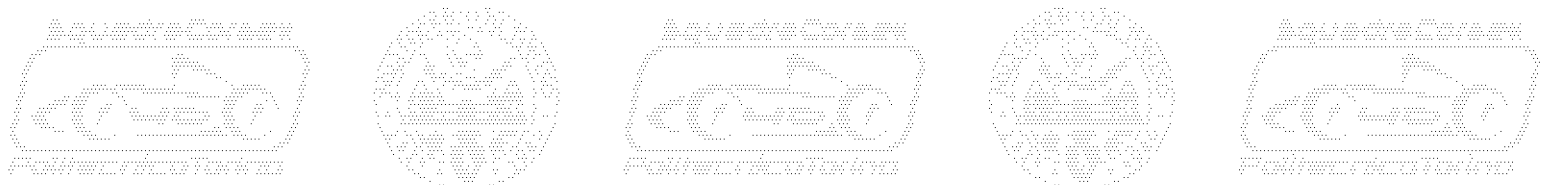
Next phase is the most thrilling of the entire competition, **“Dynamic events”**. In this phase antagonistic spirit and unexpected plot twists convert a “leitmotiv” design competition into a real race. Like previous phases, dynamic too is structured on different tests. In order to make vehicle performance more relevant than racer performance, driver is changed once in each test.

- **“Acceleration”**: car needs to run over along a 75 [m] straight, starting from stationary position. Fine tuned traction and launch control, coupled with a good sensitivity of the driver make the difference on this test. Maximum score assigned is 75/1000.



Picture 1.1-9: Wet skid-pad test, Formula Student Germany, Hockenheim 2014 (<https://www.pistonudos.com/>).

- **“Skid-Pad”**: is a conventional test, widespread in automotive field. Its target is to cause distress to cornering behaviour of the vehicle. This purpose is achieved exploiting a very high lateral acceleration at relatively low speed. Car runs on very tight 8-shaped track: internal radius of circles is 15,25 [m]. Two laps are ride in a clockwise sense, two laps in the opposite. In this phase, a good match of tire, and suspension kinematics allows the driver to perceive the limit of the tire, achieving a good performance. In addition, set-up of the car needs to be very balanced on both sides of the vehicle. Anyway, a good tuning of traction control helps the driver to keep the vehicle on the fastest lane. Additional difficulty is that skid-pad and acceleration test are scheduled in parallel. It’s clear that optimal set up parameters, camber in particular, needs to be very different between two tests and unfortunately, time is not enough to modify the set up. For this reason team



members have to be very able to find the best trade-off between acceleration set-up and skid-pad set-up.

This test rewards the fastest cornering vehicle. Overall lap time achieved in the test, represents the calculated average between best clockwise lap and best anti clockwise lap. Maximum score is obviously assigned to the car which achieved the lowest overall lap time, it consists of 50/1000.

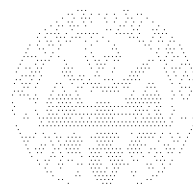
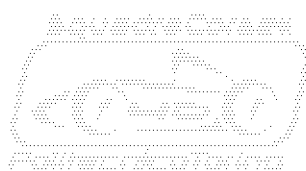
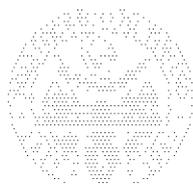
- **“Autocross”**: it’s a sort of time attack, similar to a “super-pole” performed on a point-to-point agility track. In this test, driver needs to exploit the overall dynamic performances of the car. Tight corners, straights and fast slaloms are going to reveal the potential of the car on the track. Ranking provided by this test determines the starting order of endurance event. In this way, vehicles which obtained similar lap times race each other with less interferences due to disparity of performances. Maximum score assigned is 150/1000.
- **“Endurance”**: is the test aimed to evaluate the reliability of the car. It’s the most severe of dynamic tests, because car needs to run a 22 [km] race. It’s not so trivial for a student built prototype. Differently from other tests, the car is not lonely on the track. There are 4-5 cars racing together trying to complete the test in the shortest time. Anyway, overtaking are not free, these are regulated by a procedure aimed to ensure always the maximum safety. Maximum score assigned is 300/1000.



Picture 1.1-10: SC12e and eta2012 (TU Darmstadt) fighting for the podium, Formula SAE Italy, Varano 2012 (<https://www.facebook.com/SCPolito/>).

- **“Fuel Economy”**: fuel or electric energy of cars that completed endurance test are measured. In this way it’s possible to reward the most efficient car too. To achieve a good score It’s necessary to find a good trade-off between endurance performance and fuel or energy consumption. Maximum score assigned is 100/1000.

Clearly, winning team is the one gained the highest score. Even so, any single team member of any single team, gained a personal victory. As a matter of fact, any competition is a very challenging and very formative experience. Participation to a competition is therefore an important event in the job career and in the personal life of any single competitor.



1.2. Squadra Corse – Polytechnic University of Turin.

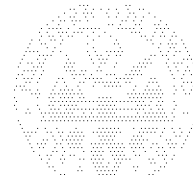
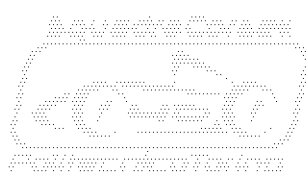
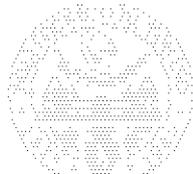
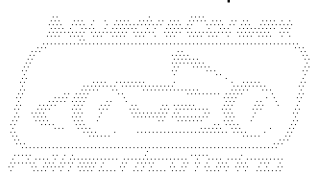
Squadra Corse, S.C. for members, is the academic team established in Polytechnic University of Turin with the purpose of competing in Formula S.A.E. events. Like many other initiatives offered by the athenaeum, it's a voluntary activity not mandatory in order to obtain the graduation title. Anyway, subjects faced during the participation can be a good topic for a graduation thesis, like in this case. To be a team member of S.C. it's necessary to pass positively a severe selection process. Every years hundreds of students apply for the recruitment, but the 10% only is eligible to be part of the team. Judges of this hard selection are veteran members in collaboration with the academic responsible of the team, the "Faculty Advisor". The selection process is structured in order to evaluate the personal experiences, the technical knowledge, the operational skills and the motivating force above all. It's easy to understand that it's quite hard conciliate, academic career, work in the team and personal life.



Picture 1.2-1: Members of the first team pose with S.C.05, IMEche Formula Student, Bruntinghorpe Aerodrome 2005 (<https://www.facebook.com/SCPolito/>).

The story of the team begins in October 2003. A small group arranged by ten students from Automotive Engineering course, coordinated by the "Faculty Advisor" Prof. Ing. Andrea Tonoli, started the design of a single-seater. The car, called **S.C.05**, was able to run in early months of 2005 and to take part in competitions organized by S.A.E. during that year.

The first car of Squadra Corse displays an elegant **red bodywork**. It's a tribute to the most noble Italian racing tradition, made a legend by bespoke brands like Alfa Romeo, Ferrari, Maserati, Lancia, Cisitalia, Itala and other glories lost in the past. A number plate with the **"46"** number dominates the bodywork. Two are the main explanations about the choice of number. The first is a tribute to Cole Trickle, legendary NASCAR driver, portrayed by Tom Cruise in the movie **"Days of Thunder"** (Tony Scott – 1990). Second explanation is a tribute to **Valentino Rossi**, the famous Italian rider who won 9 world championships in the years between 1997 and 2009. Red livery and "46" number were shared by many of Squadra Corse cars and nowadays are one of the most beloved tradition of the team.





Picture 1.2-2: Squadra Corse cars equipped with internal combustion engine, from 2005 to 2011.

From the first single-seater “wearing” red bodywork and “46” race number to the actual “*scdiciasette*”, eleven cars were built. Any car, compared with its previous, displays a continuous technical evolution in all the fields of the design.

The first field of evolution regards the **power-train**, starting from motorcycle internal combustion engines, arriving to electric traction motors. The first single-seater, S.C.05, was equipped with a 4-stroke, 2-cylinders Guzzi V2 engine. From the second car, **S.C.06**, the 4-stroke, 4-cylinders, Honda engine is the base for power-train developments. During 6 years of continuous research and tests, 4-cylinder engines reached important targets of performance and efficiency. Improving of engine performance have been achieved by mechanical and control strategy tuning

First step in the direction of the electric traction, have been done in 2009 when Squadra Corse set up a specific crew with the purpose of compete in the **Formula Student Hybrid**. For this reason **S.C.08** was modified to house the electric power-train which provided a sort of boost to the conventional internal combustion engine. **S.C.08H** was born.

With **S.C.12e** Squadra Corse faces the future of automotive and motorsport, the full electric traction. Two Magneti Marelli electric motors, specific for automotive traction, were installed to make S.C.12e and **S.C.R.** run on the track. The final step of this amazing technical evolution is the 4-motors, 4-wheel drive single-seater. This extremely innovative car architecture was developed by Squadra Corse with **S.C.X.V.** and continues nowadays in the design of future cars.

Another element important for the traction is the **transmission**. Early cars was equipped by a stock gear-box that, in most of cases, was modified in order to lower the total mass of the vehicle. Gear-box faced a specific Formula SAE limited slip differential, with a simple and reliable chain transmission. The most important step of evolution in S.C. transmissions was the introduction of the electro-pneumatic actuation gear-box. This amazing system, was firstly introduced



by **S.C09** and was inspired by most modern high-end race cars. The advantage of an electro-pneumatic actuated gear-box allows the driver to change gear instantaneously, with no need of loose grab on the steering wheel. With the introduction of the electric traction motors, multispeed gear-boxes was

useless. By the way, multi-speed stock gear-boxes were replaced by mono-speed gear-boxes, purposely designed and manufactured by Squadra Corse. From S.C.R. an important knowledge on gear design was collected by the team. The final step of this technical path is the double stage planetary gear-box which equipped new cars since S.C.X.V.

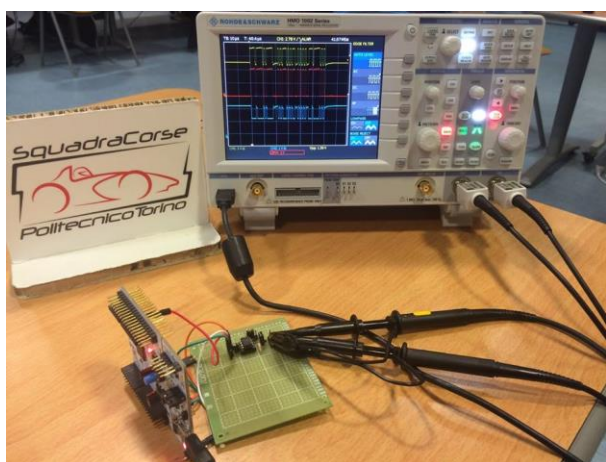


A performing and efficient power-train needs a light but strong **chassis**. S.C.05 was realized by a square-section steel space frame, that solution was widely conventional in single-seaters of many years ago. Then, chassis design was tuned and square-section pipes was replaced by round section pipes. Year after year, packaging, ergonomic and safety issues was important drivers to improve the chassis of previous cars. However, main target of the chassis design is the ratio between torsional stiffness and weight. The main evolution of this technical field was the first **mono-coque** realized using carbon fibre reinforced polymers (C.F.R.P.). It was introduced firstly in 2013 on S.C.R. project. This solution was inspired by top performance formula single-seaters.

Picture 1.2-3: S.C.X. chassis laying on the welding jig. It's the most typical example of steel tubular space frame of a formula student car (<https://www.facebook.com/SCPolito/>).

Another strong point of S.C. single-seaters are **suspensions**. Inspired by actual formula cars, double wishbone arms is the standard configuration. In most of cases hydraulic dampers were faced with push rods layout. Only two cars in S.C. history deviated from this pattern, adopting a pull-rod layout: **S.C.07** and S.C.R. Independently from adopted layout, suspensions was always developed studied in S.C. projects. Kinematic studies and very realistic lap time simulations allows the team to reach important targets of performance.

Last but not least is **electronic**. In early cars electronic was restricted to a basic engine control. During years, as done for mechanic, electronic of the car was step by step developed. CAN-BUS communication, real backbone of nowadays cars electronics, was finally introduced on S.C. projects. In this way it's possible to implement a strong data acquisition system, essential for reliability tests and fine mechanical tuning of the car. However a fine mechanical tuning may not be enough to be competitive or winner. Differently from many championships, a very open system of rules, allows the development of refined electronic controls



Picture 1.2-4: Debug of electronic components of Squadra Corse car (<https://www.facebook.com/SCPolito/>).



applied to chassis and engine. On many single-seaters, performance of the driver is supported by launch control and traction control. In many cases, electric traction formula student features a real electronic differential, the "Torque Vectoring". Differently from early vehicles, nowadays S.C. cars represent an articulated electronic system in which controls holds the largest majority of importance.

Growing in car design implicated a significant team growth. The little group of ten race enthusiasts became a real organized team which is composed by approximately fifty students. Origin of students is very spread, by academic and by geographical point of view. Students came from different courses of study like mechanic, automotive, energetic, electronic, telecommunications, industrial design, engineering management and others. On the other hand, team is not composed by only Italian members. During years of activity, team integrated members from China, South America, Spain, France and many other countries.

Analogously of what happens in professional motorsport team, two main tasks of members are "technical" and "management". The technical crew acts on all the technical issues concerning car and competitions. Typical activities performed by technical crew are design, manufacturing and testing. On the other side, the management crew acts on sponsor relationships, promotional activities, paperwork, logistic and planning of competitions.

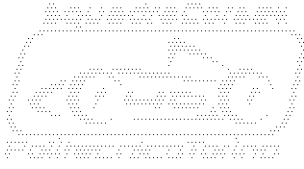
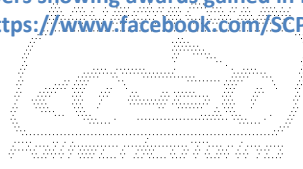
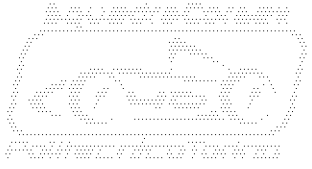
Despite this apparent split, Squadra Corse members need to work jointly together. Common targets, but friendship above all, make the team stronger and able to face problems and difficulties lead to F.S.A.E. season. For that reason, formula student is not only an occasion of growth or a strong passport for the labour market, formula student is an excellent human experience.

During so many years, team renovated personnel many times. Many members, completing the academic path, needs to quit the team to start the job adventure. By the way spirit of Squadra Corse is always the original:

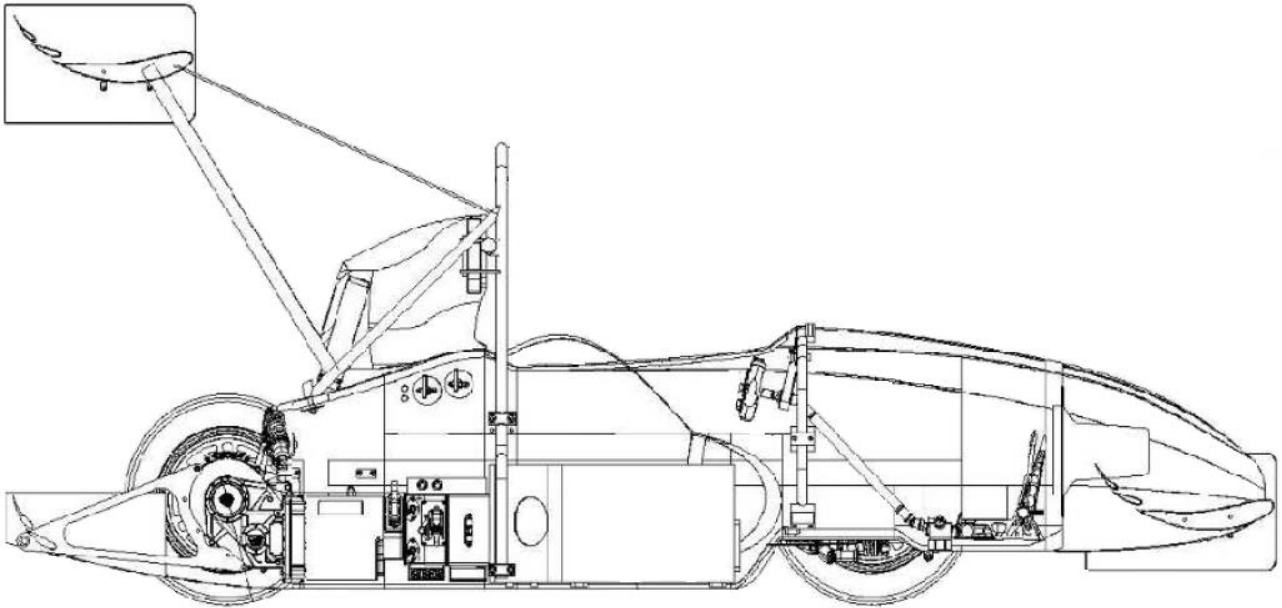
"Abbiamo sempre puntato a superare gli altri ed i nostri stessi limiti. – [ENG.]: We've always tried to overcome other competitors and our own limits."



Picture 1.2-5: Team members showing awards gained in Formula SAE Italy, Varano 2012 (<https://www.facebook.com/SCPolito/>).



1.3. S.C.R. and S.C.R. evo.



Picture 1.3-1: Side view of S.C.R.

Usually, the acronym that identifies a Squadra Corse car is composed by letters “S” and “C” followed by two numbers which identify the year of production. The subject in question is born to be a point of break, starting from its identification acronym. In this case letter “R”, which replaces the usual numbers, means “**Revolution**”, revolution in the design.

In order to appreciate main features of S.C.R. project, it’s necessary to briefly explain how it’s usually made a F.S.A.E. car, compliant with rules described by Ref.[1]. Like it was revealed in advance at Chapter 1.1, that kind of vehicles are open wheel single-seaters.

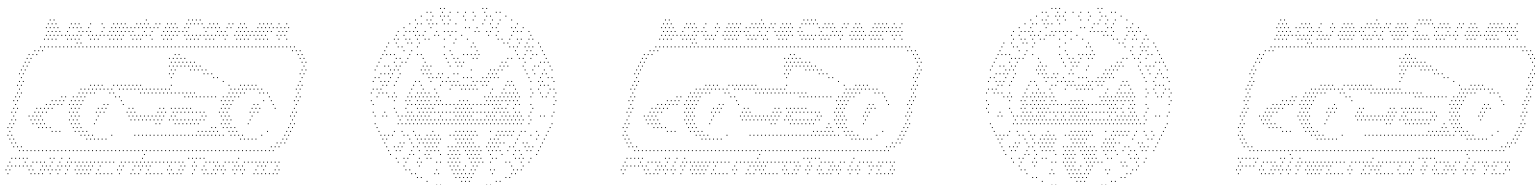


Picture 1.3-2: Comparison of dimensions between kart, formula student and Formula Renault 2.0.

Like it’s shown by Picture 1.3-2, dimensions are higher than a Kart but lower than an entry level formula car like Formula Renault, Formula4, and others. It’s the same about weights, F.S.A.E. car represents a compromise between a kart and a basic formula car. Despite dimensions and performances are more similar to a kart, architecture of the vehicle is typical of a formula car. Survival cell, double wish-bone independent suspensions, 13 [inches] racing wheels and aerodynamic pack are the typical formula car features which are widespread in F.S.A.E.

By technical point of view, F.S.A.E. vehicle can be ideally split in three main fields: “frame”, “power-train” and “controls”. Purpose of this chapter is explain widely each field of the vehicle.

“**Frame**” consists of the main structural parts of the car like chassis, suspensions, un-sprung weights, steering system, pedal box, aerodynamic pack and bodywork.



“Power-train” is the system of the car which provides the traction. Usually, main power-train components are of an internal combustion car are: motorbike engine, fuel tank, intake system, exhaust system, cooling system, gear-box, limited slip differential and axles. Power-train regarding an electric formula S.A.E. car is quite different and it’s composed on: motor which can be more than one, accumulator, controller which may not be single, transmission and cooling system.

“Control” consists of software and hardware components necessary to drive the systems of the car in order to obtain reliability and performance of the vehicle.



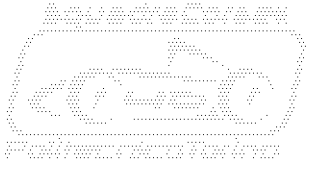
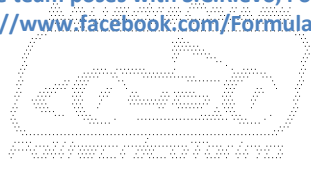
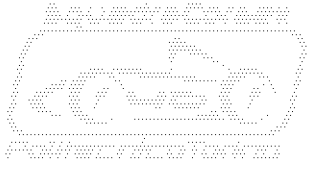
Picture 1.3-3: Squadra Corse team poses with S.C.R., Formula Student Germany, Hockenheim 2013 (<https://www.facebook.com/FSGeV/>).

S.C.R. project started in first months of 2012. It was based on some research and development studies: composite material chassis, gear-train and aerodynamic pack. Anyway, the real rush of the project started in autumn 2012, after the admission of the new team members. Finally S.C.R. was officially presented on July 15th of 2013, in Museo dell’ Automobile, in Turin.

After a strong rebuild and many modifications on original design of components, S.C.R. returned on the track in 2014 for its second season. The car was launched with the name of S.C.R.evo.

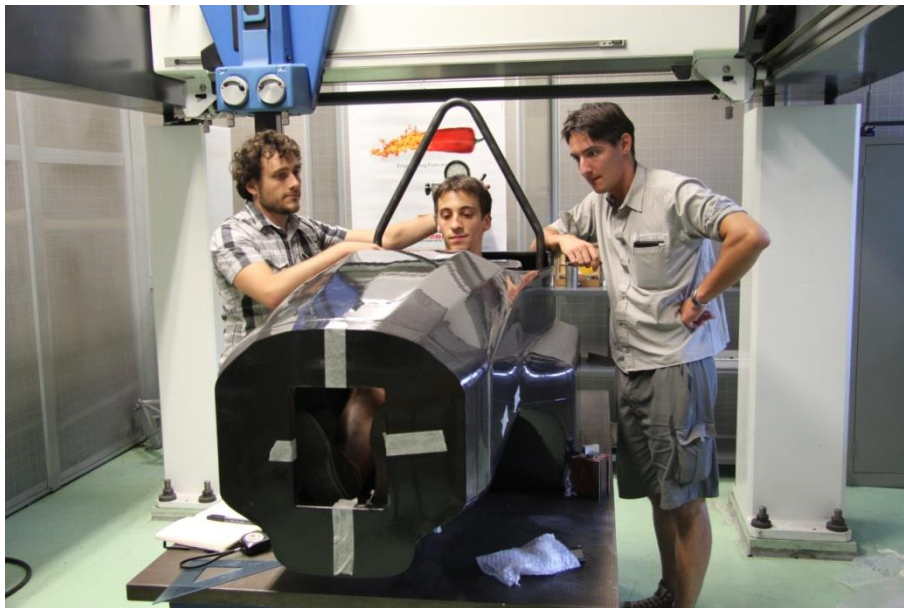


Picture 1.3-4 Squadra Corse team poses with S.C.R.evo, Formula S.A.E. Italy, Varano 2014 (<https://www.facebook.com/FormulasAEItaly/>).



As explained before, S.C.R. was a “revolution” if compared to previous Squadra Corse project. By the way “revolution” is, first of all, intended as an evolution in previous designs. Following it’s important remark the main differences with S.C.12e, the previous Squadra Corse project.

Traditionally **chassis** of Squadra Corse cars was built welding pipes of 25CrMo4 together on a proper jig. This layout was improved season by season, reaching very important targets of “**torsional stiffness/weight**” ratio. With S.C.12e, steel chassis performances achieved the peak. A radical change of technology was necessary to improve more. Inspired by top performance modern race cars, the mono-coque of S.C.R. is realized by carbon fibre reinforced plastic technology.



Picture 1.3-5: Jonathan, Alessandro and Daniele performing first checks on the mono-coque of S.C.R.

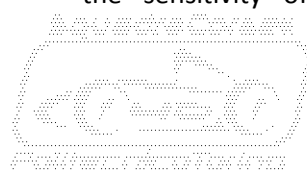
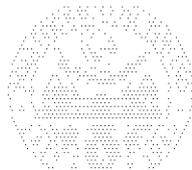
This technology is based on the lamination of carbon fibre skins on a desired shape mould. Internal and external carbon fibre layers are spaced by an honeycomb texture core which has a specific width. This kind of layout is known as “**sandwich structure**” and it’s displayed by Picture 1.3-6. Honeycomb, usually made of Kevlar fibre or aluminium, is, in some cases, subrogated by polyurethane solid foam panels. Advantage of foam panels is the capability of be machined. In this way, machined panels can be used as filler in complex geometry areas.



Picture 1.3-6: Composite material panel manufactured with “Sandwich Structure” (<https://aerospaceengineeringblog.com/>).

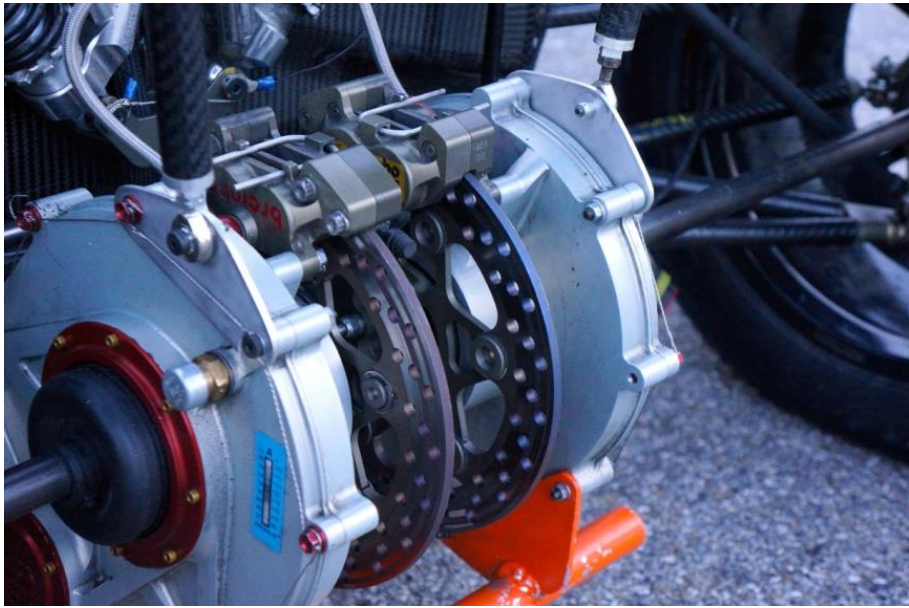
Carbon fibre can be purchased in rolls by form of pure texture or by form of “pre-preg”. This last solution is made up of texture impregnated of resin, which enables an easier application of the material. Geometry and sizes of texture are different and depend on the specific application.

Choice of materials depends logically by performance targets and budget issues. Design of chassis, entirely performed by S.C. members, was a challenging process in which tests on materials was performed in parallel with complex F.E.M. and draping analysis. The aim of tests was collect data on performances of materials and understand the sensitivity of material to different manufacturing



techniques. By previous calculations, optimized carbon fibre layers are split in skins of a well determined geometry. Any skin owns its precise position on the chassis. Then, It's fundamental determine the thickness of layers and skins but that's not enough. It's necessary to know that carbon fibre, which is product on the form of "fabric", is not an isotropic material. By virtue of that, its performances varies on the base of texture orientation. For this reason, many steps of material optimization, are required to determine the exact orientation of any patch of carbon fibre.

Anyway the technology of composites displays higher costs of materials and an higher manufacturing complexity if compared with welded pipe technology. Despite the higher complexity, chassis was entirely and successfully manufactured by team members.

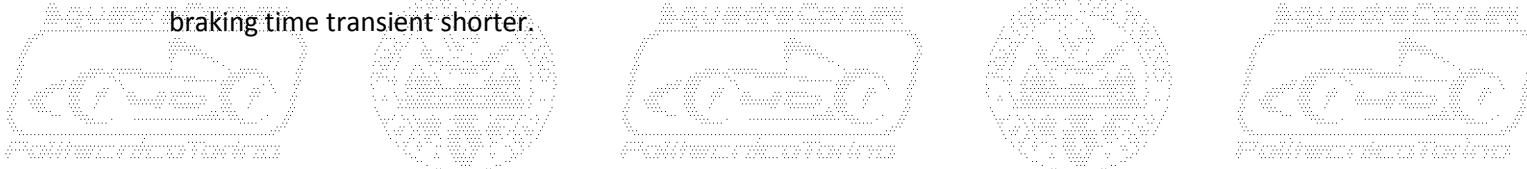


Picture 1.3-7: On-board brakes mounted on S.C.R. gear-box.

Braking system of S.C.R. is assembled with top performance motorbike calipers and racing car pumps, supplied by one of the main sponsors, the bespoke Brembo company. These excellent components are widespread in Squadra Corse projects, but S.C.R. is the unique car that can display **"on-board brake technology"**. Rear brake calipers are fixed to the gear-box structure instead to upright. Brake discs are bounded to transmission axles. This solution allows to save weight on un-sprung masses with important benefits on handling and traction. The main drawback of this solution is the augmented stress on axles that can bring to fatigue failures.

Another important improvement in braking system is the **"brake bias electronic distribution"**, that allows to vary the brake bias distribution by the steering wheel. Front/Rear brake distribution, in racing car, is often adjusted by a main screw that connects brake pumps and brake pedal, the "balance-bar". It works varying the length of the lever arms corresponding to front or rear brake pump. Usually balance bar is actuated by a steel wire connected to a rotating knob mounted on the instrument panel. This mechanical link, on S.C.R. was replaced by a small DC motor housed in the pedal box and controlled by an electronic knob housed on the steering wheel. In this way it is possible to adjust the brake balance quicker, without losing grip on the steering wheel.

The entire system is then completed by specific motorsport fittings and steel braid reinforced pipes. The high stiffness of this specific pipes, avoids displacements caused by brake pressure, making the braking time transient shorter.





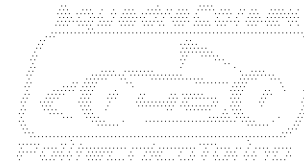
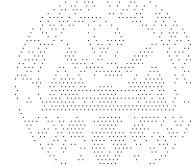
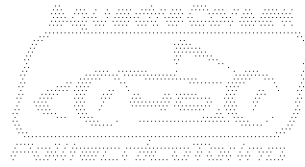
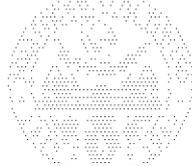
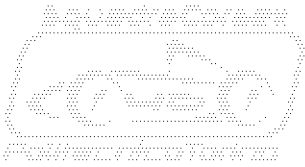
Picture 1.3-8: S.C.R. wheel hubs, front and rear (<https://www.facebook.com/SCPolito/>).

Like it was revealed in advance, lightweight **un-sprung masses** are fundamentals in a competitive race car. For this reason, components are manufactured with the most performing technologies and materials. Uprights are realized machining a monolithic block of Al7075-T651 Ergal, one of the strongest alloys of aluminium. Uprights are designed in order to tune the set up of the vehicle quickly, adding or removing narrow metal shims.

The other very important component of un-sprung masses is the wheel hub. It is designed to support the wheel, holding it with a single centre locknut. This solution is very widespread on top level Formula cars or Gran Turismo cars. Main feature is the quick tire replacement. Wheel hubs, like uprights, are totally designed by team members. Are obtained machining a monolithic round of Ti-6Al-4V Titanium alloy. Titanium Alloy is an excellent compromise between strength and weight and it's the real middle-ground between steel and aluminium.



Picture 1.3-9: S.C.R. upright during an intermediate step of manufacturing (<https://www.facebook.com/SCPolito/>).



Another main feature of this material is the excellent corrosion resistance that makes the alloy largely employed on biomedical and aerospace fields. The wheel hub is sustained by a “O-mounted” couple of high precision hybrid spherical bearings. That solution guarantees a very rigid coupling and ceramic spheres feature extremely low friction combined with low weight.

Rims, 13x7” size, are produced by another bespoke partner of Squadra Corse, OZ Racing. The technology employed in the production of these rims is the magnesium casting. Magnesium, is another interesting material employed in most extreme engineering fields. Weaker than aluminium, magnesium is therefore lighter and very suitable for cast manufacturing.

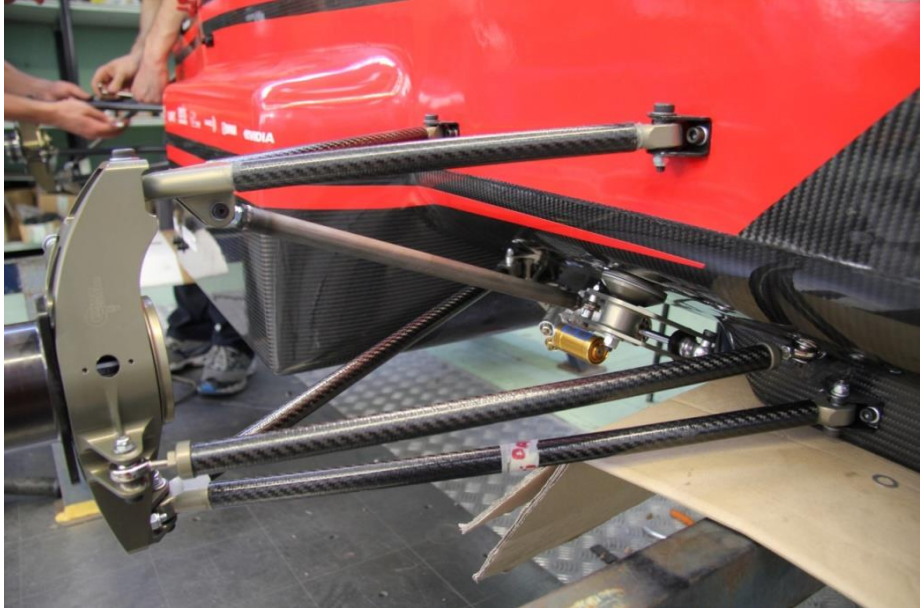
Finally it’s necessary a mention about tires. Made by the legendary Italian Pirelli, supplier of Formula1, Superbike Championship and World Rally Championship. The strong point of these tires is the compound, an extremely soft blend used in motorbike competitions that guarantees an excellent grip in any condition of the tarmac. Obviously, tires are supplied in “slick” and “wet” version.

Suspensions are realized in double wish-bone configuration, with push-rod on the rear and pull-rod on the front. Suspension hard-points that are a key point in the car design, are determined evolving from previous cars configurations. Target is to improve handling features of the car. Taking into account S.C.12e dynamic performances, S.C.R. design needs to be finalized to:

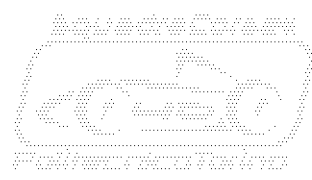
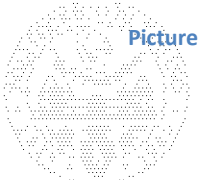
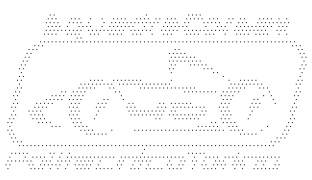
- Weaken the **“under-steering”** behaviour at end of corners.
- Increase the **“pitch effect”**, in order to improve the braking feeling.
- Increase the **“sensitivity”** on the steering wheel.

In order to better understand previous issues, it would be recommended consultation of *“W.F. Milliken & D.L. Milliken - Race Cars Vehicle Dynamics”*, Ref.[2] and *“G. Genta - Meccanica dell’Autoveicolo”*, Ref.[3].

The approval of suspension hard-points was obtained after about a month of calculations and realistic software simulations. Thanks to the software VI Grade, it has been possible to implement two vehicle models: one based on S.C.12e and one based on S.C.R. Two models was compared by lap simulations performed on real F.S.A.E. tracks.



Picture 1.3-10: Detail of front-left suspension of S.C.R.



However, main improvement of suspension system, regards roll rate. It's grown from $0.6 [deg/g]$ to $1 [deg/g]$ and to do so it was decided to vary the roll centre position. However, possibility to vary the value from $0.5 [deg/g]$ to $1.5 [deg/g]$ depending on the needs, has been maintained.

Furthermore, rear wheel track was increased as well, to improve the grip at the entering of the corner and during the acceleration test. Anti-Dive value too was increased of about 2% with the respect to S.C.12e, that feature improves the pitch and braking feeling. Like in the case of S.C.12e suspensions are designed in order to have the lower control arm as long as possible, in order to avoid large variations of track and roll centre. Outer hard-points need to be as near as possible to the centre of the wheel, that reduces dimension and mass of un-sprung weights. In front suspension king pin axle was reduced in order to decrease the load on the steering wheel.

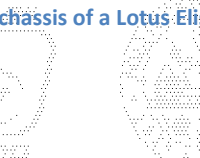


Picture 1.3-11: Detail of front-left rocker assembly with rear lower-control arm, push-rod, damper and anti-roll bar connection rod, S.C.R.evo.

Choice of pull-rod in front suspension, displayed on Picture 1.3-11, is quite atypical in S.C. cars. However it's a good solution by aerodynamic and weight distribution point of view. In this way the damper-rocker system is "hidden" under the nose of the car, in a specific slot realized between the pedal-box and the driver seat. That improves the aerodynamic efficiency, reducing considerably the drag. More relevant issue to consider is that the groups of dampers, rockers, anti-roll bar are a mass difficult to neglect. For this reason, house these components in a lower position helps to lower the centre of gravity of the car. This feature represents a notable advantage by handling point of view.



Picture 1.3-12: Structural bonding applied to the aluminium chassis of a Lotus Elise (<https://framess.co/>).



Suspensions, which influence main dynamic performances of the car, are interesting by the point of view of manufacturing too. Control arms are assembled with aluminium inserts glued to carbon fibre pipes. Aluminium inserts are machined from monolithic blocks and are necessities to house steel spherical joints. By the way the key of this exotic lightweight design is adhesive.

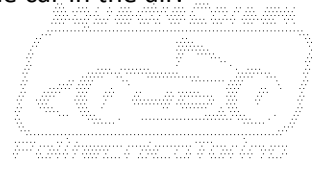
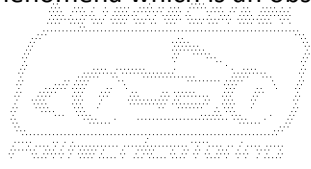
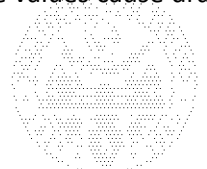
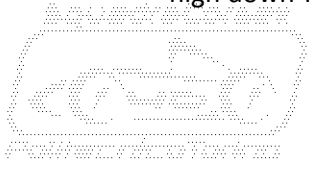
Structural bonding is obtaining an increasing success in automotive industry nowadays. One of the most iconic example is the Lotus Elise chassis, displayed on Picture 1.3-12, realized by extruded aluminium beams bonded together and then riveted in order to ensure a safe mechanical backup. Like other S.C.R. car components, glue too is an extremely high technologic product: a two-components structural adhesive especially designed for heavy duties. In that kind of manufacturing, it's necessary to respect a rigid bonding protocol. Indeed a soil surface, a worst application of the catalyst or a wrong environment temperature can be very dangerous for bonding effectiveness. Due to low reliability of the process, following cars made by S.C. abandoned that innovative design, preferring more conventional solutions.

Anti Roll-Bars, A.R.B., like it was revealed in advance, act on rockers through a simple rod and are bear by polymeric bushings housed in lightweight chassis brackets. Therefore, design of A.R.B.s is much more conventional than control arms one. A.R.B.s are manufactured by steel levers welded to a round pipe. Geometry of levers is specific to obtain a quick A.R.B. tuning, one of the most performed intervention during track events.



Picture 1.3-13 S.C.12e performing aero-test in Centro Ricerche Fiat wind tunnel, Orbassano 2012 (<https://www.facebook.com/SCPolito/>).

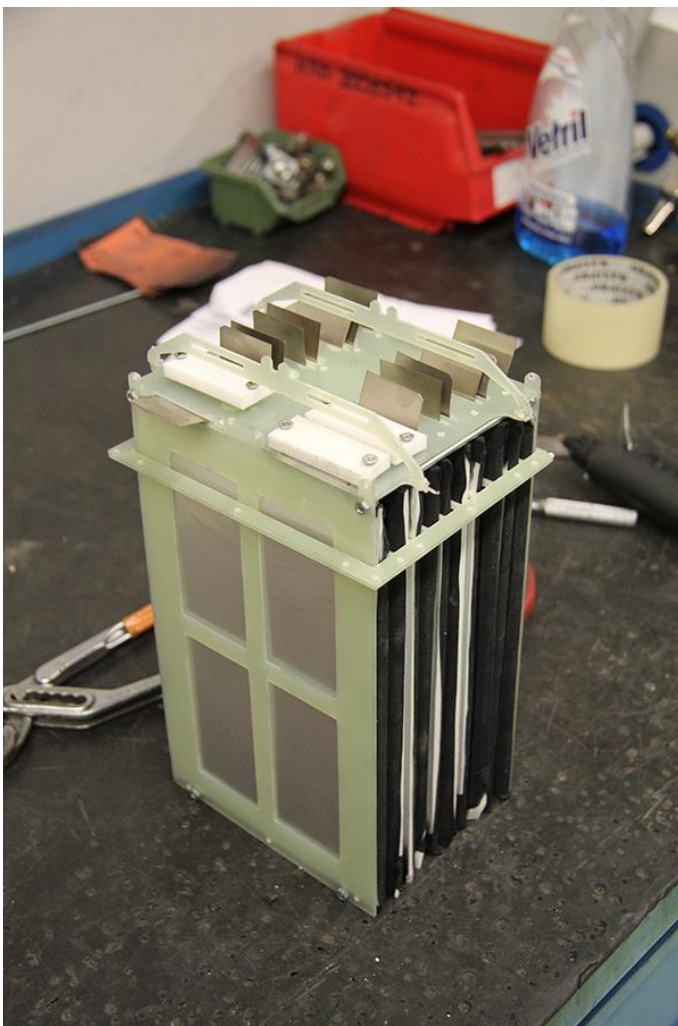
Another field that is widespread in formula F.S.A.E. nowadays is **Aerodynamic**. According to “J. Smith – *Fundamentals of Motorsport Engineering*”, Ref.[4], main target in the work of aerodynamic is to find the best trade-off between “down-force” and “drag”. Aerodynamic devices exploit, above all, down-force that improves the grip of tires pushing the car to the ground. Moreover, devices featuring too high down-force values cause drag phenomena which is an obstacle to penetration of the car in the air.



Such behavior finally affects negatively the energy consumption. Like revealed at chapter 1.1, in F.S.A.E. competitions, consumption is very important, especially for an electric vehicle. Many CFD analysis and lap-time simulation was performed, choosing the more suitable wing profiles.

Finally CFD model was evaluated comparing it to the model obtained by a real test in FIAT wind tunnel. The result was a vehicle equipped with: front wing, rear wing, flat bottom and rear diffuser. Aerodynamic devices are realized by carbon fibre profiles, bonded to aluminium inserts in order to feature a strong and rigid structure. To ensure a more accurate tuning of the car, wing profile angles can be easily adjusted, ensuring more degrees of freedom in set-up of the car. The complete aerodynamic kit was manufactured and assembled only in 2014, in order to equip the rebuilt S.C.R.evo.

Power-train of S.C.R. is intended in rear drive independent wheels. Both driving wheels are actuated by an independent motor-controller system. The ability of drive wheels autonomously allows to implement a real electronic differential known with the name of **“Torque Vectoring”**. The importance of this feature is the abatement of the friction losses that are very serious in a mechanical differential transmission. In addition, tuning of the differential can be adjusted by the cockpit, with no need of long time mechanical interventions. This fact is extremely important in order to achieve a good performance. An heavy mechanical component, like the differential is then replaced by a weightless algorithm based on vehicle dynamic equations.

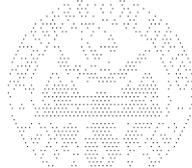


By the point of view of the hardware, S.C.R. power-train is based on specific automotive components supplied by Magneti Marelli: two **“TMG-Small-Size”** motors (that will be widely described in chapter 2.7) and two **“Proto-C”** controllers.

Other main component of the Power-Train is the accumulator, or **“battery pack”** that consists of 96 Lithium-Polymer battery cells packed together in order to satisfy safety, packaging and weight distribution requirements. The accumulator is packaged in three main modules. Any main module is assembled with sub-modules like that shown in Picture 1.3-14.

Main modules are split in two main volumes. Lower part of structures houses core of the cells, for this reason is provided by electric fans that features a cooling effect. Upper part houses contacts of cells and, for these reason needs to be insulated from the external environment. Accumulator modules surround the driver on three sides. For this reason, structures have to be strong enough to guarantee mechanical restraint and electric insulation of cells. Finally, structures need to allow a simplified maintenance and a quick cell replacement.

Picture 1.3-14: Accumulator sub-module before the final assembly.





Picture 1.3-15: S.C.R.evo radiators.

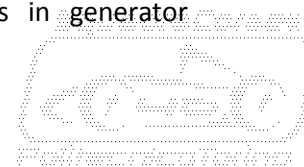
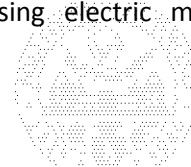
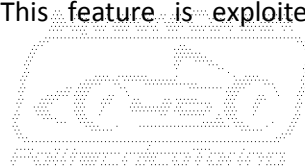
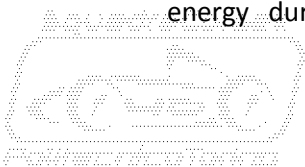
Accumulator is one of the most complicated system on F.S.A.E. cars. In order to solve some reliability issues and lower the weight, in 2014 S.C.R.evo was equipped with a brand new accumulator.

While a simple air cooling can be enough for the accumulator, motor and inverters need a proper liquid **cooling system**. The target is to satisfy reliability and efficiency requirements of main power-train components. Data necessities for a fine calculation have been obtained logging more temperature sensors on S.C.12e. It's necessary to remember that S.C.12e shared the same traction components. Data has been necessities to perform a model of the cooling system, useful to calculate cooling liquid flow and dimensions of the radiators. Layout of cooling system is split on two main symmetrical branches. Any branch connects an hydraulic pump, a controller and a motor. Branches gather together at entry and split at exit of the radiator. The system is filled and bleed from a pressure cap, welded on the top of the cooling fluid reservoir. In order to

improve performances, the plant is pressurized to $1,3 [bar]$. The unique radiator was originally housed behind the helmet of the driver, in order to obtain good cooling performances without compromise aerodynamic efficiency. By the way a single plant with a single radiator wasn't enough. For this reason in 2014, S.C.R.evo cooling system was split in two different plants. Essentially, controllers was served by an autonomous secondary plant, which is provided of a water pump and a single radiator. The main plant, which serves motors, is still split in two branches. Every branch is provided by a own radiator, but the pump is single. Radiators are housed on both sides of the car, in the area between suspension points and roll bar bracings.

Electric and electronic systems of the car can be grouped in two main areas: high voltage electric part and low voltage electric part. High voltage main components it's obviously the accumulator. The nominal voltage of the accumulator is $350 [V]$, with a peak voltage of $398 [V]$. It's important to remember that, in comparison with S.C.12e, the nominal voltage is grown of about $100 [V]$. That's because motors exploit the best efficiency in the range between $350 [V]$ and $420 [V]$. Capacity is bounded by F.S.A.E. rules to a maximum value of $7,5 [kWh]$. The choice of designers was to exploit all the allowed capacity.

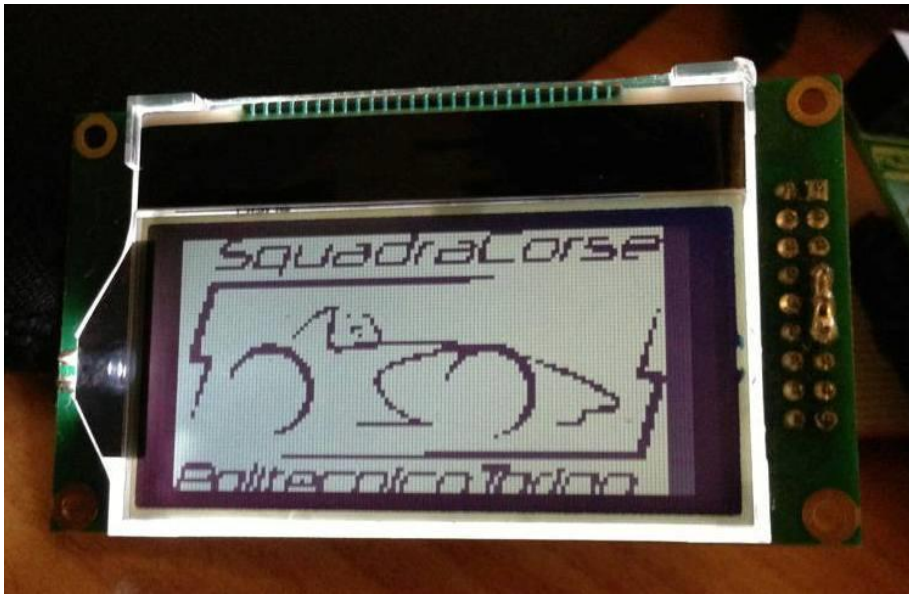
Another very important component is the **"Vehicle Management Unit"**, V.M.U., which governs the power-train controllers sending messages by CAN bus. **"Electronic differential"** and **"traction control"** are implemented inside V.M.U. Anyway, the most innovative feature adopted on S.C.R. is the **"kinetic energy recovery system"**, K.E.R.S. Developed in F1 and LMP1 vehicles, K.E.R.S. allows to recover kinetic energy during the brake phase. This feature is exploited using electric motors in generator



configuration. In this way, a large amount of the kinetic energy of the car, that usually is wasted by brakes in heat generation, is recovered and stored into the accumulator. Two main benefits of K.E.R.S. are the extended autonomy of the accumulator and the downsizing of the mechanical elements in the braking system. The drag torque of electric motors employed in configuration of generator is an important aid during the brake. For this reason, components can be downsized in order to set an important weight saving on un-sprung masses. High voltage electric part is completed by the discharge circuitry, a very important device that allows to work on the car in safety, with all the stored electric energy circumscribed to accumulator only.

Obviously high and low electric parts are kept in communication and the medium is established by three **CAN buses**. Main controls of the vehicle works measuring the accelerations of the car, for this reason low voltage electric parts includes an **"Inertial Measurement Unit"**, I.M.U. Such a unit is constituted by a tri-axial MEMS sensor which measures linear and angular accelerations of the vehicle.

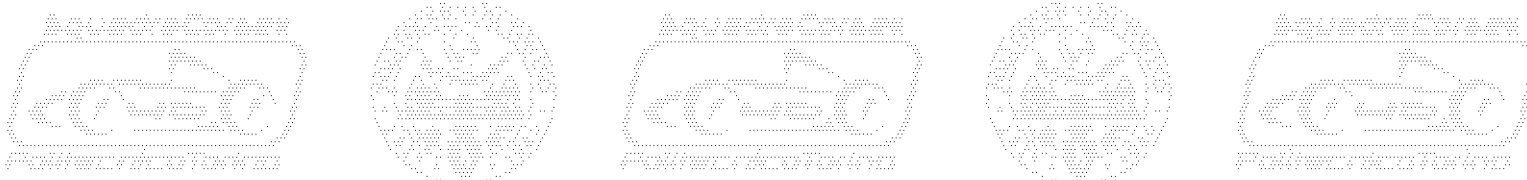
Another important low voltage component is the **"Temperature Measurement Unit"** a device utilized to monitor temperature of tires during tests. T.M.U. is based on three infrared sensors mounted in proximity of each wheel, one points the external tire tread, one the central tread, the last points the internal tread. These measurements are fundamentals to understand behaviour of the tires and tune the suspension set-up scrupulously.



Picture 1.3-16: LCD display of S.C.R.

"Battery Management Systems" B.M.S. are two and are applied to low voltage and high voltage accumulators. These devices control the state of charge and the voltage of service of the accumulators. B.M.S.s work essentially during charge phases but are employed in safety issues too. In case of any failure, B.M.S. sends an alert message to V.M.U. that shuts down the car, avoiding dangerous issues.

Like the late majority of racing cars, S.C.R. is equipped by a **"data-logger"**, a system which collects data from all the sensors installed in all the systems of the vehicle. The same system can store data on a SD card or send them to an access point which creates a suitable net. In this way it's possible to collect a reliable data back up and read live data by remote position.



A small **L.C.D. display**, housed in the centre of the cockpit, completes the low voltage parts of the car. This display allows the driver to monitor the main information regarding the running car. Very useful is the visualization of the parameters set by the cockpit.

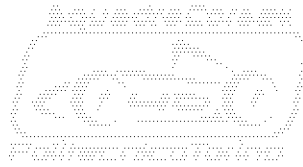
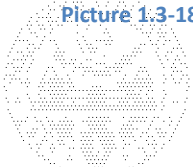
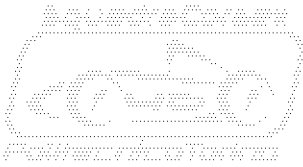
It's important to remember that all units are designed, manufactured, programmed and tested by the members of the team, like the late majority of mechanical components.



Picture 1.3-17: S.C.R. in the day of public presentation, Museo dell 'Automobile di Torino, 2013.



Picture 1.3-18: S.C.R.evò testing in Barauda track, Moncalieri, 2014.



1.4. Design evolution in Squadra Corse transmissions.

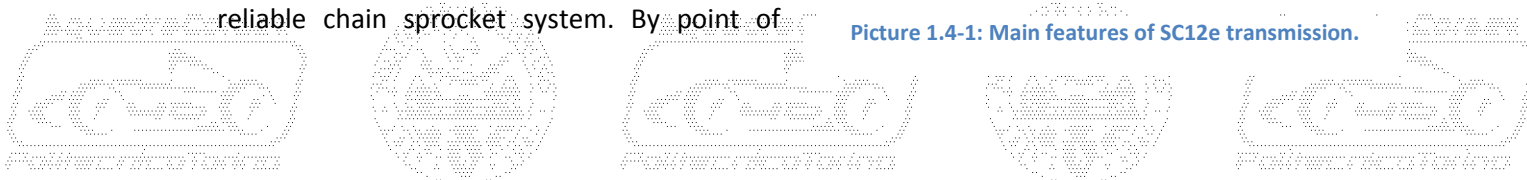
The main topic of this work, are transmissions. To better understand the importance of S.C.R. project, it's useful explain how transmission designs evolved in Squadra Corse team. How explained in advance at Chapter 1.3, internal combustion engine vehicles needed multi-speed gear-boxes coupled with limited slip differentials. Main components of the transmission was therefore derived by stock components or modified stock components. The main feature of electric motors is the highest torque, supplied from "zero rpm". Moreover, rpm range is very wide compared to a conventional internal combustion engine (2-3 times higher). It's known that in F.S.A.E. events, elevate top speed isn't important like in other motorsport competitions. Top speed is reached occasionally, during the "acceleration" test, 160 [km/h] are enough to gain an excellent lap. These motivations make a conventional multi-speed gear-box worthless on a F.S.A.E. vehicle. Clutch too is useless since electric motor doesn't need an idle revolution regime. In addition, is no more possible buy or modify stock transmission components found on the market, anything between motor and wheel have to be specifically designed.

1.4.1. S.C.12e.

The first step of the evolution corresponds to the first electric car designed by Squadra Corse, S.C.12e. In order to save time and contain dangerous uncertainties derived by the new power-train, the vehicle was strictly derived by the previous car, the rear wheel drive S.C.X.X. Basically, the new electric power-train components was fitted into the car avoiding strong modifications of the layout and of the chassis. From nose to the back of the driver, electric car is very similar to the previous internal combustion engine vehicle. Accumulator was stored in the position previously occupied by the fuel tank, behind driver's back. Two Magneti Marelli TMG small size motors are placed in transversal configuration, in the lowest free space behind the accumulator. Controllers that have a mass lower than motors, are packed together and placed over the motors. As explained in Chapter 1.3, two motors electric car doesn't need a mechanical differential, for this reason any motor is equipped with its own independent transmission. Wheels are moved by specific half-shafts provided by classical tripod joints on both sides. This solution allows the operation of the axle independently by suspension movement. Motors and axles are faced by a strong and reliable chain sprocket system. By point of



Picture 1.4-1: Main features of SC12e transmission.



view of the tuning, this system is very smart because allows to change the gear ratio quickly in a very cost efficient way. Indeed It's enough change the pinion and the sprocket , or the sprocket only, in order to obtain the desired ratio. Moreover, a set of sprocket with different number of teeth is a low-cost solution, because motorcycle sprockets can be easily found on the market. Such a kind of system, represents a very lightweight solution, due to the simplicity of the components and due to the needlessness of a proper oil sump.

Anyway, this kind of solution features some drawbacks, the first is related to efficiency. It's well known that chain-sprocket mechanism is affected by strong friction, that friction grows if the system isn't accurately clean up and lubricated. But the main drawback is the limited gear ratio which It's possible to obtain, S.C.12e features a maximum of 6:1.

1.4.2. S.C.R.

S.C.R. project is a very significant step by many points of view of the design. It was affected by severe issues which compromised agonistic performances. Anyway, such experience provided to the team many benefits by knowledge point of view.

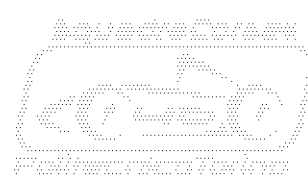
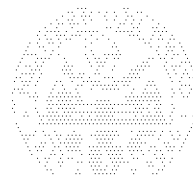
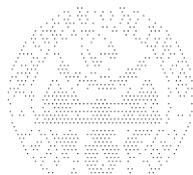
The architecture of the car is strongly different by previous cars, that is due to a new layout deeply explained in Chapter 1.3.

Anyway the car is still a rear-drive vehicle with two motors and two independent transmissions. Main difference is related to layout of the motors installed in longitudinal position. However, motors are the same of the previous project. In order to increase the gear ratio between motors and wheels, another reduction stage is added, featuring a total gear ratio of 9:1. The new layout of motors impose that the first stage is realized by a set of bevel gear, while the second is realized by a set of spur gear. Such design is more complicated if compared to previous chain-sprocket system. Manufacturing needs deep knowledge about gears and about their specific design. Unfortunately, gear system allows less possibilities of tuning. Replacement parts are custom and, for this reason very expensive. Errors in esteem or calculations of parameters have to be avoided at any cost.

Anyway S.C.R. is the first Squadra Corse vehicle equipped by a gear-box completely designed by the team. That it's an important step because provides a good starting point in the work on transmissions for next vehicles.



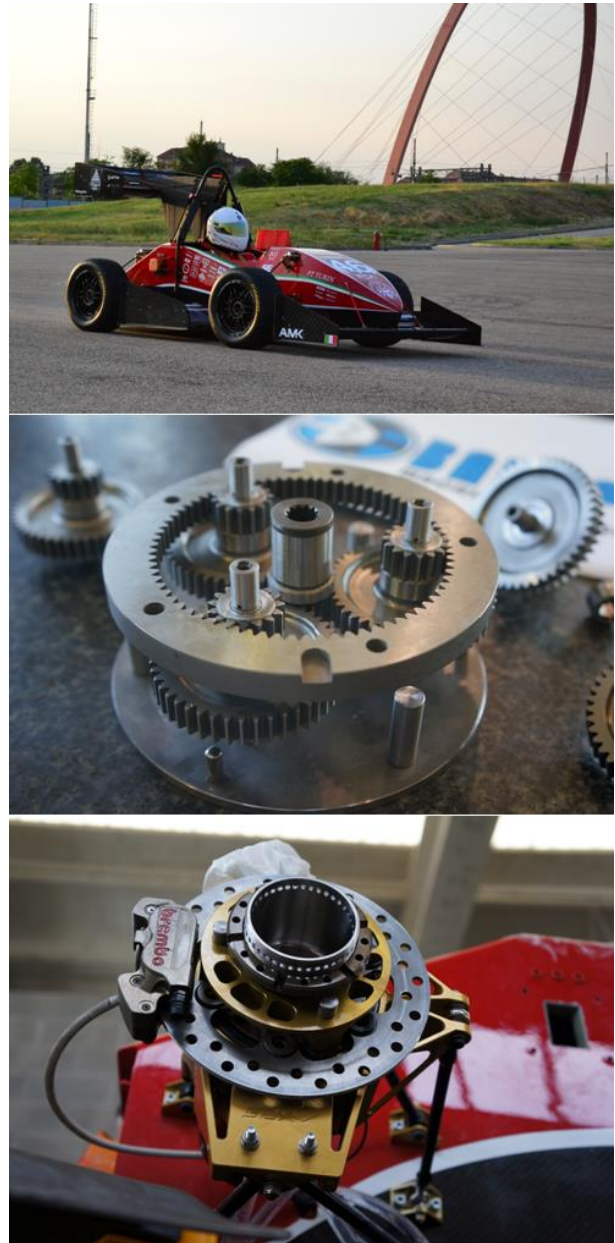
Picture 1.4-2: Main features of S.C.R. transmission.



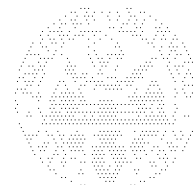
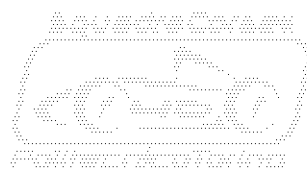
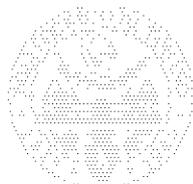
1.4.3. S.C.X.V.

Following the trend of the most important F.S.A.E. teams, availing the knowledge gained on S.C.R. project, in 2015 Squadra Corse was able to produce one of the most interesting car of its history, S.C.X.V. In order to improve traction ability and dynamic behaviour, a four wheel drive vehicle was designed. The integral traction is exploited connecting a motor to each wheel. In order to simplify architecture of the chassis, motors are installed on the uprights, directly on the un-sprung masses. Motors, that have to be very compact and light, are supplied by the German manufacturer A.M.K., Arnold Muller Kirkenheim. Controllers are provided by the same company.

Any motor can deliver a maximum power of 35 [kW], but is limited to 20 [kW] due to regulations. Peak torque is around 21 [Nm] while maximum revolution speed is over 19.000 [rpm]. The particular, layout of the car and performance of the motors, need a transmission which is compact, light and features an high gear ratio. The best solution to conciliate all of these features is a co-axial double stage, three branches, epicyclic gear-box. Sun gear is connected rigidly to motor and is supported by two tight bearings housed in the gear carrier. Gear carrier, composed by two parts, is connected rigidly to the vehicle wheel and supports three planetary shafts. Ring rear is fix, rigidly connected to the upright, which works as sump. Such a delicate system needs to be assembled carefully with components of high accuracy, in order to obtain the desired reliability. Components are in large majority manufactured by machining of several high technologic materials. Upright is a monolithic block of Al7075-T651 Ergal, derived from that of S.C.R. Wheel hub too, which has the function of planetary carrier, is assembled with two components, one machined by Al7075-T651 Ergal billet, the other machined by Ti-6Al-4V Titanium billet. Gears are manufactured by carburized 18CrNiMo7 steel, and internal faces of teeth are rectified in order to tear down the friction. Although layout of the gear-box is quite complex, technology of manufacturing processes and materials is the same utilized for the production of S.C.R. gears. That's an additional evidence that S.C.R. gear design is a milestone in the knowledge of Squadra Corse.



Picture 1.4-3 main features of SCXV transmission.



1.5. Bench Mark.

Starting with a brand new project, it's useful study solutions adopted by opponent main teams. For this reason, most interesting cars that took place in 2011 and 2012 events was deeply studied on the basis of pictures found on the net or shoot made on the circuit.

1.5.1. D.U.T. Racing, Delft University of Technology, Netherlands.

T.U. Delft is one of the most eminent athenaeum of the Europe. This university It's particularly famous for have been the base of Professor Hans B. Pacejka researches. The illustrious professor



Picture 1.5-1: Detail of the back of 2012 DUT Racing car (<https://www.facebook.com/FSteamDelft/>).

gave an important contribution to the automotive industry studying deeply the behaviour of tires. In Formula S.A.E. team from Delft was one of the first to take part in European events. It was one of the first to switch from internal combustion engine to full electric traction. Advanced knowledge on vehicle dynamics, combined with a huge experience in Formula S.A.E., make the team of Delft one of the most winning in Europe and in the world.

By Picture 1.5-1, It's important to observe the gear-box coming out from the back of the mono-coque. It's necessary to appreciate the tripod joint housing, which is integrated inside the hub of the output gearwheel. That solution looks suitable for a simpler assembly and for the reduction of un-necessary components. Car from D.U.T. Racing is one of the first four wheel-drive F.S.A.E. cars. Motors are four and are installed on un-sprung masses in front axle. Motors of the rear axle are fitted into the mono-coque. For this reason, it's credible that small size motors of the rear axle can be housed inside the mono-coque with a transversal layout. By consequence of this, it's easy imagine that the gear-box includes a couple of double stage twin transmissions assembled with simple and efficient spur gears.

1.5.2. A.M.Z., Eidgenössische Technische Hochschule Zürich, Switzerland.



Picture 1.5-2: Sump of A.M.Z. car gear-box (<https://www.facebook.com/amzracing/>).

E.T.H. of Zurich is, like the previous athenaeum, one of the five best university of Europe. Formula Student team from Zurich is, like that from Delft, one of the first teams to join Formula Student Electric. for this reason is one of the most skilled in the world.

2012 A.M.Z. car was a basic rear wheel drive car in which carbon fibre mono-coque houses all the power-train components. It' important to know that drive wheels are controlled by a motor for each.

By a small investigation based on Picture 1.5-2, it's easy to guess the transversal layout of the motors. Anyway, It's necessary consider that A.M.Z.

By a small investigation based on Picture 1.5-2, it's easy to guess the transversal layout of the motors. Anyway, It's necessary consider that A.M.Z.

By a small investigation based on Picture 1.5-2, it's easy to guess the transversal layout of the motors. Anyway, It's necessary consider that A.M.Z.

By a small investigation based on Picture 1.5-2, it's easy to guess the transversal layout of the motors. Anyway, It's necessary consider that A.M.Z.



develops and installs homebuilt motors with external rotor. Such motors are very short in longitudinal dimension, that is an important advantage in terms of packaging. Sump is assembled by three components manufactured from milling billets of aluminium alloy. Observing the gear-box output opening, it's easy to guess that tripod housing is integrated inside the output hub, similarly to the car of D.U.T. Racing. It's not difficult to guess the layout of gears. Like in the previous case, a couple of double stage twin transmissions assembled with simple spur gears.

1.5.3. Green Team, Universität Stuttgart, Germany.

University of Stuttgart owns the most winning team in the history of Formula Student in Europe, Renn Team Stuttgart. A couple of years ago, the University set up a specific team which competes in the Formula Student electric, The Green Team. Car deployed in 2012 by team of Stuttgart was a two wheel drive vehicle, with drive wheels controlled independently.



Picture 1.5-3: Motors and gearbox of Green Team assembled together on a test rig (<https://www.facebook.com/greenteamstuttgart/>).

By Picture 1.5-3 it's possible to appreciate the group of motor and gear-box assembled together on a test rig. The first aspect to highlight is that motors are positioned following a longitudinal layout, differently from cars analyzed above. For this reason, it's right to guess that transmission is realized by a couple of twin gear-boxes. A bevel gear is installed in the first stage and a spur gear in the second. In order to keep motors in the lowest position as possible, with axis parallel to the ground, axis of two stages don't lay on the same plan identified by axis of the motors. Output of the gear-box is positioned in higher position, in order to allow the half-shaft to work parallel to the ground. Housing of the tripod joint is integrated inside the hub of output, In this solution too. Back to the Picture

1.5-3, it's important observe the opening below the gear-box output. It's easy to guess that is the opening necessary to calibrate preload of angular contact bearings. Last deductive reasoning have to be made around the sump. It's an assembly of two huge components manufactured by monolithic blocks of aluminium alloy. Surface of joint between two components is the plan that lays between the central and the output shaft.

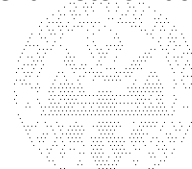
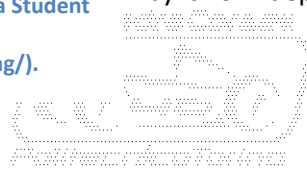
1.5.4. T.U.G. Racing, Technische Universität Graz, Austria.



Picture 1.5-4: The back of T.U.G. car at Formula Student Hungary, Gyor 2012 (<https://www.facebook.com/tugraz.racing/>).

Technical University of Graz is one of the first athenaeums to take part of Formula Student in Europe. Internal combustion engine cars from Graz duelled against those of Stuttgart to claim the first positions, for a decade. In last years the team built some electric traction cars, starting from chassis of combustion cars.

By Picture 1.5-4, it's important to meditate about the layout of the car which is a rear wheel drive equipped by two independent motors. It's easy to guess that



motors are positioned in parallel longitudinal position, like in the case studied at Chapter 1.5.3. Transmissions is composed by two independent twin gear-boxes. It's right suppose that the gear-train is split in two stages, first realized by bevels, the second realized by spurs. Differently from the previous case, all the gears lays on the same plane. For this reason, the plan which houses axis of the gear-train components have to be tilted. That allows the half-shaft to reach the centre of the wheel hub. Half-shafts which work in angled position don't feature their best work condition. Anyway, this solution is excellent to keep masses as low as possible. Finally, It's important to consider that this solution can be effective on a car equipped with 10 [inches] rims only. That's due to the limited angle of operation of half-shafts

1.5.5. Ka-Raceing, Karlsruher Institut für Technologie, Germany.

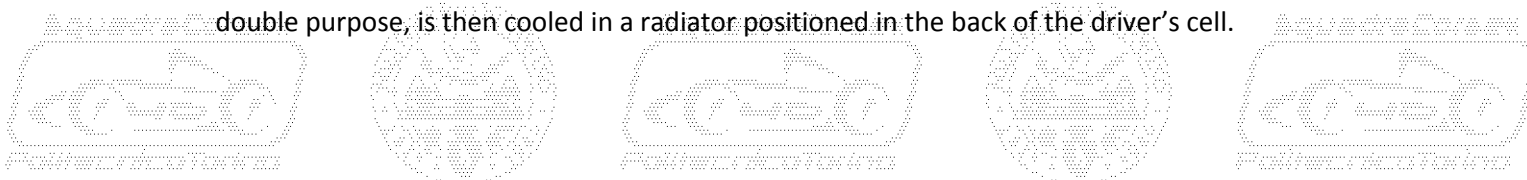
Another important athenaeum in the European overview is the Institute of Technology of Karlsruhe. By a couple of years this university deploys two very interesting Formula Student cars, one equipped by internal combustion engine, one equipped by electric motors.



Picture 1.5-5: Rear of the car of KA-Raceing (Squadra Corse PoliTo Archive).

First of all, it's important to appreciate the non ordinary solutions adopted in these cars. Motors are assembled together sharing the liquid cooling jacket and the box of the contacts. Gear-boxes are independent and symmetric, positioned in external position referred to the centre plan of the car. But the most original feature of the power-train module is the structural purpose. It's interesting appreciate that mounts of rear upper control arms are positioned on the sump structures. Rear lower control arms are assembled on a tubular frame that includes the jacking bar. Tubular frame is then bounded to the power-train. Observing the picture more in detail, it's possible to notice that rear wing attachments are bounded to power-train module too. About gear-train it's necessary observe that motor and half-shaft lay on the same axis. Is therefore reasonable that gear-train is realized by planetary layout, with a fixed internal crown.

Another important detail to focus in, is the presence of the hoses on the sumps. It's sure that the cover of the motors houses a liquid cooling jacket. But, observing position of the hoses it's right to suppose that the cooling liquid and the transmission oil are the same fluid. The fluid with this double purpose, is then cooled in a radiator positioned in the back of the driver's cell.



1.5.6. DART Racing, Technische Universität Darmstadt, Germany.

Another interesting team to take in example is DART Racing from Darmstadt. Like many others, a couple of years ago, this team switched from the conventional power-train to the electric one with good results. It's possible appreciate in Picture 1.1-10 the duel for the podium between S.C.12e and eta2012. during Formula S.A.E. Italy of 2012.

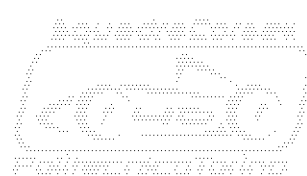
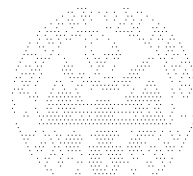
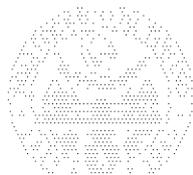


Picture 1.5-6: Disassembled gear-box from DART Racing car. Note the scavange rotary pump circled in red (<https://www.facebook.com/TUDarmstadtRacingTeam/>).

Motors shown in Picture 1.5-6 features a very tight axial dimension but quite large radial. It's obvious that chosen layout is the transversal one. All power-train components are roomed inside the monocoque chassis. That solution, which is very similar to the one described at Chapter 1.5.2, is in reality more interesting and refined.

Basically, layout adopted is the same shown in chapters 1.5.1 and 1.5.2, but there are some details that make the solution of DART very interesting. Analysis starts from the sump, which is assembled by only two components, machined by billets of aluminium alloy. Central wall of the sump, displayed in the solution of A.M.Z., is therefore removed. As consequence, there isn't a central support to house bearings. From deep observation of Picture 1.5-6, it's possible to notice that twin gear-trains feature a single stage of reduction with offset grown by idle gear. Moreover, it's possible to notice that gearwheels aren't equal to their homologues. One gearwheel is provided by an integral shaft which is shared with the homologue wheel too. In order to guarantee that two homologue wheels on the same shaft are decoupled, one of the wheels is supported by a radial and an axial bearings.

Returning to analyze the sump, it's possible to appreciate the labyrinth walls under the gear-box input opening. It's sure that these barriers protect the admission of a scavange pump by the oil surging. As matter of fact, it's possible notice a small rotary oil pump which in the picture is underlined by a red circle. It's sure enough that the rotor of the pump is connected to the idle shaft of the gear-box. That solution which looks very interesting by point of view of the packaging but impairs the efficiency of the two "branches" of the gear-train. Another detail to appreciate is the couple of spray nozzles useful to lubricate heavily stressed gear in meshing zone. That example is very relevant by lubrication point of view. Traditionally, gear-boxes exploited on Formula Student vehicles are lubricated by the classic wet sump. It's now useful take in consideration the possibility of install a system devoted to cool and to direct gear-box lubrication oil.



1.5.7. Racetech, Technische Universität Bergakademie Freiberg, Germany.



Picture 1.5-7: Gear assembly from Racetech car (<https://www.facebook.com/Racetech.Racingteam/>).

By point of view of materials and technology, some of the most interesting cars are made by the Technical University of Freiberg.

Gears shown in Picture 1.5-7 suggest a layout of the transmission like that described in Chapter 1.5.3. As explained in advance, students of TU Freiberg are particularly skilled in the choice of the materials and in the employ of advanced manufacturing technologies. Gears shown in Picture 1.5-7 are supported in a quite sophisticate sump produced by additive manufacturing of magnesium alloy.

Gears shown, are quite conventional by point of view of geometry which exploits sp-lined profiles and spiral bevel profiles of tooth. The most interesting detail to take in consideration, is the finish of the gears. Seen from the picture, it looks a PVD coating which is fundamental in order to tear down the friction. That leads to a higher efficiency and to a lower wear that affects the components.

1.5.8. R.M.I.T. Racing, University of Melbourne, Australia.

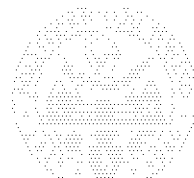


Picture 1.5-8: R.M.I.T Racing partially assembled gearbox (<https://www.facebook.com/RMITElectricRacing/>).

R.M.I.T. Racing is the team of the Melbourne University which competes in the Formula Student Australasia, unique event to take place in Oceania.

Layout of motors and of Gear-train looks very similar to examples shown in chapters 1.5.3 and 1.5.7. Components, gears in particular, looks quite heavy to be installed on a race car.

Anyway, it's important appreciate the sump. Differently from the example described in chapter 1.5.3, it's useful observe how sump is disassembled. In this example, the surface of joint is perpendicular to that of Green Team gear-box. This fact simplify a lot the manufacturing of the sump because housing of bearings are integral. Another detail to notice in the sump, is the spacing of the screws. Bolts are very near each others, in order to ensure the proper stiffness in the connection of the different components of the sump. That ensures the proper operation of the bevel gears and the retain of lubricant oil.



2. Choice of electric motors.



Plot 1.5-1: MGU 012 motor (<https://www.magnetimarelli.com>).

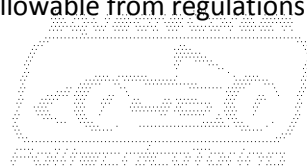
2.1. Magneti Marelli Deal.

As explained in advance at Chapter 1.3, S.C.R. power-train is strictly derived from S.C.12e one. The choice of the S.C.12e electric motors dates back to 2011. After the successful experience of the SC08H, an hybrid prototype built from the chassis of 2008 Squadra Corse car, Italian manufacturer Magneti Marelli offered a deal based on the following points:

- **Two electric motors** TMG Small, MGU 012, and **two controllers** are provided for the 2012 F.S.A.E. season.
- **Technical support** is offered to optimize the entire project.
- **Data** collected by Squadra Corse on the track must be shared Magneti Marelli to test the electric units, which will be used in future road and racing cars.

2.2. F.S.A.E. rules and restrictions.

Being partner of a giant of electric and electronics like Magneti Marelli has enabled the developers to opt for a cheap and competitive power-train. Nevertheless it's right to point out that some drawbacks are present, due to the great advance of the decision for the 2012 season. Electric motors have been chosen in 2011 when total power is limited to $100 [kW]$, as prescribed by "SAE – 2011 Formula SAE Rules", Ref.[5]. Since then, there have been some changes and the power limit has been lowered to $85 [kW]$, how It's prescribed by Ref.[1]. This modification has forced developers to adapt motors to the new restrictions. Therefore, nominal tension has been lowered to $230 [V]$, thus limiting the nominal power of a single motor to $38 [kW]$. This choice has enabled the team to keep the initial project of chassis and transmission, even if it doesn't represent the best combination in all respects. Anyway, nominal tension of the accumulator have been elevate to $350 [V]$ during development of S.C.R. project. That allows to exploit all the power allowable from regulations depicted by Ref.[1].



2.3. Electric motors and manufacturers.

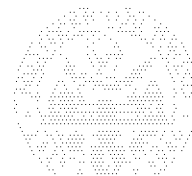
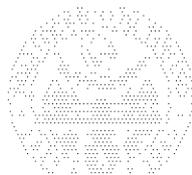


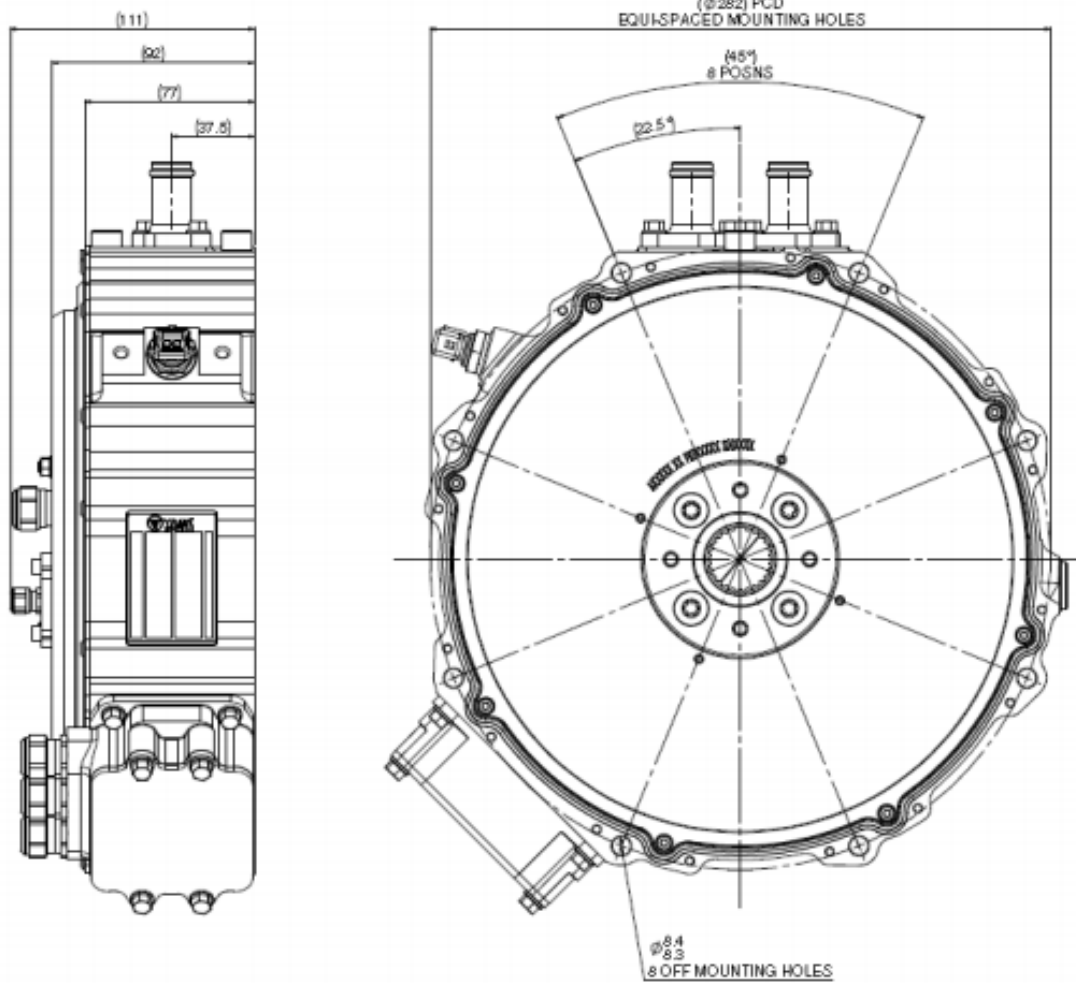
Picture 2.3-1: motor of the Renault Formula E (circled in red). Dimension are similar to that of the 18 inches rims (<https://www.pinterest.it/>).

Electric traction in automotive and motorsport is still an innovative field. For this reason it's not easy to find devoted products. An usual Formula E car, which is one of the rare electric vehicles in motorsport, has a mass of 900kg and a maximum power of about 200 [kW].

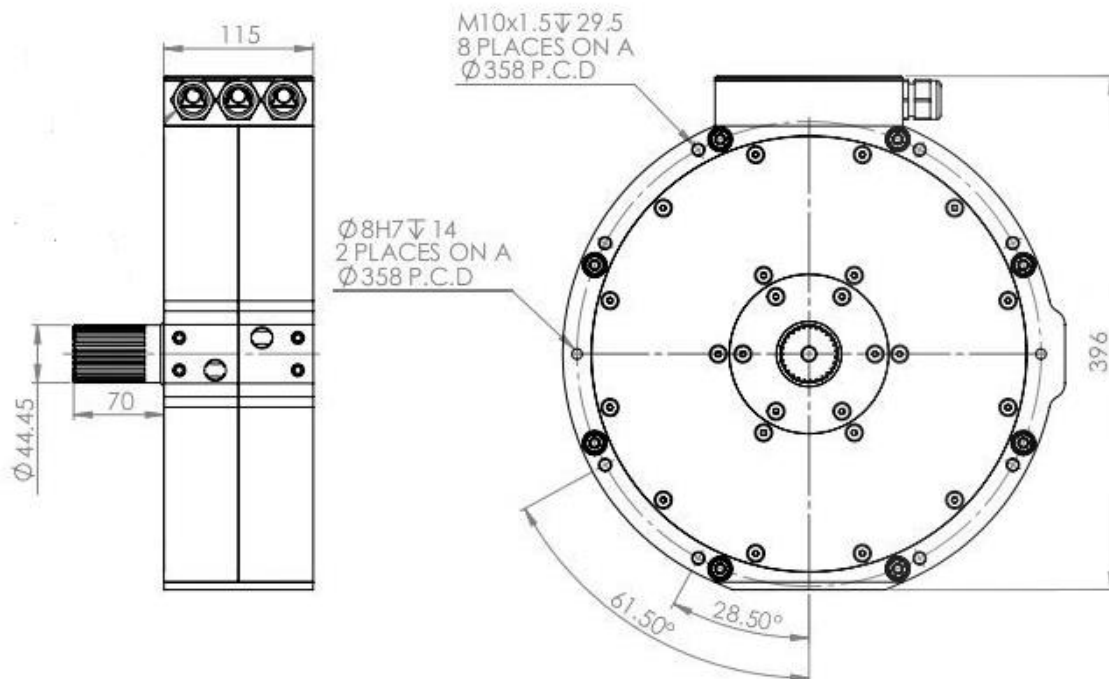
Performance of that kind of vehicle are too far from Formula Student regulations, depicted by Chapter 2.2. Therefore, It' easier to find more suitable products in the hybrid vehicle field. Power-units of Formula 1 cars are provided by traction electric motors. Such motors, utilized in the Kinetic Energy Recovery System, K.E.R.S., features 60 [kW] with a very limited weight. However this technology is very expensive and concealed, not suitable for a F.S.A.E. project.

Another field in which it's possible to find many good solutions to apply in F.S.A.E. power-trains is the industry. Modern machine tools employ very interesting revolution speed varying motors, these motors are utilized by many F.S.A.E. teams. That's an important occasion for manufacturers to test their products on a different field of employ. For this reason, different solution have been studied and evaluated at the start of the project, such **YASA 400** and **Evo Electric AFM140**.

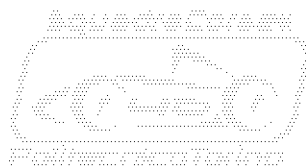




Picture 2.3-2: Main dimensions of YASA 400 motor (<https://www.yasa.com/>).



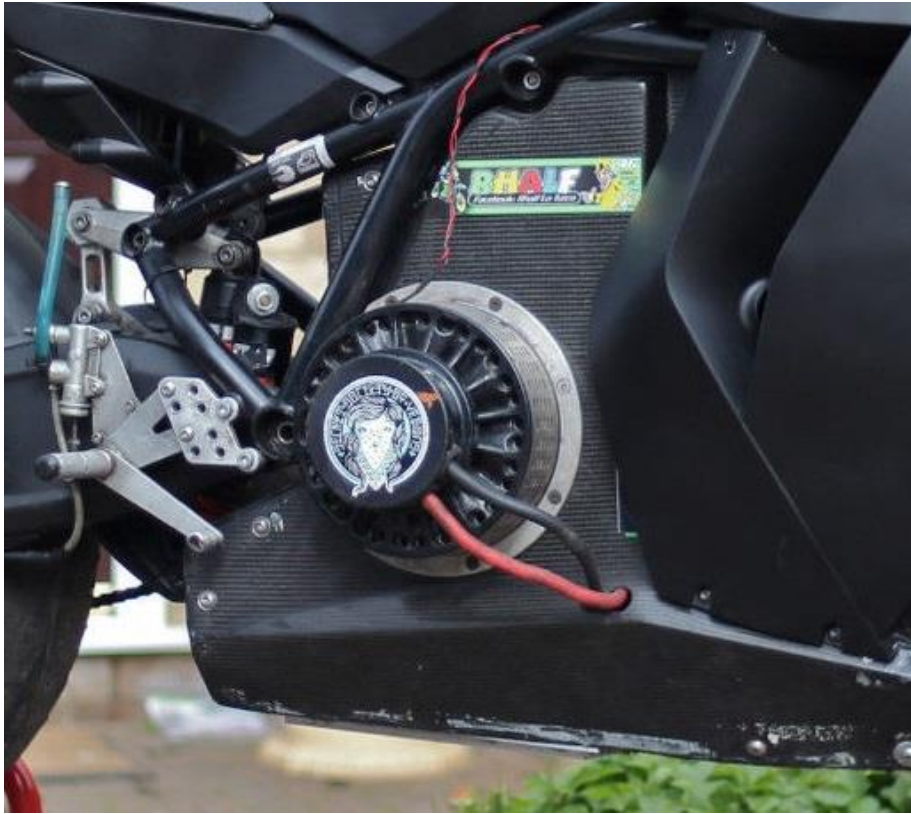
Picture 2.3-3: Main dimensions of Evo Electric AFM140 (<https://avidtp.com/>).



Some other motors that has been evaluated, in example **Wittenstein MRSF049**: this unit features high power and low weight for this reason it would represent a competitive choice. One further motor that has been evaluated is the **AMK DT7-72-20-RxW-5000**, which is similar to the Magneti Marelli one, and quite cheap respect to the others. By the way, as of previous explanation, Squadra Corse chose Magneti Marelli motors, specific for hybrid cars. Italian motors, for Squadra Corse, represent the better trade-off between packaging, performances and business themes.

2.4. Different types of electric motors.

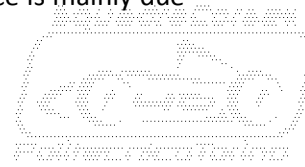
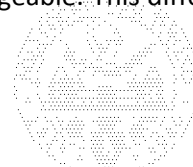
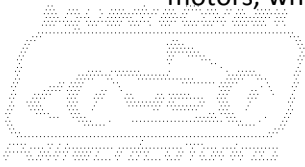
All the units that have been evaluated are three-phase AC synchronous motors. The reasons of this boundary are explained here below. Available **direct current** motors don't feature power ratings suitable for a racing car. Moreover, need to be used under steady load condition, in order to obtain the best performance level. This lack of flexibility led many car manufacturers to discard this kind of motors and prefer the alternating current ones.



Picture 2.4-1: AGNI DC which is employed on a motor bike(<https://www.groen7.nl/>).

Among the DC motors, **AGNI** and **Lynch** units have been evaluated but, as previously explained, didn't match requirements proper of a race car. Lacks are displayed in terms of power, which is often below 30 [kW], and in terms of energy demand. This last issue is related to the presence of brushes in almost all DC motors. Some positive aspects, though, are the easy fitting and power supplying connection. Moreover, DC motors are usually smaller and less noisy, even if exploit some lacks for what concerns cooling and isolation. One more positive aspect of DC motors is the need of less cables and connectors, in spite of their homologues.

Usually, **AC motors** feature bigger size, and this forces developers to manage with more attention the available room into the chassis. Usually, DC motors tend to stress the transmission more than AC motors, whose torque delivery can be more progressive and manageable. This difference is mainly due



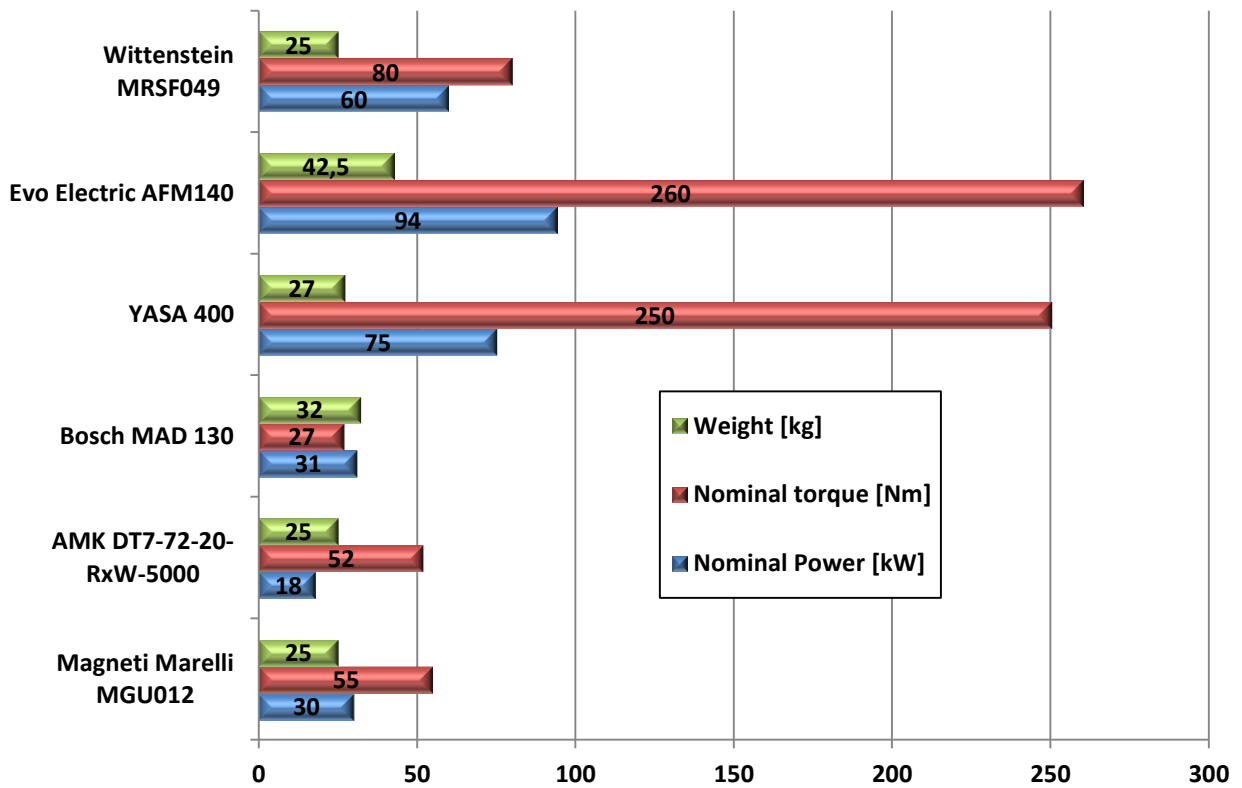
to the presence of easily programmable inverters linked to AC motors, instead of DC controllers. Benefits are evident for both the battery pack and the drive-train system.

2.5. Permanent magnet motors.

AC motors and DC motors can both feature permanent magnets instead of windings of electrical wires. This is a further distinction that leads to different options. Permanent magnet motors feature high torque, high efficiency and low power consumption. On the negative side, magnets can be demagnetized in case of high temperature inside the stator. In this case, more electromagnetic interference is generated by permanent magnets. S.C.12e motors belong to the permanent magnet category and this choice led to an accurate analysis on cooling system. Design of cooling has been assisted by track test gathered data, in order to prevent damages on magnets. Anyway, It's important to remember that temperature is not important for reliability only, temperature strongly affects efficiency.

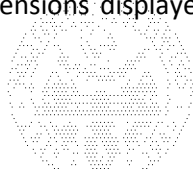
2.6. Comparative chart.

As previously explained at Chapter 2.3, basic technical information about performances have been collected from different manufacturers and organized in the following comparison. A range of different motors have been evaluated and compared to Magneti Marelli TMG Small, MGU 012. It's necessary to clarify that performances refers to an input tension of 350 [V].



Plot 2.6-1: Comparative chart of electric motors.

The comparative Plot 2.6-1 shows that Evo Electric motor features good performances. However, weight and dimensions displayed in Picture 2.3-3 make this motor difficult to fit into a small single-



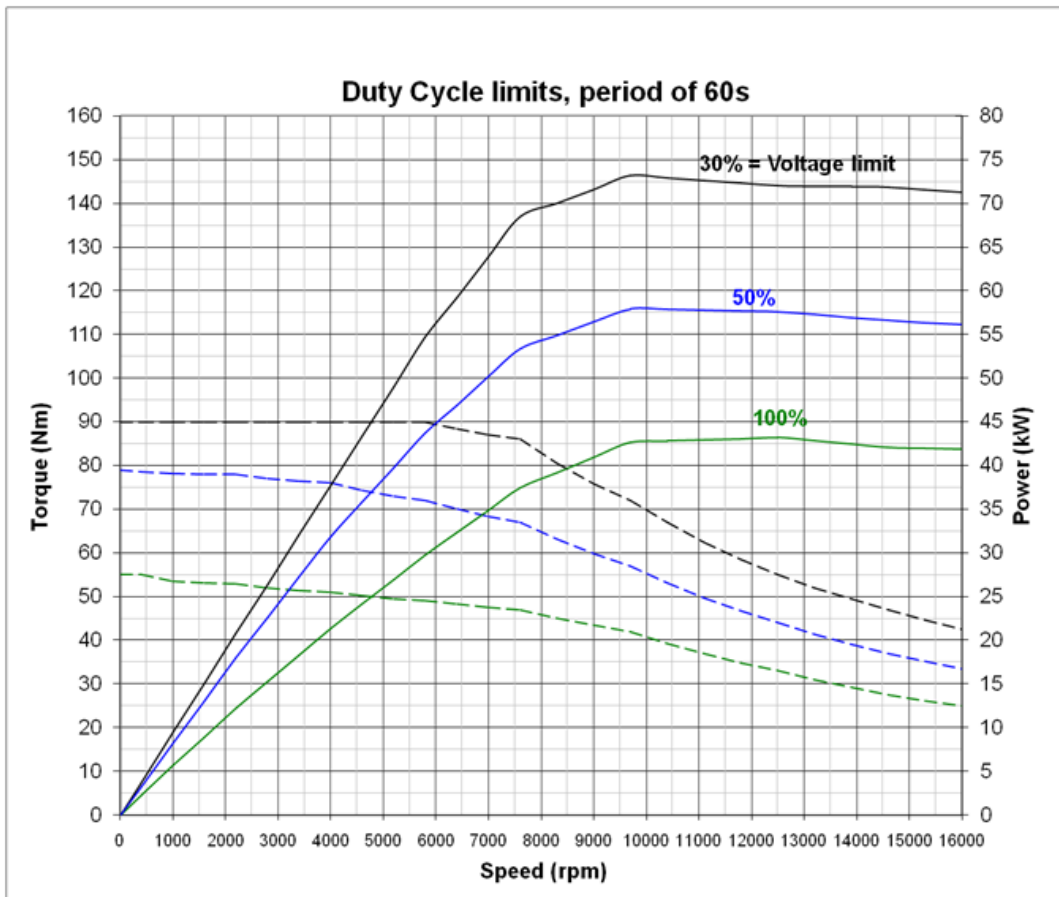
seater vehicle. In order to overcome these drawbacks, Yasa motor has been evaluated. That features similar performances by the point of view of power and torque. However Yasa is much more lighter and compact, as it's shown in Picture 2.3-2. Anyway, taking into account chapter 2.2, it's clear that these two kinds of motor are oversized for a car exploiting a two independent motors layout.

A valiant solution to take into account may be the Wittenstein motor. Weight and torque are very interesting but the power makes this motor too weak for a single-motor layout and oversized for the case of two.

It's clear that it's necessary to evaluate smaller motors. One opportunity may be the motor from Bosch, but the weight it's too high if compared to performances which are suitable for the desired layout.

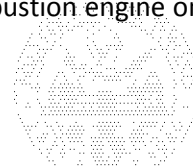
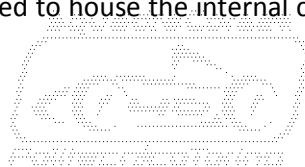
By virtue of that, final challenge regards AMK versus Magneti Marelli. First of all It's necessary underline that biggest issue of AMK motor regards tension. If AMK is operated around 350 [V] tension displays a dramatic drop of power. For this reason, AMK motors are a good solution by point of view of torque output and weight but are much more less competitive than Magneti Marelli units by point of view of exploited.

2.7. Magneti Marelli TMG small size (MGU012).



Plot 2.7-1: Performance of Magneti Marelli MGU 012.

Magneti Marelli automotive traction motors take their origins from the experience acquired in Formula 1. Indeed M.M. is the exclusive supplier of K.E.R.S. systems for all the teams of F1 world championship from 2009 season. That makes the company able to fit electric power-train solutions in tight volumes, with the maximum save of room and weight. That feature is especially useful when it's necessary to fit an hybrid system on a vehicle designed to house the internal combustion engine only. Motors supplied



to Squadra Corse are the result of decades of experience in the electric field, combined to the modern techniques of FEM calculation and simulation. M.M. MGU 012 small size is a motor specific for hybrid power-trains of road cars. Design of such motor, that is still to prototypal stage, is oriented to fulfil requirements of the mass production by virtue of low investments needed. Another important characteristic, required by the automotive field, is the modularity. M.M. motors are designed to be easily fitted on different platforms, featuring short times required for the validation of test results.

Most relevant features about chosen M.M. MGU 012 small size motors are:

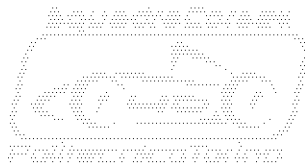
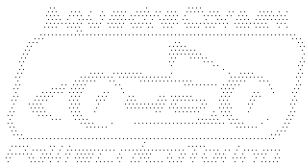
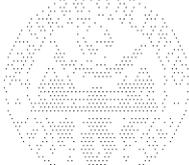
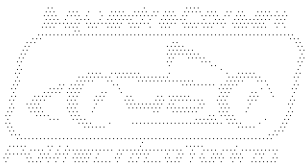
- High **power density**: up to 5 [kW/kg].
- Reduced **size**: up to 15 [kW/l].
- Large rpm **range**: 0 to 16.000 [rpm].
- Good peak **torque**: 90 [Nm].

By mechanical point of view, design of the motor is quite conventional. In the large aluminium casted core, a smart system of cooling ducts is housed. By the exterior, it's possible remark the two brass fittings that feature the inlet and the outlet of the liquid coolant. In the front, a large flange houses the threaded holes necessary to fasten motor on its specific housing. The mechanical output is represented by a steel grooved shaft that hangs out from the front flange. Output shaft is bounded by two slim radial spherical bearings located externally to the rotor. On the back side of the motor, an insulated plastic box contains the connections of the three phases and the plug of the rotational speed sensor.

Differently from Picture 2.7-1, contact boxes have been modified in order to receive one only three-phase cable. Such a cable is much easier to route and fit into a tight race car layout.



Picture 2.7-1: One of the two MGU 012 electric motors delivered to Squadra Corse. Data in the label refers to 350V input (<https://www.facebook.com/SCPolino/>).



3. Design Targets.

In order to deeply understand design solutions performed on S.C.R., it's useful to clarify which are targets of the project. Some of these topics can be understood reading previous chapters, anyway, the aim of following chapters is ordering and explaining main design targets.

3.1. Performance.

Word **“performance”** must be the key word in the definition of a racing vehicle. By virtue of that, It's the main target in the design of a race car. Any component of any system have to be designed in order to exploit the maximum of the reachable performance. Strong limitations are imposed by the official rules, as described by Ref.[1], anyway designers must be able to obtain the maximum by their car, respecting common regulations.

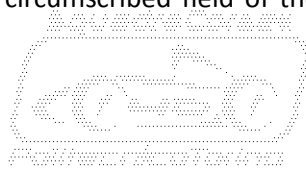
3.2. High efficiency.

A modern vehicle, electric in particular, have to be focused on the efficiency. New scenario of world energy crisis requires vehicles able to tear down energy consumption. In motorsport events too, endurance races especially, low consumption means a huge advantage. A race car which features a good efficiency can reduce the loss of time due to refuelling in pit lane. In F.S.A.E. efficiency has a greater importance because, as explained in Chapter 1.1, allows to gain precious scores in the **“Fuel Economy”** test. For this reason, energy consumption affects race strategy during the “Endurance Test”. Car and drivers, assisted by the data engineer, have to find the better trade-off between race performance and consumption. By the way, it's very likely that the most efficient car can face the endurance laps with more grit, avoiding risk to obtain a bad score in “fuel economy” and avoiding risk to quit endurance due to low state of charge in the accumulator.

Transmission design allows many options to improve efficiency. Like explained at Chapter 5.4, friction, which is the first cause of efficiency loss, can be contained with a proper choice of gear module. Mechanical efficiency can be increased during manufacturing process too. Like it's explained at Chapter 6.2, finish teeth surfaces is the most effective way to tear down loss by friction. Other factors which need be considered optimizing the overall efficiency, depend on bearings, size of gaskets, quality and quantity of lubricant.

3.3. Technical evolution.

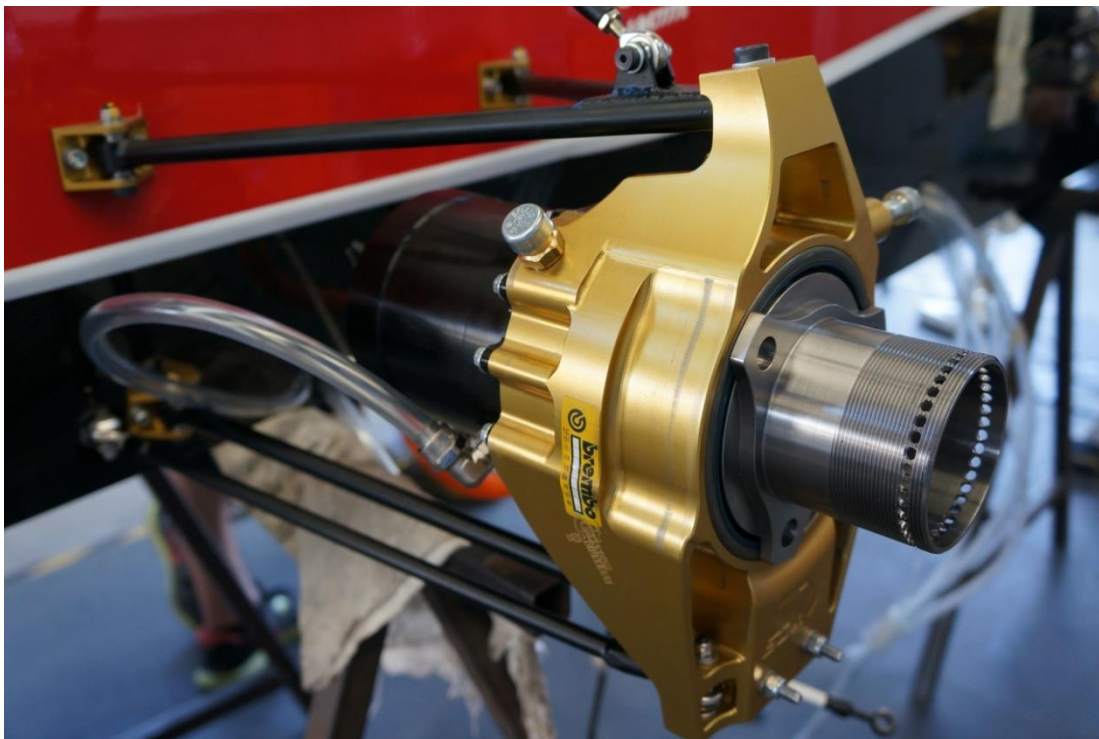
F.S.A.E. is an important step in the career of a young designer, due to the range of opportunities that are available. Usually, teams collaborate with companies which offer their product and their technologies to realize vehicle components. Some examples applied to transmissions are widely described by Chapter 1.5. Mainly, benefits achieved by companies due to F.S.A.E. involvement are related to marketing and image. Anyway, collaboration with a F.S.A.E. team, may offer precious field tests on the specific courts of automotive and motorsport. On the other hand, a young designer takes advantages by the occasion of testing materials and technologies which can be exotic in the conventional daily work. Moreover, judges involved on “Engineering Design” tests appreciate very much innovative solutions. At any event, most original realizations are awarded by very rich scores and dedicated prizes. With reference to circumscribed field of the team, first target to achieve, must be



technical evolution of the car from previous season. Focusing to S.C.R. project, gear-box especially represents an important evolution aimed to upgrade of the sprocket-chain transmission that equips S.C.12e.

3.4. High level of integration.

A F.S.A.E vehicle that features a wheelbase of about $1600 [mm]$ is a very tight ambient of work. For this reason, different systems which are essential for the operation of the car, have to be accurately positioned and integrated. The typical example on S.C.R. is described in Chapter 1.2, on-board rear brakes, which integrates the transmission with the components of the braking system. Another important example is described at Chapter 1.4.3. The “corner” of S.C.X.V. integrates functions typical of un-sprung mass components and power-train components. That represent a an important save of weight and money due to the reduced number of components.



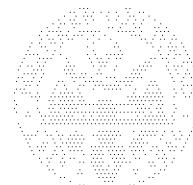
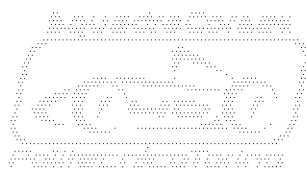
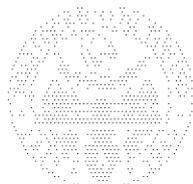
Picture 3.4-1: S.C.X.V. un-sprung weight.

3.5. Higher gear ratio.

As revealed in advance at Chapter 1.4.2, tests and races shown that torque discharged from S.C.12e to the ground wasn't enough to exploit good acceleration performances. For this reason, one of the target in S.C.R. design is the increase of gear ratio from 6:1 to a value around 9:1. That is a quite complex goal which cannot be reached by a simple chain-sprocket system or by a single stage gear-box.

3.6. Best weight stiffness trade off.

It's simple to image that main requirement of a race car is the save of weight. In addition F.S.A.E. official regulations don't impose a minimum weight.



Extreme research of lightness is congruent but the light weight isn't the only requirement to fulfil. Thinking to the entire vehicle, the main requirement it's, of course, driver safety but that's not all. Then It's important reflect on operation of the components. Considerably lightened components can operate differently from what intended by the designer, that's due basically by displacements. For example, a suspension arm, like many other components, cannot be considered infinitely stiff. It deforms in operation, but if it isn't stiff enough it may deform more than necessary. This condition may produce undesired displacement of suspension hard-points housed on the un-sprung mass.

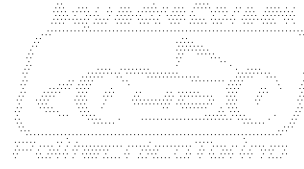
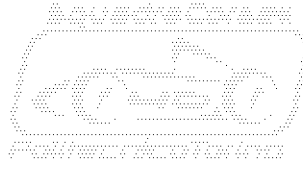
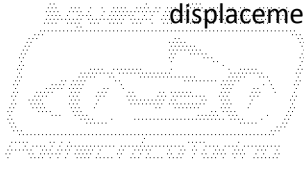
Precise position and bounded movement of suspension hard-points is essential for the good operation of the entire suspension. Undesired displacements on the suspension can dangerously affect dynamic performances of the car causing loss of driver feeling and worsening of handling. Another example can be applied to transmission, a poor matching between bearings and case can cause a too high displacement of gearwheels. Such issue can drive to severe problems in reliability, efficiency and noise. By virtue of that, designer haven't to consider weight of components only, but he must take into account stiffness too. Therefore, the target of a good design have to be set on the ***"best trade-off between weight and stiffness"***.



Picture 3.6-1: Dimensional checks on S.C.R. gear-train components.

3.7. Easy and accurate assembly.

Transmissions, gear-boxes in particular, are a very delicate topic in mechanic field. In the entire range of the vehicle, in a electric car especially, transmission is the most complex system by mechanical point of view. Usually transmission exploits a large range of mechanical components like gears, bearings, gaskets springs, levers and pneumatic actuators. In addition, a wider range of electronic components like sensors, control units, looms are integrated in order to increase performances and reliability of the system. How It's widely described by "L. Morello – Progetto della Trasmissione Meccanica" Ref.[6], good operation of a transmission depends on a wide range of issues like thermal dissipation, displacements, backlashes and wear.



Anyway, transmission designers haven't to care about operational problems only. First of all they need to concentrate on manufacturing issues too. A well engineered transmission layout have to be envisioned caring about assembly and tuning issues. A transmission such that of S.C.R. is based on bevel gears and angular contact bearings. By assembly and manufacturing point of view, these kinds of components needs to be installed on accurate machined housings. Furthermore, gears and bearings need a proper set preload in order to achieve an efficient and reliable operation. By virtue of that S.C.R. gear-box case needs to be designed ensuring measurement ability and needs to be manufactured following highest standards of accuracy. On the other hand S.C.R. gear-box needs to be simple enough to be assembled quickly using the minimum number of tools and custom devices.

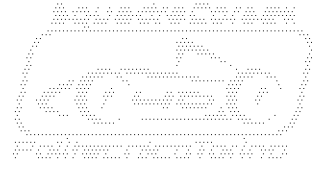
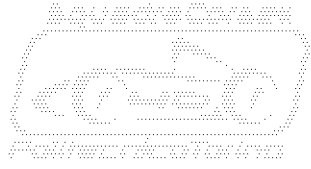
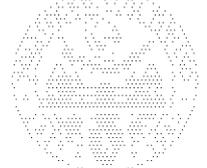
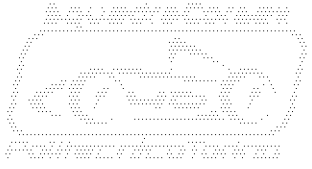


Picture 3.7-1: Squadra Corse crew making interventions on S.C.X.V. before a performance test. Lingotto 2015 (<https://www.facebook.com/SCPolino/>).

3.8. Fast maintenance and tuning.

Unfortunately race cars, prototypes especially, needs interventions of maintenance and tuning any time. During tests and races, events are more dense and times are very tight. For this reason, times devoted to maintenance have to be shorter as possible.

Systems need to be simple enough to ensure the ability of intervention on the track too, where workshop equipments are more lacking and where multiple operators need to work on the car at the same time, as depicted by Picture 3.7-1. S.C.R. is therefore designed trying to match different maintenance requirements. With reference to Chapter 1.3, suspension are one of the most effective examples of easy and fast intervention. Such system is designed to ensure wheel and brakes quick replacement. In addition, few dozens of minutes are enough to regulate set-up parameters of the vehicle: camber, toe, ride height, A.R.B. stiffness and hydraulics. About transmission, all the system can be disassembled from the vehicle in ten minutes only. These features ensure a strong ability of tuning and maintenance of the car.



4. Design boundaries.

In this chapter, all the boundaries of design of S.C.R. transmission are wide explained. In particular boundaries related to performances of the motors and boundaries related to the packaging of the different components in the car.

4.1. Gear ratio calculation.

“Gear ratio” is the first parameter needed in order to set up the design of a transmission. It affects mainly the structural aspects of the design and it has strong impact on packaging choices too

With reference to “G. Belforte – Meccanica Applicata alle Macchine” Ref.[7], It’s necessary clarify definition of gear ratio, indicated with u in the text, is actually defined with i . Factors involved in definition too are declared by different notation with equivalent physical meaning. Definitely gear ratio is defined by the following relation:

$$\text{Eq. 4.1-1} \quad i = \frac{n_i}{n_o} = \frac{T_o}{T_i}$$

Where:

- n_i is “input shaft rotational speed” of transmission, measured in [rpm].
- n_o is “output shaft rotational speed” of transmission, measured in [rpm].
- T_i is “input torque” of transmission, measured in [Nm].
- T_o is “output torque” of transmission, measured in [Nm].

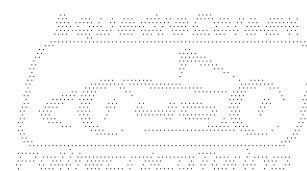
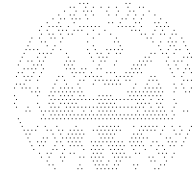
It’s necessary to evidence that, in next calculations efficiency of the transmission is going to be considered equal to one, It’s clearly a simplification but It’s coherent with the target of high efficiency explained at Chapter 3.2.

Typically, an automotive transmission is a particular kind of transmission: a speed reducer. Motors or, more commonly employed engines, feature a rotational speed much more higher than the rotational speed needed to make the vehicle run at desired linear speed. By virtue of that, wheels need to turn at a rotational speed inferior to rotational speed of the engine. By other hand, torque generated by engines is very low if compared to the torque needed to accelerate the vehicle. Basically the automotive transmission is a device that transforms a “high speed/low torque” input into a “low speed/high torque” output, for this reason It can be defined “speed reducer”. Following relation describes i_{SR} the “speed reducer gear ratio”:

$$\text{Eq. 4.1-2} \quad i_{SR} = \frac{T_w}{T_m} = \frac{n_m}{n_w}$$

Where:

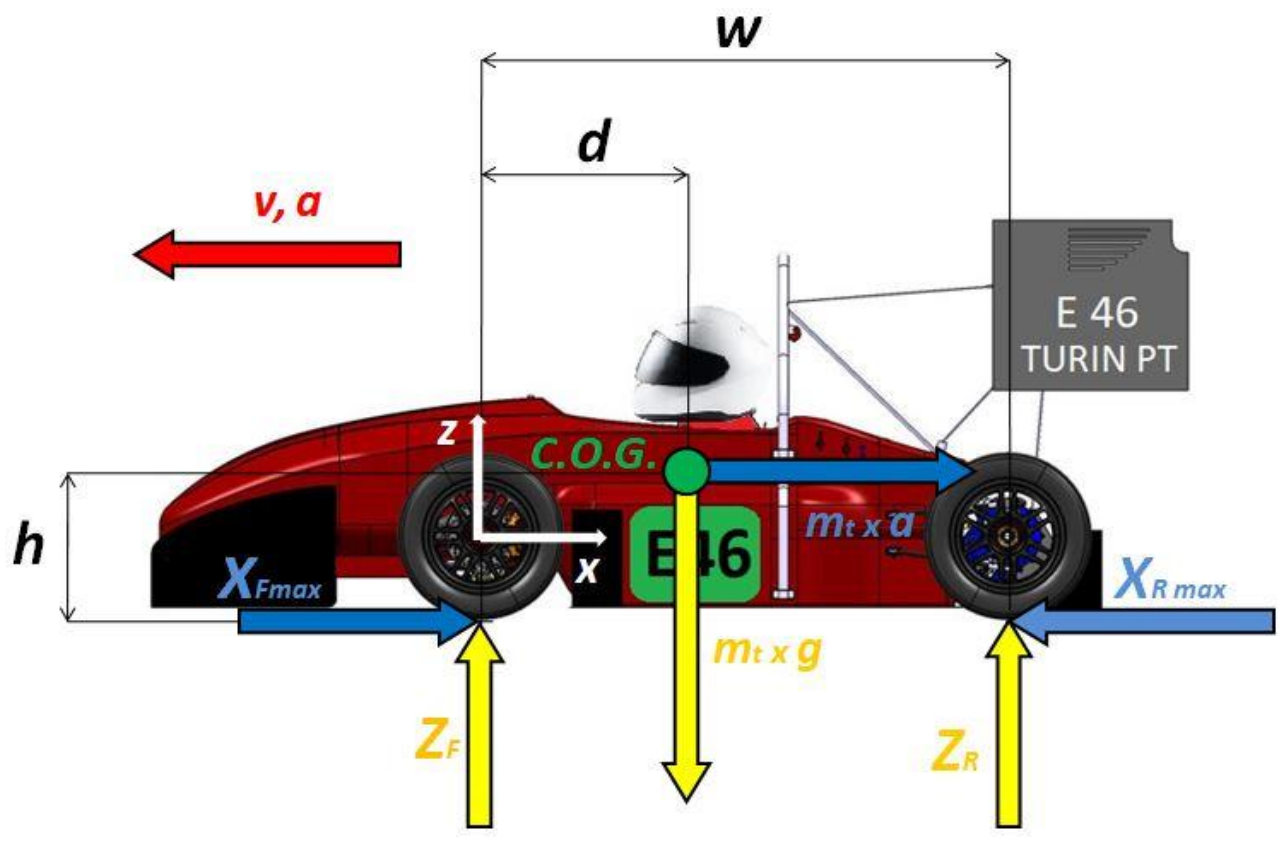
- T_w is “torque on wheel”, measured in [Nm].
- T_m is “torque of motor”, measured in [Nm].
- n_m is “rotational speed of motor”, measured in [rpm].
- n_w is “rotational speed of wheel”, measured in [rpm].



It's shown that value of gear ratio is strongly affected by performances of the electric motors: Torque and rotational speed. Anyway, Eq. 4.1-2 displays that value of gear ratio depends by other fundamental components of the car, wheels. It's necessary to clarify that wheels are intended to be the assembly of tire and rim. **Wheels**, on the basis of their dimensions, rule maximum torque possible dischargeable to the ground and maximum speed that vehicle can reach. Anyway, maximum torque is strongly ruled by features of tire and condition of the track, of course.

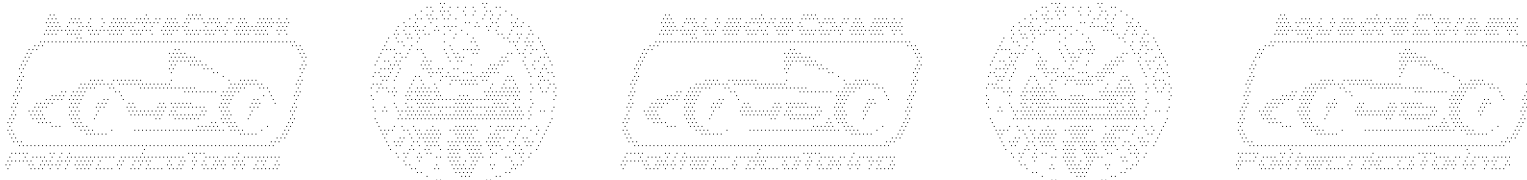
It's clear that, S.C.R. is a race car, purposely designed to perform extremely fast accelerations. As declared in advance, key to reach this target of performance is exploitation of the **tires**. For this reason, it's important that transmission provides to wheels the maximum torque that is possible discharge to the ground. Therefore, gear ratio of transmission must be dimensioned to keep tire operation as close as possible to **"incipient slip"** condition.

Anyway, value of maximum torque which vehicle can discharge to ground doesn't depend by wheels only, as widely described by Ref.[2] and Ref.[3]. Main features of vehicle regarding weights, distances and aerodynamics strongly affect operation of tires. For simplification, aerodynamic effects are neglected during actual dissertation. That's why, by analysis of telemetry data, strongest accelerations are exploited during low speed regimes, when influence of aerodynamic devices is very narrow.



Plot 4.1-1: Two dimensions model of S.C.R. focused on longitudinal load transfer, acceleration case.

On the basis of previous considerations, It's clear that a believable value of maximum torque discharged by a rear wheel, can be obtained by a rough calculation. Such calculation needs to be set on a basic two dimensions model, that is shown in the Plot 4.1-1 inspired by models depicted by Ref.[3]. Model is a free-body diagram which represents the **"longitudinal load transfer"** of the vehicle. Fundamental related variables of calculus are:



- Z_F is “**vertical force on front axle**” of the car, measured in $[N]$.
- Z_R is “**vertical force on rear axle**” of the car, measured in $[N]$.
- X_{Fmax} is “**maximum tangential force of front axle**” of the car, measured in $[N]$.
- X_{Rmax} is “**maximum tangential force on rear axle**” of the car, measured in $[N]$.
- a is “**acceleration**” of the car, measured in $[m/s^2]$.

It's necessary to underline that model depicted by Plot 4.1-1 is specific for a “**rear wheel drive vehicle in acceleration condition**”. That's clear by sense of X_{Rmax} vector which is opposite to x-axis of the car. Such a vector opposes to movement of wheel torque which exploits the “**drive condition**”. On the other hand, vector X_{Fmax} features a sense concordant with x-axis, that's the case of wheel in “**driven condition**”. To turn the two dimension model into the specific case of four wheel drive vehicle in acceleration condition, sense of X_{Fmax} vector must be opposite to x-axis and concordant with sense of X_{Rmax} . While it would be necessary turn the model to “**braking condition**”. In this case, wheels have to be modelled in driven condition thus, sense of X_{Fmax} and X_{Rmax} must be concordant to x-axis. Anyway, that's not enough to provide a proper model of the situation, It's necessary to consider $m_t \cdot a$, the “**inertia vector**”. In braking condition, inertia tends to keep the vehicle running along the road, for this reason inertia vector needs to be opposite to sense of x-axis.

By quantitative point of view, model is based on main parameters of the car, some esteemed by previous experiences, some fixed as input of the design of the vehicle. Total mass of the car, longitudinal friction coefficient and position of centre of gravity are esteemed. Weight distribution of the vehicle, crucial parameter of the longitudinal load transfer, is a free choice parameter fixed around 52% to the rear.

Input data are so declared:

- $r_d = 0,254 [m]$ is “**radius of deformed tire**”.
- $m_t = 330 [kg]$ is “**total mass of vehicle**”, driver included.
- $\mu_{Xmax} = 1.6 [dim. less]$ is “**longitudinal friction coefficient**” between tire and ground.
- $w = 1,620 [m]$ is “**wheel-base**” of the car.
- $d = 0,850 [m]$ is “**distance**” between front axle and centre of gravity of the vehicle.
- $h = 0,250 [m]$ is “**height**” of the centre of gravity.
- $g = 9.81 [m/s^2]$ is “**acceleration of gravity**”.

It's suitable to notice that parameters are declared according to unit of measure set on following equations. From knowledge of previous elements, It's possible to write a five-equations system based on the two dimensional model of Plot 4.1-1.

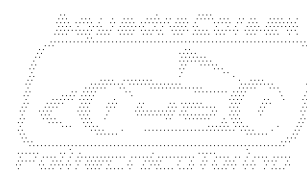
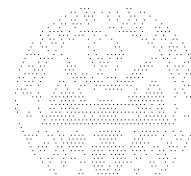
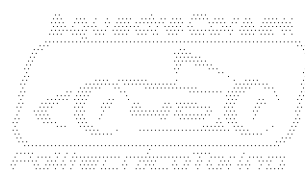
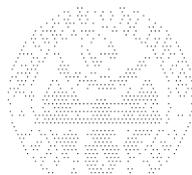
$$\text{Eq. 4.1-3} \quad m_t \cdot g \cdot d + m_t \cdot a \cdot h - Z_R \cdot w = 0$$

$$\text{Eq. 4.1-4} \quad Z_F - m_t \cdot g + Z_R = 0$$

$$\text{Eq. 4.1-5} \quad X_{Fmax} + m_t \cdot a - X_{Rmax} = 0$$

$$\text{Eq. 4.1-6} \quad X_{Fmax} = \mu_{Xmax} \cdot Z_F$$

$$\text{Eq. 4.1-7} \quad X_{Rmax} = \mu_{Xmax} \cdot Z_R$$



Eq. 4.1-3 regards the equilibrium to the rotation around the front tire-ground contact point. Eq. 4.1-4 regards the equilibrium of vertical forces. Eq. 4.1-5 is the equation which rules the equilibrium of longitudinal forces. Eq. 4.1-6 and Eq. 4.1-7 are equations relative to front and rear wheels, describing the relation between vertical force and tangential force.

It's suitable to take notice that a system of five linear equations, with five variables, have been set. It's easy to solve the system by a basic matrix calculus performed by Office Excell. Anyway, first step through resolution of the system is setting of matrices. To easily detect terms and coefficients it's necessary to rewrite previous equations in a more comfortable form.

Eq. 4.1-8 $-Z_R \cdot w + m_t \cdot a \cdot h = -m_t \cdot g \cdot d$

Eq. 4.1-9 $Z_F + Z_R = m_t \cdot g$

Eq. 4.1-10 $X_{Fmax} - X_{Rmax} + m_t \cdot a = 0$

Eq. 4.1-11 $-\mu_{Xmax} \cdot Z_F + X_{Fmax} = 0$

Eq. 4.1-12 $-\mu_{Xmax} \cdot Z_R + X_{Rmax} = 0$

Starting from previous equations, it's easy to write **A**, the "matrix of variable coefficients":

Eq. 4.1-13 $A = \begin{vmatrix} 0 & -w & 0 & 0 & m_t \cdot h \\ 1 & 1 & 0 & 0 & 0 \\ 0 & 0 & 1 & -1 & m_t \\ -\mu_{Xmax} & 0 & 1 & 0 & 0 \\ 0 & -\mu_{Xmax} & 0 & 1 & 0 \end{vmatrix}$

Then it's necessary to write **B**, the "matrix of known terms":

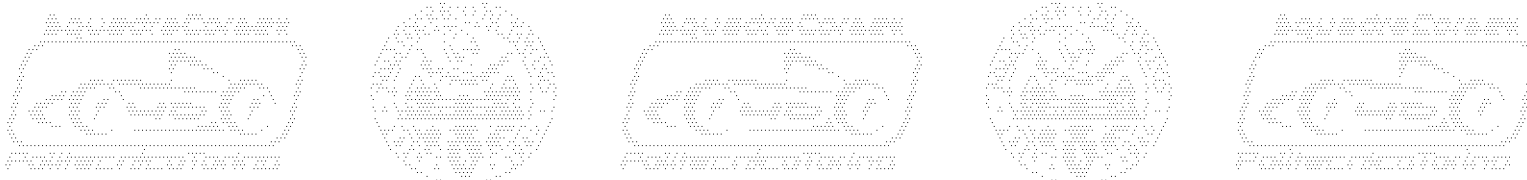
Eq. 4.1-14 $B = \begin{vmatrix} -m_t \cdot g \cdot d \\ m_t \cdot g \\ 0 \\ 0 \\ 0 \end{vmatrix}$

By the software it's easy to solve the following matrix equation:

Eq. 4.1-15 $A \cdot x = B$

Where **x** is the "vector of solutions" of the system.

Solutions are then displayed by following equations, extracted from vector **x**:



Eq. 4.1-16 $Z_F = 1461 [N]$

Eq. 4.1-17 $Z_R = 1777 [N]$

Eq. 4.1-18 $X_{Fmax} = 2337 [N]$

Eq. 4.1-19 $X_{Rmax} = 2842 [N]$

Eq. 4.1-20 $a = 1,53 [m/s^2]$

In order to proceed with the calculation of gear ratio, most interesting result is represented Eq. 4.1-19. It describes numerical value of X_{Rmax} , the “**maximum tangential force of rear axle**”. At this point, introducing some trivial equations and some new parameters, it’s easy to calculate the gear ratio.

- T_{max} is “**maximum torque dischargeable to ground**” by rear axle, measured in $[Nm]$.
- T_{maxW} is “**maximum torque dischargeable by single rear wheel**” to the ground, in the hypothesis that torque generated by each motor is identical. Condition of each tire must be identically the same by point of view of inflating pressure, temperature and wear. Condition of tarmac have to be the identical under each wheel. Such torque is measured in $[Nm]$.
- $T_{maxM} = 90[N \cdot m]$ is “**maximum torque of motor**”.

Eq. 4.1-21 $T_{max} = X_{Rmax} \cdot r_d = 722[N \cdot m]$

Eq. 4.1-22 $T_{maxW} = \frac{T_{max}}{2} = 361 [N \cdot m]$

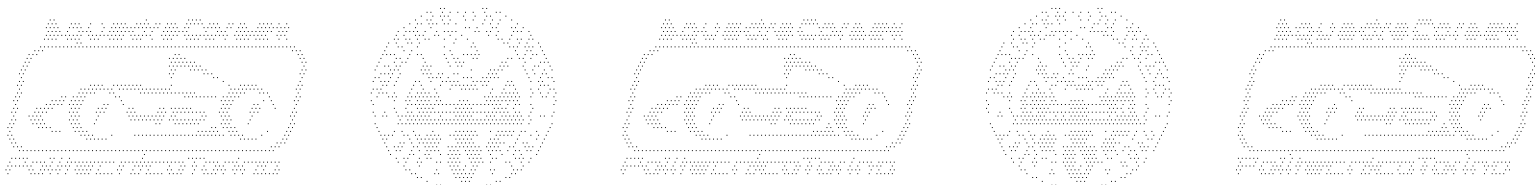
From Eq. 4.1-2 it’s possible to obtain that “**speed reducer gear ratio**”:

Eq. 4.1-23 $i_{SR} = \frac{T_{maxW}}{T_{maxM}} = 4,01 [dim. less]$

That value is not so far from to that obtained in S.C.12e gear ratio calculation. Anyway, as revealed in advance at Chapters 1.3. and Chapter 3, value of the gear ratio isn’t large enough and it must be increased. That incongruity cannot be imputed to the calculus set on two-dimensional model which, in first instance, can appear trivial. The incongruity derives by the fact that gear ratio has been calculated on the base of the maximum torque exploitable by the motor. With reference to Plot 2.7-1, it’s possible to reflect on the operation of the electric motor, on the “**duty cycles**” in particular. It’s evident that the gear ratio calculated by Eq. 4.1-23 is suitable for the acceleration test which lasts less than 18 seconds. It’s known that S.C.12e suffered a lack of torque in low rpm regimes during the endurance/autocross tests. For this reason it’s necessary to consider the first part of the green dashed line that represents the torque of the motor in “**continuous operation**” duty cycle. With reference to Plot 2.7-1 it’s possible to introduce a new parameter, T_{end} defined as “**endurance torque**”.

- $T_{end} \cong 40[N \cdot m]$ is a medium value assumed on the $0 \div 16.000 [rpm]$ range of the Plot 2.7-1. How It’s depicted by Plot 6.1-1, It’s the maximum value of torque exploited by S.C.12e during endurance test.

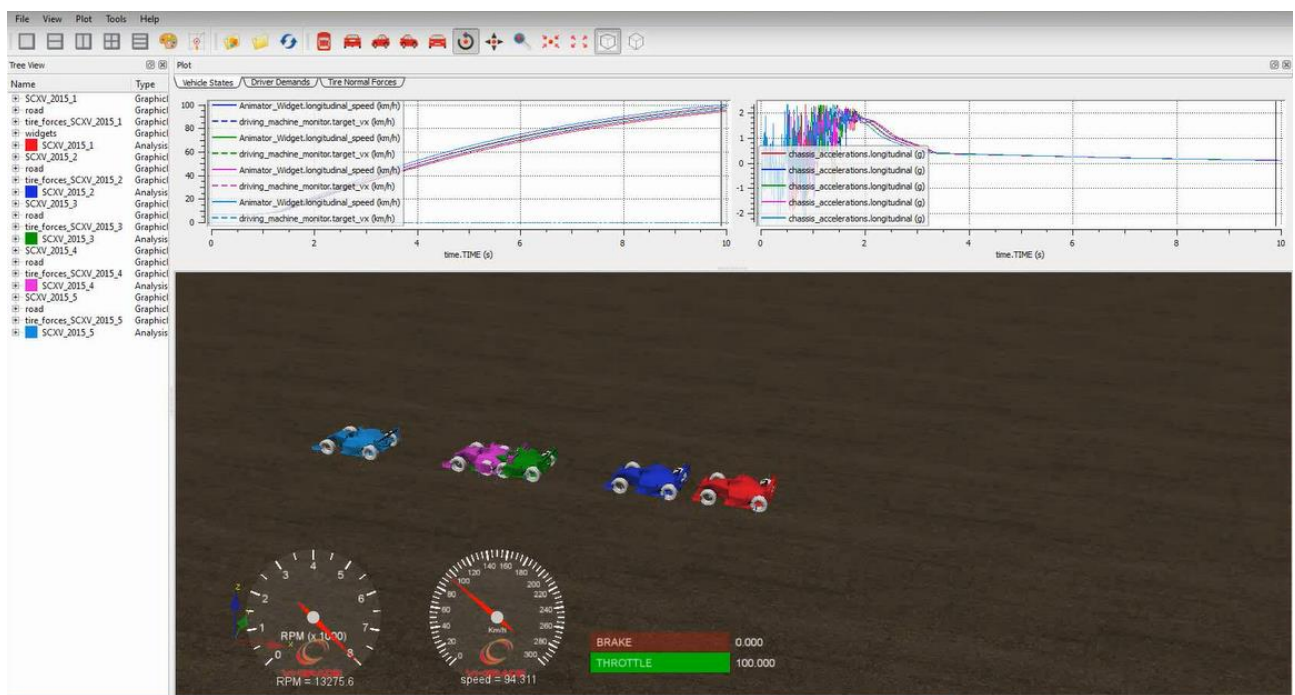
It’s now necessary to write a new equation based on Eq. 4.1-2. Then introduce a new value of gear ratio, suitable to increase traction during endurance sessions: i_{end} defined as “**endurance gear ratio**”.



$$\text{Eq. 4.1-24} \quad i_{end} = \frac{T_{maxW}}{T_{end}} = 9,02 \cong 9 \text{ [dim. less]}$$

It's possible to highlight that the original result of Eq. 4.1-24 have been rounded off to the greater integer. That's why, in the reality, the maximum torque discharged to the ground is affected by efficiency of the system. Moreover, the result of previous equation represents the minimum value to achieve in order to exploit the desired traction. Anyway, the exceeding torque can be cut off in electronic way, implementing a tuneable traction control.

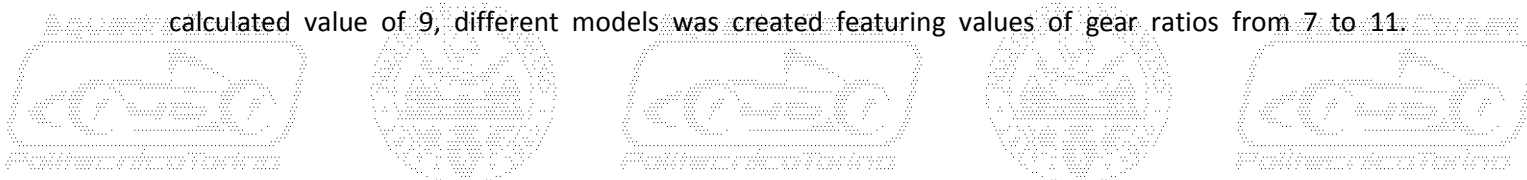
In order to have an additional check on the obtained result, different values of gear ratio was tested on the dynamic model of the car performed by a proper software. VI-Grade is a software which includes templates and methods for the modelling and simulation of vehicle multi-body systems through dynamic events. Main features of this software are the effects of controls, hydraulics, flexibility, contacts, and nonlinear behaviour. Methods and templates have been developed with industry partners with the purpose of develop models of sport cars and race cars. Moreover, by VI-Grade software, starting from main parameters of power-train and gear-train, It's possible to set up a basic model of energy consumption of the vehicle. That's fundamental in the choice of main vehicle variables like gear ratio.



Picture 4.1-1: Simulation performed in VI-Grade, in order to choose the most suitable gear ratio.

In the specific, the dynamic model of the car was built around the main parameters of the cars which regard weight distribution, suspension and power-train. Part of these parameters was exploited in two-dimension model displayed on the actual chapter. Main variables of the project was tested and chosen running the model on different circuits. Circuits was modelled on the base of data collected by S.C.12e during the races. Choice of design variables was aimed to perform the best lap time on F.S.A.E. Italy circuit of Varano.

Obviously, one of the main design variables was **“endurance gear ratio”**. In order to find the solution most suitable on the chosen track, different values of gear ratios was tested. Focusing around the calculated value of 9, different models was created featuring values of gear ratios from 7 to 11.



Simulations made possible to appreciate that gear ratio value of 9 exploits good performances in corners and in straights too. That's easy to check observing virtual cars running, as depicted by Picture 4.1-1. On the other hand, It's known that value of gear ratio affects **"energy consumption"** of the accumulator. For this reasons, chosen value of endurance gear ratio needs to be the **best trade-off between dynamic performance and energy consumption**.

To finally deliberate the choice, It's useful make some calculations, in order to verify the value of v_{max} which represents the **"maximum speed of vehicle"**. Concerning to Chapter 2.7 It's necessary to introduce a new parameter, in order to perform the calculation:

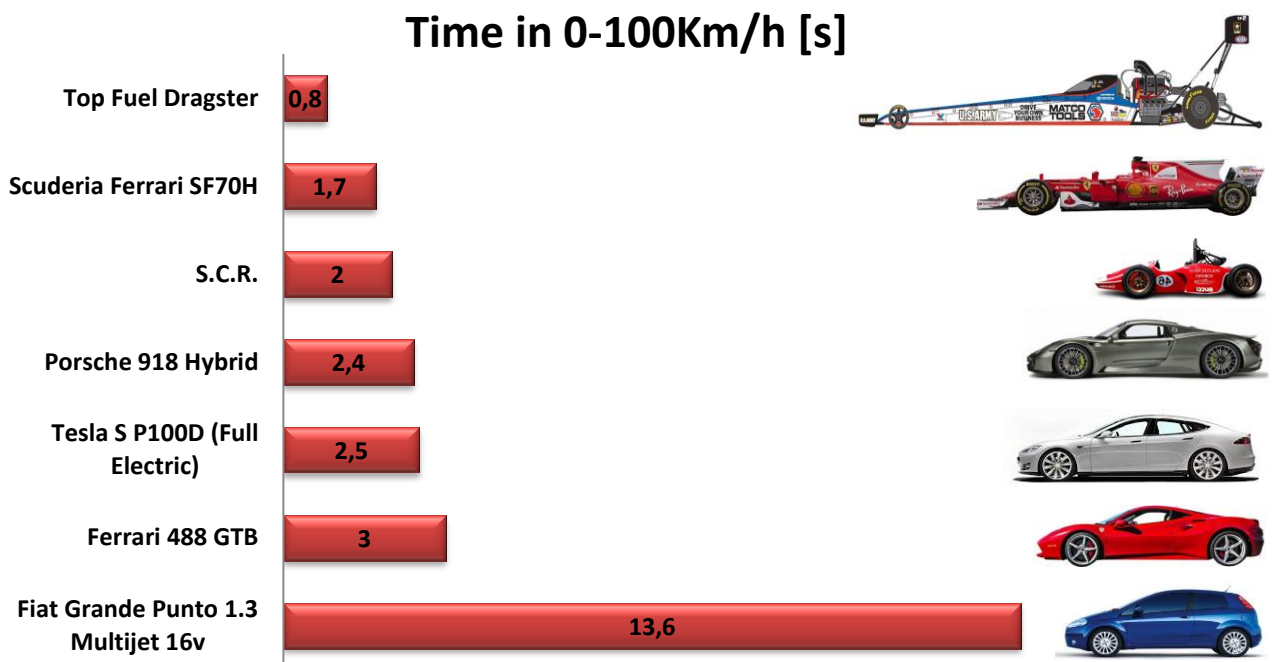
- $n_{max} = 16.000 [rpm]$ it's **"maximum rotational speed of motor"**.

Other parameters of the calculus are known. Then, it's possible to proceed with the verification calculus:

$$\text{Eq. 4.1-25} \quad v_{max} = 2 \cdot \pi \cdot r_d \cdot \frac{n_{max} \cdot 3.6}{i_{end} \cdot 60} \cong 171 [km/h]$$

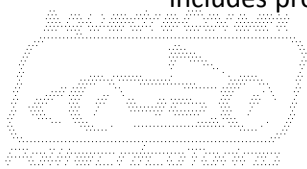
By experience of F.S.A.E., it's known that it's necessary to cover the 75 [m] in less than 3.5 [s], in order to achieve a good result in acceleration test. That means that it's necessary reach a top speed which is around 160 [Km/h], at least. In automotive field, the widespread test to measure acceleration of vehicles is the 0-100 [Km/h] test.

On the base of statements explained before, S.C.R. can be able to perform 0-100 [km/h] test in about 2 [s]. This value of time can be senseless if It's not compared to those of other vehicles. For this reason Plot 4.1-2 have been built, collecting different 0-100 [km/h] records found on the web.



Plot 4.1-2: Comparison of different type of vehicles in 0-100Km/h test.

Characters displayed by the plot are iconic models, different specific type of vehicles. The range includes prototypes, high-end race cars, high-end sport cars and common a passenger car too. Vehicles



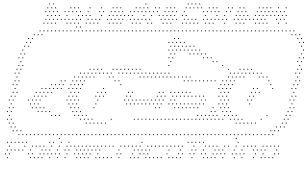
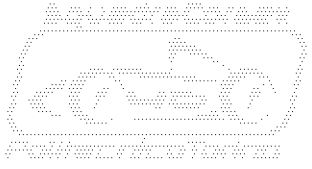
have been chosen by virtue of their power-train, in order to display performances on a wide range of different propulsion.

Dragster is equipped by V8 top-fuel combustion engine, feed by a mix of methanol and nitro-methane propellant. **Ferrari F1** runs an example of high-tech hybrid power-train specific for racing use. A small displacement turbocharged V6 engine is integrated by two kinetic energy recovery systems. One acts on the turbocharger, the other acts on the rear axle. Recovered energy is stored in a battery by form of electric energy. Such energy feeds an electric motor which provides traction to the rear axle, working in parallel with the conventional combustion engine. **Porsche** features a good example high performance hybrid power-train, specific for road use. Large displacement V8 combustion engine is integrated with two electric motors. Motors exploit the role of energy recovery and road traction both, one acts on front axle, other acts on rear axle. **Tesla** probably represents the state of art of fully electric passenger car, featuring excellent performances, remarkable autonomy and interesting price. **Ferrari** is the traditional sport coupé, equipped by a classic high performance V8 twin-turbo engine. It's basically a road car which offers some excellent racing variants. Finally, **FIAT** plays an important role on the comparison because it's a very widespread car. It's very likely that the reader of this thesis would be a owner of this car, if not he probably drove once in his experience of driver. By virtue of that, reader knows well performances of the small displacement turbocharged engine, feed by diesel propellant.

By results of Plot 4.1-2, It's clear that performances of a F.S.A.E. car represent an excellence in the racing and automotive fields. In order to demonstrate that fact, in June 22th 2016 the vehicle of Akademische Motorsportverein Zurich (A.M.Z.) team was able to complete a 0-100 [km/h] test in 1.513[s]. That endeavour assigned the **"Fastest 0-100 [Km/h] acceleration – electric car"** Guinness World Record to the Swiss team. It's necessary to remember that this exceptional result was obtained out of a F.S.A.E. competition, removing the limitations which fix maximum power to 85 [kW].



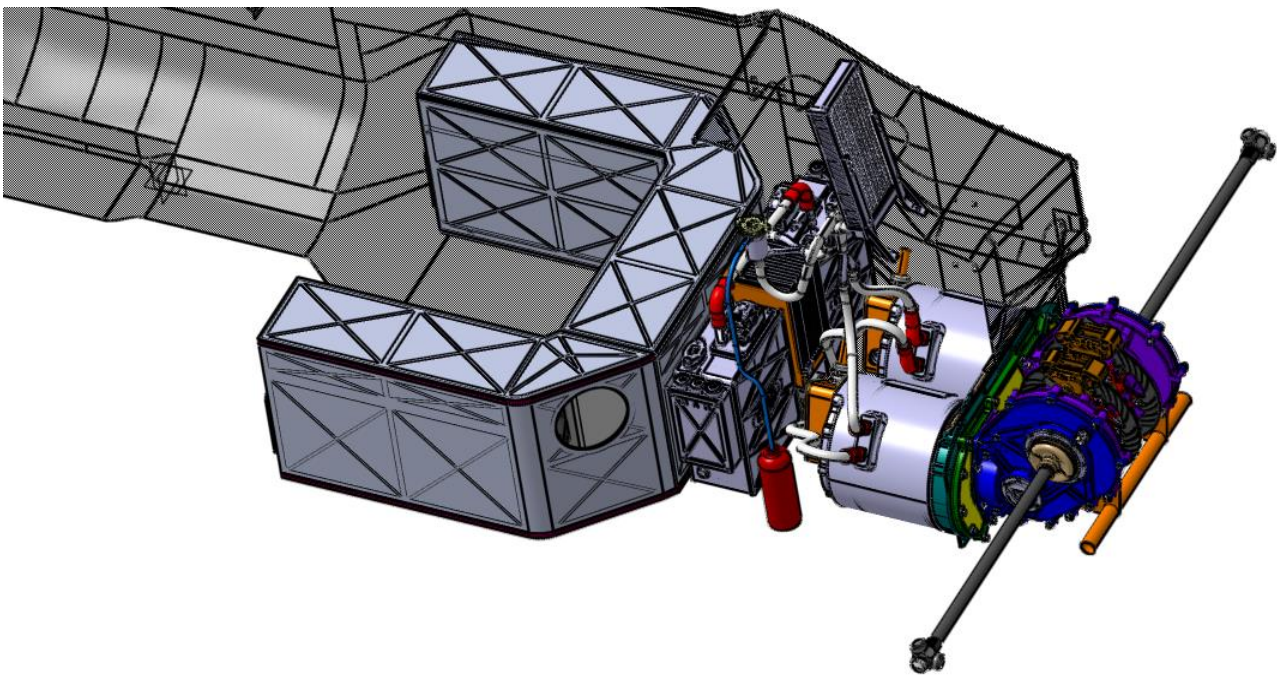
Picture 4.1-2: "Grimsel" the car of A.M.Z. team that claimed the "Fastest 0-100Km/h acceleration – electric car" Guinness World Record (<https://www.facebook.com/amzracing/>).



Moreover, this performance was strongly helped by tire heaters application, devices banned in official F.S.A.E. competitions. Furthermore, like It's possible to notice by Picture 4.1-2, aerodynamic set-up of the car was strongly modified compared to that exploited during events. It's possible underline that rear wing was removed in order to reduce the aerodynamic drag and save weight. However, front wing is maintained, that's necessary to balance the longitudinal weight transfer, providing load on the front axle where a couple of traction motors operate.

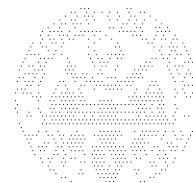
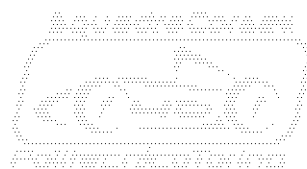
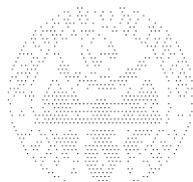
Concluding topic about gear ratio, it's necessary remark that the chosen value is enough to guarantee a good traction in autocross-endurance tests. Moreover a suitable final speed is guarantee.

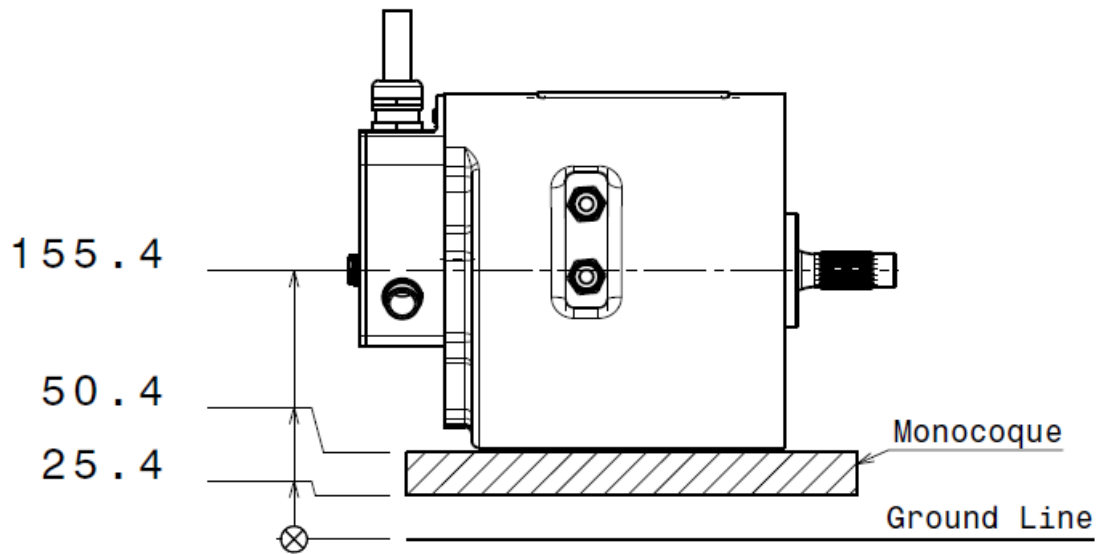
4.2. Packaging of the vehicle.



Picture 4.2-1: Accumulator, controllers, motors and transmission fitted inside a monocoque.

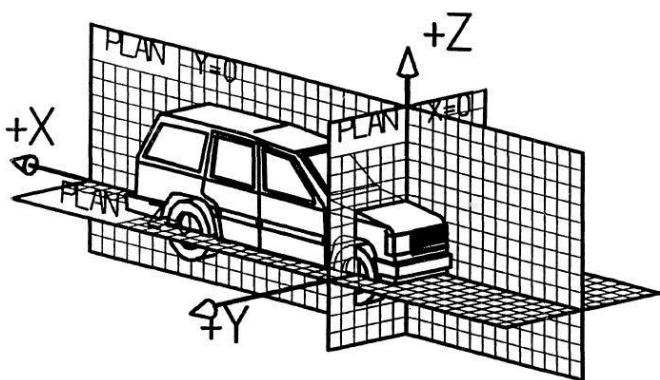
As revealed in advance at Chapter 3.4, one of the target in vehicle project is to reach a high level of integration between components. For this reason, once the gear ratio is determined, it's important to understand where motors have to be placed. That choice is going to affect the entire design of the transmission and of the vehicle. Mass of motors is $50 [kg]$ for both, that mass is so relevant, for this reason its placement strongly affects the dynamic performances of the vehicle. Accumulator features the same weight of the two motors, but exploits a larger volume. As revealed in advance at Chapter 1.3, this component is realized by three modules placed around the driver. Just behind the central module, controllers are housed in vertical position. Controllers feature a mass of $20 [kg]$ for both. Vertical placement grows the inertia of the vehicle around the roll axe but allows to keep masses centred in longitudinal direction. This solution allows to maintain weight distribution around the intended value of 52% to the rear.





Plot 4.2-1: Position of the motor into the monocoque.

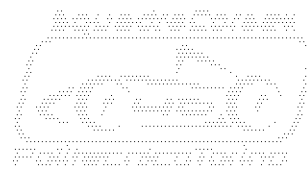
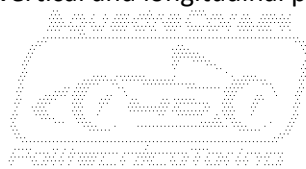
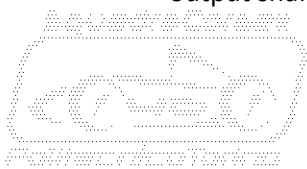
Dissertation is going to be developed around the placement of motors. In order to simplify the topic, next statements are going to be focused on one half of the car, with one only motor and one only transmission. In accordance with Plot 4.1-1, reference system adopted on the vehicle is depicted by Picture 4.2-2, x,y,z-axis and relative plans which are mentioned in the following dissertation coincide with those displayed on the picture. In addition, It's necessary to clarify that output shaft of the motor is intended to be parallel to x-axis.

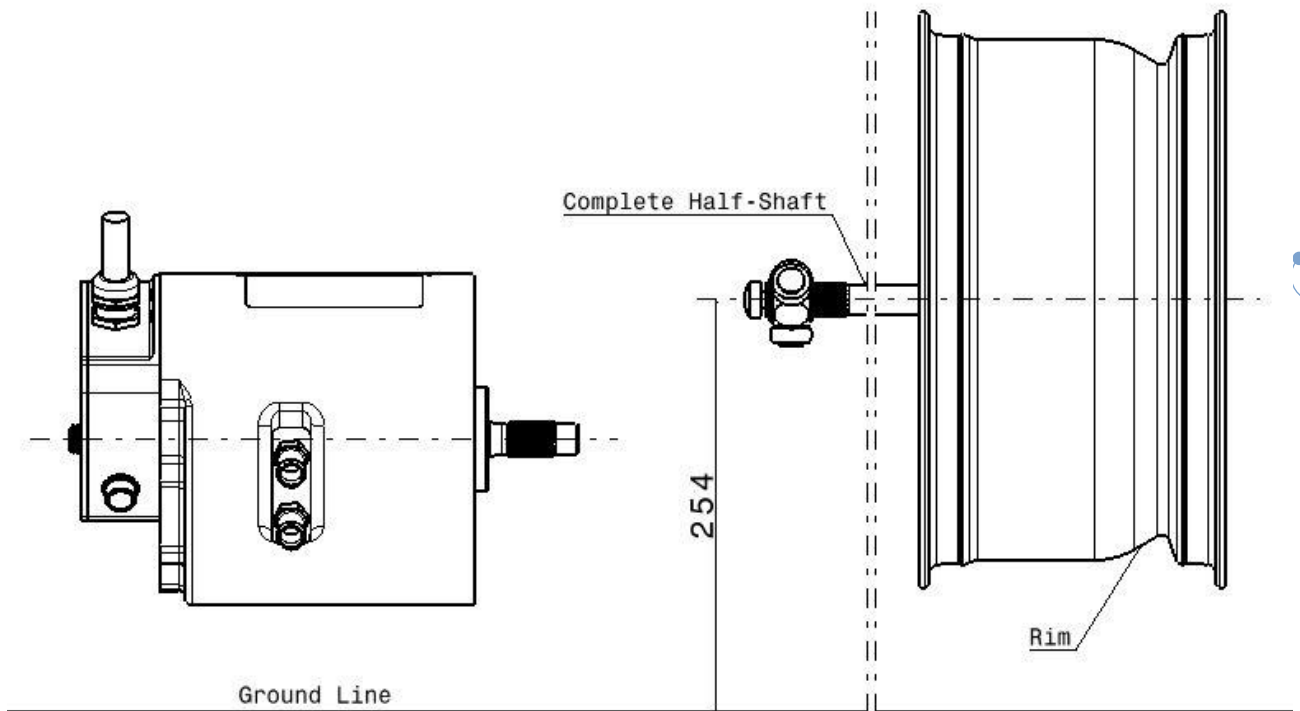


Picture 4.2-2: XYZ axis convention for a vehicle (<https://www.motor-talk.de/>).

By point of view of vehicle dynamics, it's clear that motor, due to its own mass, have to be placed in the lowest position inside the chassis. In order to keep as low as possible the centre of gravity of the vehicle. Some important information are available in order to define accurately placement. By Ref.[1], minimum ride height of the car, "**ground clearance**", it's imposed: value is set to 1,0 [inch.] which corresponds to 25,4 [mm]. Thickness of floor of the monocoque depends mainly by thickness of chosen honeycomb, like it was revealed at Chapter 1.2. So, overall thickness can be roughly esteemed to be around 25 [mm].

Lowest point internal to the monocoque can be easily calculated along z-axis with the sum of ground clearance and floor thickness. As consequence, position of motor output shaft along z-axis is well determined, as depicted in the Plot 4.2-1. Position of motor output shaft along y-axis have to be chosen as close as possible to the mid plane of the car, in order to limit the inertia around the roll axe of the vehicle, Ref.[2] Ref.[3]. Main boundary is dimension of the front flange, for this reason position of motor is well determined. Longitudinal position, along x-axis, is a bit more complex to determinate. By virtue of that, It's necessary to perform some evaluations and packaging studies that are going to be deeply described in the following Chapters. Congruously with this level of the study, position of motor output shaft is clearly determined in vertical and longitudinal position (yz-axis).





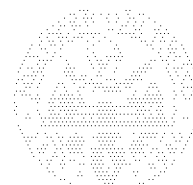
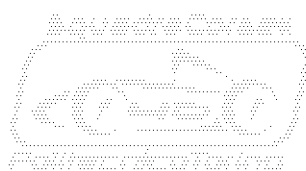
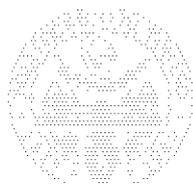
Plot 4.2-2: Position of rim and half-shaft.

Ideally, transmission axle or **“half-shaft”**, needs to operate parallel to the axis of the wheel that drags. This condition guarantee top efficiency of tripod joints around the complete field of rear suspension operation. Preliminary design of the vehicle, depicted in Plot 4.2-2, establish that rear wheels were bounded to $y=0$ plan, in parallel position. It means that the half-shaft works parallel to y -axis and that the axis of the half-shaft coincides with the axis of the rear wheel. Wheelbase of the car is known, therefore coordinates of the transmission output shaft on x -axis and z -axis, are clearly determined.

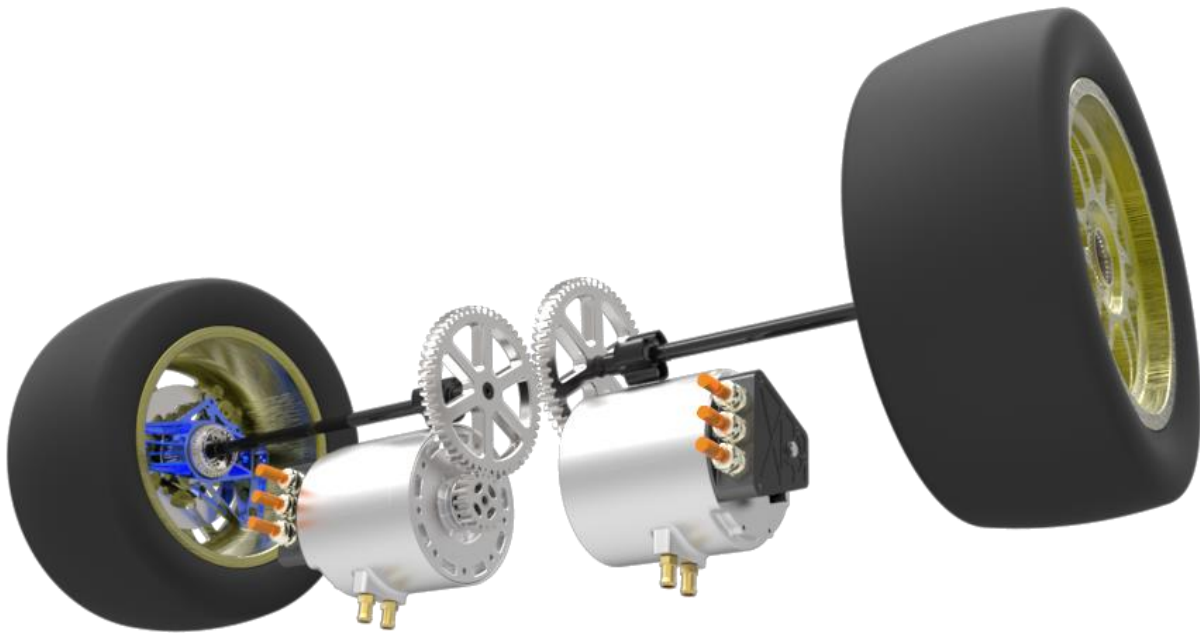
Basic design boundaries are fixed, It' s now possible to evaluate some different solutions in order to find the best configuration for motor/transmission layout. That is going to be the main topic of following chapters.



Picture 4.2-3: Example of tripod joint employed on F.S.A.E. car.



4.2.1. Transversal with internal transmission.



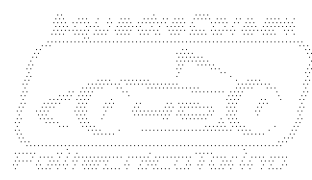
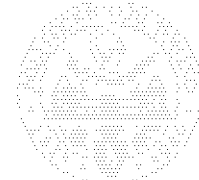
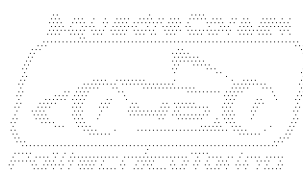
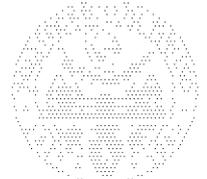
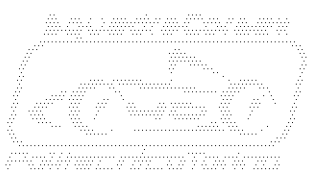
Picture 4.2-4: Transversal motors with internal transmission.

That is the configuration adopted by S.C.12e project and observed in chapters 1.5.1, 1.5.2 and 1.5.6. Transversal layout means that motors are positioned perpendicular to the road axis, parallel to y-axis of the vehicle. Obviously, input and output shafts need to be parallel among them. In this configuration, gears of the transmission are all cylindrical and probably spur in a project oriented on a motorsport application. By virtue of that, actual represents the best solution by point of view of transmission **mechanical efficiency**, Ref.[6].

Main drawback of this solution is represented by distance between motors and rear axle. Such dimension is controlled by the size of gears. As revealed previously by Chapter 3.1, the main target in a race car design is the performance. For this reason, dimension of gears needs to be kept as compact as possible, in order to save weight and limit inertia. By other hand, dimension of motor front flange is quite large. Compact gears and large flange causes issues in the offset between output shaft of motor and rear axle of the vehicle. In first approximation calculus, this dimension tends to be shorter than needed. That causes a serious lack of space, with important difficulties in the housing of transmission components. Indeed the space in which floating half-shaft needs to be free may be too tight. That leads to probability of **dangerous interferences** between motor and transmission axle.

Short offset between output shaft of motor and rear axle of the vehicle doesn't lead to packaging problems only. It leads to an important displacement along x-axis of the centre of gravity of the vehicle. In this way, intended value of front/rear **weight distribution** is difficult to achieve.

Such issues, in S.C.12e project, were overcome by the adoption of a drive chain transmission system. Anyway, as explained at Chapter 1.4.1, this solution is not suitable by point of view of mechanical efficiency, which is one of the main design targets of S.C.R. Moreover, drive chain transmission system may cause issues regarding the recovery of kinetic energy. Alternatively, it would be suitable to evaluate a transmission provided of drop gears, like shown at Chapter



1.5.6. Anyway, this solution too is lacking by point of view of mechanical efficiency. Moreover, may suffer an excessive weight.

Another great issue of this solution derives from aerodynamic aspects. Motors would be housed in low rear position. This layout doesn't leave enough space to install a **rear under-body diffuser** which features proper dimensions and related efficacy.

In accordance with dissertations dealt in this chapter, it's possible to establish that transversal layout with internal transmissions may be the better solution by point of view of mechanical efficiency. Anyway it's quite improper by point of view of packaging, vehicle dynamics and aerodynamic efficacy. Drawbacks look to be more than benefits.

4.2.2. Transversal with external transmission.



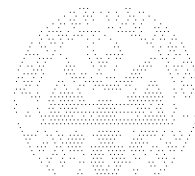
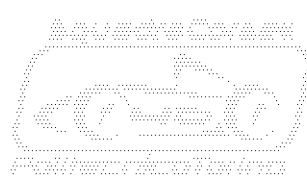
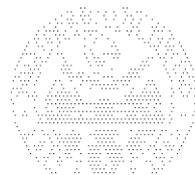
Picture 4.2-5: Transversal motors with external transmission.

House transmission on external position may be the proper solution to solve issues about lacking of space. In this way, interferences between half-shaft and motor are surely avoided. In addition, mass of transmission axle is significantly reduced decreasing inertia of the entire transmission system.

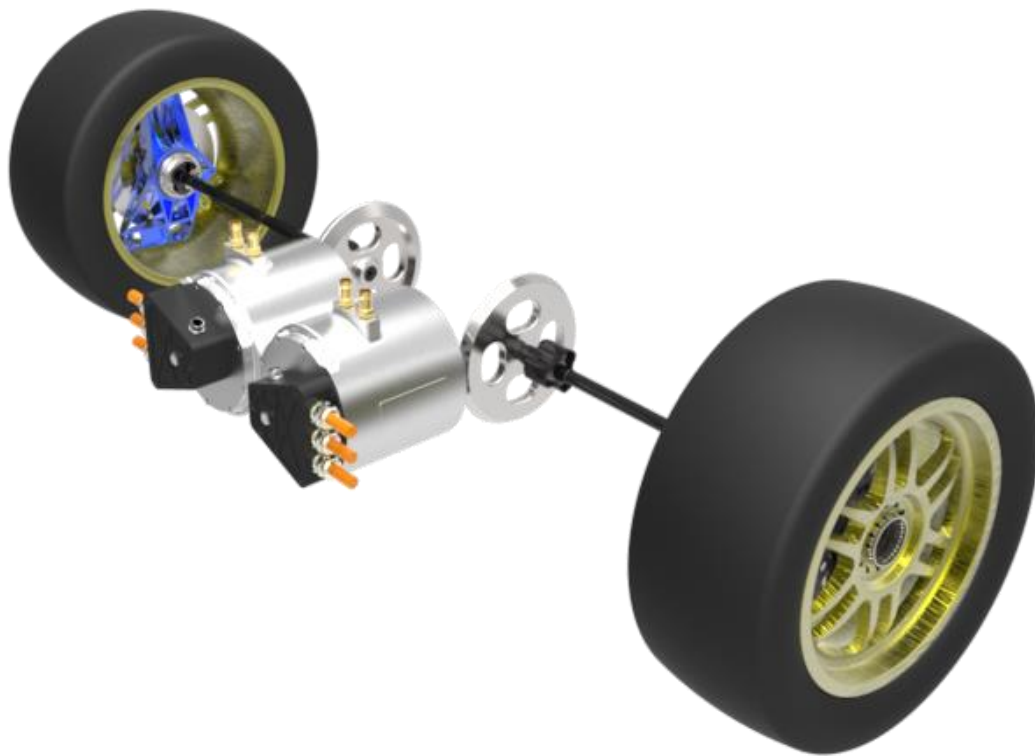
Mechanical efficiency still represents the strong point of this solution, especially in case of spur gears application.

By point of view of weight distribution situation is still worsen, because mass of motors is located in the same position. While mass of gear-box is shifted towards external of the car. In this way, **inertia of the vehicle around roll axis** is significantly increased, with a probable deterioration of handling performance.

Issues related to aerodynamic are identical and still unsolved. For reasons explained above, it's possible to conclude that this type of solution results improper for the studied application.

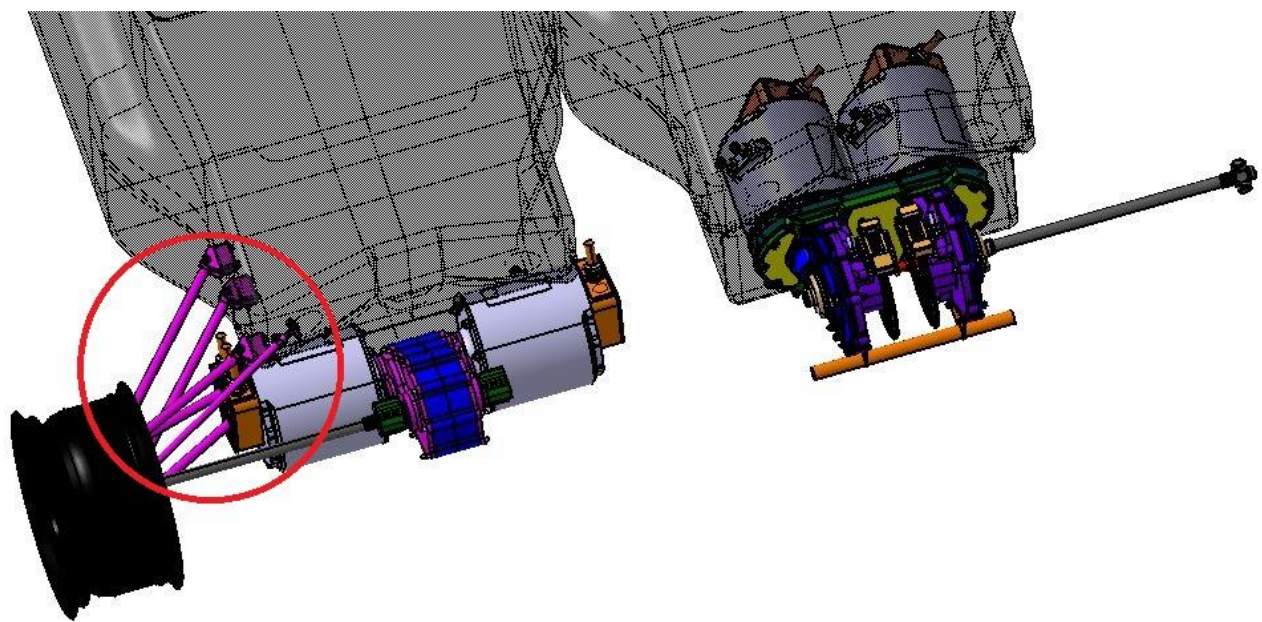


4.2.3. Longitudinal.



Picture 4.2-6: Longitudinal motors.

This layout features motors installed in position parallel to the road axis. The consequence is that input and output shafts need to be orthogonal. This kind of configuration can be appreciated with some examples described at Chapters 1.5.3, 1.5.4, 1.5.7 and 1.5.8. A configuration based on longitudinal motors is surely worse in terms of mechanical efficiency. Power through orthogonal axes is usually transmitted by bevel gears which feature a lower efficiency compared to cylindrical spur gears.



Picture 4.2-7: Transversal vs. Longitudinal motors fitted with monocoque and suspension.



Loss of efficiency is quantified between 5% and 6%, Ref.[6]. Anyway efficiency is comparable with a drop gear solution and it's surely higher than a drive chain configuration.

Moreover this solution is worse in terms of transmission **overall mass** too. By experience, It's possible to notice that, on equal terms of tooth face width, bevel gear is weaker than cylindrical one. At the same time, bevel gears need to be installed on angular contact bearings that are usually bulky compared to radials bearing comparable loads. Angular contact bearings are installed to oppose to axial component of force generated by bevels and absent in spur gears. Moreover It's necessary remind that gear-box cases needs to be reinforced in order to bear axial loads. By virtue of explained issues, transmissions including bevel gears are often heavier than full spur gears transmissions.

Anyway by point of view of **weight distribution**, longitudinal configuration ensures some advantages. First of all, It's necessary to remember that all evaluated solutions features motors positioned on the floor of the chassis. For this reason, distribution of weights along z-axis is mainly the same. The real benefit of longitudinal solution is the installation of motors in forwarded position, closer to the centre of gravity of the vehicle. That feature allows to maintain intended value of front/rear weight distribution. Furthermore, masses of motors are closer to the mean plan of the car, $y=0$. That reduces significantly inertia of the vehicle around the roll axis, with important benefits by handling point of view.

About **packaging** issues, it's convenient analyze Picture 4.2-7. It's extremely clear that a transversal layout, suitable for a tubular space frame, is not adequate for the tapered shape of the monocoque. But the most significant aspect is that dimensions of motors and gear-box cause issues of integration with frame and suspensions. Furthermore affordability of electric contact boxes the maybe compromised.

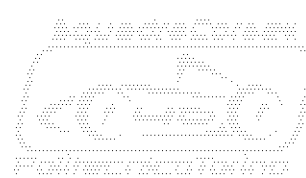
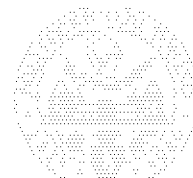
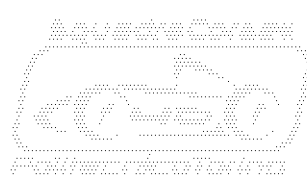
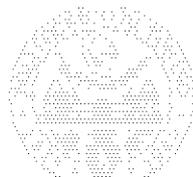
By aerodynamic point of view, motors shifted forward offer more space to design a suitable **diffuser**. This item generates important benefits for overall performances of a formula car.

At the end of this deep evaluation it's clear that longitudinal configuration is the best solution suitable in S.C.R. project. Issues related to mechanical efficiency and weight are widely overcome by benefits of layout, weight distribution and aerodynamic.

4.3. Technology of gears.

Gears represent the most iconic field of mechanic and establish a path of continuous evolution during millenniums. Following chapters provide knowledge of most important steps that characterize the evolution of gears in the history.

In order to perform a detailed design, starting from configuration chosen at Chapter 4.2, it's necessary to own a deep knowledge about gears and mechanical solutions. For this reason, following chapters are oriented to provide some notions of technical culture and to provide a panoramic knowledge about technologies available nowadays. Displayed topics are oriented through the design of S.C.R. transmission. Complete knowledge of gear field is out of this thesis target.



4.3.1. Evolution of gears.

After a brief research performed on the web, some basic information about evolution of gears have been collected and gathered. Large majority of following information have been reported according with source "<https://www.wikipedia.org/>", Ref.[8].

Starting step of this history can be surely represented by early prototypes found in China. Such artefacts can be dated around the 4th. century B.C. during the Zhang Guo times, Late East Zhou dynasty and have been preserved at the Luoyang Museum of Henan Province. Examples of mould of bronze gears dated around 2th. century B.C., during the early Han Dynasty, are displayed in the Shanghai Museum.

First European samples of gears technology can be found in the Antikythera Mechanism. It's a complex and intricate device found in 1900 in the sea that surrounds Antikythera island in the Aegean sea, not far from Crete. Device it's dated between the 2nd. and the 1st. century B.C. Anyway, duties and operations aren't been clearly understood still now. Most respected hypothesis assert that the mechanism is a sort of planetarium designed to calculate sun rising, moon phases, planet movements, equinoxes, months and days with unexpected accuracy. Parts of the bronze mechanism, fossilized on a stone, have been preserved in the National Archaeological Museum of Athens, in Greece.



Picture 4.3-1: Antikythera Mechanism (<http://www.namuseum.gr>).

Inside technical literature, gears can be found in some works connected with Hero from Alexandria who lived in the Roman Egypt around the A.D. 50. Anyway, other examples of gears can be traced back to the works of the Alexandrian School. That's a collective designation used to identify literary, philosophic, medic and scientific works created in the Ptolemaic Egypt, during the 3rd. century B.C. Many of these works can be ascribed to the well-known Greek polymath Archimedes who lived between 287th. And 212th. year B.C.

Returning to China it's remarkable the "South Pointing Chariot", an ancient two wheeled vehicle that mounted a movable point to indicate the south direction. The chariot, supposedly used as moving compass, is ascribed to the mythological engineer Ma Jun, who lived around the 250th. year B.C. The relevance of this invention it's the first example of differential gear ever installed.



It's necessary wait the A.D. 725 to find the first example of the most refined gear technology, clock technology. The first clock was created by Chinese engineers Yi Xing and Liang Lingzang, it's based on a water-powered gearwheel that works as escapement mechanism.

Another step of this amazing evolution is the water lifting device invented by the Mesopotamian engineer Al-Jazari. His invention operates the first example of segmental gears of the history and it's dated around A.D. 1206.

Gears of the type realized with the actual shape appeared in the European Middle Ages and was operated in the gigantic clock mechanism of cathedrals. Bronze and brass used to manufacture gearwheels was then replaced by the more robust steel during the industrial revolution and the cast manufacturing was replaced by more refined machining. Evolution continued in the 20th. century, thanks to a refinement in the profile of the teeth and thanks to a well-established knowledge in the sciences of materials. Nowadays plastic or metal gears are operated in the large majority of devices employed by humans, from the little domestic electrical appliances to the colossal merchant ships.

4.3.2. Orthogonal axes.

Chapter 4.2.3 explains briefly main drawbacks about configuration based on longitudinal motors. Orthogonal position between input and output shafts it's clearly the most complex feature of the chosen transmission layout. With reference to Chapter 4.2.3, preliminary evaluations performed on longitudinal configuration were based on the installation of bevel gears which are widespread. However, choice of a gear suitable to transmit power between orthogonal axes is not single. According to Ref.[7], next chapters display some solutions which technology of gears propose to overcome the issue of orthogonal axis.

4.3.2.1. Worm Screw.

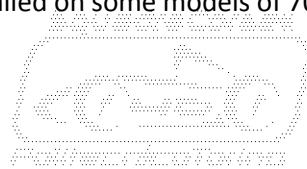
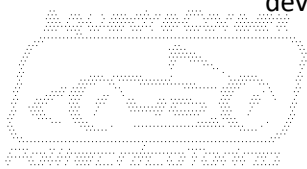
This solution is based on a endless screw featuring trapezoid profile, connected to the input, that operates a gearwheel. This solution, simple and effective, is widespread in all the industrial field. Main feature is the possibility to obtain very high gear ratios in a single

reduction stage (10:1÷20:1 and more). For this reason, the solution is very convenient in terms of **weight** and **volume**. Anyway, this mechanism is **not reversible** and that is a strong boundary to the employ of this technology. In any case, most significant drawback is the **efficiency**. Very high values of friction acts in the screw-gear contact and the efficiency may fall down to 50%. A strategy operated to limit efficiency loss is shown in the Picture 4.3-2. Gear is machined by a billet of brass, a material which interfaced with steel, features a very low friction coefficient. Unfortunately, featured mechanical efficiency it's extremely inadequate for a



Picture 4.3-2: Example of worm-screw (<http://www.altraex.com>).

continuous operation transmissions. This solution is more suitable in mechanisms which operate in discontinuous way. Anyway, It's necessary to remind that Peugeot exploited this device on transmissions installed on some models of 70's, according with Ref.[8].



4.3.2.2. Bevel Gears.

It's the most ordinary solution to transmit power between orthogonal axes. External shape of wheels is conical, differently to the cylindrical shape used to transmit power between parallel



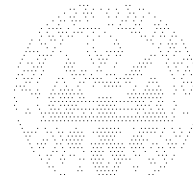
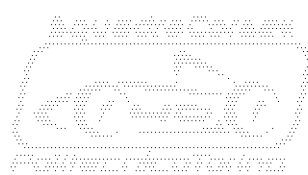
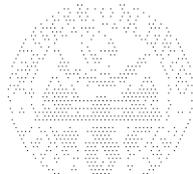
Picture 4.3-3: Example of bevel gears (<https://dir.indiamart.com/>).

or skew axes. This technology too allows to design a compact solution. Anyway, **gear ratio** that's convenient realize by a single stage is much more lower respect to the worm screw. Range of ratios is often included between $1:1$ to $4:1$. However, mechanical **efficiency** of a single gear is greater than 90% , according with Ref.[6]. This value is considerably higher respect to that featured by worm screw solution. Anyway, as declared in advance at Chapter 4.2, it's necessary to remember that efficiency of bevel gears is lower than efficiency of cylindrical gears which is around 98% . An important drawback of bevel gears it's the axial touch between pinion and driven wheel. It must respect well determined values during all the operation scenarios. That fact affects **manufacturing** and **assembly** procedures which must to be very precise and accurate. It's necessary

to reiterate that, for nowadays racing gear-box too, most delicate component is the bevel set coupled on the differential, which is the output of the system. A racing bevel set installed improperly, shows serious damages in a limited number of kilometres, maybe between $2.000 [km]$ and $3.000 [km]$. Some modern racing gear-boxes, coupled with high performance longitudinal engines, adopt a transversal layout in which shafts carrying ratios are parallel to y-axis. This solution allows to position the bevel set on the input of the gear-box, in order to improve car weight distribution. On the other hand, a longitudinal configuration gear-box houses the bevel set directly on the power output. By definition of gear ratio exploited at Chapter 4.1, it's clear that bevel set installed on the input of the gear-box is much less stressed than bevel set installed on the output. It was explained that input torque applied to an automotive gear-box is lower than output torque.

By virtue of issues explained in advance, **layout of a transmission** which houses a bevel gear, become more complicated if compared to a transmission realized by cylindrical spur gears only. Proper operation of a bevel gear inside a transmission needs angular contact bearings, preload devices, shims and well determined measure points.

Range of bevel gears is very wide, those in Picture 4.3-3 are the most basic example, straight bevels. Anyway, tooth profile of bevel gears evolved in different variants: zerol, spiral bevels, helical bevels and hypoid bevels. Benefits and drawbacks of different variants are going to be explained in next chapters, following the evolution of the design.



4.3.2.3. Face Gears.

According to “L. Baldassini – Vademecum per Disegntori e Tecnici 19° edizione”, Ref.[9], another option can be taken into account. That solution works substantially like the previous one, a conventional bevel gear. Main difference is represented by geometry of drive wheel which is a basic cylindrical spur pinion. On the other hand, driven wheel features a quite complicate geometry. It’s useful to image teeth of a spur gear, parallel to wheel axis, revolved of 90°. Axis of teeth which were parallel each other’s and parallel to wheel axis, are now perpendicular to wheel axis and converge on an unique point which lays on wheel axis. By virtue of that, geometry of driven wheel teeth features cuneiform shape.



Picture 4.3-4: Example of face gears (<http://www.assag.ch>).

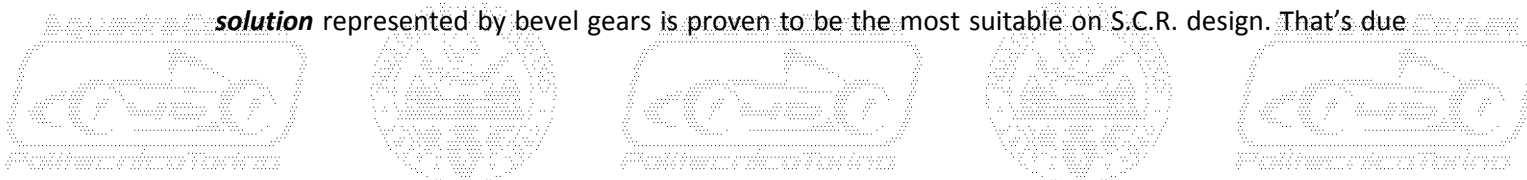
Differently from what explained at previous Chapter 4.3.2.2, a face gear set doesn’t need a well determined **axial touch** to operate properly. That’s due to drive wheel geometry which allows large freedom on its axial positioning. By point of view of bearings, configuration featured by face gears, looks simplified because driven gear only is loaded by **axial force**. For this reason, angular contact bearings are necessary on driven wheel installation only.

By virtue of previously explained benefits, face gears technology looks to be perfect applied to S.C.R. transmission design. Anyway, exhaustive **information** about this type of solution are difficult to find, probably because technology is quite young. **Formulae** and **standards** of calculation are very difficult to find like exhaustive data about **efficiency** or **reliability**. An additional issue is that, **manufacturers** skilled to produce face gears are very rare in Italy. For these reasons manufacturing looks difficult to realize in a short time.

No	Type	Normal Ratio Range	Efficiency Range
1	Spur	1:1 to 6:1	94-98%
2	Straight Bevel	3:2 to 5:1	93-97%
3	Spiral Bevel	3:2 to 4:1	95-99%
4	Worm	5:1 to 75:1	50-90%
5	Hypoid	10:1 to 200:1	80-95%
6	Helical	3:2 to 10:1	94-98%
7	Cycloid	10:1 to 100:1	75% to 85%

Table 4.3-1: Gear Ratio and Efficiency exploited by main types of gears, (<http://www.meadinfo.org>).

Back to the topic regarding design issues, previous research material is exhaustive enough to choose one of the described options. Differently from what declared on Chapter 3.3, **conventional solution** represented by bevel gears is proven to be the most suitable on S.C.R. design. That’s due



to **lack of time** and **lack of experience** which usually affect F.S.A.E. projects. Anyway, this case too, demonstrates that most experienced solution is the most suitable in motorsport oriented projects.

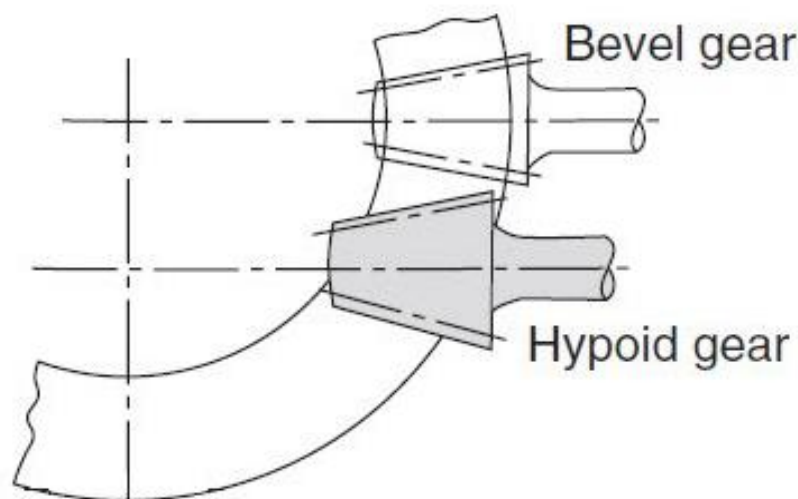
In order to conclude topic about face gears option, which represent the most innovative solution, It needs to be taken into account as a good starting point for an eventual design of development.

4.4. Distribution of Gear Ratio.

With reference to Eq. 4.1-24, value of gear ratio have been established. Anyway, knowledge on gears suggests that a gear ratio of 9:1 It's not convenient to be realized by a simple single-stage of reduction. As matter of fact, dimensions of gears in a stage are proportional to the value of gear ratio. In particular, high gear ratio affects strongly dimensions of driven wheel.

Plot 4.2-1 shows that motors are very close to the ground. For this reason, a very large driven wheel is very difficult to fit in accordance with car layout. It's therefore clear that transmission structures have to build up to vertical position. It's necessary to catch up with the fixed output axis position. That coincides with the position along z-axis of the half-shaft displayed in the Plot 4.2-2.

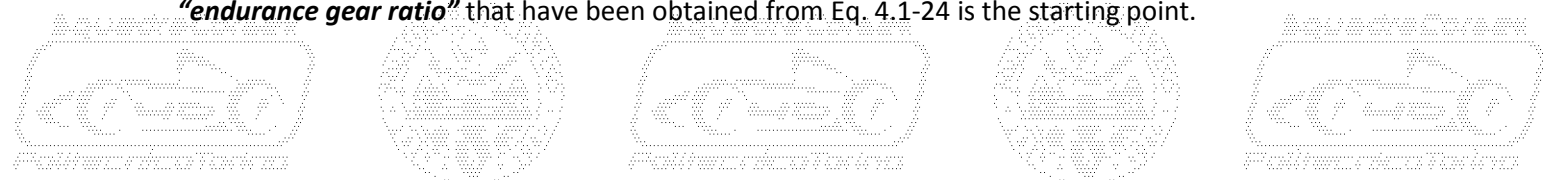
According with Ref.[9], hypoid bevel gears can be useful to solve these issues of packaging in a single stage solution. As depicted in Plot 4.4-1, main feature of hypoid bevel gears is the axis of the pinion that can be spaced out from axis of the driven wheel. Instead, axis of conventional bevel gears have to lie on the same plan. Unfortunately, as shown in Table 4.3-1, hypoid bevel gears feature a very low efficiency located in the range 80÷95%. Moreover it's necessary to consider that a large driven wheel of a single stage transmission is very improper by the point of view of the inertia. That's a crucial aspect on a vehicle oriented to fast accelerations. These arguments are relevant enough to exclude hypoid solution.



Plot 4.4-1 Difference between bevel and hypoid (<http://www.meadinfo.org>).

Split transmission in two stages, may be useful to solve depicted issues. First stage may be realized by bevel gears, second stage by spur cylindrical gears. Packaging configuration, technology of gears and total gear ratio are now set. By virtue of that, It's necessary to consider some other topics, with the purpose of extract some data useful in gears calculations.

Actual issue is choosing the more convenient way to split the gear ratio. The value of i_{end} the "**endurance gear ratio**" that have been obtained from Eq. 4.1-24 is the starting point.



$$\text{Eq. 4.4-1} \quad i_{end} = i_{1,2} \cdot i_{3,4} = 9,00 \text{ [dim. less]}$$

$$\text{Eq. 4.4-2} \quad i_{1,2} = \frac{d_2}{d_1}$$

$$\text{Eq. 4.4-3} \quad i_{3,4} = \frac{d_4}{d_3}$$

- $i_{1,2}$ is “**gear ratio of first stage**” of transmission, it’s a dimensionless parameter.
- $i_{3,4}$ is “**gear ratio of second stage**” of transmission, it’s a dimensionless parameter.
- d_1 is “**pitch diameter of wheel 1**”, drive wheel of the first stage, it’s measured in [mm].
- d_2 is “**pitch diameter of wheel 2**”, driven wheel of the first stage, it’s measured in [mm].
- d_3 is “**pitch diameter of wheel 3**”, drive wheel of the second stage, it’s measured in [mm].
- d_4 is “**pitch diameter of wheel 4**”, driven wheel of the second stage, it’s measured in [mm].

It’s necessary to find the most suitable values of $i_{1,2}$ and $i_{3,4}$.

Regarding first stage of reduction, It’s important consider that dimensions of the drive wheel, “**pinion**”, are geometrically bounded by dimensions of output shaft of the motor. On the other hand, it’s known that z_1 which is “**number of teeth of wheel 1**” is bounded by a minimum value, as explained at Chapter 5.3. Obviously, z_1 affects dimension of pitch diameter of wheel 1. Moreover, dimensions of the pinion are proportional to T_1 the “**torque on the pinion**” axis. To be conservative enough, it’s necessary to state that the maximum torque acting on the pinion coincides with maximum torque generated by the motor in endurance setting. The dimension which is more influenced by the torque it’s the pitch diameter, as shown by Chapters 5.4 and 5.5.

$$\text{Eq. 4.4-4} \quad D_1 \propto T_1 = T_{end}$$

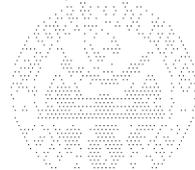
By previous dissertations it’s clear that D_1 , pitch diameter of wheel 1 can’t be lower than a well determined value. Accurate value is going to be calculated accurately in next Chapter 6. For the moment, it’s important understand that pinion dimension is bounded. It’s now useful consider another parameter of Eq. 4.4-2: diameter of the driven wheel.

By Eq. 4.4-2 it’s obvious that a large gear ratio leads to larger **dimensions of driven wheel** with a consequent increase of the mass. By virtue of that, a larger ratio on the first stage keeps low the centre of gravity of the transmission, with important benefits on dynamic performances of the car.

On the other hand, as explained previously, it’s clear that a too large dimension of driven gear leads to packaging problems because overall dimensions of the transmission may exceed the space limited by the minimum ride height of the car. For this reason, maximum value of external diameter of the driven wheel, have been set to be nearly tangent to monocoque floor. After these considerations, it’s possible to conclude that D_2 , pitch diameter of wheel 2 is bounded too.

To better evaluate a range of suitable dimensions, an advanced spreadsheet have been created on the basis of equations explained in chapter 5. Target is obtain a quicker esteem on the overall dimensions of gearwheels. Data which aren’t available at this stage of design, have been guessed on the basis of the maximum torque. For example $m_{1,2}$ which is “**modulus of first stage**” have been fixed:

$$\text{Eq. 4.4-5} \quad m_{1,2} = 3,00 \text{ [mm]}$$

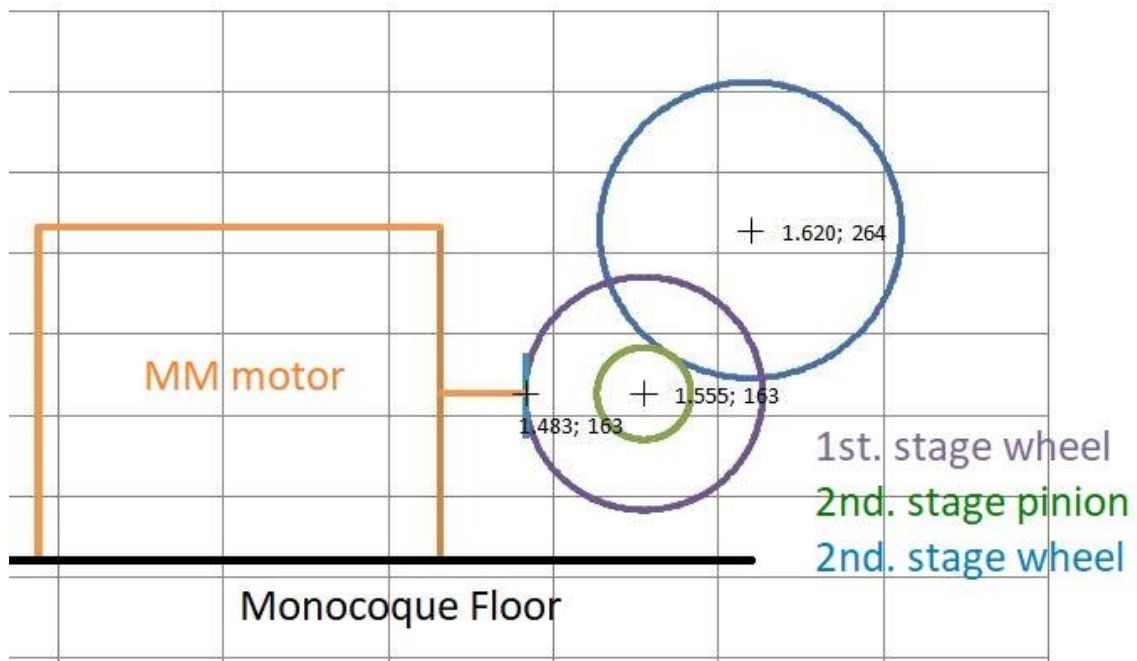


Output, shown in Plot 4.4-2, is a basic plot in which it's possible to compare dimensions of gears and dimensions of the motor positioned into the monocoque. In this way it's easier to estimate which is the maximum value suitable for first stage gear ratio. After many attempts, gear ratio distribution has been fixed:

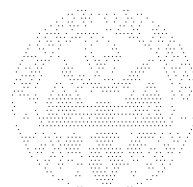
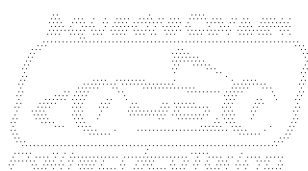
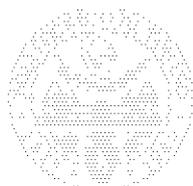
Eq. 4.4-6 $i_{1,2} = 2,80$ [dim. less]

Eq. 4.4-7 $i_{3,4} = \frac{i_{end}}{i_{1,2}} \cong 3,20$ [dim. less]

Values displayed by Eq. 4.4-6 and Eq. 4.4-7 underline that total gear ratio value can be quite evenly split on both stages. Need of keeping down masses would suggest that gear ratio of first stage would be greater than value of second stage. Anyway, as explained before, accurate analysis of likely dimensions led to privilege packaging requirements.



Plot 4.4-2: Output of the spreadsheet necessary to evaluate overall dimensions.

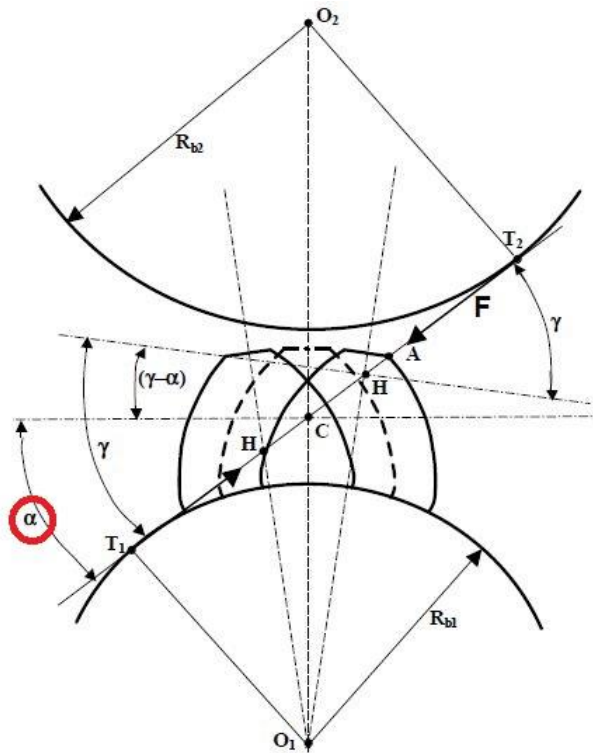


5. Basics of gears calculations.

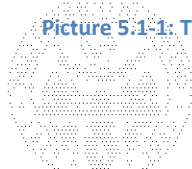
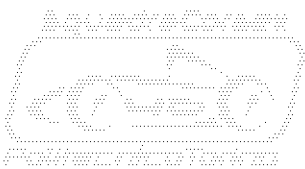
In the gears calculation the main parameter to be considered is gear ratio. The choice of this parameter is widely explained in the previous Chapter 4.1 and Chapter 4.4. Anyway, many other parameters have to be chosen or esteemed, in order to set up a proper calculation. The purpose of this chapter is to explain main equations that stand behind the algebraic calculations of gears. Calculations are aimed to determine the strength of the gears. The study is based on relations specific of cylindrical gears, from chapter 5.1 to 5.10. Furthermore, equations specific of bevel gears are displayed in chapter 5.11. Aim of following chapters is provide an exhaustive view of main parameters which rules gear design and gear operation.

5.1. Geometrical and design parameters.

According with Ref.[7], It's necessary to introduce some parameters that are going to affect the calculation of the designed gears. The most important is α , the "pressure angle". It's defined by the angle between "line of action", which is the straight line tangent to the "base circles" of the two wheels, and the horizontal line perpendicular to the "line of centres". That's parameter affects heavily the shape of the tooth. A low value of α leads to a shape in which the tooth is very thin in the root section but it's enough thick around the outside section. On the contrary, a high value of α leads to a tooth that is very strong on the root section but it's quite spiky on the outside section. Such a tooth profile it's effective in terms of stiffness of the single tooth but makes worse the meshing characteristic of the entire gear, transverse contact ratio in particular. Pressure angle is determined by geometry of the tool employed to manufacture the gear, for this reason values of α are well determined. Any angle needs a specific tool. Here the most commonly used in automotive and industrial application: $.5^\circ$, 15° , 18° , 20° , 22.5° and 30° .



Picture 5.1-1: The alpha parameter (<https://www.engineersedge.com/>).



The next geometrical parameter have to be assumed according to the requirement of the packaging. It's λ , the "**Face Width/Module Ratio**", a dimensionless parameter which is defined as follow:

$$\text{Eq. 5.1-1} \quad \lambda = \frac{b}{m}$$

- b is "**face width**" of the tooth, it's measured in [mm].
- m is "**module**" of the gear, it's measured in [mm].

Modulus It's the variable which needs to be calculated. Lambda is a parameter useful to perform preliminary calculus only. Assumed a certain value of module which satisfy packaging requirements, the definitive value of face width have to be confirmed by some verifications.

The real design parameter is the "**Safety Coefficient**", It's a dimensionless quantity which has no geometrical meaning. Suitable value needs to be assumed in the preliminary calculus of the module:

$$\text{Eq. 5.1-2} \quad S.C. \geq 1,2 \text{ [dim. less]}$$

Chosen value may appear too tight if compared with values normally assumed in automotive or industrial fields. Anyway, It's always necessary to realize that the gears to design are employed on a race car. Moreover the breakdown of the gear-box cannot lead safety issues for the driver or for other involved persons. With a reasonable amount of risk, it can be possible reduce considerably weight of the components.

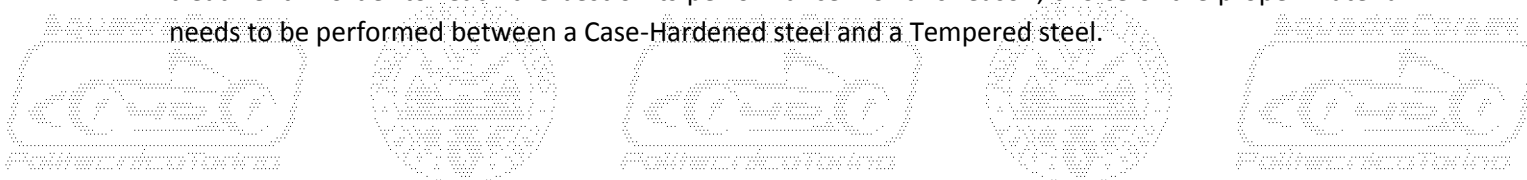
5.2. Importance of materials and preliminary evaluations.

Material strongly affect performance and dimension of gears, in order to obtain the best trade-off between strength and weight, the choice of the material is fundamental.

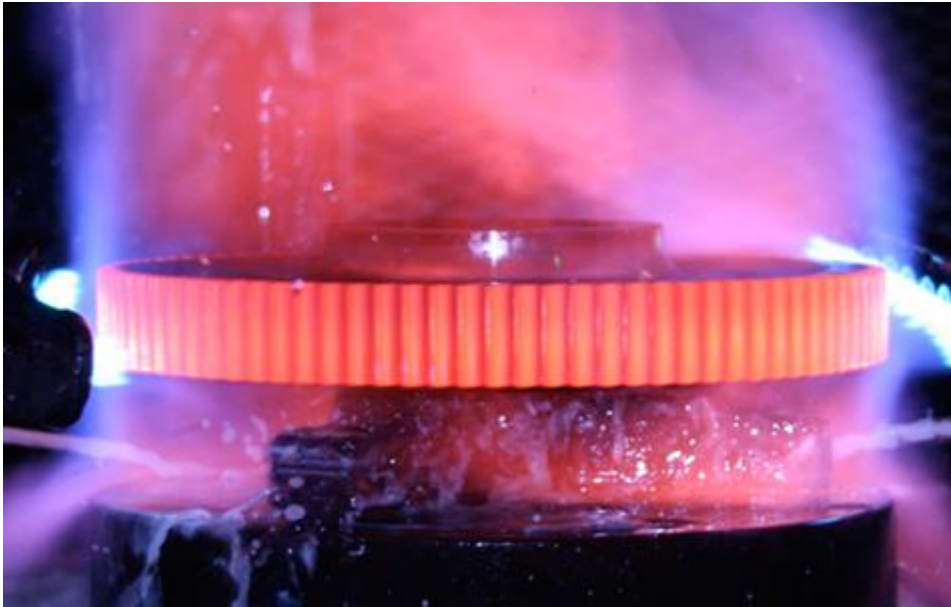
How it's going to be explained forward, the most stressed part in the wheel is the tooth. It needs to be tenacious in order to bear the bending caused by the gear meshing. In addition, tooth needs to be resilient in order to sustain the impact due to the backlash between teeth. Last but not least, tooth needs to be hard enough to tolerate the strong pressure between faces of teeth belonging different wheels.

The most suitable material for heavy duties have to be, obviously, **metal**. A racing transmission is a very stressed component, for this reason it's necessary reject aluminium alloys to evaluate **titanium alloys** and steel. Titanium alloys are an optimum trade-off between performance and weight. Moreover, it exhibits many issues in manufacturing, indeed machinability is difficult if compared to that of aluminium and steel. For this reason, it's necessary to machine titanium components by specific tools, in order to obtain good results. Cost and availability of specific tools may represent two huge issues. On the other hand, a material suitable for gears needs specific heat treatments, and those specific for titanium are not so widespread nowadays. The pursuit of partners provided by specific tools and skilled in specific heat treatments hadn't good results, for this reason more conventional materials were preferred in the choice.

Most widespread metallic materials used to manufacture gears are **steel alloys**. A good engineered steel, which combines all the features enlisted at the beginning of the chapter, needs an efficient heath treatment in order to reach the best of its performance. For this reason, choice of the proper material needs to be performed between a Case-Hardened steel and a Tempered steel.



Case-Hardened is a kind which includes structural steels alloyed with a content of carbon lower than 0.30%. It's usually employed in the production of gears, axles, pins and bushes. External surface of components is hardened by a carbon enrichment obtained by quenching in furnace atmosphere. That features high hardness of the surface, necessary to sustain the wear caused by friction. Hardness of surface after the Case-Hardening treatment, is usually higher than 650 HV points. Low content of carbon in the core of the component features high tenacity. Most performing alloys of this family are 18NiCrMo7 and 16MnCr5.



Picture 5.2-1: Heat treatment of a gear (<http://gearsolutions.com>).

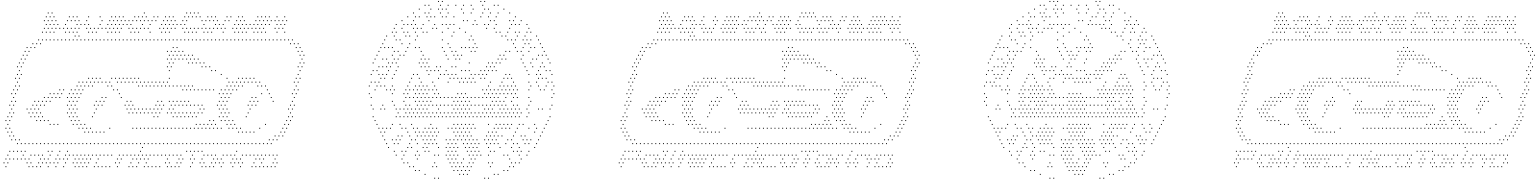
Tempered is a family of steels suitable for the oil quenching. These materials are widely employed in automotive industry, in the production of engine components particularly. That's due to the good results in machinability. Anyway, These materials suffer serious brittleness after the hardening process. Large portions of crystalline structure of material have been transformed in martensite. In order to overcome this issue, components are subject to a treatment of **"annealing"**. That consists of heating steel again to a room temperature between 300÷600°C, then a very slowly cooling down process takes place. Total annealing process may last for several days.

The main feature of these steels is the ability of maintain best performances in large raw components with thickness between 20mm and 80mm. Different alloys feature different aptitude to quenching process and, of course, different levels of deformation after the treatment. Most performing alloys of this family are 42CrMo4, 36CrNiMo6 and 30NiCrMo8.

5.3. Minimum number of teeth.

According with Ref.[7], a critical condition of interference may happen in the meshing between drive and driven wheels. This issue is exhibit on gears obtained by modular calculation. Critical condition happens when the outer diameter of the driven wheel interferes with the gear hollow of the drive wheel, the pinion.

That kind of interference decreases when the number of teeth of the drive wheel is increased. From a certain value to above, interference disappears. That value is Z_{min} which is defined as **"minimum**



number of teeth". It can be calculated in function of gear ratio i , defined in Chapter 4.1, and pressure angle α , defined and Chapter 5.1.

$$\text{Eq. 5.3-1} \quad z_{min} = \frac{\frac{2}{i}}{-1 + \sqrt{1 + \frac{\sin^2 \alpha}{i} \left(2 + \frac{1}{i}\right)}}$$

It's necessary to consider that result of Eq. 5.3-1 is a minimum value, for this reason the decimal number needs to be round off the greater whole number. The rounded value is the number of teeth of the drive wheel, the pinion, z_1 . It's now possible write the equation of the gear ratio in this form:

$$\text{Eq. 5.3-2} \quad i = \frac{z_1}{z_2}$$

- i is "**gear ratio**", a dimensionless parameter defined in chapter 4.1.
- z_1 is "**number of teeth of wheel 1**", drive wheel of the reduction stage, usually defined "**pinion**".
- z_2 is "**number of teeth of wheel 2**", driven wheel of the reduction stage.

Due to manufacturing process, some errors may happen. For this reason, it's necessary to avoid that a certain tooth of the pinion works always with the same tooth of the wheel, because that can amplify the error. For this reason it's necessary to chose a number of teeth of the pinion which is a prime number, for example: 17, 19, 23 and so on.

5.4. Module.

In the modular dimensioning of gears, parameters which can be free or bounded, have to be established on the base of a unified norm. Main targets are guarantee a complete interchange-ability of the gears and the application of a standard in the manufacturing process. That leads to an important saving in the cost of manufacturing. By virtue of that, the base of gear dimensioning is m the "**module**" parameter, defined by the following relation.

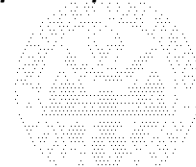
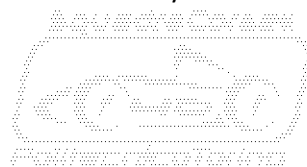
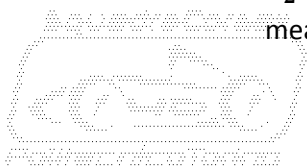
$$\text{Eq. 5.4-1} \quad m = \frac{p}{\pi}$$

- p is "**pitch**", the distance between two homologue points that are owned by two consecutive teeth, measured on the pitch diameter. Pitch is a dimension common to the gear, have to be the same in both drive and driven wheel. It's measured in [mm].

Empirical calculation of the modulus is based on the "**Theory of Lewis**", according to "R. G. Budynas, J. K. Nisbett – *Shigley's Mechanical Engineering Design 9^{ed.}*", Ref.[10]. Such theory describes a mathematical model in which tooth is treated as a fixed beam. F_t is the "**tangential gear force**" which is applied to the unbounded end of the beam. It's measured in [N].

$$\text{Eq. 5.4-2} \quad F_t = \frac{T_1}{d_1} = \frac{T_2}{d_2}$$

- T_1 is "**torque on drive wheel axis**". Usually known as "**input torque**" of the gear. It's measured in [Nm].
- T_2 is "**torque on driven wheel axis**". Usually known as "**output torque**" of the gear, It's measured in [Nm].



- d_1 is “pitch diameter of wheel 1”, drive wheel of the reduction stage, it’s measured in [mm].
- d_2 is “pitch diameter of wheel 2”, driven wheel of the reduction stage, it’s measured in [mm].

Obviously, the most stressed area is the bounded end which corresponds to the root of the tooth. Result of the Lewis theory is the equation which determines σ_{LW} the stress in the root area, defined as “Stress of Lewis”. Dimension of this stress is [MPa].

$$\text{Eq. 5.4-3} \quad \sigma_{LW} = \frac{F_t}{b \cdot m} \cdot Y_{LW}$$

- b is “face width” of the tooth, it’s measured in [mm].
- m is “module” of the gear, it’s measured in [mm].
- Y_{LW} is “coefficient of Lewis” which is a dimensionless parameter chosen in the Table 5.4-1. Input of such table are two. One is the number of teeth of the drive wheel Z, Z_v . Other is the normal pressure angle α_n .

Z, Z_v	$\alpha_n=20^\circ$			Z, Z_v	$\alpha_n=20^\circ$		
	$1/y_{LW}$	y_{LW}	k		$1/y_{LW}$	y_{LW}	k
12	0,245	4,08	0,88	28	0,352	2,84	0,588
13	0,261	3,83	0,839	30	0,358	2,79	0,571
14	0,276	3,62	0,803	34	0,371	2,70	0,541
15	0,289	3,46	0,773	38	0,383	2,61	0,516
16	0,295	3,39	0,751	43	0,396	2,53	0,49
17	0,302	3,31	0,73	50	0,408	2,45	0,451
18	0,308	3,25	0,712	60	0,421	2,38	0,43
19	0,314	3,18	0,695	75	0,434	2,30	0,395
20	0,32	3,13	0,679	100	0,446	2,24	0,355
21	0,327	3,06	0,663	150	0,459	2,18	0,307
22	0,33	3,03	0,651	300	0,471	2,12	0,242
24	0,336	2,98	0,629	8	0,484	2,07	
25	0,346	2,89	0,606				

Table 5.4-1: Choice of the coefficient of Lewis, Ref.[10].

Anyway, it’s necessary to transform Eq. 5.4-3 in a design equation. First step is the following relation that ensures the structural integrity of the tooth.

$$\text{Eq. 5.4-4} \quad \sigma_{LW} \leq \sigma_{all}$$

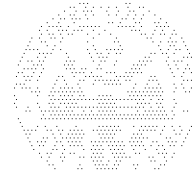
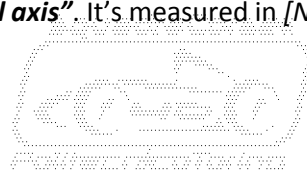
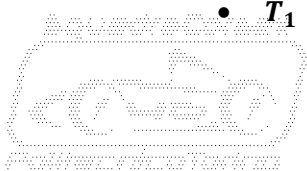
$$\text{Eq. 5.4-5} \quad \sigma_{all} = \frac{R_{P02}}{S.C.}$$

- σ_{all} is “allowable stress”, it’s measured in [MPa].
- R_{P02} is “yield strength”, it’s a feature of the chosen material and It’s obtained by experimental tests. It’s measured in [MPa].
- $S.C.$ is “safety coefficient”, a dimensionless parameter displayed in Chapter 5.1.

The Eq. 5.4-3 becomes the following design equation:

$$\text{Eq. 5.4-6} \quad m = \sqrt[3]{\frac{T_1 \cdot Y_{LW} \cdot 2}{\lambda \cdot \sigma_{all} \cdot z_1}}$$

- T_1 is “torque on drive wheel axis”. It’s measured in [Nm].



- λ is “**Face Width/Module Ratio**”, a dimensionless parameter described by Eq. 5.3-2.
- z_1 is “**number of teeth of wheel 1**”, described in chapter 5.3.

In this case, torque is assumed to be the maximum for reasons of safety.

$$\text{Eq. 5.4-7} \quad T_1 = T_{Mmax}$$

- T_{Mmax} is “**maximum torque**” generated by motor or by engine, It’s measured in $[Nm]$.

As explained at the beginning of this chapter, module is a standard dimension. Like pressure angle, It depends by the tool used to machine teeth. The result of Eq. 5.4-6 needs to be round off choosing one of the values of the Table 5.4-2. Such a table shows standard modules defined by **U.N.I. 6587** standard, dimensions re in millimetres.

<i>0.5</i>	<i>2.5</i>	<i>6</i>
<i>0.75</i>	<i>2.75</i>	<i>6.5</i>
<i>1</i>	<i>3</i>	<i>7</i>
<i>1.125</i>	<i>3.25</i>	<i>8</i>
<i>1.25</i>	<i>3.5</i>	<i>9</i>
<i>1.375</i>	<i>3.75</i>	<i>10</i>
<i>1.5</i>	<i>4</i>	<i>11</i>
<i>1.75</i>	<i>4.5</i>	<i>12</i>
<i>2</i>	<i>5</i>	<i>14</i>
<i>2.25</i>	<i>5.5</i>	<i>16</i>

Table 5.4-2: Standard modules from regulations (UNI 6587:1969).

Anyway, special applications need custom values of the module. It may not be a big issue by point of view of the cost, if number of produced components is large enough to make cost of tooling inconsistent. For this reason, It’s quite usual find custom module gears in automotive applications,

5.5. Radial dimensions.

Once modulus is chosen, it’s possible to calculate typical dimensions of gears according with Ref.[7]. Subject of this chapter are radial dimensions. It’s important underline that, parameters which constitute following equations don’t show subscripts because are generic can be referred to both wheels of the gear. By parameters extracted in previous parameters, it’s possible to calculate r defined as “**pitch radius**”. This dimension is measured in $[mm]$.

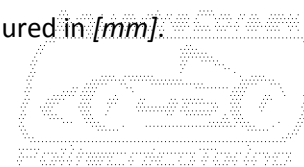
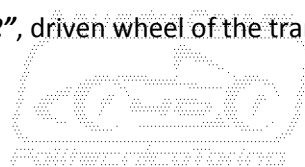
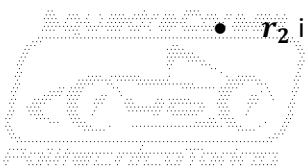
$$\text{Eq. 5.5-1} \quad r = \frac{m \cdot z}{2} = \frac{d}{2}$$

Before the calculation of next parameter, It’s necessary to clarify that, pitch diameters of the wheels of the same gear are tangent each others. For this reason, the sum of the two pitch radius measured on the pitch diameter, is $o_{1,2}$ that is the “**offset**” of the gear, measured in $[mm]$.

$$\text{Eq. 5.5-2} \quad o_{1,2} = r_1 + r_2$$

Where:

- r_1 is “**pitch radius of wheel 1**”, drive wheel of the transmission stage, it’s measured in $[mm]$.
- r_2 is “**pitch radius of wheel 2**”, driven wheel of the transmission stage, it’s measured in $[mm]$.



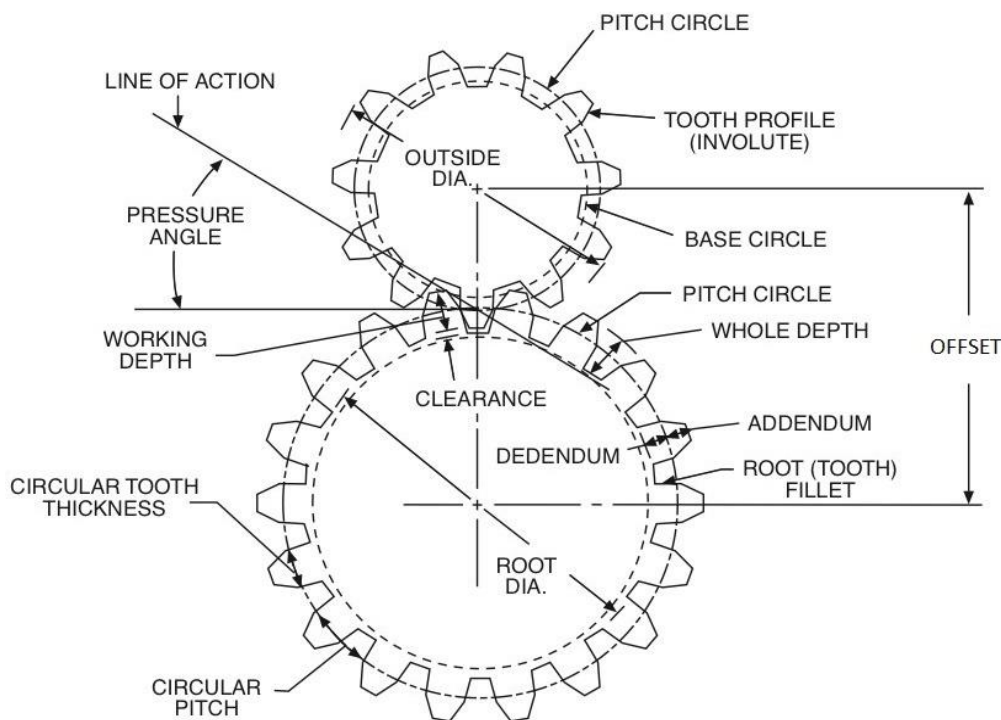
Another important parameter to calculate is h , the “**height of the tooth**” which is related to other two measures ha which is the “**addendum**” and hd which is the “**dedendum**”. All parameters are proper of the gear, for this reason are common to drive and driven wheel. All parameters are measured in [mm].

Eq. 5.5-3 $h = ha + hd$

Eq. 5.5-4 $ha = m$

Eq. 5.5-5 $hd = 1,25 \cdot m$

Addendum which is defined by Eq. 5.5-4 is the distance between top diameter and pitch diameter. Analogously, Eq. 5.5-5 defines dedendum, which represents the distance between pitch diameter and root diameter. In relation to dedendum parameter, the choice of multiply modulus for 1,25 is safety measure which avoids that top of tooth collides with root of related wheel.



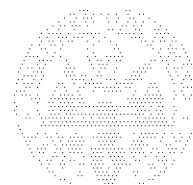
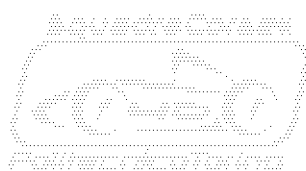
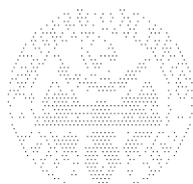
Picture 5.5-1: Main radial dimensions of gears (<https://www.quora.com/>).

On the base of previous calculations, It’s possible to obtain main radial dimensions of gear. In particular, r_t the “**tip radius**”, which represents the outer diameter of the gearwheel. Then, r_r the “**root radius**” and r_b the “**base radius**”. This last dimension, differently from other two owns a meaning in the design only. The straight line tangent of two base diameters of the gear is the direction where the force exchanged by the wheels lays. Measures are proper to the gear in this case too and dimension is [mm].

Eq. 5.5-6 $r_t = r + ha$

Eq. 5.5-7 $r_r = r - hd$

Eq. 5.5-8 $r_b = r \cdot \sin \alpha$



5.6. Axial Dimension.

While module of gear have been determinate, another important parameter related to gear strength have to be fixed, **b** which is the “**face width**”. Once the module is fixed, face width is well determined by Eq. 5.1-1. It’s necessary remind that value of λ have been chosen arbitrarily.

For this reason, face width is to be considered a variable yet. Some verifications are going to be performed in next chapters, the purpose is to evaluate the proper value of face width. That’s why, when design arrives to verification stage, It’s no more convenient vary the value of modulus. In addition, value of face width can be varied continuously, with no need to respect standardized values, like for modulus.

5.7. Overlap ratio.

After the calculations of main geometric dimensions of the gear, it’s necessary to perform some checks ad verifications. One of these is based on the “overlap ratio” which will be deeply explained forward. In order to obtain the overlap ratio, one geometric parameter still have to be obtained: **p**, known as the “**pitch**”. Knowing the value of module, it can be obtained revolving Eq. 5.4-1. Like it was declared in advance at Chapter 5.4, It’s measured in [mm].

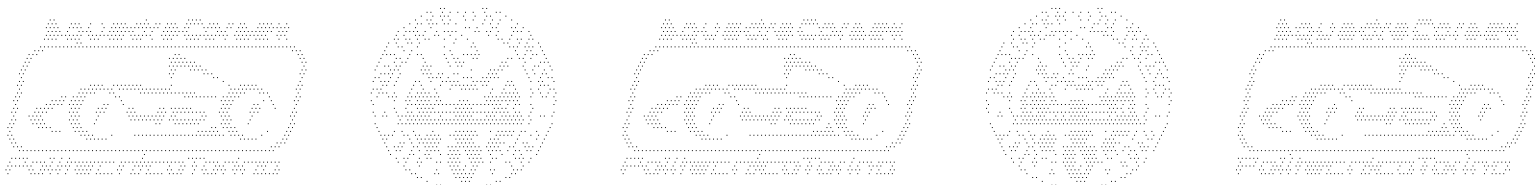
Eq. 5.7-1
$$p = m \cdot \pi$$

Starting by data obtained by previous equations, it’s possible to calculate parameter ϵ which is known as “overlap ratio”.

Eq. 5.7-2
$$\epsilon = \frac{\sqrt{r_{t1}^2 - r_{b1}^2} + \sqrt{r_{t2}^2 - r_{b2}^2} - (r_1 + r_2) \cdot \sin \alpha}{p \cdot \cos \alpha}$$

- r_{t1} is “**tip radius of wheel 1**”, drive wheel of the reduction stage, it’s measured in [mm].
- r_{b1} is “**base radius of wheel 1**”, drive wheel of the reduction stage, it’s measured in [mm].
- r_{t2} is “**tip radius of wheel 2**”, driven wheel of the reduction stage, it’s measured in [mm].
- r_{b2} is “**base radius of wheel 2**”, driven wheel of the reduction stage, it’s measured in [mm].
- r_1 is “**pitch radius of wheel 1**”, drive wheel of the reduction stage, it’s measured in [mm].
- r_2 is “**pitch radius of wheel 2**”, driven wheel of the reduction stage, it’s measured in [mm].
- α is “**pressure angle**” of the gear. In this case is intended to be considered as α_n which is the “**normal pressure angle**”. This parameter is measured in [°].

Overlap ratio is a dimensionless parameter referred to the gear and not to single wheels only. It represents an index of gear good operation. Value obtained by Eq. 5.7-2 indicates how many teeth per wheel are simultaneously involved in the gear meshing. It’s clear that one only couple of teeth meshing each others as supposed in chapter 5.4 it’s a really conservative assumption. In the reality it would cause lacks in the gear contact which is consequently restored by impact. If the result of the previous equation is, at least, 2.0 it means that a couple of teeth per wheel is in contact with the corresponding couple of the related gear. Unfortunately this small value leads to a noisy gear operation. For these reasons, the overlap ratio of a good operating automotive gear is included between 3.0 and 4.0.



5.8. Fatigue verification in bend.

Back to mathematical model mentioned at Chapter 5.4, concept of beam bounded to an extremity is developed and applied to a fatigue case, in order to study behavior of teeth loaded by cyclic bending stresses. That kind of verification is strictly referred to standard "U.N.I. – UNI Sperimentale 8862-2:1987", Ref.[11] and it's performed by the following main relation:

$$\text{Eq. 5.8-1} \quad \sigma_F \leq \sigma_{FP}$$

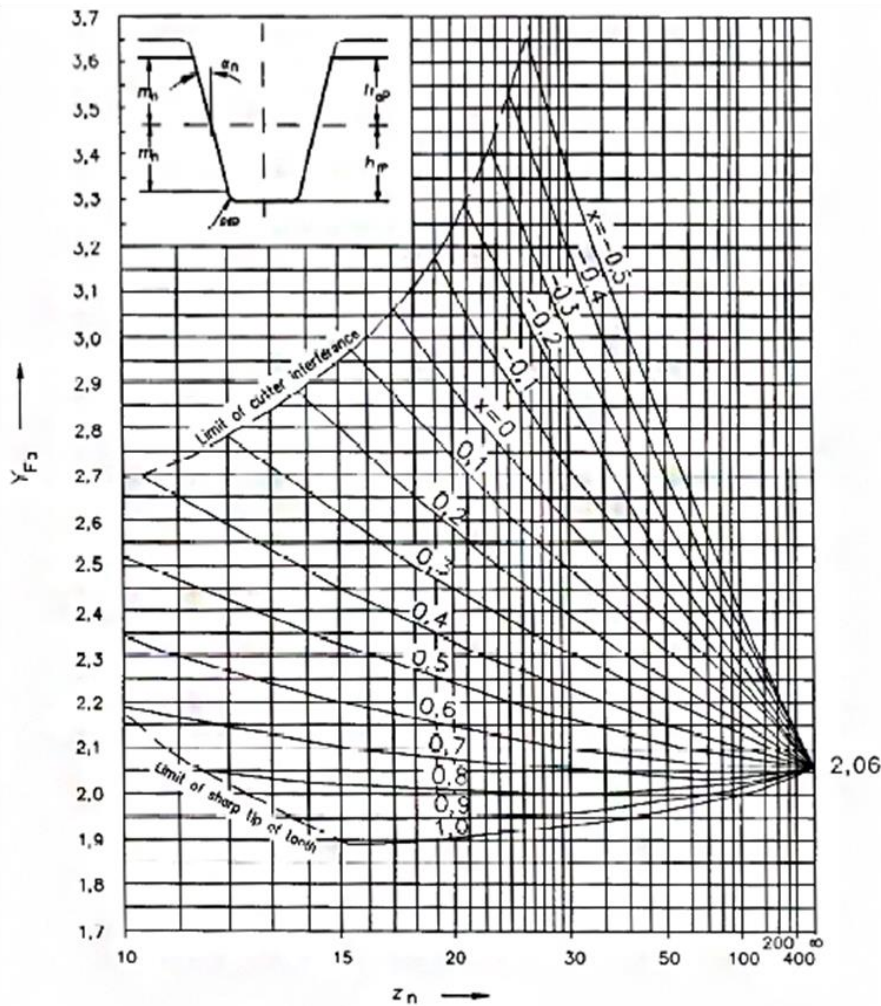
- σ_F is "equivalent stress in root section" of the tooth.
- σ_{FP} is "pulsating bending fatigue limit" and it's also known as "allowable stress" but it must be distinguished by allowed stress of Chapter 5.4.

Both terms of Eq. 5.8-1 can be considered as stress, for this reason are measured in [MPa].

Equivalent stress in root section of the tooth is obtained by a well structured equation deeply described as follows.

$$\text{Eq. 5.8-2} \quad \sigma_F = \frac{F_{Tm}}{b \cdot m} \cdot Y_{Fa} \cdot Y_{Sa} \cdot Y_\epsilon \cdot Y_\beta \cdot (K_a \cdot K_v \cdot K_{f\beta} \cdot K_{f\alpha})$$

- b is "face width" which represents the parameter that needs to be checked measured in [mm].
- m is "module" . In this calculus can be considered a fixed parameter. It's measured in [mm].



Plot 5.8-1: Y_{Fa} factor displayed in function of z_n quantity and x factor, Ref.[11].

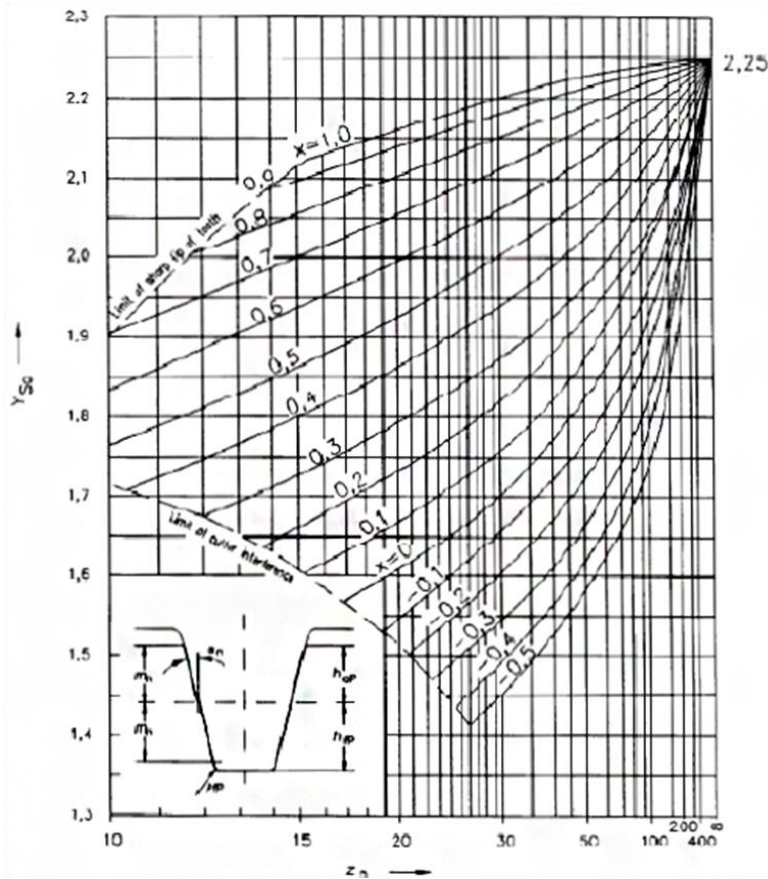


- F_{Tm} is “**mean tangential gear force**”. It’s measured in $[N]$ and, differently from tangential force calculated by Eq. 5.4-2, it’s described as follows:

Eq. 5.8-3
$$F_{Tm} = \frac{T_{1m}}{\frac{d_1}{2}}$$

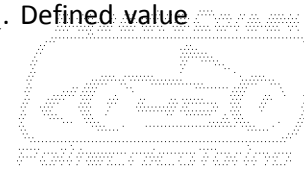
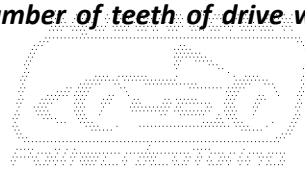
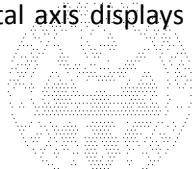
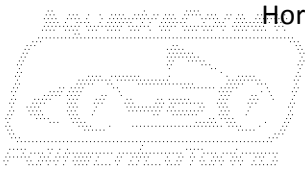
- T_{1m} is “**mean torque on wheel 1**”. That datum it’s difficult to own in the design preliminary phase. It needs to be esteemed or extracted by data of a similar vehicle. Risk is that, an over-esteemed value can lead to an over-sized gear. It’s measured in $[Nm]$.
 - d_1 is “**pitch diameter of wheel 1**”, drive wheel of the reduction stage, It’s measured in $[mm]$.
- Other factors of Eq. 5.8-2 have to be chosen on the basis of plots supplied by Ref.[11] standards.

- Y_{Fa} is “**tooth form factor**”. It relates the geometry of the tooth to the nominal bending stress. It can be extracted by Plot 5.8-1. Horizontal axis displays “**number of teeth of drive wheel**”, indicated with Z_n . Defined value needs to be crossed with curves of “**gear profile shift**”, indicated with X . Detailed information about that dimensionless parameter can be found at Chapter 5.12. Point identified by number of teeth and gear profile shift needs to be shifted horizontally toward vertical axis on which value of tooth form factor can be read. It’s suitable remember that this factor is a dimensionless parameter.



Plot 5.8-2: Y_{Sa} factor displayed in function of z quantity and x factor, Ref.[11].

- Y_{Sa} is “**stress correction factor**”. It’s necessary for the conversion of the nominal stress applied to tooth root. It’s determined by the application of load at the outer point of single pair of tooth in contact. Analytic calculus of this factor is quite complex and, in first approximation, it’s more useful chose the value with the help of Plot 5.8-2. As explained in the case of Y_{Fa} , Horizontal axis displays “**number of teeth of drive wheel**”, indicated with Z_n . Defined value



needs to be crossed with curves of “**gear profile shift**”, indicated with **X**. Point identified by number of teeth and gear profile needs shift to be shifted horizontally toward vertical axis on which value of stress correction factor can be read. It’s suitable remember that this factor is a dimensionless parameter.

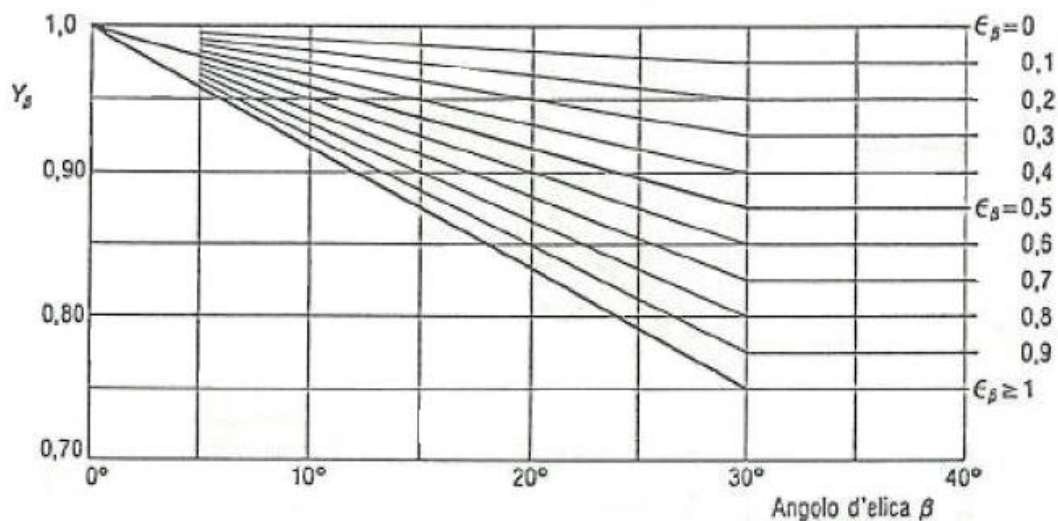
- Y_ϵ is “**overlap ratio factor**” which is a dimensionless parameter. Let image that meshing is extended over a single couple of teeth, condition of maximum stress appears it the root of teeth. This factor takes into account that, in the reality, force due to gear meshing isn’t applied to the top of the tooth, but in another point of the profile. To calculate the factor, standard provides this relation:

Eq. 5.8-4

$$\begin{cases} Y_\epsilon = 0,25 + \frac{0,75}{\epsilon} \leftrightarrow \epsilon < 2 \\ Y_\epsilon = 0,5 \leftrightarrow \epsilon \geq 2 \end{cases}$$

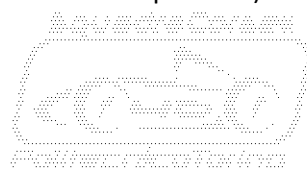
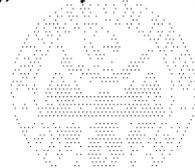
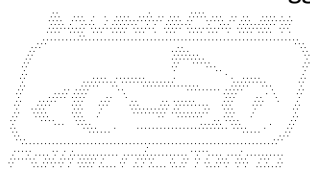
- Y_β is “**helix angle factor**” which takes into account the effect of helix profile on the distribution of the stress. Its value can be extracted by Plot 5.8-3. Horizontal axis displays “**helix angle**”, indicated with β . Defined value needs to be crossed with broken lines which represent the “**overlap ratio**”, indicated with ϵ_β . Point identified by number of teeth and gear shift profile needs to be shifted horizontally toward vertical axis on which value of helix angle factor can be read. It’s suitable remember that this factor is a dimensionless parameter.

In the particular case of a spur gear with straight profile teeth, value of the factor is 1.



Plot 5.8-3: Y_β factor displayed in function of β quantity and Y_ϵ factor, Ref.[11].

- K_a is “**load application factor**”. It takes into account the presence and the entity of overloads in the operational life of the gear. These overloads can be due to the operation of the drive machine, motors for example . Operational condition of the drive machine can be split in three cases: uniform (“uniforme”), light overloads (“sovraccarichi leggeri”), heavy overloads (“sovraccarichi pesanti”). On the other hand, operation of the driven machine, in which gear is housed, can be affected by overloads. In the same way, operational condition of the driven machine can be split in three cases: uniform (“uniforme”), light overloads (“sovraccarichi leggeri”), heavy overloads (“sovraccarichi pesanti”).



Caratteristiche di funzionamento del motore	Caratteristiche di funzionamento della macchina azionata		
	uniforme	sovraccarichi leggeri	sovraccarichi forti
	Valori orientativi di K_A * •		
Uniforme	1,0	1,25	1,75
Sovraccarichi leggeri	1,25	1,5	2,0 o più
Sovraccarichi forti	1,5	1,75	2,25 o più

* I valori indicati non sono validi per ingranaggi funzionanti a velocità prossime alle velocità di risonanza.
 • Per ingranaggi moltiplicatori, moltiplicare i valori indicati per 1,1.

Table 5.8-1: Y_{Fa} factor displayed in function of z quantity and x factor, Ref.[11]

Once operational cases of drive and driven machine are determined, value of load application factor can be chosen on the Table 5.8-1. This factor is a dimensionless parameter.

- K_v is “dynamic factor” which takes into account the effect due to rotating masses of the gear. In first approximation it’s possible to calculate dynamic factor by following Eq. 5.8-2, where v_p it’s the “gear maximum tangential speed”, calculated on the pitch diameter.

Eq. 5.8-5
$$K_v = \frac{5,6 + \sqrt{v_p}}{5,6}$$

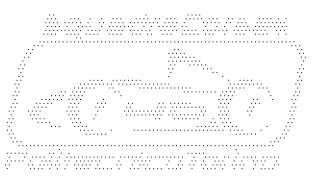
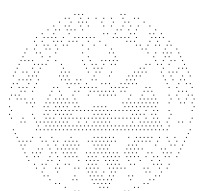
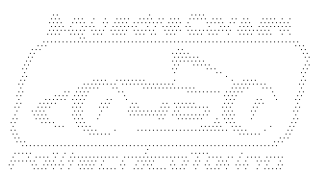
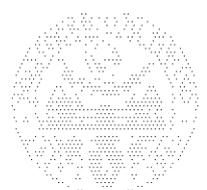
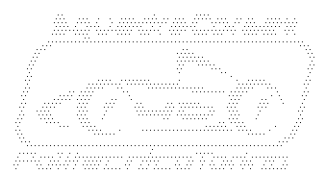
- $K_{f\beta}$ is “longitudinal load distribution factor”, it’s a dimensionless factor which takes into account of non-uniformity of the load application along the tooth profile. It can be calculated in different methods displayed in **U.N.I. 8862** standard. Fine determination of this parameter is outside from thesis target.
- $K_{f\alpha}$ is “transversal load distribution factor”, it’s a dimensionless factor which takes into account of non-uniformity in pitch errors and non-uniformity in load application. It can be calculated in different methods displayed by **U.N.I. 8862** standard. Fine determination of this parameter is outside from thesis target.

Back to Eq. 5.8-1, it’s necessary to describe accurately the second term of the equation σ_{FP} the “pulsating bending fatigue limit”.

Eq. 5.8-6
$$\sigma_{FP} = \frac{\sigma_{flim} \cdot Y_{st} \cdot Y_{nt}}{S.C.} \cdot Y_{\delta relT} \cdot Y_{RrelT} \cdot Y_x$$

Factors of the equation are going to be explained in following words.

- σ_{flim} is “limit of stress in bending fatigue” and depends by the chosen material. Value of the factor can be easily determined reading on Table 5.8-2. Different types of material are, substantially, cast iron and steel. Steel types are distinguished by heat treatments like carburizing, quenching, tempering and nitriding. Moreover, performance of any different treated materials depend on surface hardness. It’s measured in [MPa].

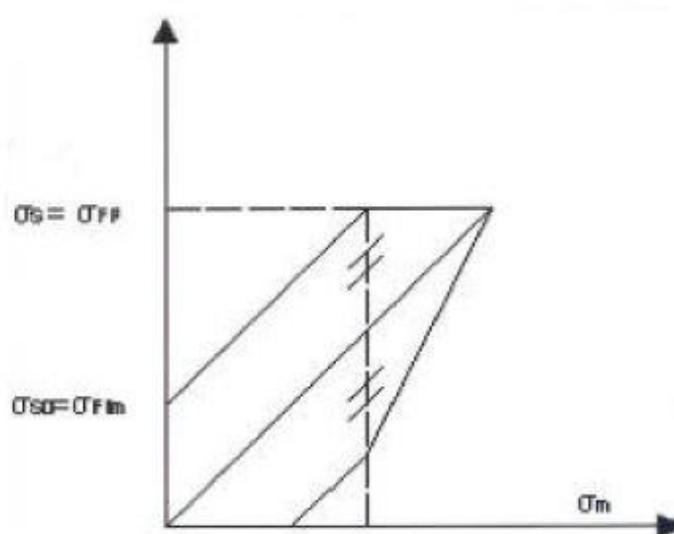


Materiale	Durezza superficiale	σ_{Hlim} N/mm ²	σ_{Flim}^* N/mm ²
Acciaio non legato di base	HB = 150 HB = 200	480 550	205 200
Acciaio in getti	HB = 150	415	170
Ghisa grigia	HB = 190 HB = 230	410 460	90 100
Ghisa a grafite sferoidale	HB = 200 HB = 250	560 630	215 230
Acciaio al carbonio bonificato	HB = 150 HB = 200	560 600	240 255
Acciaio legato bonificato	HRC $\begin{cases} 25 \\ 30 \end{cases}$ HB $\begin{cases} 253 \\ 286 \end{cases}$	800 850	320 335
Acciaio bonificato con tempra superficiale (temprato ad induzione o alla fiamma)	HRC = 50 HRC = 55	1 320 1 370	375 415
Acciaio legato cementato*	HRC = 58 ÷ 62	1 650	525
Acciaio bonificato nitrurato	HV1 = 700 ÷ 850	1 450**	470

* Per tensione alterna (per esempio ruote oziose) assumere il 70% dei valori indicati. Per senso di rotazione reversibile, apportare una riduzione di minor entità.
 ** Valori validi per indurimenti estesi al piede del dente. Nel caso in cui l'indurimento è limitato ai fianchi del dente, il valore di σ_{Flim} è generalmente minore di quello dell'acciaio bonificato base e a volte nettamente minore.
 • Valori validi per spessori efficaci di indurimento da 0,15 fino a 0,25 m_n al termine delle lavorazioni.
 •• Valore valido (eccetto per gli acciai all'alluminio) per nitrurazione gassosa prolungata o per un adeguato spessore di indurimento (da 0,4 fino a 0,6 mm per m_n da 2 fino a 5 mm) e per ingranaggi con interasse modesto.

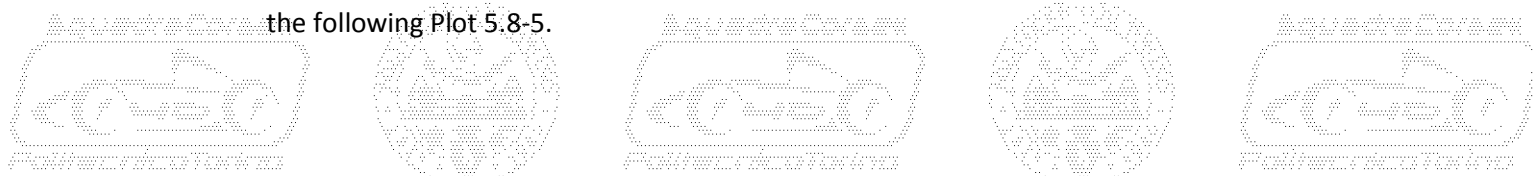
Table 5.8-2: σ_{Flim} and σ_{Hlim} displayed in function of the chosen material, Ref.[11].

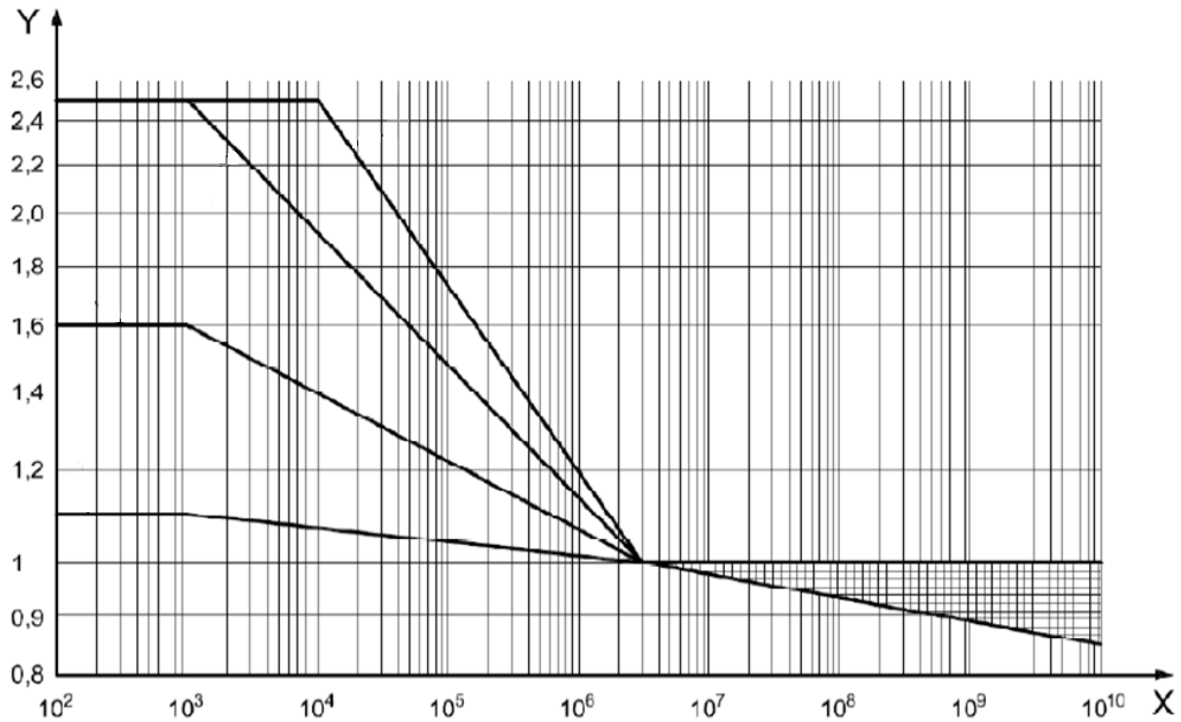
- Y_{st} is "stress correction factor", it's a dimensionless factor which takes into account the nature of the stress: uniform, pulsating, alternated, positive alternated, and so on. It's possible find the value of this factor on the Smith-Goodman diagram displayed in Plot 5.8-4. Following plot is strictly related to the chosen material.



Plot 5.8-4: Smith-Goodman diagram of a generic steel, Ref.[11].

- Y_{nt} is "endurance factor" or "Woehler factor". This dimensionless factor can be extracted by the following Plot 5.8-5.





Plot 5.8-5: Woehler diagram related to the bending of the teeth, Ref.[11].

First parameter to choose is the “**number of cycles**” which is displayed on horizontal axis in elevations of base ten. Determined value needs to be crossed with one of broken lines which depend on chosen material. Identified point needs to be shifted horizontally toward vertical axis, in order to locate the value of endurance factor.

- **S.C.** is the “**safety coefficient**” a dimensionless factor, which function have been widely explained at Chapter 5.1.
- $Y_{\delta relT}$ is the “**relative notch sensitivity factor**”. It is the ratio of the notch sensitivity factor Y_{δ} of the gear under design compared to that of the standard test $Y_{\delta T}$, which specifies the amount by which the theoretical stress at fatigue breakage exceeds the fatigue stress. $Y_{\delta relT}$ is function of the material and of the stress gradient concerned, and can be approximated using values between 0,95 and 1,0. It’s a dimensionless factor.

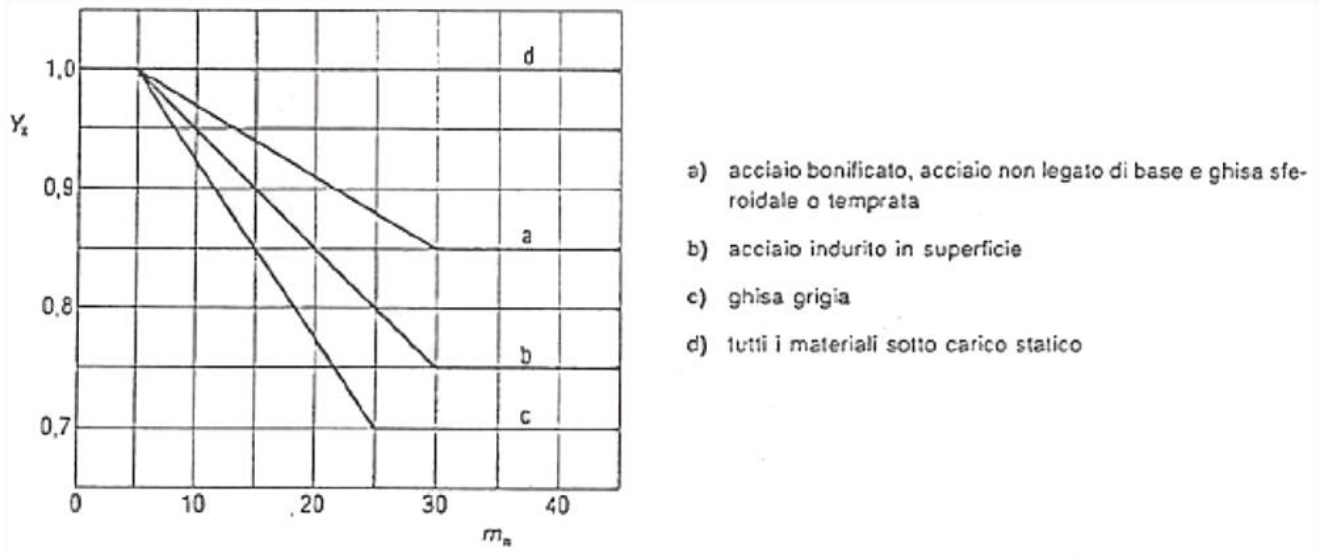
Designation	Formula
Relative surface condition factors for $R_z < 1 \mu\text{m}$	$Y_{RelT1,2} = 1.12$ for heat-treated and case hardened steels $Y_{RelT1,2} = 1.07$ for constructional steels $Y_{RelT1,2} = 1.025$ for grey cast iron and nitrocarburized steels
Relative surface condition factors for $1 \mu\text{m} < R_z < 40 \mu\text{m}$	$Y_{RelT1,2} = 1.674 - 0.529(R_{z1,2} + 1)^{1/10}$ for heat treated and case hardened steels
	$Y_{RelT1,2} = 5.306 - 4.203(R_{z1,2} + 1)^{1/100}$ for constructional steels
	$Y_{RelT1,2} = 4.299 - 3.259(R_{z1,2} + 1)^{1/200}$ for grey cast iron and nitrocarburized steels

Table 5.8-3: Y_{RelT} in function of material and treatment, Ref.[11].



Y_{RelT} is the “**relative surface condition factor**”. This factor considers the influence of the surface quality, especially roughness in the tooth root, on the possible root tooth stress. It is a function of the material and may be determined from the following Table 5.8-3. It’s necessary to clarify that parameter R_z on which is based the calculus is the roughness on the root of the tooth.

- Y_x is the “**dimensional factor**”. It depends on dimensions of the gearwheel. Value of this factor can be extracted by Plot 2.6-1.



Plot 5.8-6: Y_x in function of the module and of the material, Ref.[11].

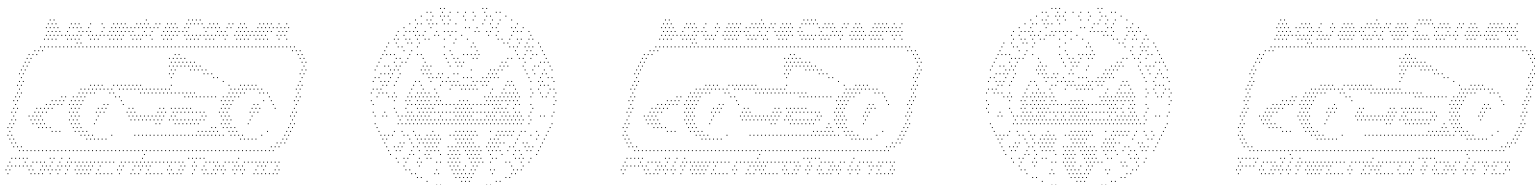
First step is locate the proper value of the module on the horizontal axis. Then, value of module needs to be vertically crossed with broken lines which depend on different materials. “a” curve refers to tempered steel, non-alloyed base steel and ductile iron. “b” curve refers to surface hardened steel. “c” curve refers to grey cast iron. “d” curve suitable for any loaded material. Point located by module and quality of material, needs to be horizontally shifted toward vertical axis, in order to read the proper value of dimensional factor.

5.9. Static verification on Hertzian contact.

Bend isn’t the only stress which acts on teeth. According with Ref.[10]., It’s necessary to take into account about pressure of contact among teeth faces causes another important type of stress. Excessive “**specific contact pressure**” leads to deterioration of the tooth face surface. That cannot be accepted in order to warrant the optimal operation of the gear.

Calculus of specific contact pressure is based on the **Hertzian theory**. The specific reference case is contact between cylinders. In the mathematical model width of cylinders coincides with the pace width of gears. Hertzian theory applied to gears is based on some simplifications enlisted as follows:

- Perfect elasticity of the material.
- Absence of friction forces.
- Contact surface dimension smaller compared to bodies in contact dimensions.



Strength verification is exploited by the following mathematical relation, which express the inequality between two stresses measured in [MPa]:

$$\text{Eq. 5.9-1} \quad \sigma_H \leq \sigma_{all}$$

σ_H is the “**specific contact pressure**”, which depends on geometrical parameters and on material of the gear. It can be obtained by the following relation:

$$\text{Eq. 5.9-2} \quad \sigma_H = 0,629 \cdot 0,418 \cdot \sqrt{\frac{F_T \cdot E \cdot \left(\frac{1}{r_1} + \frac{1}{r_2}\right) \cdot \frac{1}{\sin \alpha}}{b}}$$

- F_T is “**tangential force**” exchanged by meshing teeth. It’s described by Eq. 5.4-3 and It’s measured in [N].
- α is “**pressure angle**” of the gear described by Picture 5.1-1. It’s measured in [°].
- E is “**Young’s modulus**” of the material of the gear, measured in [MPa].
- r_1 is “**pitch radius of wheel 1**”, drive wheel of the reduction stage, It’s measured in [mm].
- r_2 is “**pitch radius of wheel 2**”, driven wheel of the reduction stage, It’s measured in [mm].
- b is “**face width**” of the gear, measured in [mm].

σ_{all} , the “**allowable stress**” which is the second member of Eq. 5.9-1 is described by the following equation.

$$\text{Eq. 5.9-3} \quad \sigma_{all} = \frac{\sigma_0}{S.F.}$$

- σ_0 is “**compression strength**” of the material. It’s value is higher than yield strength one and it’s measured in [MPa].
- $S.C.$ is “**safety coefficient**”, a dimensionless factor which is been widely explained in Chapter 5.1.

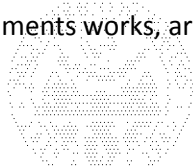
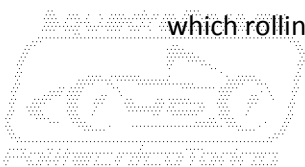
5.10. Fatigue verification on Hertzian contact.

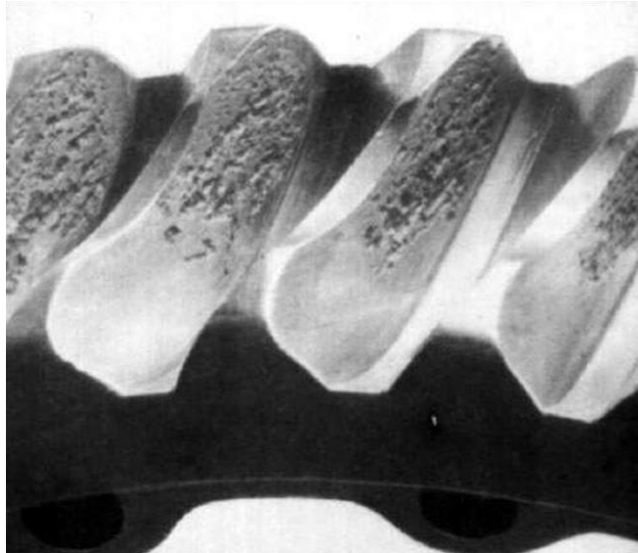
How It was shown regarding bending stress, It’s necessary take into account about fatigue phenomena related to hertzian contact.

By virtue of that, Ref.[11] standard describes the fatigue verification on Hertzian contact too. Fatigue damage caused by Hertzian contact is known with the name of “**pitting**”. Such a term is inspired by medical sphere and is due to the superficial detriment that occurs on the face of the tooth. That superficial detriment call to mind damages caused by variola to the skin of the infirm.

Such a damage displays small craters very close each others. That compromises the surface finish with issues on the good operation of the gear. Indeed damaged surface is source of high friction and noise.

The first scientist who faced this issue was Heinrich Rudolf Hertz. He discovered for first that this kind of matter can be reduced or cancelled. The key to solve this problem is the contact pressure which arises between meshing teeth. Such a pressure needs to be limited on the base of following criteria. Pitting isn’t a damage specific in gears only. It is displayed in every mechanic component which undergoes to high pressures of contact. Bearings displays most significant examples because cups on which rolling elements works, are very stressed by contact pressure.





Picture 5.10-1: Effects of pitting on the driven wheel of a worm gear (<http://www.tribology.co.uk>).

Unavoidably pitting begins to manifest on surface of the cup. Damage is deteriorated by lubrication oil that, pressurized by the contact between rollers and cup, penetrates in the small cracking. Inside such a small crevices, lubrication oil acts removing material. That phenomena is quite serious and may cause the mechanical failure of the bearing. Example of damage cup is displayed by Picture 5.10-2.

Pitting may also found its causes in the chemistry. It may be produced by localized corrosive hazards derived from phenomena of electrochemical nature.

Analogously to previous chapters, verification process is started setting up the following main relation:

$$\text{Eq. 5.10-1} \quad \sigma_{HF} \leq \sigma_{HP}$$

Where σ_{HF} is “*fatigue contact pressure*”, it’s measures in [MPa] and can be extracted by the following relation:

$$\text{Eq. 5.10-2} \quad \sigma_{HF} = Z_H \cdot Z_E \cdot Z_\varepsilon \cdot Z_\beta \cdot \sqrt{\frac{F_{Tm} \cdot i+1}{d \cdot b \cdot i}} \cdot \sqrt{K_a \cdot K_v \cdot K_{h\beta} \cdot K_{h\alpha}}$$

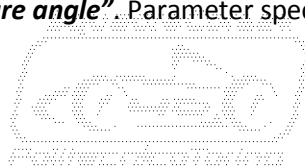
- Z_H is “*zone factor*” an dimensionless factor which is function of characteristic angles of gears. This parameter takes into account effects due to the relative curvature of flanks of teeth in the point of primitive gear meshing. Standard prescribes an empiric relation of general purpose.

$$\text{Eq. 5.10-3} \quad Z_H = \sqrt{\frac{2 \cdot \cos \beta_b \cdot \cos \alpha_t'}{\cos^2 \alpha_t \cdot \sin \alpha_t'}}$$

$$\text{Eq. 5.10-4} \quad \tan \alpha_t = \frac{\tan \alpha_n}{\cos \beta}$$

$$\text{Eq. 5.10-5} \quad \cos \alpha_t' = \frac{d}{d'} \cdot \cos \alpha_t$$

- β_b is “*base helix angle*”. Parameter specific for helix gears, measured in [°].
- α_t is “*transversal pressure angle*”. Parameter specific for helix gears, measured in [°].
- α_n is “*normal pressure angle*”. Parameter specific for helix gears, measured in [°].



- d is “pitch diameter” of reference gear, measured in [mm].
- d' is “operation pitch diameter” of reference gear, measured in [mm].
- $apex'$ is referred to shifted profile parameters.
- Z_E is “elasticity of material factor”, a dimensionless parameter which is function of the modulus of the material.

Eq. 5.10-6
$$Z_E = \sqrt{\frac{1}{\pi \cdot \left(\frac{1-\nu_1^2}{E_1} + \frac{1-\nu_2^2}{E_2} \right)}}$$

- E_1 is “Young’s modulus” of the material of the drive wheel, measured in [MPa].
- E_2 is “Young’s modulus” of the material of the driven wheel, measured in [MPa].
- ν_1 is “Poisson’s modulus” of the material of the drive wheel, it’s dimensionless.
- ν_2 is “Poisson’s modulus” of the material of the driven wheel, it’s dimensionless.

It’s important remark that Eq. 5.10-6, needs to be set up in situations where material of drive wheel is different from material of driven wheel. If materials of wheels coincide: $Z_E = 1$.

- Z_ε is “overlap ratio factor” and it’s a dimensionless factor. Its relations depends from the overlap ratios and from the helix angle of the gears.

Eq. 5.10-7
$$Z_\varepsilon = \sqrt{\frac{4-\varepsilon_\alpha}{3}} \rightarrow \beta = 0$$

Eq. 5.10-8
$$Z_\varepsilon = \sqrt{\frac{4-\varepsilon_\alpha}{3} \cdot (1 - \varepsilon_\beta) + \frac{\varepsilon_\beta}{\varepsilon_\alpha}} \rightarrow \varepsilon_\beta < 1$$

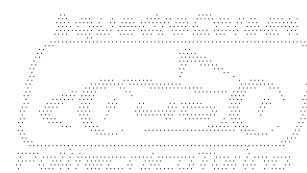
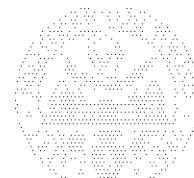
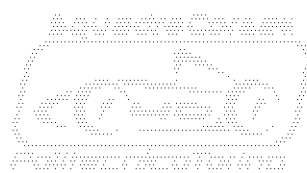
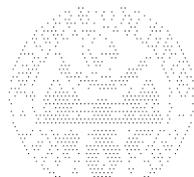
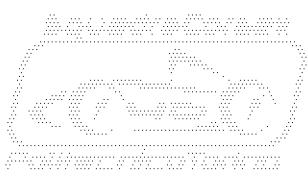
Eq. 5.10-9
$$Z_\varepsilon = \sqrt{\frac{1}{\varepsilon_\alpha}} \rightarrow \varepsilon_\beta \geq 1$$

- ε_α is “transversal overlap ratio”, it’s a dimensionless factor.
- ε_β is “normal overlap ratio”, it’s a dimensionless factor.
- β is “helix angle”, measured in [°].

- Z_β is “helix angle factor”, a dimensionless parameter described by the following relation:

Eq. 5.10-10
$$Z_\beta = \sqrt{\cos \beta}$$

- F_{Tm} is “mean tangential gear force” displayed at Chapter 5.8. and measured in [N].
- d is “pitch diameter” of the reference wheel. In this specific case, reference wheel have to be the most stressed, the drive wheel, or pinion. It’s measured in [mm].
- b is “face width” of the gear, measured in [mm].
- i is “gear ratio” and it’s a dimensionless parameter.
- K_α is “load application factor”, a dimensionless parameter which it’s possible to extract by Table 5.8-1.
- K_v is “dynamic factor” a dimensionless parameter which it’s possible to extract by Eq. 5.8-5.



- $K_{f\beta}$ is “**longitudinal load distribution factor**”, a dimensionless parameter that have to be determined with same criteria explained at Chapter 5.8.
- $K_{f\alpha}$ is “**transversal load distribution factor**”, a dimensionless parameter that have to be determined with same criteria explained at Chapter 5.8.

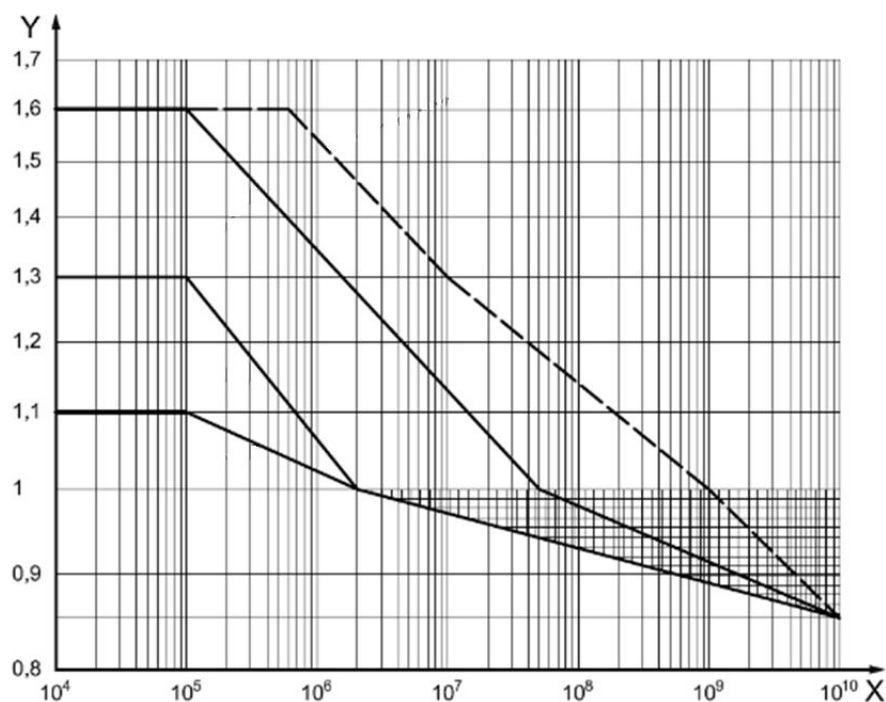


Picture 5.10-2: Example of pitting on bearing internal raceways (<https://maschinendiagnose.de/>).

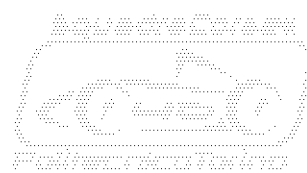
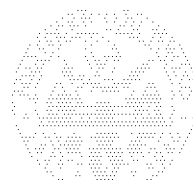
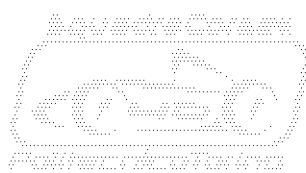
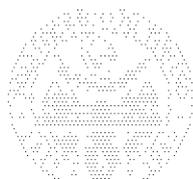
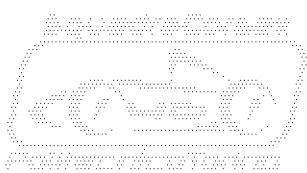
Back to Eq. 5.10-1 it's necessary to describe the second member of the relation, σ_{HP} which is defined as “**allowable pulsating compression stress**”.

Eq. 5.10-11
$$\sigma_{HP} = \frac{\sigma_{Hlim} \cdot Z_n}{S_{Hmin}} \cdot Z_l \cdot Z_r \cdot Z_v \cdot Z_w \cdot Z_x$$

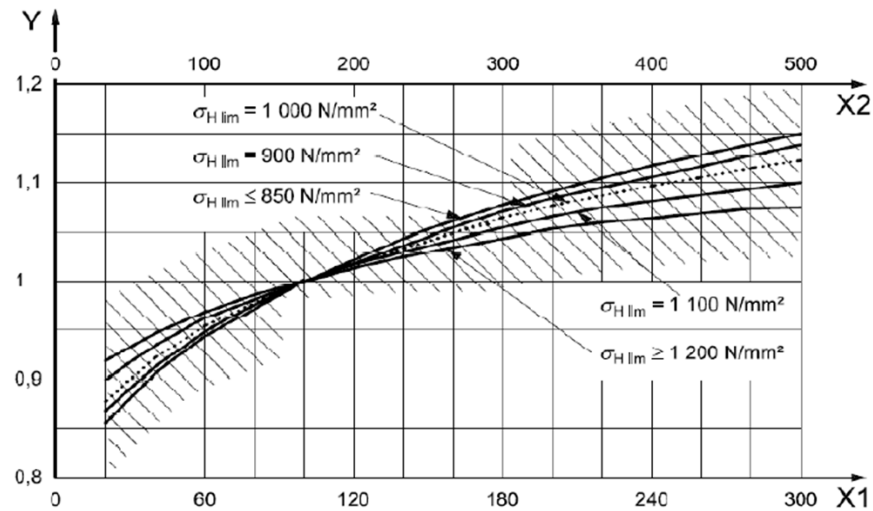
- σ_{Hlim} is “**limit pressure of base superficial fatigue**”. The proper value can be chosen in the Table 5.8-2. and It's measured in [MPa].
- S_{Hmin} is “**minimum safety coefficient**” related to pitting fatigue. This dimensionless parameter It's usually chosen equal to 1 or equal to 1.1 in order to be conservative.



Plot 5.10-1: Woehler diagram related to the pitting of the teeth, Ref.[11].

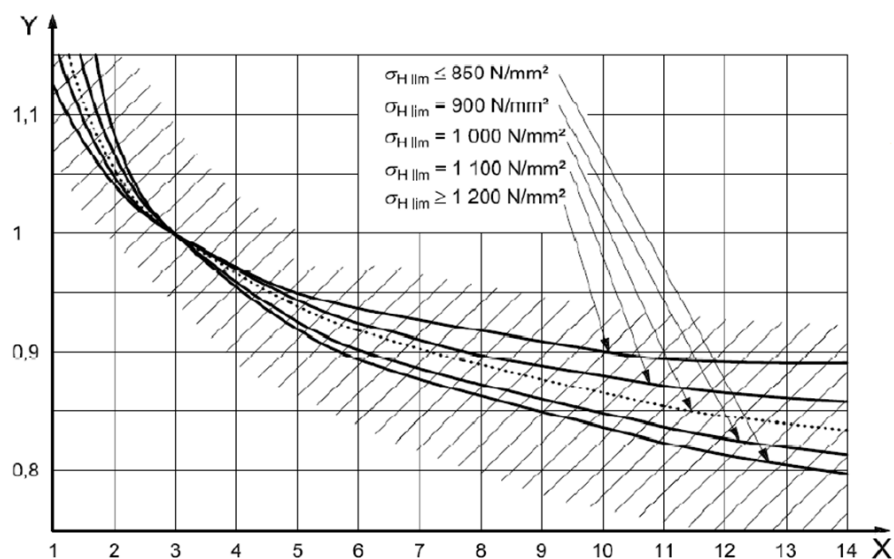


- Z_n** is “**endurance factor**” a dimensionless parameter which is totally analogue to that described in Chapter 5.8. Therefore, such factor is extracted by the Woehler diagram specific for pitting, displayed in the Plot 5.10-1. First of all, it’s necessary to determine **X** the “**desired number of cycles**” plotted on the horizontal axis. Chosen value needs to be crossed with one of the broken lines. Different broken lines are related to material of the gear. Identified point needs to be translated horizontally towards the vertical axis. Endurance factor coincides with the located value of **Y** .

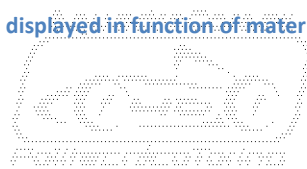
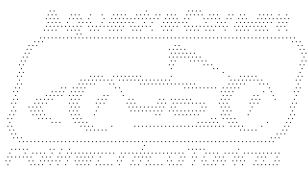


Plot 5.10-2: Lubrication factor displayed in function of material and kinetic viscosity of lubrication oil, Ref.[11].

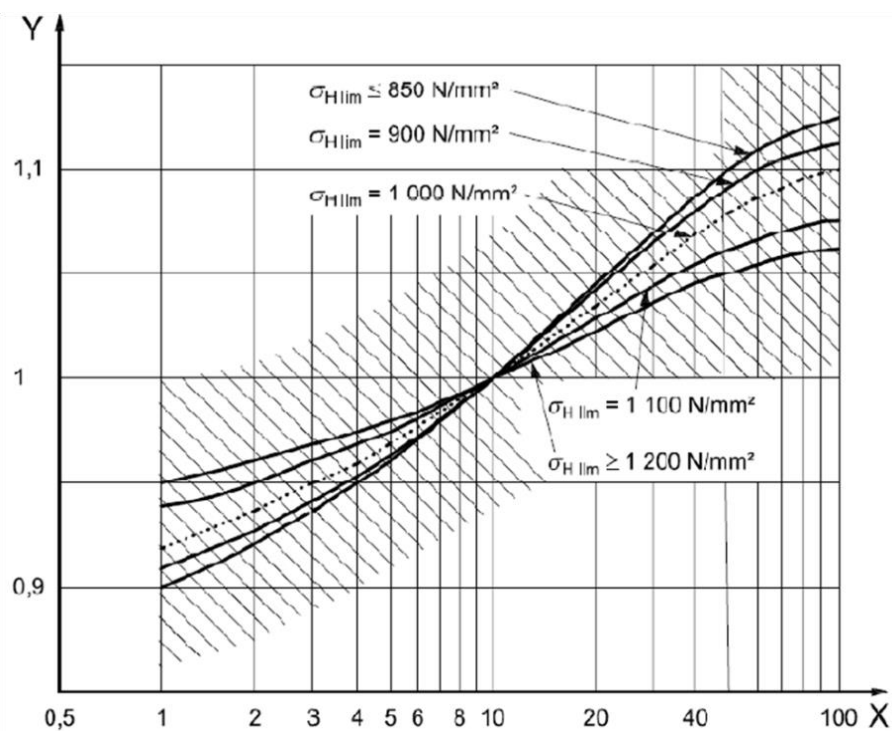
- Z_l** is “**lubrication factor**” and can be extracted from Plot 5.10-2. High horizontal axis displays “**kinetic viscosity measured at 50°C**” of lubrication oil, indicated with **$X2$** . Low horizontal axis displays “**kinetic viscosity measured at 40°C**” of lubrication oil, indicated with **$X1$** . Both values of viscosity are measured with $[\text{mm}^2/\text{s}]$. Chosen value of viscosity needs to be crossed with the curve related to σ_{Hlim} which is “**pressure of base superficial fatigue**”. Its value can be extracted by Table 5.8-2. Value of lubrication factor is indicated by **Y** and can be read on the vertical axis of the plot.



Plot 5.10-3: Roughness factor displayed in function of material and surface finish of teeth, Ref.[11].



- Z_r is “**roughness factor**” and can be extracted from Plot 5.10-3. Horizontal axis displays X the “**surface roughness on the flank of teeth**” which is measured in $[\mu m]$. Value of roughness needs to be crossed with the curve related to σ_{Hlim} which is “**pressure of base superficial fatigue**”. Its value can be extracted by Table 5.8-2. Value of roughness factor is indicated by Y and can be read on the vertical axis of the plot.
- Z_v is “**speed factor**” and can be extracted from Plot 5.10-4. Horizontal axis displays X the “**maximum tangential speed of the gearwheel calculated on the pitch diameter**”. Such parameter is calculated on the base of the maximum rotational speed of the gear and it’s measured in $[m/s]$. Value of speed needs to be crossed with the curve related to σ_{Hlim} which is “**pressure of base superficial fatigue**”. Its value can be extracted by Table 5.8-2. Value of speed factor is indicated by Y and can be read on the vertical axis of the plot.

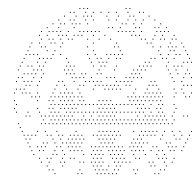
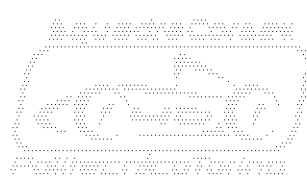
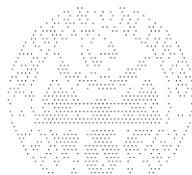


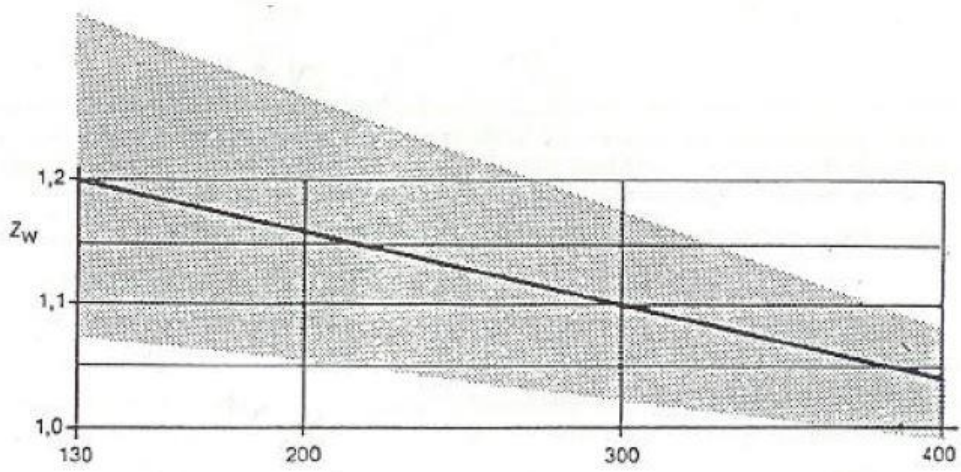
Plot 5.10-4: Speed factor displayed in function of the material and of the tangential speed of the gearwheel, Ref.[11].

- Z_w is “**hardness ratio factor**” and depends by the surface hardness of both wheels of the gear. This parameter can be calculated by Eq. 5.10-12 on the basis of Brinell hardness HB . In order to be conservative, this parameter is assumed to be the surface hardness of the softest wheel.

$$\text{Eq. 5.10-12} \quad Z_w = 1,2 \cdot \frac{HB-130}{1700}$$

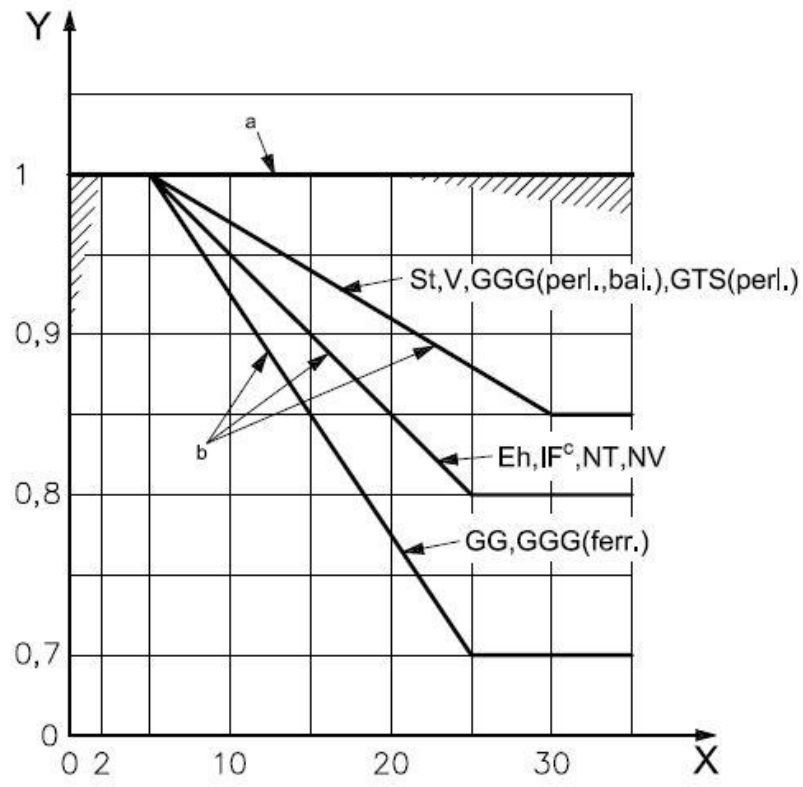
Alternatively, hardness ratio factor can be extracted by the Plot 5.10-5. Horizontal axis displays different values of HB hardness. Chosen value which needs to be crossed with black oblique line. From identified point, it’s necessary to move horizontally towards vertical axis where the value of the factor can be read.



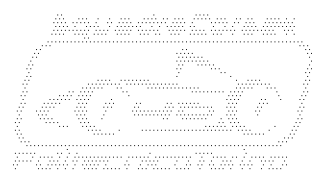
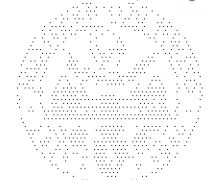
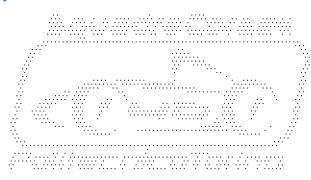
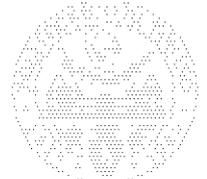
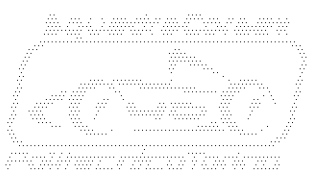


Plot 5.10-5: Hardness parameter displayed in function of hardness HB (horizontal axis), Ref.[11].

- Z_x is the **“size factor”** , a dimensionless parameter which takes into account the influence of size on the distribution of weak points in the structure of the material. In accordance with strength of materials theory, the stress gradients decrease with increasing dimensions. Quality of the material is determined by the extension, effectiveness of forging, presence of defects, etc. The value of size factor can be extracted from Plot 5.10-6. Horizontal axis displays X the **“module”** of the gear which is measured in [mm]. Value of module needs to be crossed with the broken lines related to σ_{Hlim} which is **“pressure of base superficial fatigue”**. Its value can be extracted by Table 5.8-2. Value of size factor is indicated by Y and can be read on the vertical axis of the plot.

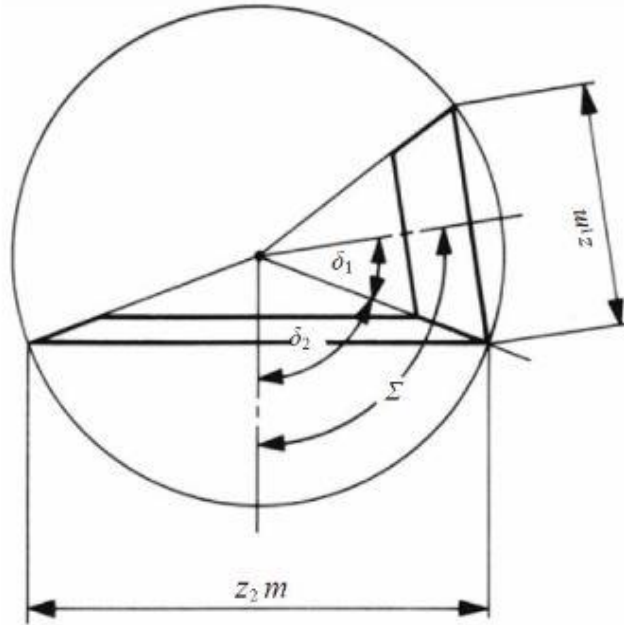


Plot 5.10-6: Size factor displayed in function of the material and of the module, Ref.[11].



5.11. Calculations on bevel gears.

Formulas and parameters displayed in previous chapters are specific for cylindrical gears. In this chapter it will be possible to find some useful relations regarding the geometry of bevel gears, according with source “<https://khkgears.net>”, Ref.[12]. Detailed verifications on the strength of teeth are outside from purposes of this thesis. The full verification procedure can be found in the norms **I.S.O. 10300-1-2-3**.



Picture 5.11-1: Pitch cones of a bevel gear Ref.[12].

About cylindrical gears, main dimension is represented by a diameter. Concerning bevel gears, which are more complex by point of view of geometry, main dimension have to be a surface. For this reason, homologue of the “pitch diameter” is the “pitch surface”. Such a surface, logically, needs to have a cone shape. It’s for this reason that pitch surfaces are defined “pitch cones”. Such cones are used to drive intersecting axis of both wheels of the gear, like it’s displayed in Picture 5.11-1.

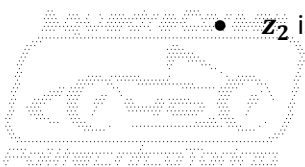
Analogously to cylindrical gear, meshing of teeth in a bevel gear is intended as the contact of the two pitch cones which roll each others. First step in calculation is aimed to calculate dimensions of pitch cones.

Eq. 5.11-1
$$\tan \delta_1 = \frac{\sin \Sigma}{\frac{z_2}{z_1} + \cos \Sigma}$$

Eq. 5.11-2
$$\tan \delta_2 = \frac{\sin \Sigma}{\frac{z_1}{z_2} + \cos \Sigma}$$

Where:

- δ_1 is “angle of the pitch cone of wheel 1” drive wheel of transmission stage, measured in [°].
- δ_2 is “angle of the pitch cone of wheel 2” driven wheel of transmission stage, measured in [°].
- Σ is “shaft angle” of the gear. It’s the angle between axis of wheels, measured in [°].
- z_1 is “number of teeth of wheel 1”, drive wheel of the reduction stage, the pinion.
- z_2 is “number of teeth of wheel 2”, driven wheel of the reduction stage.



In the largest majority of cases, “shaft angle” needs to be assumed equal to 90° . It’s the same for the gear-box in exam which features orthogonal axis, as explained at Chapter 4.3.2. For this reason, Eq. 5.11-1 and Eq. 5.11-2 evolve as follows:

Eq. 5.11-3 $\delta_1 = \tan^{-1} \left(\frac{z_1}{z_2} \right)$

Eq. 5.11-4 $\delta_2 = \tan^{-1} \left(\frac{z_2}{z_1} \right)$

By definition of “*gear ratio*”:

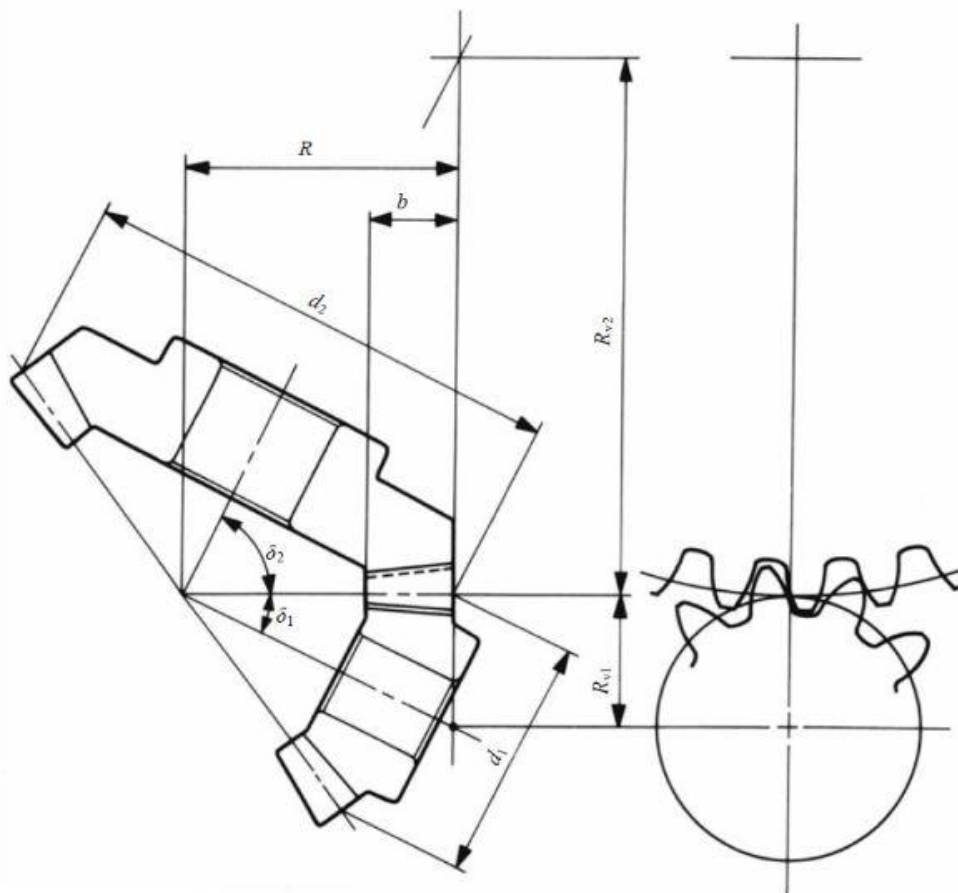
Eq. 5.11-5 $i = \frac{z_2}{z_1}$

For this reason Eq. 5.11-3 and Eq. 5.11-4 can be written in the following way.

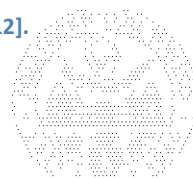
Eq. 5.11-6 $\delta_1 = \tan^{-1} \left(\frac{1}{i} \right)$

Eq. 5.11-7 $\delta_2 = \tan^{-1}(i) = \Sigma - \delta_1$

First aspect to take into account is that dimension of pitch cones depends on the gear ratio. For this reason, wheels have to work always in the same couple.



Picture 5.11-2: Meshing of bevel gears, Ref.[12].



Knowing dimensions of pitch cones, δ_1 and δ_2 , it's possible to calculate the distance of the common apex of pitch cones R . This dimension is defined "**cone distance**".

$$\text{Eq. 5.11-8} \quad R = \frac{d_1}{2 \cdot \sin \delta_1} = \frac{d_2}{2 \cdot \sin \delta_2}$$

$$\text{Eq. 5.11-9} \quad d_1 = m \cdot z_1$$

$$\text{Eq. 5.11-10} \quad d_2 = m \cdot z_2$$

- m is "**module**" of the gear, measured in [mm].
- d_1 is "**pitch diameter of wheel 1**", drive wheel of the reduction stage. It's measured in [mm].
- d_2 is "**pitch diameter of wheel 2**", driven wheel of the reduction stage. It's measured in [mm].

In the right part of Picture 5.11-2 it's possible to observe the facial view of teeth. In this view, meshing of teeth looks very similar to spur gears. Indeed missing dimensions can be found choosing proper parameters, similarly to the case of spur gears:

- α is "**pressure angle**" of the gear, measured in [°].
- b is "**face width**" of the gear. It wouldn't overcome three times the value of the cone distance. This parameter is measured in [mm].

$$\text{Eq. 5.11-11} \quad b \leq 3 \cdot R$$

Thanks to the choice of the previous parameters, it's possible to calculate ha_2 which is the "**addendum**" of the driven wheel. Such parameter is measured in [mm].

$$\text{Eq. 5.11-12} \quad ha_2 = 0,540 \cdot m + \frac{0,460 \cdot m}{\left(\frac{z_2 \cdot \cos \delta_1}{z_1 \cdot \cos \delta_2}\right)}$$

Consequently, it's possible to obtain ha_1 the "**addendum**" of the drive wheel, measured in [mm].

$$\text{Eq. 5.11-13} \quad ha_1 = 2 \cdot m - ha_2$$

On the opposite side of pitch cones, it's possible proceed with the calculation of hf_1 , "**dedendum**" of the drive wheel which derives by Eq. 5.11-14. hf_2 is "**dedendum**" of the driven wheel and it's calculated by Eq. 5.11-15. Both dimensions are measured in [mm].

$$\text{Eq. 5.11-14} \quad hf_1 = 2,188 \cdot m - ha_1$$

$$\text{Eq. 5.11-15} \quad hf_2 = 2,188 \cdot m - ha_2$$

As consequence, the "**dedendum angle**" of the drive wheel θ_{f1} is calculated by Eq. 5.11-16. "**dedendum angle**" of the driven wheel θ_{f2} , is obtained by Eq. 5.11-17. Both parameters are measured in [°].

$$\text{Eq. 5.11-16} \quad \theta_{f1} = \tan^{-1} \left(\frac{hf_1}{R} \right)$$

$$\text{Eq. 5.11-17} \quad \theta_{f2} = \tan^{-1} \left(\frac{hf_2}{R} \right)$$



Dimension “**addendum angle**” is equal to “**dedendum angle**” of the corresponding wheel, as displayed in Eq. 5.11-18 and Eq. 5.11-19. Both parameters are measured in [°].

$$\text{Eq. 5.11-18} \quad \theta a_1 = \theta f_1$$

$$\text{Eq. 5.11-19} \quad \theta a_2 = \theta f_2$$

Starting from previous parameters, by Eq. 5.11-20, it's possible calculate δ_{a1} which is the “**tip angle**” of drive wheel. By Eq. 5.11-21 it's possible to calculate δ_{a2} the “**tip angle**” of driven wheel. Both parameters are measured in [°].

$$\text{Eq. 5.11-20} \quad \delta a_1 = \delta_1 + \theta a_1$$

$$\text{Eq. 5.11-21} \quad \delta a_2 = \delta_2 + \theta a_2$$

Similarly to previous relations, by Eq. 5.11-22, it's possible to calculate δ_{f1} the “**root angle**” of drive wheel. By Eq. 5.11-23 it's possible to calculate δ_{f2} the “**root angle**” of driven wheel. Both parameters are measured in [°].

$$\text{Eq. 5.11-22} \quad \delta f_1 = \delta_1 - \theta f_1$$

$$\text{Eq. 5.11-23} \quad \delta f_2 = \delta_2 - \theta f_2$$

By means of angular dimensions It's possible to calculate linear dimensions. By Eq. 5.11-24 it's obtained d_{a1} which is the “**tip diameter**” . At the same way, by Eq. 5.11-25 it's obtained d_{a2} which is the “**tip diameter**” of the driven wheel. Both parameters are measured in [mm].

$$\text{Eq. 5.11-24} \quad da_1 = d_1 + 2 \cdot ha_1 \cdot \cos \delta_1$$

$$\text{Eq. 5.11-25} \quad da_2 = d_2 + 2 \cdot ha_2 \cdot \cos \delta_2$$

Then, by Eq. 5.11-26, it's possible to calculate Y_1 which is the “**distance between pitch apex and crown**” of the drive wheel. By Eq. 5.11-27 derives Y_2 , the “**distance between pitch apex and crown**” of the driven wheel. Both parameters are measured in [mm].

$$\text{Eq. 5.11-26} \quad Y_1 = R \cdot \cos \delta_1 - ha_1 \cdot \sin \delta_1$$

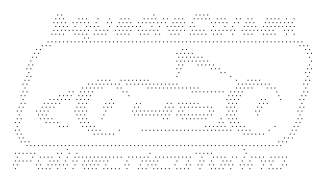
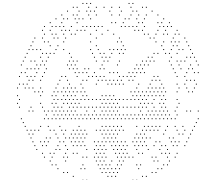
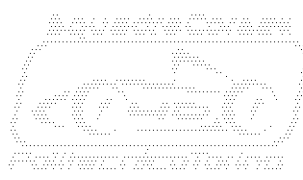
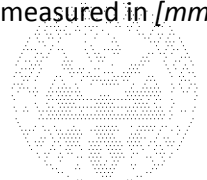
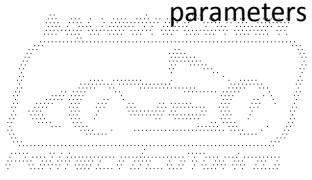
$$\text{Eq. 5.11-27} \quad Y_2 = R \cdot \cos \delta_2 - ha_2 \cdot \sin \delta_2$$

Next dimension, obtained by Eq. 5.11-28, is Y_{b1} the “**axial face-width**” which is the projection of the face width on the axis of the drive wheel. Analogously, by Eq. 5.11-29Eq. 5.11-28, it's possible to obtain Y_{b2} the “**axial face-width**” related to the driven wheel. Both parameters are measured in [mm].

$$\text{Eq. 5.11-28} \quad Yb_1 = \frac{b \cdot \cos \delta a_1}{\cos \theta a_1}$$

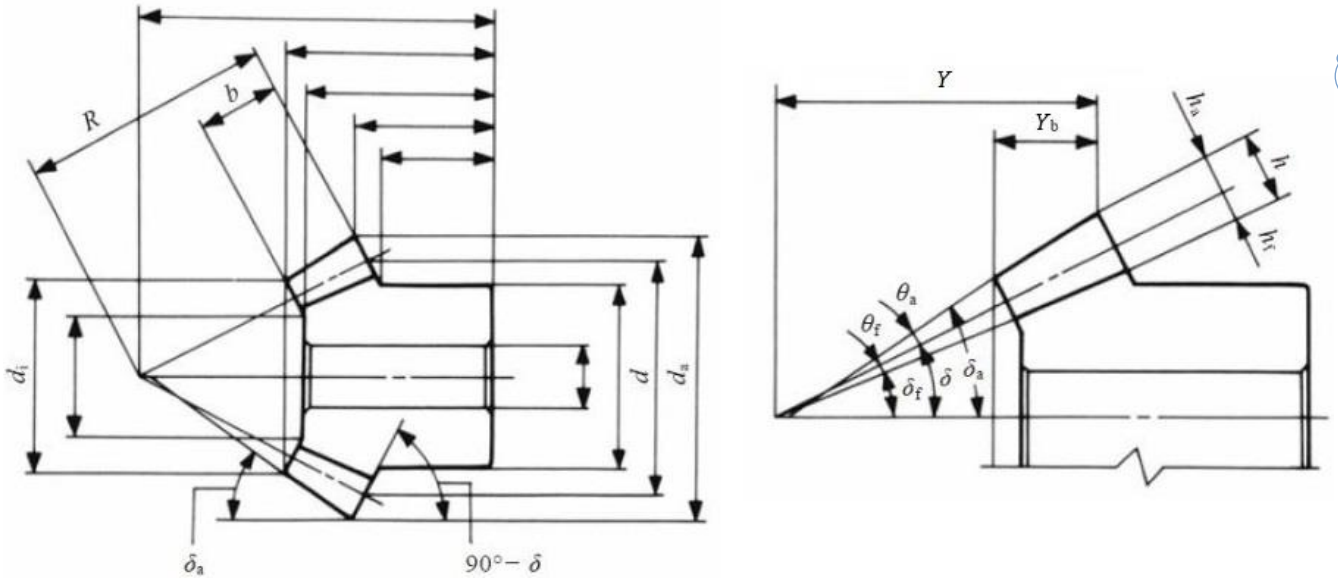
$$\text{Eq. 5.11-29} \quad Yb_2 = \frac{b \cdot \cos \delta a_2}{\cos \theta a_2}$$

Last dimension that it's necessary to calculate is di_1 the “**inner tip diameter**” of the drive wheel, obtained by Eq. 5.11-30. By Eq. 5.11-31, derives di_2 the “**inner tip diameter**” of the driven wheel. Both parameters are measured in [mm].



Eq. 5.11-30
$$di_1 = da_1 - \frac{2 \cdot b \cdot \sin \delta a_1}{\cos \theta a_1}$$

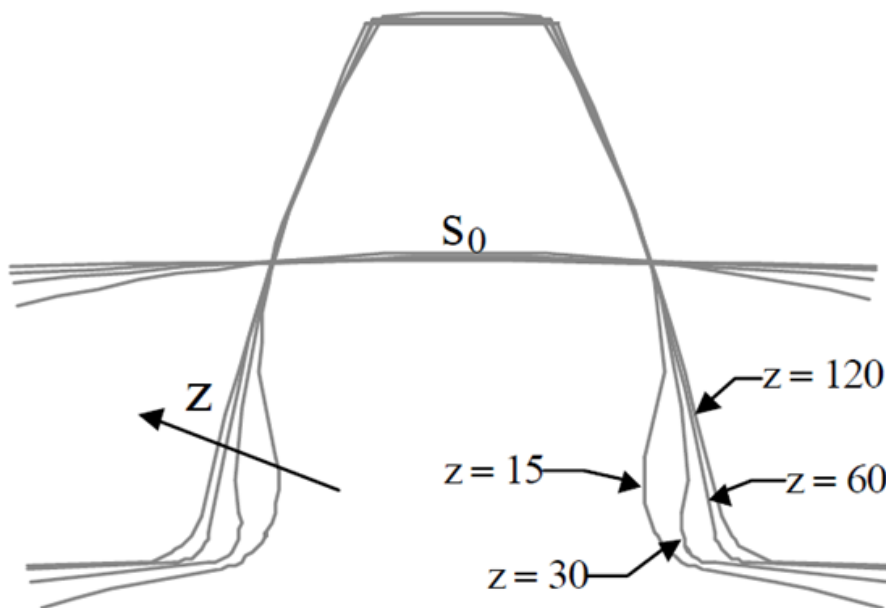
Eq. 5.11-31
$$di_2 = da_2 - \frac{2 \cdot b \cdot \sin \delta a_2}{\cos \theta a_2}$$



Picture 5.11-3: Main dimensions of bevel gears, Ref.[12].

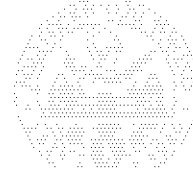
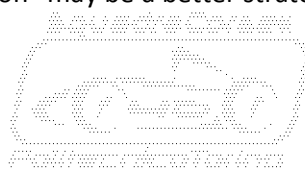
Dimensions displayed and calculated in the previous chapter, are well represented in the Picture 5.11-3.

5.12. Profile correction factor of gears.



Plot 5.12-1: Variation in profile due to number of teeth, Ref.[12].

Growth of module or face width aren't the only options in order to improve strength and stiffness of teeth. Application of "profile correction" may be a better strategy.

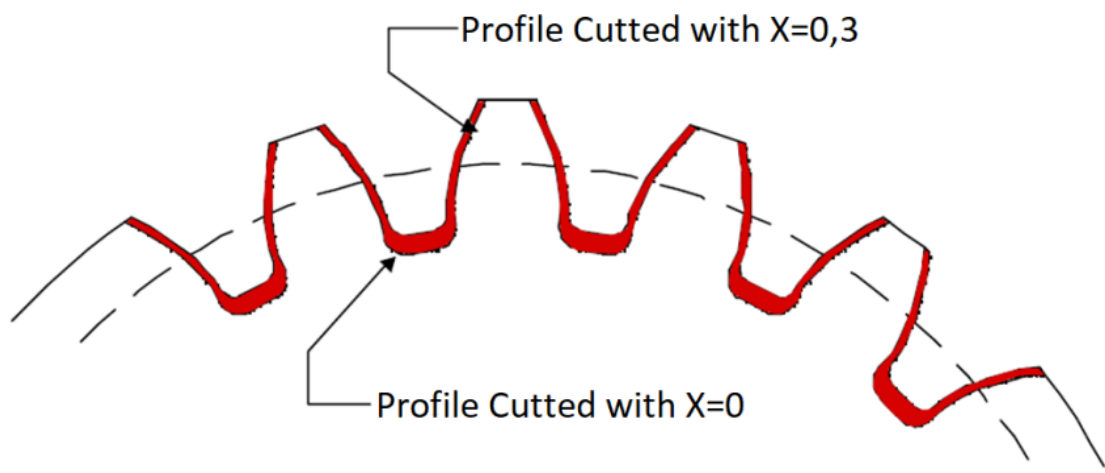


Bending strength of the tooth is localized in the tightest section. Generally, such a section coincides with the root of the tooth. Moreover, this section is the farthest from the contact area of teeth. That fact makes the bending moment greater in root section.

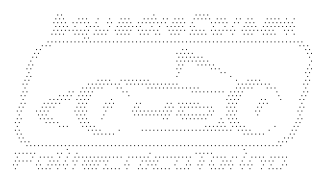
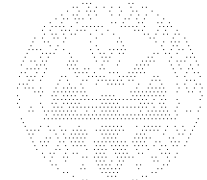
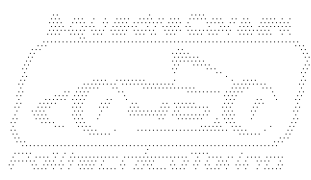
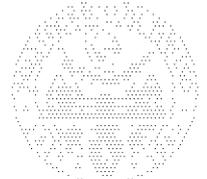
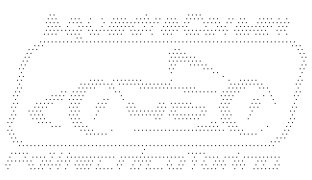
Plot 5.12-1 shows how profile of teeth varies with the number of teeth. Amplitude of root section, obviously, depends on profile of the tooth. It's possible to observe that tight root sections correspond to low values in number of teeth. As explained at chapter 5.3 it's not possible reduce number of teeth under a certain calculated value. However, sometimes, a very stressed gear needs to be housed in a tight space. For this reason, the calculated minimum number of teeth may be too huge for the available room. Try to improve area of the root section growing module or face width has no sense. Indeed distribution of material is not well balanced and the large majority of it is localized in less stressed sections.

Most suitable solution is very smart and consists on the shift of the profile of the tooth. Shifting profile of the pinion toward tip of teeth, causes a growth in the area of the stressed root section. That strategy allows to optimize the distribution of material and it's cost effective too. Indeed correction in profile of gears doesn't need particular tools or machines. Parameter which describes correction is usually indicated with letter *X*. A positive value indicates a shift of the profile towards the external, as depicted by Plot 5.12-2.

About dimensions calculated by relations of Chapter 5.5 and Chapter 5.11, these are no longer valid in case of shifted profiles.



Plot 5.12-2: Positive versus zero correction, Ref.[12].



6. Software aided calculation.

One of the biggest issue in Formula S.A.E. is that concurrent cars are prototypes, nevertheless, components need to be reliable for the entire race calendar. Frequently, there is no time and no money to produce



Picture 6: Cover page of KISSOFT Release 3/2011 software (<http://www.kisssoft.ch>).

spares or verify reliability with experimental tests. For this reason calculations and simulations need to be very accurate and reliable. Relations and parameters displayed in Chapter 5 are usually employed to set up advanced spreadsheets implemented by Microsoft Office Excell. Anyway, variety and spectrum of parameters is too wide and specialized firms only (Graziano, Hewland, Sadev, Cima, X-trac, Holinger, Ricardo et cetera) can easily set up efficient and reliable advanced spreadsheets, on the basis of their own experiences.

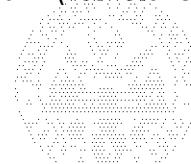
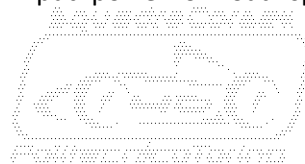
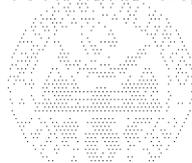
For a small work group, like a Formula S.A.E. team, the best solution is certainly a software dedicated to the calculation of gears. In this need, Squadra Corse has been supported by the worldwide leader of gear calculation software, the Swiss firm KISSOFT A.G.

KISSOFT A.G. is a company specialized in the development of calculation software addressed to designers and engineers of different mechanical fields. Gears and transmissions designed with the help of KISSOFT products, can be found from heavy industrial machines to Formula 1 cars with a wide spectrum of dimensions that goes from funicular railway gears to miniature gears of Mars Pathfinder rover.

Calculations of gears are in compliance with current norms **D.I.N.**, **I.S.O.**, **A.G.M.A.** and the architecture of the software allows high flexibility on calculus. Parameters and outputs are well represented with the help of plots, in this way it's possible to find quickly the best **trade-off between performance and reliability**.

One important advantage of the KISSOFT software application is that a reliable calculation doesn't need the setting of all parameters described at Chapter 5. Calculation is split in two main steps: **"rough design"** and **"precision design"**. The main advantage of begin with raw design step is that, software proposes a large number of different solutions on the base of few main input parameters. Solutions are different through basic parameters, like the number of teeth, module, face width, overall dimensions and others. Task of the designer is to choose the solution which is more suitable to requirements of the project. Chosen solution is then processed in precision design step in order to obtain the best performance from raw dimensioned gear.

The typical output of KISSOFT software are the numerical reports like those annexed in Appendix 1 and Appendix 2. These documents display: input power or load spectrum (**"Collettivo di carico"**), safety



coefficients (“*Sicurezza...*”), information about geometry of teeth and material (“*Geometria del dente e materiale*”), information of lubrication system and technical features of the lubricant, backlash, forces acting on the gear (“*Fattori d’influsso generali*”), control measures on thickness of teeth (“*Misure di controllo per spessore del dente*”) and tolerance on teeth (“*Tolleranze Dentatura*”). All information included in the report are useful for designer to trace parameters of the project but are useful to gear manufacturer too, who can find all the dimensions useful to produce and check the gear performing the best of its quality. An additional module is able to export a 3D model of the gearwheels, very useful to match associated components like bearings, gasket, fasteners and to design the case.

Beginning with rough design, first parameter to be set is the input torque which value have been replaced by load spectrums widely described in next chapter.

6.1. Collection data and set up of input power.

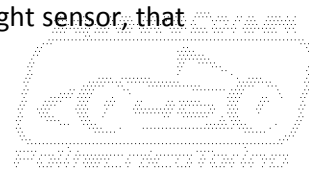
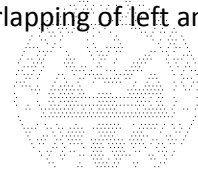
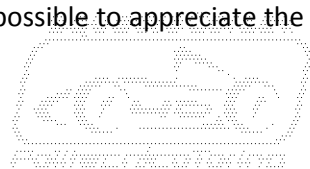
The first aspect to take into account is that an accurate calculation needs to be based on an accurate set up of input data. One of the strongest point of Kisssoft software is that input torque of the gear-box can be set through a single value or through a spectrum. It’s easy to understand that, a single value of torque, can be enough in the industrial application where the input torque can be considered steady for all the operational life of the machinery. Moreover, design gears on the basis of maximum torque generated by motors, can be unsuitable for a motorsport application. Indeed how it’s explained at Chapter 4.1, not all the torque can be discharged to the ground in any condition and that leads to an undesirable over-sizing.

For these reasons, one of the most appreciated features of Kisssoft software is the opportunity of set a detailed load spectrum (“*Collettivo di carico*”) as input. This sort of “*load history*” is modelled on different levels, any level is defined by 3 parameters: torque, rotational speed and frequency, which is intended as percentage of the total life of the gear. Total life of the gear is esteemed around 100 [h] which correspond to 4000 [Km] of ride between races and performance tests. In this way, software owns all data needed to trace a Woehler curve of the gear. Then, using *Miner-Haibach Theory* as described by *A.G.M.A. 2001* standard, software calculates a model of “*accumulated damage*” due to loads. It’s necessary underline that methods of fatigue calculation used by the software, are described by *A.G.M.A. 2003-C10* for bevels and are described by *I.S.O. 6336:2006 B Method* for spur gears.

First issue is obtain values of the torque necessary to set the load spectrum. It’s well known that S.C.12e car throttle is equipped by two rotary potentiometer sensors indicated as “*Left sensor*” and “*Right sensor*”. Left sensor provides signal to the controller, right sensor works as back up of the left. Signal from sensor represents the torque demanded by the driver during the ride. Therefore, starting from telemetry data of S.C.12e, it’s possible to obtain torque requested by the driver during a reference race or during a performance test.

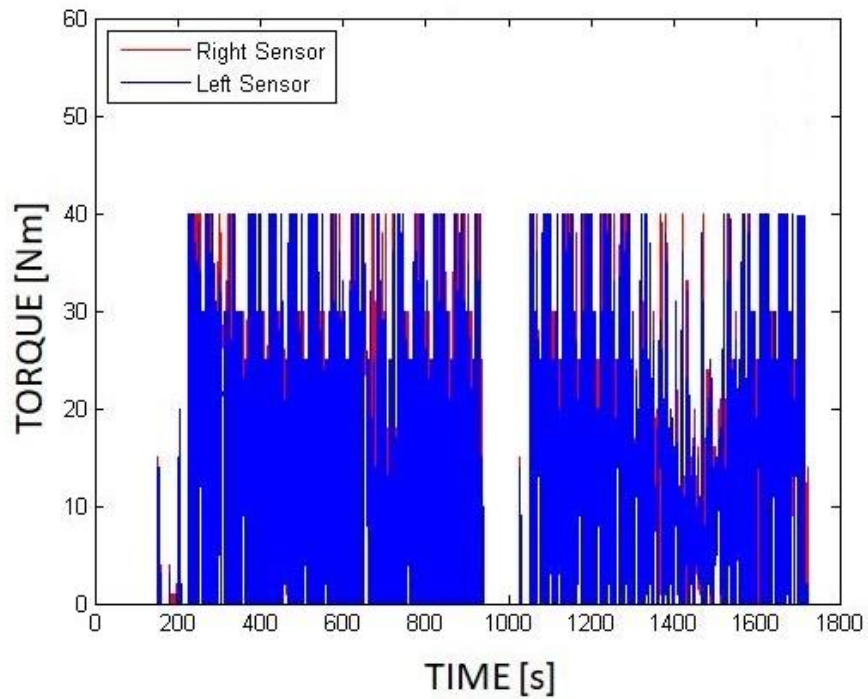
In order to be accurate enough, it’s useful extract data from endurance test of F.S.A.E. Italy 2012. Track fitted on Varano Circuit displays a good variety of situations because it features high speed sectors and a very low speed sector in which the car needs to pass through a “*minimum radius corner*”.

Taking into exam Plot 6.1-1, vertical axis displays value of the torque, while horizontal displays the progressive value of the time. Scale of time axis is very narrow, for this reason values of potentiometer signal look represented as distinct vertical lines instead of a continuous signal which displays bright increase and decrease. Anyway, it’s possible to appreciate the overlapping of left and right sensor, that

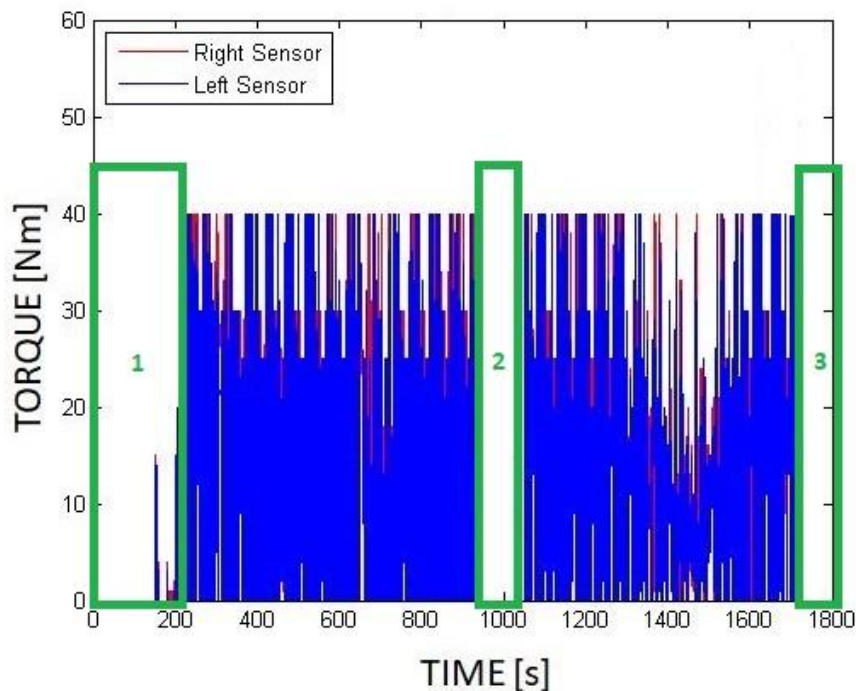


means a regular operation of the throttle pedal. If an important difference between signal from left and right sensor is detected, a safety system shuts down the power supply of motors.

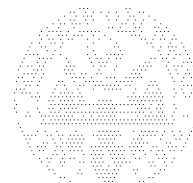
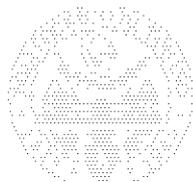
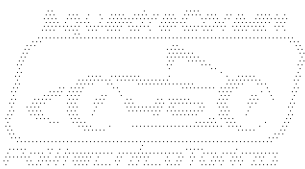
Angle measured by a rotary potentiometer is converted to a percentage of throttle pedal stroke. Then it's translated to a percentage of the torque supplied by motors. Observing the scale of vertical axis, it's possible to detect that maximum value of torque is limited to $40[Nm]$. That is a strategy to preserve the state of charge of the battery, which is crucial during the endurance test. Therefore, in endurance configuration, 100% of throttle, "flat out", corresponds to a torque of $40[Nm]$.



Plot 6.1-1: Request of torque during the endurance test of F.S.A.E Italy 2012.



Plot 6.1-2: Car stopped events.

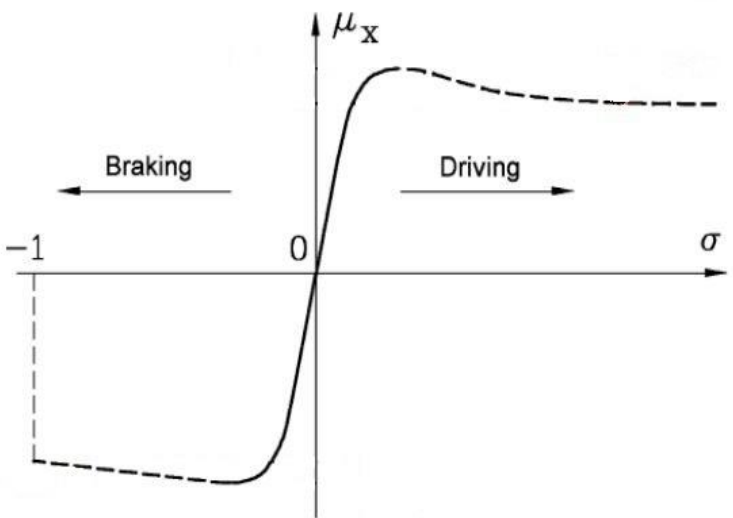


As declared in advance, horizontal axis shows the entire time since the car was switched on. For this reason, data recording includes three main events in which the car is switched on but stopped. To quick detection, events are highlighted by green squares in Plot 6.1-2. **Event 1** is the time necessary to deploy the car on the track. In this event, car moves slowly from the paddock to the track entry. **Event 2** represents the time necessary to change the driver in the mid of endurance test, car is switched on but completely stopped. **Event 3** represents the time between the end of the endurance test and the switching off of the car. Car is stopped in the paddock waiting that marshal switches off the energy system. It's important remark that in any event the throttle pedal is released or almost released.

It's known that a kinetic energy recovery system needs to be implemented on S.C.R. This system easily operates when throttle pedal is released. Anyway, energy recovery system cannot be considered operating in any release of the throttle pedal, read on data. Therefore, event 1, 2, and 3 have to be distinguished by other events in which throttle sensors read a 0% signal. So it's important to exclude events 1,2 and 3 from collected data. In this way, entire life of the gear is intended as 100 [h] net of operation in the Endurance Track of F.S.A.E. Italy.

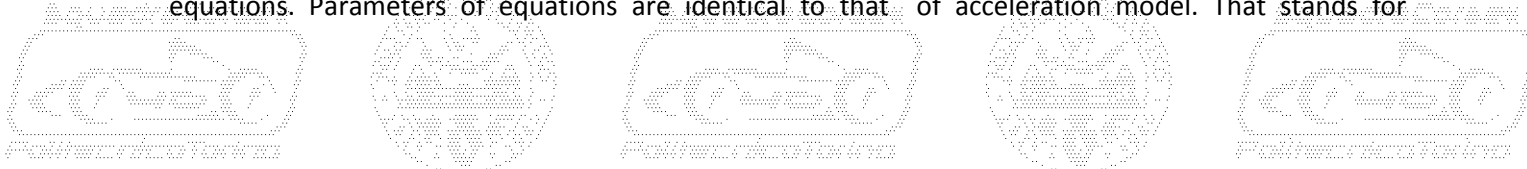
Anyway, values of torque demanded by driver are known, but that isn't still enough to set up an accurate load spectrum. Missing variable is maximum torque exploitable by rear wheels during energy recovery event. In order to find a suitable value, It's necessary to study S.C.R. behaviour during braking event. For this purpose, a two dimensions model similar to that displayed by Plot 4.1-1, have to be set up. Anyway, It's necessary remind that in this case longitudinal load transfer is modelled on "**vehicle in braking condition**".

As depicted in advance at Chapter 4.1, model of braking condition features two main differences respect to "**rear wheel drive vehicle in acceleration condition**" model. First is related to rear wheel which needs to be represented in "driven condition" and not in "drive condition". By virtue of that, sense of X_{Fmax} and X_{Rmax} must be concordant to x-axis. Second difference regards sense of inertia vector which needs to be represented opposite to x-axis, differently from previous case.

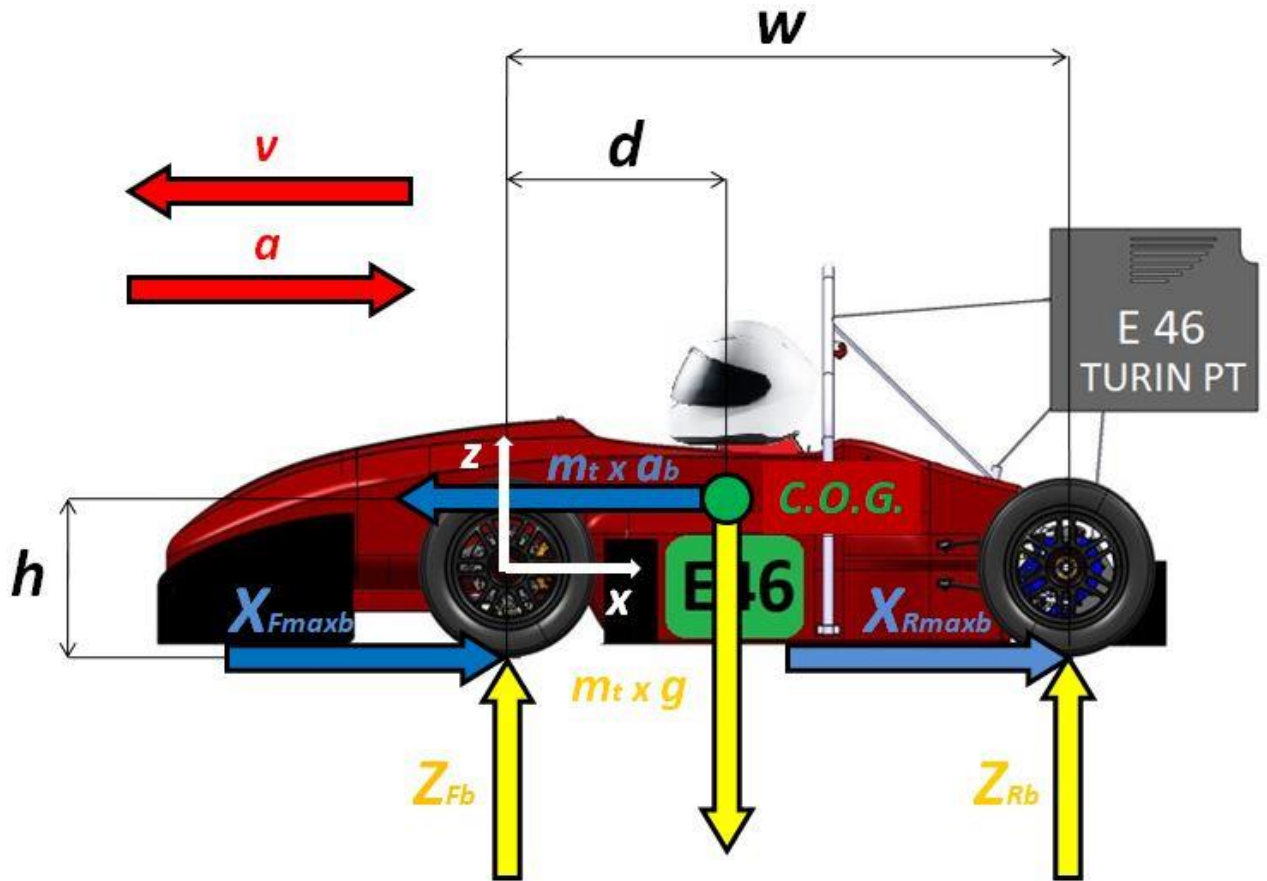


Plot 6.1-3: Behaviour of the tire in driving and in braking condition Ref.[2].

On the base of Plot 6.1-4, It's possible to write a system of equations strictly similar to that of Chapter 4.1. It's possible notice that some vectors don't change sense, that fact leads to identical related equations. Parameters of equations are identical to that of acceleration model. That stands for



longitudinal friction coefficient too, indeed observing Plot 6.1-3: Behaviour of the tire in driving an in braking condition Ref.[2]. behaviour of tire is clear. By virtue of that, according with Ref.[2], module of maximum value of longitudinal friction coefficient is the same in case of acceleration and braking both. About variable parameters, It's necessary to underline the employ of letter "b" on subscripts. That means "braking" condition.



Plot 6.1-4 Two dimensions model of S.C.R. focused on longitudinal load transfer, braking case.

Equations derived by Plot 6.1-4 are displayed as follows:

$$\text{Eq. 6.1-1} \quad -m_t \cdot a_b \cdot h + m_t \cdot g \cdot d - Z_{Rb} \cdot w = 0$$

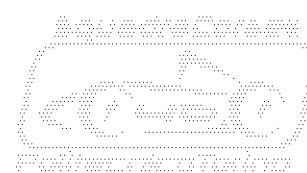
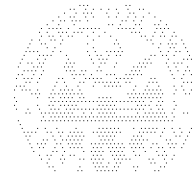
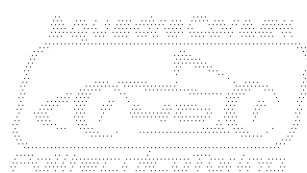
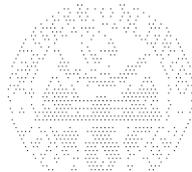
$$\text{Eq. 6.1-2} \quad Z_{Fb} - m_t \cdot g + Z_{Rb} = 0$$

$$\text{Eq. 6.1-3} \quad X_{Fmaxb} - m_t \cdot a_b + X_{Rmaxb} = 0$$

$$\text{Eq. 6.1-4} \quad X_{Fmaxb} = \mu_{Xmax} \cdot Z_{Fb}$$

$$\text{Eq. 6.1-5} \quad X_{Rmaxb} = \mu_{Xmax} \cdot Z_{Rb}$$

Therefore It's useful to remind meaning of equations. Eq. 6.1-1 regards the equilibrium to the rotation around the front tire-ground contact point. Eq. 6.1-2 regards the equilibrium of vertical forces. Eq. 6.1-3 is the equation which rules the equilibrium of longitudinal forces. Eq. 6.1-4 and Eq. 6.1-5 are equations relative to front and rear wheels, describing the relation between vertical force and tangential force. Next step is order previous equations, to easily write the related matrix.



Eq. 6.1-6 $Z_{Rb} \cdot w + m_t \cdot a_b \cdot h = m_t \cdot g \cdot d$

Eq. 6.1-7 $Z_{Fb} + Z_{Rb} = m_t \cdot g$

Eq. 6.1-8 $X_{Fmaxb} + X_{Rmaxb} - m_t \cdot a_b = 0$

Eq. 6.1-9 $-\mu_{Xmax} \cdot Z_{Fb} + X_{Fmaxb} = 0$

Eq. 6.1-10 $-\mu_{Xmax} \cdot Z_{Rb} + X_{Rmaxb} = 0$

Starting from previous equations, It's easy to write A_b , the "matrix of variable coefficients", referred to braking condition:

Eq. 6.1-11 $A_b = \begin{vmatrix} 0 & w & 0 & 0 & m_t \cdot h \\ 1 & 1 & 0 & 0 & 0 \\ 0 & 0 & 1 & 1 & -m_t \\ -\mu_{Xmax} & 0 & 1 & 0 & 0 \\ 0 & -\mu_{Xmax} & 0 & 1 & 0 \end{vmatrix}$

Then It's necessary to write B_b , the "matrix of known terms", referred to braking condition:

Eq. 6.1-12 $B_b = \begin{vmatrix} m_t \cdot g \cdot d \\ m_t \cdot g \\ 0 \\ 0 \\ 0 \end{vmatrix}$

With the help of excell software It's easy solve the following matrix equation:

Eq. 6.1-13 $A_b \cdot x_b = B_b$

Where x_b is the "vector of solutions" of the system, referred to braking condition.

Solutions are then displayed by following equations, extracted from vector x :

Eq. 6.1-14 $Z_{Fb} = 2338 [N]$

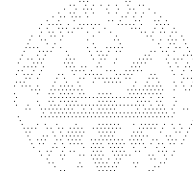
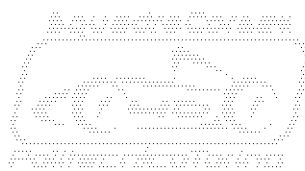
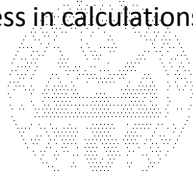
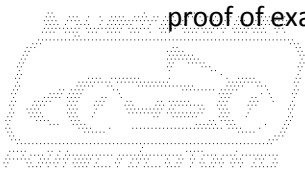
Eq. 6.1-15 $Z_{Rb} = 899 [N]$

Eq. 6.1-16 $X_{Fmaxb} = 3741 [N]$

Eq. 6.1-17 $X_{Rmaxb} = 1439 [N]$

Eq. 6.1-18 $a_b = 15,69 \left[\frac{m}{s^2} \right]$

On the contrary to previous case of Chapter 4.1, It's necessary notice that load of the vehicle have been shifted forward, toward the front axle. That fact is coherent with expected behaviour and represents a proof of exactness in calculations.



In order to proceed with the calculation maximum torque, most interesting result is represented by Eq. 6.1-17. It describes numerical value of X_{Rmaxb} , the “**maximum tangential force of rear axle**”, related to braking condition. It’s necessary to introduce some new variables and recall old parameters.

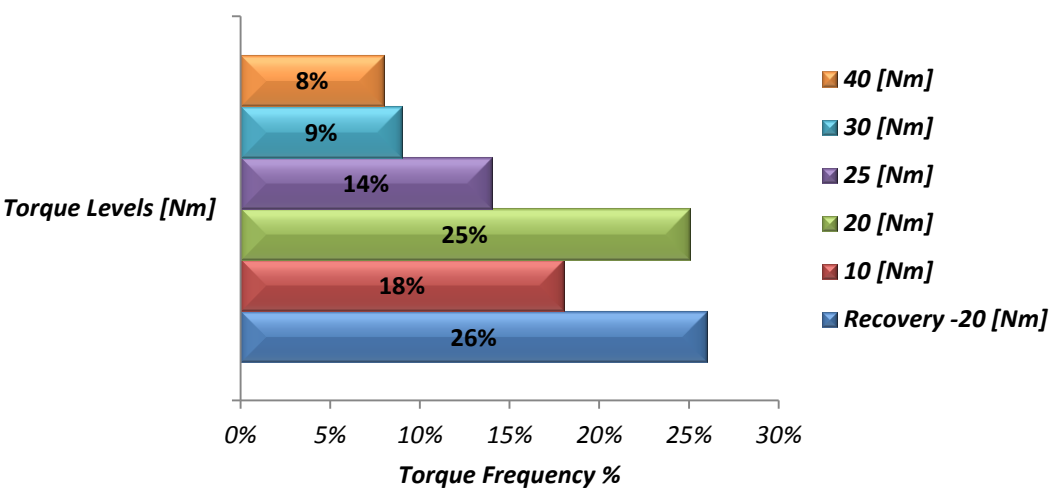
- T_{maxb} is “**maximum torque dischargeable to ground**” by rear axle in braking condition. It’s measured in [Nm].
- T_{maxbW} is “**maximum torque dischargeable by single rear wheel**” in braking condition. Main hypothesis is that condition of each tire must be identically the same by point of view of inflating pressure, temperature and wear. Condition of tarmac have to be the identical under each wheel. Such torque is measured in [Nm].
- T_{rec} is “**maximum recovered torque**”, measured in [Nm].
- $i_{end} = 9$ [dim. less] is “**endurance gear ratio**”, It’s described by Eq. 4.1-24 .

Eq. 6.1-19 $T_{maxb} = X_{Rmaxb} \cdot r_d = 366 [N \cdot m]$

Eq. 6.1-20 $T_{maxbW} = \frac{T_{maxb}}{2} = 183 [N \cdot m]$

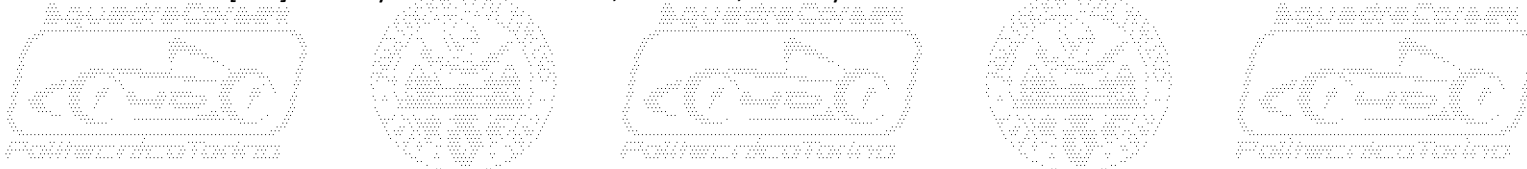
Eq. 6.1-21 $T_{rec} = \frac{T_{maxbW}}{i_{end}} = 20 [N \cdot m]$

Finally, by Eq. 6.1-24 It’s possible to extract value of maximum recovered torque. Such torque represents the negative torque that transmission needs to withstand during kinetic energy recovery. As explained in advance, kinetic energy recovery system is intended to operate when throttle pedal is depressed. That may not be totally right but it’s a conservative condition in terms of fatigue of components. Indeed It’s known that the alternation of positive and negative loads shorten total life of components.



Plot 6.1-5: Frequency on levels of requested torque.

In order to proceed with the study, filtered and calculated data are ordered on six different levels of torque request. Any level is then recorded on the basis of the frequency, as it’s shown by Plot 6.1-5. In this way, duty cycle of gear-box is modelled as a sequence of intervals of steady torque operation. Duration of intervals is determined by parameter of frequency. In example, driver needs a torque value of 40[Nm] for only 8% of the test and, of course, for only 8% of the total life.



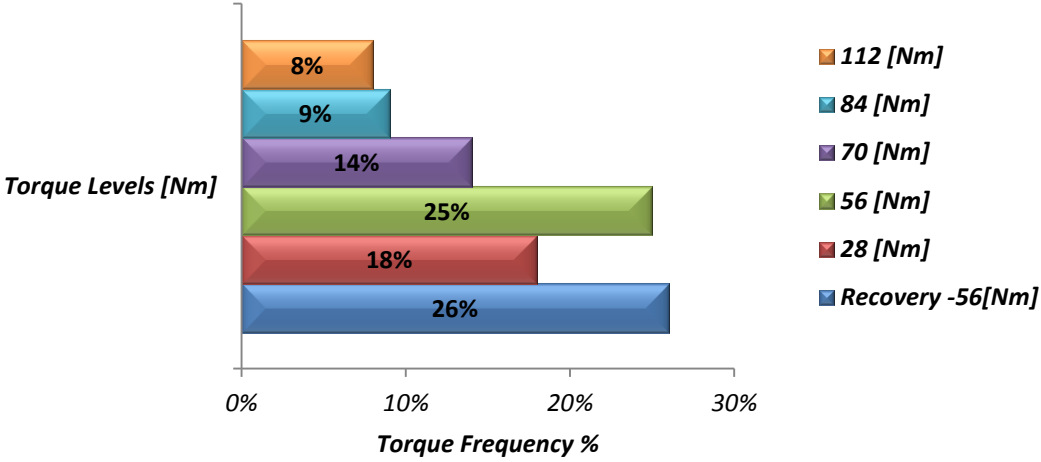
Reasonably, torque requested by the driver coincides with torque supplied by electric motors, with exception of the rare moments in which traction control operates. For this reason, It is not wrong consider that torque requested by driver coincides with input torque of the gear-box.

Last parameter to be set is the **“mean rotational speed on input shaft of first stage”, n_{1m}** . A mean value of the rotational speed needs to be assigned to any torque level. In order to simplify this step, starting from telemetry of S.C.12e referred to F.S.A.E. Italy endurance test, a mean value of rotational speed has been esteemed:

Eq. 6.1-22 $n_{1m} \cong 6.000 [rpm]$

This value is considered to be common for all six different levels of torque. That consists of an important simplification but it’s not inaccurate by point of view of fatigue model.

At this point, It’s necessary to remember that S.C.R. gear-train is split in two stages. For this reason, calculation too needs to be split on two different steps. Therefore, it’s necessary to define the load spectrum referred to second stage input.



Plot 6.1-6: Frequency on levels of requested torque, second stage.

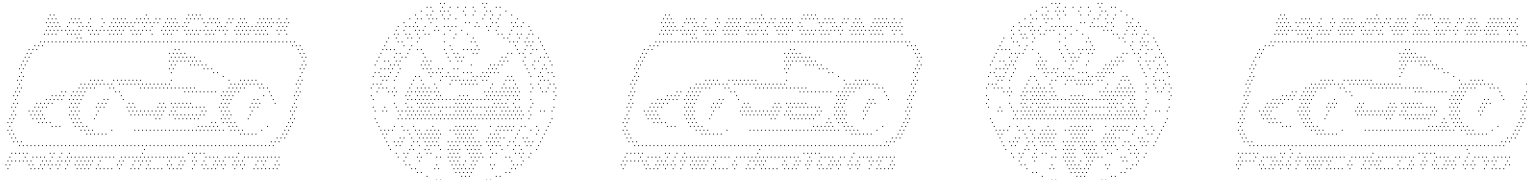
As shown by Plot 6.1-6 frequency of torque levels, of course doesn’t change. The quantity which varies is the magnitude of torque displayed in the Plot 6.1-5. Magnitude of torque levels on second stage is calculated with the following relation:

Eq. 6.1-23 $T_{2i} = i_{1,2} \cdot T_{1i}$

Where:

- T_{2i} is the generic **“magnitude of torque level”** of the second stage, measured in [Nm].
- T_{1i} is the generic **“magnitude of torque level”** of the first stage, measured in [Nm].
- $i_{1,2}$ is **“gear ratio of the first stage”**, a dimensionless parameter defined by Eq. 4.4-6.

At the same way, value of **“mean rotational speed on input shaft of second stage”, n_{2m}** is calculated by the following relation:



$$\text{Eq. 6.1-24} \quad n_{2m} = \frac{n_{1m}}{i_{1,2}} = \frac{6000}{2.8} = 2.143[\text{rpm}]$$

Where:

- n_{1m} is “mean rotational speed on input shaft of first stage”, defined by Eq. 6.1-22, measured in [rpm].
- $i_{1,2}$ is “gear ratio of first stage”, a dimensionless parameter defined by Eq. 4.4-6.

In second stage too, mean value of rotational speed is intended to be common to any level of torque.

6.2. Choice of main parameters on first stage.

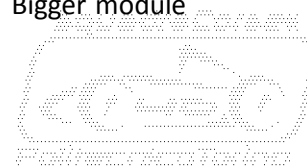
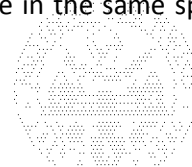
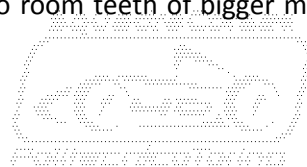
About first stage, chapter 4.3.2 explains precisely issues related to power transmissions between orthogonal axes and declares that most suitable solution is a **set of bevel gears** in the first stage. Anyway, straight profile bevel gears could be lacking by point of view of performance, indeed spiral profile bevel gears are very widespread in automotive and motorsport applications.



Picture 6.2-1: Straight profile bevel gear, spiral profile bevel gear (<https://www.machinedesign.com/>).

It's easy to understand that, while teeth of straight bevels are linear, teeth of spiral bevels follow a spiral pattern which is commonly defined with the angle of the tangent to straight line, more commonly “spiral angle” ψ . Spiral bevel gears can be manufactured by Gleason's (**Gleason-Duplex**) system. It is basically a set of standards which describes the ratios of tooth addendum, dedendum and other parameters. The main advantage that Gleason's system offers is “**coniflex**” cutting tool. That displays ends of the teeth slightly curved inward of a well defined value. That causes benefits in wheels of the gear which are more tolerant each others. Compared to straight cut teeth gears, less errors are detected in shaft alignment. In an ideal situation, the contact area of a bevel gear tested under load, will reside in the central portion of the tooth, touching neither end. As load is increased, some deflection will occur, and the contact area tends towards the outside of the gears.

Commonly, pinion of a straight bevel gear need to withstand an equation similar to Eq. 5.3-1, which prescribes the minimum number of teeth. Differently, a spiral bevel gear can work with a lower number of teeth in the pinion. That allows to room teeth of bigger module in the same space. Bigger module



leads to shorter face width, with increased structural strength. For this reason, a spiral gear is stronger than straight one with equal face width and similar overall dimensions.

First input parameter to be set is the gear ratio. All references about the choice of the value are deeply shown in Chapter 4.4. Anyway, Kisssoft needs a tolerance on the value of the “*gear ratio*”, in order to evaluate different combinations in the number of teeth.

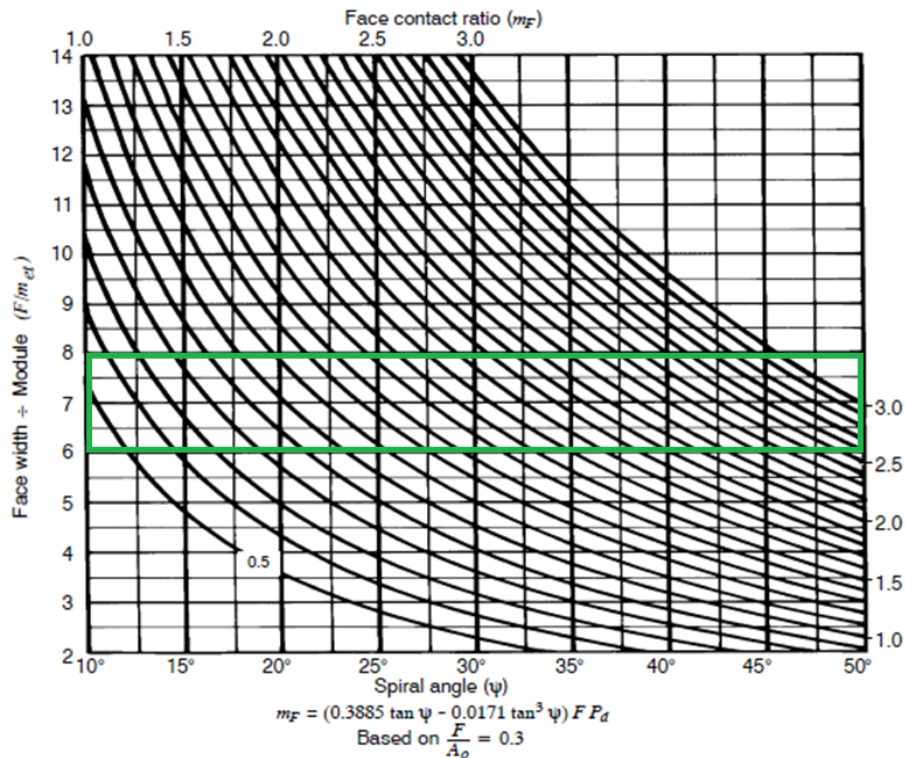
Eq. 6.2-1 $i_{1,2actual} = 2,80 \pm 0,10$ [dim. less]

Like it was revealed at Chapter 5.1, it’s necessary to set one of the most important angular parameters: the “*pressure angle*”, α . That described previously, is intended to be the “*axial pressure angle*” which is the lonely parameter in spur gear calculation. As revealed in advance at Chapter 5.10, helix or spiral profile gears, due to their geometry, identify three different parameters: “*axial pressure angle*” α , “*normal pressure angle*” α_n and “*transversal pressure angle*” α_t .

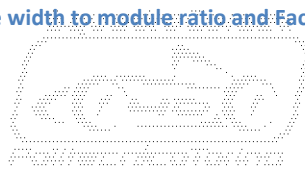
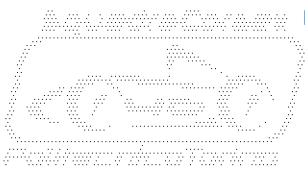
Normal pressure angle is the most relevant in calculation, for this reason it’s normally set up as input. Geometrically it’s the homologous of axial pressure angle in a spur gear but it’s measured on a plan perpendicular to the helix or to the spiral profile. Technologically, normal pressure angle too depends on the geometry of tools exploited during manufacturing process. Manufacturing of tools offers a wide spectrum in which customize the pressure angle, commonly values set on Gleason’s system varies between 14.5° and 20° . Anyway reasons of time and budget made the choice focus on the most widespread value:

Eq. 6.2-2 $\alpha_{n12} = 20^\circ$

In this way, the research of a proper gear supplier is quicker and costs of manufacturing would be logically appropriate.



Plot 6.2-1: Spiral Angle vs. Face width to module ratio and Face contact ratio. (Courtesy CRF).



By technical point of view, It's necessary to underline that the angle of 20° is the best trade-off between stiffness of the single tooth and the transverse contact ratio. That ensures reliability and efficiency of the gear both. Due to these reasons, angle 20° is the most widespread in power transmission applications.

As revealed in advance, the main parameter which describes a spiral profile is the angle of the straight line tangent to the spiral, defined as "intermediate spiral angle" ψ . This parameter is expressed on Kisssoft as: "angolo d'elica ruota 1 (medio)" and often " ψ " is replaced by " β ", " β_{m1} ".

Spiral angle needs to be obtained from Plot 6.2-1. Vertical axis displays the face width/module ratio, described by Eq. 5.1-1. It results that a compact gear suitable for motorsport applications needs a value between 6 and 8. Curved lines represent the overlap ratio, indicated as face contact ratio. As revealed in advance, at Chapter 5.7, a suitable value for this parameter is around 2. Thus the suitable value of spiral angle needs to be greater than 30°. Anyway, in order to maintain a good level of efficiency, the chosen value of spiral angle needs to be limited to 30°.

Eq. 6.2-3 $\psi = 30^\circ$

Another parameter which is important in calculations of Kisssoft is the "quality index" which basically describes the accuracy and the surface finish on the flank of teeth. Software uses a scale parameter which it's based on **I.S.O. 17485:2006** standard.

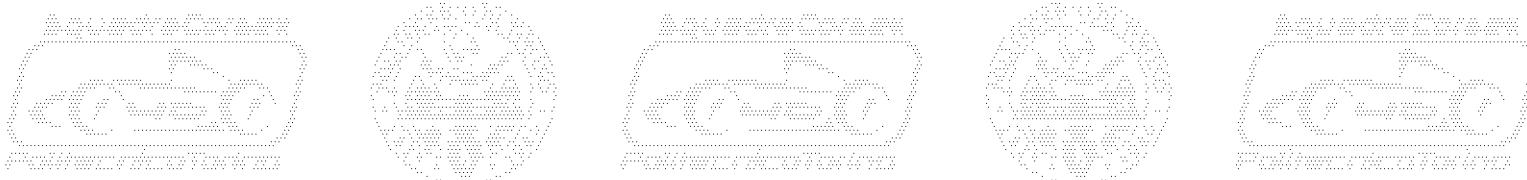
Norm establishes a classification system that can be used to communicate geometrical accuracy specifications of unassembled bevel gears, hypoid gears, and gear pairs. It defines gear tooth accuracy terms, and specifies the structure of the gear accuracy grade system and allowable values. **I.S.O. 17485:2006** provides the gear manufacturer and the customer with a mutually advantageous reference for uniform tolerances. Ten accuracy grades are defined, numbered 2 to 11 in order of decreasing precision.

Gears which features high performances , after the basic manufacturing process, need to be delivered to Lafer S.p.a., an Italian company specialized in surface finishing treatments. Components, first of all, are exposed to a "superfinish" process, then to a "coating" process. To better explain processes carried out by Lafer S.p.a. it's necessary to exploit the notion of roughness.



Plot 6.2-2: Basic scheme of roughness.

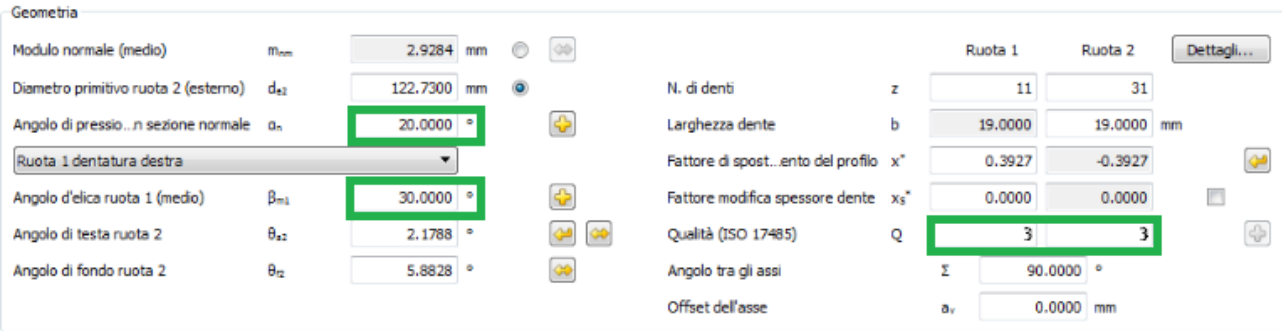
Roughness of a component can be basically described by Plot 6.2-2. Zero line is the nominal dimension of the component. Around this line, actual surface of the component floats between positive values "peaks" and negative values, "valleys". The target of the superfinish process is to flatten all positive peaks, respecting the mechanical tolerance of the component.



In order to have a flat and smooth surface on the component, it's necessary to eliminate the issue of negative valleys. Therefore an additional treatment is needed, **Carbonlafer** which is the commercial name of a WC/C coating process. By chemical point of view, this treatment It's based on the sediment of an amorphous multi layer of tungsten carbide, which thickness varies between 1 [μm] and 3 [μm].

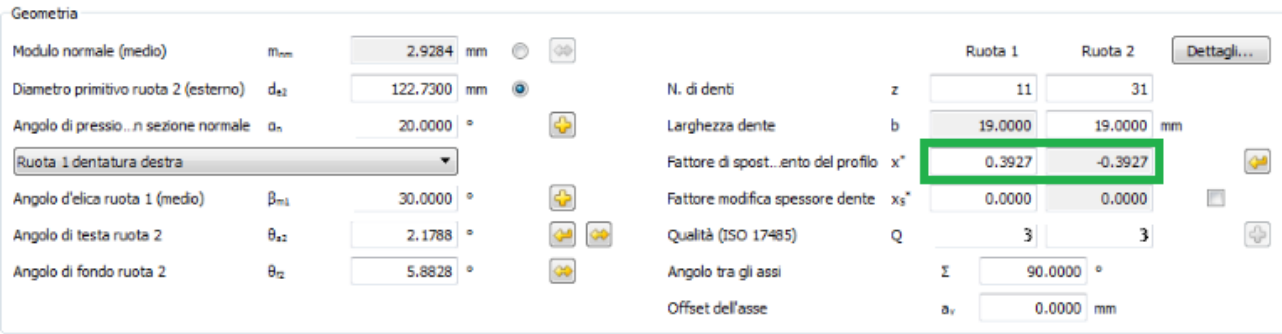
According with website "<http://www.lafer.eu/>", Ref.[13], this process is suitable in any application where it's necessary to reduce the friction between mechanical components and limit the employ of lubricants. It's normally employed for gears, hydraulic pumps, bearings, worm screws and sliding guides. Main feature of Carbonlafer is a very low **coefficient of friction**, C.O.F., measured around 0.15 on dry steel. Then, hardness of the surface is increased by a value included between 200HV and 300HV points which represent a surplus of 15÷20% in the total hardness of the material surface. Strong adhesion of the coating layers can be obtained at relative low temperature, 180°C and this ensures that unwanted displacements could not appear. Anyway, coating is very stable under high temperatures, that allows to treated components to work until 380°C.

Returning to focus on the software, to the setting of input parameters in particular, a value of quality set on 3 can be congruent to the treatments performed on the gear. Value of 3 instead of 2 is a preventive measure, knowing that cutting of spiral bevel gears is a very delicate process by point of view of technology. Surface finish of first manufacturing process is often a bit scratched and not all deep scratches can be sealed by coating. Parameters actually set on the software are displayed on Picture 6.2-2.

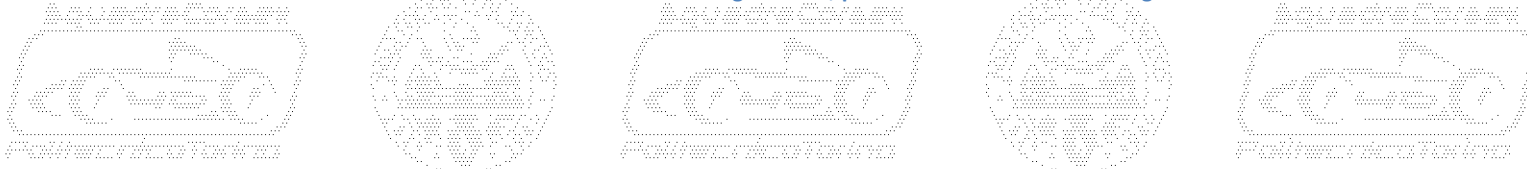


Picture 6.2-2: Detail on Kisssoft dialog window, input geometric parameters are highlighted by green squares.

A brief clarification needs to be done about **profile correction factor** which Kisssoft indicates with "**Fattore di spostamento del profilo**", widely described at Chapter 5.12. Software acts selecting two different options of correction: one maximizes the structural strength of the tooth, the other maximizes the efficiency of the gear.



Picture 6.2-3: Detail on Kisssoft dialog window, profile correction factor setting.



Chosen option is symmetrical:

$$\text{Eq. 6.2-4} \quad X_1 = 0,3927 \text{ [dim. less]}$$

$$\text{Eq. 6.2-5} \quad X_2 = -0,3927 \text{ [dim. less]}$$

Where:

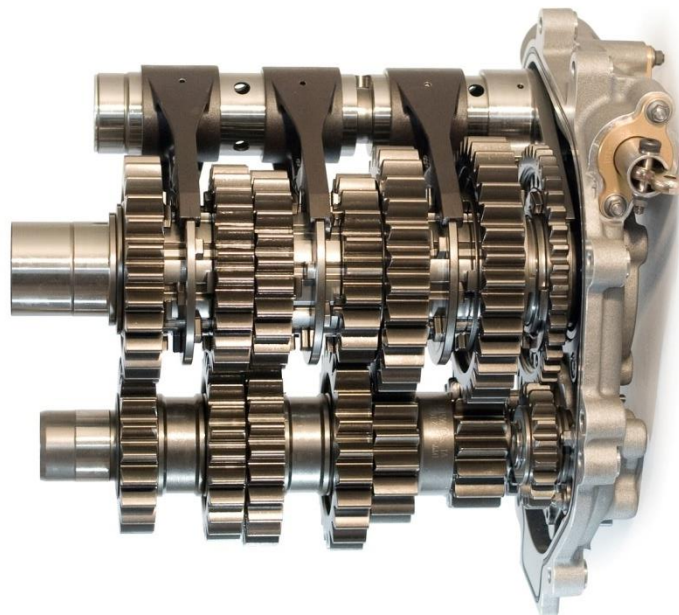
- X_1 is “**profile correction factor of wheel 1**” drive wheel of first stage. It’s a dimensionless parameter.
- X_2 is “**profile correction factor of wheel 2**” driven wheel of first stage. It’s a dimensionless parameter.

Determined value allows to maximize strength of teeth, through the strengthening of roots.

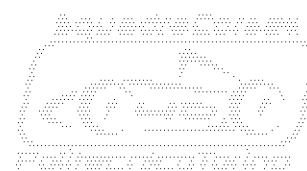
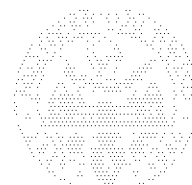
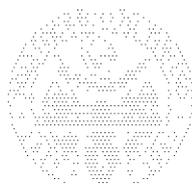
Profile of gear, on the basis of calculations, have been modelled in accordance with **I.S.O. 23509:2006 Q4-7** standard.

6.3. Choice of main parameters on second stage.

Before starting a deep examination of design parameters on second stage gear, it’s appropriate introduce briefly spur gears which have been chosen to realize the second stage of the gear-box. Road cars and, more commonly, passenger cars are equipped with specific road gear-boxes. Design of such transmissions is oriented on reliability and, in particular, on comfort, according with Ref.[6]. A gear-box designed around comfort includes devices like synchronizers that make the gear shifting more linear and progressive. Employ of these devices is excluded by racing use. In order to save weight and time on the shifting, synchronizers are replaced by simpler devices called “dog rings”. Gears related to ratios are different too.



Picture 6.3-1: Gear cluster of a racing gear-box manufactured by Hewland Engineering (<https://www.hewland.com/>).



Gear-box of passenger cars are assembled with helix profile cylindrical gears. These items ensure a smoother transmission of forces between drive and driven wheel of the gear. Important benefits are achieved by point of view of comfort, noise and vibrations.

Sport motorbikes and racing cars don't need to withstand to particular design drivers determined by issues of noise and comfort. For this reason, related gear-boxes are assembled with ratios realized by cylindrical spur gear sets. These particular kind of gear feature two main benefits. First is related to efficiency because friction between teeth is lower compared to a helix profile gear. Second is related to axial forces because spur gears don't feature forces in axial direction. That allows to save weight in the design of bearings and gear-box case. Finally, first input parameter in the design of second stage gear is fixed: **"helix angle" β** .

Eq. 6.3-1 $\beta = 0^\circ$

Going forward with setting of input parameters, to determine the gear ratio, it's necessary to return back to Chapter 4.4, to Eq. 4.4-7, in particular. With reference of what explained in previous Chapter 6.2, software needs that **"gear ratio"** was set up with a suitable tolerance value.

Eq. 6.3-2 $i_{3,4actual} = 3,20 \pm 0,10$

In order to determine a suitable pressure angle, it's necessary return back to Chapter 6.2. Principles about choice of the parameter are identical. Anyway, it's necessary to underline that , in a spur gear, **"pressure angle"** to set up is the axial one.

Eq. 6.3-3 $\alpha_{n34} = 20^\circ$

Identical considerations can be done on quality index of second stage gear which have been involved in the same cycles of surface coating. Therefore, value of quality index to set up is 3.

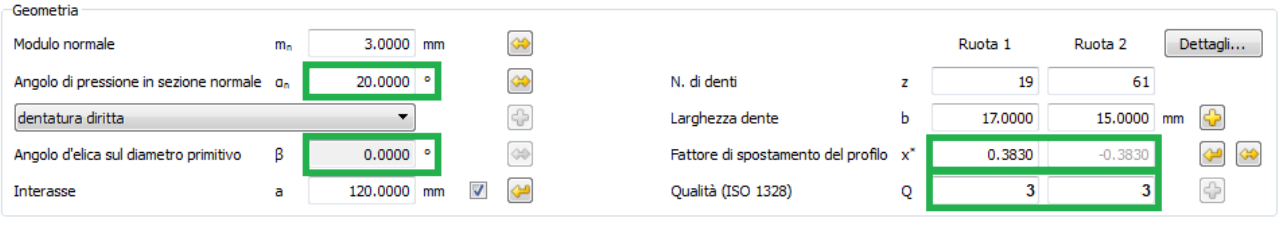
In this stage too, correction profile factor have been chosen in order to maximize the strength of teeth, for this reason:

Eq. 6.3-4 $X_3 = 0,3830 [dim. less]$

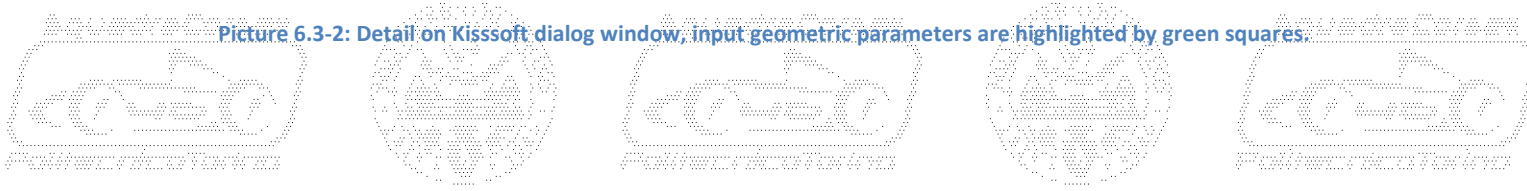
Eq. 6.3-5 $X_4 = -0,3830 [dim. less]$

Where:

- X_3 is **"profile correction factor of wheel 3"** drive wheel of second stage, It's a dimensionless parameter.
- X_4 is **"profile correction factor wheel 4"** driven wheel of second stage, It's a dimensionless parameter.



Picture 6.3-2: Detail on Kisssoft dialog window, input geometric parameters are highlighted by green squares.



Returning back to Chapter 4.2 and Chapter 4.4, it's clear that a minimum offset between axis of the gear needs to be fixed. Kisssoft software offers the opportunity to exchange input parameters on the basis of requirements of the designer. Offset, which is normally an output, in this situation has been chosen to become an input parameter. Some studies, performed on the layout of the car, established that a well determined value of offset a is needed. First aim is to catch up position of centre of semi axle, which is relatively far on z-axis. Second aim is keep motors as far as possible from rear axle of the car. For these reasons, minimum value of "offset" a is:

$$\text{Eq. 6.3-6} \quad a = o_{34} = 120,00 \text{ [mm]}$$

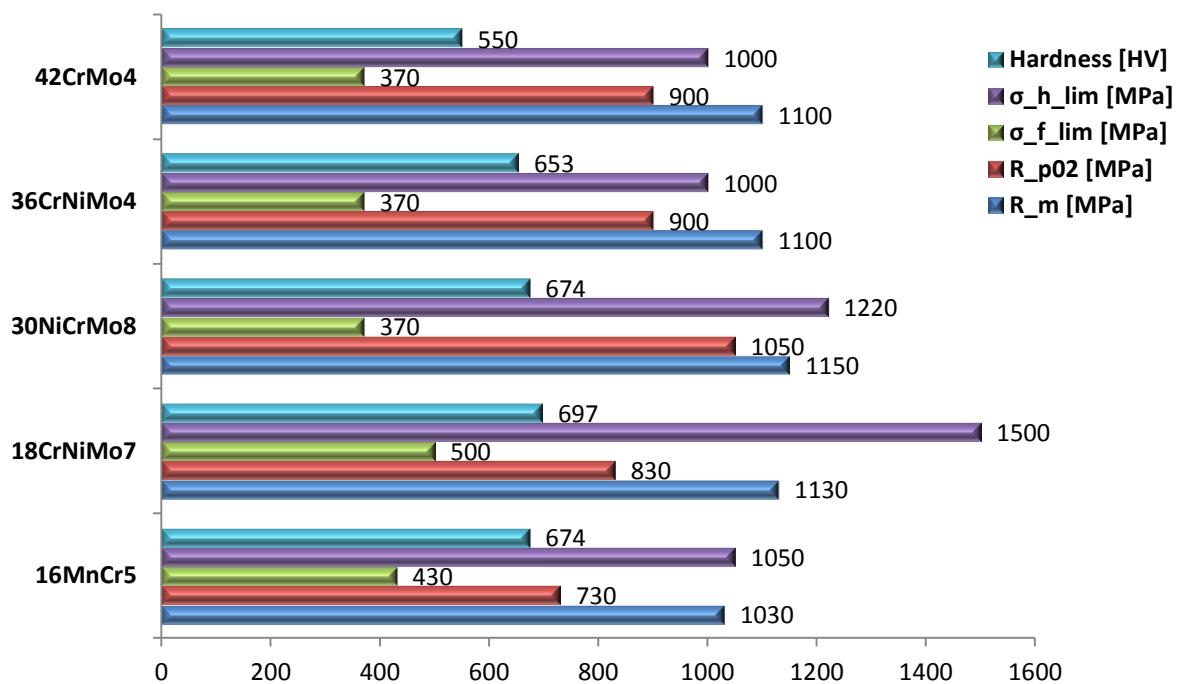
Geometria		Ruota 1		Ruota 2		Dettagli...	
Modulo normale	m_n 3.0000 mm	N. di denti	z 19	61			
Angolo di pressione in sezione normale	α_n 20.0000 °	Larghezza dente	b 17.0000	15.0000 mm			
dentatura dritta		Fattore di spostamento del profilo	x^* 0.3830	-0.3830			
Angolo d'elica sul diametro primitivo	β 0.0000 °	Qualità (ISO 1328)	Q 3	3			
Interasse	a 120.0000 mm						

Eq. 6.3-7: Detail on Kisssoft dialog window, minimum offset setting

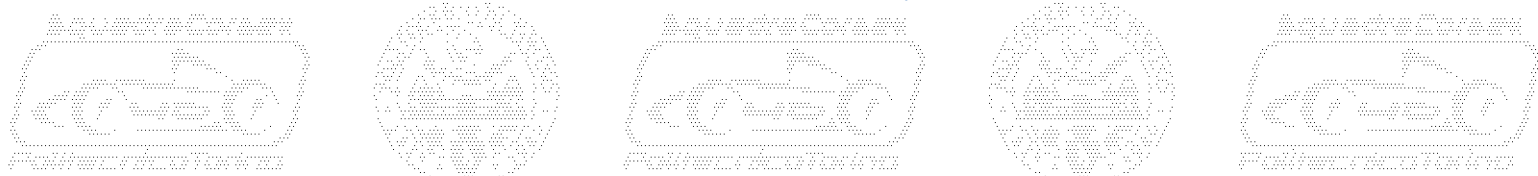
To conclude it's necessary to remember that profile of gear of second stage have been modelled in accordance with **D.I.N. 3967:1978 CD2** standard.

6.4. Choice of material.

Review on calculation of gears displayed on Chapter 5, underlines the relevance of material in technology of gearwheels. Chapter 5.2, in particular, explains why in this project, steel is more suitable than other metals. The same chapter describes briefly main features needed by a steel suitable for the production of gears. Moreover, a large selection of best performing steels have been introduced.



Plot 6.4-1: Performances of evaluated materials, data from Kisssoft software.



Target of actual chapter is evaluate any single feature of any introduced steel, in order to perform the more suitable choice for the project.

Previous, Plot 6.4-1 displays evaluated steels by point of view of numeric performances, extracted by database of Kisssoft software. Plotted parameters are:

- **“Hardness”**, which is measured in HV points.
- σ_{Hlim} is **“Pressure of base superficial fatigue”**, described an Chapter 5.10., measured in [MPa].
- σ_{flim} the **“Limit of stress in bending fatigue”**, described in Chapter 5.8., measured in [MPa].
- R_{p02} the **“Yield strength”**, measured in [MPa].
- R_m the **“Ultimate tensile strength”**, U.T.S, measured in [MPa].

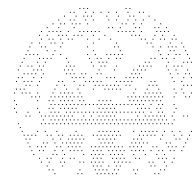
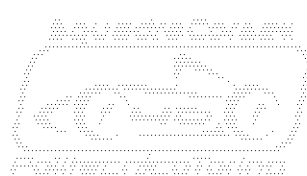
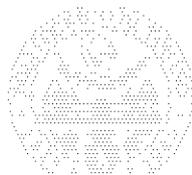
One other important feature of Kisssoft software is the database of materials and treatments. Data stored into the database derive from **I.S.O. 6336-5 “Strength and quality of materials”** standard. The relevance of data imported on Kisssoft database is that values are referred to materials after the treatments performed on them. That’s very important because data which are often provided by steel manufacturers and dealers, are related to the natural state of the material, ignoring benefits produced by different treatments. For any material, different options related to the treatment can be chosen, in order to find the most suitable solution by point of view of the designer. Indeed data about σ_{Hlim} and σ_{flim} , which are relevant by point of view of fatigue, are often excluded by the large majority of data sheets.

Observing values of σ_{Hlim} and σ_{flim} displayed by Table 5.8-2, deriving from Ref.[11], It’s necessary to notice that are higher respect to values displayed by Plot 6.4-1, deriving from I.S.O. 6336-5. That’s not so relevant because table shows one only value for each family of steel, while data from Kisssoft database are distinguished for any alloy of the family. Anyway, I.S.O. 6336-5 results more modern than U.N.I. 8862, Ref.[11], for this reason exploits a research performed with more modern methods of investigation. It’s therefore right considerate that more recent standard may be more accurate. On the other hand, values displayed by I.S.O. 6336-5 tends to be more cautionary, for this reason are more suitable to a design process which includes fatigue.

By the Plot 6.4-1 it’s clear that 16MnCr5 features good performances by point of view of fatigue behaviour and hardness, but it’s quite lacking by point of view of yield strength. Anyway this material can represent good performance balanced steel.

Very high performances are featured by 18CrNiMo7. It looks particularly strong by point of view of hardness and fatigue contact pressure. Good performances about yield strength and U.T.S.

Anyway, case-hardened steels, like 18CrNiMo7 and 16MnCr5, gain their hardness by a very aggressive heat treatment, in which temperature arises around 900°C . Process is often performed on finished components. Therefore a gear related to this project will surely accumulate undesired displacements during the treatment. In order to avoid displacements on most important working areas, it is necessary treat a raw gear which is provided of a large over-material in order to increase the stiffness. Then is necessary a machining process to remove the surplus material. Main issue is that, treated material, case hardened in particular, is very difficult to remove by machine tool, for this reason it isn’t a cheap solution.

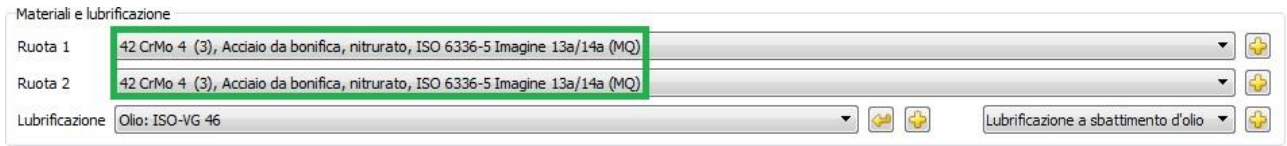


Going forward with the analysis of Plot 6.4-1, it's possible to detect that 30CrMo8 may be the better choice in the family of tempered steels. Anyway, this steel is very rare to find, it's sold in large quantities only and, in addition, it's very expensive.

In order to close this chapter, it's necessary underline that choice needs to be performed between 36CrNiMo4 and 42CrMo4. Both materials can withstand a nitriding process with good results. This Treatment doesn't cause displacements in the shaped gear because reached working temperature is around 500°C.

Standing by Plot 6.4-1 it's clear that performances of 36CrNiMo4 and 42CrMo4 are quite similar. The only important difference is that 42CrMo4 is weaker by point of view of hardness. Anyway, surface hardening of 42CrMo4 can surely be improved by WC/C coating process. Moreover, 42CrMo4 is a very cheap and widespread material, it probably represents the best trade-off between **performance** and **price**. For this reasons, 42CrMo4 is the best practice proposed by **Euren S.p.a.**, the partner in gear manufacturing which performs the role of the sponsor too.

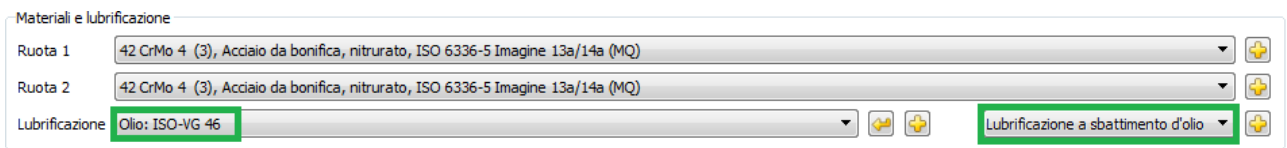
Picture 6.4-1 shows the portion of command window of the software, where it's possible to set up the material , indicated with the related thermal treatment .



Picture 6.4-1: Detail on Kisssoft dialog window, choice of material highlighted by green square.

6.5. Choice of lubrication and lubricant.

Observing portion of command window displayed on Picture 6.5-1, it's possible to notice two popup menus related to lubrication. Variables to choose are essentially two, one located in low right position describes the type of lubrication, one located in low left position describes the type of lubrication oil. With reference to previous topics, relevance of lubrication emerged from Chapter 5.10. Lubrication is a wide and complex argument, purpose of this chapter is provide main information about this topic and explain design choices related to gear-box project.

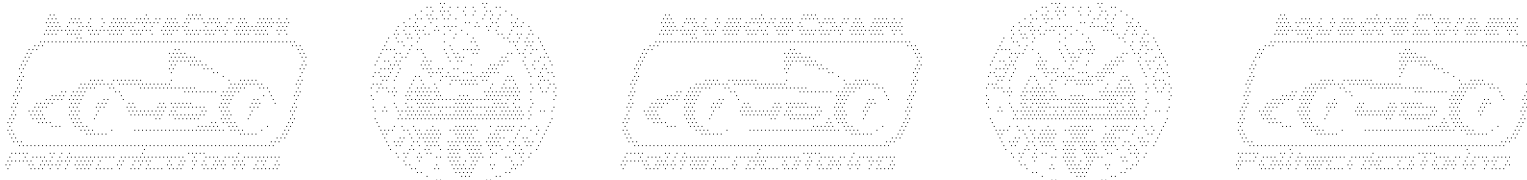


Picture 6.5-1 : Detail on Kisssoft dialog window, information about lubrication are highlighted by green squares.

Precondition to topic dissertation is knowledge of lubrication main tasks. One is related to the reduction of friction between sliding metal parts. Other is related to cooling down of heated surfaces on components. Tasks are strictly related because It's necessary consider that heat is generated by friction.

6.5.1. Lubrication systems.

Back to Picture 6.5-1, importance of lubrication system It's widely clear. Following paragraphs are oriented on the comparison of the two possible solutions, **“forced lubrication system with dry sump”** and **“splash lubrication with wet sump”** (“lubrificazione a sbattimento d’olio”).



From bench mark analysis performed on Chapter 1.5, it's clear that a gear-box provided of forced lubrication system with dry sump, pump and oil radiator is a quite exotic solution in F.S.A.E. neighbourhood. Moreover It may be over-engineered. Definitely, this refined solution, which is widespread in high-end motorsport vehicles, is more efficient than the classic splash lubrication solution.

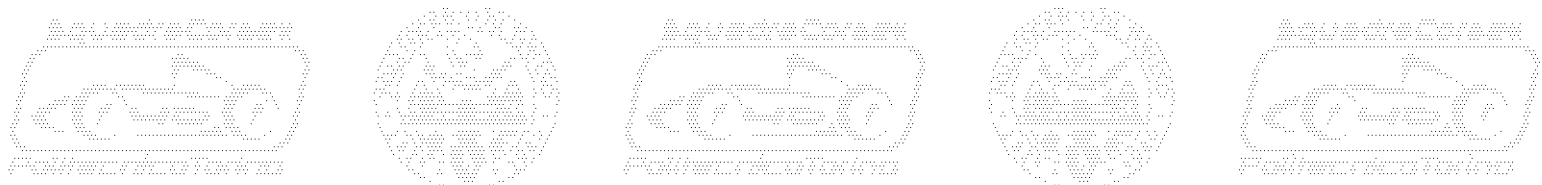
It's important to remind that dry sump is extremely important in racing engines. According with Ref.[4], this solution make the engine more compact and, for this reason, allows to lower **centre of gravity position** on z-axis of about dozen of millimetres. Engine, is one of the heaviest components on the car. Lower its own centre of gravity produces extremely high benefits in the handling performance of the car. Identical considerations can be performed on gear-box too, even if benefits are quite smaller. Due to mechanical layout and lower operation temperatures, usually gear-boxes don't need large pans to store lubrication oil.



Picture 6.5-2: Bench test on Minardi F1 gear-box featuring dry sump. Central section of the case is manufactured in plastic transparent material. That solution allows to observe behaviour of lubrication oil, in order check the proper operation and perform optimizations of the oil delivery system (<https://www.crpmeccanica.com/>).

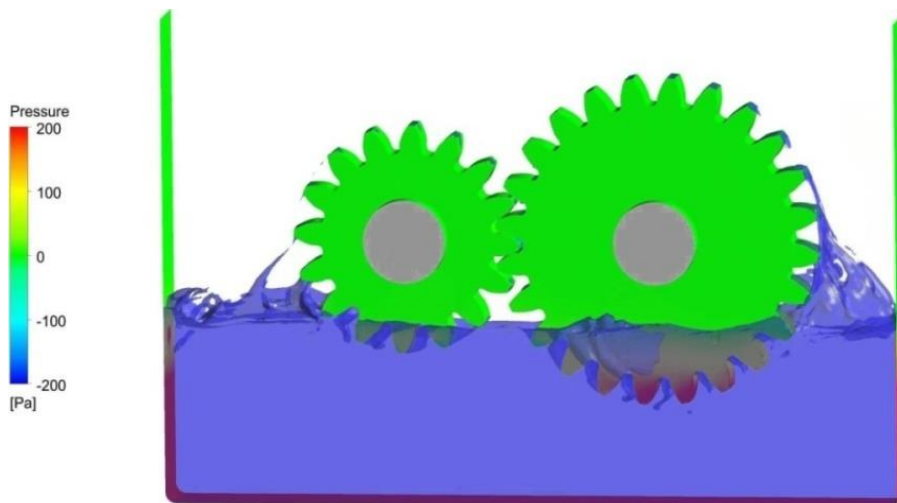
Forced lubrication system needs, to work without problems, a sophisticate layout of **baffles** integrated in the sump, as depicted in Picture 1.5-6. Baffles prevent the surging of oil which may exhibit at admittance of scavenge pump during the track operation. Moreover, a well designed baffle system helps lubricant to release air trapped into the foam. To work properly, forced lubrication system needs to be integrated by an efficient **system of ducts** in which lubricant is forced by scavenge pump and distributed around gear-box. Ducts are terminated by special **rails** or **nozzles** which are able to spray lubrication oil with stunningly precision.

It's important consider that forced solution, limits the **presence of lubrication oil** to circumscribed crucial zones. Such zones, like bearing rings or contact patches of teeth, are subject to high friction and, of course, to high temperatures. Jets of oil sprayed by nozzles and rails, are oriented on such zones. In splash solution, lubricant is spread around and slammed randomly into the gear-box case, as depicted by simulation of Picture 6.5-3. Splash is caused by the impact between gear teeth and mass of oil in the stored in the sump. Such operation mode causes friction losses between oil and gearwheels and leads to foam formation. Therefore, main drawback is due to presence of lubricant which may not be guaranteed in crucial zones.



By virtue of that, an important aspect of dry sump solution needs to be considered. **Quantity of oil** in the gear-box is reduced, with a non negligible save of weight. Anyway, a F.S.A.E. transmission features reduced number of ratios, reduced dimensions of gears and tight times of track operation. By virtue of that, F.S.A.E. designer may esteem that lubricant needed is a quantity around or lower the litre. Instead, large gear-boxes installed on high-end race vehicles need more or less, dozens of litres of lubricant. In this case, the difference of weight is consistent and makes dry sump solution more relevant in overall performance of the car.

About dry sump solution, lubricant which operates in circumscribed areas has a great **cooling capability**, because it comes directly from a radiator where oil it's cooled down by fresh air. Differently, lubrication oil in a wet sump, takes advantage of its own mass and of gear-box surfaces to cool down itself. To make this solution efficient, gear-box needs to be reached by a continuous stream of fresh air. That's quite difficult to realize because, often, gear-box is housed in the tight engine bay, which is the hotter zone of the car.



Picture 6.5-3: CAE simulation of oil slam in wet sump gear-box.

Another important feature of forced lubrication system is the **filtering capability**. By the way, It's necessary to explain that impurities and debris are meshed with operating lubrication oil. That's mainly due to service life of components which causes wear and consequent spread of debris. To overcome such issue, oil picked up by scavenge pump is forced to pass through a cartridge filter which entraps any contaminant. Differently, in a wet sump system, arrests of the vehicle are exploited to leave contaminants deposit on the lower point of the sump. That works only if contaminants are heavier than lubricant. Lower point of the sump, houses the discharge oil plug which is usually provided of a small magnet. This item is able to attract metallic contaminants in its neighbourhood but it's totally ineffective with any other type of contaminant.

To finally conclude this topic, it's necessary underline that gear-box of a F.S.A.E. car, custom designed for the first time, needs to be simpler as possible. By point of view of calculations, It's clear that an efficient lubrication system improves resistance to high pressure fatigue stresses. By structural point of view, It means tighten dimension of teeth of some millimetres, without any reduction of safety coefficients. Despite of its efficacy, forced lubrication system with dry sump, pump and oil radiator is a quite improper solution, by point of view of design complexity, manufacturing of components and costs. **Complexity related to design** and **tuning of the system** is proved by Picture 6.5-2: Bench test on Minardi F1 gear-box featuring dry sump. Central section of



the case is manufactured in plastic transparent material. That solution allows to observe behaviour of lubrication oil, in order check the proper operation and perform optimizations of the oil delivery system. Tuning and optimization of a forced lubrication solution requires hours of test bench with a large employ of time, human and economic resources. By virtue of that, It's clear that splash solution is less efficient but simplifies the entire project leaving designers focus on issues with larger priorities.

6.5.2. Operation of lubrication oil.

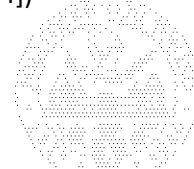
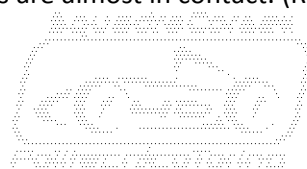
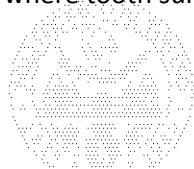
Like it was declared in advance, main tasks of lubricant are **reduction of friction** and **cooling of components**. Anyway, a good transmission oil needs to exploit some more other features.

According to "H. Naunheimer, B. Bertsche, J. Ryborz, W. Novak – Automotive Transmissions", Ref.[14], suitable lubricant must **prevent possible damages** of a mechanism. If It's already damaged, oil must prevent or delay further damages. Another important task for transmission lubricant, especially when employed in wet sump gear-box, is **prevention to foam formation**, due to violent impacts with teeth. Moreover, lubricant must be **resistant to oxidation and ageing**. It's known that oils employed manual gear-boxes of modern passenger cars last for all operational life of the vehicle, with an important contribution to environment preservation. Additionally, lubrication oil must **protect components** from their own oxidation and corrosion. That can be exploited featuring good **water separation** capabilities. **Good adherence** is fundamental in order to maintain oil in contact with rotary components, opposing to centrifugal force. On the other hand, lubricant needs to operate like a good cleanser because it may exploit good **dirt removal and dirt absorption features**. At the same time, lubricant must be **non-aggressive** to seals and rubber rings. A requirement which is particularly important in motorsport and industrial vehicles is **stability at high and low temperatures**. It's known that viscosity of lubricant is strongly affected by operation temperatures, an high performance oil must maintain values of viscosity independently from them. Finally, It's known that some automotive lubricants need to be able to **reduce noise** and **lighten actuation force** necessary to gearshift.

Anyway, most important feature of lubrication oil , especially for gear-box applications, is the **behaviour under high pressures and high speeds**. According with Ref.[14], during meshing of teeth, two types of movement take place: rolling and sliding. Regarding flank of tooth, sliding speed is at its maximum at the beginning and the end of contact. Beginning area of contact is located near root, while end of contact is located near the apex of tooth. Wear increases as the sliding speed increases. By virtue of that, most favourable conditions for lubrication, arise in coincidence of pitch diameter, near centre of tooth flank. On the contrary, conditions are less favourable at tooth root and tip. That's due to meshing impact and high temperatures resulting from higher sliding speed.

Reflecting about friction, It's possible to individuate three different zones located on tooth flank:

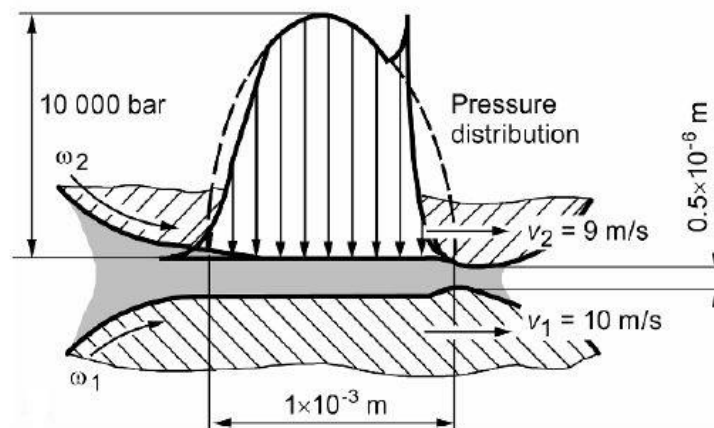
- **"Boundary friction"**: It's the zone which displays dry friction. Tooth flanks are separated by a boundary layer of chemical reaction products only. Such layer features few nanometres of thickness, intended to prevent metal-to-metal contact. Boundary lubrication is related to this zone. (Ref.[14])
- **"Mixed friction"**: It's the zone where tooth flanks are partially separated by a film of lubricant oil. There is liquid friction and dry friction at the same time. Obviously, boundary lubrication appears where tooth surfaces are almost in contact. (Ref.[14])



- **“Fluid friction”**: it’s the zone in which tooth flanks are completely separated by a film of lubricant. This condition is defined as **“elasto-hydrodynamic lubrication”**. (Ref.[14])

From previous dissertations, It’s possible to conclude that lubricant exhibits a two-fold effect in reducing friction and wear at the tooth flanks: “elasto-hydrodynamic lubricant film” and “chemical protective film”. Gearwheels often operate in the mixed friction range, even if proportion of elasto-hydrodynamic lubrication along the contact path is high. When a gearwheel spins at circumferential speeds $> 4 [m/s]$, proportion is more than 60%. Proportion is not impaired by high stress levels and It may often arise around 80÷95%.

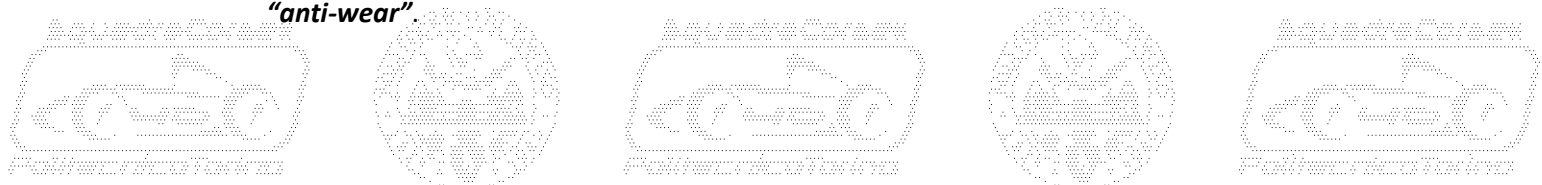
- **“elasto-hydrodynamic lubricant film”**: E.H.D. lubricant film, It’s mainly a physic phenomena. Lubrication process results to be discontinuous since the bearing film needs to be re-established at each meshing action. Elasto-hydrodynamic lubrication theory needs to be applied due to high values of contact pressures. Elasto-hydrodynamic lubrication is characterized by two fundamental facts. First regards **viscosity of the oil film which increases dramatically due to high surface stresses**. Second regards **elastic deformation occurs at the tooth flank contact points**. That’s due to high surface stress. For this reason, engaged tooth flanks flatten under load. Tooth flanks are kept out of direct contact by the increase on contact surface and load capacity of the lubricant film, related to its viscosity. Formation of the lubrication gap, depicted in light grey, and pressure distribution in the contact zone are displayed by Plot 6.5-1. By the image, It’s possible to detect a pressure peak arisen before the end of the lubrication gap. Another particular to take into account is the contraction at end of the gap of the lubricant outlet, that’s due to elastic deformation of tooth flank.



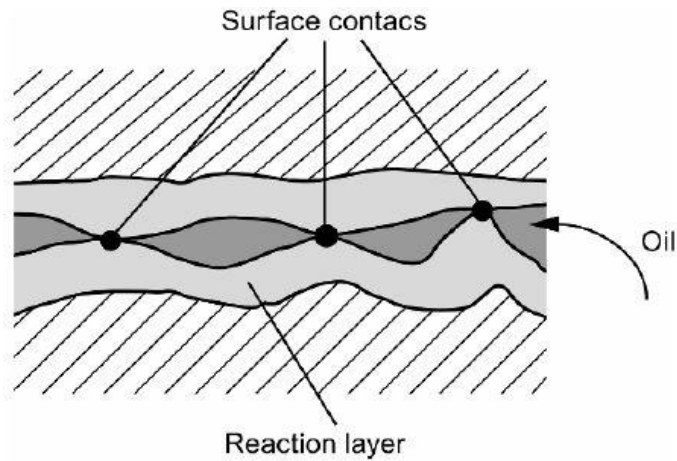
Plot 6.5-1: Formation of the lubrication gap with elasto-hydrodynamic lubrication Ref.[14].

To conclude this topic It’s necessary to underline that thickness of the film of lubrication oil depends mainly by: tooth geometry, viscosity of the lubricating oil, circumferential speed, contact pressure, tooth flank temperature and surface roughness. (Ref.[14])

- **“chemical protective film”**: frequently named boundary layer or reaction layer, It’s mainly a chemical phenomena. When surfaces of meshing teeth gets in touch with mixed friction or boundary friction, wear-reducing additives of lubricant begin their operation. Indeed a chemical protective layer is created on the tooth flanks. Wear-reducing additives are named **E.P.** which stands for **“extreme pressure”**. Alternatively, It’s often employed term **A.W.**, which stands for **“anti-wear”**.



As depicted by Plot 6.5-2, such additives prevent bonding of contact surfaces, forming surface reaction layers which exploits lower shear strength than pure materials. Highly reactive E.P./A.W. additives lead to measurable reaction layers even before their trigger temperature is reached.

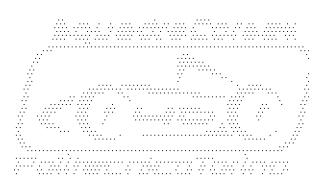
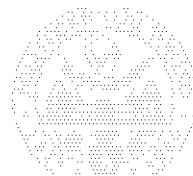
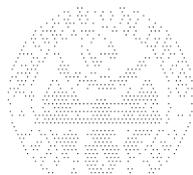


Plot 6.5-2: Mixed friction surface reaction layer, Ref.[14].

Reaction layer is abraded at any cycle of meshing by very high stresses, anyway additives needs to be able to quick regenerate layers. High temperatures due to friction, are very dangerous for the boundary layer. That is going to be destroyed if characteristic temperature of lubricant is exceeded. Composition of the reaction layers depends mainly by mechanical conditions, materials, temperature, lubricant base fluid and, of course, additives. (Ref.[14])

6.5.3. Damages caused by improper lubrication.

By previous dissertations, It's clear that, in field of gears, choice of proper material and proper treatments may not be enough if features of lubrication oil aren't suitable. For this reason, properties of chosen lubrication oil are one of the main input parameters of gear calculation. With reference to Chapter 5.10, importance of lubrication is related to resistance to pitting. By virtue of that, relation for fatigue verification on Hertzian contact, includes a lubrication coefficient. Indeed such coefficient is extracted by Plot 5.10-2, crossing value of σ_{Hlim} with kinetic viscosity of lubrication oil





Picture 6.5-4: Scuffing on tooth flank of the wheel, Ref.[14].

. Anyway, importance of lubrication oil is not limited to pitting resistance, some other damages affect operation of gears. According with Ref.[14], failures in flank lubrication of tooth lead to severe consequences known with the name of **“Scuffing”**.

Failures dependant from wear caused by circumferential speed, are known as **“cold scuffing”**. Wear occurs mostly at low circumferential speeds, $< 5 [m/s]$ and when unsuitable lubricants are applied.

Anyway, scuffing can exhibit in another form known as **“hot scuffing”**. This kind of phenomena arises when lubricant film breaks down due to high temperatures or excessive stresses. This leads to metal-to-metal contact, local welding, and flaking of the tooth flanks. Typical damage caused by hot scuffing is shown by Picture 6.5-4.

Such phenomena is caused by physical and especially chemical processes. At this point, It's necessary to differentiate between two levels of scuffing:

- **“Scoring”**: Individual scoring or clusters of scoring appear in the sliding direction of the tooth flanks. This kind of phenomena can vary from minor to serious. Scoring appears in combination with additive-treated oils and circumferential speeds $< 30 [m/s]$. (Ref.[14])
- **“Scuffing”**: This phenomena exhibits in three different ways. One displays individual fine lines, known as “scuffing lines”. Other displays clusters, known as “heavy scuffing”. Last displays areas across the full face width, known as “scuffing zones”. The main feature of the scored areas is a matt appearance. Scuffing appears in combination with non-additive treated and additive-treated oils both. Usually appears at circumferential speeds $> 30 [m/s]$. (Ref.[14])

By previous dissertation, It's clear that scuffing process is critically affected by the gearwheels heating up. The critical temperature is known with name of “tooth flank constant temperature” or “tooth mass temperature”. Tooth flank is constantly exposed to this temperature, even when It's not engaged in gear meshing.

6.5.4. Selection of lubricant characteristics.

Back to Picture 6.5-1 it's time to focus on popup menu located in lower left position of command window. It points to a database in the software where different oils are stored with their own



features and data. Different oils of software database are identified by **I.S.O. 3448** standard, even if automotive and motorsport lubricants are often commercialized with **S.A.E. J306** identification. Following with the topic, it would be important make a clarification about equivalences on different standards. Table 6.5-2 is going to be the key.

In order to perform a good choice about lubricant, It's suitable have a good knowledge about their composition. According with Ref.[14], modern lubricants are made up of several constituents, starting point is a base oil meshed with proper additives. By the way, lubricants are distinguished on two main families: "**mineral oils**" and "**synthetic oils**".

Basically, mineral oils are used as base oil for manufacturing gear-box oils. Various qualities of mineral oils are distinguished by their **V.I.**, the "**viscosity index**". Such dimensionless parameter describes the properties of the base oil depending temperatures. As declared in advance at Chapter 6.5.2, lubrication oil needs to be stable independently from temperature variation. A quality oil needs to be liquid enough at low temperatures, without becoming excessively liquid at high temperatures. Low value of V.I. means large variation of viscosity due to temperature, while an high value means a very tight variation. Values of V.I. for a good mineral oil are approximately around $95 \div 105$. While high-quality mineral oils display a V.I. greater than 150 . Synthetic oils are employed where extremes of temperatures, below -20°C and above 140°C are reached.

Characteristics of gear-box oils are strongly affected by "**additives**" and "**packages**", as previously declared at Chapter 6.5.2. Term package refers to a gear-box oil in which additives represent $2 \div 10\%$ of the entire volume. Most common additives for gear-box lubricants are:

- **E.P.** additives for improving high-pressure characteristics.
- **Corrosion inhibitors** for preventing rust, verdigris and harmful products of oxidation.
- **D.D.**, detergent and dispergent, are additives for removing dirt.
- **Friction modifiers** which reduce friction and wear.
- **V.I. improver** to improve high and low temperature performance. (Ref.[14])

Employ of additives enables to create oils for different purposes. Anyway, action of the various additives should be complementary.

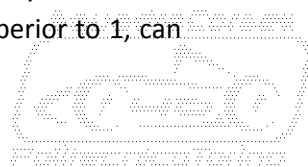
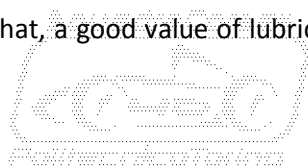
Most important feature of gear-box oil is its flow-ability, or **viscosity**. Such parameter describes the internal friction of a fluid. As declared in advance, lubrication oils are classified on the base of their viscosity and are divided into different viscosity groups. The kinetic nominal viscosity can determined as a function of the surface stress and the sliding speed.

Gearwheels to design are specific for motorsport employ, that means slim thickness of teeth which leads to high surface pressures applied on flanks of teeth. For this reason, oil film needs to be strong enough to sustain high values of applied pressure, without loose the continuity on the stressed area. Proper value for thickness of the lubricant film can be determined applying elasto-hydrodynamic theory. According with Ref.[14], parameters to take into account are:

- Mechanical stress.
- Circumferential speed.
- Effective temperature.
- Kinematic viscosity of the lubricant: high viscosity, high thickness.

Value of film thickness can be adequate when it is larger than the average surface roughness of the tooth flank surface. Alternatively, the lubricant viscosity required to provide a bearing film of sufficient thickness for a given gear system, can be determined when the operating conditions are known. Resistance to scuffing and pitting of gears is improved by viscosity increase.

With reference to Chapter 5.10, which treats verification to pitting, It's possible to analyze Plot 5.10-2 again. It's easy to notice that, a good value of lubrication factor, equal or superior to 1, can

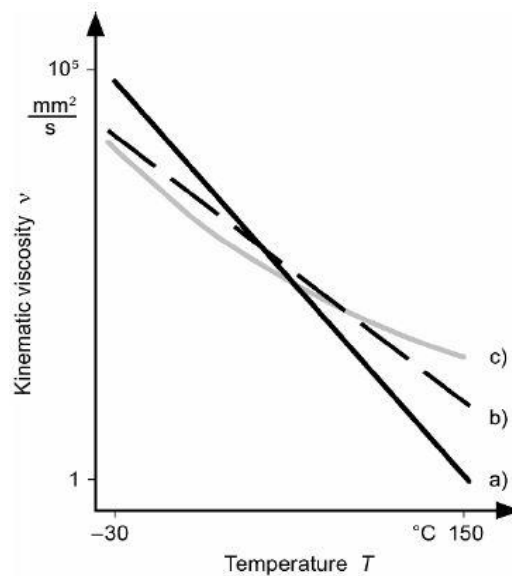


be obtained only through an high value of kinetic viscosity. Anyway It's necessary to notice that viscosity values are sensibly higher to that employed for gears nowadays.

However, It's not so useful employ oils with too high values of viscosity, if It is too great negative effects can be exploited. It's necessary to remind that high viscosity leads to high friction between lubricant and gearwheels. That's a very dramatic condition for efficiency and temperature.

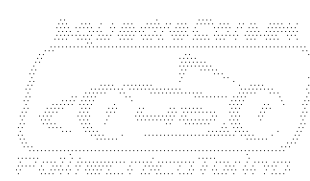
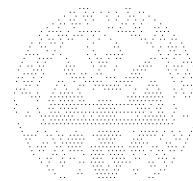
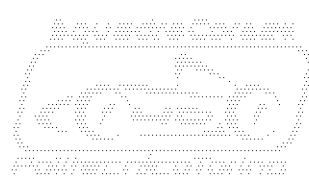
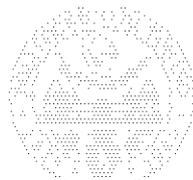
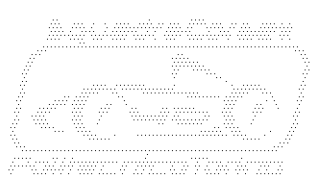
For these reasons, selection of a lubricant provided of a right value of viscosity is always a compromise between different factors.

By virtue of that, It can be useful knowing behaviour of viscosity depending on **temperature**. Basically, viscosity exponentially decreases as temperature increases. By the way, It's useful examine the log-log Ubbelohde diagram of Plot 6.5-3 which displays three curves: a) is the profile related to mineral based oils, b) is related to synthetic oils based on poly- α -olefins, c) is related to synthetic oils based on polyglycol. From a brief analysis, It's clear that stability of mineral based oils is not so high, while stability of polyglycol-based oils is considerably better.



Plot 6.5-3: Temperature dependent behaviour of different families of lubricant, Ref.[14].

On the other hand, It can be useful analyze some numeric values. Table 6.5-1 shows behaviour under temperature variation of different types of lubrication oils. Red values represent standard viscosity which identifies the lubricant at 40°C, according to **I.S.O. 3448** standard. Moreover, plot can be useful to evaluate spectrum of viscosity regarding different gear-box lubricants.



Viscosità cinematica Kinetic viscosity		5	10	22	32	46	68	77	100	150	220	320	460
- 20 °C	cSt mm ² /s	75	310	1290	1950	5200	9900	12.200	15.600	32.000	60.000	110.000	190.000
- 10 °C	cSt mm ² /s	57	140	480	690	1650	2990	3550	4600	8900	15.000	27.500	43.000
0 °C	cSt mm ² /s	30	70	210	300	630	1090	1300	1620	2950	5100	8450	13.000
+ 20 °C	cSt mm ² /s	12	26	60	80	143	226	265	316	534	840	1300	1900
+ 40 °C	cSt mm ² /s	5	10	22	32	46	68	80	100	150	220	320	460
+ 60 °C	cSt mm ² /s	3.3	6.5	12	14	21	29.5	32.5	38.5	57	79.5	110.5	160
+ 80 °C	cSt mm ² /s	2.2	4.3	7	7.8	11.5	15.2	17	19.2	27.1	36.4	48.2	65
+ 100 °C	cSt mm ² /s	1.6	3	4.5	5	7	9	10	11	15	19.5	25	32
+ 150 °C	cSt mm ² /s	0.8	1.5	2.1	2.2	2.9	3.5	3.8	4.1	5.3	6.5	7.9	9.5

Table 6.5-1: Kinetic viscosity of lubrication oils vs. temperature.

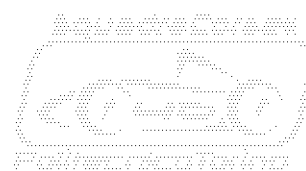
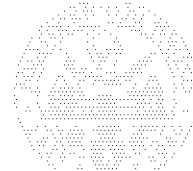
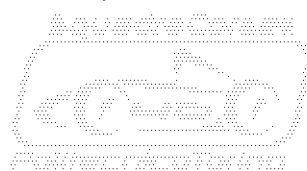
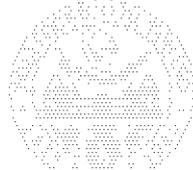
Another factor which strongly affects viscosity is **pressure**. By theory of elasto-hydrodynamic lubrication, It's known that pressure causes a dramatic increase of viscosity. Its value increases exponentially depending on tooth flank pressure. By virtue of that, It's clear that an highly stressed gear doesn't require so high values of viscosity, because the risk is a too high viscosity under operation. By the way, chosen value of viscosity needs to be well balanced. (Ref.[14])

Other two parameters to take into account are temperatures, known as "**pour point**" and "**flash point**". The pour point describes flow properties at low temperatures, It must be, at least, 5 K below the lowest operating temperature. The flash point can be ignored in all, but a few critical high-temperature applications that do not apply in automotive engineering. (Ref.[14])

In order to conclude such dissertation, It' necessary to consider that gear-box is a complex system, which integrates many components with a wide range of materials. Most critical components are seals. Indeed gaskets must not change in terms of their material characteristics under the influence of gear-box oils. In the specific, seals must not shrink, swell or become brittle. Damage gaskets shouldn't deposit any material which could lead to impairment of the oil's characteristics. For this reason, a check on **compatibility of seals** is always recommended. (Ref.[14])

Unfortunately, all data needed to perform an accurate choice on the lubricant based on numerical verifications aren't available. Some needs to be provided by supplier, other needs to be obtained by experimental tests. Anyway, this dissertation provides some guidelines useful to perform a first attempt choice. Furthermore, Kisssoft software is provided of algorithm an data necessary to perform all needed verifications on the chosen lubricant oil.

For many seasons, Squadra Corse have been supported by the Italian dealer of Motul, the famous French producer of lubricants and care products for car and motorbikes. By virtue of that, supplier recommended some products of its range, on the base of primary information regarding gear-box project. Four types of lubricant have been proposed, two are synthetic, **75W-90** and **75W-140**, two are mineral, **80W-90** and **HD 80W-90**. On the basis of datasheets included at Appendix 3, Appendix 4, Appendix 5 and Appendix 6, first attempt choice have been performed.



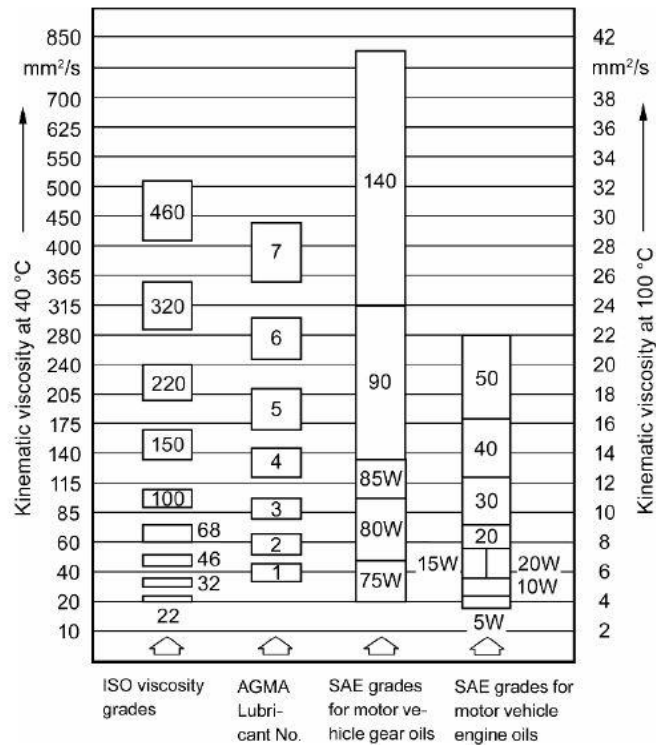


Table 6.5-2: Correlation of different standards regarding lubricants, Ref.[14].

Lubricant selected is **GEAR 300 75W-90**, a 100% synthetic oil ester based. Main features, are the very high index of viscosity which implies a wide temperature range between pour point and flash point. It's necessary underline that pour point It's not a big issue for S.C.R. project. Large majority of tests and races, first of all, take place in the summer. For this reason, lowest operation temperature is going to coincide with summer environmental temperature. On the other hand, a very large value of flash temperature is an important caution. Compatibility with gaskets is guaranteed. In addition, high finish of gears suggests that choice of lowest value of viscosity in the proposed range, is probably the best solution.

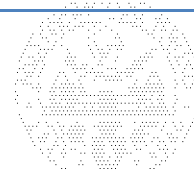
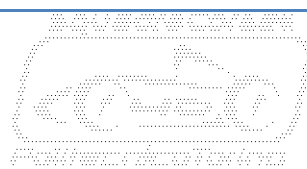
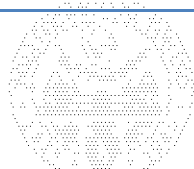
Final step of this process is find a correlation between chosen lubricant and **I.S.O. 3448** standard. By Table 6.5-2, It's clear that **75W** corresponds to **I.S.O. VG 46**, which can be set on the popup menu shown by Picture 6.5-1. Finally, lubrication choice is going to be confirmed at the end of software calculations.

6.6. Results of first stage of reduction calculus.

Parameters set up in previous chapters are sufficient to perform all calculation stages with KISSsoft software. Following, It's possible to evaluate results.

Main results have been ordered on two different tables: Table 6.6-1 is related to main geometrical dimensions, while Table 6.6-2 is related to indexes necessary to evaluate safety and performances of gearwheels. Content of tables is going to be briefly clarified and evaluated.

		Gearwheel 1	Common	Gearwheel 2	[unit]
Normal External Module	m_{et}	/	3,96	/	[mm]
Number of Teeth	z	11	/	31	[teeth]



Face Width	b	/	19	/	[mm]
Normal Pressure Angle	α_{n12}	/	20	/	[°]
Intermediate Spiral Angle	β_m	/	30	/	[°]
Shaft Angle	Σ	/	90	/	[°]
External Pitch Diameter	d_e	43,55	/	122,73	[mm]
Inner Tip Diameter	d_i	36,27	/	87,72	[mm]
Tip Diameter	d_a	52,67	/	124,01	[mm]
Pitch Angle	δ	19,54	/	70,46	[°]
Root Angle	δ_f	17,23	/	64,46	[°]
Tip Angle	δ_a	25,54	/	72,77	[°]
Profile Correction Factor	X	0,3927	/	-0,3927	[dim.less]

Table 6.6-1: Main geometrical parameters of first stage of reduction.

Analyzing Table 6.6-1, first element to take into account is module. Differently from what declared at Chapter 5.4, **module** is not a standard quantity for bevel gears. Observing geometry of tooth, value of module starts from a minimum value located in the closest to gear apex extremity. Value of module increases constantly toward opposite extremity where maximum value is located. That shown in table is maximum value, related to external position. Moreover, teeth profile is not straight, for this reason, value of module changes in relation with plan on which it's measured. Value of module displayed on the table is that measured on the plan normal to spiral profile.

Next dissertations have to be done on **number of teeth** of drive wheel. As depicted in advance at Chapter 6.2, Gleason-Duplex geometry hallows to design pinions with number of teeth considerably lower than values obtained by relation Eq. 5.3-1. Value of **11 [teeth]** calculated by Kisssoft is the clear evidence.

It's necessary to take notice that **face width** looks to be larger than expected, compared to adopted modulus. Anyway, following Table 6.6-2 is going to show that flank safety coefficients are just enough.

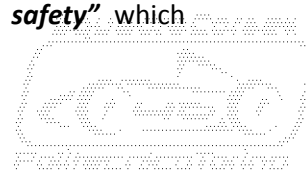
Means and choice of α_n , β_m and X parameters is widely explained at Chapter 6.2. All other variables are broadly explained at Chapter 5.11 by two dimension drafting and related formulas.

By analysis of Table 6.6-2, first index to take in consideration is **overlap ratio**, widely explained at Chapter 5.7. It's clear that resulting value is quite low, that leads to noise and vibrations of the gear. Anyway value is greater than **1,000 [teeth]** and comfort is not a priority of a motorsport project.

		Gearwheel 1	Common	Gearwheel 2	[unit]
Overlap Ratio	ϵ	/	1,1472	/	[teeth]
Root Safety Coefficient	SC_r	3,7303	/	4,0068	[dim.less]
Flank Safety Coefficient	SC_f	1,2856	/	1,3683	[dim.less]
Scuffing Safety, mean T°	SC_{sm}	/	5,7625	/	[dim.less]
Scuffing Safety, instant T°	SC_{si}	/	7,1544	/	[dim.less]
Efficiency	η	/	97,347	/	[%]

Table 6.6-2: Main performance indexes of first stage of reduction.

About safety coefficients, It's necessary to clarify that are referred to fatigue cases. **“root safety”** expressed by software terminology coincides with the safety factor of “fatigue verification in bend” widely explained at Chapter 5.8. Its value looks quite elevate for a motorsport project where safety coefficients should be around **1,2000 [dim.less]**. Anyway limiting factor is **“flank safety”** which



coincides with safety factor of **“fatigue verification on hertzian contact”**. Its value referred to drive wheel is completely suitable to the project.

“Scuffing safety” consists of two different safety coefficients calculated on the basis of theory displayed at Chapter 6.5. One coefficient refers to calculated mean temperature of the gear, other refers to calculated instant temperature around teeth meshing zone. Both values of coefficients are widely satisfying, that’s a proof of the right choice of the lubrication oil.

Anyway, all safety coefficients are greater than 1,2000 [dim.less], for this reason, It’s possible to state that gear of the first stage is going to work safely for all of 100 [h] of the esteemed operational life.

After observations about safety in operation, It’s necessary consider **“Efficiency”**. It’s possible to state that value displayed in Table 6.6-2 is satisfying compared to mean values which are displayed by Table 4.3-1.

In order to examine in deep features of first stage gear, It’s possible to consult Kisssoft report annexed at Appendix 1.

6.7. Results of second stage of reduction calculus.

Identically to what done in the previous chapter, main results of calculations have been grouped on two Tables: Table 6.7-1, Table 6.7-2.

By analysis of Table 6.7 1, first element to observe is **modulus**. Differently from previous case, value have been chosen between standard values of Table 5.4 2 as prescribed by **U.N.I. 6587** standard.

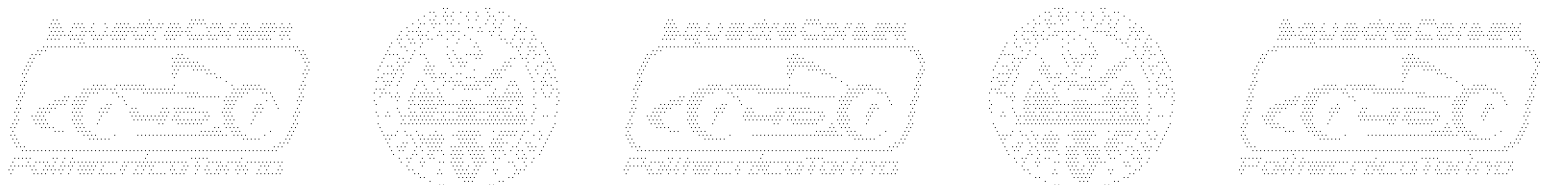
		Gearwheel 3	Common	Gearwheel 4	[unit]
Module	m	/	3,00	/	[mm]
Number of Teeth	z	19	/	61	[teeth]
Face Width	b	17	/	15	[mm]
Normal Pressure Angle	α_n34	/	20	/	[°]
Helix Angle	β	/	0	/	[°]
Pitch Diameter	d	57,00	/	183,00	[mm]
Tip Diameter	d_t	65,30	/	186,70	[mm]
Root Diameter	d_r	51,80	/	173,20	[mm]
Base Diameter	d_b	53,56	/	171,96	[mm]
Offset	o_34	/	120,00	/	[mm]
Profile Correction Factor	X	0,3830	/	-0,3830	[dim.less]

Table 6.7-1: Main geometrical parameters of second stage of reduction.

Taking into exam **number of teeth**, It's clear that value related to pinion is greater than value which It's possible to calculate by Eq. 5.3-1:

$$\text{Eq. 6.7-1} \quad z_{3min} = 15,098 \text{ [teeth]}$$

Regarding z_{3min} , It would be enough a value of 17 [teeth], anyway value have been increased to 19 [teeth] in order to satisfy the boundary fixed on $o_{3,4}$ which is the offset of the gear.



About **face width**, It's necessary notice that values related to gearwheels are different each others. Face width of drive wheel have been increased of 2 [mm] respect to face width of driven wheel. This solution has two-fold effect. First is related to lubrication, pinion is in contact with oil in the sump. A larger face width helps to improve splashing of lubrication oil. Second effect is structural, while pinion is always the most stressed gearwheel, larger face width obviously improve strength of teeth.

About other parameters and variable quantities displayed on Table 6.7-1, nothing of unusual have been noticed, for this reason It's useful going on with analysis of performance indexes.

		Gearwheel 3	Common	Gearwheel 4	[unit]
Overlap Ratio	ϵ	/	1,5778	/	[teeth]
Root Safety Coefficient	SC_r	2,0502	/	1,7029	[dim.less]
Flank Safety Coefficient	SC_f	1,5341	/	1,267	[dim.less]
Scuffing Safety, mean T°	SC_{sm}	/	3,6254	/	[dim.less]
Scuffing Safety, instant T°	SC_{si}	/	4,8192	/	[dim.less]
Efficiency	η_{34}	/	98,862	/	[%]

Table 6.7-2: Main performance indexes of second stage of reduction.

About **overlap ratio**, value is increased if compared to previous case, anyway It's still lower than 2,000 [teeth]. By virtue of that, operation of second stage too is going to be affected by noise and vibrations.

About **root safety** and **flank safety**, It's possible to notice that limiting factor is flank in this case too. Differently from previous case and from usual, coefficients of the drive wheel are greater than coefficients of driven. Reason is trivial to be understood, because face width of drive wheel is greater than driven, as explained in advance. Anyway coefficients are well balanced because range of values varies from 1,2670 [dim.less] to 2.0502 [dim.less].

Values of coefficients related to **scuffing safety** are large enough. By virtue of that, It's possible to state that working of gear, is going to be safe for all operational life of the vehicle, which is esteemed around 100 [hours].

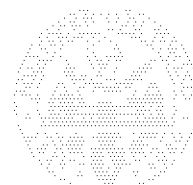
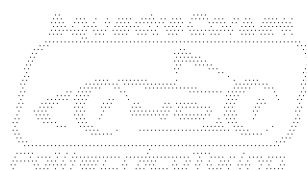
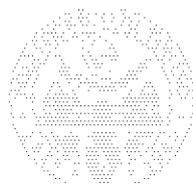
In order to gain a more complete idea about performance of gears, It's necessary to take into account parameter of **efficiency**, on Table 6.7-2. Displayed value represents displays a magnitude suitable with target of the project, like expected. It's then possible calculate η_{tot} which represents the "**total efficiency of gear-train**":

$$\text{Eq. 6.7-2} \quad \eta_{tot} = \eta_{1,2} \cdot \eta_{3,4} = 96,239 \text{ [%]}$$

To finally conclude actual dissertation, It's useful calculate i_{act} the "**actual gear ratio of gear-train**", as done for efficiency parameter.

$$\text{Eq. 6.7-3} \quad i_{act} = \frac{z_2}{z_1} \cdot \frac{z_4}{z_3} = 9,05 \text{ [dim. less]}$$

It's possible to observe that result of Eq. 6.7-3 is about 5% higher than ideal value declared by Eq. 4.4-1. By virtue of that, with reference to values displayed by Eq. 6.2-1 and Eq. 6.3-2, total tolerance on the gar ratio value can be considered fully respected.



7. Design of shafts.

Once mechanical and packaging boundaries are defined, gears are designed, It's possible to design shafts. Forces transmitted by gears are those acting on shafts, generating stresses and displacements.

Typical layout of a two stages gear-box consists of three shafts. Input shaft, identified as **"shaft 1"** needs to be coaxial with motor, like displayed by Plot 4.2-1. Such shaft represents the link between motor and first stage of reduction. For this reason, shaft 1 needs to integrate female sp-lined profile of the motor and drive wheel of first stage, indicated as **"gearwheel 1"**.

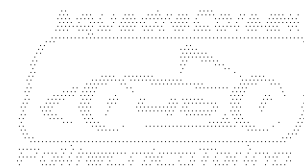
Intermediate shaft, identified as **"shaft 2"**, lays on the plan identified by axis of two motors. Such shaft represents the link between first stage and second stage of reduction. By virtue of that, shaft 2 integrates driven wheel of first stage, indicated as **"gearwheel 2"**, and drive wheel of second stage, indicated as **"gearwheel 3"**. Both wheels are rigidly connected in order to spin at the same angular speed.

Output shaft, identified as **"shaft 3"**, lays on a plan parallel to the ground. Position on z-axis of such plan is identified by radius of deformed tire, as depicted by Plot 4.2-2. Shaft 3 represents the mechanical link between second stage of reduction and half shaft. For this reason, It needs to integrate driven wheel of second stage, indicated as **"gearwheel 4"** and tripod housing of half shaft. Moreover, as depicted by Picture 1.3-7, shaft 3 needs to integrate rear brake disc which transmits additional forces and stresses.



Plot 6.7-1: Gearwheels nomenclature.

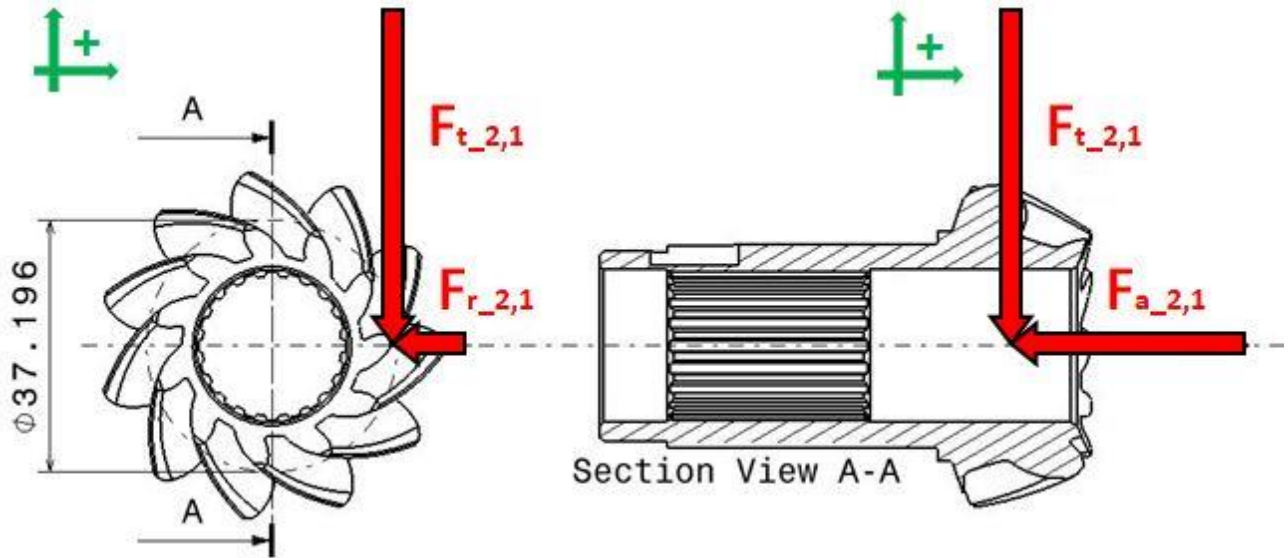
Anyway, design of shafts cannot be performed on the base of gears only. Design of shafts must take into account external boundaries and any other issue related to packaging. However, first aspect to consider is integration with bearings. By virtue of that, diameters of shafts are bounded by bore diameters of bearings. Moreover, mounting configuration of bearings strongly affects design of shafts. Angular contact bearings, in particular, needs to operate under a well determined preload which requires calibrated shims or ring nuts to be properly tuned. Anyway, first step of design is calculation of loads acting on transmission. How It's possible to notice by following chapters, three different cases are analyzed.



7.1. Forces acting on shafts, driving case.

Another important output of calculation performed by Kisssoft software is represented by system of forces exchanged by gearwheels during operation. Actual Chapter 7.1 analyzes system of forces generated by gears during driving condition, that occurs when motors supply power.

Such system of forces is derives by application of T_{end} , which is the maximum torque which is possible discharge to the ground, as widely explained at Chapter 4.1. In order to proceed in a organized way, It's necessary to study each shaft by a free-body plot. By virtue of that, It's necessary proceed studying forces inducted by gear meshing on shaft 1.



Plot 7.1-1: Gear meshing forces on Shaft 1, driving condition.

Analyzing Plot 7.1-1, It's possible to notice two different views of the shaft that are useful to display all meshing forces acting on drive wheel of first stage of reduction. Like It was declared in advance at Chapter 4.2.3, meshing of bevel gears generates a force which needs to be fractionate on 3 components: tangential, radial and axial.

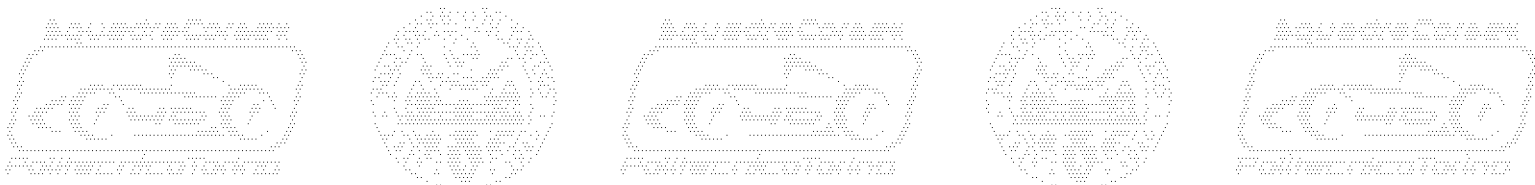
- $F_{t2,1}$ is **“tangential force of first gear in driving condition”** which driven wheel 2 transmits to drive wheel 1. It's defined by relation Eq. 5.4-2.
- $F_{r2,1}$ is **“radial force of first gear in driving condition”** which driven wheel 2 transmits to drive wheel 1.
- $F_{a2,1}$ is **“axial force of first gear in driving condition”** which driven wheel 2 transmits to drive wheel 1.

Basically, previous forces represent components of reaction force which driven wheel 2 opposes to drive wheel 1 during gear operation.

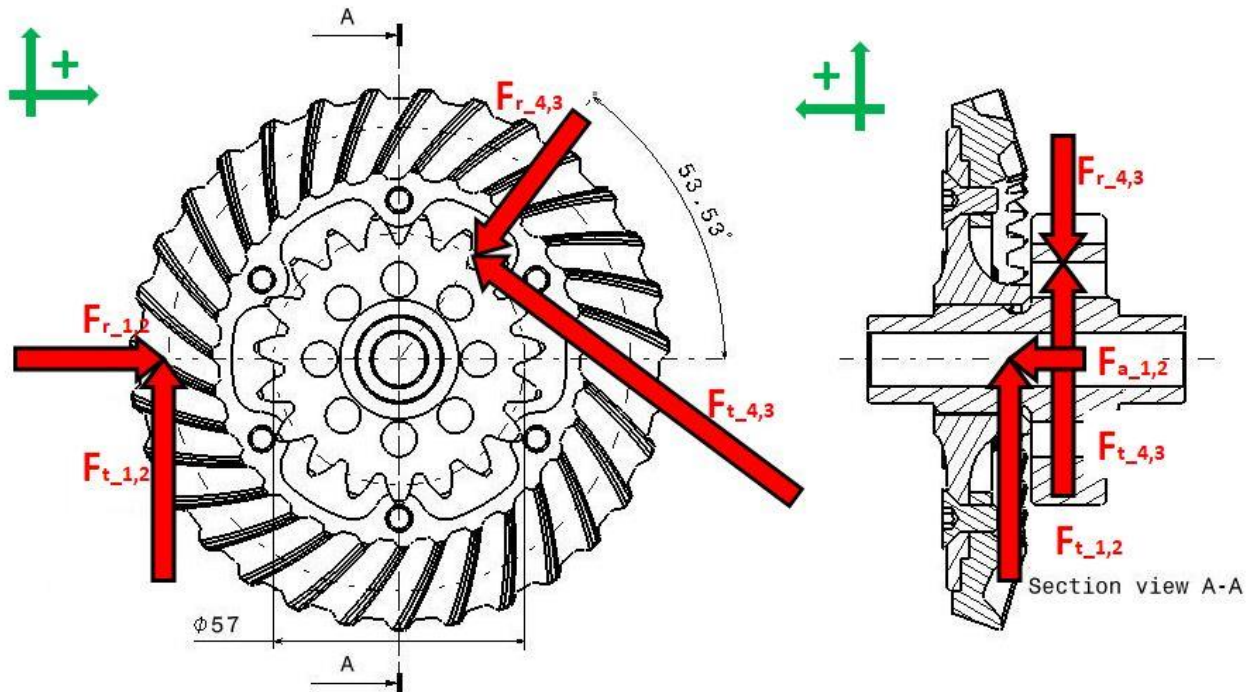
Eq. 7.1-1 $F_{t2,1} = -2.151[N]$

Eq. 7.1-2 $F_{r2,1} = -439[N]$

Eq. 7.1-3 $F_{a2,1} = -1.492[N]$



The same way to operate can be applied to shaft 2, which is depicted by Plot 7.1-2. By exam of the plot, first aspect to take into account is that shaft 2 integrates two gearwheels, for this reason system of forces is more complex than previous case. As declared in advance, every bevel gearwheel is subject to a force that needs to be fractionate on 3 vectors.

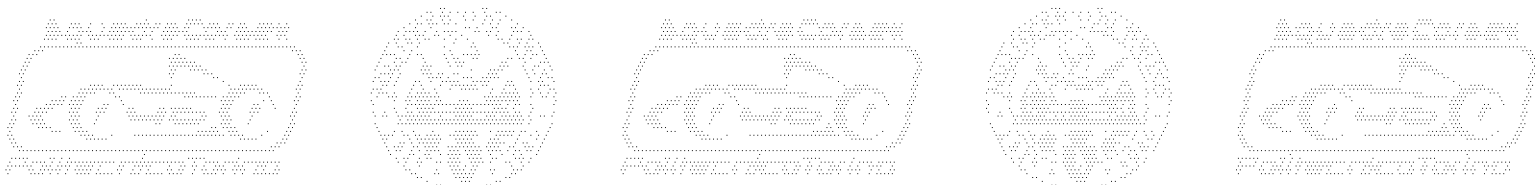


Plot 7.1-2: Gear meshing forces on Shaft 2, driving condition.

In the specific, vectors need to be opposite in sign respect to vectors displayed on Plot 7.1-1. Other gearwheel acting on shaft 2 is spur, for this reason meshing force needs be fractionate on 2 only vectors, tangential and radial. It's necessary to notice that offset of second stage of reduction features a diagonal position referred to car axis system. Plot 7.1-2 display meshing force of second stage of reduction, fractioned along gear offset and perpendicular direction. Therefore, intermediate shaft is subject to 5 gear meshing vectors in total:

- $F_{t1,2}$ is “**tangential force of first gear in driving condition**” which drive wheel 1 transmits to driven wheel 2.
- $F_{r1,2}$ is “**radial force of first gear in driving condition**” which drive wheel 1 transmits to driven wheel 2.
- $F_{a1,2}$ is “**axial force of first gear in driving condition**” which drive wheel 1 transmits to driven wheel 2.
- $F_{t4,3}$ is “**tangential force of second gear in driving condition**” which driven wheel 4 transmits to drive wheel 3. It's defined by relation Eq. 5.4-2.
- $F_{r4,3}$ is “**radial force of second gear in driving condition**” which driven wheel 4 transmits to drive wheel 3.

Basically forces acting on bevel gearwheel represent forces which propel intermediate shaft, while forces acting on spur gearwheel represent reaction which driven wheel 4 opposes to drive wheel 3.



Eq. 7.1-4 $F_{t1,2} = 2.151[N]$

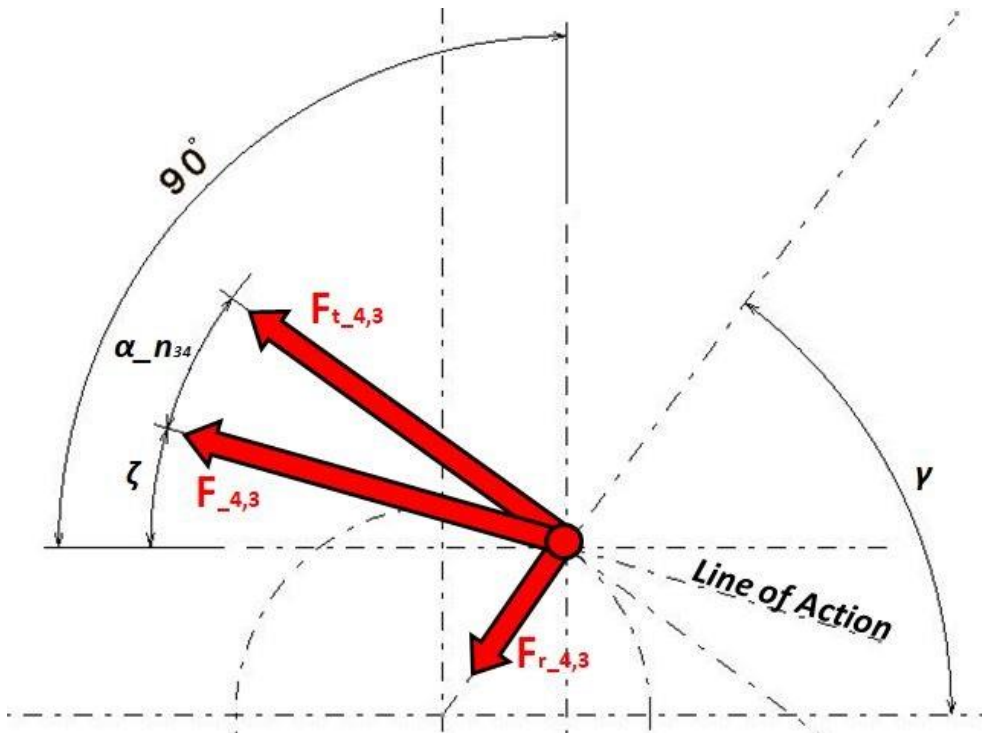
Eq. 7.1-5 $F_{r1,2} = -F_{a2,1} = 1.492[N]$

Eq. 7.1-6 $F_{a1,2} = -F_{r2,1} = 439[N]$

Eq. 7.1-7 $F_{t4,3} = 3.955[N]$

Eq. 7.1-8 $F_{r4,3} = 1.467[N]$

Observing Plot 7.1-2, It's possible to notice that reaction forces on gearwheel 3 aren't parallel to conventional axis. For this reason, It's clear that gear meshing forces acting on gearwheel 3 need to be decomposed along, X and Z axis in order to be parallel to corresponding forces applied on gearwheel 2. By virtue of that, first step is composition of $F_{t4,3}$, displayed by Eq. 7.1-7, and $F_{r4,3}$, displayed by Eq. 7.1-8, along line of action of second stage gear.



Plot 7.1-3: Composition of forces along line of action, driving condition.

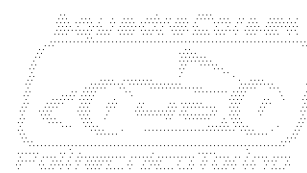
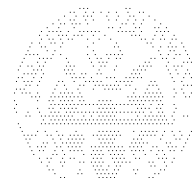
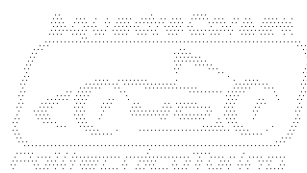
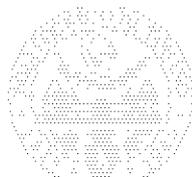
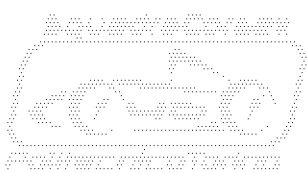
Result of composition is displayed by Plot 7.1-3, $F_{4,3}$ which is the **“total force of second gear in driving condition”**. Its module can be calculated thanks to knowledge of following geometric parameter:

- $\alpha_{n34} = 20^\circ$ is **“normal pressure angle of second stage”** defined at 132Chapter 6.7.

Calculation of module can be performed:

Eq. 7.1-9 $F_{4,3} = \frac{F_{t43}}{\cos \alpha_{n34}} = 4.218 [N]$

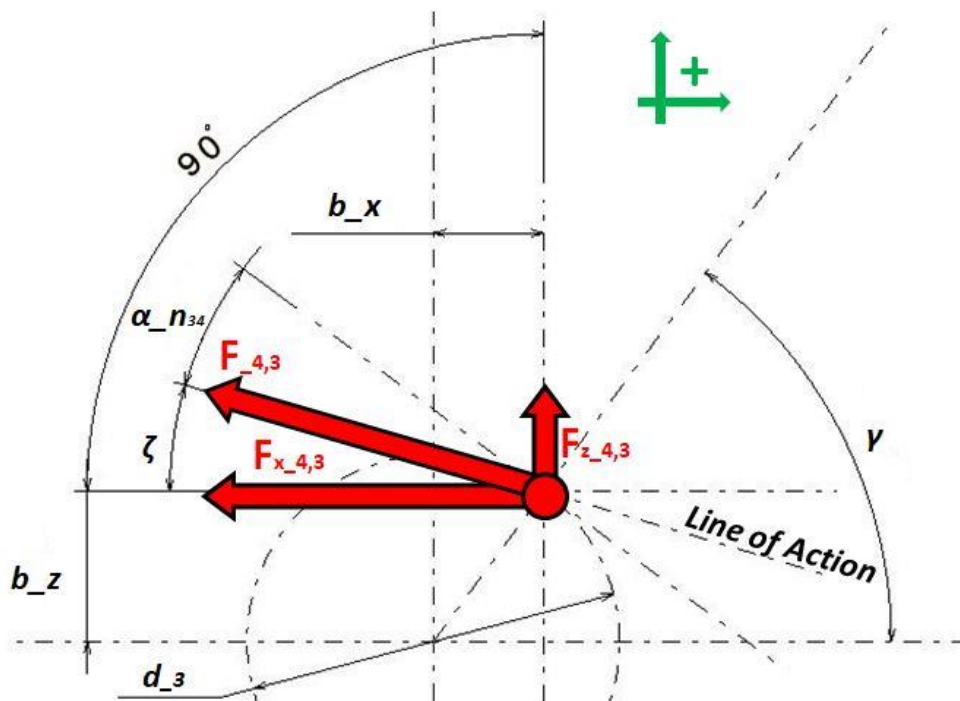
Once $F_{t4,3}$ and $F_{r4,3}$ are composed in $F_{4,3}$ vector, It's necessary doing the opposite operation, decomposing $F_{4,3}$ along X and Z axis. Result of such operation is represented by:



- $F_{x4,3}$ is “**component along x of total force of second gear in driving condition**”. It’s measured in [N] and It’s displayed by Plot 7.1-4.
- $F_{z4,3}$ is “**component along z of total force of second gear in driving condition**”. It’s measured in [N] and It’s displayed by Plot 7.1-4.

Observation of Plot 7.1-4 indicates sense of previous vectors, sign is ruled by convention depicted in green. In order to calculate modulus of $F_{x4,3}$ and $F_{z4,3}$, It’s necessary to present another geometric parameter:

- $\gamma = 53, 53^\circ$ is “**inclination of second stage**” respect to XY plan.



Plot 7.1-4: Decomposition of gear meshing force along XY axis, driving condition.

Calculations can proceed as follows:

Eq. 7.1-10 $\zeta = 90 - \alpha_{n34} - \gamma = 16,47 [^\circ]$

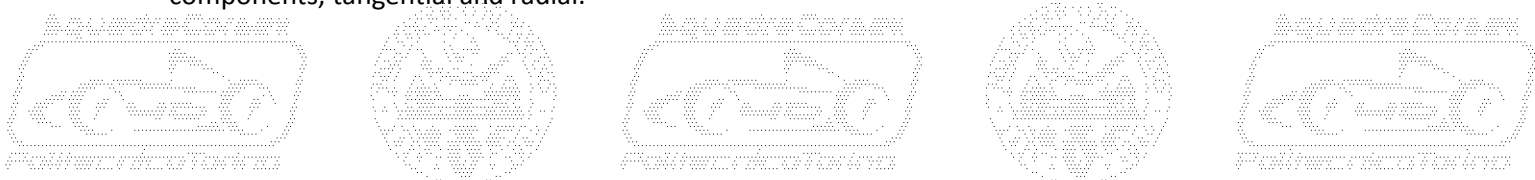
Eq. 7.1-11 $F_{x4,3} = F_{43} \cdot \cos \zeta = -4.045 [N]$

Eq. 7.1-12 $F_{z4,3} = F_{43} \cdot \sin \zeta = 1.196 [N]$

By an accurate analysis of Plot 7.1-4, It’s possible notice other two elements useful for free body diagram set up, levers of forces acting on gearwheel 3:

- $b_x = 16,940 [mm]$ is “**lever parallel to x**”.
- $b_z = 22,919 [mm]$ is “**lever parallel to z**”.

Finally, gear meshing forces acting on shaft 3 can be analyzed. One gearwheel only is connected to shaft 3, the cylindrical spur gearwheel 4. By virtue of that, gear-train acts on the shaft with only two components, tangential and radial:



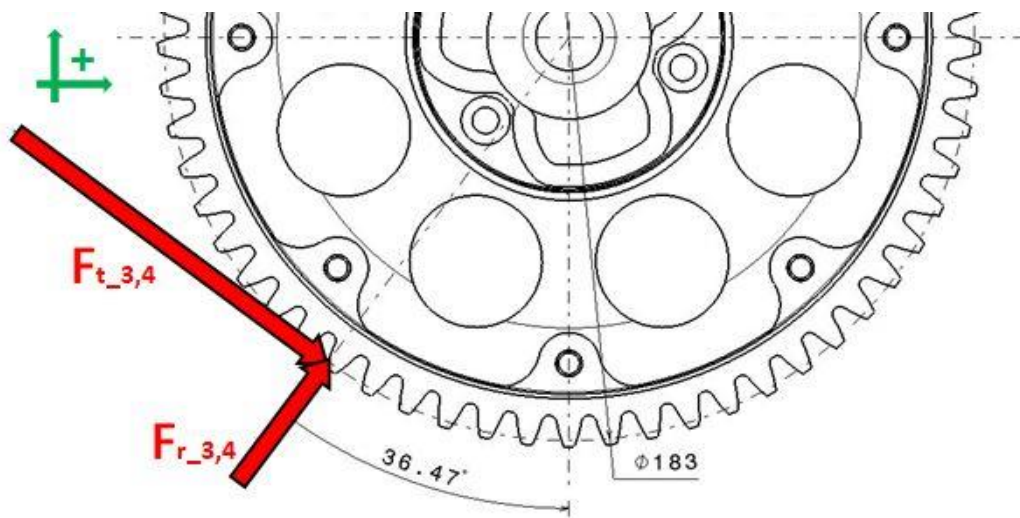
- $F_{t3,4}$ is “*tangential force of second gear in driving condition*” which drive wheel 3 transmits to driven wheel 4.
- $F_{r3,4}$ is “*radial force of second gear in driving condition*” which drive wheel 3 transmits to driven wheel 4.

Such components derive by the fraction of the force which propels the output shaft.

Eq. 7.1-13 $F_{t3,4} = 3.955[N]$

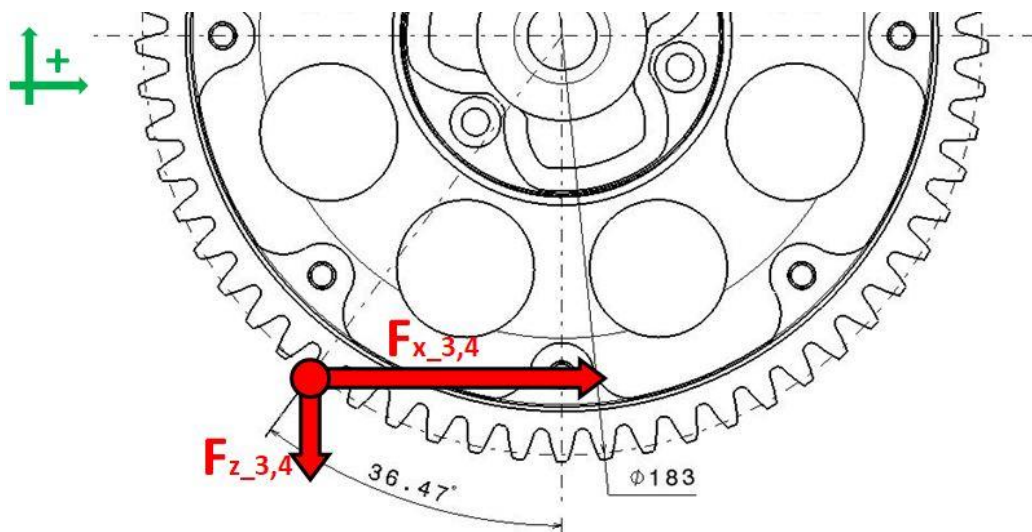
Eq. 7.1-14 $F_{r3,4} = 1.467[N]$

Obviously, propelling forces features contrary signs respect to opposing forces.

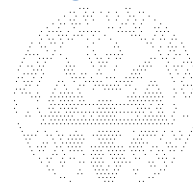
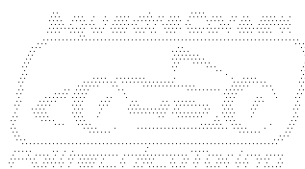
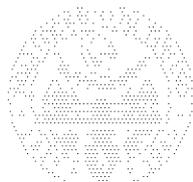


Plot 7.1-5: Gear meshing forces on Shaft 3, driving condition.

As depicted in the previous case, component of forces parallel to X and Z axis are needed to perform calculations.



Plot 7.1-6: Gear meshing forces on Shaft 3, along X and Z axis, driving condition.



By analysis of Plot 7.1-6, It's necessary to observe that displayed vectors are equal, to vectors displayed by Plot 7.1-4 by point of view of module and direction, signs are opposite. By virtue of that:

- $F_{x3,4}$ is "component along x of force transmitted by gearwheel 3 to 4 in driving condition". It's measured in [N].
- $F_{z3,4}$ is "component along z of force transmitted by gearwheel 3 to 4 in driving condition". It's measured in [N].

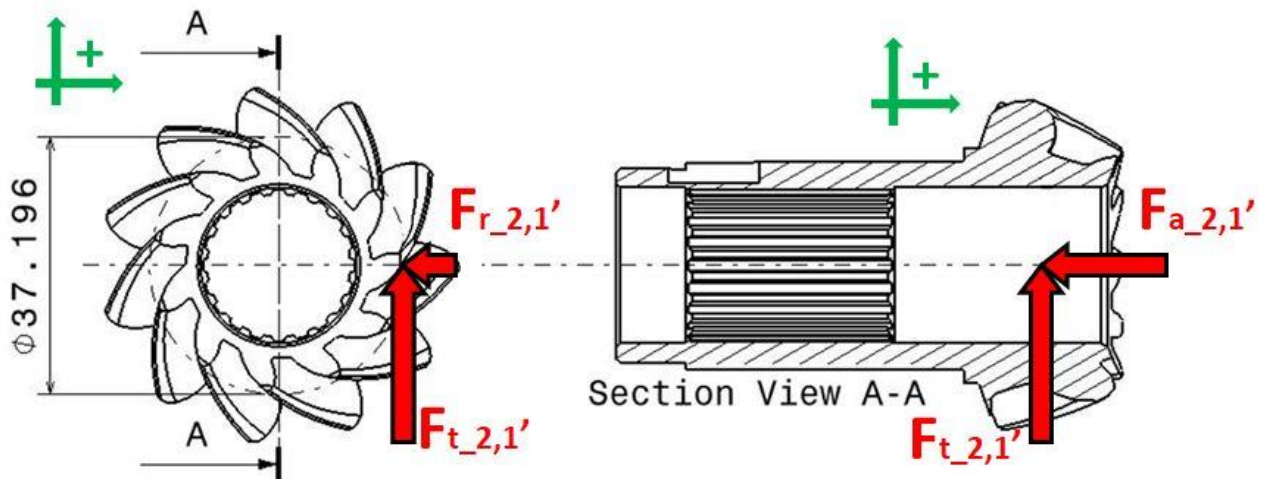
Eq. 7.1-15 $F_{x3,4} = 4.045 [N]$

Eq. 7.1-16 $F_{z3,4} = -1.196 [N]$

Anyway, as declared in advance, shaft 3 integrates rear brake disk too. For this reason, It's necessary to take into account effect of braking events on the entire system.

7.2. Forces acting on shafts, energy recovery case.

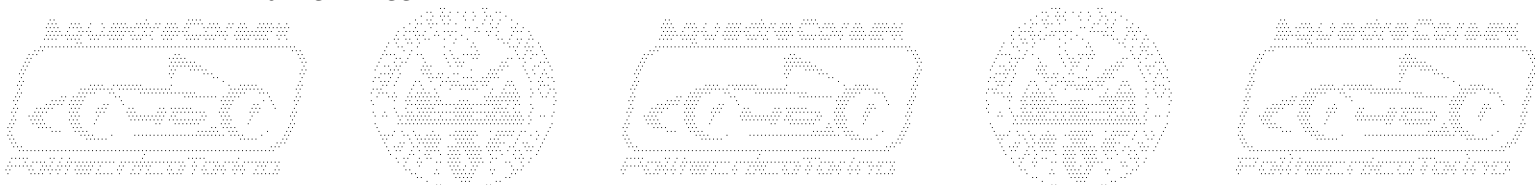
Other operational condition to take into account during calculations is energy recovery case. Such condition needs to be distinguished from driving case because happens when throttle pedal is released and motors are employed to recovery energy. Maximum torque acting on input shaft during recovery condition have been calculated at Chapter 6.1 and is displayed by equation Eq. 6.1-21. It's necessary to observe that value of torque is half respect to value exploited during driving condition, that's due to load transfer which shifts weight from rear to front axle, limiting maximum torque that rear wheels can bear without slip. Half magnitude of torque leads to half magnitude of transmitted forces during gear meshing. Anyway It's necessary to take into account that, during recovery condition, sign of torque is opposite respect to driving condition. That means a change in sign of tangential components of gear meshing forces. Sign of axial and radial components remains the same. Furthermore, It's necessary underline a change in definition of drive and driven wheel.



Plot 7.2-1: Gear meshing forces on Shaft 1, energy recovery condition.

It's possible to notice that Plot 7.2-1 derives from Plot 7.1-1, with inversion of tangential force sign.

- $F'_{t2,1}$ is "tangential force of first gear in recovery condition" which drive wheel 2 transmits to driven wheel 1.



- $F'_{r2,1}$ is “radial force of first gear in recovery condition” which drive wheel 2 transmits to driven wheel 1.
- $F'_{a2,1}$ is “axial force of first gear in recovery condition” which drive wheel 2 transmits to driven wheel 1.

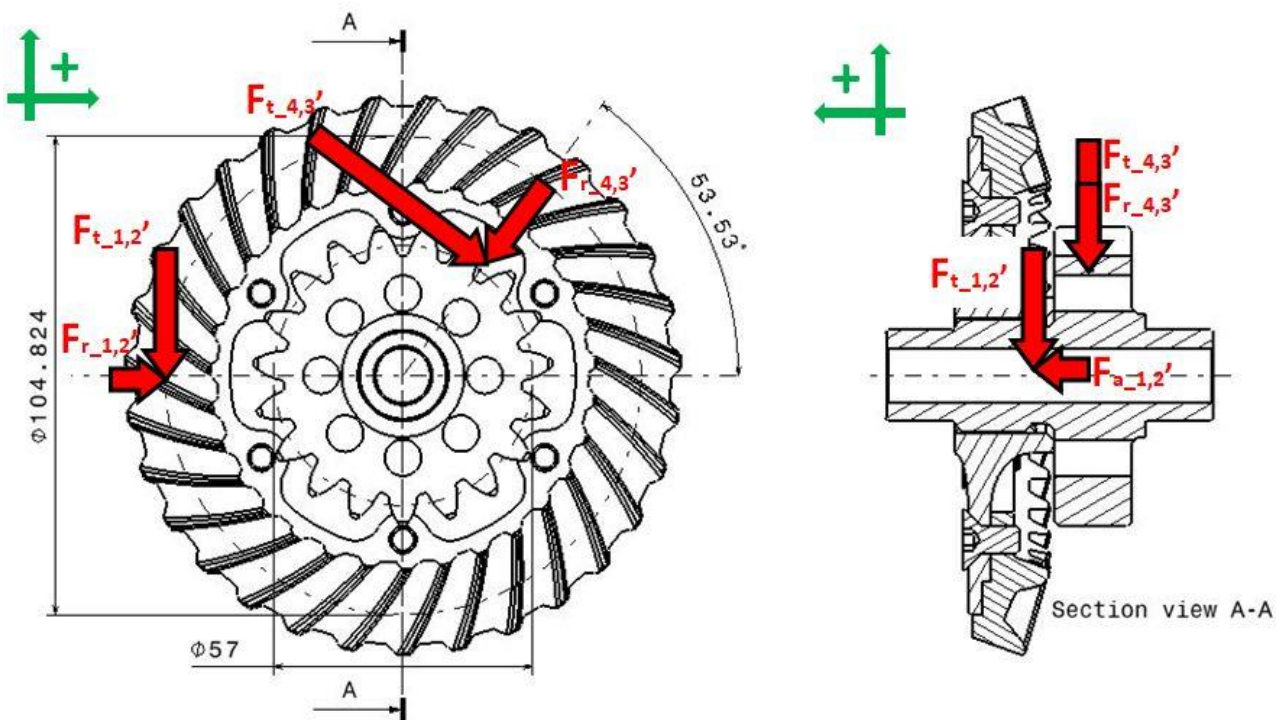
Magnitude of forces is described by following equations:

Eq. 7.2-1 $F'_{t2,1} = 1.076[N]$

Eq. 7.2-2 $F'_{r2,1} = -220[N]$

Eq. 7.2-3 $F'_{a2,1} = -746[N]$

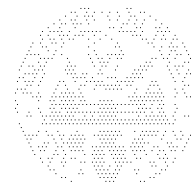
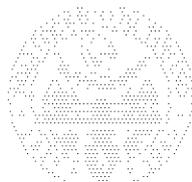
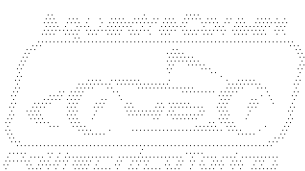
The same way to operate can is applied to shaft 2, which is depicted by Plot 7.1-2.



Plot 7.2-2: Gear meshing forces on Shaft 2, energy recovery condition.

Comparing Plot 7.1-2 and Plot 7.1-2 It's necessary to notice that sign of tangential forces has changed.

- $F'_{t1,2}$ is “tangential force of first gear in recovery condition” which driven wheel 1 transmits to drive wheel 2.
- $F'_{r1,2}$ is “radial force of first gear in recovery condition” which driven wheel 1 transmits to drive wheel 2.
- $F'_{a1,2}$ is “axial force of first gear in recovery condition” which driven wheel 1 transmits to drive wheel 2.
- $F'_{t4,3}$ is “tangential force of second gear in recovery condition” which drive wheel 4 transmits to driven wheel 3. It's defined by relation Eq. 5.4-2.
- $F'_{r4,3}$ is “radial force of second gear in recovery condition” which drive wheel 4 transmits to driven wheel 3.



Basically forces acting on bevel gearwheel represent reaction forces which driven wheel 1 opposes to drive wheel 2, while forces acting on spur gearwheel represent forces which propel shaft 2.

Eq. 7.2-4 $F'_{t1,2} = -1.076[N]$

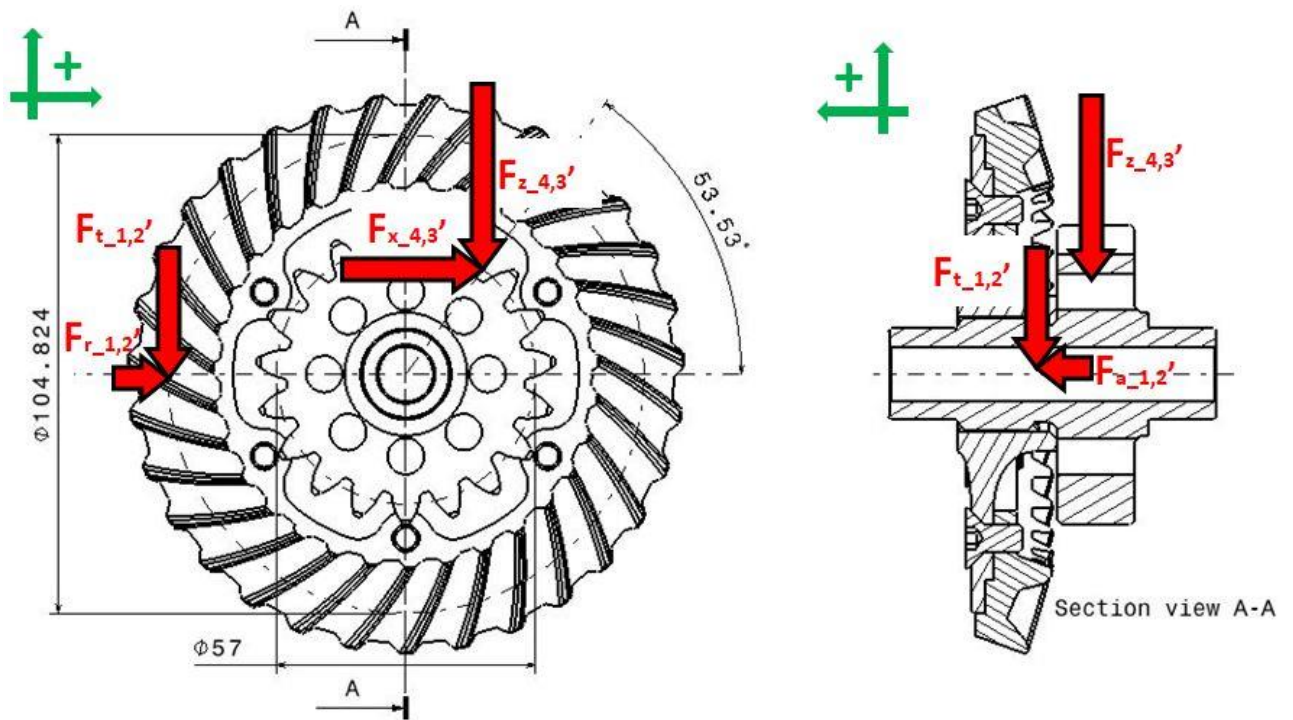
Eq. 7.2-5 $F'_{r1,2} = -F'_{a1,2} = 746[N]$

Eq. 7.2-6 $F'_{a1,2} = -F'_{r1,2} = 220[N]$

Eq. 7.2-7 $F'_{t4,3} = 1.978[N]$

Eq. 7.2-8 $F'_{r4,3} = 736[N]$

Like It was shown by previous case, components of reaction forces on $F'_{t4,3}$ and $F'_{r4,3}$ needs to be parallel to X and Z axis. In order to simplify actual dissertation, operations of composition and decomposition of vectors are omitted, final result is directly shown.



Plot 7.2-3: Gear meshing forces on Shaft 2 decomposed along X and Z axis, energy recovery condition.

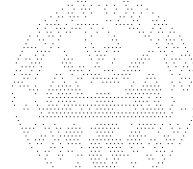
Result of the operation is a system of two vectors:

- $F'_{x4,3}$ is “**component along x of total force of second gear in recovery condition**”. It’s measured in $[N]$, direction and sign are displayed by Plot 7.2-3.
- $F'_{z4,3}$ is “**component along z of total force of second gear in recovery condition**”. It’s measured in $[N]$, direction and sign are displayed by Plot 7.2-3.

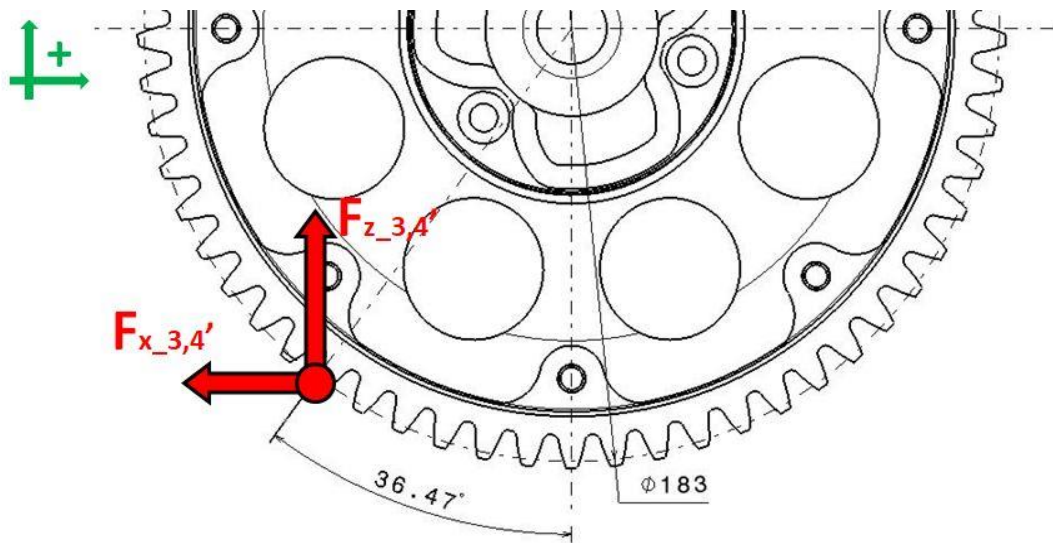
Magnitude of vectors is displayed by following equations.

Eq. 7.2-9 $F'_{x4,3} = 1.165[N]$

Eq. 7.2-10 $F'_{z4,3} = -1.738[N]$



Finally, It's necessary to study Shaft 3 in order to have the complete scenario of gear meshing forces during energy recovery condition.



Plot 7.2-4: Gear meshing forces on Shaft 3, along X and Z axis, recovery condition.

In this case too, It's necessary to notice that vectors are equal to homologous of Plot 7.2-3, for what concerns direction and magnitude. How expected sign is opposite. By virtue of that is useful introduce:

- $F'_{x3,4}$ is “**component along x of force transmitted by gearwheel 3 to 4 in recovery condition**”. It's measured in [N], direction and sign are displayed by Plot 7.2-4.
- $F'_{z3,4}$ is “**component along z of force transmitted by gearwheel 3 to 4 in recovery condition**”. It's measured in [N], direction and sign are displayed by Plot 7.2-4.

Magnitude of vectors is displayed by following equations.

Eq. 7.2-11 $F'_{x3,4} = -1.165[N]$

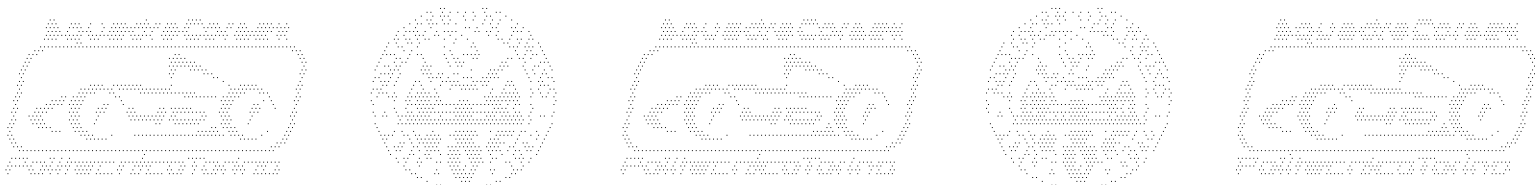
Eq. 7.2-12 $F'_{z3,4} = 1.738[N]$

7.3. Forces acting on shafts, braking case.

Braking and driving condition are in theory two distinguished events, thus It's necessary to study which of the two events represents the worst load case for the gear-box.

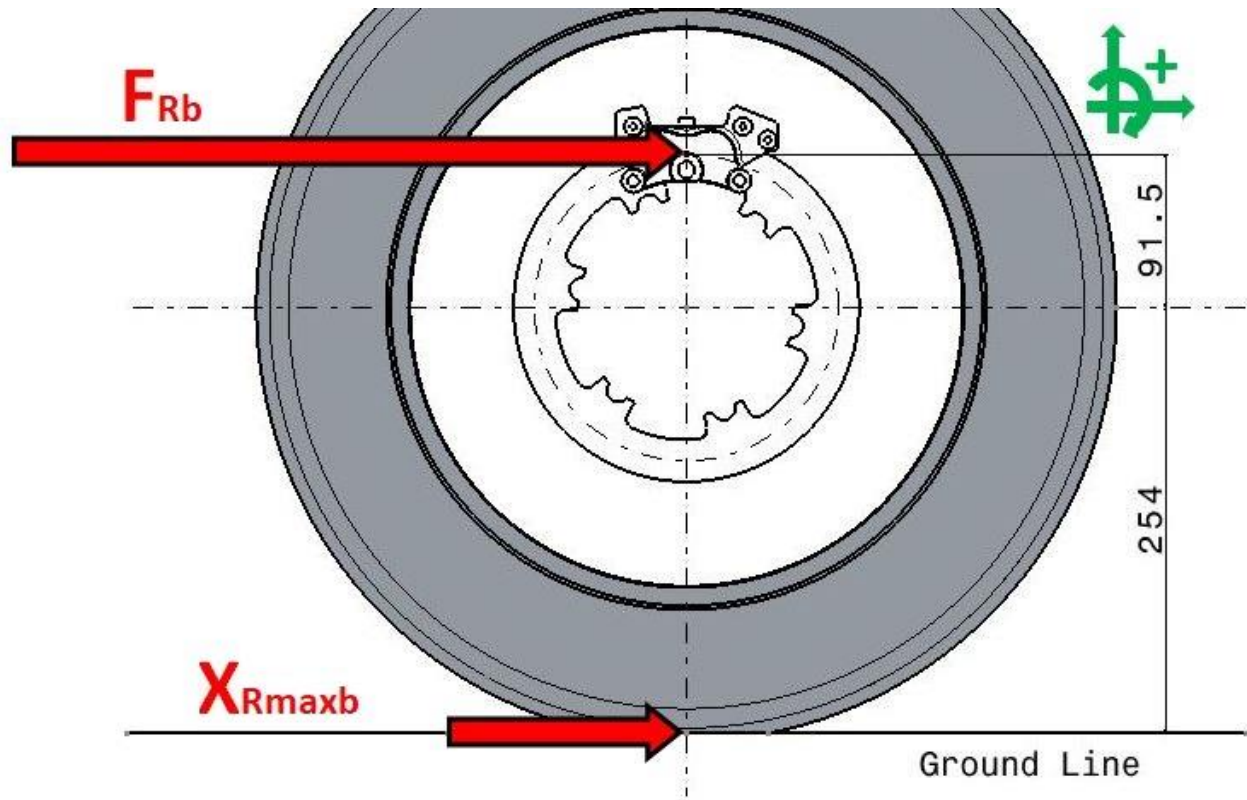
First of all, It's necessary to study braking behaviour of S.C.R. car, in order to calculate F_{RbW} which is “**maximum rear braking force per wheel**” acting on shaft 3. In order to briefly obtain braking force, It's necessary to set up a basic two dimensions model, depicted by Plot 7.3-1. Such model consists of two elements only, tire and brake disk. Tire is imaged to be rigidly bound to rear brake disc. Deformation of tire have been taken into account, all other deformations related to brake components are obviously neglected. Geometrical known parameters are:

- $r_d = 0,254 [m]$ is “**radius of deformed tire**”.
- $r_{Rbd} = 0,0915 [m]$ is “**radius of rear brake disc**”.



Analyzing Plot 7.3-1, It's possible obtain F_{Rb} the "maximum rear braking force" which acts on rear axle, by knowledge of X_{Rmaxb} , which is the "maximum tangential force on rear axle during braking condition". Its value can be recalled by Eq. 6.1-17 of Chapter 6.1. and derives by longitudinal load transfer model depicted by Plot 6.1-4. By virtue of that:

- $X_{Rmaxb} = 1439 [N]$



Plot 7.3-1: Two dimensions model of braking on rear axle.

By previous dissertation, all elements are available to solve the equation of equilibrium around tire axis, displayed as follows.

$$\text{Eq. 7.3-1} \quad F_{Rb} \cdot r_{Rbd} - X_{Rmaxb} \cdot r_d = 0$$

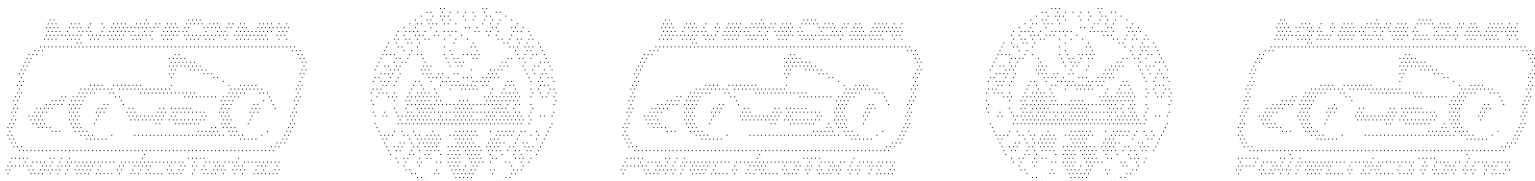
Solution of Eq. 7.3-1 is easily written in following equation:

$$\text{Eq. 7.3-2} \quad F_{Rb} = \frac{X_{Rmaxb} \cdot r_d}{r_{Rbd}} = 3994 [N]$$

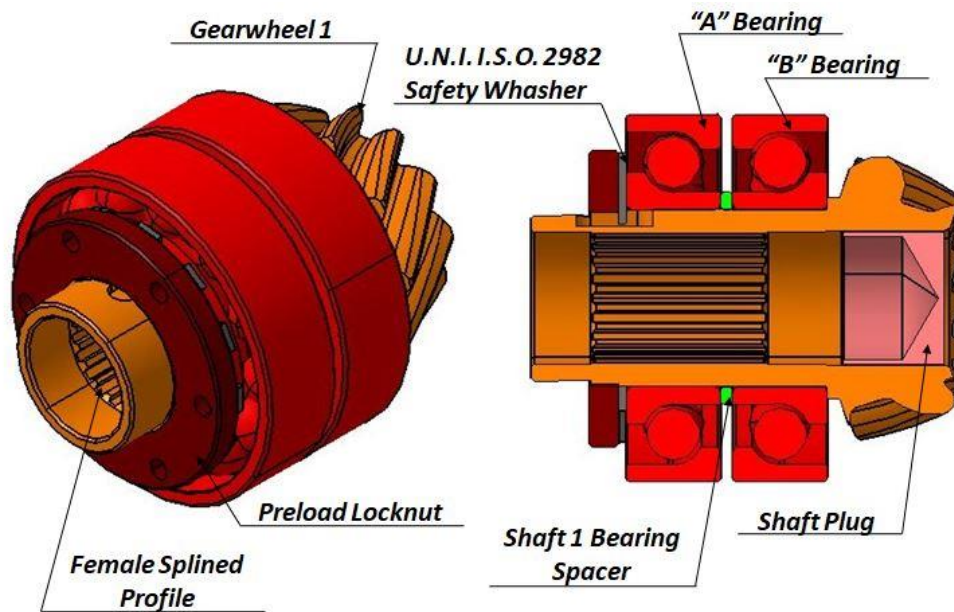
Result of previous Eq. 7.3-2 is related to the entire rear axle, to obtain force referred to single brake disc, It's necessary following equation:

$$\text{Eq. 7.3-3} \quad F_{RbW} = \frac{F_{Rb}}{2} = 1997 [N]$$

Forces calculated in previous chapters are going to be employed in the study of transmission shafts, described by following chapters.

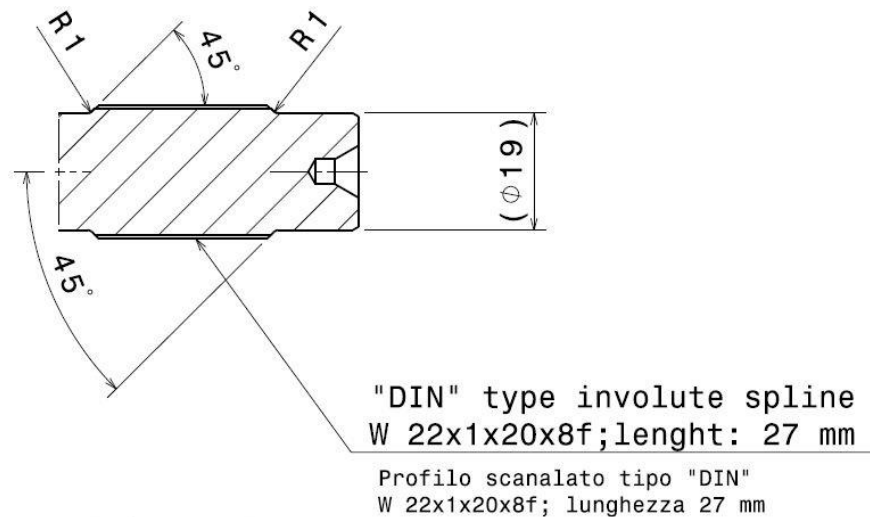


7.4. Shaft 1.



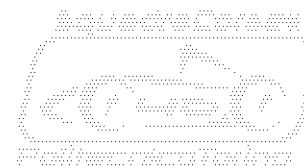
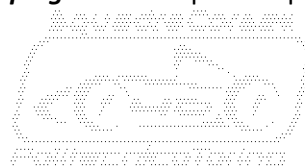
Plot 7.4-1: Details of assembled Shaft 1 core.

By previous brief description of Chapter 7, “*shaft 1*” is one assembly of different components which represents the mechanical link between motor and first stage of reduction. By the way, “*gearwheel 1*” integrates teeth of drive wheel and female sp-lined profile which couples with motor. Indeed output of motor is realized by a cantilever male sp-lined shaft depicted by Plot 7.4-2.

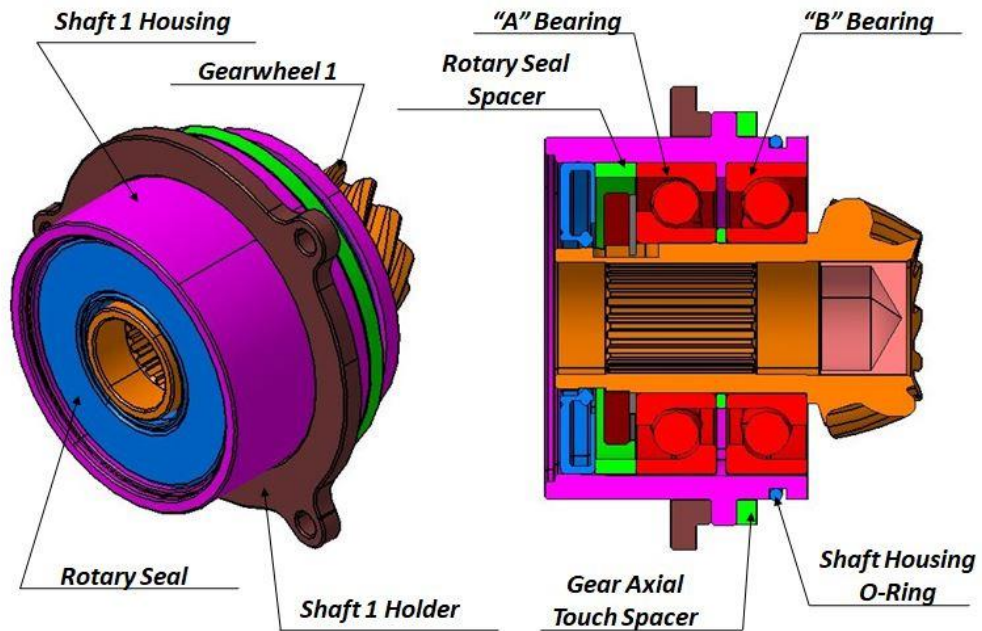


Plot 7.4-2: Motor sp-lined output shaft.

It's necessary to notice that female sp-lined profile realized on “*Gearwheel 1*” is a strong bound to design of components. First of all, broach which realizes the profile needs to operate in a through hole. That represents an important issue for bearings positioning and for lubricant oil sealing. Indeed It's necessary to observe that gearwheel 1 constitutes a link between internal environment of the gear-box and external environment. By virtue of that, sealing needs to be accurately studied around shaft 1. It's known that sp-lined profile joints feature some backlashes in coupling, for this reason, oil leakage through the joint is ensured. “*Shaft plug*” is a component purposely designed in order to overcome

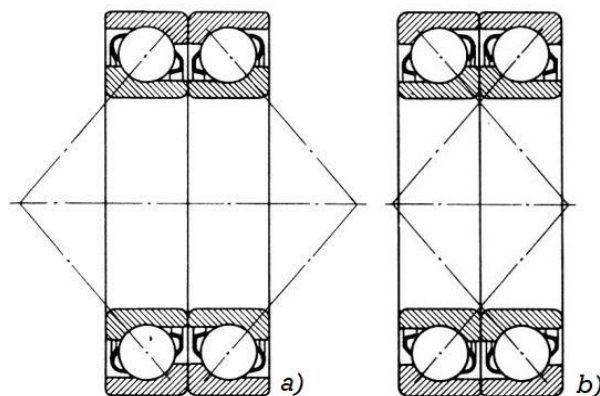


such issue. Component is realized by an aluminium cylindrical cap machined to feature low weight due to thin walls. Shaft plug is bounded to gearwheel 1 by a tight radial interference of $0,01 [mm]$, measured at room temperature. Anyway choice of material isn't an issue of weight only. Aluminium features a thermal linear displacement which is double respect to steel. By virtue of that, an aluminium plug forced into a steel housing never going to lose bounding interference.



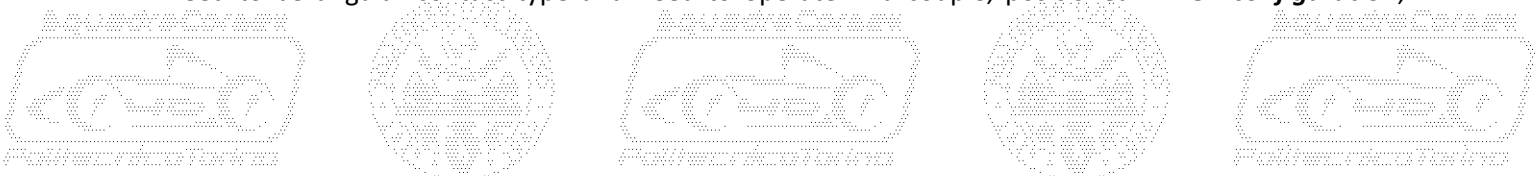
Plot 7.4-3: Details of assembled Shaft 1 into its housing.

Another important topic about Shaft 1 layout is represented by bearings. In order to reduce Tilting momentum on motor output, shaft 1 is provided of its own bearings: "A bearing" and "B bearing". Due to axial through hole which allows operation of broach, it's very difficult position a proper dimension bearing on the right end of gearwheel 1. By structural point of view, gearwheel 1 operates like a cantilever shaft.



Plot 7.4-4: Angular contact bearings mounted in "O" configuration a) and in "X" configuration b).

Unfortunately space to room components is very tight, for this reason bearings are spaced by only $2 [mm]$. Such a tight space between boundaries may amplify tilting momentum caused by gear meshing forces. In order to overcome tilting momentum, according with "Rolling Bearings", Ref.[15], bearings need to be angular contact type and need to operate in a couple, positioned in "O" configuration,



depicted by Plot 7.4-4. Stiffness of a shaft loaded by tilting momentum depends by contact angle of bearings and distance between them. Moreover, such choice about type and configuration of bearings allows to overcome axial component of gear meshing force, displayed by Plot 7.1-1. Indeed It's known that radial bearings are weak in axial direction and are able to bear only small axial forces.

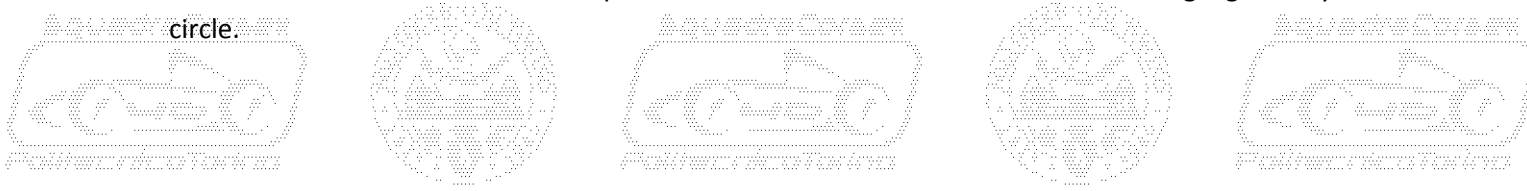
"O" configuration of bearings, as depicted by Plot 7.4-3 works in the following way. Internal raceway of "B" bearing is in contact with collar of gearwheel 1, while external raceway is in contact with collar of "shaft 1 housing". A bearing is positioned in symmetric way, with external raceway in contact with collar of shaft 1 housing, while internal raceway is in contact with "U.N.I. I.S.O. 2982 safety washer". "O" shape can be noticed observing diagonal axis of bearings, displayed on Plot 7.4-4. Anyway, safety washer haven't a structural task, It's only a security measure to ensure the positive locking of "preload locknut". That's a female threaded metal ring which operates providing an axial bound to the entire stack of bearings, housing and spacer. Metal ring is tighten to M30x1 thread displayed on Plot 7.4-5 and, how suggested by name, ensures preload of angular contact bearings.

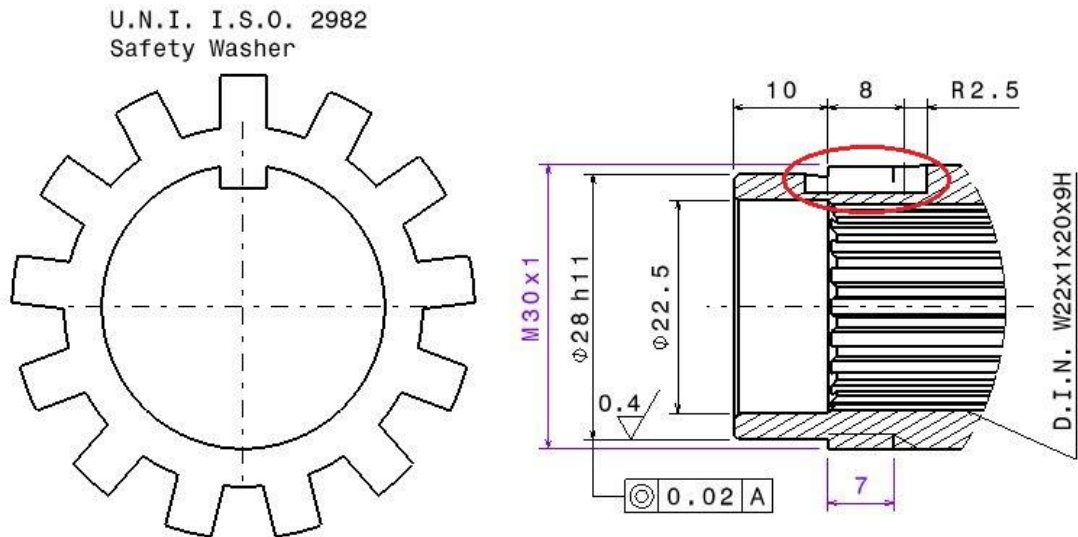
It's known that angular contact bearings couples need to operate under a well determined value of preload. That ensures proper rigidity of the system and long operational life of bearings. In this configuration, value of preload which is a length, is controlled by thickness of "shaft 1 bearing spacer", a thin steel ring positioned between internal raceway of bearings, as depicted by Plot 7.4-1. Preload value is represented by difference of thickness between bearing spacer and collar of housing which holds external raceway of bearings. Value of preload is determined after calculations and accurate measuring of bearings and housing. Precision needed by preload value is often around 0,01 [mm]. In order to preserve exact value of preload, locknut needs to be tighten with a precise torque. Low torque may lead to unscrewing, on the other hand high torque may lead to unwanted increase of preload. Increase of preload leads to a worsening of gear-train efficiency and damages raceways of bearings due to high pressure. For this reason, preload locknut needs to be fasten by a torque wrench set on 10 [Nm]. Due to lack of spaces, a conventional female hexagon socket tool cannot be used to fasten the locknut. Therefore, two special tools have been designed, one interfaces locknut and torque wrench, other holds gearwheel 1 by sp-lined profile.

To conclude this small dissertation about influence of bearings on design, It's necessary notice that $\Phi 30$ [mm] diameter of shaft integrated on gearwheel 1 have been defined by bore diameter of bearings. Chosen bearings represent smallest size offered by SKF catalogue of standard products. Often, inner bearing, "A" bearing, is downsized respect to outer one because large majority of load is supported by outer constraint. Chosen configuration exploits a couple of identical bearings in order to simplify manufacturing and assembly of entire shaft. After a brief analysis of supported loads, displayed on SKF catalogue, chosen bearings may result to be quite oversized, by static point of view. Anyway, information about code, description and verification of each bearing is going to be provided in detail by next Chapter **Errore. L'origine riferimento non è stata trovata.**

By the way, It's necessary to clarify that SKF range is able to offer smaller products, which may be more suitable on a motorsport project. Anyway, lead times of special products are aren't compatible with tight times of a F.S.A.E. project. For this reason, less performing standard products, which are constantly in stock, are preferred to more performing special ones.

By accurate analysis of Plot 7.4-5, It's possible to notice that U.N.I. I.S.O. 2982 safety washer requires a radial slot to hold the tooth which protrudes on the bore diameter. Such slot is highlighted by a red circle.





Plot 7.4-5: Details of Gearwheel 1: Thread, grind, safety washer with housing.

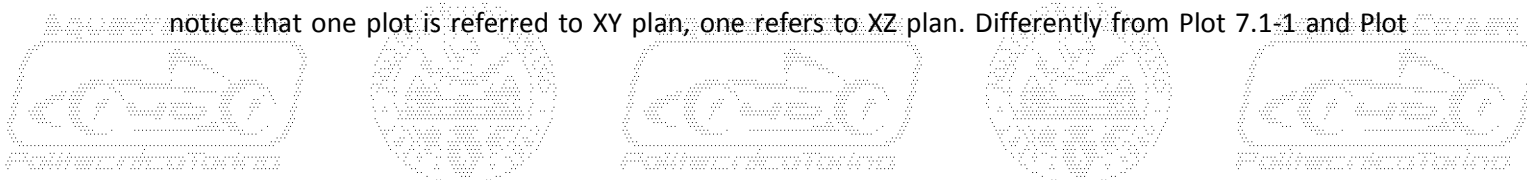
Other detail to take into account is grinded $\Phi 28$ [mm] diameter which represents the working diameter of “rotary seal”. Such gasket is bounded to shaft housing by interference and “Rotary Seal Spacer” guarantees a proper distance by A bearing. It’s necessary to remind that bearings are not provided by their own seals. For this reason, purpose of rotary seal is avoid leakages between external diameter of gearwheel 1 and bore diameter of shaft housing.

Knowledge of bevel gears, briefly described at Chapter 4.3.2.2, suggest that axial touch of gearwheels needs to be verified and regulated. “Axial touch” is often the distance between drive wheel and a reference on the gear-box case. Value of such distance rules relative position of bevel gearwheels. By virtue of that, axial touch rules position of tooth contact patch along face width. Optimal operation of a bevel gear needs a contact patch located in the middle of face width. Some measures and some experimental tests needs to be done before reach optimal position.

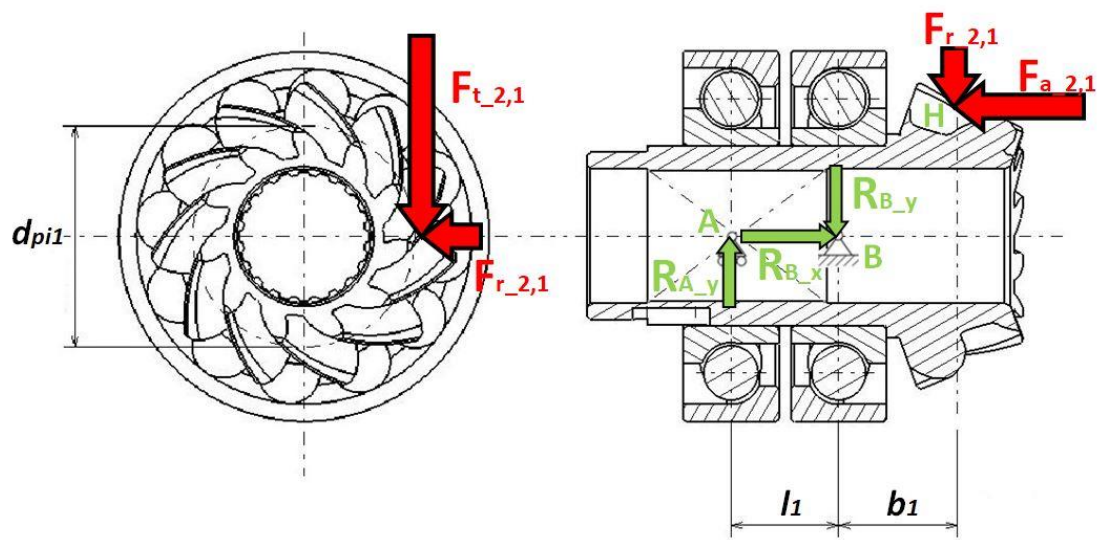
Observing Plot 7.4-3 It’s necessary notice that assembly of shaft, provided of housing and fasteners, represents a rigid integrated system. This solution is studied to easily control position of the shaft assembly along motor axis, which coincides with gearwheel 1 axis. A simple ring shim, inserted on outer diameter of shaft 1 housing is able to regulate axial position of the entire shaft assembly. Definitely, thickness of “gear axial touch spacer” defines position between gear-box case, where shaft 2 is bounded, and gearwheel 1. Adjustment of axial touch is therefore provided.

At this point of dissertation, layout of shaft 1 can be considered widely described by qualitative point of view, for this reasons some basic **verifications** needs to be performed. Purpose of verifications is understand if chosen diameters of gearwheel 1 integrated shaft could be suitable to gear-box loads. In case of negative result, internal diameter can’t be decreased due to described design constraints. On the other hand, a change of material can be performed but It’s not recommended by virtue of facts explained at Chapter 6.4. Easier solution to take into account is increase of $\Phi 30$ [mm] diameter with an increase of bearing bore diameter too, as consequence. Anyway, more accurate and more time lasting, F.E.M. simulations can be performed later if needed.

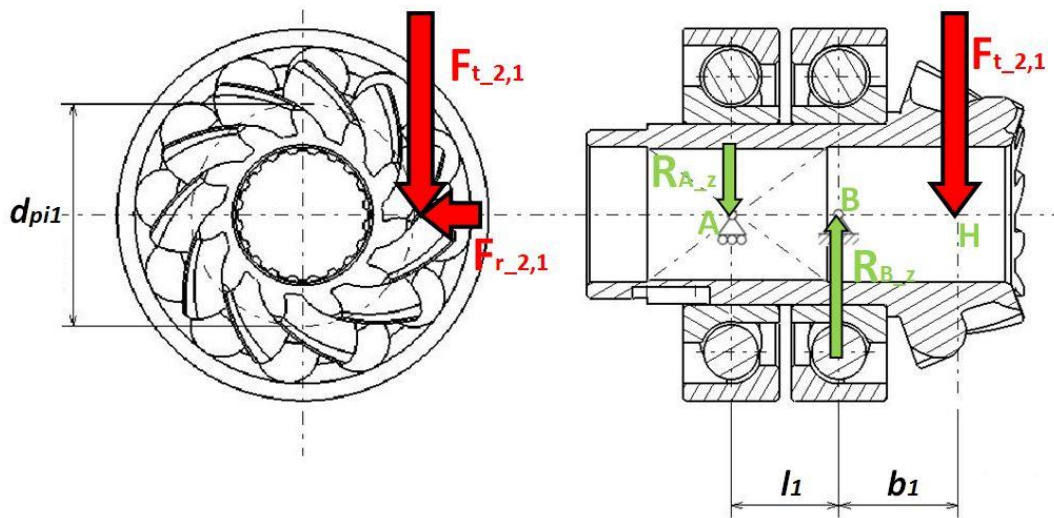
First step is set up “free body diagrams” of gearwheel 1, based on driving condition. It’s possible to notice that one plot is referred to XY plan, one refers to XZ plan. Differently from Plot 7.1-1 and Plot



7.2-1, a free body diagram includes reaction forces exploited by constraints A and B. Such forces are applied on mid section of bearings which are represented by two simple points, "A" and "B" displayed by Plot 7.4-6 and Plot 7.4-7. By knowledge of geometric parameters and knowledge of gear meshing forces displayed at Chapter 7.1, It's possible calculate reaction forces on constraints which are green vectors displayed by Plot 7.4-6 and Plot 7.4-7. Procedure is applied in accordance with "G. Curti F. Curà – Fondamenti di Meccanica Strutturale", Ref.[16].



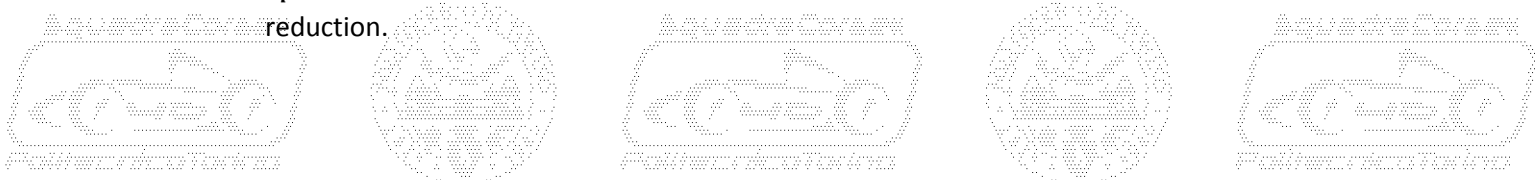
Plot 7.4-6: Free body diagram of gearwheel 1 in driving condition, vectors lay on XY plan.



Plot 7.4-7: Free body diagram of gearwheel 1 in driving condition, vectors lay on XZ plan.

It's necessary to clarify that subscripts x,y,z indicate direction of reaction force vectors. Geometrical parameters which It's necessary to introduce are:

- $l_1 = 18,00 [mm]$ is "distance of points A-B".
- $b_1 = 19,77 [mm]$ is "distance of points A-H".
- $d_{pi1} = 37,20 [mm]$ is "intermediate pitch diameter of wheel 1" drive wheel of first stage of reduction.
- $r_{pi1} = 18,60 [mm]$ is "intermediate pitch radius of wheel 1" drive wheel of first stage of reduction.



Analyzing Plot 7.4-6 and Plot 7.4-7, It's possible to write a system of five equilibrium equations, very similar to those explained by Chapter 4.1 and Chapter 6.1. Resolution of the system is analogue to cases treated by previous chapters. Therefore, in order to simplify actual dissertation, system and its resolution is going to be omitted. Anyway, magnitude of reaction forces on boundaries are displayed as follows:

Eq. 7.4-1 $R_{Ay} = 1.059 [N]$

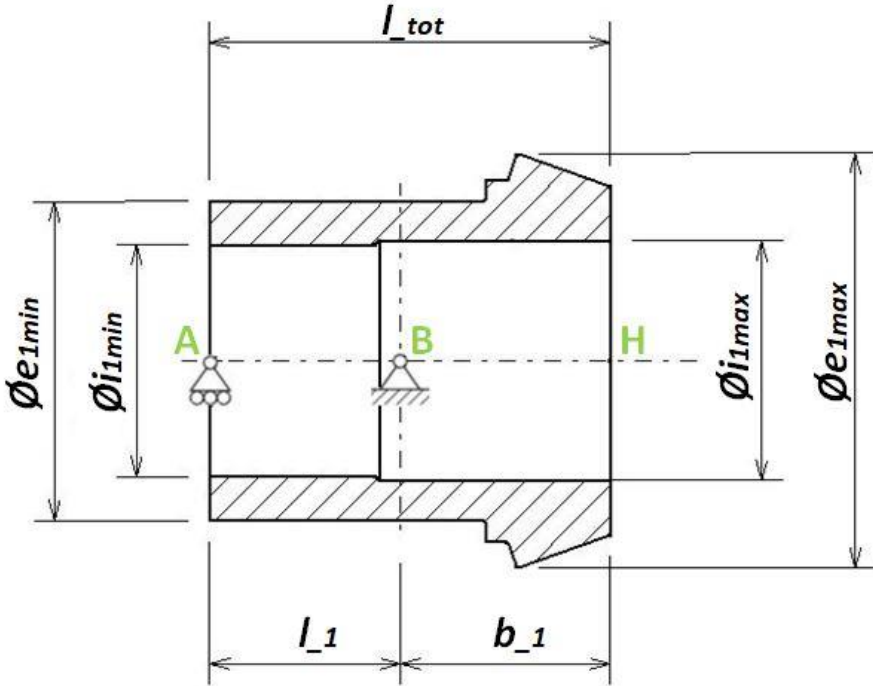
Eq. 7.4-2 $R_{Az} = 2.363 [N]$

Eq. 7.4-3 $R_{Bx} = 1.492 [N]$

Eq. 7.4-4 $R_{By} = 620 [N]$

Eq. 7.4-5 $R_{Bz} = 4514 [N]$

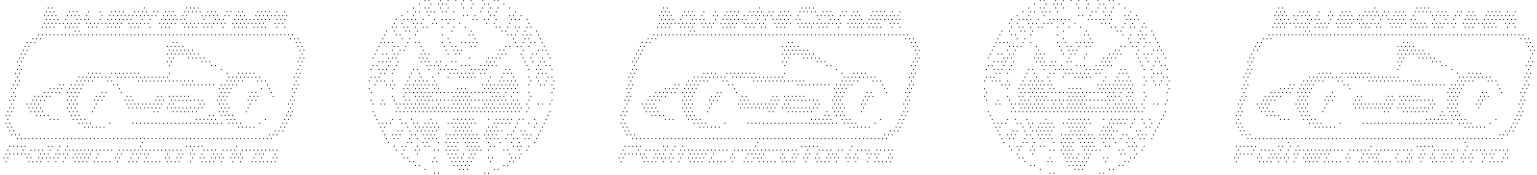
Positive sense of reaction forces is in accordance with green vectors displayed by Plot 7.4-6 and Plot 7.4-7.



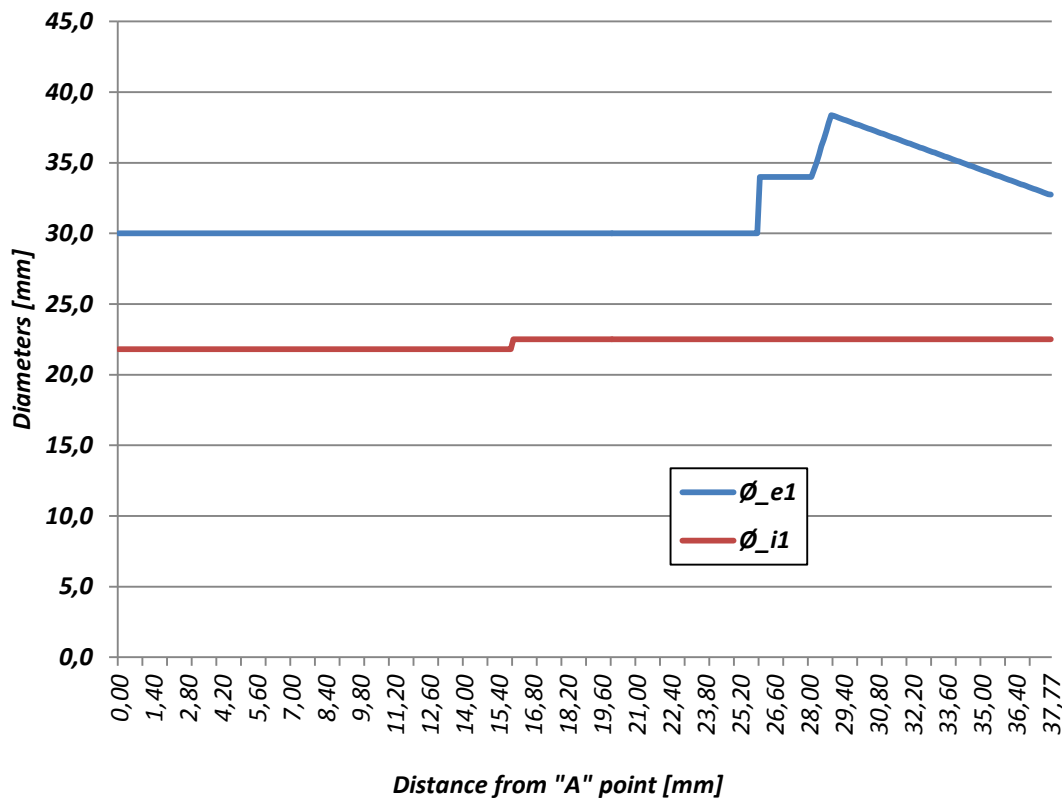
Plot 7.4-8: Structural model of Gearwheel 1.

By knowledge of previous information, It's possible to set up an empiric model referred to structure of gearwheel 1. Such model, displayed by Plot 7.4-8, can be analyzed like a beam which features multiple different sections. First aspect to take into account is that model of beam haven't to include all the component sections. It represents the portion of component included between point "A" and "H". Simplification of the model establish that sections external to points "A" and "H", need to be considered unloaded. It's necessary to clarify that point "H" represents the force application point of gearwheel 1.

Structural model of Gearwheel 1 have been expressed in function of two diameters:



- \varnothing_{e1} is “**external diameter of gearwheel 1**”. Such dimension is measured in [mm] and varies along the beam.
- \varnothing_{i1} is “**internal diameter of wheel t**”. Such dimension is measured in [mm] and varies along the beam.

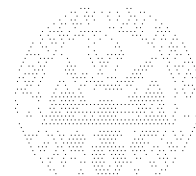
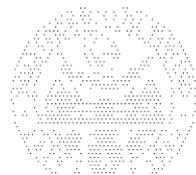


Plot 7.4-9: Variation of diameters of gearwheel 1 implemented on Microsoft Excell Spreadsheet.

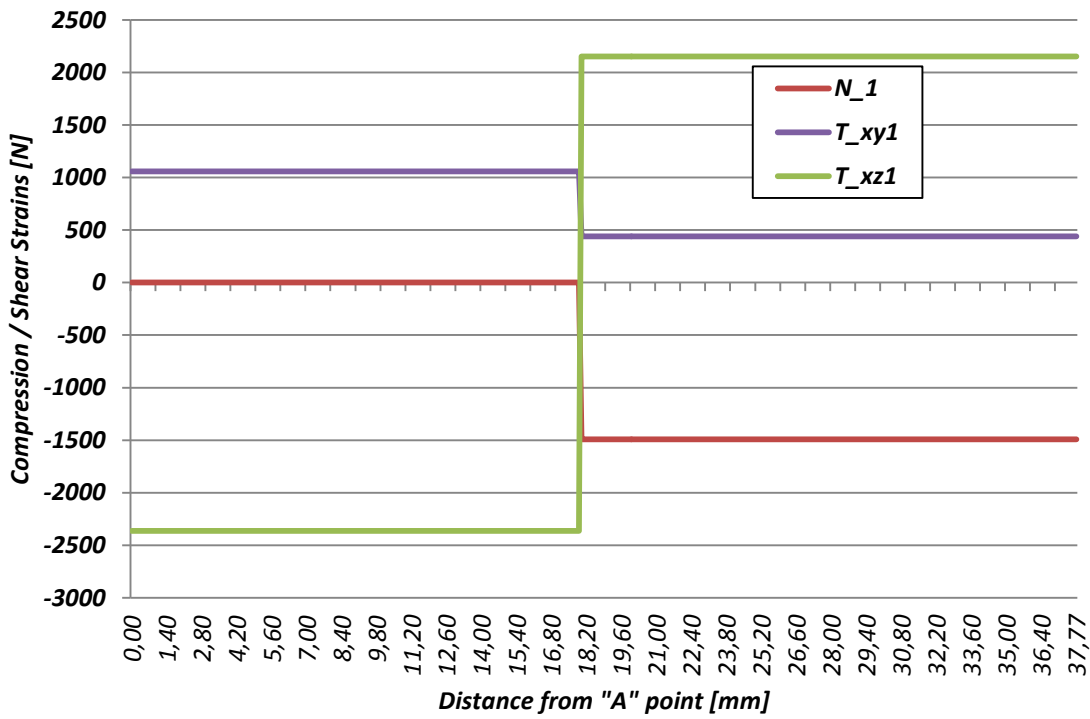
Model have been implemented by an advanced spreadsheet of Microsoft Excell software. Portion of gearwheel 3 displayed by Plot 7.4-8 have been split on **379 sections** perpendicular to x axis and **spaced of 0,1 [mm]** each other. Result is displayed by Plot 7.4-9. Such technique ensures a good accuracy of calculation and a good definition of the extracted plots. It's necessary to underline that model displayed by Plot 7.4-8 represents a very extreme condition by point of view of sections, which are reduced to the minimum. Model is intended to be conservative while material represented by teeth of sp-lined profile and gear have been neglected.

Next step is determination of different strains acting on the model, caused by gear meshing forces during driving condition, according with Ref.[16]:

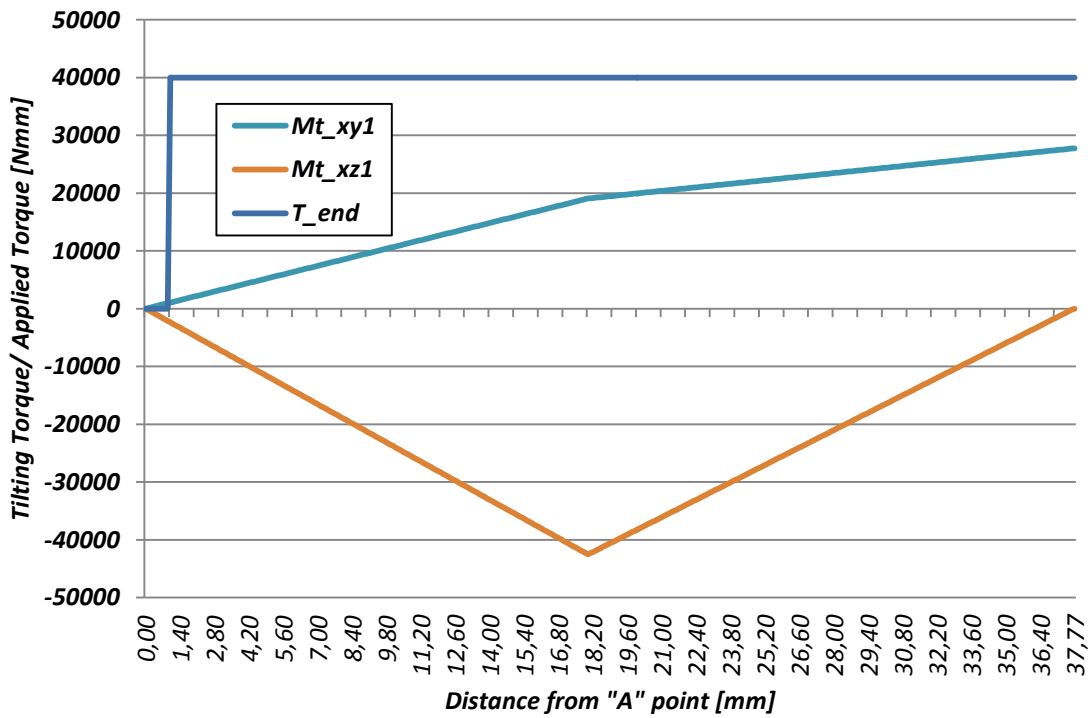
- N_1 is “**strain normal to section of gearwheel 1 in driving condition**”. It's measured in [N] and represents the compression caused by axial force which gearwheel 2 transmits to gearwheel 1.
- T_{xy1} is “**shear strain on xy plan of gearwheel 1 in driving condition**”. It's measured in [N] and represents shear caused by forces laying on xy plan.
- T_{xz1} is “**shear strain on xz plan of gearwheel 1 in driving condition**”. It's measured in [N] and represents shear caused by forces laying on xz plan.
- M_{txy1} is “**tilting momentum on xy plan of gearwheel 1 in driving condition**”. It's measured in [Nmm] and represents tilting momentum caused by forces laying on xy plan.



- M_{txz1} is “tilting momentum on xz plan of gearwheel 1 in driving condition”. It’s measured in [Nmm] and represents tilting momentum caused by forces laying on xz plan.
- T_{end} is “endurance torque”. It’s measured in [Nmm] and refers to studies of Chapter 4.1.

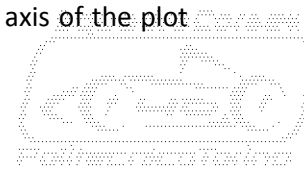
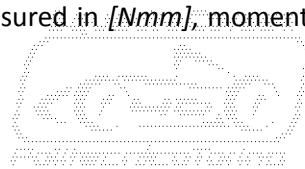
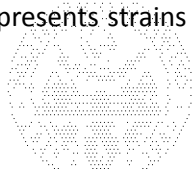


Plot 7.4-10: Strains acting on gearwheel 1, measured in [N] and referred to driving condition.



Plot 7.4-11: Strains acting on gearwheel 1, measured in [Nmm] and referred to driving condition.

Strains are displayed on two different plots: Plot 7.4-10 which depicts strains measured in [N] and Plot 7.4-11 which represents strains measured in [Nmm], moments and torque. Horizontal axis of the plot

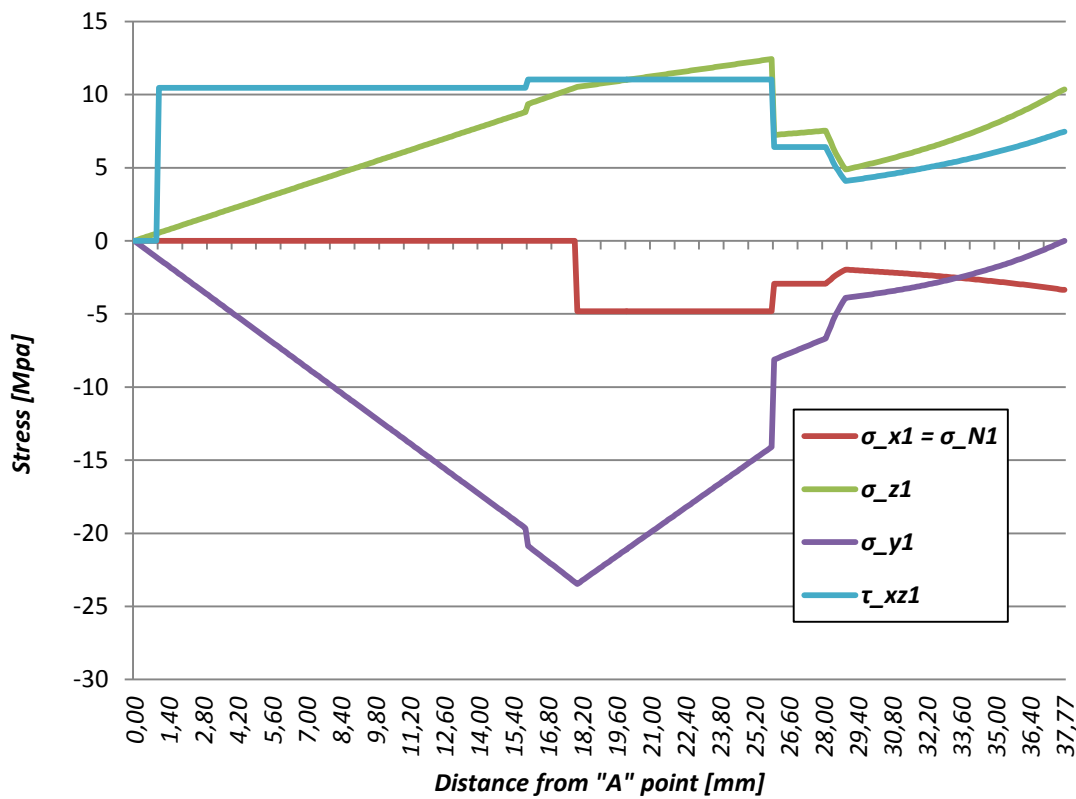


represents distance from point "A", maximum value represents position of point "H" referred to "A". Strains and successively stresses are represented on the vertical axis.

By Plot 7.4-10, It's necessary to observe that normal strain acts in the portion of beam included between point "B" and point "H". That's because axial strain is supported by "B" bearing. By the way, not all the model is subject by compression. Magnitude of shear strains varies in coincidence with gear forces application points, as expected.

By Plot 7.4-11, It's necessary to observe which driving torque is considered to be applied in the mid section of female sp-lined shaft. By virtue of that, torque affects large majority of the beam. Another detail to take into account is behaviour of M_{txy1} which is different from zero on point "H". That's due to tilting momentum applied by axial force acting on gearwheel 1.

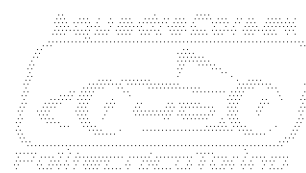
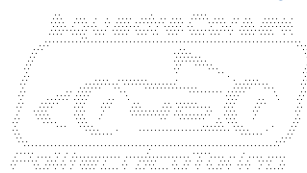
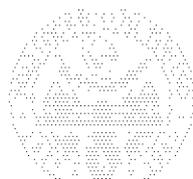
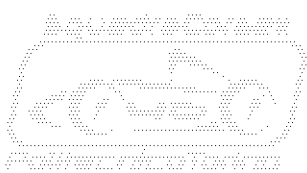
Next step is study of stresses caused by strains displayed on previous plots. Stresses are strongly affected by main diameters displayed by models displayed by Plot 7.4-8 and Plot 7.4-9. Such dimensions affect area, area momentum of inertia, torsion strength modulus and bending strength modulus. By virtue of that, It's interesting **study behaviour of stresses section by section**, according with Ref.[16].



Plot 7.4-12: Stresses acting on gearwheel 1, referred to driving condition.

Plot 7.4-12 represents four different stresses acting on gearwheel 1 displayed in function of distance from point "A". σ_{x1} is the "compression stress acting on gearwheel 1 in driving condition" generated by N_1 , strain normal to section. Stress is calculated by following function:

Eq. 7.4-6
$$\sigma_{x1}(x) = \frac{N_{1i}(x)}{A_{1i}(x)} = \frac{N_{1i}(x)}{\pi \frac{\phi(x)^2_{e1} - \phi(x)^2_{i1}}{4}}$$



Where:

- $N_{1i}(x)$ is **“strain normal to i section of gearwheel 1 in driving condition”**. It’s measured in $[N]$ and is function of x , because depends from portion of the beam on which is applied, as depicted by Plot 7.4-10.
- $A_{1i}(x)$ is **“area of i section of gearwheel 1”**. It’s measured in $[mm^2]$ and is function of x , because depends by distance from point “A” due to dimension of diameters ϕ_{i1} and ϕ_{e1} .

How expected, value of the stress is different from zero in the portion of beam included between points “B” and “H”. Then It’s possible to observe that value is affected by variations of section which stand in proximity of toothed sections. Values different from zero are always negative because stress is a compression. Anyway, maximum value of stress is not alarming, due to large diameters of the component and due to strength of material.

σ_{z1} is the **“bending stress in driving condition”** generated by M_{txy1} , tilting momentum acting on xy plan. Stress is calculated by following function:

$$\text{Eq. 7.4-7} \quad \sigma_{z1}(x) = \frac{M_{txy1i}(x)}{W_{f1i}(x)} = \frac{M_{txy1i}(x)}{\pi \frac{\phi(x)^4_{e1} - \phi(x)^4_{i1}}{32 \cdot \phi(x)_{e1}}}$$

Where:

- $M_{txy1i}(x)$ is **“tilting momentum acting on xy plan referred to i section of gearwheel 1 in driving condition”**. It’s measured in $[Nmm]$ and is function of x , because depends from distance from point “A”, as depicted by Plot 7.5-11.
- $W_{f1i}(x)$ is **“bending strength modulus referred to i section of gearwheel 1”**. It’s measured in $[mm^3]$ and is function of x , because depends by distance from point “A” due to dimension of diameters ϕ_{i1} and ϕ_{e1} .

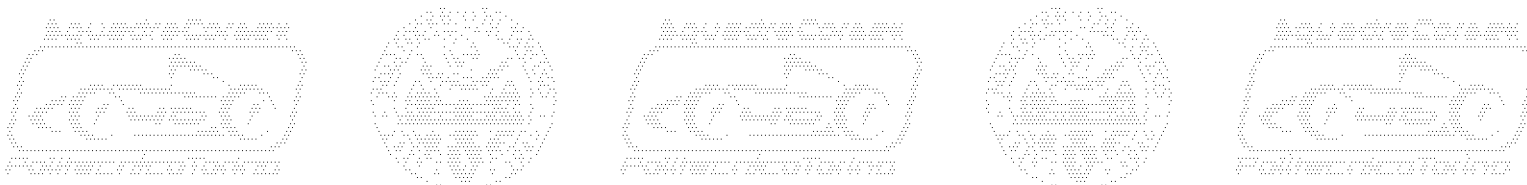
Value of stress is always positive, because naturally affected by M_{txy1} . Value of stress varies in a quite continuous way along all the beam, anyway It’s possible to observe some points where trend of stress displays “step” behaviour. That’s due to changes in dimension of diameters ϕ_{i1} and ϕ_{e1} . Peak value of the stress is localized in concomitance with point “B”, but its value isn’t dangerous for the safe operation of the component.

σ_{y1} is the **“bending stress in driving condition”** generated by M_{txz1} , tilting momentum acting on yz plan. Stress is calculated by following function:

$$\text{Eq. 7.4-8} \quad \sigma_{y1}(x) = \frac{M_{txz1i}(x)}{W_{f1i}(x)} = \frac{M_{txz1i}(x)}{\pi \frac{\phi(x)^4_{e1} - \phi(x)^4_{i1}}{16 \cdot \phi(x)_{e1}}}$$

Where:

- $M_{txz1i}(x)$ is **“tilting momentum acting on xz plan referred to i section of gearwheel 1 in driving condition”**. It’s measured in $[Nmm]$ and is function of x , because depends from distance from point “A”, as depicted by Plot 7.4-11.



Value of stress results null in coincidence with mid section of bearings. It is continuously negative along large majority of the beam and peak appears in coincidence with point “B”. Changes of slope inclination and steps are localized in correspondence with changes of section diameters. In this case too, values of studied stresses doesn’t appear important by point of view of safety.

τ_{yz1} is the “**torsion stress in driving condition**” generated by T_{end} . Stress is calculated by following function:

$$\text{Eq. 7.4-9} \quad \tau_{yz1}(x) = \frac{T_{end}(x)}{W_{t1i}(x)} = \frac{T_{end}(x)}{\pi \frac{\phi(x)^4_{e1} - \phi(x)^4_{i1}}{32 \cdot \phi(x)_{e1}}}$$

Where:

- $T_{end}(x)$ is “**driving torque acting on input shaft**”. It’s measured in $[Nmm]$ and is function of x , because depends from portion of the beam on which is applied, as depicted by Plot 7.4-11.
- $W_{t1i}(x)$ is “**torsion strength modulus referred to i section of gearwheel 1**”. It’s measured in $[mm^3]$ and is function of x , because depends by relative position with point “A” due to dimension of diameters ϕ_{i1} and ϕ_{e1} . It’s possible to notice that value is double respect to $W_{f1i}(x)$.

Following trend of torsion strain, stress acts in the large majority of the beam. By observation of Plot 7.4-12, It’s possible to notice that stress is strongly affected by variation of diameters along the section. In particular, It’s possible notice a large drop in correspondence of toothed section, near “H” point.

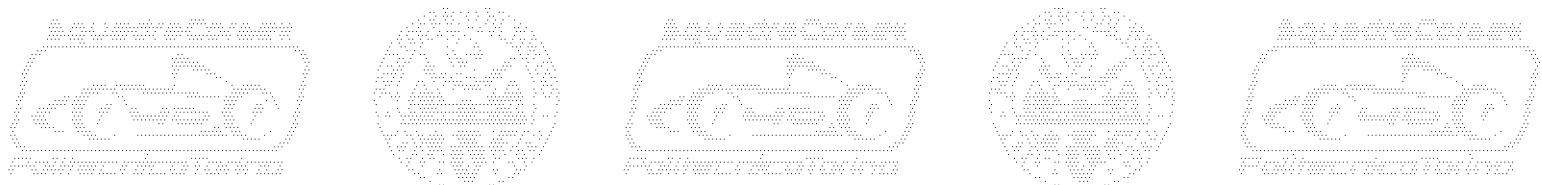
After this wide dissertation about trend of single stress, It’s important to observe that application of single stress, is not able to compromise safety of the structure, indeed peak value between stresses is about 30 times smaller than allowable stress of the material. For this reason, It’s necessary to calculate a function of stress which takes into account contribution of single stresses, σ_{eq1} which is the “**equivalent stress on gearwheel 1 in driving condition**”. It can be calculated according to Ref.[16], through to following relation:

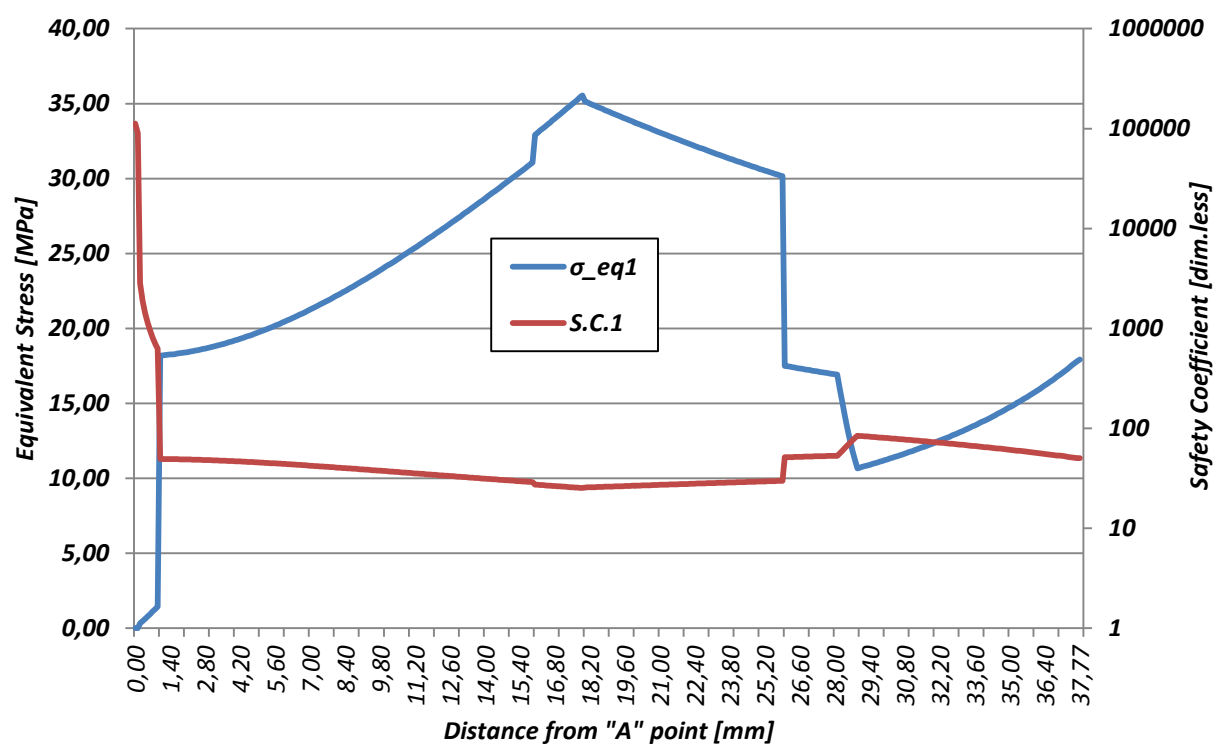
Eq. 7.4-10

$$\sigma_{eq1} = \frac{1}{\sqrt{2}} \sqrt{(\sigma_{x1} - \sigma_{y1})^2 + (\sigma_{y1} - \sigma_{z1})^2 + (\sigma_{z1} - \sigma_{x1})^2 + 6 \cdot (\tau_{xy1}^2 + \tau_{yz1}^2 + \tau_{zx1}^2)}$$

It’s necessary remind that, in the actual case, Eq. 7.4-10 Eq. 7.5-14 represents a function with distance from point “A”. It’s necessary notice that equation have been written in entire form, even if values of τ_{xy1} and τ_{zx1} are null.

By virtue of that, stresses displayed by Plot 7.4-12, combined according to Eq. 7.4-10, give as result blue curve displayed by Plot 7.4-13. It’s possible to notice that values of σ_{eq1} combines maximum values of positive sign stresses. By analysis of the curve, point “B” coincides with most stressed section. Next step is study of safety coefficient which is displayed by red curve on Plot 7.4-13, its trend, displayed on logarithmic scale, is obviously opposite to trend of equivalent stress. It’s possible to notice that levels of safety are enormously high on extremity sections.

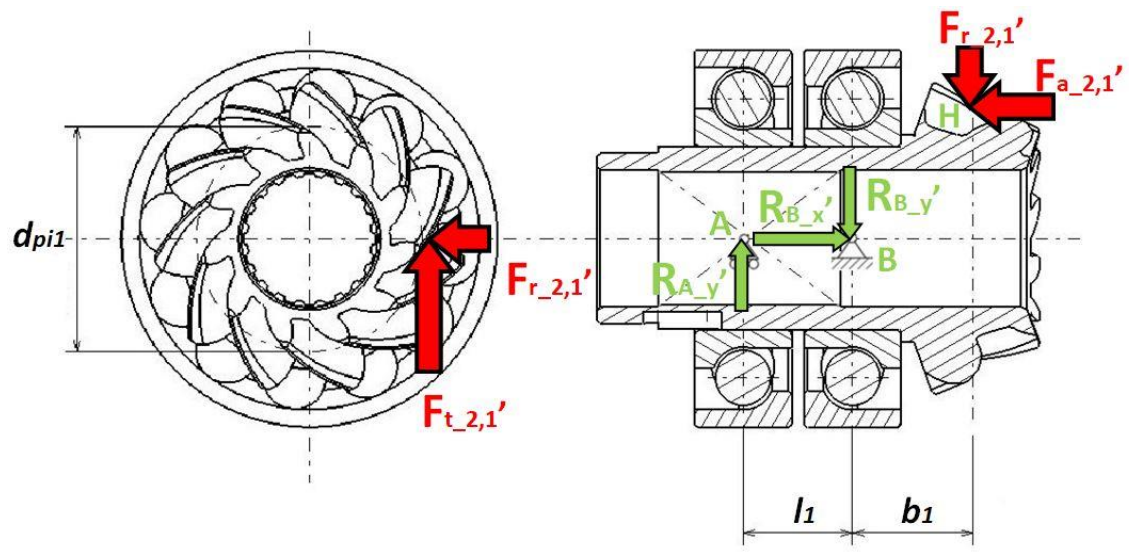




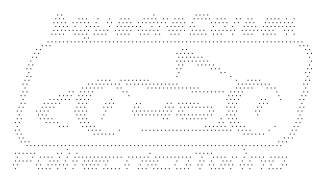
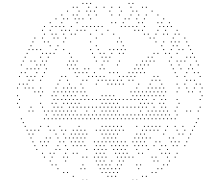
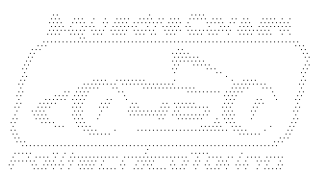
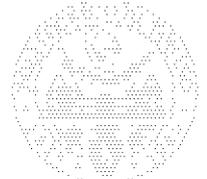
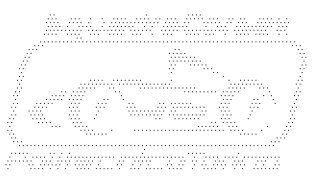
Plot 7.4-13: Equivalent Stress and Safety Coefficient acting on gearwheel 1, referred to driving condition.

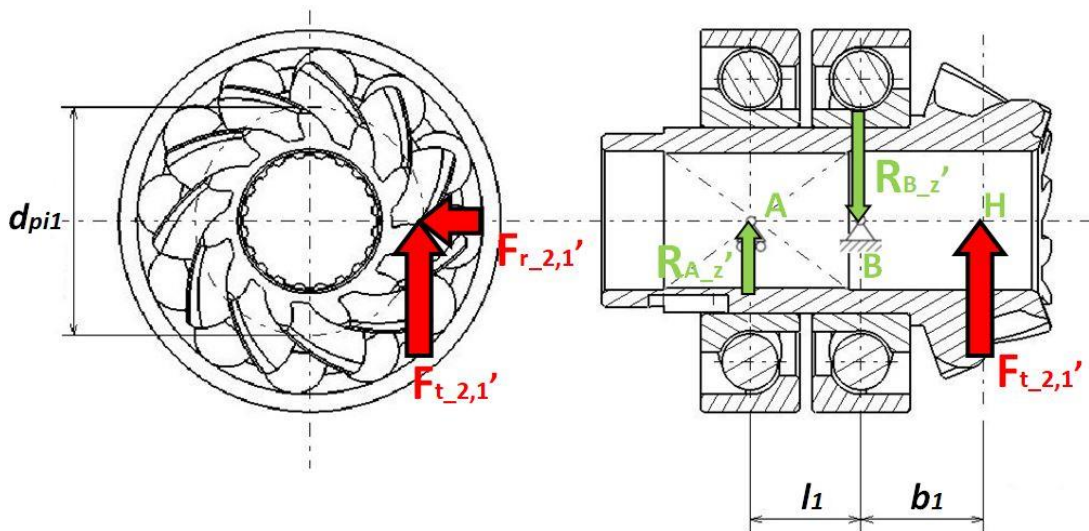
Anyway, It's clear that gearwheel 1 operates in safe conditions when bears static loads due to driving condition. Indeed minimum value of safety coefficient is about 20 times larger than minimum allowable coefficient.

How it was revealed by previous chapters, driving condition isn't the only load case which acts on transmission.



Plot 7.4-14: Free body diagram of gearwheel 1 in energy recovery condition, vectors lay on XY plan.





Plot 7.4-15: Free body diagram of gearwheel 1 in energy recovery condition, vectors lay on XZ plan.

By virtue of that, It's necessary to study energy recovery condition, widely explained at Chapter 7.2. To this purpose, two more "free body diagrams" needs to be set up. Plot 7.4-14 represents the homologous of Plot 7.4-6 and Plot 7.4-15 represents the homologous of Plot 7.4-7. By observation of Plot 7.4-14 is necessary notice that sign of constraint reaction forces isn't changed respect to Plot 7.4-6. Differently, It's possible to notice that change of sign in gear meshing tangential force, causes a change of sign in boundary reaction forces displayed by Plot 7.4-15.

How It was done in previous case, It's possible write a system of five equations based on Plot 7.4-14 and Plot 7.4-15. In order to simplify actual dissertation again, system and its resolution is going to be omitted. Anyway, magnitude of reaction forces on boundaries are displayed as follows:

Eq. 7.4-11 $R'_{Ay} = 530 [N]$

Eq. 7.4-12 $R'_{Az} = 1.181 [N]$

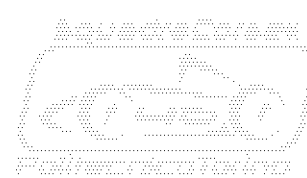
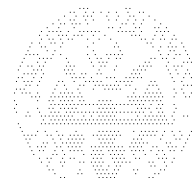
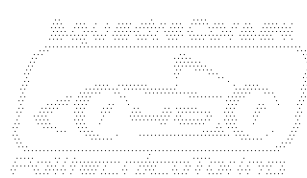
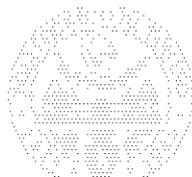
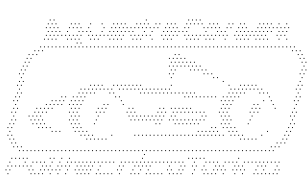
Eq. 7.4-13 $R'_{Bx} = 746 [N]$

Eq. 7.4-14 $R'_{By} = 310 [N]$

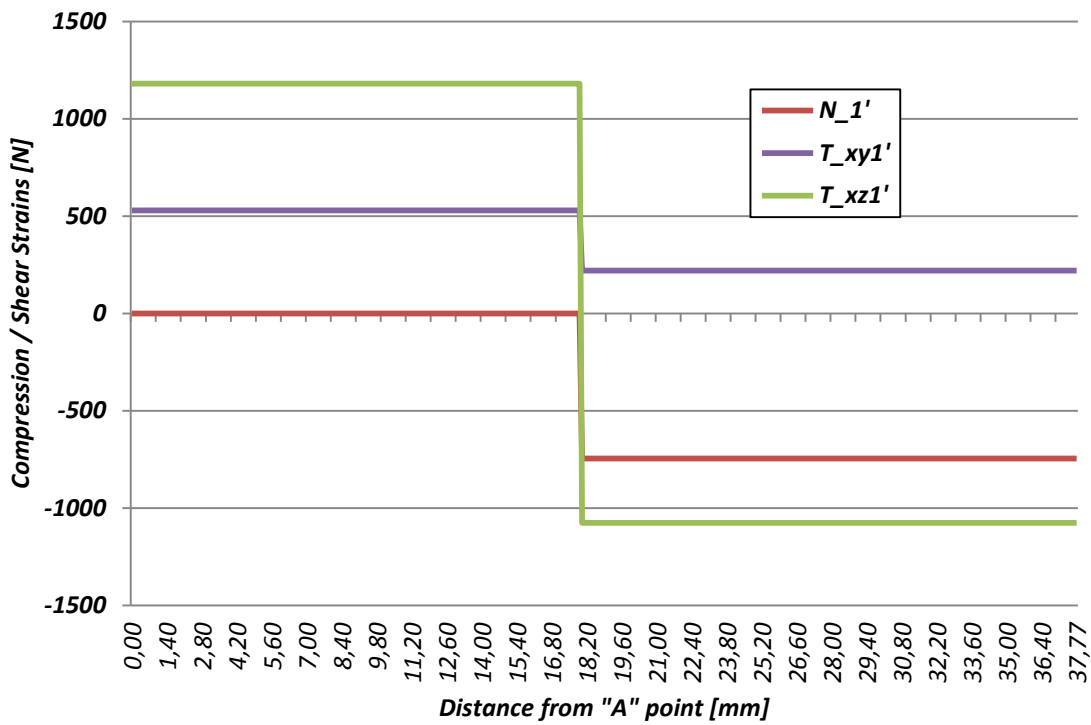
Eq. 7.4-15 $R'_{Bz} = 2.257 [N]$

Once constraint reaction forces are known, It's easy calculate strains related to energy recovery condition. Structural model is the same adopted in the study of driving case and depicted by Plot 7.4-8. How done before, strains acting on the model are declared:

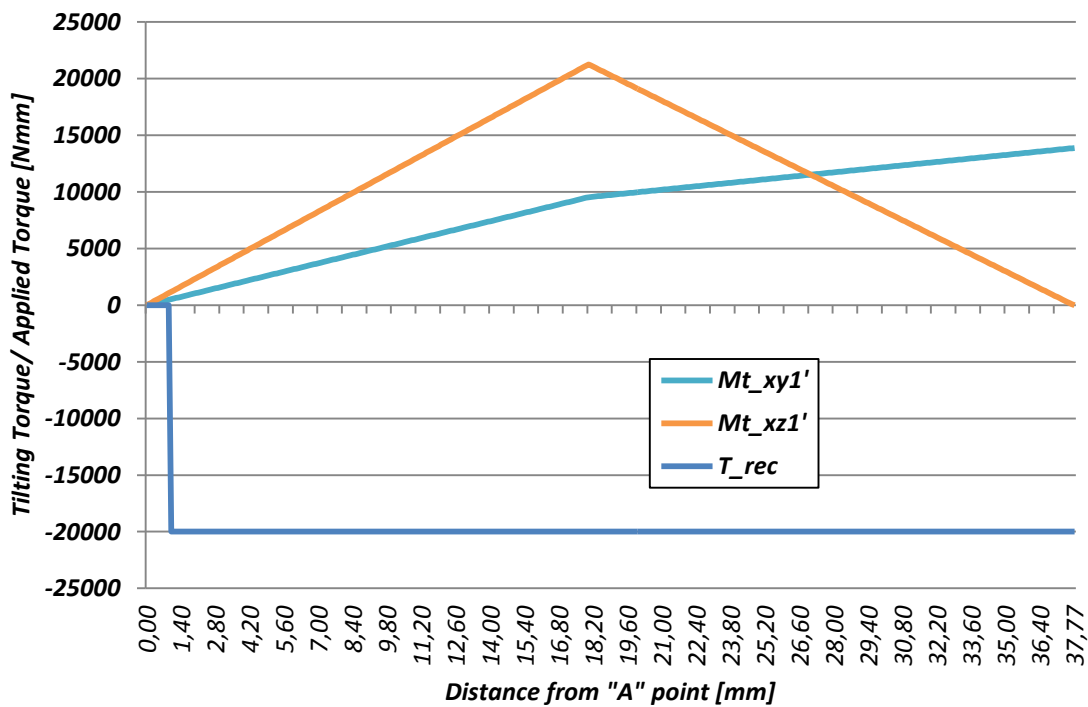
- N'_1 is "strain normal to section of gearwheel 1 in recovery condition". It's measured in $[N]$ and represents the compression caused by axial force which gearwheel 2 transmits to gearwheel 1.
- T'_{xy1} is "shear strain on xy plan of gearwheel 1 in recovery condition". It's measured in $[N]$ and represents shear caused by forces laying on xy plan.
- T'_{xz1} is "shear strain on xz plan of gearwheel 1 in recovery condition". It's measured in $[N]$ and represents shear caused by forces laying on xz plan.



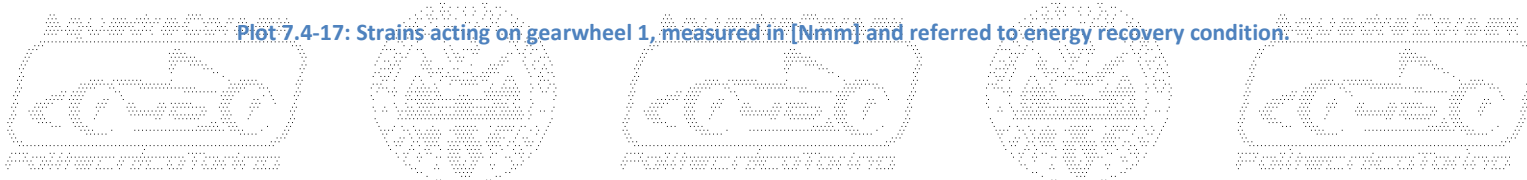
- M'_{txy1} is “tilting momentum on xy plan of gearwheel 1 in recovery condition”. It’s measured in [Nmm] and represents tilting momentum caused by forces laying on xy plan.
- M'_{txz1} is “tilting momentum on xz plan of gearwheel 1 in recovery condition”. It’s measured in [Nmm] and represents tilting momentum caused by forces laying on xz plan.
- T_{rec} is “maximum recovered torque”, It’s measured in [Nmm] and refers to studies of Chapter 6.1.



Plot 7.4-16: Strains acting on gearwheel 1, measured in [N] and referred to energy recovery condition.



Plot 7.4-17: Strains acting on gearwheel 1, measured in [Nmm] and referred to energy recovery condition.



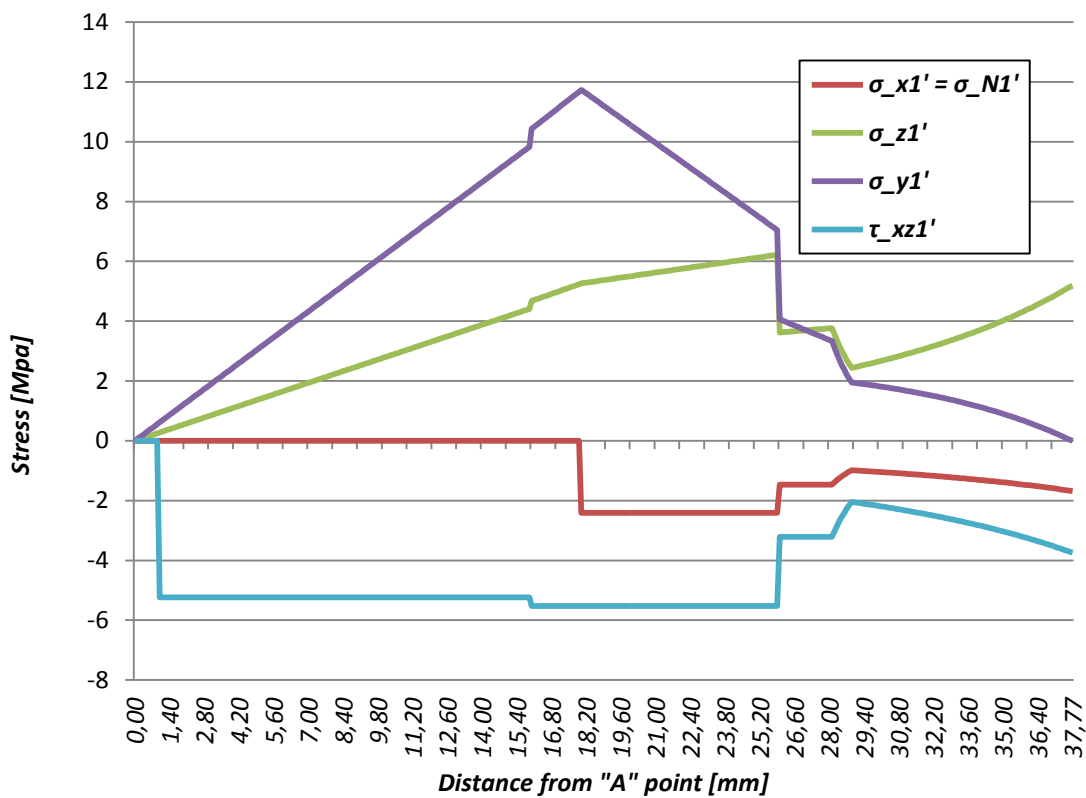
Analogously to the previous case, strains are displayed on two different plots: Plot 7.4-16 and Plot 7.4-17. Plot 7.4-16 is the homologous of Plot 7.4-10 and Plot 7.4-17 is the homologous of Plot 7.4-11.

Comparing Plot 7.4-16 and Plot 7.4-10 It's necessary notice that overall trend of N'_1 and T'_{xy1} is maintained but magnitude is halved. Main difference of two plots is represented by trend of T'_{xz1} which is literally inverted on Plot 7.4-16. Such behaviour is expected because depends by change of sign of tangential component of the force.

By comparison between Plot 7.4-17 and Plot 7.4-11, It's possible notice that main difference is sign of M'_{txz1} which is positive along all the beam. At the same way, value of T_{rec} changes its sign from positive to negative, but the trend remains the same. Instead trend of M'_{txy1} remains the same with important changes in magnitude.

A general observation that can be done on the value of strains related to energy recovery condition, is that values of magnitude are considerably lower than driving condition.

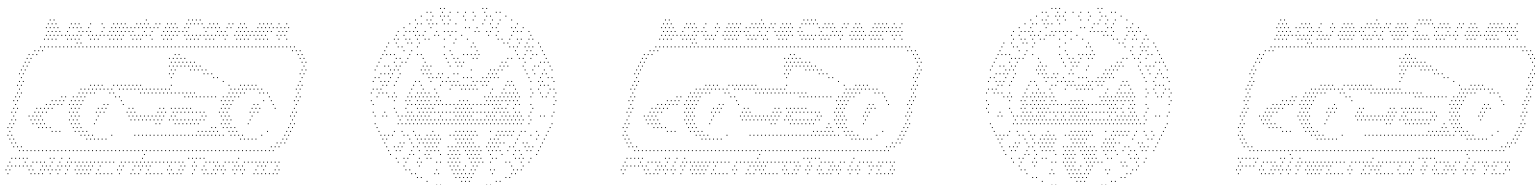
Next step is study of stresses caused by gear meshing forces during energy recovery condition.



Plot 7.4-18: Stresses acting on gearwheel 1, referred to energy recovery condition.

Plot 7.4-18 is the homologous of Plot 7.4-12, trend and magnitude of stresses acting on gearwheel 1 are displayed in function of distance from "A" point.

σ'_{x1} is the "compression stress acting on gearwheel 1 in recovery condition" generated by N'_1 , strain normal to section. Stress is calculated by following function:



$$\text{Eq. 7.4-16} \quad \sigma'_{x1}(x) = \frac{N'_{1i}(x)}{A_{1i}(x)} = \frac{N'_{1i}(x)}{\pi \frac{\phi(x)^2 e_1 - \phi(x)^2 i_1}{4}}$$

Where:

- $N'_{1i}(x)$ is “**strain normal to i section of gearwheel 1 in recovery condition**”. It’s measured in [N] and is function of x, because depends from portion of the beam on which is applied, as depicted by Plot 7.4-16.

How expected, trend of the stress is the same of σ_{x1} , anyway It’s necessary to notice that values of magnitude are halved.

σ'_{z1} is the “**bending stress in recovery condition**” generated by M'_{txy1} , tilting momentum acting on xy plan. Stress is calculated by following function:

$$\text{Eq. 7.4-17} \quad \sigma'_{z1}(x) = \frac{M'_{txy1i}(x)}{W_{f1i}(x)} = \frac{M'_{txy1i}(x)}{\pi \frac{\phi(x)^4 e_1 - \phi(x)^4 i_1}{32 \cdot \phi(x) e_1}}$$

Where:

- $M'_{txy1i}(x)$ is “**tilting momentum acting on xy plan referred to i section of gearwheel 1 in recovery condition**”. It’s measured in [Nmm] and is function of x, because depends from distance from point “A”, as depicted by Plot 7.4-17.

How expected, trend of stress doesn’t change in recovery condition but value of magnitude is halved.

σ'_{y1} is the “**bending stress in recovery condition**” generated by M'_{txz1} , tilting momentum acting on yz plan. Stress is calculated by following function:

$$\text{Eq. 7.4-18} \quad \sigma'_{y1}(x) = \frac{M'_{txz1i}(x)}{W_{f1i}(x)} = \frac{M'_{txz1i}(x)}{\pi \frac{\phi(x)^4 e_1 - \phi(x)^4 i_1}{16 \cdot \phi(x) e_1}}$$

Where:

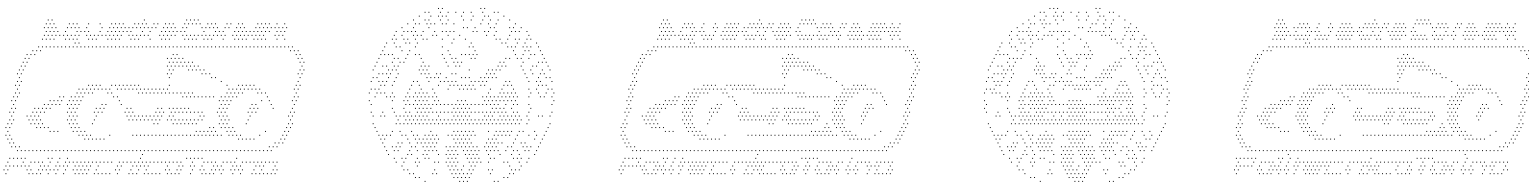
- $M'_{txz1i}(x)$ is “**tilting momentum acting on xz plan referred to i section of gearwheel 1 in recovery condition**”. It’s measured in [Nmm] and is function of x, because depends from distance from point “A”, as depicted by Plot 7.4-17.

Contrary to driving case, sign of stress is positive, due to change in sign of tangential force.

τ'_{yz1} is the “**torsion stress in recovery condition**” generated by T_{rec} . Stress is calculated by following function:

$$\text{Eq. 7.4-19} \quad \tau'_{yz1}(x) = \frac{T_{rec}(x)}{W_{t1i}(x)} = \frac{T_{rec}(x)}{\pi \frac{\phi(x)^4 e_1 - \phi(x)^4 i_1}{32 \cdot \phi(x) e_1}}$$

Where:



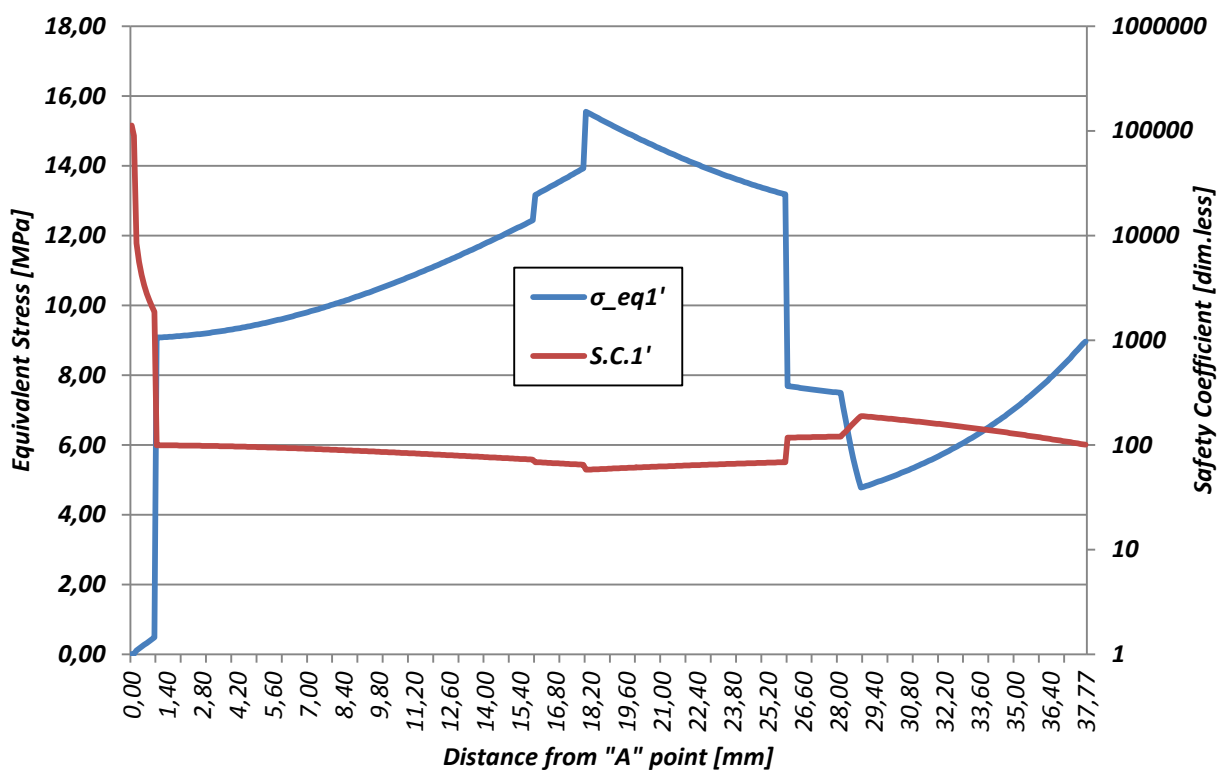
- $T_{rec}(x)$ is “**recovery torque acting on input shaft**”. It’s measured in [Nmm] and is function of x , because depends from portion of the beam on which is applied, as depicted by Plot 7.4-17.

Trend of stress is identical compared to Plot 7.4-12, while sign is negative and magnitude is halved.

After this wide dissertation about trend of single stress, It’s necessary calculate σ'_{eq1} which is the “**equivalent stress on gearwheel 1 in recovery condition**”. It can be calculated through relation displayed by Eq. 7.4-20 and result is displayed by Plot 7.4-19.

Eq. 7.4-20

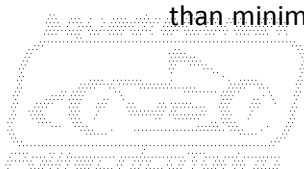
$$\sigma'_{eq1} = \frac{1}{\sqrt{2}} \sqrt{(\sigma'_{x1} - \sigma'_{y1})^2 + (\sigma'_{y1} - \sigma'_{z1})^2 + (\sigma'_{z1} - \sigma'_{x1})^2 + 6 \cdot (\tau'_{xy1}^2 + \tau'_{yz1}^2 + \tau'_{zx1}^2)}$$



Plot 7.4-19: Equivalent Stress and Safety Coefficient acting on gearwheel 1, referred to recovery condition.

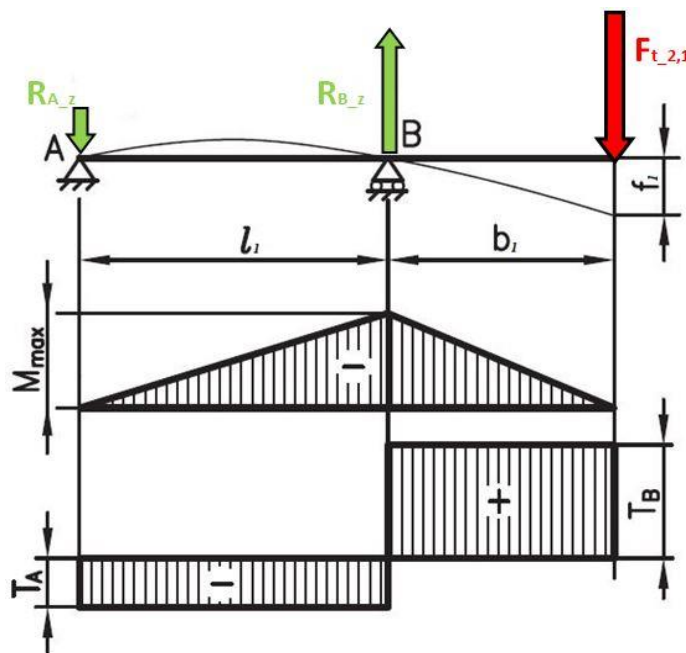
Comparing Plot 7.4-19 with Plot 7.4-13, It’s possible to notice that trend of equivalent stress is slightly different in the central part of the beam. That’s due to change in sign of σ'_{y1} . Other observations can be done on magnitude of the stress which is halved respect to Plot 7.4-13, how It’s expected. By value of equivalent stress, It’s possible obtain value of safety coefficient which is displayed by red curve on Plot 7.4-19.

It’s possible conclude dissertation about stresses on shaft 1 claiming that highest values are exploited during drive condition. That’s due to higher value of transmitted torque, which It’s double respect to recovery case. Anyway observing safety coefficient, It’s clear that gearwheel 1 operates in safe during energy recovery condition too. Indeed minimum value of safety coefficient is about 50 times larger than minimum allowable coefficient. Arguing about safety coefficient, It can be adopted as parameter



to study level of optimization of the component. By virtue of that, It's clear that material is scarcely optimized along the component sections. Anyway, basic technological issues don't allow to equalize value of safety coefficient. Indeed, gearwheel 1 is designed to be easily realized by conventional manufacturing technologies, in order to be cost effective and reliable.

As It was declared in advance, gearwheel 1 can be considered safe by structural point of view, anyway, It's useful understand if operating conditions are proper. With reference to topic treated on Chapter 3.6, It's necessary evaluate stiffness of the component. By previous dissertations, It's clear that relative position of bevel gearwheels is fundamental for the proper operation of the system. Anyway, tilting momentum caused by gear meshing may cause a dangerous displacement which could impair operation of gears. For this reason, target of next verification is esteem value of f_1 which is **"deflection of gearwheel 1 in driving condition"**.

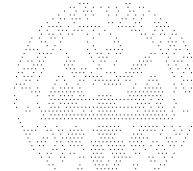
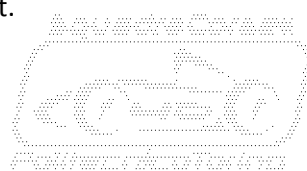
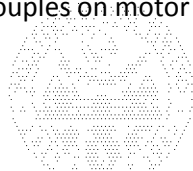
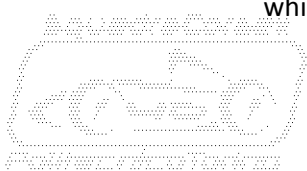


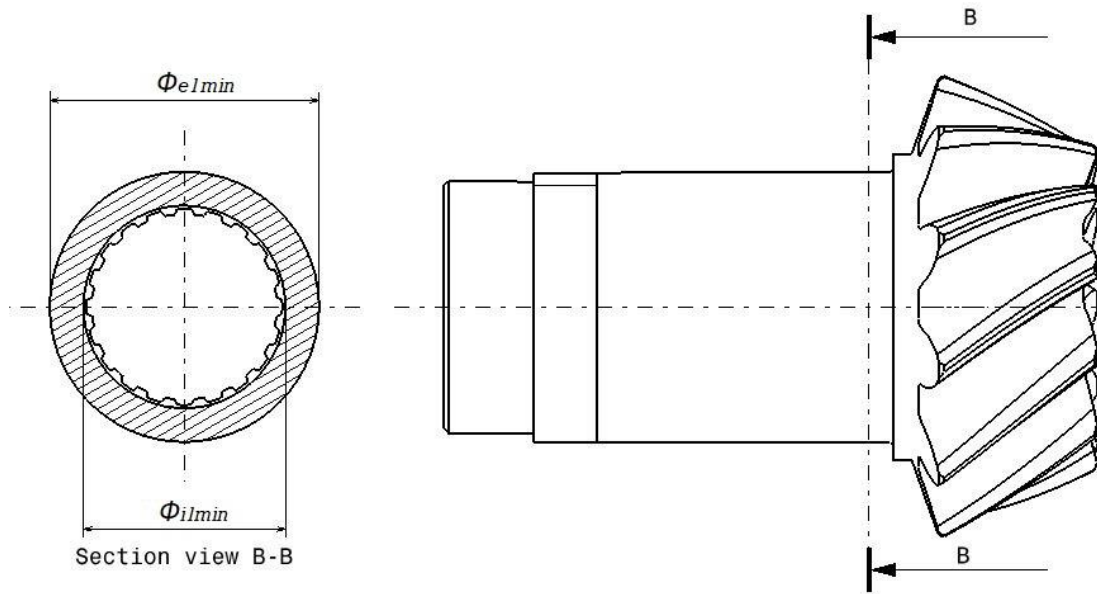
Plot 7.4-20: Model of a cantilever beam loaded on its extremity, Ref.[17].

Plot 7.4-20, from "<http://www.hoeplicuola.it/>" Ref.[17], displays the model of a cantilever beam, which is suitable to represent gearwheel 1 with sufficient accuracy. It's clear that worst case of loads is represented by forces acting on xz plan during drive condition. In particular, module of tangential force, displayed by Eq. 7.1-1, owns highest value.

Despite variations on thickness in gearwheel 1 section, worst case of stressed section is depicted by Plot 7.4-21, which displays **"critical section"**, the thinnest one. To be precautionary enough and to simplify the verification, entire component is modelled as a constant ring section beam, where constant section is represented by critical section. Plot 7.4-21 displays dimensions needed to calculate I_1 which is **"area momentum of inertia"** referred to mentioned section :

- $\varnothing_{e1min} = 30,00[mm]$ is **"minimum external diameter of wheel 1 integrated shaft"** measured in correspondence with critical section. It corresponds with bore diameter of bearings.
- $\varnothing_{i1min} = 22,50[mm]$ is **"minimum internal diameter of wheel 1 integrated shaft"** measured in correspondence with critical section. It's ruled by root diameter of female sp-lined shaft which couples on motor shaft.





Plot 7.4-21: Critical section of gearwheel 1.

By previous data:

$$\text{Eq. 7.4-21} \quad I_{1min} = \pi \cdot \frac{\Phi_{e1min}^4 - \Phi_{i1min}^4}{64} = 27.180 \text{ [mm}^4\text{]}$$

Missing data necessary to calculus of deflection, is:

- $E = 206.000 \text{ [MPa]}$ which is the “steel Young’s module” related to chosen material.

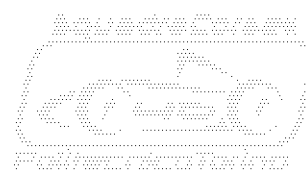
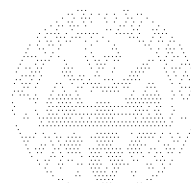
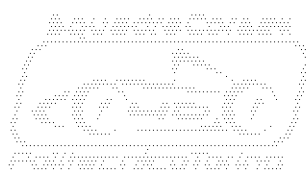
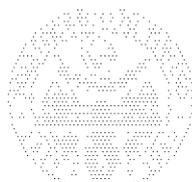
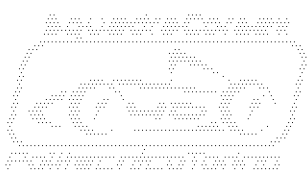
All data necessary to solve Eq. 7.4-22 are available, It’s possible going forward with calculus.

$$\text{Eq. 7.4-22} \quad f_1 = \frac{F_{t2,1}}{E \cdot I_{1min}} \cdot \frac{(l_1 + b_1) \cdot b_1^2}{3} = 1,890 \cdot 10^{-3} \text{ [mm]} \text{ Ref.[17]}$$

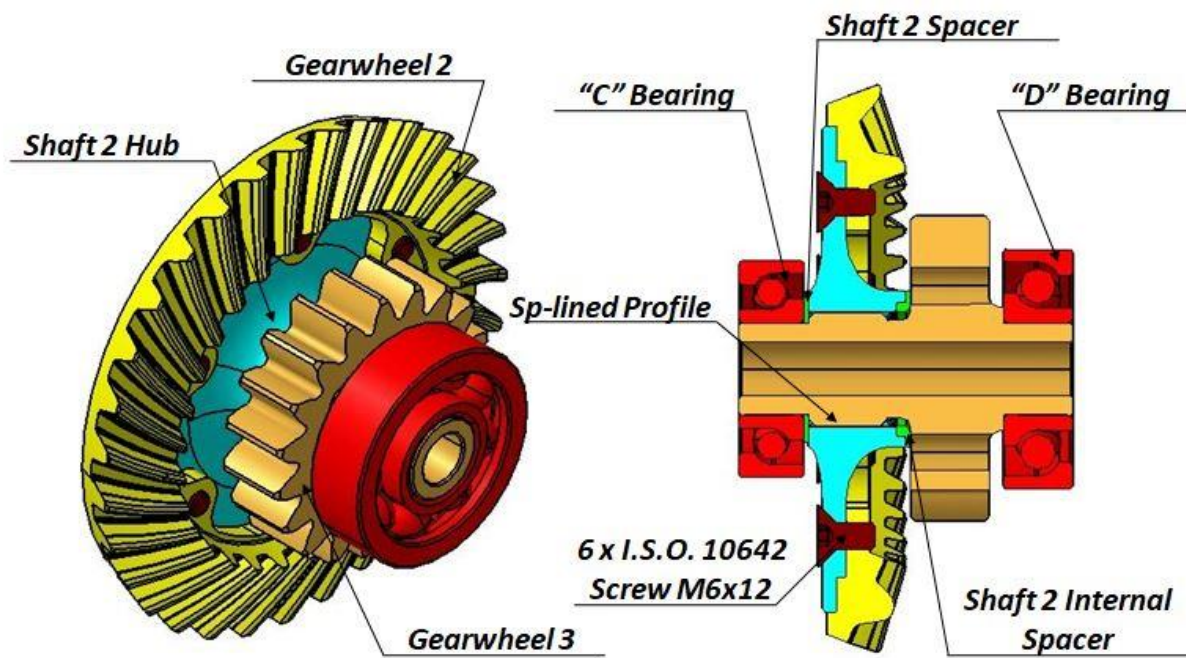
Result of Eq. 7.4-22 indicates that calculated displacement of application point of gear meshing forces is quite small, even if all critical condition was adopted to set up calculation. f_{1all} which represents “maximum allowable result for Eq. 7.4-22” can be 7-8 times larger:

$$\text{Eq. 7.4-23} \quad f_{1all} = 1,500 \cdot 10^{-2} \text{ [mm]}$$

By values of previous basic verifications, is clear that shaft integrated on gearwheel 1 is stiff enough to guarantee the optimal operation of first stage of reduction gear. On the other hand, gearwheel 1 total weight is about 240 [g] which is a considerably light weight. A little percentage of weight saving may complicate the component by point of view of view of manufacturing and, of course, costs. On the other hand, a reduction of bearings bore diameter may lead to a weight saving inferior to 10%. Anyway It would complicate situation by point of view of locknut and rotary seal integration. To conclude actual dissertation, It’s necessary to state that design of gearwheel 1 It’s not convenient to be modified.



7.5. Shaft 2.



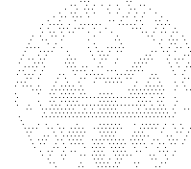
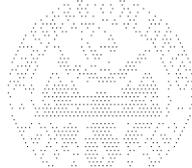
Plot 7.5-1: Details of assembled Shaft 2.

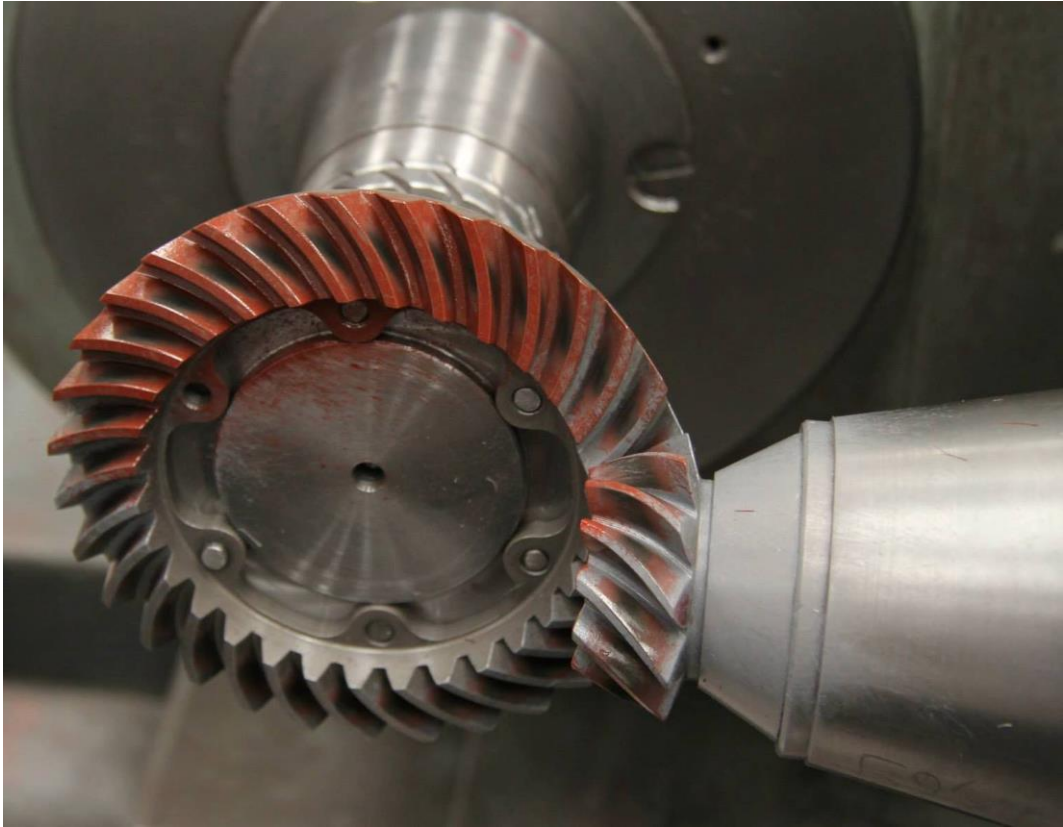
“**Shaft 2**” represents mechanical link between first and second stage of reduction. Indeed shaft 2 is designed assembling “**gearwheel 2**” which is driven wheel of the first stage and “**gearwheel 3**”, drive wheel of the second stage.

By analysis of Plot 7.5-1, It’s possible to notice that steel core of gearwheel 2 have been removed and replaced by a light-weight aluminium flange, “**shaft 2 hub**”. Proper radial position of gearwheel 2 is ensured by a centring diameter machined on the hub. Linkage between gearwheel and hub is ensured by six “**I.S.O. 10642 screw M6x12**” secured by Loctite 271 thread-lock.

“**Gearwheel 3**”, like gearwheel 1 is designed to integrate the main shaft which supports the rotation of all components and which houses bearings. Like any other component, gearwheel 3 is designed to be as lighter as possible, avoiding issues about manufacturing and cost

Linkage between gearwheel 3 and shaft 2 hub is ensured by “**D.I.N. 5482 25x22 sp-lined profile**”, Ref[9]. Anyway sp-lined profile is a slide linkage which allows to shaft 2 hub an axial displacement. Such degree of freedom is useful to control exact position of gearwheel 2 and allows to compensate manufacturing tolerances. To better understand this feature, It’s necessary to take into account “**C Bearing**” which is the reference to determine position of entire shaft 2 inside the gear-box case. “**C Bearing**” is coupled to gearwheel 3 pin by interference, and its internal raceway holds in position shaft 2 hub. Anyway, It’s necessary to notice that hub isn’t the only component between “**C bearing**” internal raceway and gearwheel 3 toothed surface. Indeed, It’s possible to observe a stack of three different components: shaft 2 hub, “**shaft 2 spacer**” and “**shaft 2 internal spacer**”, both coloured by light green on Plot 7.5-1. Entire stack must feature a precise thickness which is determined by measure of gear-box case and bearings. Thickness of shaft 2 hub needs to be accurately measured and It’s considered a bounded dimension. By virtue of that, total thickness of the stack is controlled by spacers which are accurately machined by flat grinding.



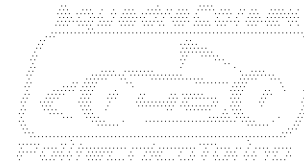
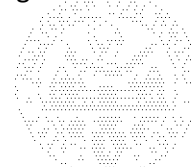
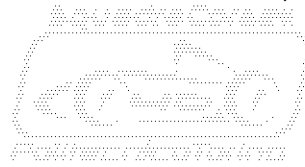
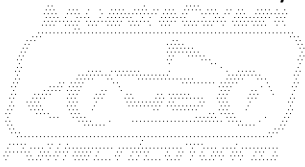


Picture 7.5-1: Test of axial touch by magenta red paint.

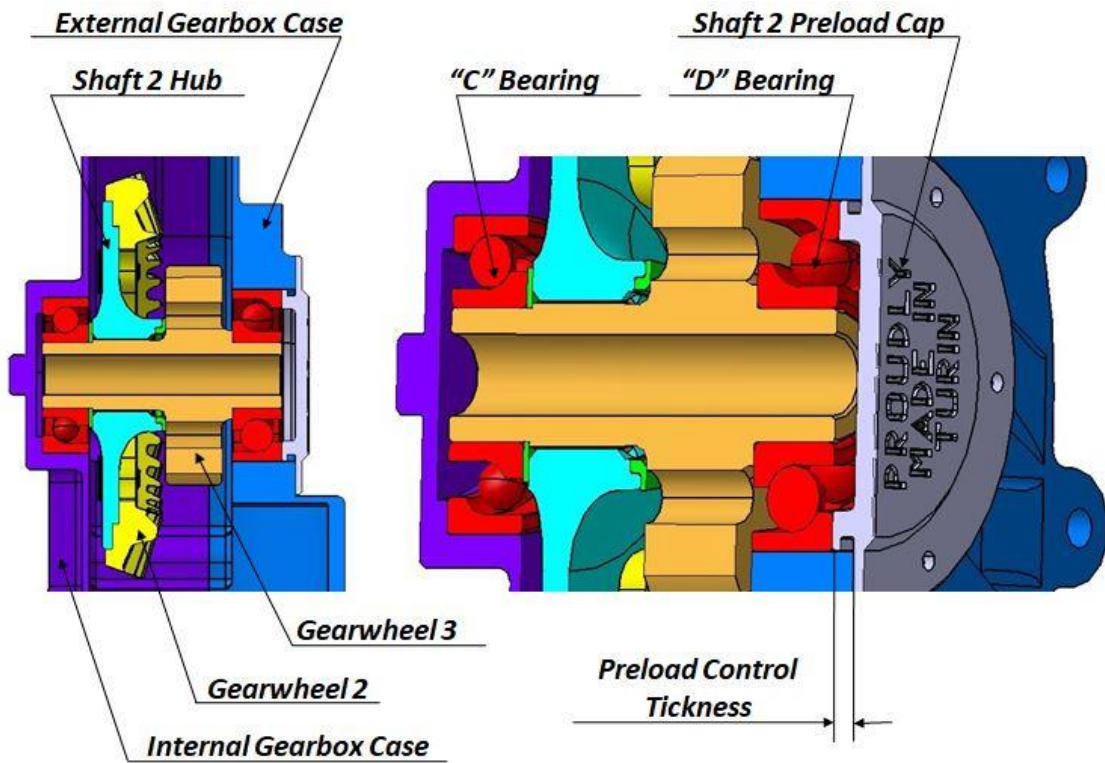
Furthermore, different thickness of spacers is used to control relative position of gearwheel 2 respect to gear-box components. It's the same function performed by axial touch spacer displayed by Plot 7.4-3. It's known that production of bevel gears, prototypes in particular, may lead to some unavoidable manufacturing errors. For this reason, test shown by Picture 7.5-1 is performed to verify exact position of contact patch along face width of driven wheel. Test bench allows to vary relative position of gearwheels and allows to measure difference between design position and optimal operation position. By virtue of that, first indication about thickness of axial touch spacer, shaft 2 spacer and shaft 2 inner spacer is given by previous test. Anyway, test of axial touch must be repeated on assembled gear-box, in order to determine definitive measure of spacers. Obviously, any assembly of gearwheels, flanges and components of the case owns its proper set of custom spacers.

Actual dissertation needs to continue focusing on bearings. Differently from previous case, configuration of bearings needs to be changed. That's due to loads which are no more applied in cantilever position but are applied in central position between two constraints. Chosen bearings layout is known as **"X" configuration** and It's obtained tilting of 180° bearings in "O" configuration, as depicted by Plot 7.4-4 and according with Ref.[15].

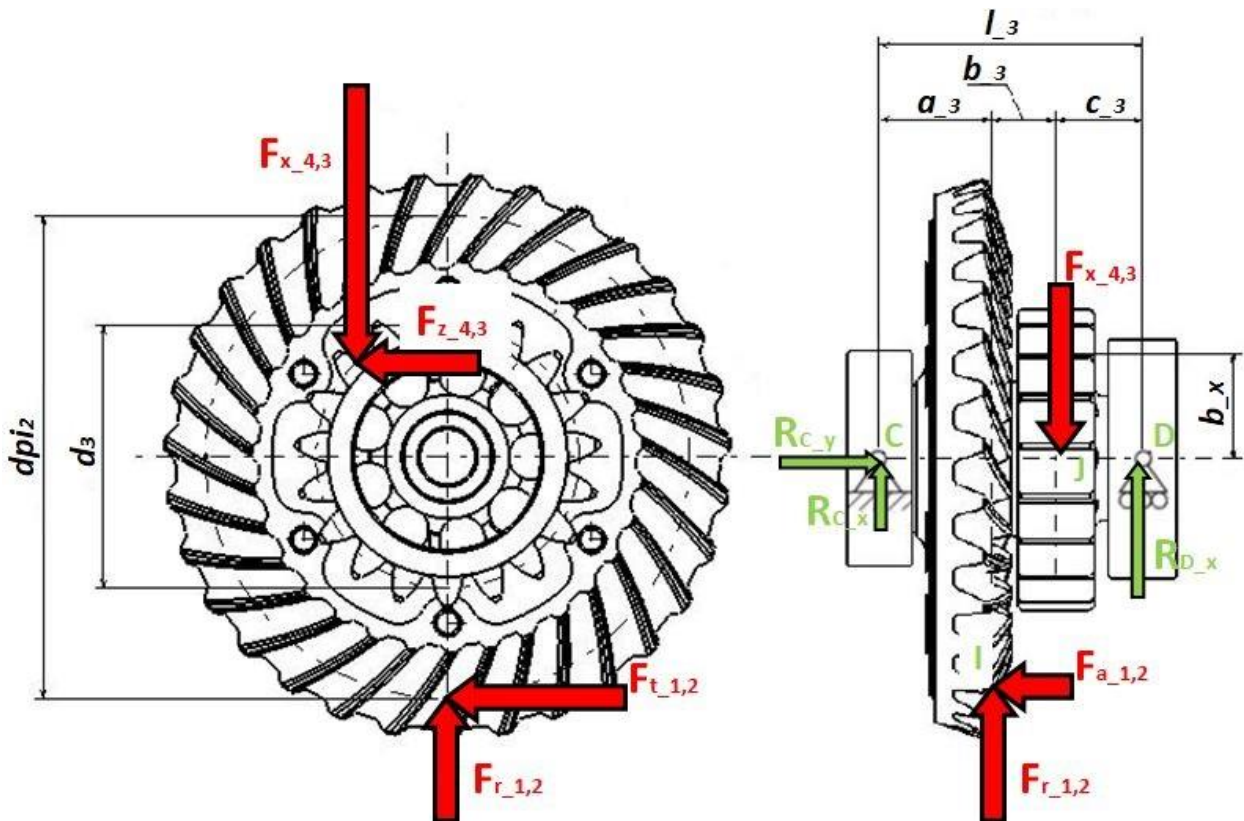
Basically, "C" bearing is in contact with gear-box case by external raceway, while internal raceway is in contact with components of the shaft. At the same way, internal raceway of "D" bearing is in contact with gearwheel 3 while external raceway is in contact with **"shaft 2 preload cap"**. By an accurate observation of Plot 7.5-2 It's possible to notice that all components of shaft 2 are stacked and hold between "C" and "D" bearings. Preload of bearings, in this case too is intended to be a distance which is controlled by dimension of shaft 2 preload cap: **"preload control thickness"**. Such dimension is accurately determined after precise measurements of case, bearings and assembled stack of shaft 2



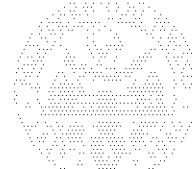
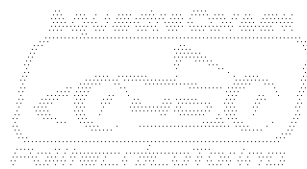
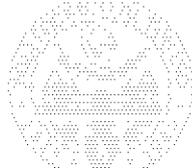
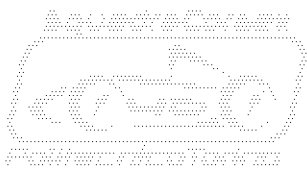
components. Measurement procedure is the core of assembly procedure and is going to be widely described in next Chapter 10.

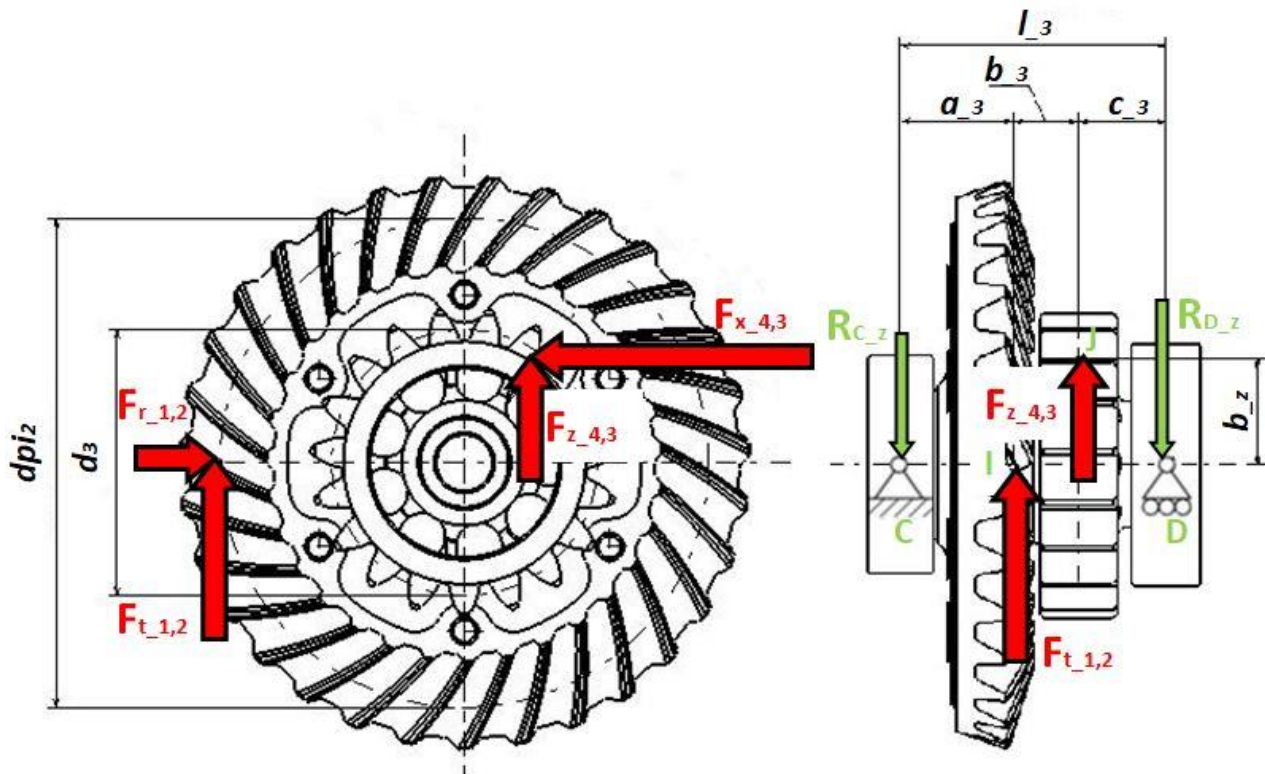


Plot 7.5-2: Details of shaft 2 inside gear-box case.



Plot 7.5-3: Free body diagram of shaft 2 in driving condition, vectors lay on XY plan.





Plot 7.5-4: Free body diagram of shaft 2 in driving condition, vectors lay on YZ plan.

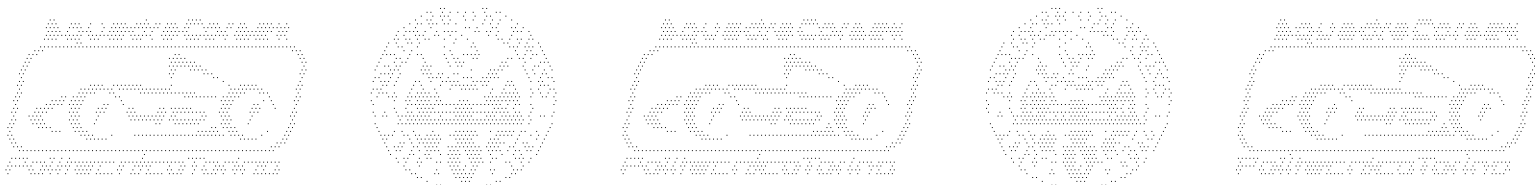
Like in the previous case of Chapter 7.4, next step is analysis of **“free body diagrams”** of shaft 2, according with Ref.[16]. Gear meshing forces displayed at Chapter 7.1 and 7.2 are a known parameter, therefore It’s possible calculate reaction forces on constrains “C” and “D”.

Analogously to previous case, It’s necessary to clarify that subscripts x,y,z indicate direction of reaction force vectors. Furthermore, It’s necessary to observe characteristic points of the model. Point “C” corresponds with mid section of “C” bearing, the same is for point “D”. Point “I” corresponds to force application point of gearwheel 2, while point “J” corresponds to force application point of gearwheel 3.

New geometrical parameters which It’s necessary to introduce to perform the calculus are:

- $l_3 = 57,50 [mm]$ is **“distance of points C-D”**.
- $a_3 = 24,40 [mm]$ is **“distance of points C-I”**.
- $b_3 = 14,10 [mm]$ is **“distance of points I-J”**.
- $c_3 = 19,00 [mm]$ is **“distance of points J-D”**.
- $d_{pi2} = 104,82 [mm]$ is **“intermediate pitch diameter of wheel 2”** driven wheel of first stage of reduction.
- $d_3 = 57,00 [mm]$ is **“pitch diameter of wheel 3”** drive wheel of second stage of reduction.

Analyzing Plot 7.5-3 and Plot 7.5-4 which are referred to driving condition, It’s possible to write a system of five equilibrium equations, homologous to Chapter 7.4. Resolution of the system is analogue to cases treated by previous Chapters 4.1 and 6.1. Therefore, in order to simplify actual dissertation, system and its resolution is going to be omitted. Anyway, reaction forces applied on boundaries are displayed as follows:



Eq. 7.5-1 $R_{Cx} = 78 [N]$

Eq. 7.5-2 $R_{Cy} = 439 [N]$

Eq. 7.5-3 $R_{Cz} = 1.633 [N]$

Eq. 7.5-4 $R_{Dx} = 2.476 [N]$

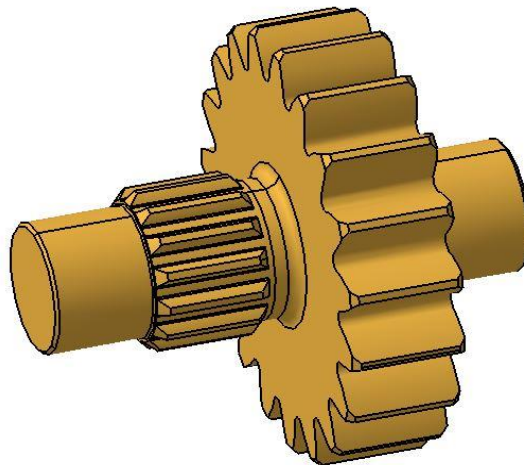
Eq. 7.5-5 $R_{Dz} = 1.714 [N]$

Positive sense of reaction forces is in accordance with green vectors displayed by Plot 7.5-3 and Plot 7.5-4. Such reaction forces, in this case too, are useful to perform structural verifications on shaft 2. By a brief examination about magnitude of reaction forces on boundaries, It's now possible perform a first approximation choice on bearings, those need to be accurately verified in next Chapter **Errore. L'origine riferimento non è stata trovata..**

Component which mainly affect mechanical properties of shaft 2 is gearwheel 3. Design of integrated shaft which bears gearwheel 2 and gearwheel 3 is fundamental to control proper operation and reliability of the entire system. First aspect to take into account is material of gearwheel 3, steel 42CrMo4.

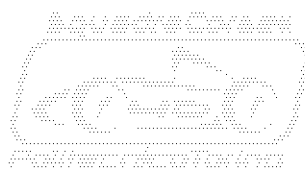
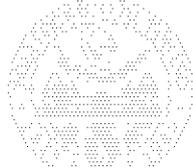
Due to choice of material, gearwheel 3 may be potentially heavy, for this reason, total weight needs to be scrupulously optimized. By virtue of that, eight axial holes have been drilled under the root of teeth. Axial holes are a very cost effective solution because are very easy to manufacture and equilibrate.

Aim of actual topic is explain technique adopted to choose dimension of lightning holes machined on "bulky" component depicted by Plot 7.5-5.

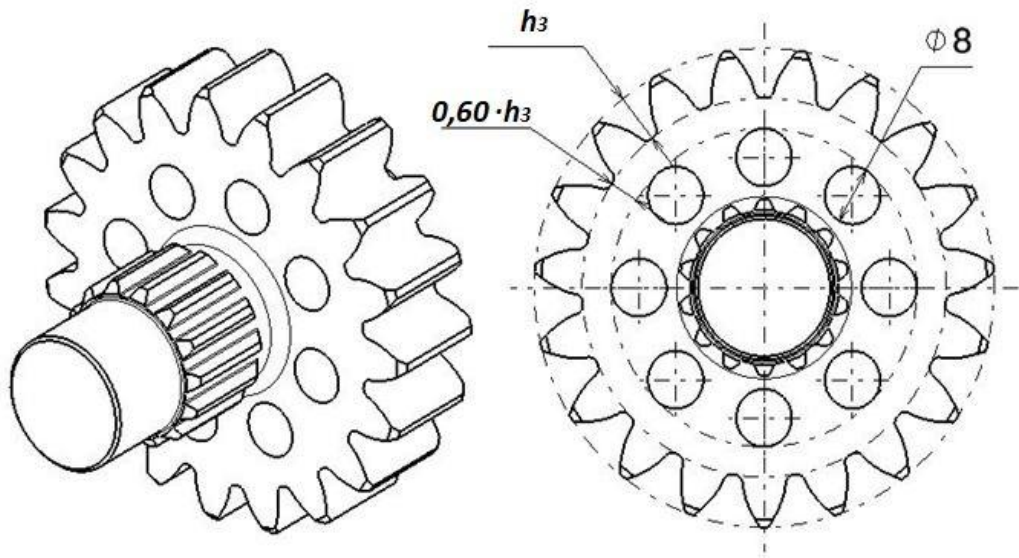


Plot 7.5-5: Raw Gearwheel 3, "bulky" version.

Plot 7.5-6 shows axial holes drilled under root of gearwheel 3 teeth. It's possible to notice that, in order to avoid excessive stress and displacements of teeth, material which lays under roots needs to respect a minimum value of thickness which is related to tooth height. Other bound to respect is fillet which links toothed surface with housing of "D" bearing. Between these two bounds It's possible to position a crown constituted by eight $\Phi 8 [mm]$ axial holes. How It's going to be shown in following Plot 7.5-25,

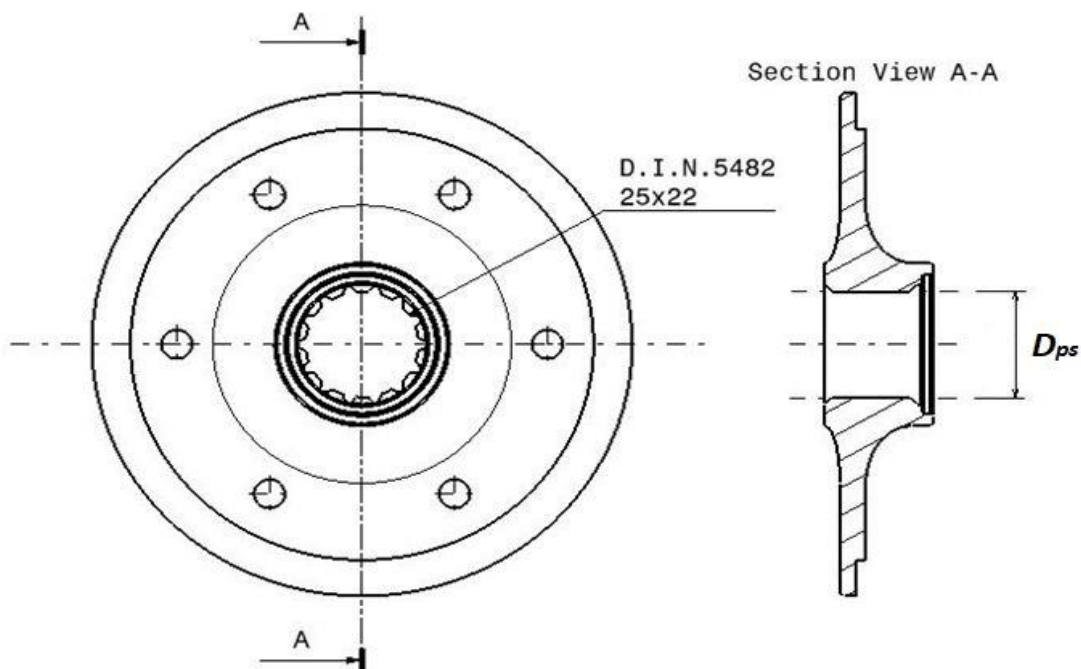


axial holes ensure a weight saving of about 10%. Anyway, most relevant benefit is related to inertia momentum.

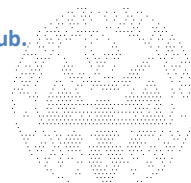


Plot 7.5-6: Crown of lightening axial holes.

Position of axial holes, which are far enough respect to rotation axis of component, ensures an important reduction of inertia, quantified around 10% respect to configuration shown by Plot 7.5-5. This reduction improves dynamic behaviour of gearwheel 3, a very important benefit during transients of the track activity. **Dimensions of shaft integrated on gearwheel 3** is the other aspect that needs to be accurately studied in order to achieve an important weight saving. External diameter is mainly affected by **bore diameter of chosen bearings, $\Phi 20$ [mm]**, and by **dimension of sp-lined profile** which needs to be verified. Like it was explained in advance, D.I.N. 5482 profile links gearwheel 3 with shaft 2 hub which is manufactured by a billet of light weight aluminium alloy, Al7075 T651 Ergal. Of course, weakest side of the joint is the aluminium female sp-lined profile displayed by Plot 7.5-7.



Plot 7.5-7: Female sp-lined shaft on shaft 2 hub.



Data needed to perform verification are:

- $R_{p02.7075} = 450$ [MPa] is “**Al7075 yield strength**” material of shaft 2 hub.
- $D_{psp} = 22,40$ [mm] is “**pitch diameter of sp-lined profile**” machined on gearwheel 3 integrated shaft.
- $l_{sp} = 14,00$ [mm] is “**length of sp-lined profile**” machined on gearwheel 3 integrated shaft. Such dimension depends mainly by axial dimension of gearwheel 2.
- $S.C. = 1,2$ [dim. less] is the “**safety coefficient**” adopted in all performed verifications.

First variable to calculate is $\sigma_{all.7075}$ the “**Al7075 allowable stress**”:

$$\text{Eq. 7.5-6} \quad \sigma_{all.7075} = \frac{R_{p02.7075}}{S.C.} = 375 \text{ [MPa]}$$

Main stress which sp-lined profile bears is a torsion, by the way It’s necessary to transform result of Eq. 7.5-6 into $\tau_{all.7075}$ the “**Al7075 allowable tangential stress**”:

$$\text{Eq. 7.5-7} \quad \tau_{all.7075} = \frac{\sigma_{all.7075}}{\sqrt{3}} = 216 \text{ [MPa]}$$

It’s necessary take in consideration that input torque of the verification doesn’t coincide with endurance torque T_{end} but It’s defined as T_{is} which is “**torque acting on intermediate shaft in driving condition**”:

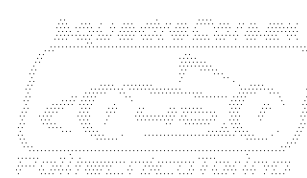
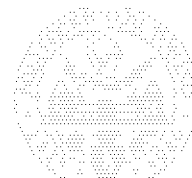
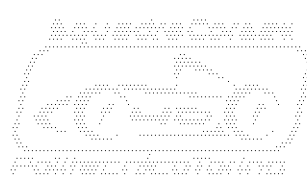
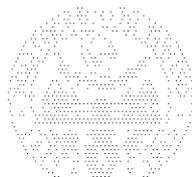
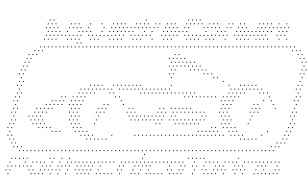
$$\text{Eq. 7.5-8} \quad T_{is} = T_{end} \cdot i_{1,2} = 112.727 \text{ [Nmm]}$$

All information needed to calculate τ_{sp} the “**Maximum tangential stress on sp-lined profile**” are known, then It’s possible to write:

$$\text{Eq. 7.5-9} \quad \tau_{sp} = \frac{16 \cdot T_{is}}{\pi \cdot (D_{psp})^2 \cdot l_{sp}} = 82 \text{ [MPa]}$$

By comparison of results of Eq. 7.5-7 and Eq. 7.5-9, It’s clear that female sp-lined profile machined on shaft 2 hub is **widely safe in static conditions of load**. Indeed its actual safety coefficient exceeds value of 2 [dim.less]. To level out such value to the minimum declared at Chapter 5.1, It would be useful reduce length of sp-lined profile. Anyway this solution is useless because reduction of profile doesn’t allow save of space along y axis. That’s because gearwheel 2 and gearwheel 3 are already distanced by a minimum clearance of about 2,2 [mm]. Furthermore, reduction of weight is very marginal. By virtue of that, It’s cautionary keep length of sp-lined profile extended for all the available space. On the other hand, can be useful reduce radial dimensions, with a consequent reduction of number of teeth. Anyway that’s not possible because dimension of root diameter of sp-lined profile needs to be larger than bore diameter of chosen bearings, which is $\phi 20$ [mm]. That ensures the proper assembly of all shaft 2 components. Previous topic about dimension of sp-lined profile can be concluded by statement that linked components operate in wide safety conditions and no one parameter of first approximation design is going to be modified.

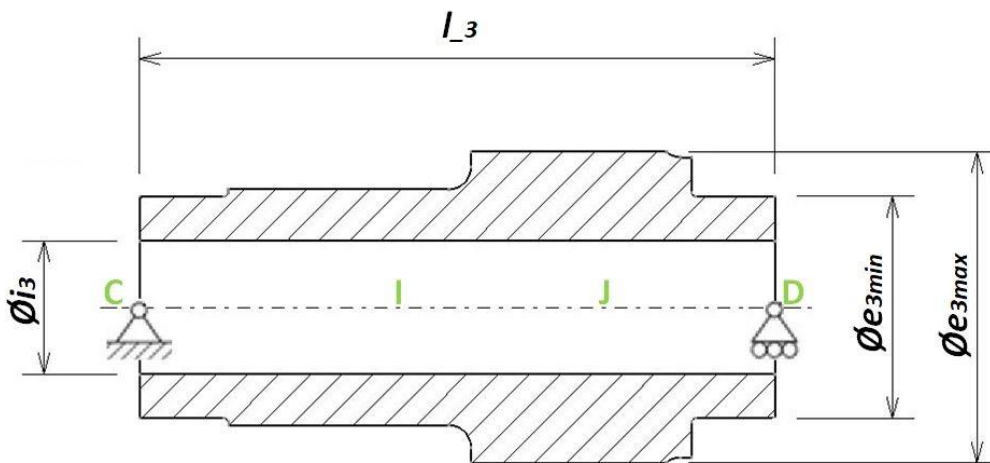
Back to the topic treated before, sp-lined profile verification, It’s necessary proceed with the study of gearwheel 3 lightening. By virtue of that, It’s necessary return on Plot 7.5-5, by image It’s clear that a huge quantity of material is still present in proximity of integrated shaft. An **axial hole** which passes



through integrated shaft, can be an optimal solution to save precious weight, with a small difference of complexity and cost.

By point of view of inertia momentum, benefit is much less important, differently from case of crown of holes. That's due to position of removed material which is distributed very close to rotational axis of gearwheel 3. Anyway, dimension of lightening axial hole cannot be chosen arbitrarily because affects **strength and stiffness** of the entire shaft 2 assembly.

To better study such issue, a **F.E.M. model** may be set up. However, this solution lasts a lot of precious time because, 3D models of component needs to be re-meshed from zero after any modification which involves the structure. For this reason, It's more convenient set up a **parametric model** analogue to that displayed at previous Chapter 7.4. Structural model of gearwheel 3, depicted by Plot 7.5-8, have been set up in a very simple way. With reference to Plot 7.5-3 and Plot 7.5-4, It's possible notice that model includes the part internal to points "C" and "D" only.

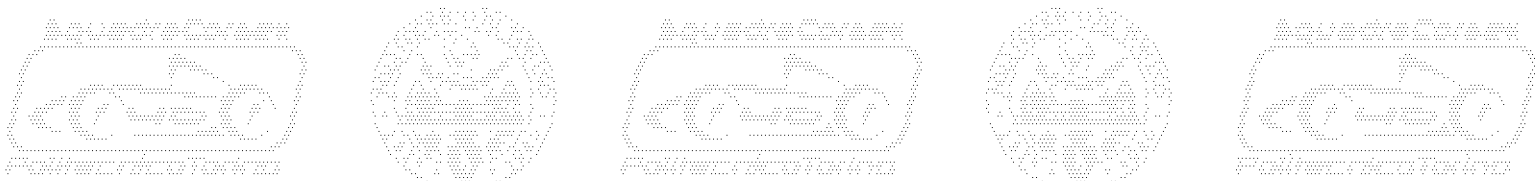


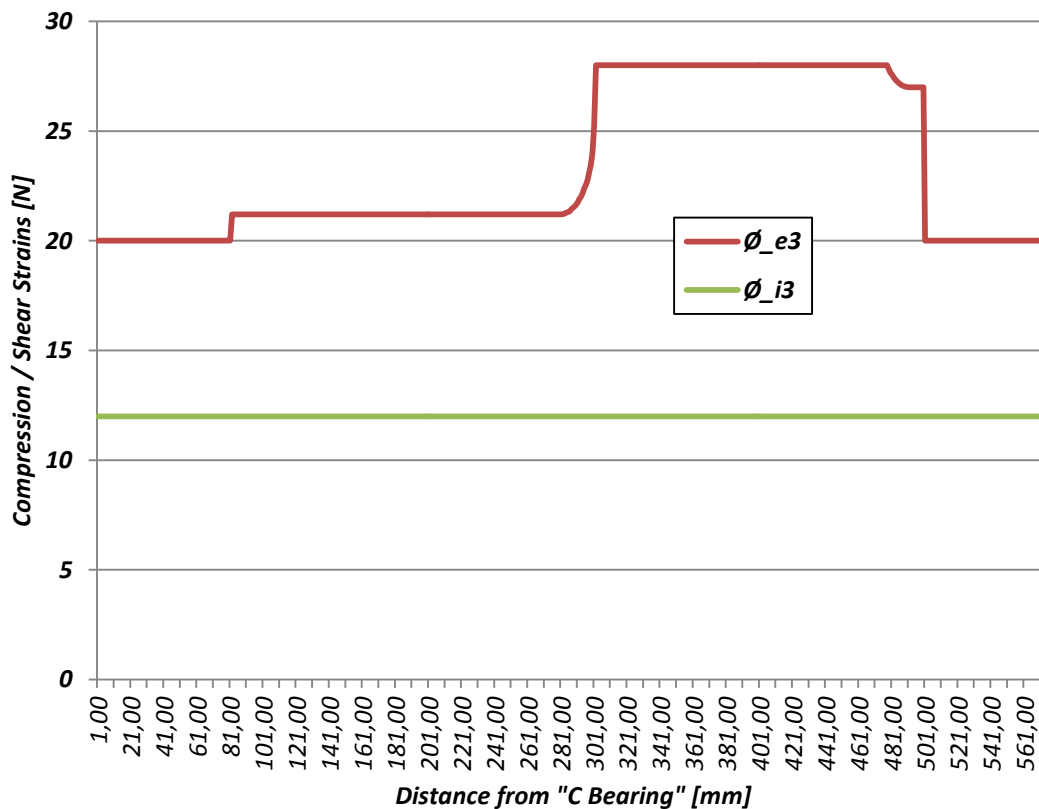
Plot 7.5-8: Simplified structural model of gearwheel 3.

Key diameters to take into account are only 3:

- $\varnothing_{e3min} = 21,20 [mm]$ is "**minimum external diameter of wheel 3 integrated shaft**". Such dimension is constant and corresponds to bearing bore diameters.
- $\varnothing_{e3max} = 28,00 [mm]$ is "**maximum external diameter of wheel 3 integrated shaft**". Such dimension is constant and includes all the material internal to axial holes crown. It's necessary to underline that such representation is cautionary enough, because contribution of material located in toothed part have been neglected.
- \varnothing_{i3} is "**internal diameter of wheel 3 integrated shaft**". Such dimension is measured in $[mm]$ and represents the variable of the study. Diameter needs to be constant along all beam, due to manufacturing issues.

Model have been implemented by an advanced spreadsheet of Microsoft Excell software. Portion of integrated shaft displayed by Plot 7.5-8 have been split on **576 sections** perpendicular to y axis and **spaced of 0,1 [mm]** each other. Such technique ensures a good definition of the extracted plots. Aim of the spreadsheet is provide a versatile instrument to study strength and stiffness of modelled beam. Result of section modelling is depicted by Plot 7.5-9.





Plot 7.5-9: Variation of diameters of gearwheel 3 implemented on Microsoft Excell Spreadsheet.

Dimension of \varnothing_{i3} is varied with increasing steps of about 1 [mm], starting from a beam which features $\varnothing_{i3} = 0$. Gear meshing forces and constraint reaction forces are the same depicted by free body diagrams of Plot 7.5-3 and Plot 7.5-4.

It's necessary to underline that model displayed by Plot 7.5-8 represents a very extreme condition by point of view of sections, which are reduced to the minimum. Anyway, the aim of the study is briefly understand which could be the suitable value of \varnothing_{i3} . Potential calculations of weight optimization can be successively performed by F.E.M. analysis.

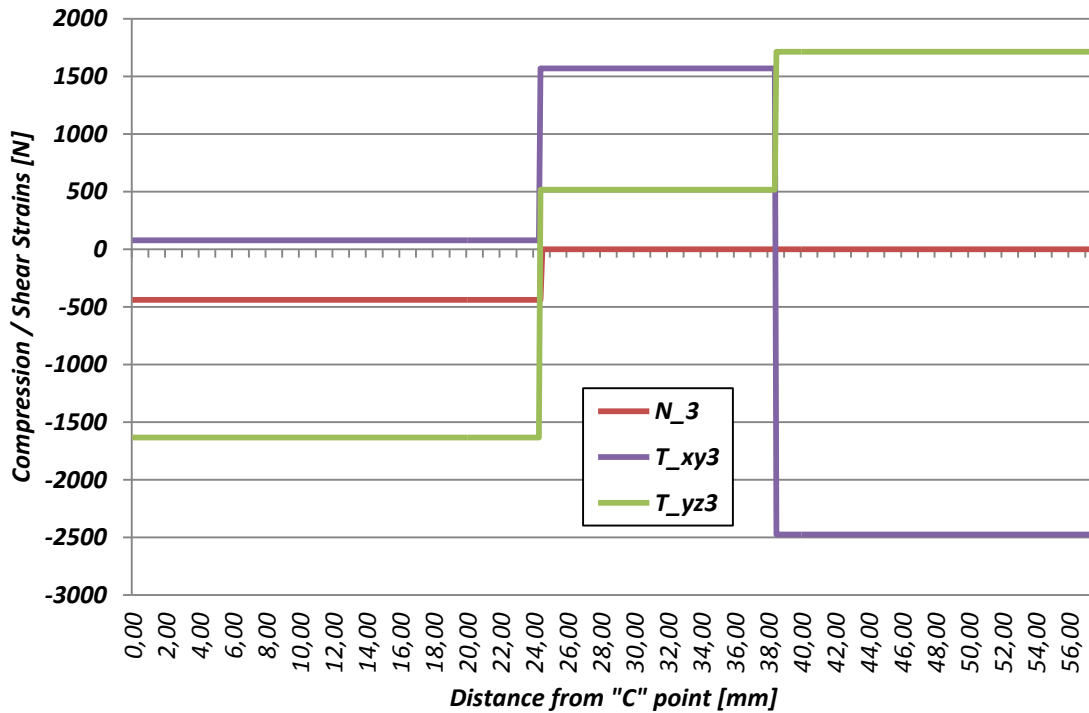
Next step is determination of different strains acting on the model, caused by gear meshing forces, according with Ref.[16]:

- N_3 is "strain normal to section of gearwheel 3 in driving condition". It's measured in [N] and represents the compression caused by axial force which gearwheel 1 transmits to gearwheel 2.
- T_{xy3} is "shear strain on xy plan of gearwheel 3 in driving condition". It's measured in [N] and represents shear caused by forces laying on xy plan.
- T_{xz3} is "shear strain on xz plan of gearwheel 3 in driving condition". It's measured in [N] and represents shear caused by forces laying on xz plan.
- M_{txy3} is "tilting momentum on xy plan of gearwheel 3 in driving condition". It's measured in [Nmm] and represents tilting momentum caused by forces laying on xy plan.
- M_{txz3} is "tilting momentum on xz plan of gearwheel 3 in driving condition". It's measured in [Nmm] and represents tilting momentum caused by forces laying on xz plan.
- T_{is} is "torque acting on intermediate shaft in driving condition". It's measured in [Nmm] and is the same parameter calculated in the verification of sp-lined profile.

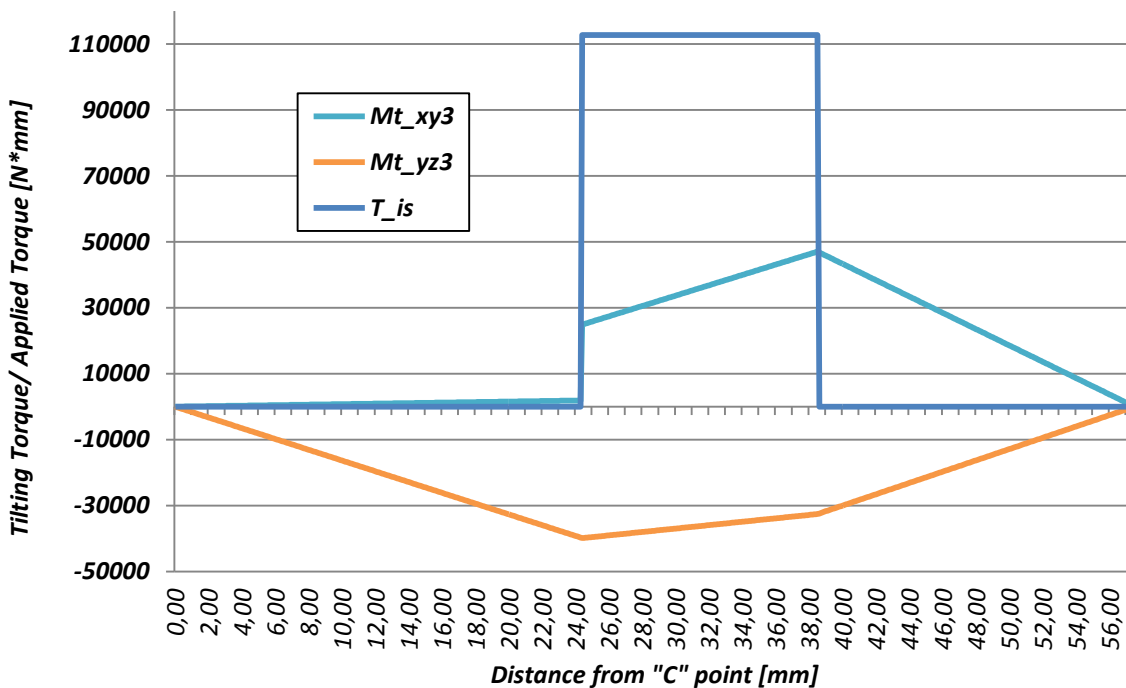


Strains are displayed on two different plots: Plot 7.5-10 which is the homologous of Plot 7.4-10 and Plot 7.5-11 which is the homologous of Plot 7.4-11.

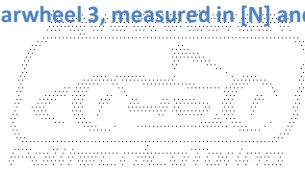
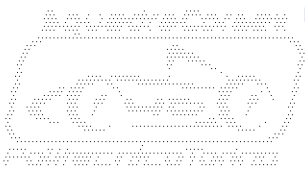
About Plot 7.5-10, It's necessary to observe that normal strain acts in the portion of beam included between point "C" and point "I", force application point related to gearwheel 2. By the way, not all the model is subject by compression. Magnitude of shear strains varies in coincidence with gear forces application points, as expected.



Plot 7.5-10: Strains acting on gearwheel 3, measured in [N] and referred to driving condition.



Plot 7.5-11: Strains acting on gearwheel 3, measured in [N] and referred to driving condition.



Next step is study of stresses caused by strains displayed on previous plots. Stresses are strongly affected by main diameters displayed by the model of Plot 7.5-8. Such dimensions affect area, area momentum of inertia, torsion strength modulus and bending strength modulus. By virtue of that, It's interesting **study behaviour of stresses depending on ϕ_{i3}** dimension. Four plots have been generated, ϕ_{i3} varies from 0 [mm] to 18 [mm].

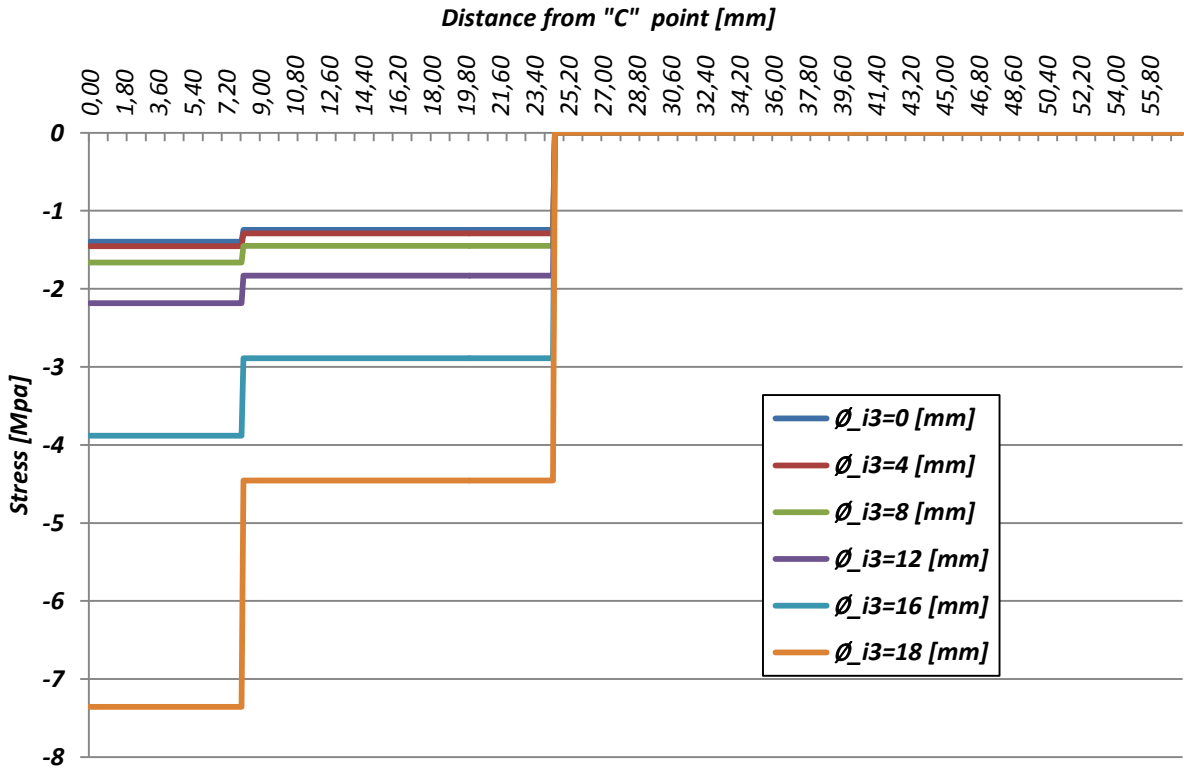
Plot 7.5-12, Plot 7.5-13, Plot 7.5-14 and Plot 7.5-15 have been created, It would be useful analyze each of them in the detail. Analogously to previous Plot 7.5-10 and Plot 7.5-11, horizontal axis shows distance from point "C".

Plot 7.5-12 displays trend of σ_{y3} which is the **"compression stress acting on gearwheel 3 in driving condition"** generated by N_3 , strain normal to section. Stress is calculated by following function:

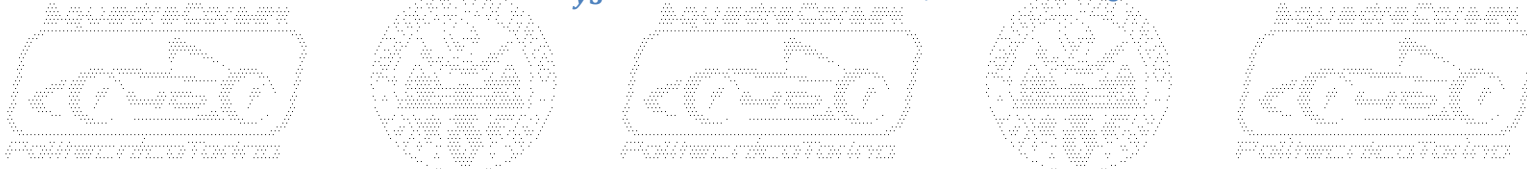
$$\text{Eq. 7.5-10} \quad \sigma_{y3}(y) = \frac{N_{3i}(y)}{A_{3i}(y)} = \frac{N_{3i}(y)}{\pi \frac{\phi(y)^2 e_3^2 - \phi_{i3}^2}{4}}$$

Where:

- $N_{3i}(y)$ is **"strain normal to i section of gearwheel 3 in driving condition"**. It's measured in [N] and is function of y, because depends from portion of the beam on which is applied, as depicted by Plot 7.5-10.
- $A_{3i}(y)$ is **"area of i section of gearwheel 3"**. It's measured in [mm²] and is function of y, because depends by distance from point "C" and, of course, by dimension of internal diameter ϕ_{i3} .



Plot 7.5-12: Behaviour of σ_{y3} in function of internal diameter, referred to driving condition .



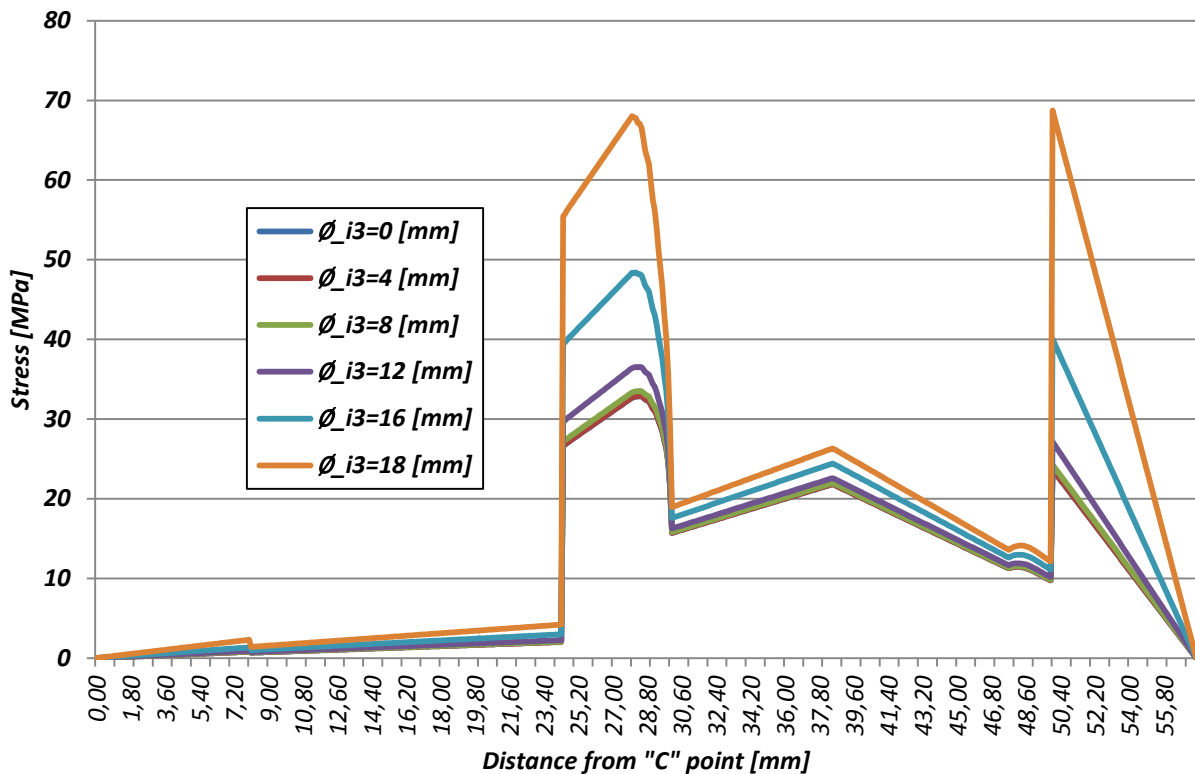
Value of the stress different from zero only in the section between point “C” and point “I”, as expected. Negative value of the stress is influenced by changing on section amplitude. General trend of the stress is not influenced by internal diameter \varnothing_{i3} , difference can be appreciated observing magnitude of the stress only. It’s necessary notice that internal diameters included between 0 [mm] and 4 [mm] are practically irrelevant by point of view of stress magnitude. It’s possible to notice an important increase of stress when internal diameter varies between 16 [mm] and 18 [mm]. Anyway, maximum value of stress is not alarming, due to quite low magnitude.

Plot 7.5-13 displays trend of σ_{z3} which is the “**bending stress acting on gearwheel 3 in driving condition**” generated by M_{txy3} , tilting momentum acting on xy plan. Stress is calculated by following function:

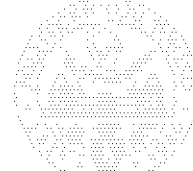
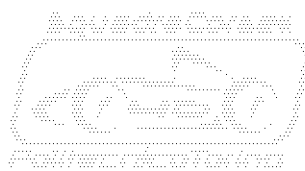
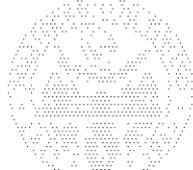
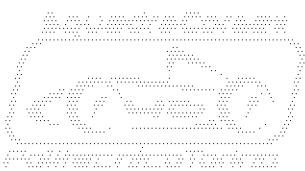
$$\text{Eq. 7.5-11} \quad \sigma_{z3}(y) = \frac{M_{txy3i}(y)}{W_{f3i}(y)} = \frac{M_{txy3i}(y)}{\pi \frac{\varnothing(y)^4_{e3} - \varnothing^4_{i3}}{32 \cdot \varnothing(y)_{e3}}}$$

Where:

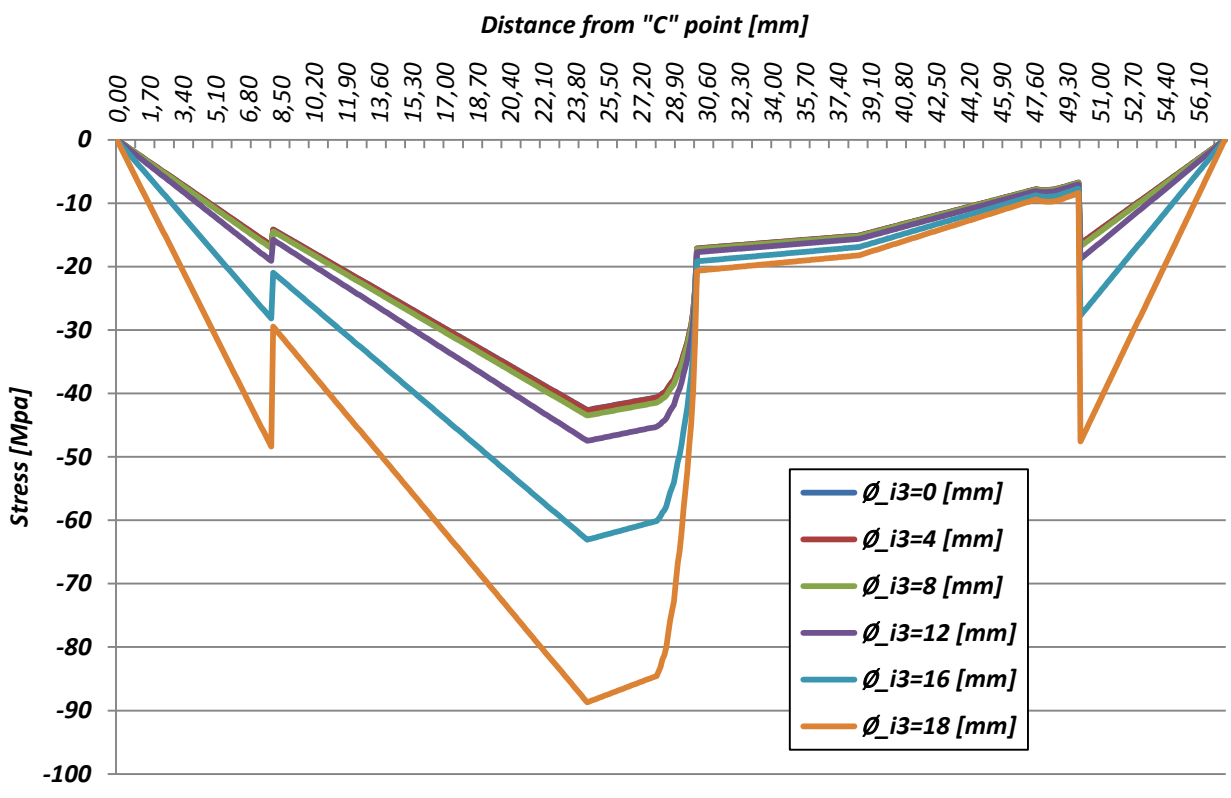
- $M_{txy3i}(y)$ is “**tilting momentum acting on xy plan referred to i section of gearwheel 3 in driving condition**”. It’s measured in [Nmm] and is function of y, because depends from distance from point “C”, as depicted by Plot 7.5-11.
- $W_{f3i}(y)$ is “**bending strength modulus referred to i section of gearwheel 3**”. It’s measured in [mm³] and is function of y, because depends by distance from point “C” and, of course, by dimension of internal diameter \varnothing_{i3} .



Plot 7.5-13: Behaviour of σ_{z3} in function of internal diameter, referred to driving condition.



Value of stress, naturally affected by M_{txy3} trend, varies along all the beam displaying step variations and important spikes. Anyway, value is positive along all the component and displays null value in correspondence with mid section of bearings, following the trend of M_{txy3} . First important step variation exhibits in correspondence with point "I" and It's due to tilting momentum caused by meshing forces of gearwheel 2. Other important spike arises in correspondence of a consistent section reduction, where housing of "D" bearing is placed. It's possible to notice an important drop in the stress value, localized between 28,10 [mm] and 49,90 [mm]. Cause is the important change on external diameter of the beam, due to toothed section of the component. It's possible notice effect of fillet which causes a smoother change in the stress value. Like It was shown by previous case, internal diameter value doesn't influence general trend of the stress, internal diameter influences magnitude only. Anyway, values of internal diameters included between 0 [mm] and 8 [mm] are practically irrelevant by point of view of stress magnitude. On the other hand, value of 18 [mm] is able to double the stress. In this case, values of stress are considerably higher than previous case, and safety of most stressed section needs to be accurately verified.

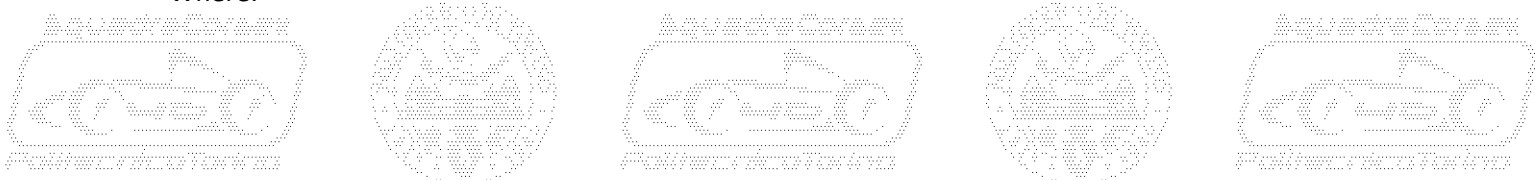


Plot 7.5-14: Behaviour of σ_{x3} in function of internal diameter, referred to driving condition.

Plot 7.5-14 displays trend of σ_{x3} which is the "bending stress acting on gearwheel 3 in driving condition" generated by M_{tyz3} , tilting momentum acting on yz plan. Stress is calculated by following function:

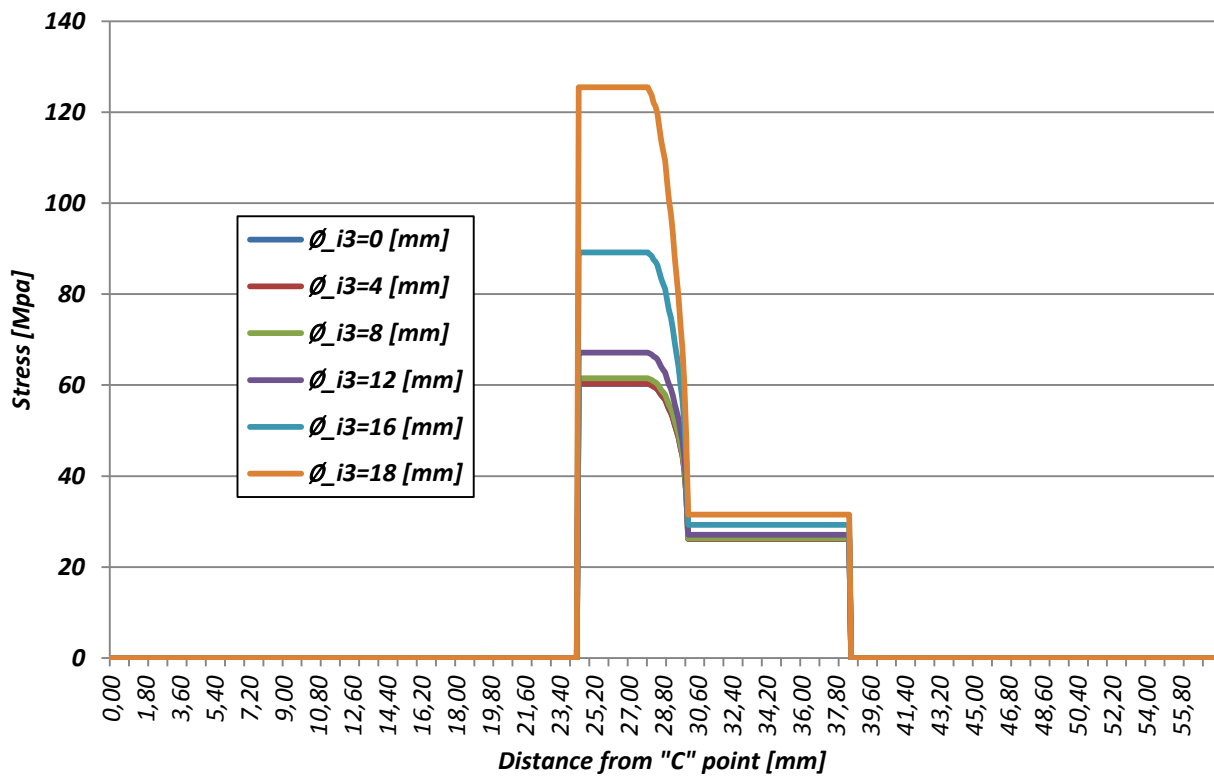
Eq. 7.5-12
$$\sigma_{x3}(y) = \frac{M_{tyz3i}(y)}{W_{f3i}(y)} = \frac{M_{tyz3i}(y)}{\pi \frac{\emptyset(y)^4 e3 - \emptyset i3^4}{16 \cdot \emptyset(y) e3}}$$

Where:



- $M_{tyz3i}(y)$ is “tilting momentum acting on yz plan referred to i section of gearwheel 3 in driving condition”. It’s measured in [Nmm] and is function of y, because depends from distance from point “C”, as depicted by Plot 7.5-11.

Analogously from previous case, value of stress results null in coincidence with points “C” and “D”. Value is negative along all beam and displays some spikes. Anyway, peak value appears in coincidence with forces application point “I” while pikes are localized in coincidence with changes of section area. In this case too, general trend of the stress isn’t influenced by values of internal diameter and magnitude of the stress isn’t influenced by values of internal diameters included between 0 [mm] and 8 [mm]. Analogously from previous case, value of 18 [mm] is able to double the stress. Values of stress studied in actual case, doesn’t appear important by point of view of safety.



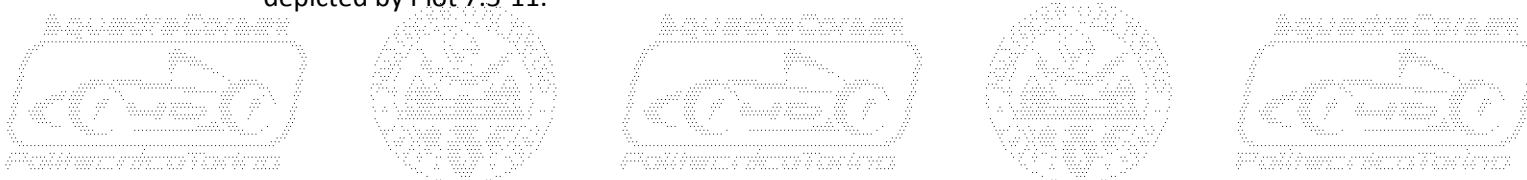
Plot 7.5-15: Behaviour of τ_{xz3} in function of internal diameter, referred to driving condition.

Plot 7.5-15 displays trend of τ_{xz3} which is the “torsion stress acting on gearwheel 3 in driving condition” generated by T_{is} , drive torque which acts on shaft 2. Stress is calculated by following function:

$$Eq. 7.5-13 \quad \tau_{xz3}(y) = \frac{T_{is}(y)}{W_{ti3}(y)} = \frac{M_{tyzi}(y)}{\pi \frac{\phi(y)^4 e3 - \phi_{i3}^4}{32 \cdot \phi(y) e3}}$$

Where:

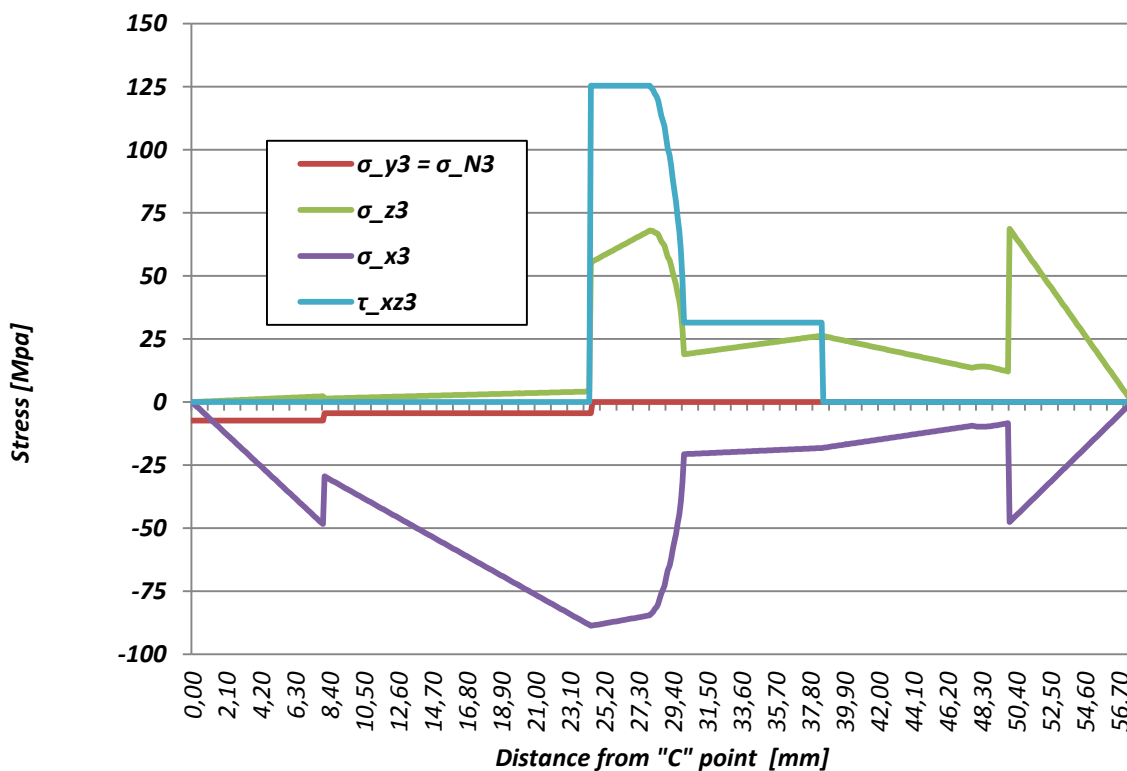
- $T_{is}(y)$ is “driving torque acting intermediate shaft in driving condition”. It’s measured in [Nmm] and is function of y, because depends from portion of the beam on which is applied, as depicted by Plot 7.5-11.



- $W_{ti3}(y)$ is **“torsion strength modulus referred to i section of gearwheel 3”**. It’s measured in $[mm^3]$ and is function of y , because depends by distance from point “C” and by dimension of internal diameter \emptyset_{i3} . It’s possible to notice that value is double respect to $W_{fi3}(y)$.

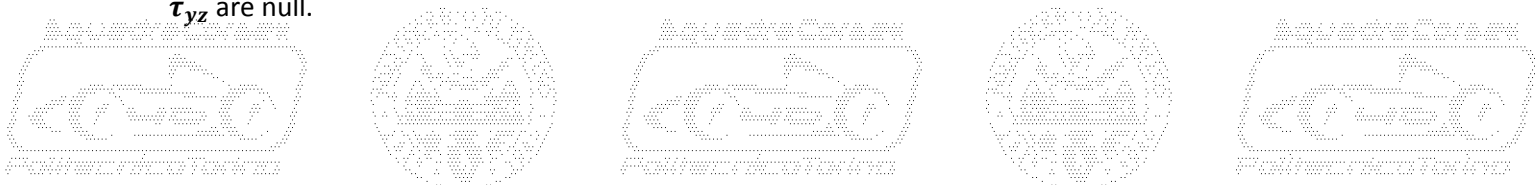
While driving torque is applied between gear force application points, “I” and “J”, value of torsion stress is different from zero in the central part of the beam only. It’s necessary to observe that stress would be constant along all the central part of the beam. Anyway, increase of section due to toothed part of the component, make stress value collapse. It’s important appreciate smoothing function of the fillet in this case too. Despite sudden changes in stress magnitude, peak value is located in correspondence with force application point of gearwheel 2. About influence of internal diameter, It’s irrelevant on the general trend in this case too. However, It’s important to notice that values smaller than $8 [mm]$ are irrelevant by point of view of stress increase, like in previous cases. In this case, value of $18 [mm]$ causes an increase in the stress which is more than double, and overall magnitude of stress suggest a scrupulous verification of safety.

After this wide dissertation about trend of single stresses, It’s important to observe that application of single stress, is not able to compromise safety of the structure, indeed peak value between stresses is $6\div7$ times smaller than allowable stress of the material. How It was displayed by previous Chapter 7.4, It’s necessary to calculate a function of stress which takes into account contribution of single stresses, σ_{eq3} which is the **“equivalent stress on gearwheel 3 in driving condition”**. It can be calculated thanks to following relation displayed by Eq. 7.5-14.



Plot 7.5-16: Stresses related to $\emptyset_{i3} = 18 [mm]$, referred to driving condition.

It’s necessary remind that, in the treated case, Eq. 7.5-14 represents a function with distance from “C” bearing. It’s necessary notice that equation have been written in entire form, even if values of τ_{xy} and τ_{yz} are null.

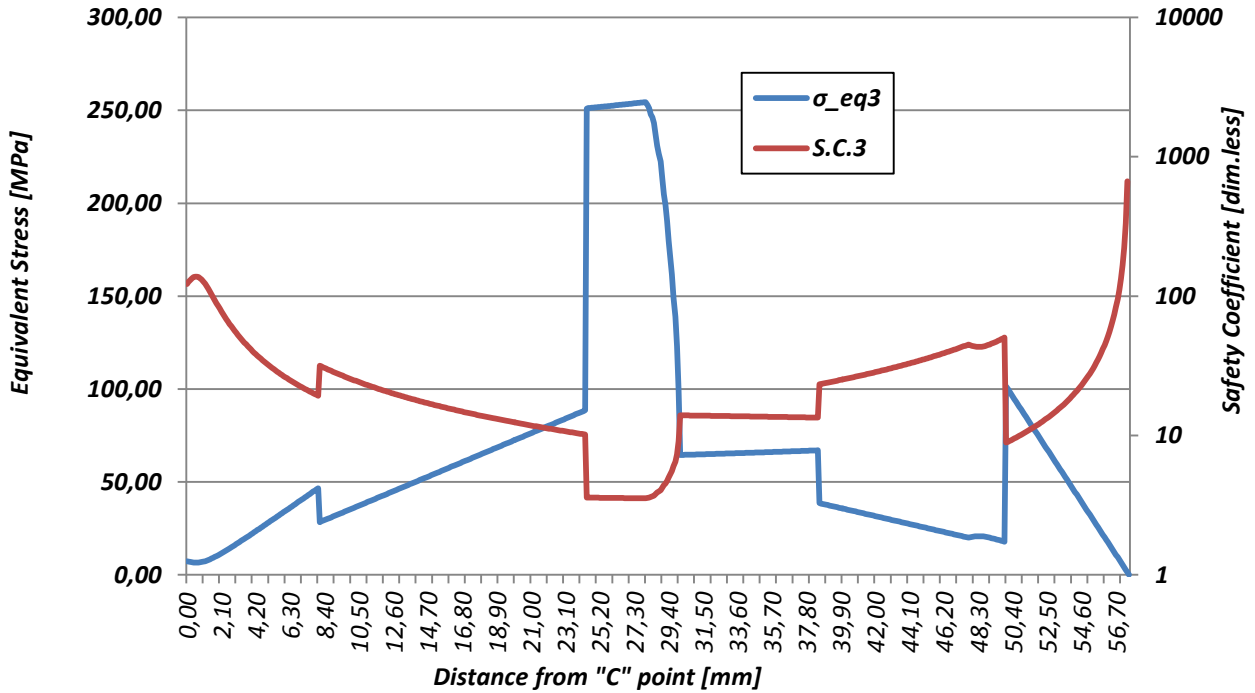


Eq. 7.5-14

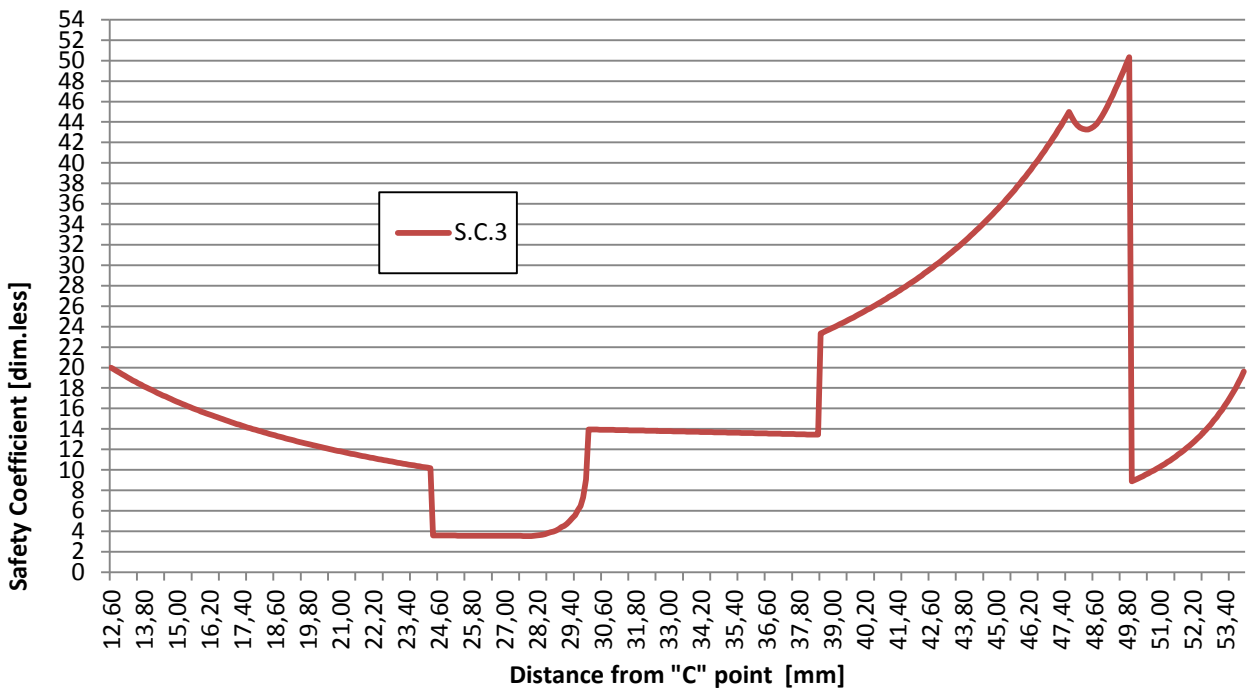
$$\sigma_{eq3} =$$

$$\frac{1}{\sqrt{2}} \sqrt{(\sigma_{x3} - \sigma_{y3})^2 + (\sigma_{y3} - \sigma_{z3})^2 + (\sigma_{z3} - \sigma_{x3})^2 + 6 \cdot (\tau_{xy3}^2 + \tau_{yz3}^2 + \tau_{zx3}^2)}$$

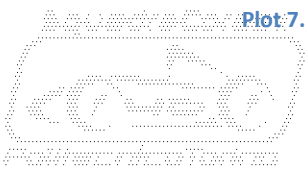
By virtue of that, stresses of Plot 7.5-16, combined according to Eq. 7.5-14 give as result blue curve displayed by Plot 7.5-17.



Plot 7.5-17: Equivalent Stress and Safety Coefficient related to $\phi_{i3} = 18$ [mm], referred to driving condition.



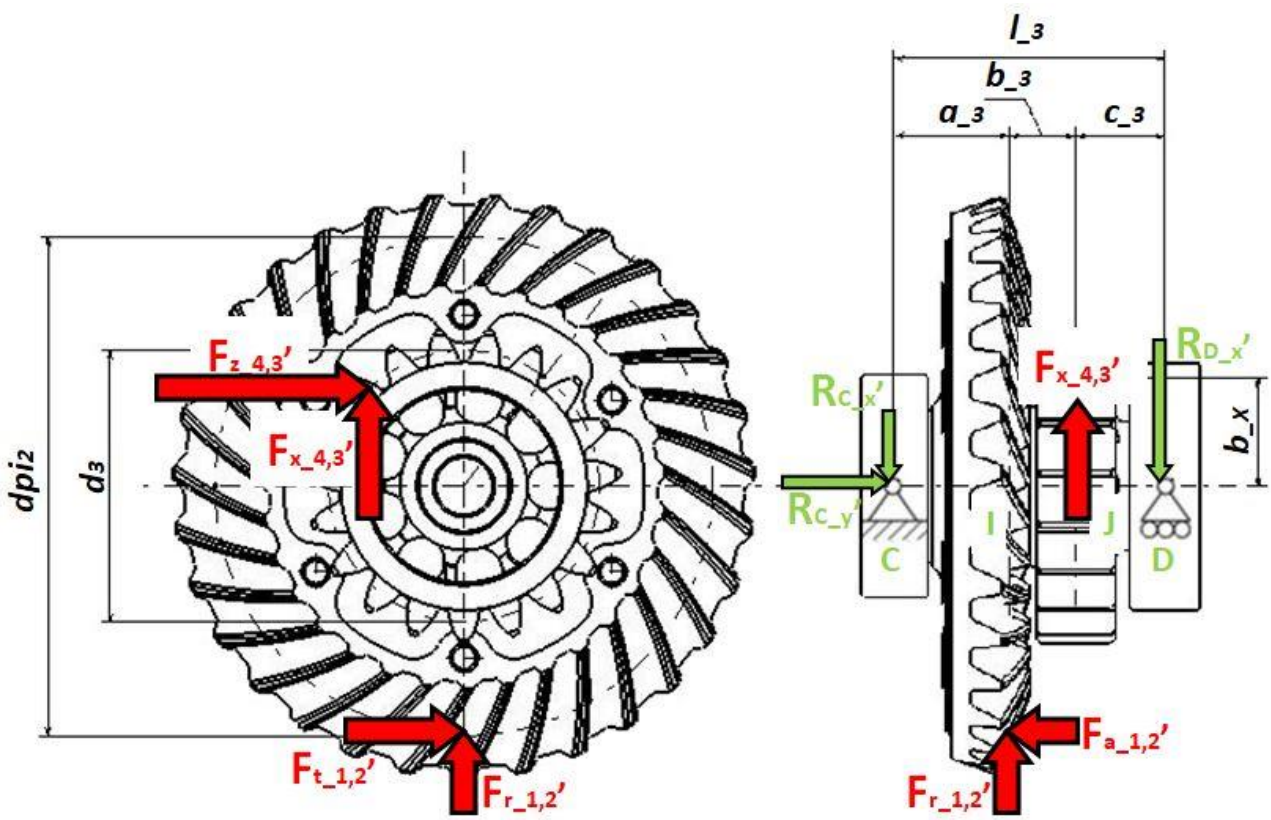
Plot 7.5-18: Values of S.C. included between force application points of gears related to $\phi_{i3} = 18$ [mm].



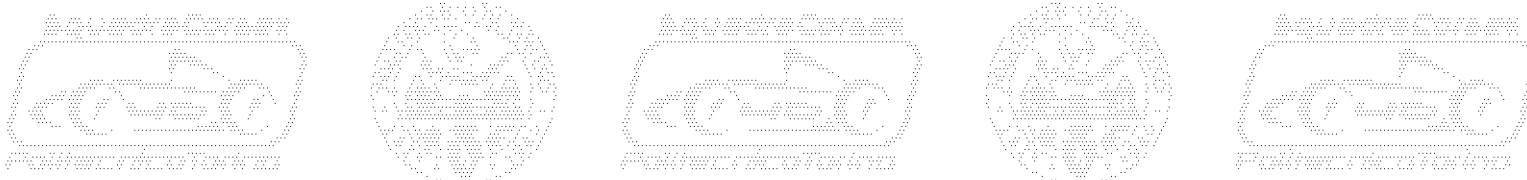
It's possible to notice that values of σ_{eq3} combines maximum values of positive sign stresses. How expected, force application point of gearwheel 2 coincides with most stressed section. Next step is study of safety coefficient which is displayed by red curve on Plot 7.5-17, its trend is obviously opposite to trend of equivalent stress. It's possible to notice that levels of safety are extremely high in two sections of beam included between points "C-I" and points "J-D". By virtue of that, It's surely useful study values of safety coefficient of sections included between points "I" and "J". In order to study the detail of safety coefficient values, Plot 7.5-18 have been created.

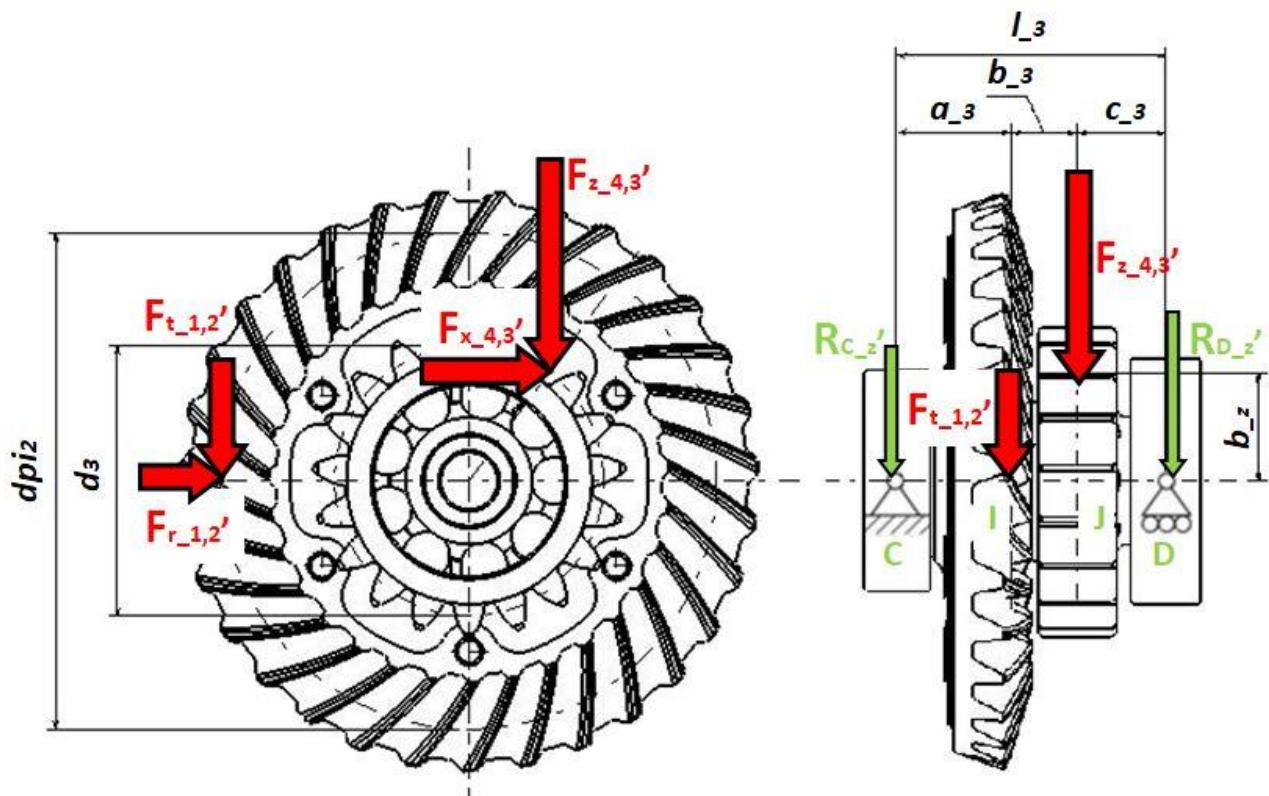
By analysis of Plot 7.5-18, It's clear that gearwheel 3 operates in safe conditions when bears static loads generated by driving condition. Indeed minimum value of safety coefficient is about 3,54 [dim.less]. Minimum value is located in correspondence of point "I", while step variations exploit in correspondence of section changes.

Dissertation about stresses acting on shaft 2 cannot be considered concluded without an analysis performed on energy recovery condition. Direction, sign and magnitude of gear meshing forces is widely explained by Chapter 7.2. Similarly to previous cases, first step is the study of free body diagrams. Two plots are generated: Plot 7.5-19 is homologous of Plot 7.5-3, while Plot 7.5-20 is homologous of Plot 7.5-4. Observing two plots related to energy recovery condition It's possible to notice that change in orientation of tangential forces, causes inversion in signs of large majority of vectors.



Plot 7.5-19: Free body diagram of shaft 2 in energy recovery condition, vectors lay on XY plan.





Plot 7.5-20: Free body diagram of shaft 2 in energy recovery condition, vectors lay on YZ plan.

Analyzing Plot 7.5-19 and Plot 7.5-20, It's possible to write a system of five equilibrium equations, homologous to Chapter 7.4. Resolution of the system is analogue to cases treated by previous Chapters 4.1 and 6.1. Therefore, in order to simplify actual dissertation, system and its resolution is going to be omitted. Anyway, reaction forces applied on boundaries are displayed as follows:

$$\text{Eq. 7.5-15} \quad R'_{Cx} = 1.014 [N]$$

$$\text{Eq. 7.5-16} \quad R'_{Cy} = 220 [N]$$

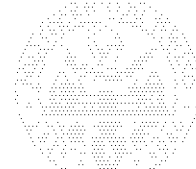
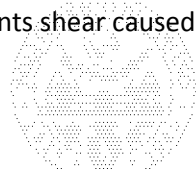
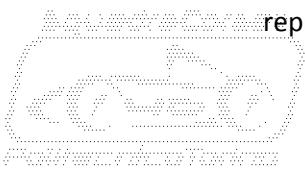
$$\text{Eq. 7.5-17} \quad R'_{Cz} = 1.193 [N]$$

$$\text{Eq. 7.5-18} \quad R'_{Dx} = 897 [N]$$

$$\text{Eq. 7.5-19} \quad R'_{Dz} = 1.620 [N]$$

Positive sense of reaction forces is in accordance with green vectors displayed by Plot 7.5-19 and Plot 7.5-20. Once constraint reaction forces are known, It's easy calculate strains related to energy recovery condition. Structural model is the same adopted in the study of driving case and depicted by Plot 7.5-8. How seen before, strains acting on the model are declared:

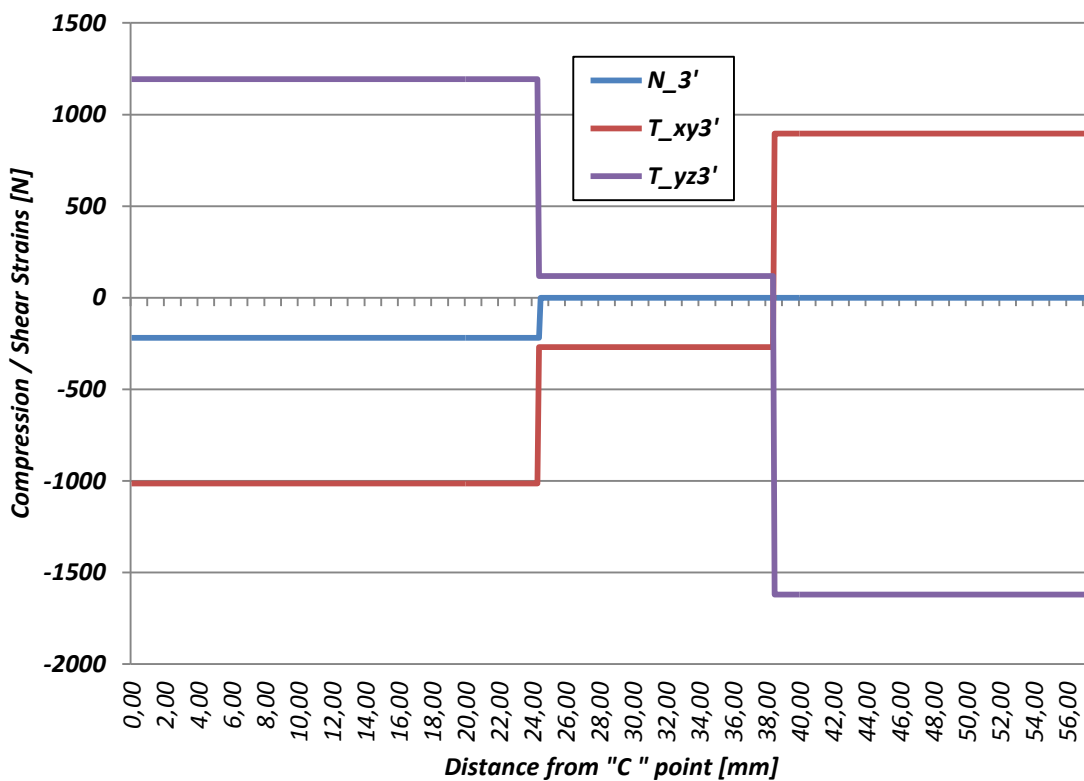
- N'_3 is "strain normal to section of gearwheel 3 in recovery condition". It's measured in $[N]$ and represents the compression caused by axial force which gearwheel 1 transmits to gearwheel 2.
- T'_{xy3} is "shear strain on xy plan of gearwheel 3 in recovery condition". It's measured in $[N]$ and represents shear caused by forces laying on xy plan.
- T'_{yz3} is "shear strain on yz plan of gearwheel 3 in recovery condition". It's measured in $[N]$ and represents shear caused by forces laying on xz plan.



- M'_{txy3} is “tilting momentum on xy plan of gearwheel 3 in recovery condition”. It’s measured in [Nmm] and represents tilting momentum caused by forces laying on xy plan.
- M'_{tyz3} is “tilting momentum on yz plan of gearwheel 3 in recovery condition”. It’s measured in [Nmm] and represents tilting momentum caused by forces laying on xz plan.
- T'_{is} is “maximum recovering torque on intermediate shaft”, It’s measured in [Nmm] and needs to be calculated as follows.

Eq. 7.5-20 $T'_{is} = T_{rec} \cdot i_{1,2} = 56.364 [Nmm]$

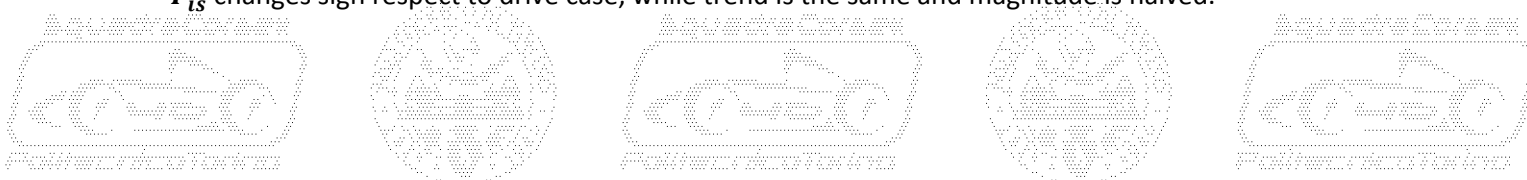
By virtue of that, all elements needed to plot diagram of strains are available.

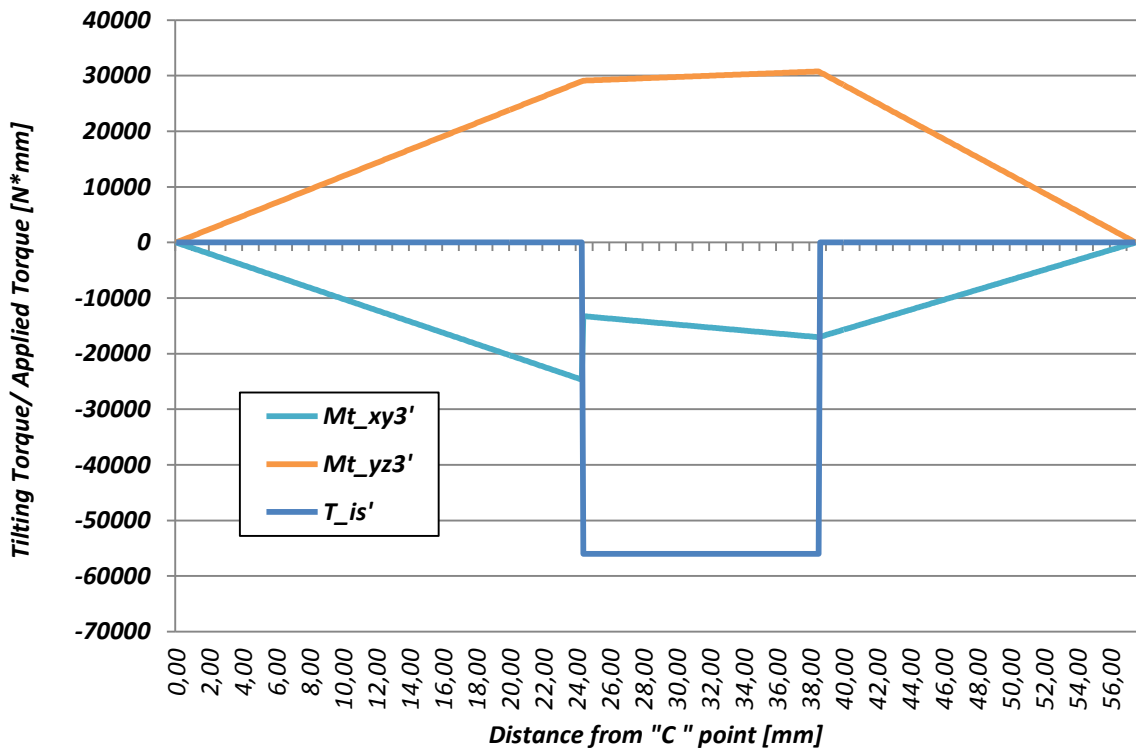


Plot 7.5-21: Strains acting on gearwheel 3, measured in [N] and referred to recovery condition.

Comparing Plot 7.5-21 and Plot 7.5-10 It’s necessary notice that overall trend of N'_3 only remains the same, while magnitude is halved, how expected. Anyway, It’s possible to notice that trends magnitude of T'_{xz3} and T'_{xy3} are totally different. That’s due to sign of tangential components which have been inverted. Anyway, It’s possible notice that maximum values are considerably lower during recovery condition.

By comparison between Plot 7.5-22 and Plot 7.5-11 It’s necessary to notice an important change of trend of M'_{txy3} which exploits a change of sign from positive to negative . Peak value of the strain is located in correspondence with point “I” and no more in correspondence with point “J”. Similarly, It’s possible to notice that M'_{tyz3} changes its sign from negative to positive. At the same way peak value is located in correspondence with point “J” and no more with point “I”. Analogously from previous cases, T'_{is} changes sign respect to drive case, while trend is the same and magnitude is halved.





Plot 7.5-22: Strains acting on gearwheel 3, measured in [Nmm] and referred to recovery condition.

Next step is analysis of stresses, how it was done in previous studied cases. Driving condition shows that certain values of internal diameter ϕ_{i3} don't exhibit important changes on values of stresses. By virtue of that, the only case taken in consideration is going to be $\phi_{i3} = 18 [mm]$. By virtue of that, it's necessary to introduce some new variables of the study.

σ'_{y3} is the "compression stress acting on gearwheel 3 in recovery condition" generated by N'_{3i} , strain normal to section. Stress is calculated by following function:

$$Eq. 7.5-21 \quad \sigma'_{y3}(y) = \frac{N'_{3i}(y)}{A_{3i}(y)} = \frac{N'_{3i}(y)}{\pi \frac{\phi(y)^2 e_3 - \phi_{i3}^2}{4}}$$

Where:

- $N'_{3i}(y)$ is "strain normal to i section of gearwheel 3 in recovery condition". It's measured in [N] and is function of y, because depends from portion of the beam on which is applied, as depicted by Plot 7.5-21.

By comparison between red curves of Plot 7.5-23 and Plot 7.5-16, it's possible to notice that general trend hasn't changed. How expected values of magnitude is halved.

σ'_{z3} is the "bending stress acting on gearwheel 3 in recovery condition" generated by M'_{txy3} , tilting momentum acting on xy plan. Stress is calculated by following function:

$$Eq. 7.5-22 \quad \sigma'_{z3}(y) = \frac{M'_{txy3i}(y)}{W_{f3i}(y)} = \frac{M'_{txy3i}(y)}{\pi \frac{\phi(y)^4 e_3 - \phi_{i3}^4}{32 \cdot \phi(y) e_3}}$$



Where:

- $M'_{txy3i}(y)$ is **“tilting momentum acting on xy plan referred to i section of gearwheel 3 in recovery condition”**. It’s measured in $[Nmm]$ and is function of y , because depends from distance from point “C”, as depicted by Plot 7.5-22.

By comparison between green curves of Plot 7.5-23 and Plot 7.5-16, It’s possible to notice the change of sign from positive to negative. General trend of the stress displays an important peak in correspondence with point “I”. In this point, magnitude of the stress is similar to maximum value exploited during driving case. Spike generated by reduction of stressed section in correspondence with “D” bearing housing is much less pronounced compared to driving case.

σ'_{x3} is the **“bending stress acting on gearwheel 3 in recovery condition”** generated by M'_{tyz3} , tilting momentum acting on yz plan. Stress is calculated by following function:

$$\text{Eq. 7.5-23} \quad \sigma'_{x3}(y) = \frac{M'_{tyz3i}(y)}{W_{f3i}(y)} = \frac{M'_{tyz3i}(y)}{\pi \frac{\phi(y)^4 e3 - \phi_{i3}^4}{16 \cdot \phi(y) e3}}$$

Where:

- $M'_{tyz3i}(y)$ is **“tilting momentum acting on xy plan referred to i section of gearwheel 3 in recovery condition”**. It’s measured in $[Nmm]$ and is function of y , because depends from distance from point “C”, as depicted by Plot 7.5-22.

Comparing violet curves of Plot 7.5-23 and Plot 7.5-16, It’s possible to notice the change of sign from negative to positive. That’s mainly due to change in sign of boundary reaction forces. Profile of the trend and vale of magnitude is quite the same.

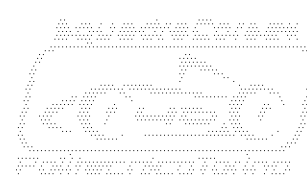
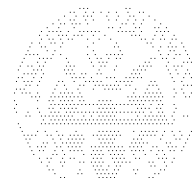
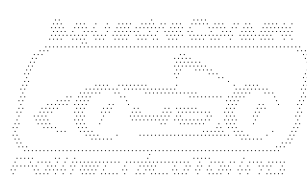
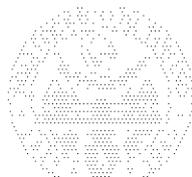
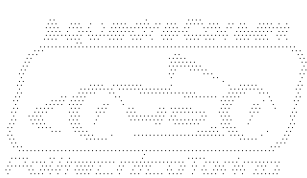
τ'_{xz3} is the **“torsion stress acting on gearwheel 3 in recovery condition”** generated by T'_{is} , torque which acts on shaft 2. Stress is calculated by following function:

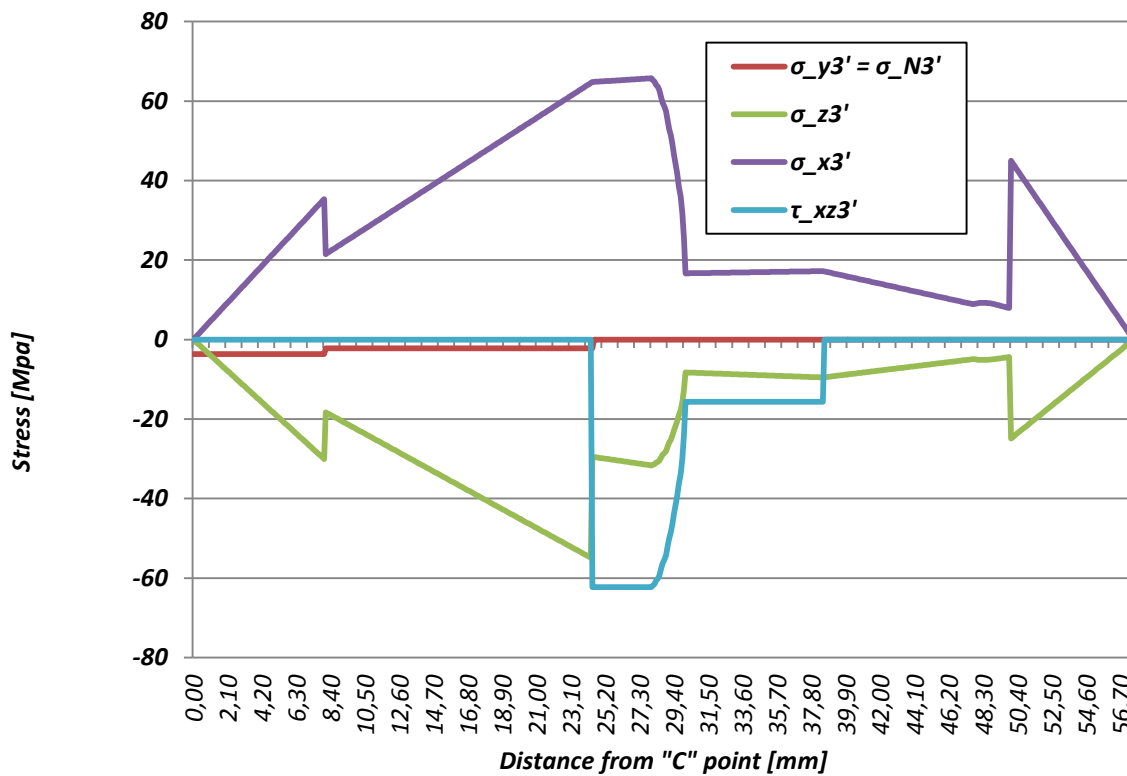
$$\text{Eq. 7.5-24} \quad \tau'_{xz3}(y) = \frac{M'_{tyzi}(y)}{W_{ti3}(y)} = \frac{M'_{tyzi}(y)}{\pi \frac{\phi(y)^4 e3 - \phi_{i3}^4}{32 \cdot \phi(y) e3}}$$

Where:

- $T'_{is}(y)$ is **“driving torque acting intermediate shaft in recovery condition”**. It’s measured in $[Nmm]$ and is function of y , because depends from portion of the beam on which is applied, as depicted by Plot 7.5-22.

A brief comparison between azure curves of of Plot 7.5-23 and Plot 7.5-16, It’s possible to notice a change in sign, first of all. Anyway general trend of the stress doesn’t change even if values of magnitude are halved.





Plot 7.5-23: : Stresses related to $\phi_{i3} = 18$ [mm], referred to driving condition.

After this wide dissertation about trend of single stress, It's necessary calculate σ'_{eq3} which is the "equivalent stress on gearwheel 3 in recovery condition". It can be calculated through relation of displayed by Eq. 7.5-25 and result is displayed by Plot 7.5-24.

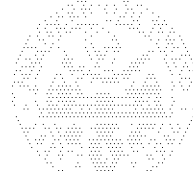
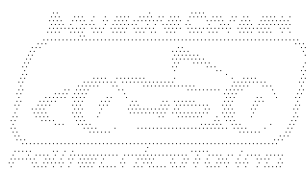
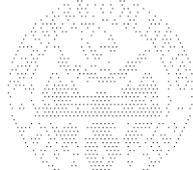
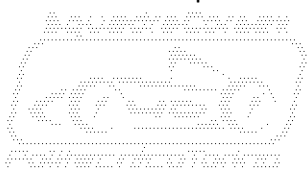
Eq. 7.5-25

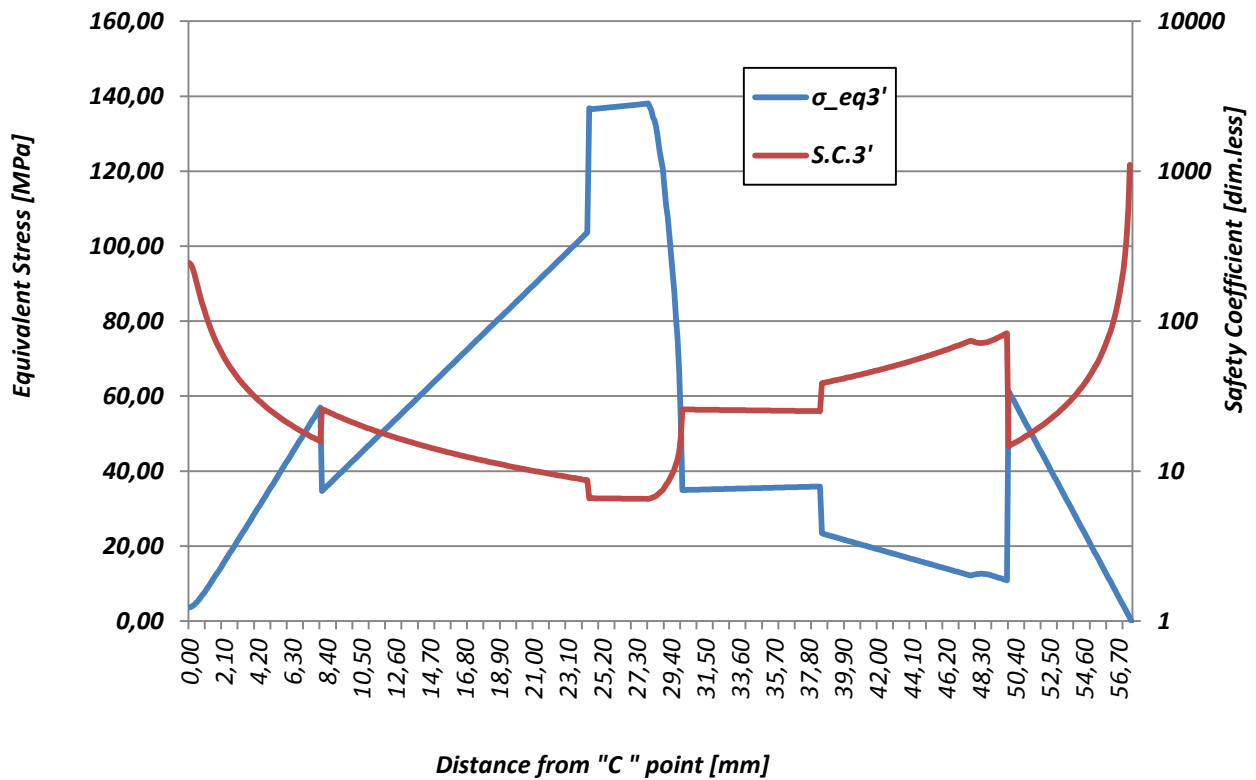
$$\sigma'_{eq3} =$$

$$\frac{1}{\sqrt{2}} \sqrt{(\sigma'_{x3} - \sigma'_{y3})^2 + (\sigma'_{y3} - \sigma'_{z3})^2 + (\sigma'_{z3} - \sigma'_{x3})^2 + 6 \cdot (\tau'_{xy3}{}^2 + \tau'_{yz3}{}^2 + \tau'_{zx3}{}^2)}$$

A brief comparison between Plot 7.5-24 and Plot 7.5-17 shows that beam section included between "C" point and "I" point is a bit more stressed during recovery condition. Anyway, all other portions of the beam are more stressed in driving condition. Indeed, a comparison performed on maximum stressed section, which remains the same, shows a difference of more 40% in the equivalent stress. Anyway, general trend of curves displayed by Plot 7.5-24 is the same respect to Plot 7.5-17, despite changing in sign on tangential forces. Finally, It's possible to notice that minimum safety coefficient is about two times respect to driving condition. By virtue of that, It's clear that energy recovery condition is considerably safer than driving condition, by point of view of stresses on Shaft 2.

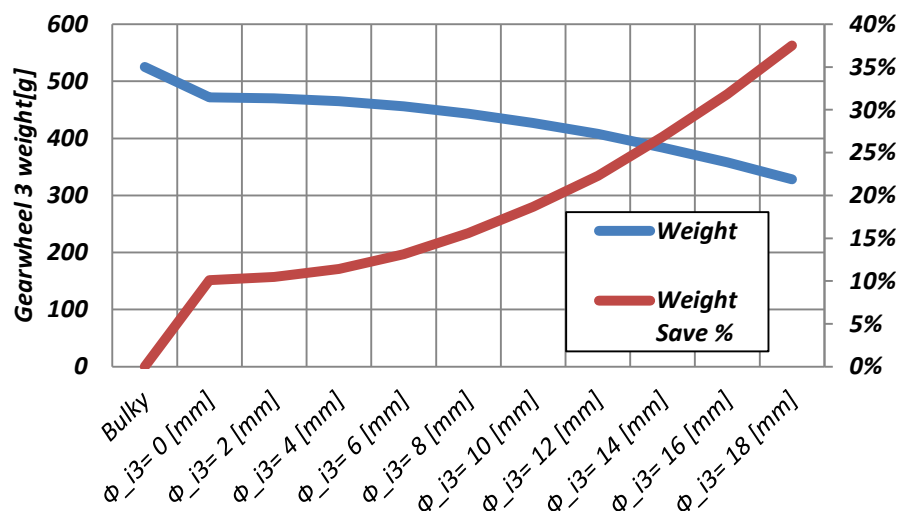
Like in the case of previous dissertation performed on Chapter 7.4, safety coefficient can be adopted as parameter to study optimization of the component. By virtue of that, It's clear that material is scarcely optimized along the component. Anyway, basic technological issues don't allow to level out value of safety coefficient. Indeed, gearwheel 3 is designed to be easily realized by conventional manufacturing technologies, in order to be cost effective and reliable. Despite safety coefficient analysis, many other aspects need to be considered.



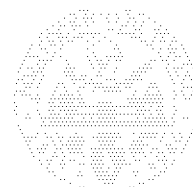
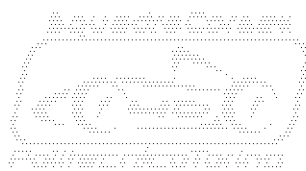
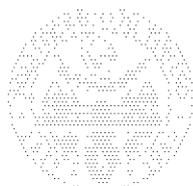
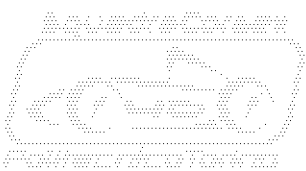


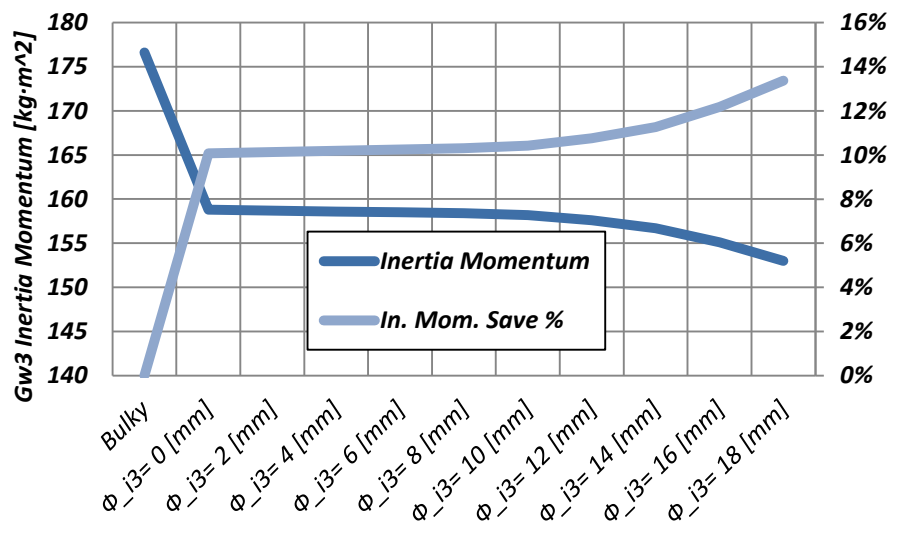
Plot 7.5-24: Equivalent Stress and Safety Coefficient acting on gearwheel 3, referred to recovery condition.

Previous Plot 7.5-16, Plot 7.5-17 and Plot 7.5-18 are referred to 18 [mm] internal diameter, anyway It's necessary to consider that diameter of bearing housings are only 20 [mm]. Despite safety coefficients, by technological point of view It would be more suitable a value around 16 [mm]. For this reason, It would be useful study differences in weight and inertia momentum conditioned by different values of ϕ_{i3} .



Plot 7.5-25: Weight in function of ϕ_{i3} .



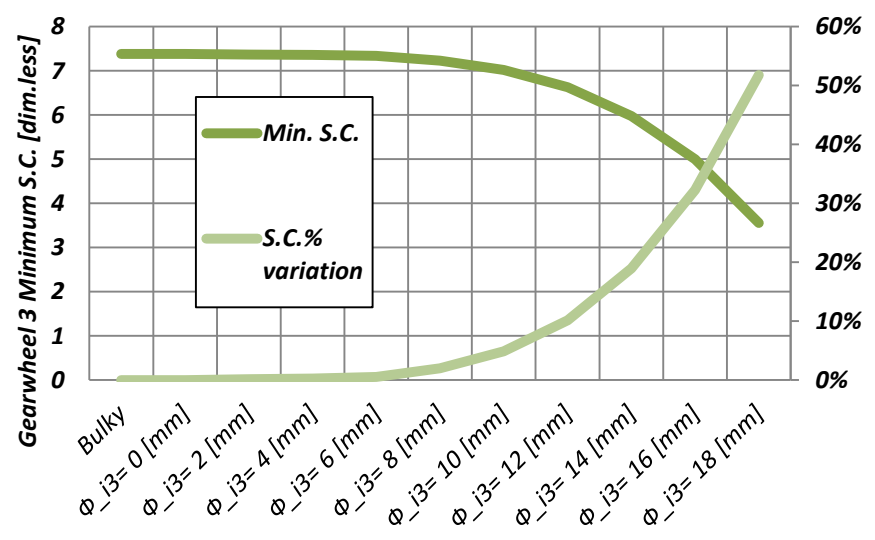


Plot 7.5-26: Gearwheel 3 inertia momentum in function of ϕ_{i3} .

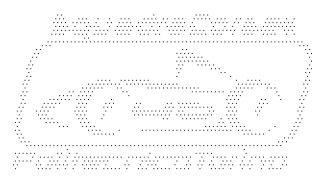
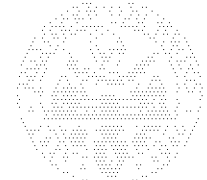
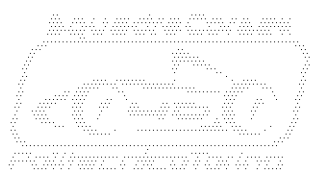
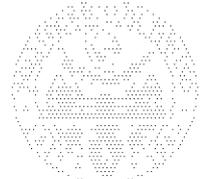
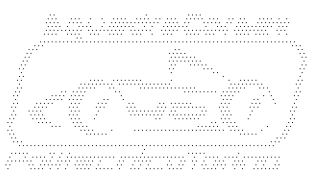
For this purpose, other two plots have been introduced: Plot 7.5-25 and Plot 7.5-26. Both plot are printed in function of ϕ_{i3} even if first values are referred to initial “bulky” configuration displayed by Plot 7.5-5. Percentages too are referred to “bulky” configuration, in order to appreciate total save of weight and save of inertia momentum.

By analysis of Plot 7.5-25, It’s possible to notice that a large contribution of weight saving is given by the crown of axial holes, how declared in advance. Anyway weight saving strongly depends by internal diameter of gearwheel 3. Analysing differences between 16 [mm] and 18 [mm] configuration, difference of weight is only about 30 [g] which represents the 5% of the initial weight only.

By analysis of Plot 7.5-26, It’s clear that large majority of inertia momentum reduction is obtained with machining of the crown of axial holes. Other modifications related to increase of ϕ_{i3} lead to very small reduction of inertia. Analysing differences between 16 [mm] and 18 [mm] configuration, difference of inertia momentum represents only 1,5% of the initial inertia momentum.

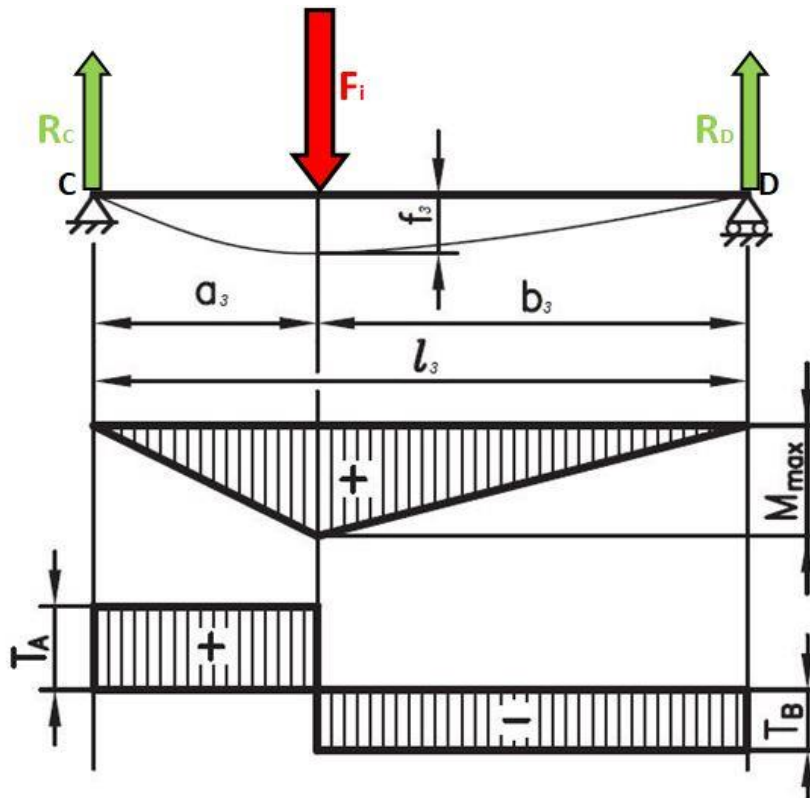


Plot 7.5-27: Trend of Safety Coefficient in most stressed section, in function of ϕ_{i3} .



By virtue of presented data, It's clear that increase of \varnothing_{i3} from 16 [mm] to 18 [mm] leads to scarce benefits with an important increase of risk. To this purpose, It's necessary introduce Plot 7.5-27.

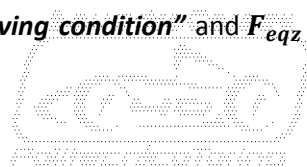
By analysis of Plot 7.5-27, It's clear that reduction of safety coefficient in the most stressed section is strongly affected by dimension of \varnothing_{i3} . In particular, difference between 16 [mm] and 18 [mm] configuration represents more than 20% respect to safety coefficient of initial configuration. That's the proof that value of 16 [mm] represents the best compromise between performance and risk.



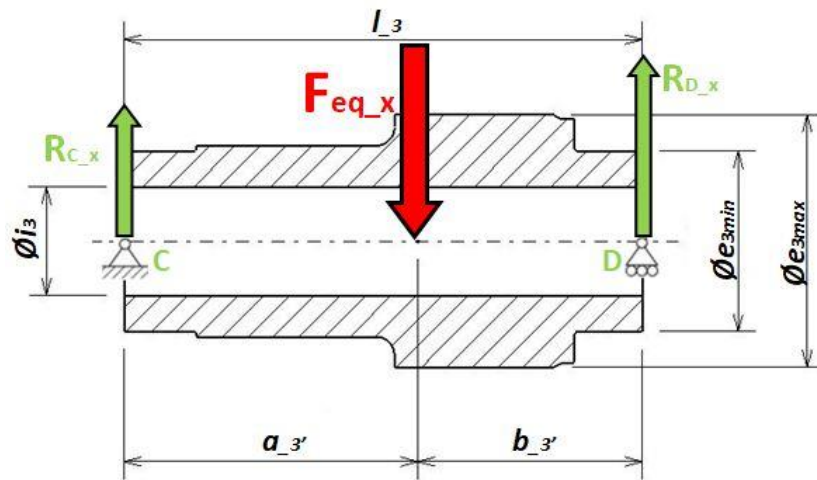
Plot 7.5-28: Model of beam bounded at extremity and loaded on central section (www.hoepliscuola.it).

Last aspect of lightening process to take into account, is stiffness of previous model derived by Plot 7.5-8. In order to confirm value of gearwheel 3 internal diameter \varnothing_{i3} , It's necessary to perform another **verification focused on displacements**. Similarly to what seen at Chapter 7.4, It's necessary to study maximum displacement of the beam due to deflection, in order to understand if optimal operation of the bevel gear is guaranteed. Model displayed by Plot 7.4-20 refers to a different case based on cantilever application of the load. For this reason It's necessary to refer verification of displacements to a different model, It's depicted by Plot 7.5-28 and is in accordance with Ref.[17]. By virtue of previous verifications regarding stresses, It's necessary underline that a verification of displacement during energy recovery condition makes no sense. For this reason the only case studied are referred to **driving condition**.

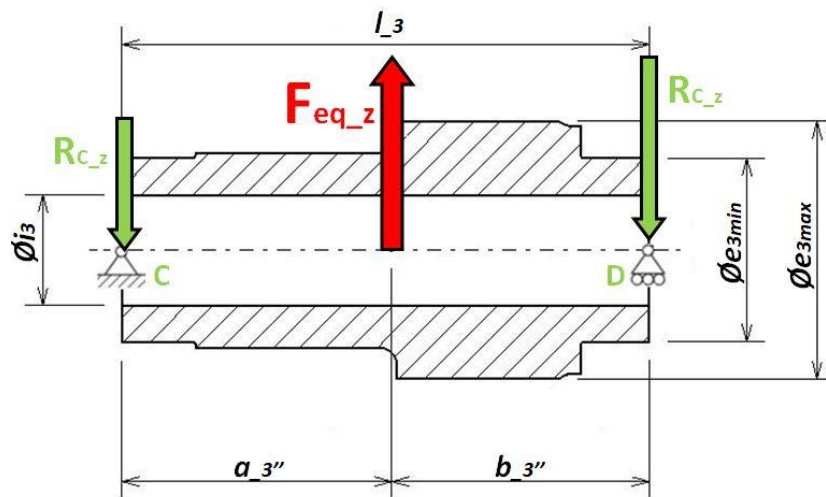
Back to free body diagrams displayed by Plot 7.5-3 and Plot 7.5-4, It's clear that such models need to be simplified according to Plot 7.5-28. By virtue of that, two simplified models are obtained, one displayed by Plot 7.5-29, one displayed by Plot 7.5-30. By analysis of following plots, It's possible to observe that applied forces displayed by Plot 7.5-3 and Plot 7.5-4, have been replaced by equivalent vectors, F_{eqx} the "equivalent force along x in driving condition" and F_{eqz} the "equivalent force along z in driving



condition". It's possible to notice that magnitude of equivalent force is the algebraic sum of applied forces, while position point of application is obtained averaging positions and magnitude of composing vectors.



Plot 7.5-29: Simplified model of beam sectioned on xy plan, referred to driving condition.

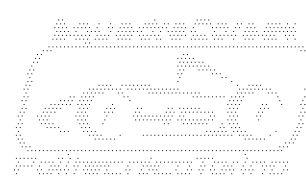
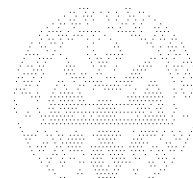
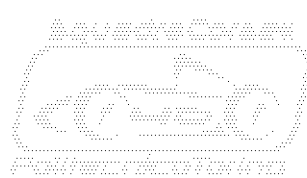
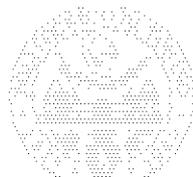
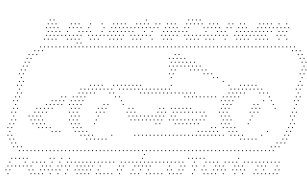


Plot 7.5-30: : Simplified model of beam sectioned on yz plan, referred to driving condition.

Next step is presentation of parameters displayed by Plot 7.5-29 and Plot 7.5-30:

- $a_{3'} = 32,64 [mm]$ is "distance of application point from C bearing".
- $b_{3'} = 24,86 [mm]$ is "distance of application point from D bearing".
- $a_{3''} = 29,44 [mm]$ is "distance of application point from C bearing".
- $b_{3''} = 28,06 [mm]$ is "distance of application point from D bearing".
- $I_{3min}(\phi_{i3} = 16 [mm]) = 4643 [mm^4]$ is "Minimum value of area momentum of inertia". It's function of ϕ_{i3} . Apply minimum value of momentum of inertia along all the beam, represents a very cautionary condition, anyway It would be more dangerous overestimate stiffness of component.

While:



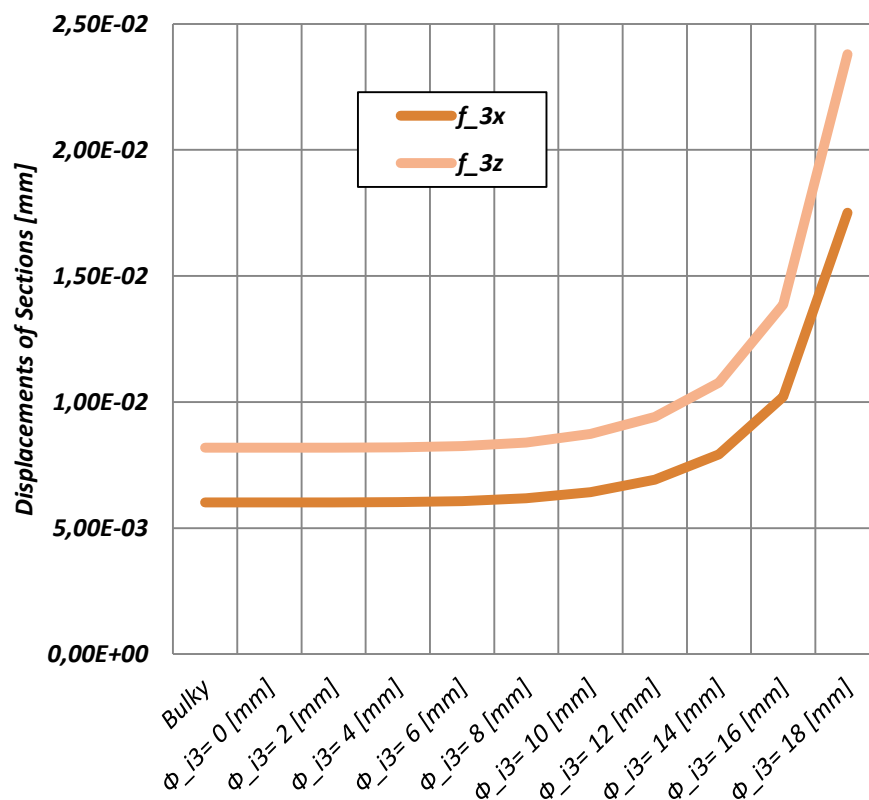
Eq. 7.5-26 $F_{eqx} = 2.553 [N]$

Eq. 7.5-27 $F_{eqz} = 3.347 [N]$

Basic formula to calculate deflection of the beam is represented by:

Eq. 7.5-28 $f_3 = \frac{1}{3} \cdot \frac{F \cdot a_3^2 \cdot b_3^2}{E \cdot I_3 \cdot l_3}$ Ref.[17]

According to models depicted by Plot 7.5-29 and Plot 7.5-30, It's possible calculate deformations in two sections and in two directions: f_{3x} which is "deflection along x axis in driving condition" of gearwheel 3 and f_{3z} which is "deflection along z axis in driving condition" of gearwheel 3.



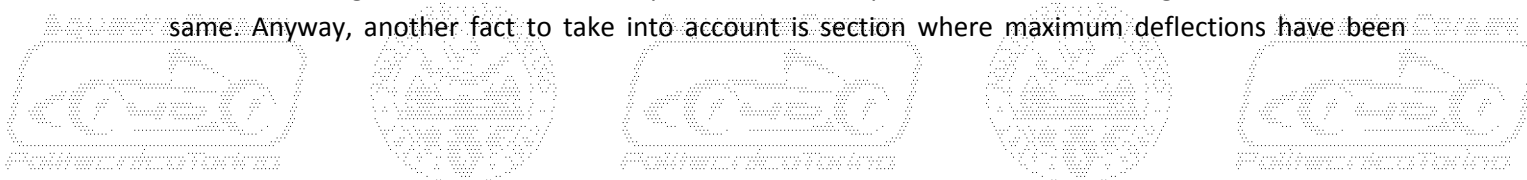
Plot 7.5-31: Maximum deflections of gearwheel 3 compared in function of internal diameter.

Then, It's possible to write:

Eq. 7.5-29 $f_{3x}(\phi_{i3} = 16 [mm]) = \frac{1}{3} \cdot \frac{F_{eqx} \cdot a_{3'}^2 \cdot b_{3'}^2}{E \cdot I_{3min} \cdot l_3} = 1,02 \cdot 10^{-2} [mm]$

Eq. 7.5-30 $f_{3z}(\phi_{i3} = 16 [mm]) = \frac{1}{3} \cdot \frac{F_{eqz} \cdot a_{3''}^2 \cdot b_{3''}^2}{E \cdot I_{3min} \cdot l_3} = 1,30 \cdot 10^{-2} [mm]$

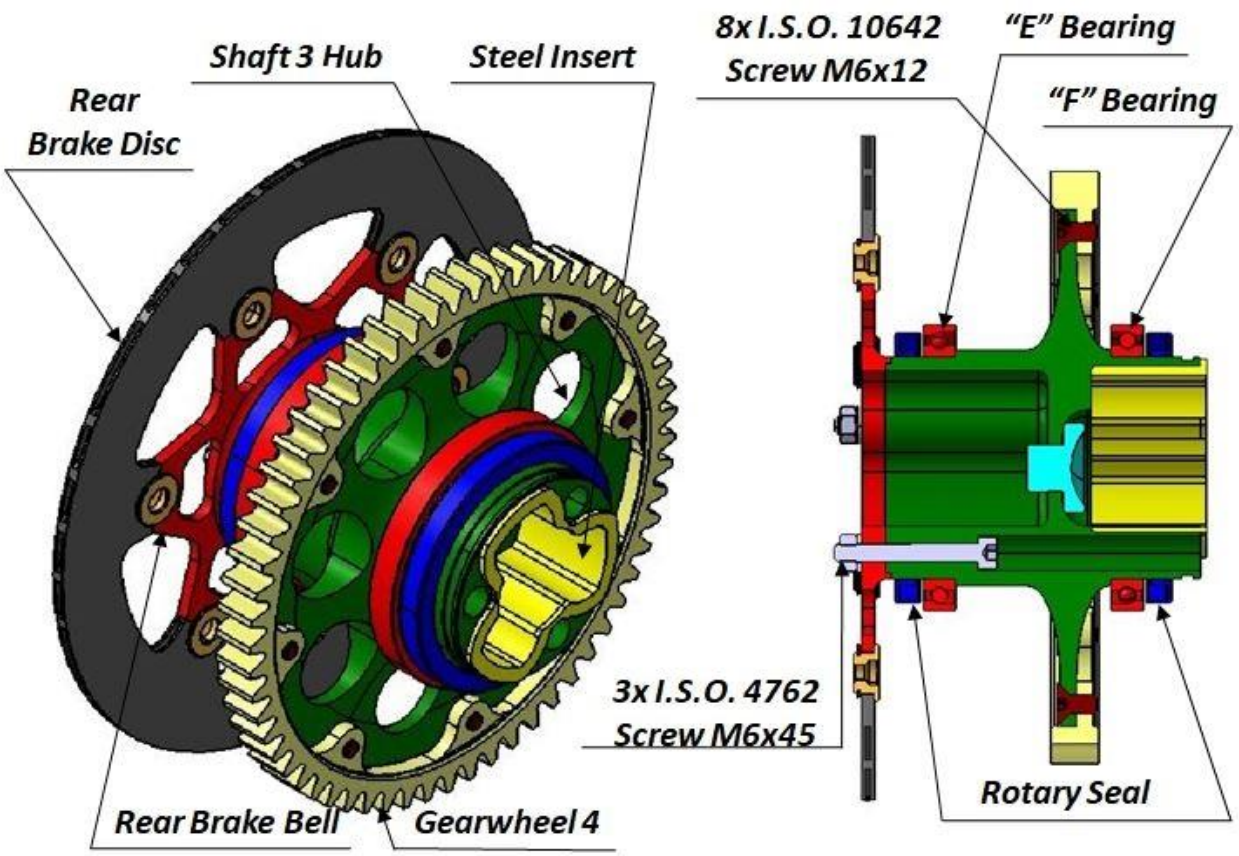
Analyzing results of previous Eq. 7.5-29 and Eq. 7.5-30, It's possible to notice that values of deflection are lower than allowable value depicted by Eq. 7.4-23. Indeed result of allowable value of displacement is about 11% greater than result of Eq. 7.5-30, and It's possible notice that magnitude order is the same. Anyway, another fact to take into account is section where maximum deflections have been



calculated. Both are quite far from force application point of gearwheel 2. By accurate observation of deflection trend depicted by Plot 7.5-28, It's sure that displacement of force application point of gearwheel 2 is going to be lower than maximum calculated deflection. In addition, It's necessary remind that value of inertia momentum employed for calculus, is the minimum along the beam.

To conclude actual dissertation, It's necessary to state that value of ϕ_{i3} internal diameter f 16 [mm] allows shaft 2 to operate in safe conditions, with no risk of undesired displacements which may compromise optimal operation of bevel gear. It would be useful evaluate a reduction of diameters of gearwheel 3 integrated shaft, but that has no sense before a scrupulous verification on bearings.

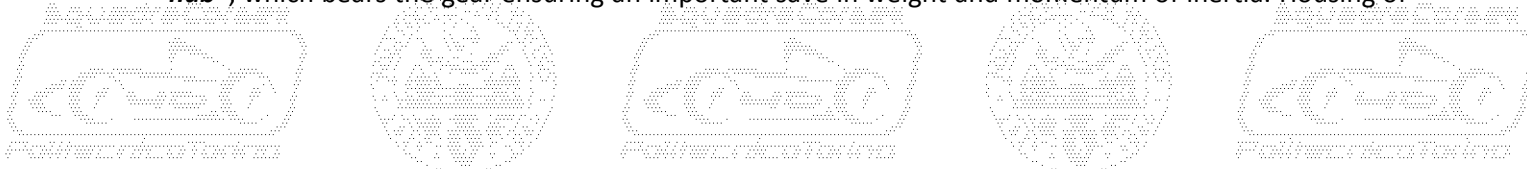
7.6. Shaft 3.



Plot 7.6-1: Details of assembled Shaft 3.

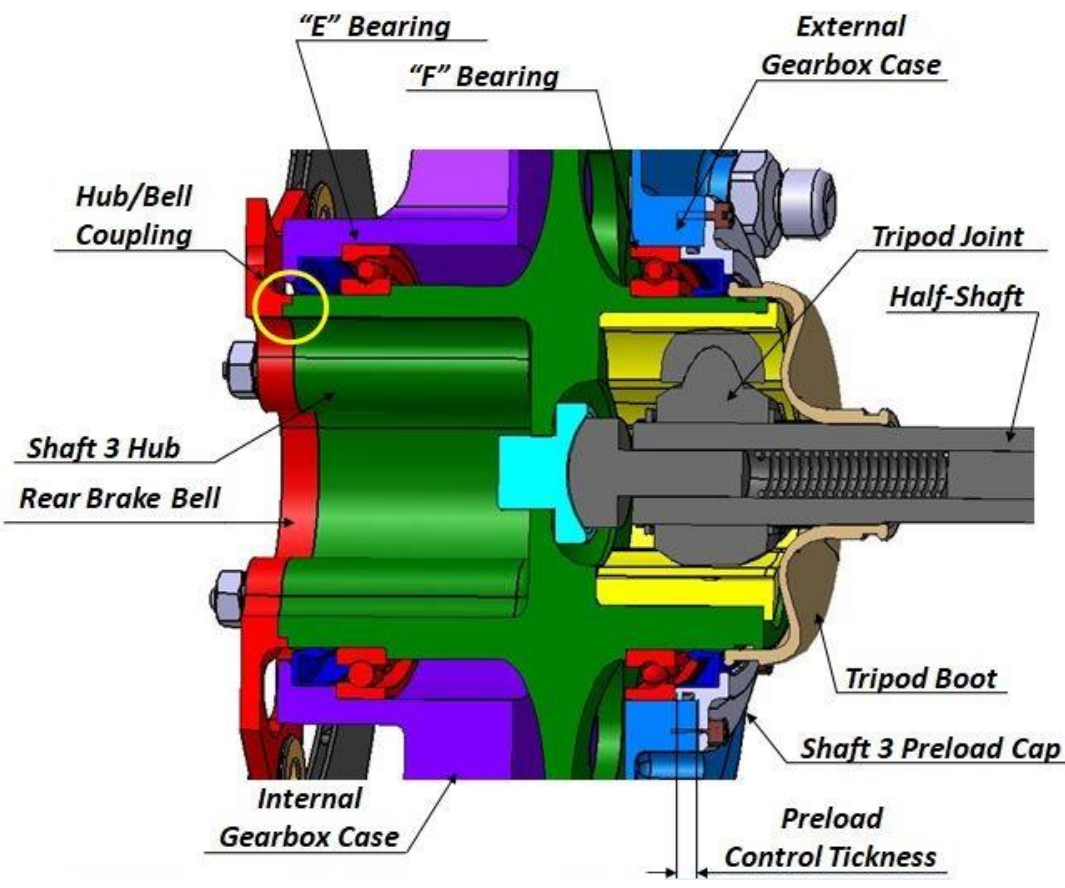
Shaft 3 represents an assembly of components with the function of linking second stage of reduction with half-shaft. By virtue of that, shaft 3 needs to integrate gearwheel 4 and "tripod joint housing". Tripod is a kind of constant velocity joint which is mainly based on the sliding of three spherical rollers into their housing, how depicted by Plot 7.6-2. It is usually employed where It's necessary to compensate small angles caused relative movement between chassis and un-sprung weights. Despite its relatively low weight, It's not suitable for steering applications.

How It's possible to observe by Plot 7.6-1, "gearwheel 4" is realized by a thin steel toothed ring provided of eight threaded holes. Steel component is fastened to an Al 7075 aluminium core, "shaft 3 hub", which bears the gear ensuring an important save in weight and momentum of inertia. Housing of



the tripod joint, is integrated into a slot centred inside the hub, realizing a solution very similar to those displayed by Picture 1.5-1, Picture 1.5-3 and Picture 1.5-6. That leads to a reduction of axial dimensions with an important simplification of layout, which reduces overall number of components and deletes issues related to assembly. Main drawback of this solution are substantially two, one is the employ of large bearings which aren't the best solution in order to reduce weight and inertia. Other is the employ of large dimension "rotary seals" which aren't the best solution by point of view of efficiency, due to high circumference of friction.

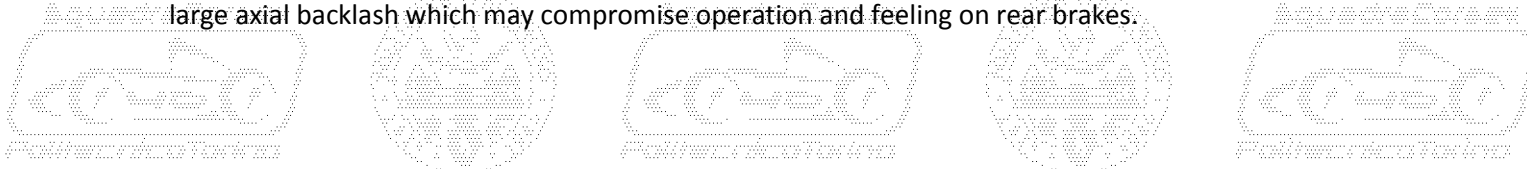
Other task which shaft 3 needs to fulfil is integration of rear "brake disc". While brake caliper is fastened rigidly to gear-box structure, floating element needs to be the disc. In order to achieve floating effect, disc is fixed to a lightweight aluminium flange known with name of "brake bell". Linkage between disc and bell is realized by six special bushings which guarantee a floating constraint due to assembly tolerances which realizes backlash. Another important benefit of floating linkage between brake disc and bell is that axial loads due to translation of brake pads, aren't transmitted to associated gear-box components. By virtue of that, axial loads on shaft 3 can be neglected.



Plot 7.6-2: Details of shaft 3 inside gear-box case.

How It's highlighted by yellow circle of Plot 7.6-2, precise coupling between brake bell and shaft 3 hub is ensured by a centring diameter machined with tight tolerances on both components. While fastening is ensured by three "I.S.O. 4762 Screw M6x45", as depicted by Plot 7.6-1. Nuts located on the on the internal side of the transmission ensure a quick and easy replacement of the disc/bell assembly.

Analogously to previous cases, a couple of angular contact bearings have been chosen to sustain shaft 3, even if axial loads are neglected. That's why a couple a large dimension radial bearings features a large axial backlash which may compromise operation and feeling on rear brakes.



Due to large dimensions of bearings, the only one solution to reduce weight and inertia is employ of a couple of high precision **hybrid bearings**, Ref.[15]. Such bearings combine high precision steel raceways with ceramic spheres, which are considerably lighter than steel ones. About bearings chosen for shaft 3, each bearing allows a weight save of about 15% compared to steel conventional solution. Anyway, most important benefit regards inertia of spinning elements which is reduced of about 30%. On the other hand, ceramic compared with steel, features **lower friction** when is contact with steel. That result is very important to reduce loss of efficiency and overcome issues deriving by poor lubrication. Poor lubrication is a scenario which may more likely happen, due to position of bearings in relation with other components of the transmission.

How It's possible to notice by Plot 7.6-2, couple of shaft 3 bearings is assembled in "X" configuration, even if "O" configuration would be applicable too. By virtue of that, external raceway of "E bearing" is in contact with "internal gear-box case" while internal is in contact with "shaft 3 hub". Internal raceway of "F bearing" is in contact with shaft 3 hub, while external is in contact with "shaft 3 preload cap". Both bearings are coupled with hub by interference on the internal raceway. How It was explained by Chapter 7.5, "X" configuration allows an easier assembly compared to "O" configuration. Moreover preload of bearings couple can be easily tuned by dimension of "preload control thickness", displayed by Plot 7.6-2.

How it was performed in previous chapters It's necessary to study constraint reaction forces acting on shaft 3 hub. By virtue of that, free-body diagrams of shaft 3 have been set up on the base of three different conditions: driving, energy recovery braking. Forces related to each condition are widely described at Chapter 7.1 Chapter 7.2 and Chapter 7.3, while geometric parameters of shaft 3 needs to be presented as follows:

- $l_4 = 81,50 [mm]$ is "distance of points K-F".
- $a_4 = 22,50 [mm]$ is "distance of points K-E".
- $b_4 = 42,50 [mm]$ is "distance of points E-L".
- $c_4 = 16,50 [mm]$ is "distance of points L-F".

How seen in previous Chapter 7.4 and Chapter 7.5, by diagrams Plot 7.6-3 and Plot 7.6-4, It's easy calculate reaction forces acting on constraints during driving condition:

Eq. 7.6-1 $R_{Ex} = 410 [N]$

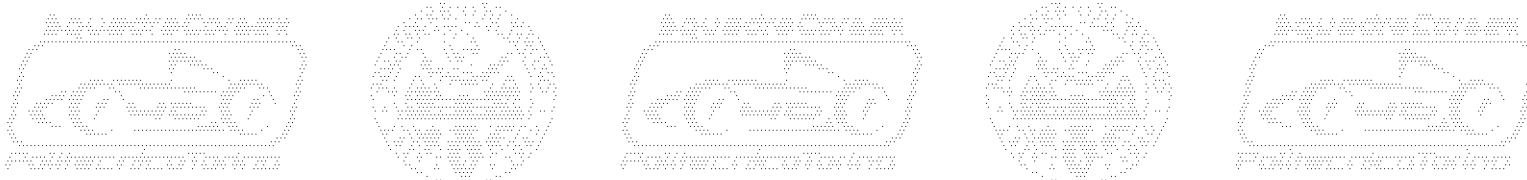
Eq. 7.6-2 $R_{Ez} = 121 [N]$

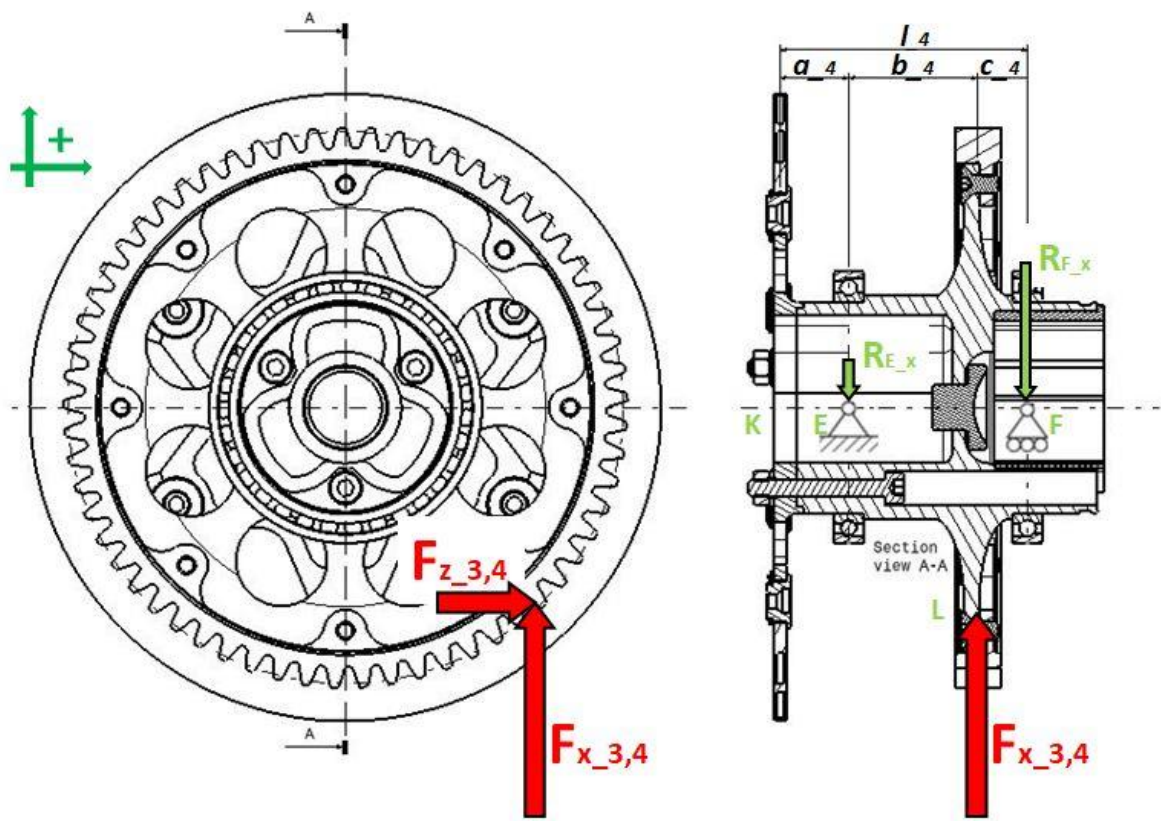
Eq. 7.6-3 $R_{Fx} = 4.455 [N]$

Eq. 7.6-4 $R_{Fz} = 1.317 [N]$

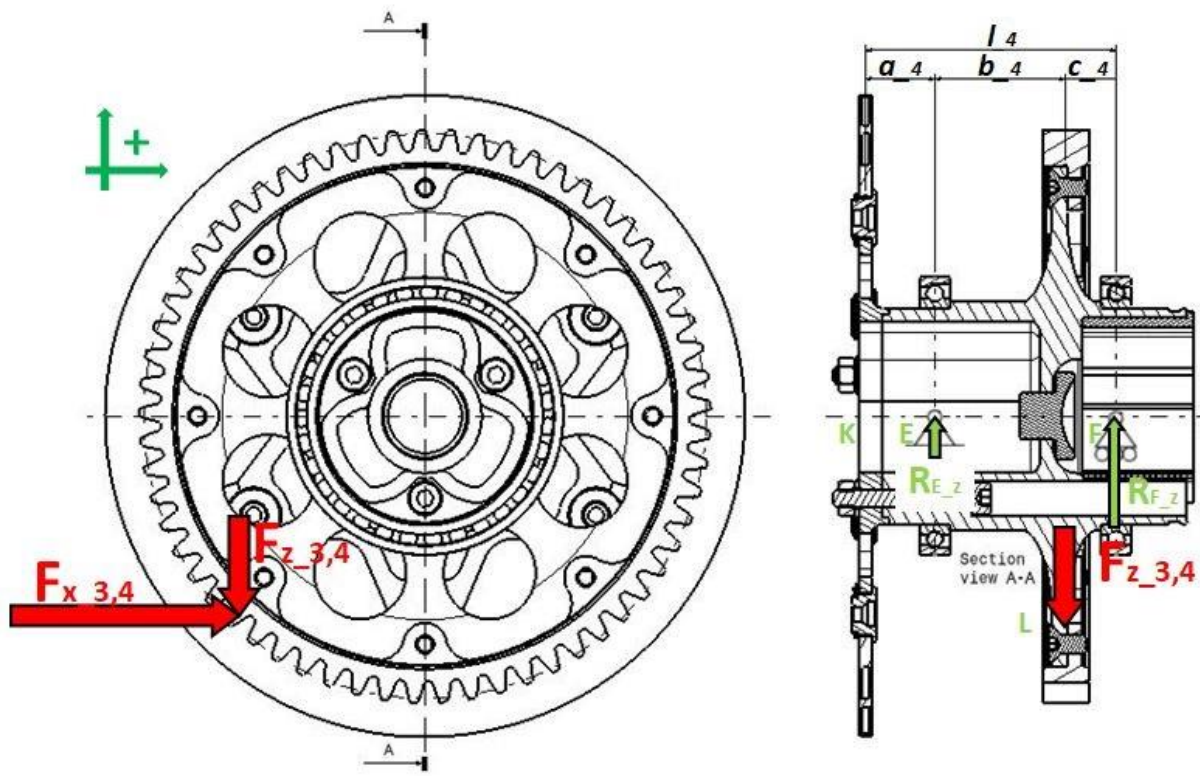
Positive sign of vectors according to signs displayed by Plot 7.6-3 and Plot 7.6-4.

By observation of magnitude of reaction forces, It's clear that driving condition stresses "F" bearing in particular . Solicitations on "E" bearing represent less than 10% in magnitude respect to "F".

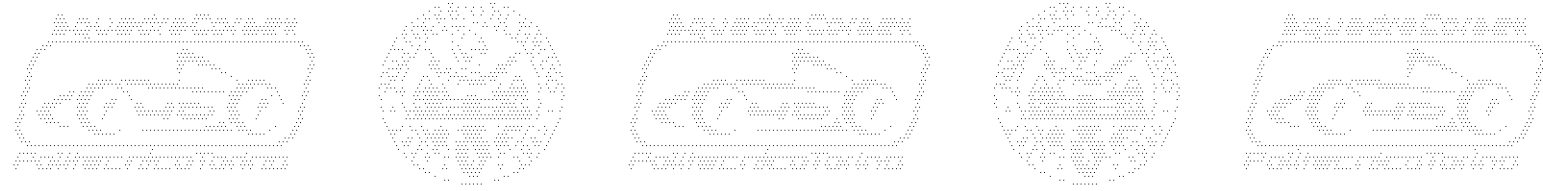


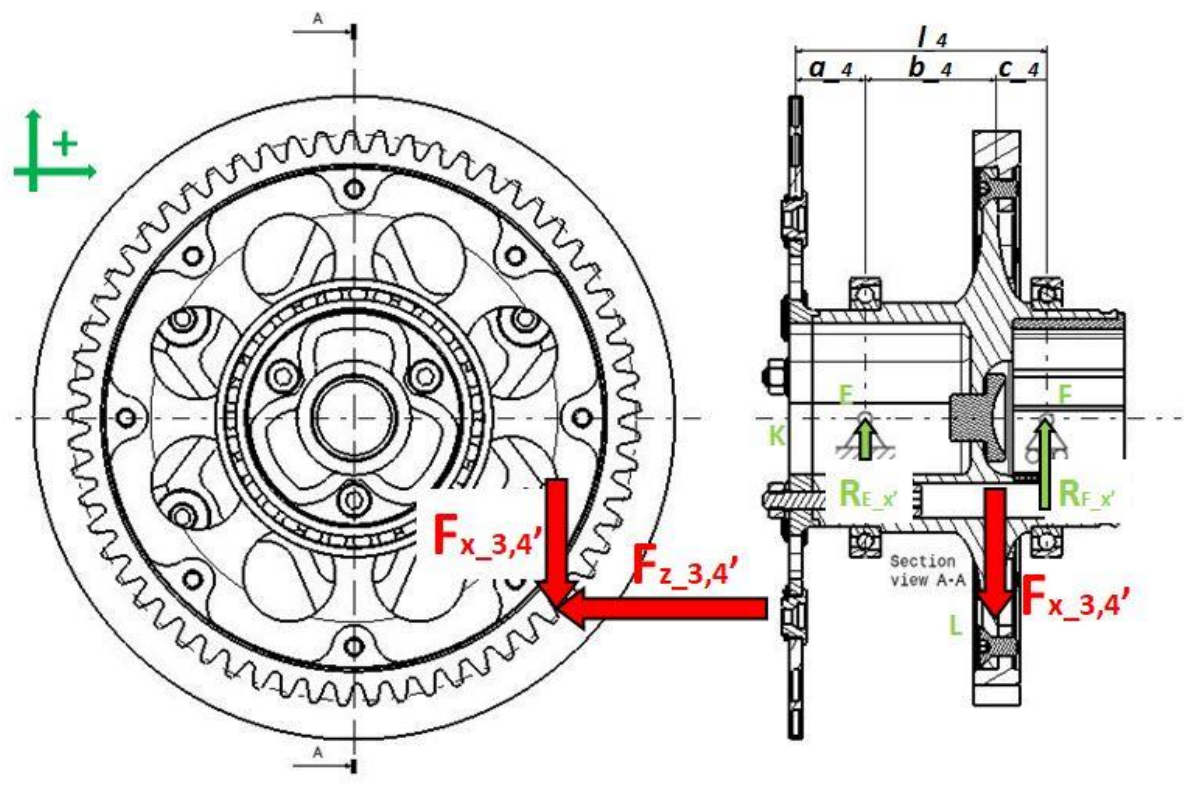


Plot 7.6-3: Free body diagram of shaft 3 in driving condition, vectors lay on XY plan.

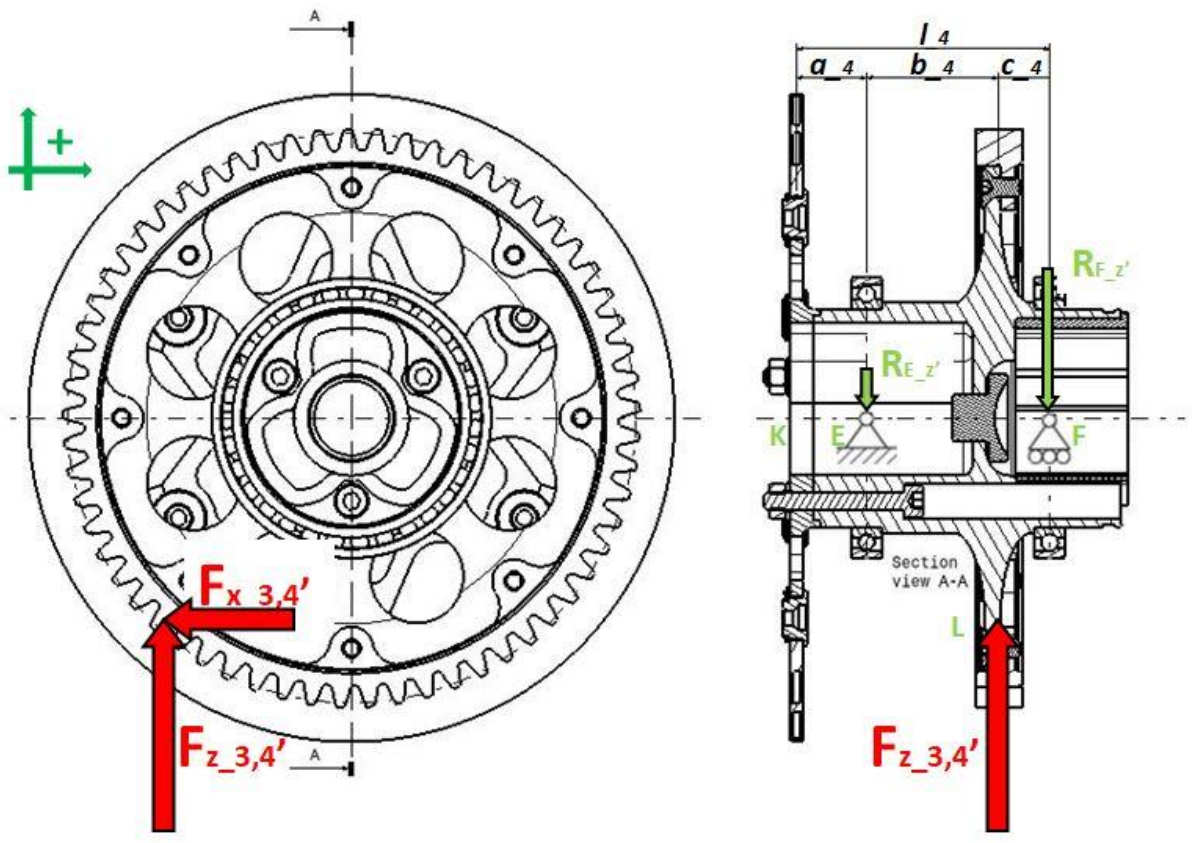


Plot 7.6-4: Free body diagram of shaft 3 in driving condition, vectors lay on YZ plan.

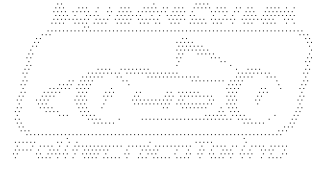
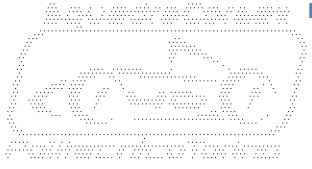


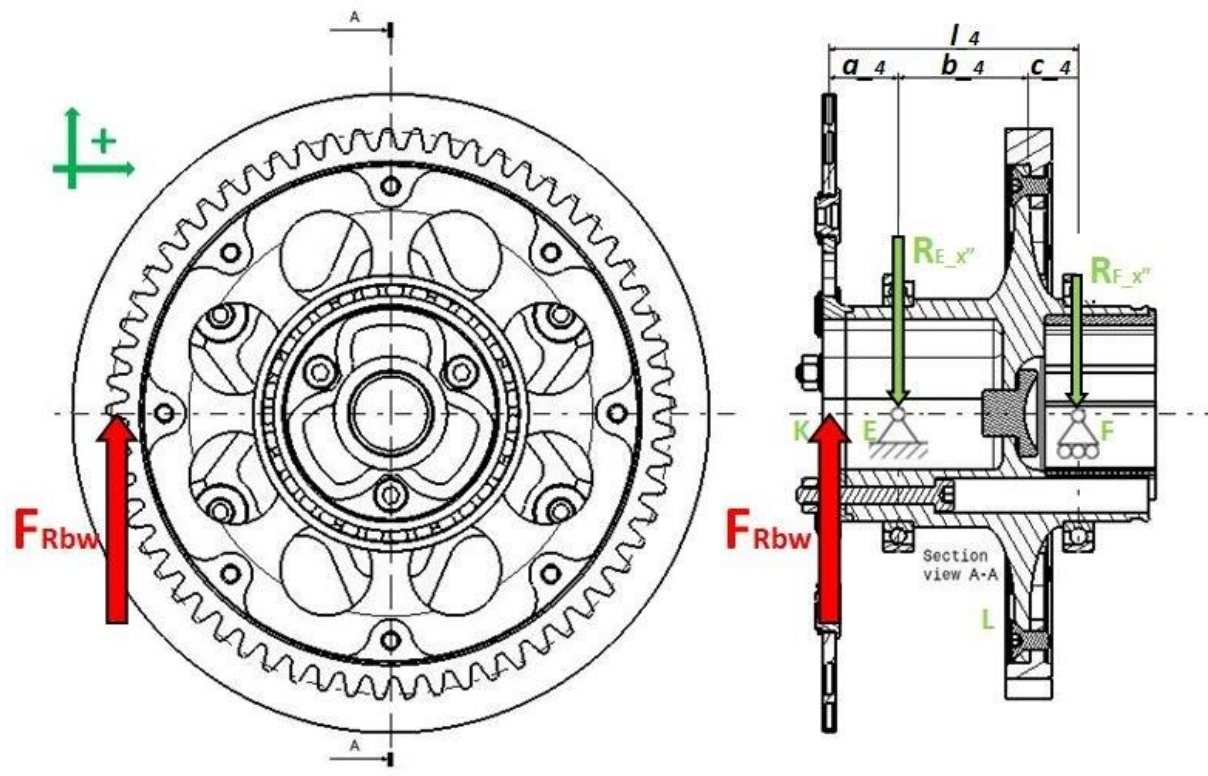


Plot 7.6-5: Free body diagram of shaft 3 in energy recovery condition, vectors lay on XY plan.



Plot 7.6-6 Free body diagram of shaft 3 in energy recovery condition, vectors lay on YZ plan.





Plot 7.6-7: Free body diagram of shaft 3 in braking condition, vectors lay on XY plan.

By free-body diagrams of Plot 7.6-5 and Plot 7.6-6, It's possible to calculate reaction forces acting on constraints during energy recovery condition:

Eq. 7.6-5 $R'_{Ex} = 118[N]$

Eq. 7.6-6 $R'_{Ez} = 178[N]$

Eq. 7.6-7 $R'_{Fx} = 1.044[N]$

Eq. 7.6-8 $R'_{Fz} = 1.932[N]$

Positive sign of vectors according to signs displayed by Plot 7.6-5 and Plot 7.6-6.

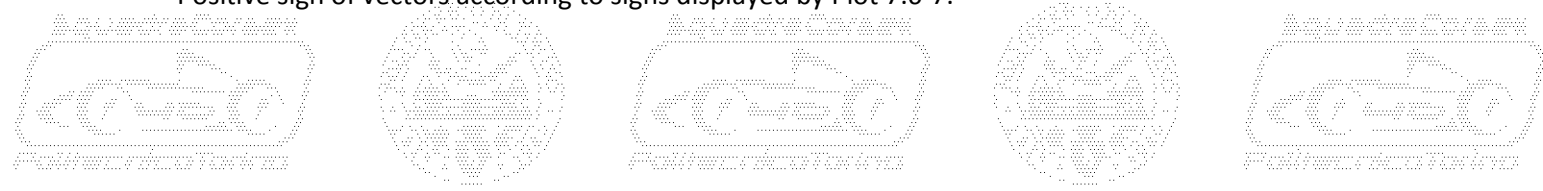
By brief analysis of magnitude of reaction forces acting during energy recovery condition, It's clear that most stressed bearing is "F", in this case too. In particular, highest magnitude of force shifts from x to z direction, that's due change in sign of tangential component of gear meshing force. Anyway, magnitude of loads acting on bearings is sensibly lower during energy recovery condition.

By free-body diagram of Plot 7.6-7, It's possible to calculate reaction forces acting on constraints during braking condition:

Eq. 7.6-9 $R''_{Ex} = 5.774[N]$

Eq. 7.6-10 $R''_{Fx} = 3.777[N]$

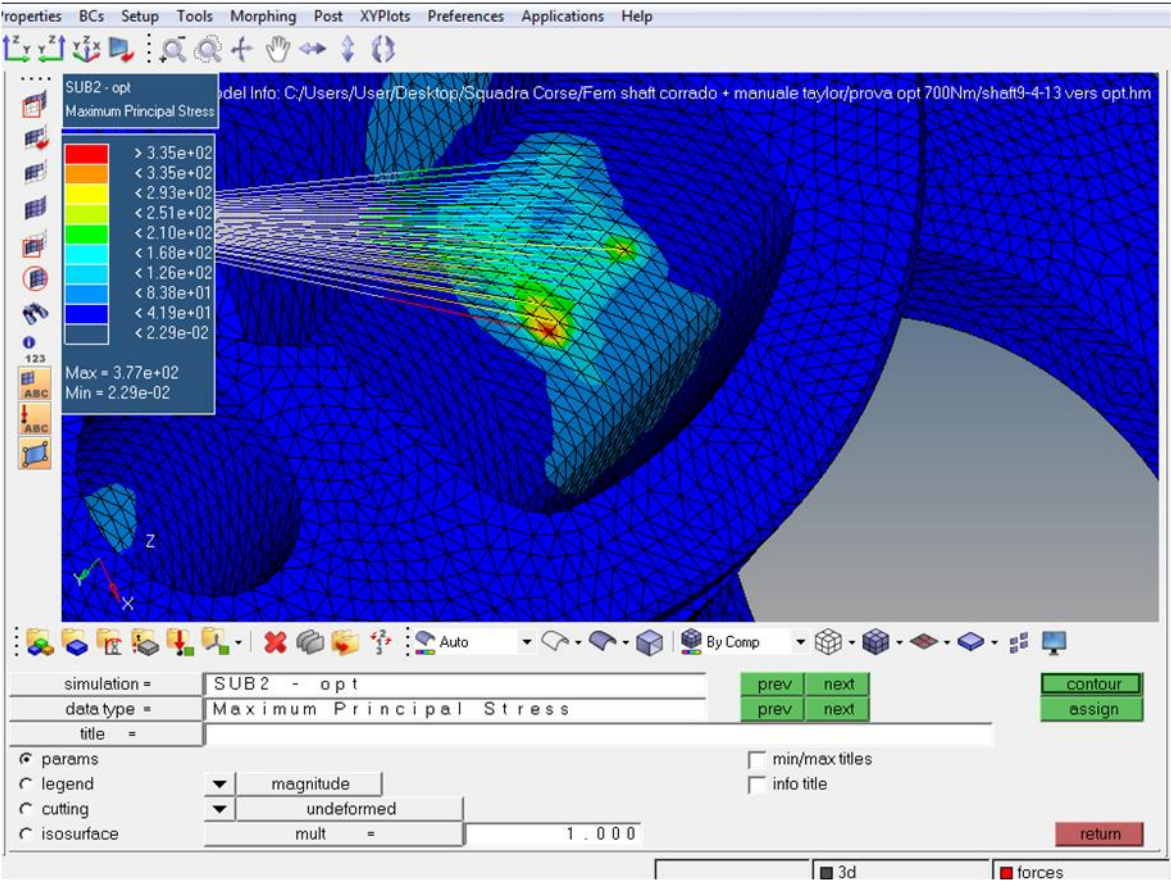
Positive sign of vectors according to signs displayed by Plot 7.6-7.



Differently from previous cases, by brief analysis of reaction forces acting during braking condition, It's possible to notice that forces act on xy plan only. By analysis of magnitude, It's clear that most stressed bearing is "E".

By virtue of elements shown in previous dissertation, It's possible to state that worst condition for "E" bearing is braking, while worst condition for "F" bearing is driving. This fact is fundamental to perform a more accurate verification on safety and duration of bearings.

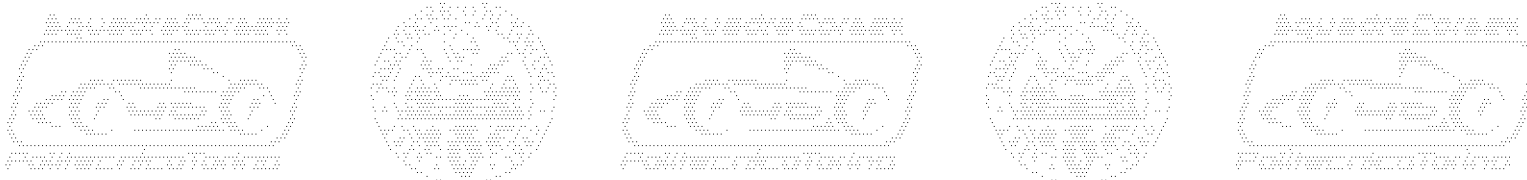
Due to complex geometry of shaft 3 hub, It's not convenient set up an empirical structural model like those analyzed by Chapter 7.4 and Chapter 7.5. Cases of driving, energy recovery and braking conditions are going to be analyzed through a more complex F.E.M. model. Most important result of structural simulations is the crown of axial holes which is possible to observe by Plot 7.6-1. Like It was declared in advance, axial holes are a simple and cheap solution to reduce total weight and inertia of a mechanical component. All portions of shaft 3 hub, work in good safety condition, even if tripod housing zone exploits a spike of stress due to roller contact, like It's displayed by Picture 7.6-1. It's known that aluminium from which shaft 3 hub is machined doesn't bear so huge stresses like steel, even if an hard oxidation coating is performed on the component.



Picture 7.6-1: F.E.M. model of shaft 3 hub in driving condition.

By virtue of that, solution was a quenched "steel insert" housed into shaft 3 hub, displayed in yellow by Plot 7.6-1.

At this level of detail, dissertation about shaft can be considered concluded. It's necessary study bearings and, if verifications are satisfying, design of shafts can be considered frozen.



8. Bearings.

How declared by previous chapters, bearings represent one of main boundaries to design freedom. On the other hand, choice of bearings is strongly affected by design issues, like coupling with other components and functional features to perform. Chapter 7.4 shows that main driver for choice of bearings on shaft 1 is represented by dimension of motor sp-lined shaft. While Chapter 7.6 displays that choice of bearings on shaft 3 is strongly affected by dimensions of tripod joint. Both cases display a choice of bearings affected by design issues and independent from loads acting on constraints. Differently from previous cases, It's necessary to remind that preliminary choice of bearings performed on shaft 2, Chapter 7.5, takes into account loads acting on constraints. Totally brand new design of the shaft allows to consider loads as design drivers.

Independently from these facts, chosen bearings needs to be accurately verified for what concerns static and fatigue load cases. Since first projects, Squadra Corse have been widely supported from bespoke Swedish bearing manufacturer **SKF** which represents a precious technical partner. Such partnership consists of supply of components like bearings, seals and one of the most important benefits, technical service. Such service allows to obtain maximum values of performance and reliability from installed bearings.

During this step of the project, is important supply to SKF engineers all available data and all transmitted information are going to be widely described by next Chapter 8.1.

8.1. Static and fatigue verification.

First information to forward to SKF technical service is designation and installation of chosen bearings.

Bearing	Designation
A	7206 BECBM
B	7206 BECBM
C	7204 BECBM
D	7304 BECBM
E	71814 CD/HCP4
F	71814 CD/HCP4

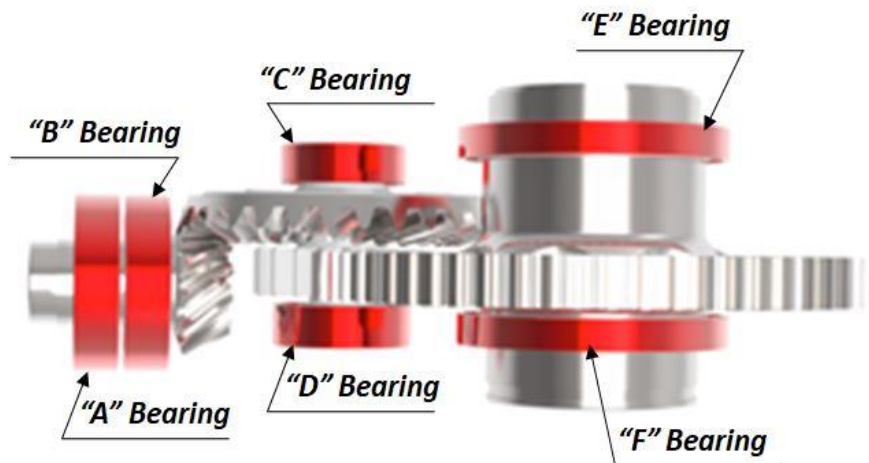
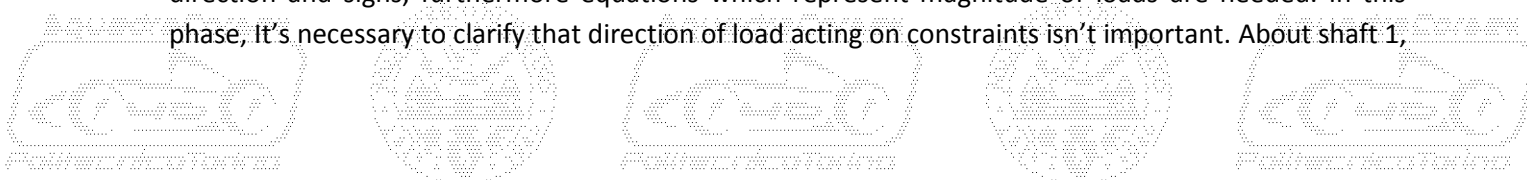


Table 8.1-1: Designation and location of bearings.

Information about installation of bearings isn't complete without information about length of shaft and position of gearwheels. By virtue of that, two dimensional drawings of shaft components were provided to SKF engineers.

In order to perform static verifications, information about worst case of loads need to be forwarded to technical service. Basically, needed information are represented by two dimension plots to indicate direction and signs, furthermore equations which represent magnitude of loads are needed. In this phase, It's necessary to clarify that direction of load acting on constraints isn't important. About shaft 1,



worst case is clearly the driving condition, for this reason all needed information are included by Plot 7.1-1, Eq. 7.1-1, Eq. 7.1-2 and Eq. 7.1-3. About shaft 2, worst case is represented by driving case too, by virtue of that, all needed information are represented by Plot 7.1-2, Plot 7.1-4, Eq. 7.1-4, Eq. 7.1-5, Eq. 7.1-6, Eq. 7.1-11 and Eq. 7.1-12. About shaft 3, situation is different, how explained by Chapter 7.6. “F” bearing is the mostly stressed during drive condition, while “E” bearing is mostly stressed during braking condition. By virtue of that, needed information are represented by Plot 7.1-6, Plot 7.3-1, Eq. 7.1-15, Eq. 7.1-16 and Eq. 7.3-3. In order to simplify transmission of data, Table 8.1-2 have been created. Reference directions and signs are those shown by Picture 4.2-2.

Case	Gearwheel	Direction	Sign	Magnitude	Unit
Driving	1	x	-	1.492	[N]
Driving	1	y	-	439	[N]
Driving	1	z	-	2.151	[N]
Driving	2	x	+	1.492	[N]
Driving	2	y	+	439	[N]
Driving	2	z	+	2.151	[N]
Driving	3	x	-	4.045	[N]
Driving	3	z	+	1.196	[N]
Driving	4	x	+	4.045	[N]
Driving	4	z	-	1.196	[N]
Braking	Br. Disc	x	+	1.997	[N]

Table 8.1-2: Loads needed to perform static load verifications.

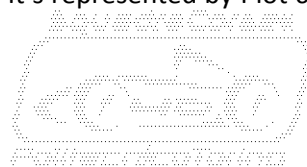
By previous data, It’s possible to perform verifications, in order to establish strength of bearings to static loads. Output of verifications are “*minimum bearing static safety coefficient*” displayed by Table 8.1-3.

Bearing	Designation	Min. Bear. Static Safety Coefficient	Unit
A	7206 BECBM	6,0	[dim.less]
B	7206 BECBM	4,6	[dim.less]
C	7204 BECBM	3,4	[dim.less]
D	7304 BECBM	2,4	[dim.less]
E	71814 CD/HCP4	5,8	[dim.less]
F	71814 CD/HCP4	5,3	[dim.less]

Table 8.1-3: Output of static bearing verifications.

By the way It’s necessary to clarify that displayed values are minimum coefficients, by virtue of that safety coefficient related to “E” bearing is referred to braking case, all others to driving case. By analysis of values it’s necessary to observe that displayed values are much higher than needed. About shaft 1 and shaft 3 explanation is written in the introduction of Chapter 8. Despite choice of driven by load about bearings of shaft 2, values of safety coefficients are higher than expected in this case too. Anyway, before a reduction of size of bearings It’s necessary to perform a verification on fatigue strength.

Technical service of SKF owns a custom software to perform fatigue verifications. It’s based on **A.F.C. Method**, which stands for “*Advanced Fatigue Calculation*”. Such method doesn’t work differently from KISSOR software, by virtue of that input for fatigue verification needs to be a duty cycle. Duty cycle of shaft 1 have been described yet and It’s represented by Plot 6.1-5. At the same way duty cycle of shaft



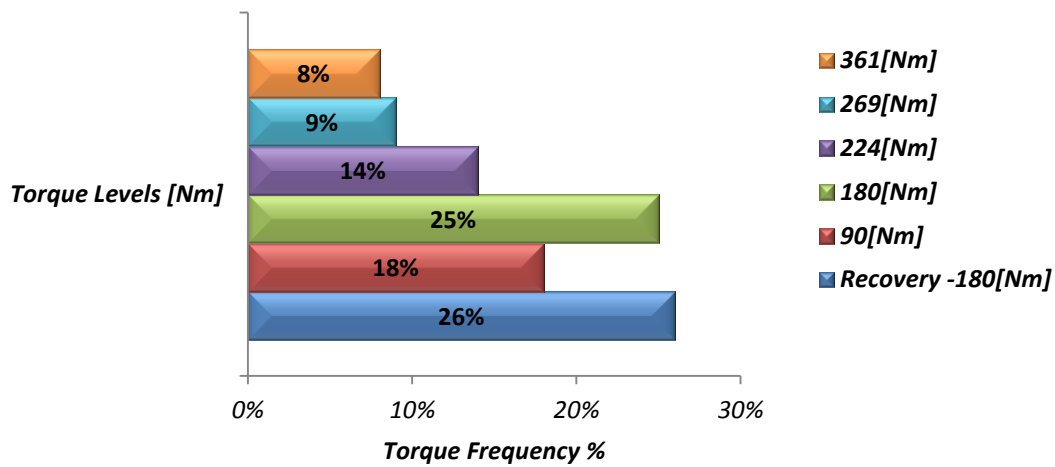
2 is represented by Plot 6.1-6. Only missing load cycle refers to shaft 3 and needs to be calculated by an homologous of Eq. 6.1-23:

$$\text{Eq. 8.1-1} \quad T_{3i} = i_{3,4} \cdot T_{2i}$$

Where:

- T_{3i} is the generic “**magnitude of torque level**” acting on shaft 3, measured in [Nm].
- T_{2i} is the generic “**magnitude of torque level**” acting on shaft 2, measured in [Nm].
- $i_{3,4}$ is “**gear ratio of the second stage**”, a dimensionless parameter defined by Eq. 4.4-7.

Result is a chart homologous to Plot 6.1-5 and Plot 6.1-6:

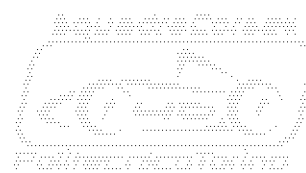
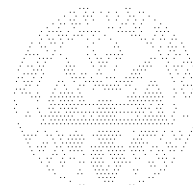
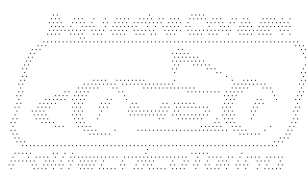
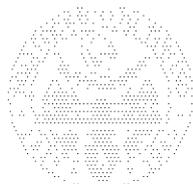
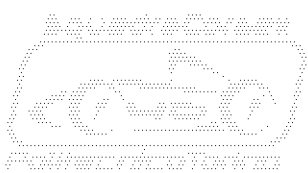


Plot 8.1-1 : Frequency on levels of requested torque, shaft 3.

Anyway, Its necessary to focus on recovery level displayed by Plot 6.1-5, Plot 6.1-6 and Plot 8.1-1. In order to be cautionary enough, recovery condition on shaft 3 needs be represented by a continuous braking phase which is known to be a worst condition respect to energy recovery. By virtue of that recovery condition of Plot 8.1-1 refers to static case of load on bearings. Differently on other shafts, recovery condition needs to be modelled on shaft 1. For this reason, It’s necessary supply to SKF engineers following data: Plot 7.2-1, Eq. 7.2-1, Eq. 7.2-2 and Eq. 7.2-3. In order to model recovery condition on shaft 2, following data are necessities: Plot 7.2-3, Eq. 7.2-4, Eq. 7.2-5, Eq. 7.2-6, Eq. 7.2-9 and Eq. 7.2-10. Analogously to previous case, data are collected on a proper chart:

Case	Gearwheel	Direction	Sign	Magnitude	Unit
Recovery	1	X	-	746	[N]
Recovery	1	Y	-	220	[N]
Recovery	1	Z	+	1.076	[N]
Recovery	2	X	+	746	[N]
Recovery	2	Y	+	220	[N]
Recovery	2	Z	-	1.076	[N]
Recovery	3	X	+	1.165	[N]
Recovery	3	Z	-	1.738	[N]

Table 8.1-4: Loads needed to model energy recovery in fatigue verification.



In order to conclude actual dissertation It's necessary to calculate maximum number of cycles that each shaft needs to sustain. Back to Chapter 6.1, It was declared that distance that S.C.R. needs to run is about 4000 [Km]. Dimension of deformed wheel is known, by virtue of that, CY_{3min} which is "minimum cycles of shaft 3" can be calculated as follows:

$$Eq. 8.1-2 \quad CY_{3min} = \frac{4000 \cdot 1000}{2 \cdot \pi \cdot r_d} \cong 2.500.000 \text{ [cycles]}$$

By virtue of that, It's possible to calculate CY_{2min} which is "minimum cycles of shaft 2" and CY_{1min} which is "minimum cycles of shaft 1".

$$Eq. 8.1-3 \quad CY_{2min} = i_{3,4} \cdot CY_3 \cong 8.000.000 \text{ [cycles]}$$

$$Eq. 8.1-4 \quad CY_{1min} = i_{1,2} \cdot CY_2 \cong 22.500.000 \text{ [cycles]}$$

It's necessary to underline that number minimum number of cycles have to be common for both bearings of the same shaft. Anyway, different size of bearings and different condition of loads, make output of verification different for each bearing.

Output of A.F.C. simulation is CY_{imax} which is the "maximum cycles sustained by generic i bearing". Values of numbers of cycles are ordered and collected by Table 8.1-5, where results of calculations of *F.S.C.i*, the "Fatigue safety coefficient of generic i bearing", are displayed. Such parameter is calculated by the following relation Eq. 8.1-5 and is a dimensionless:

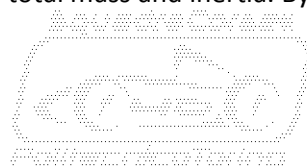
$$Eq. 8.1-5 \quad F.S.C.i = \frac{CY_{imax}}{CY_{imin}}$$

Shaft	Bearing	C_imin	C_imax	Unit	F.S.C.i	Unit
1	A	22,5	1138,0	[million cycles]	50,6	[dim.less]
1	B	22,5	91,0	[million cycles]	4,0	[dim.less]
2	C	8,0	12,0	[million cycles]	1,5	[dim.less]
2	D	8,0	11,0	[million cycles]	1,4	[dim.less]
3	E	2,5	16,0	[million cycles]	6,4	[dim.less]
3	F	2,5	13,0	[million cycles]	5,2	[dim.less]

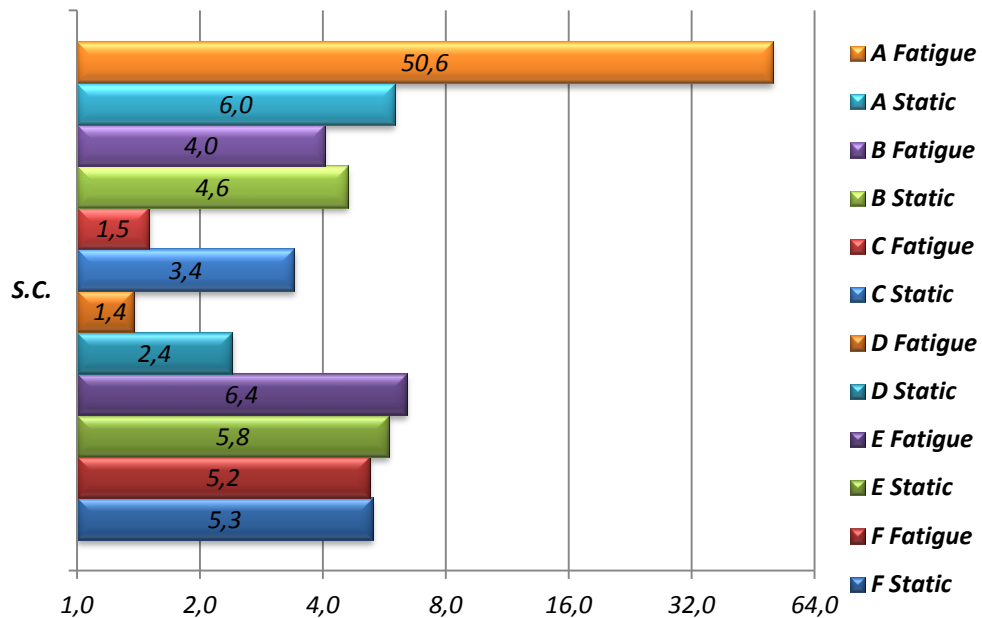
Table 8.1-5: Output of fatigue bearing verifications.

F.S.C.i parameter is very useful in the instantaneous analysis of Table 8.1-5 and practical meaning of the value is: how many times bearing can endure, compared to basic required duration CY_{imin} .

In order to have a more complete and more organized display of safety performances in static and dynamic condition, It's useful create a bar plot. By analysis of Plot 8.1-2, first aspect to take into account is magnitude of displayed coefficients. Values indicate that all bearings operate safely under static and dynamic loads. Next dissertation have to be done around safety coefficients related to shaft 1 bearings. How expected, values are much greater than needed, anyway design and commercial issues make difficult choice of alternative bearings. That's due to bore diameter of internal raceway which is tightest as possible, how explained by dissertation of Chapter 7.4. Slimmer bearings which exploit the same bore diameter aren't standard products, for these reasons, long delivery times and high costs lead to a very tight benefit in term of total mass and inertia. By virtue of that, 7206 BECBM bearings are



the better choice for installation on shaft 1. Continuing with analysis of safety coefficients of bearings, It's useful analyse those related to shaft 2. How declared in advance at Chapter 7.5, choice of bearings had more freedom respect to previous cases. Result are fatigue safety coefficients which values are very close to optimum value declared by Eq. 5.1-2. In this case too, It's not convenient evaluate slimmer bearings in order to lower value of static safety coefficient ad dynamic as consequence. By virtue of that, choice of 7204 BECBM and 7304 BECBM are confirmed.



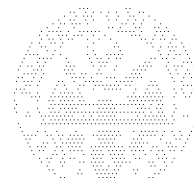
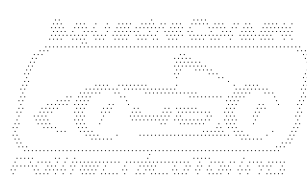
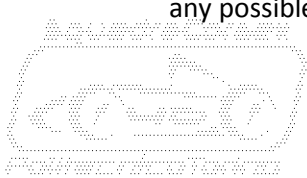
Plot 8.1-2: Comparison of fatigue and static safety coefficients.

In order to conclude actual dissertation, It's necessary analyze safety coefficients related to shaft 3 bearings. How widely explained at Chapter 7.6, main driver in choice of bearings are dimensions of tripod joints. By virtue of that, safety coefficients result oversized even if, values included 4 and 5 times minimum allowable, can be acceptable. Starting from a bounded value of internal raceway bore diameter, chosen bearings 71814 CD/HCP4 represent slimmest possible option.

8.2. Preload.

In order to introduce next dissertation, It's necessary to clarify that fatigue performances described in the previous chapter can be achieved only if any bearing operates under a right value of preload. Angular contact bearings, by own geometry feature high backlashes when not assembled. By virtue of that, a small axial load needs to be always present in order to stack crown of spinning elements between internal and external raceways. Main benefits exploited by preload are gain of stiffness, operational noise loss and precision on positioning of each shaft.

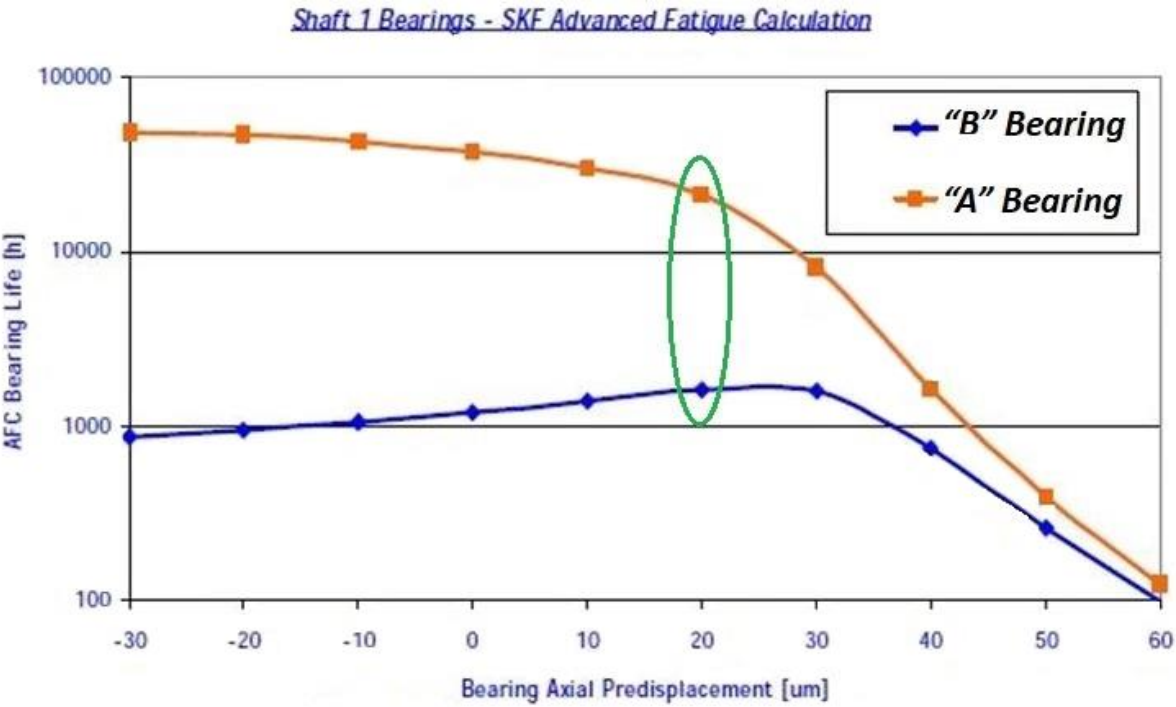
Techniques to preload a couple of angular bearings are different and depend from assembly configuration. How explained at Chapter 7.4, a couple of bearings in "O" configuration needs to be preloaded through internal raceways. While, how explained at Chapter 7.5, a couple of bearings in "X" configuration needs to be preloaded through external raceways. Both configurations, practically, require that bearings and included mechanical components are stacked together in order to eliminate any possible backlash.



By virtue of that, any available data about components, like dimensions, materials and tolerances need to be forwarded to S.K.F. engineering service. It's necessary remind that information about loads and duty cycle is still present and useful for calculation. All collected data are useful to traduce preload axial force into a distance which represents difference between length of stack of components in bench condition and length of stack in operational condition. Obviously preload distance depends by temperature. For this reason, when working on systems which feature multi material components, with different thermal displacement coefficient, It's necessary distinguish between **“preload at workshop temperature”** and **“preload in operational condition”**.

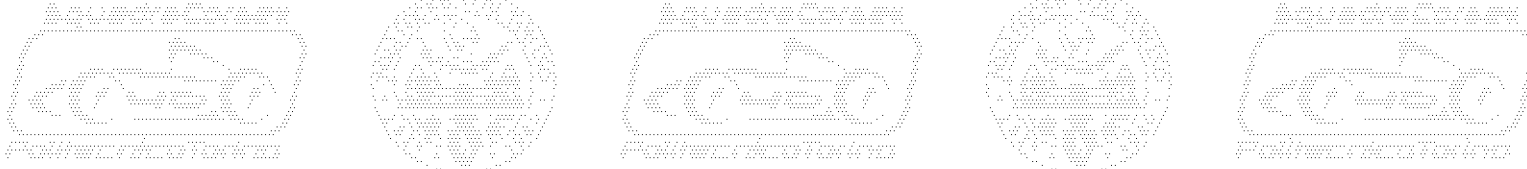
Output of calculation is a curve of bearing life in function of preload at workshop temperature value. Value of life is expressed in [hours] of operation while value of preload is expressed in [μm]. Any bearing exploits its own curve, and plots are created for every shaft: Plot 8.2-1, Plot 8.2-2 and Plot 8.2-3. By brief analysis of the plot, It's clear that higher value of axial preload needs to be applied on less loaded bearing. That's why operation of unloaded axial contact bearing tends to be affected by dangerous backlashes that compromise life of the component.

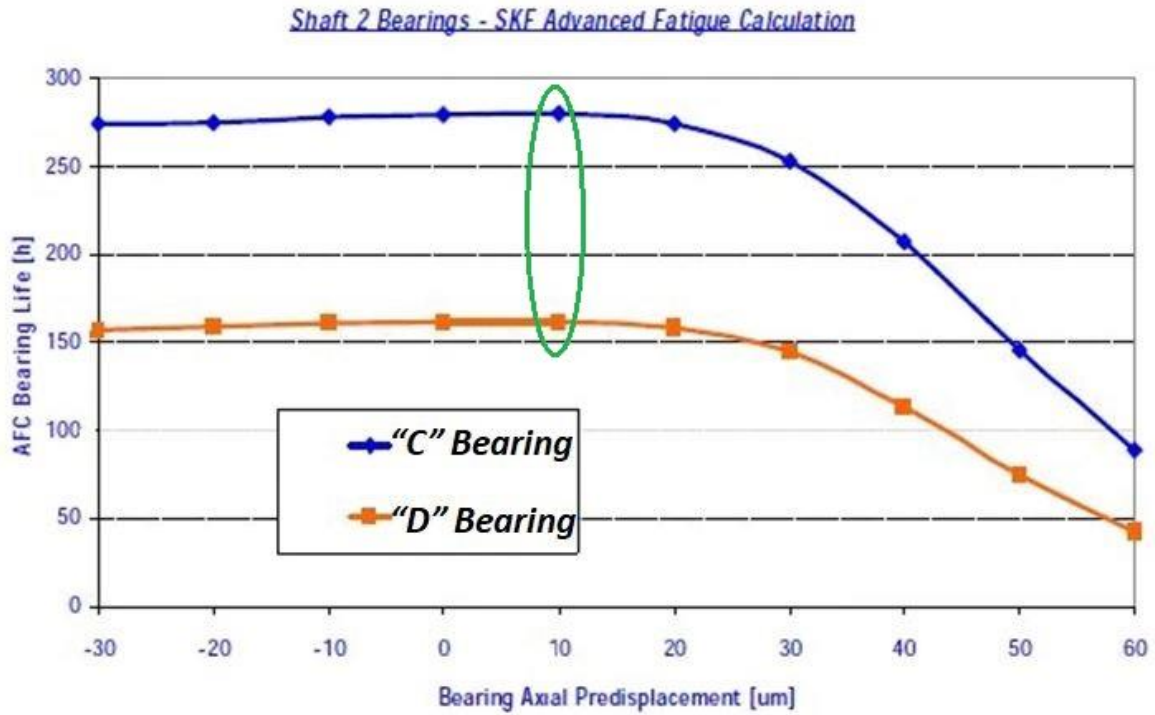
Before beginning of analysis of plots, It's necessary to clarify that total preload applied to a shaft can be considered split in two equal parts. By virtue of that, It's necessary to study Plot 8.2-1 In order to find value of preload which maximizes life of both bearings. It's clear that preload value of $20\ \mu\text{m}$ is not the best solution to maximize life of “A”, an higher value may be better. Anyway It's necessary to notice that an higher value tends to shorten life of “B” bearing. For these reasons, It's necessary to observe that a preload value of $20\ \mu\text{m}$ represents the better trade off to achieve maximum life of “A” and “B” bearings.



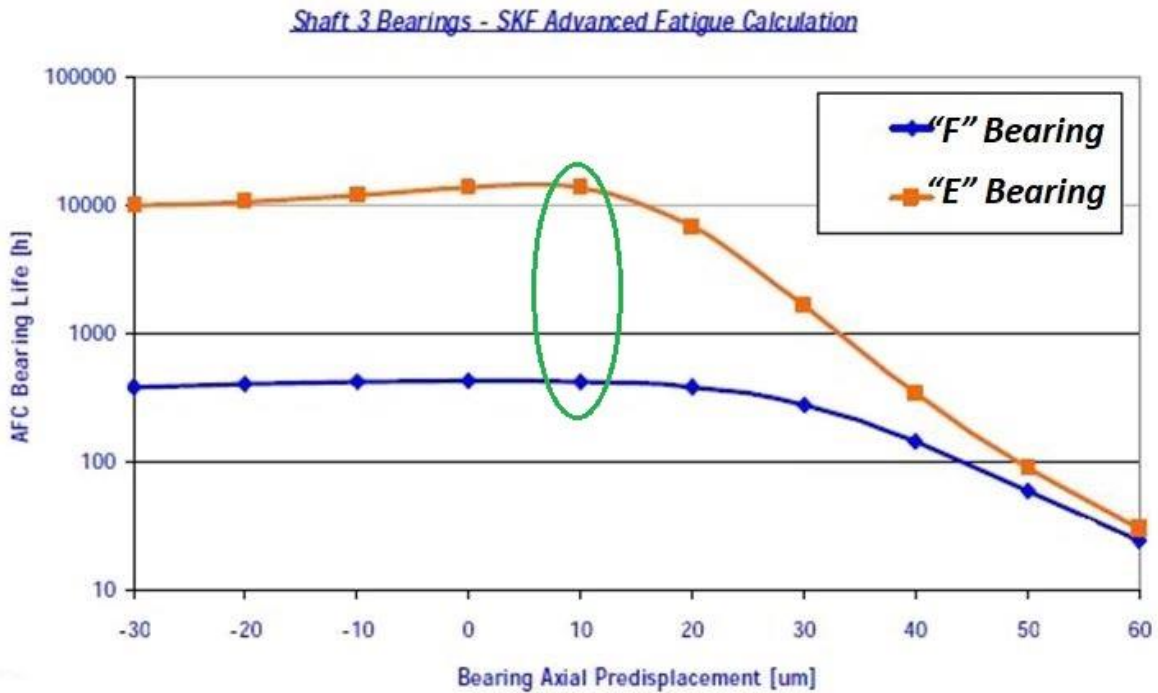
Plot 8.2-1: Preload at workshop temperature on shaft 1 bearings (Courtesy SKF).

By analysis of Plot 8.2-2, choice of axial preload doesn't represent a severe trade off because value of $10\ \mu\text{m}$ allows to obtain maximum life from both bearings of the shaft. That's why loading condition of both shafts are well balanced, differently from shaft 1.





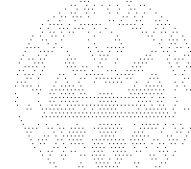
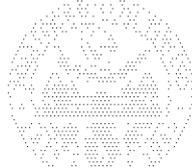
Plot 8.2-2: Preload at workshop temperature on shaft 2 bearings (Courtesy SKF).



Plot 8.2-3: Preload at workshop temperature on shaft 3 bearings (Courtesy SKF).

By analysis of Plot 8.2-3 too, choice of axial preload doesn't represent a severe trade-off. Preload at workshop temperature of $10 \mu\text{m}$ allows to obtain maximum life on both bearings.

Values and topics of previous dissertation are theoretical and stands for operational temperature only. Furthermore, It's necessary to underline that transmission assembly is performed at room temperature. By virtue of that, It's necessary to know value of axial preloads at workshop temperature.



Such values are calculated by S.K.F. engineering service under specifications of the customer, and are collected and displayed by Table 8.2-1.

Shaft	Preload at workshop temperature	Unit
1	87	[μm]
2	44	[μm]
3	10	[μm]

Table 8.2-1: Recommended preloads at workshop temperature.

Preload value recommended for shaft 1 is ruled by shaft 1 bearing spacer which is produced after a precise measurement of bearings and all associated components. Preload values recommended for shaft 2 and for shaft 3 are ruled by proper caps displayed by Plot 7.5-2 and Plot 7.6-2. In this case too, caps are accurately machined after measurement of bearings and associated components.

8.3. Description of Bearings

Actual chapter describes different types of chosen bearings. Due to relatively light applied loads, any bearing is provided of a single crown of spheres. Differences between bearings are present, how previously explained, and regard geometrical dimensions. Anyway some important design differences can be noticed. Bearings described by Table 8.3-1, Table 8.3-2 and Table 8.3-3 are typical angular contact bearings featuring standard pressure contact angle of 40°.

SKF 7206 BECBM

d	20,00 [mm]
D	62,00 [mm]
B	16,00 [mm]
d₁	42,65 [mm]
d₂	36,13 [mm]
D₁	50,10 [mm]
a	27,30 [mm]
r_{1,2}	1,00 [mm]
r_{3,4}	0,60 [mm]

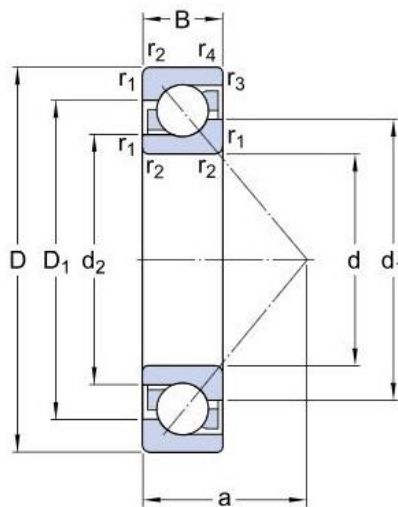
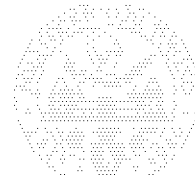
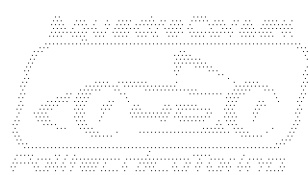
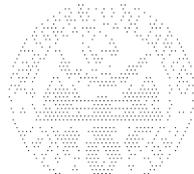


Table 8.3-1: SKF 7206 BECBM main geometrical dimensions (<http://www.skf.com>).

Therefore, It's necessary to notice that no one bearing is provided of Its own rotary seals. That's because chosen bearings operate inside the wet sump where lubrication oil needs to cross the bearing. By virtue of that, rotary seals needs to be integrated to sump components.

Bearings displayed by Table 8.3-1, Table 8.3-2 and Table 8.3-3 are from "**explores series**", the heavy duty line of S.K.F. Differently from generic bearings, those from explorer series feature a window cage with steel spheres centred. Such cage, which is machined from brass, allows to bear very high rotational speed, reducing risk of failure due to centrifugal force. That feature is particularly important on shaft 1 where rotational speed may reach 16.000 [rpm].



SKF 7204 BECBM

d	20,00 [mm]
D	47,00 [mm]
B	14,00 [mm]
d₁	30,80 [mm]
d₂	25,87 [mm]
D₁	37,00 [mm]
a	21,00 [mm]
r_{1,2}	1,00 [mm]
r_{3,4}	0,60 [mm]

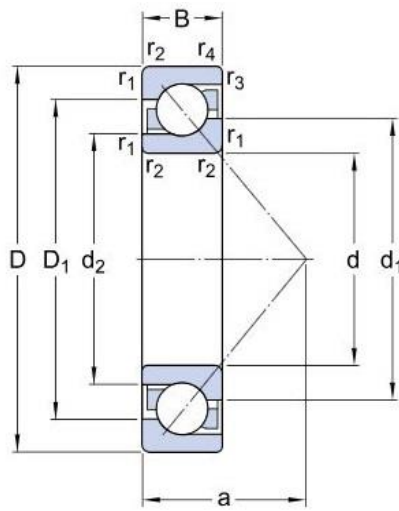


Table 8.3-2: SKF 7204 BECBM main geometrical dimensions (<http://www.skf.com>).

SKF 7304 BECBM

d	20,00 [mm]
D	52,00 [mm]
B	15,00 [mm]
d₁	33,15 [mm]
d₂	26,75 [mm]
D₁	40,50 [mm]
a	22,80 [mm]
r_{1,2}	1,10 [mm]
r_{3,4}	0,60 [mm]

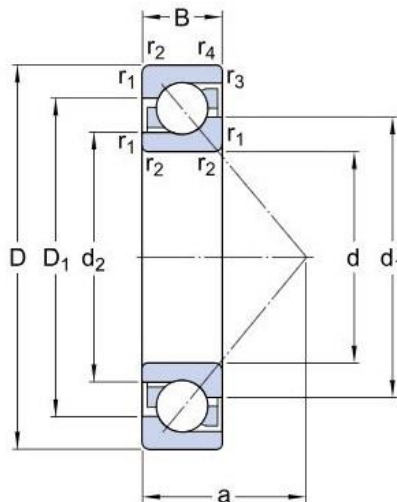
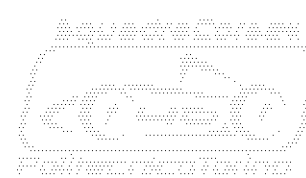
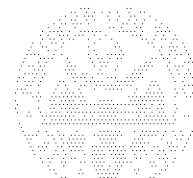
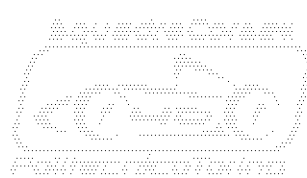
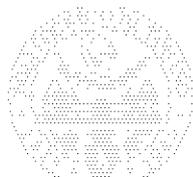
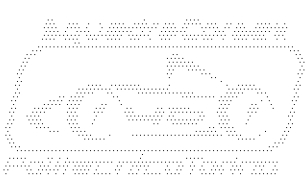


Table 8.3-3: SKF 7304 BECBM main geometrical dimensions (<http://www.skf.com>).

Finally It's necessary observe bearing displayed by Table 8.3-4. Differently from other bearings chosen for actual project, pressure contact angle is reduced to 15°. Such feature is useful in order to reduce overhanging tilting momentum due to braking event.

How declared in advance, other unique feature is that bearings assembled on shaft 3 are from **“super precision series”**. By virtue of that, feature very tight tolerances and a very accurate grade of machining. Such characteristics are particularly appreciated by machine tools manufacturers which usually employ super precision bearings in applications where extreme accuracy is needed.

How explained in previous Chapter 7.6., another important feature of chosen bearings is the employ of ceramic spheres which, combined with steel raceways make the bearing **“hybrid”** by point of view materials. Very light ceramic spheres feature lower weight and lower inertia momentum, if compared to steel ones. Anyway, main feature is **“self lubricating”** effect which reduces importance of lubrication on shaft 3 bearings.



SKF 71814 CD/HCP4

d	70,00 [mm]
D	90,00 [mm]
B	10,00 [mm]
d₁	76,70 [mm]
d₂	76,70 [mm]
D₁	83,50 [mm]
a	15,70 [mm]
r_{1,2}	0,60 [mm]
r_{3,4}	0,30 [mm]

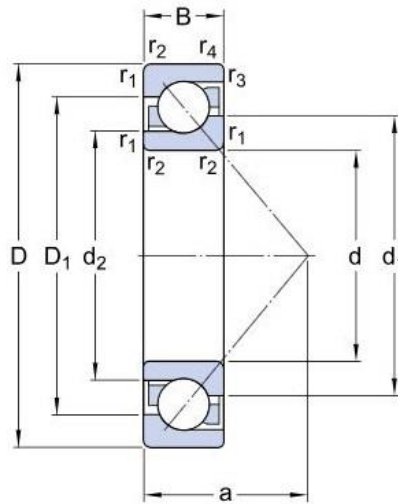
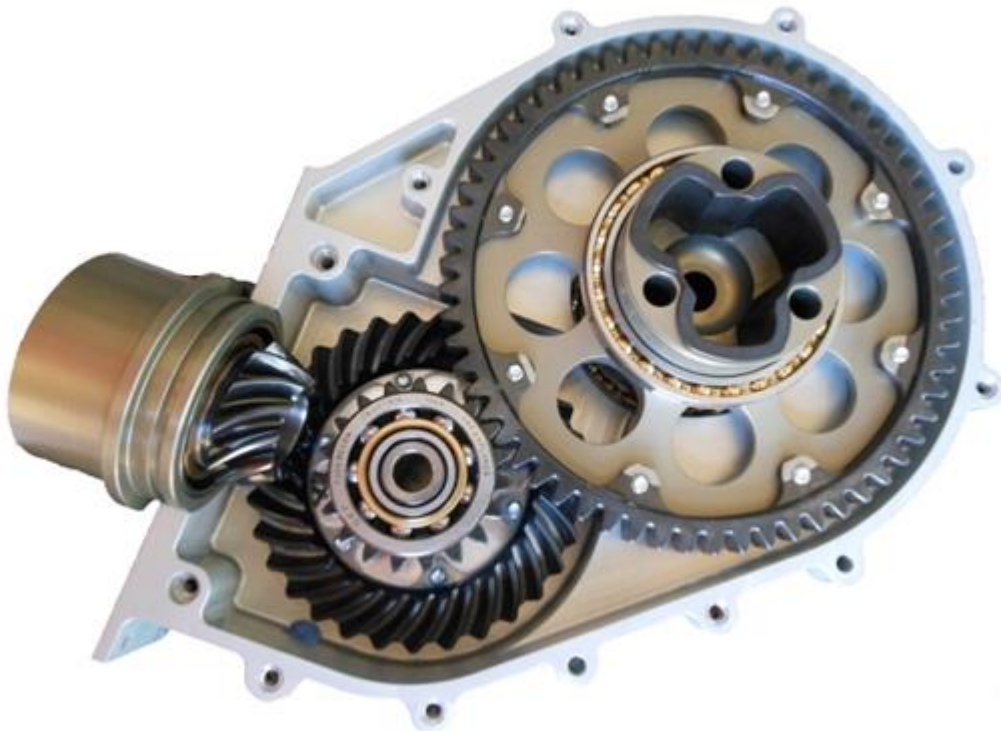
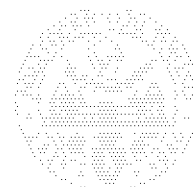
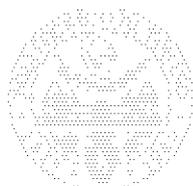


Table 8.3-4: SKF 71814 CD/HCP4 main geometrical dimensions (<http://www.skf.com>).

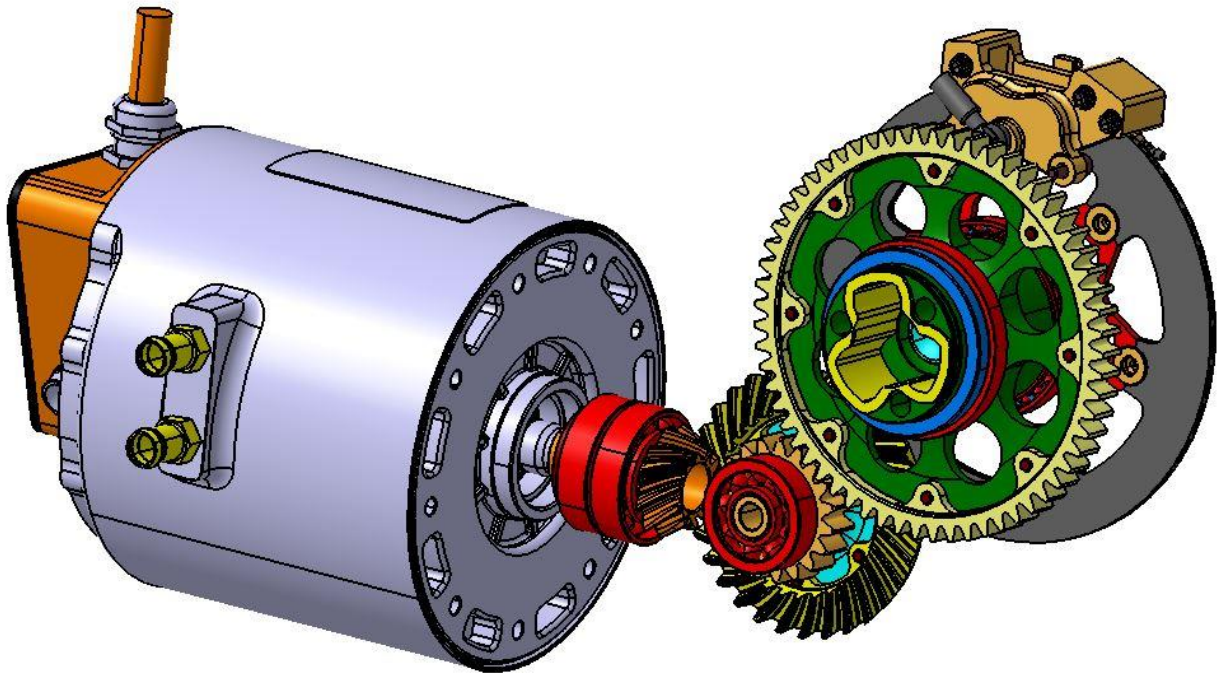
Last feature to take into account about bearings chosen for shaft 3, is material of the cage which, differently from previous cases is made from polymeric material. PA66 glass fibre reinforced ensures a very low weight compared to brass solution. It's necessary to remind that requirements on rotational speed are less severe on shaft 3 due to relatively low output speed of the transmission.



Picture 8.3-1: Assembled shafts with related bearings.



9. Gear-box case.

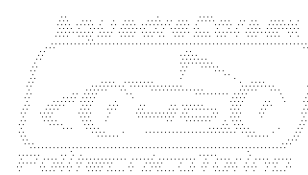
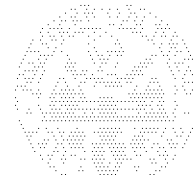
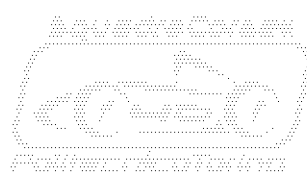
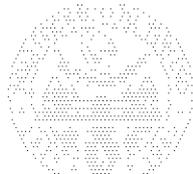
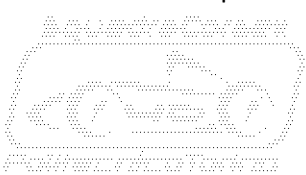


Plot 9-1: Gear-box components in position, reference for design of gear-box case.

Once design of shafts, bearings and brakes is frozen, It's necessary design the "box", a case which contains and supports all components. Main task of such a box is to bear loads from gearwheels and brakes. Furthermore, It's necessary to remind that gear-box case represents the interface between gears and chassis. Differently from some formula and prototype applications, gear-box case doesn't need to support suspension hard points. How declared in advance at Chapter 1.4.2, two independent transmissions need to be developed, one for each motor. As consequence, design of left gear-box is simply mirrored in order to obtain right one, that stands for design of gear-box case too.

Specific requirements of gear-box design are widely described at Chapter 3 and some precious references can be read on Ref.[14]. Anyway, It's useful remind that, like any other component of the transmission, gear-box case needs to be as lighter as possible. Despite weight, It's necessary to take into account that structure which supports bearings, needs to be stiff enough to ensure proper operation of bevel gear, with no risk of dangerous displacements. Another benefit related to structural stiffness is absence of oil leakages which is one of the most basic requirements for a gear-box. Integration of brake caliper is another important requirement to take into account during design, in particular by point of view of loads which are transmitted to the structure. Assembly issues too need to be taken into account because, how revealed in advance, assembly of bevel stage and angular contact bearings needs to be particularly accurate. In order to conclude actual topic about requirements, It's necessary to remind that design of gear-box case must be aimed to an easy and quick maintenance of transmission and brake components.

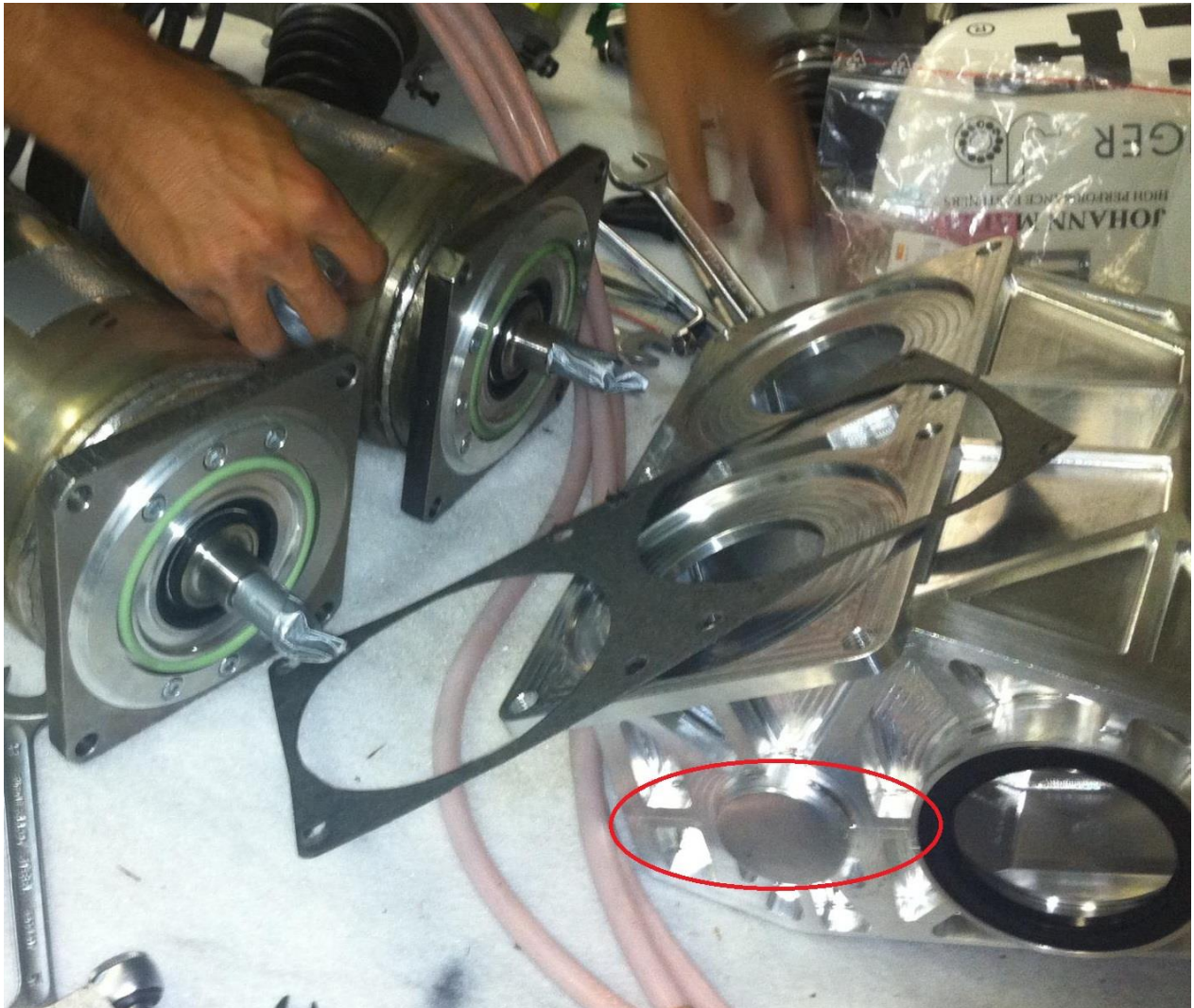
Design status coherent with actual chapter is depicted by Plot 9-1. Position of shafts, bearings and gaskets leave a large freedom on design, by virtue of that ,multiple solutions need to be accurately evaluated in next chapters.



9.1. Design concept.

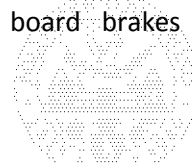
Aim of actual chapter is explain in detail main drivers which was adopted during design of gear-box case. Concept stage is the phase where all **requirements** described in previous introduction are matched to ideas coming from **bench mark work** displayed at Chapter 1.5.

By analysis of previously depicted requirements, maintenance and assembly in particular, It's clear that gear-box case needs to be an assembly of **different components**. By virtue of that each sump needs to be machined at least in two different parts. With reference to Chapter 1.5, two different solutions can have been noticed and can be evaluated.



Picture 9.1-1: Detail of transmission from Green Team of Stuttgart. Surface of joint is circled in red (<https://www.facebook.com/greenteamstuttgart/>).

First option evaluated is proposed by **Green Team of Stuttgart** and is described at Chapter 1.5.3. How declared in advance, It's necessary to notice that gear-box case is realized by only two components. Surface joint between two case parts lays between axis of intermediate shaft and axis of output shaft, how highlighted on Picture 9.1-1. Such option looks to be very functional in case of quick maintenance, anyway looks to be expensive by machining point of view. Each housing of bearing is split into two different parts, such solution requires very high precision in machining and may lead to dangerous unconformities. Another issue to take into account during observation of Picture 9.1-1. is that solution proposed by Green Team doesn't allow installation of on board brakes between mirrored



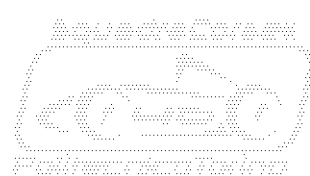
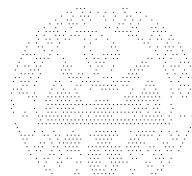
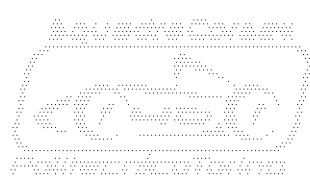
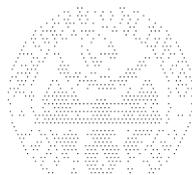
transmissions. Installation of brakes would be performed in outer position, but that solution would impair loads on bearings of output shaft. By virtue of that, solution described by Chapter 1.5.3 is not convenient to be adopted as design main driver.



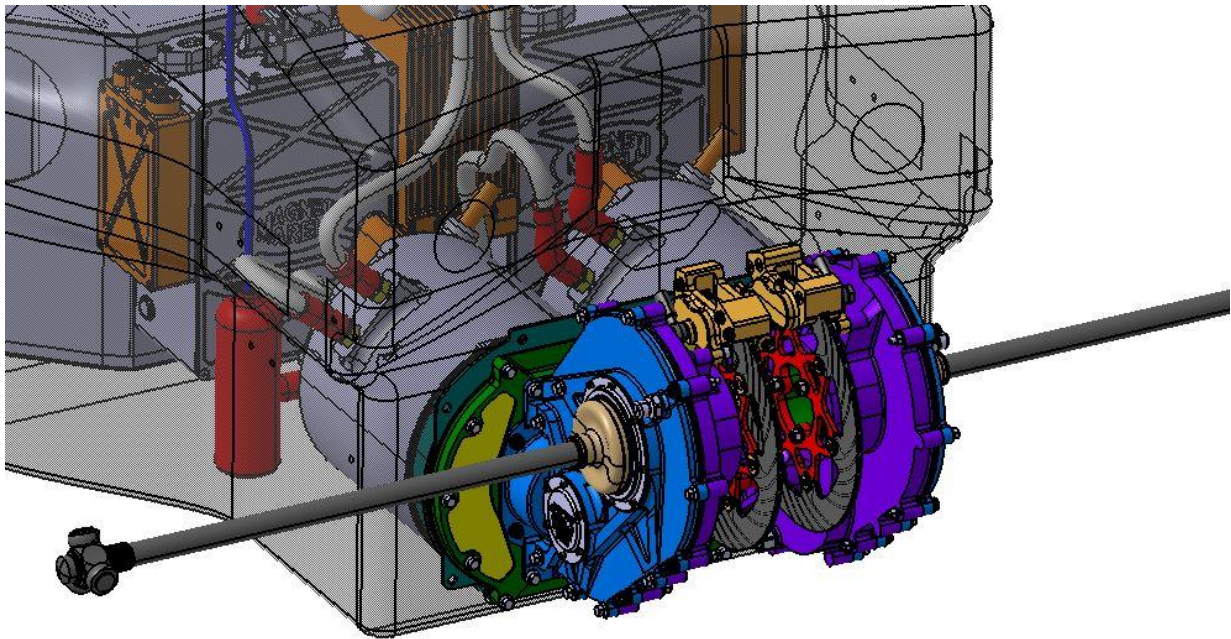
Picture 9.1-2: Photo rendering of gear-box developed by R.M.I.T. Racing Team of Melbourne (<https://www.facebook.com/RMITElectricRacing/>).

A good alternative solution to take into account is proposed by **R.M.I.T. Racing** at Chapter 1.5.8. By Picture 9.1-2, It's possible to notice gear-box case which is realized by four components, at least. Surface of joint between two different case parts is perpendicular to intermediate shaft and to output shaft. By accurate analysis of Picture 1.5-8, It's possible to notice that position of the joint surface is in correspondence with symmetry plan of input shaft . Differently from previous case, each bearing housing related to intermediate shaft and output shaft is integral and machined in one unique part. Main issue may be related to alignment of bearings of the same shaft but such issue can be solved by use basic mechanic precautions. Anyway, by observation of solution proposed by R.M.I.T. Racing, issue of split housing is still standing for bearings of input shaft. With reference to Chapter 7.4, It's necessary to remind that project of S.C.R. transmission establish an integral aluminum cylinder which supports external raceways of input shaft bearings. Observing Picture 1.5-8, It's possible to notice that case manufacturing looks to be significantly simplified respect to project depicted by Picture 9.1-1. Furthermore a R.M.I.T. style solution makes **easier integration of on board brakes** placed in internal position.

Anyway, main drawback which may affect solution based on two split gear-box cases, may be represented by **stiffness of the structure**. Indeed, high magnitude of gear mesh axial components exploited during acceleration may cause dangerous displacements which may deflect entire structure

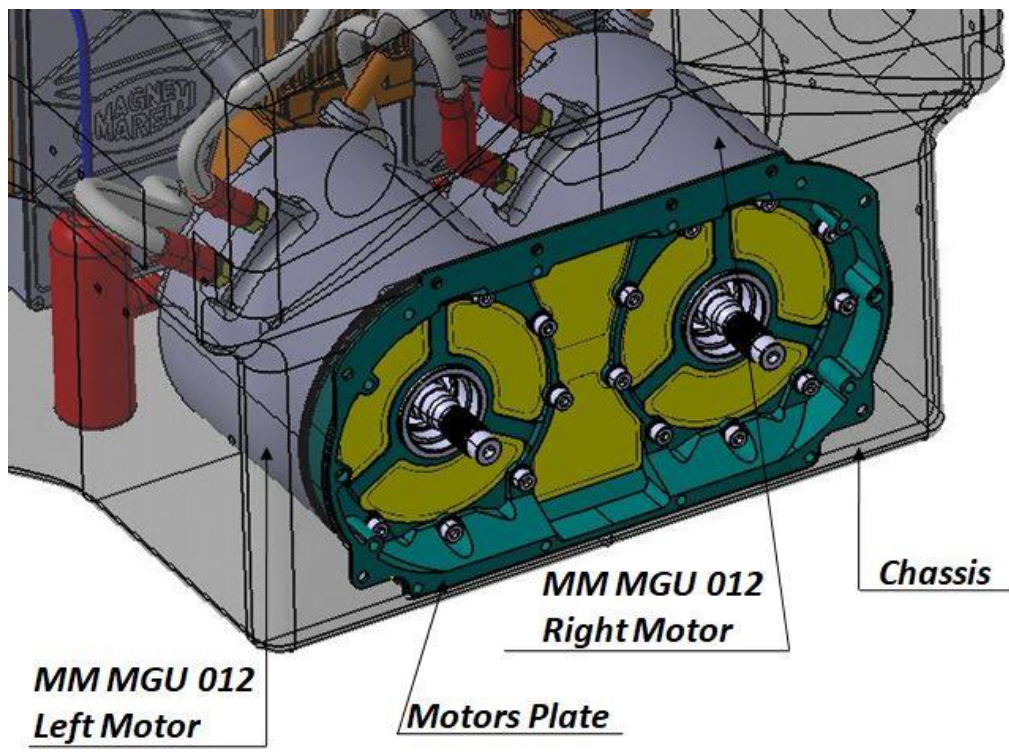


inward. Such issue can be overcome by employ of a compression beam installed coaxial with intermediate shaft.

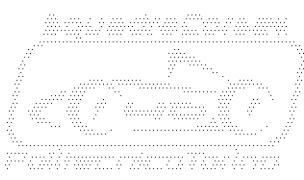
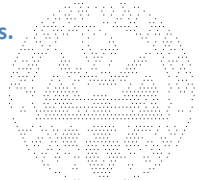
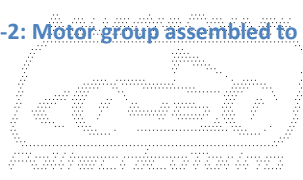
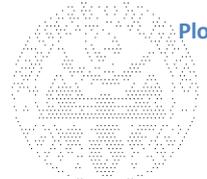
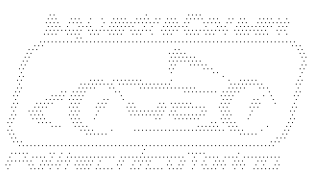


Plot 9.1-1: Back of S.C.R. with assembled motor-transmission group.

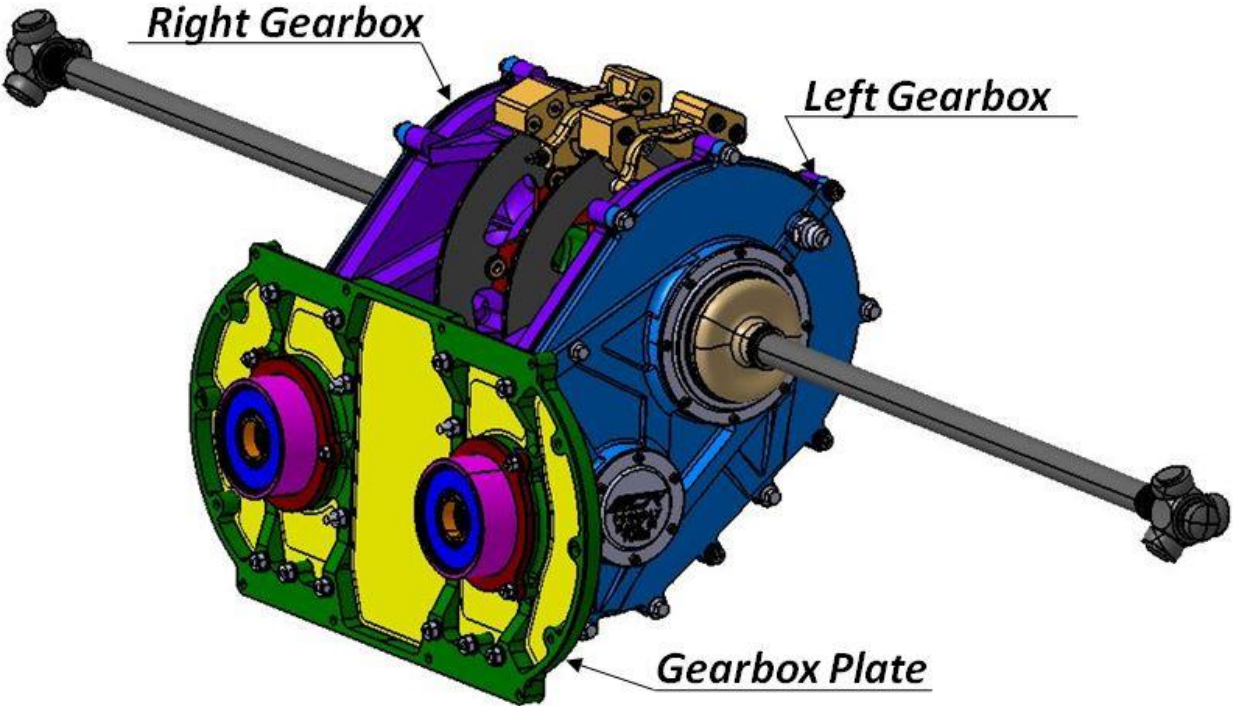
Once general layout of gear-box case is deliberated, It's necessary focus on interface between motors and chassis. Observing Plot 9.1-1, It's necessary to notice that motors are connected to power wirings and cooling system pipes which are often uncomfortable to disconnect. Furthermore, large overall weight of assembled components, make motor-transmission group difficult and dangerous to handle.



Plot 9.1-2: Motor group assembled to chassis.



By virtue of that, It's necessary to study a system which allows to separate motors and transmission in the most comfortable way. Solution of issue is very simple and consists of two large aluminum plates, one is "**motors plate**", displayed by Plot 9.1-2, supports motors and is rigidly fastened to mono-coque by use of screws. Other is "**gear-box plate**" displayed by Plot 9.1-3, It supports two sumps. Both plates are fastened together by use of a dozen of peripheral screws in order to be very quick to remove.



Plot 9.1-3: Assembled transmission group.

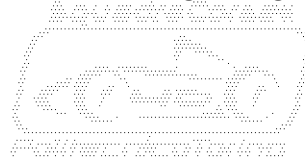
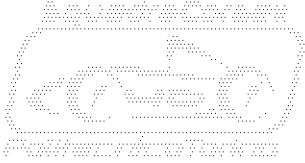
By point of view of **reliability**, probably transmission represents weakest and most complex system of car rear end, such fact is traditional in motorsport. By virtue of that, plate and counter-plate solution hallows to remove quickly transmission from car in case of mechanical breakdown, or in case of ordinary maintenance. In this way, there is no need to disconnect motors with relative pipes and plugs from chassis. Moreover, actual solution is very useful because hallows a quick check on wear of bevel stage pinions and hallows inspection of other gearwheels by passage of shaft 1 housing.

In order to make operations faster, It's necessary to study the way to remove transmission group with mounted half-shafts, as depicted by Plot 9.1-3. Complexity is removal of transmission group with no need of un-sprung masses disassembly, in order to maintain settled parameters of set-up.

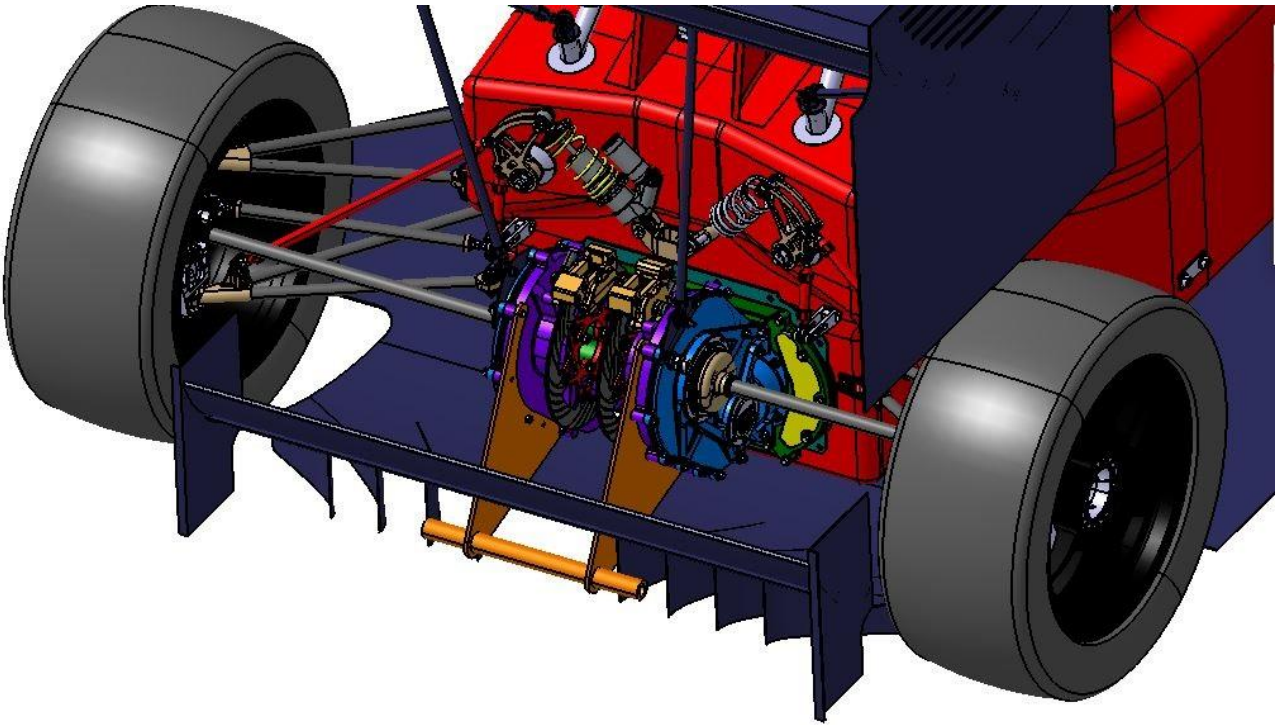
9.2. Interface with motors and chassis.

How It's declared by previous chapter, interface between transmissions and motors with chassis is realized by a smart **plate and counter-plate system**. Aim of actual chapter is provide complete and accurate information about motors plate and gear-box plate. Design philosophy, manufacturing details and calculation methods are going to be described in a satisfying way.

Before starting with calculations, It's necessary pay attention to each load that acts on transmission. By Chapter 7, all loads deriving from gears and rear brakes are known. Anyway, in this particular situation, It's necessary take into account about loads deriving from gear meshing in energy recovery condition.



That's because, in design of a structure like a gear-box case, direction of load has relevance and not highest magnitude only. According to design concept of S.C.R., gear-box case is most backward structure, how displayed by Plot 9.2-1. By virtue of that, It must provide attachment for rear wing mountings and jacking point, which is orange horizontal bar hanging in the back of diffuser in Plot 9.2-1. **Jacking point** is a safety equipment imposed by F.S.A.E. rules, It must be strong enough to lift the back of the car laying rear wheels suspended and far from ground. Such device is employed to remove stationary cars from the track or to stand car during technical scrutineering, as displayed by Picture 1.1-5



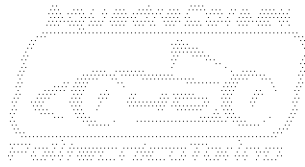
Plot 9.2-1: 3D C.A.D. of rear end of S.C.R. car

As consequence, mentioned attachments transmit non negligible loads to gear-box case structure in addition to loads due to gear meshing and braking. Moreover, observing Plot 9.2-1, It's possible to notice **rear wing attachments** installed on top of transmission group. Such attachments transmit good part of aerodynamic down-force generated by rear wing. As consequence, aerodynamic load generates a tilting momentum which tends to bend structure backward respect to wheel axis. Instead, jacking bar must sustain all weight of the car laying on front wheels only. Differently from aerodynamic load, car weight generates a tilting momentum which tends to bend structure forward respect to wheel axis.

In order to properly summarize loads which is necessary to take into account in design of gear-box case, following list have been reported:

- ***Gear meshing forces in driving condition.***
- ***Gear meshing forces in energy recovery condition.***
- ***Braking force.***
- ***Aerodynamic down-force.***
- ***Weight of jacked car.***

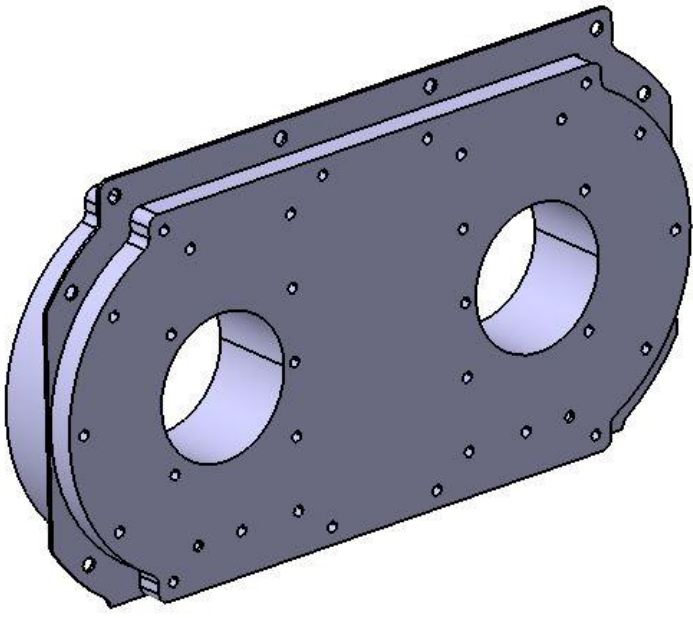
With the aim of simplify actual dissertation, analysis and calculation of unknown loads, like aerodynamic and jacking, is going to be omitted.



Calculus technology employed to design motors plate and gear-box plate, is quite forefront and is known with definition of “**topology optimization**”. Such technology is based on F.E.M. calculus method but procedure of input setting and interpretation of results is quite different.

Conventional F.E.M. analysis is set up modelling with elements technique first raw component which needs to be verified or optimized. Then, material characteristics are set up, finally boundary and loads are applied. Simulation is ready to calculation which provides a map of stresses distribution and displacements. If target of simulation is a simple verification and if displacements and stresses are lower than allowable values, analysis can be considered concluded. If target is a conspicuous weight reduction, designer have to “read” map of stresses, like that shown by Picture 7.6-1, and modify raw component removing low loaded areas or reinforcing high loaded ones. General idea is try to remove all blue, cyan and green portion of component, if design issues and chosen manufacturing process allow it. After this cycle of modification, component needs to be modelled again and submitted to a new F.E.M. simulation, with same materials, same boundaries and same loads. Again designer have to evaluate magnitude of stresses and of displacements in order to verify if component is suitable for safe operation. If verification is right, designer have to read map of stresses again in search of blue, cyan and green portions of component to eliminate. Accuracy of calculus depends by size of elements representing model, anyway large number of small elements may lead to extremely large times of computation. Depending on weight target of component, such process of optimization may endure for several cycles, with an important waste of time and human resources.

Topology optimization is an automated iterative process which reduces significantly number of calculus cycles which designer is obliged to perform in order to obtain a good level of weight optimization. In particular, such method of calculation is wide useful in case of complex geometries of components and complex application of loads. In order to better understand operation and features of calculation technique, an example is going to be fit around real cases treated in S.C.R. project.

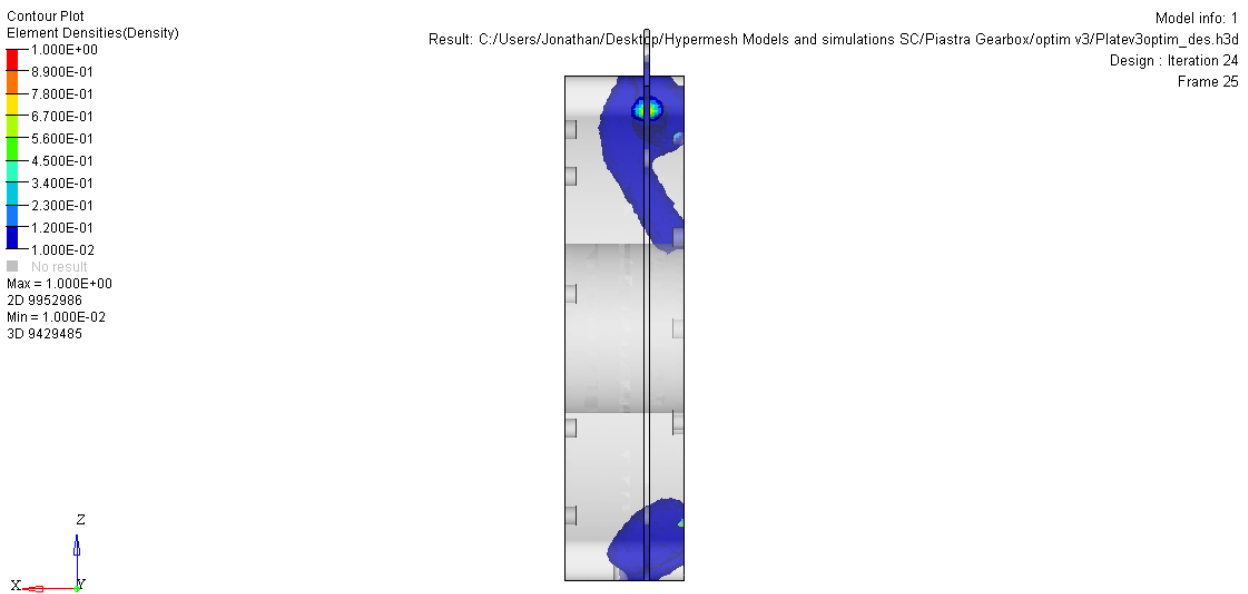


Plot 9.2-2: Raw model of plate counter-plate system.

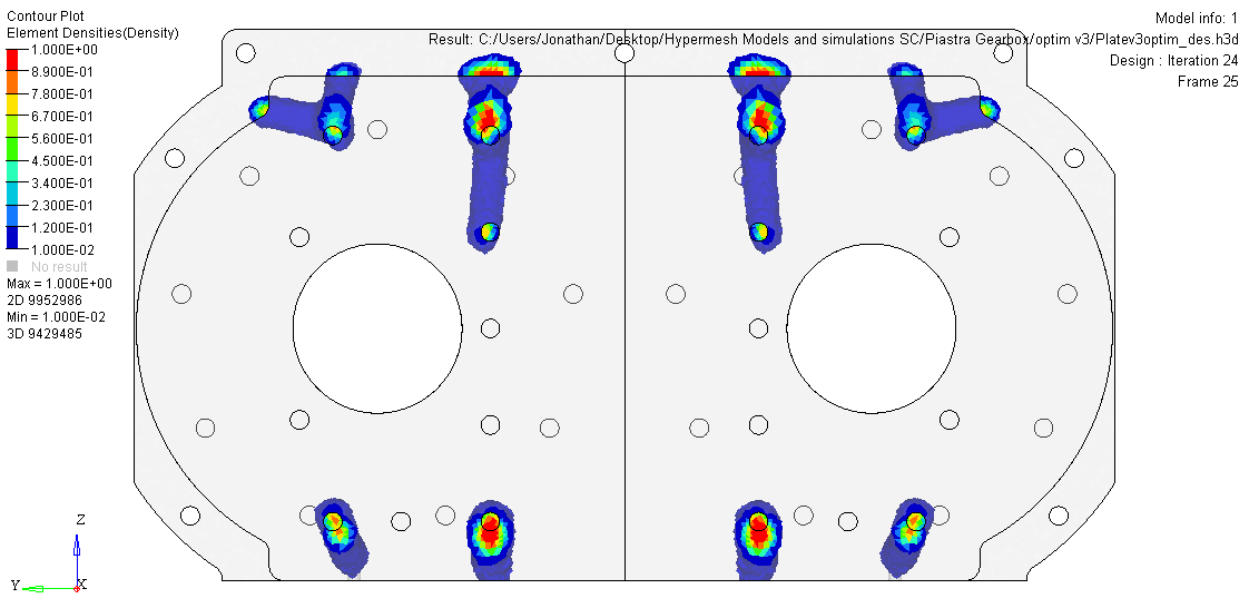
Input set-up starts with design of a **raw component** which can be assimilate to a billet of chosen material. Raw model of component is depicted by Plot 9.2-2 and represents an integral plate which includes motor plate and gear-box plate. It’s necessary notice that raw model is quite massif and surely



much more strong than needed. That's why, to design a raw model, It's necessary to occupy with material all available room, such continue volume represents **"design zone"** of optimization. By analysis of Plot 9.2-2, It's possible to notice that holes for fixing screws are present and passages of input shafts too. Such zones are defined **"non design zones"** and are excluded from process of optimization. During next step, raw model is converted into elements representation, as it's common in conventional F.E.M. analysis. Then bounds and loads are set up. It's necessary clarify that loads are ordered in five different load conditions, one for each item listed previously. Final input is assignment of a **"criteria of stiffness"**. Such criteria establish that a point internal or external to model cannot move more than a certain quantity from its original position. In the actual case, it was established that elements of rear extremity of gear-box case, doesn't move more than $0,1 [mm]$ from their original position. Then simulation is able to run. Software studies design zone, by use of several calculus iterations, in order to establish where material is really needed, by superposition of different load cases. One result of such operation is shown below by Plot 9.2-3, Plot 9.2-4 and Plot 9.2-5.

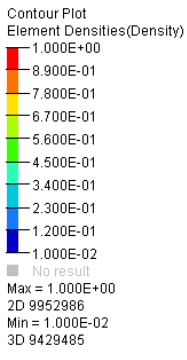


Plot 9.2-3: Topology optimization result, lateral view.

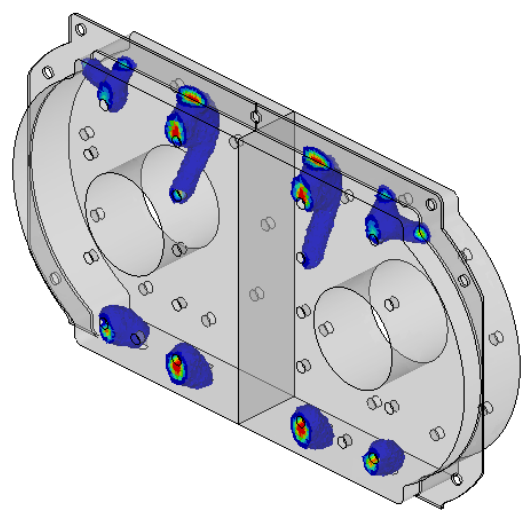


Plot 9.2-4: Topology optimization result, front view.





Result: C:/Users/Jonathan/Desktop/Hypermesh Models and simulations SC/Piastra Gearbox/optim v3/Platav3optim_des.h3d
Design : Iteration 24
Frame 25



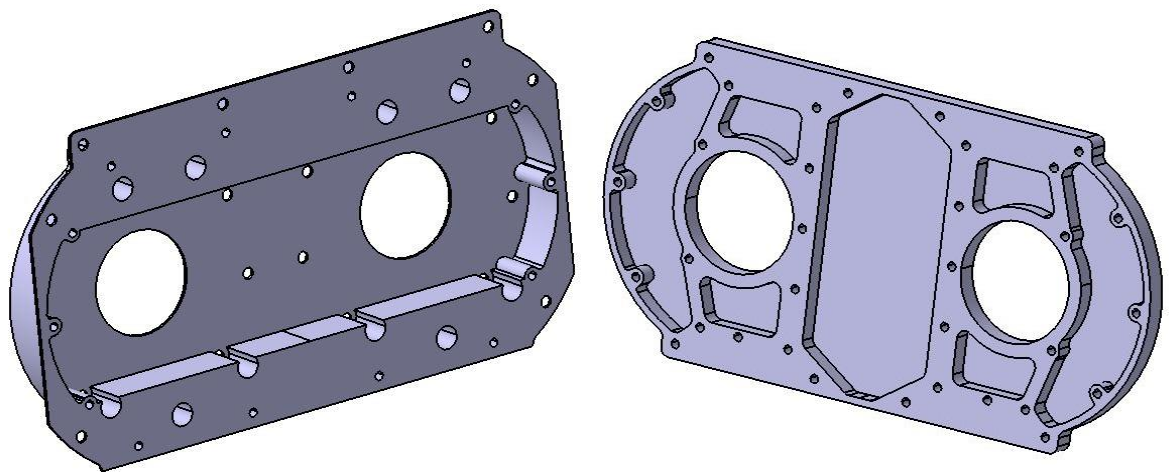
Plot 9.2-5: Topology optimization result, isometric view.

Previous images show raw model in transparency, inside it It's possible to notice some coloured elements featuring a not well defined shape. It's possible to notice that elements are located around position of screws, that is area where loads are applied, that fact give more sense to geometry of coloured elements.

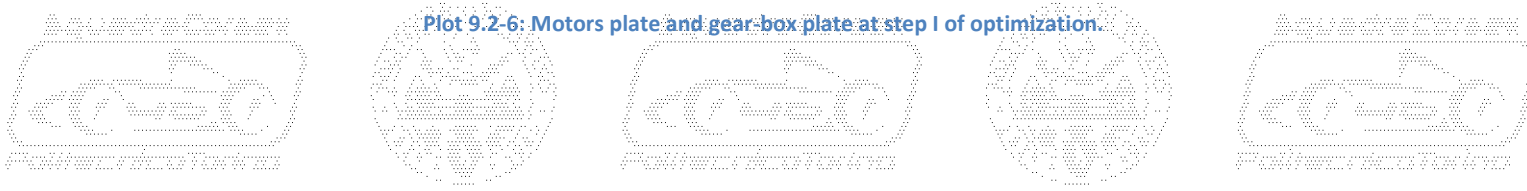
In detail It's possible to notice that colour of elements isn't constant, but it varies as in the case of a stress map. How depicted by diagram positioned on left high corner of Plot 9.2-3, Plot 9.2-4 and Plot 9.2-5, colours represent "**element density**". Such index give an idea of positions where presence material is more important, red means absolutely need of material.

It's possible to notice that not all screw holes are interested by elements, anyway number of screw is kept high in order to prevent any possible lubrication oil leakage.

Anyway It's necessary to notice that content of previous images is quite poor to completely define shape of a mechanical component. Task of previous simulation is to provide a rough idea of unloaded areas, where material is not needed and can be removed.

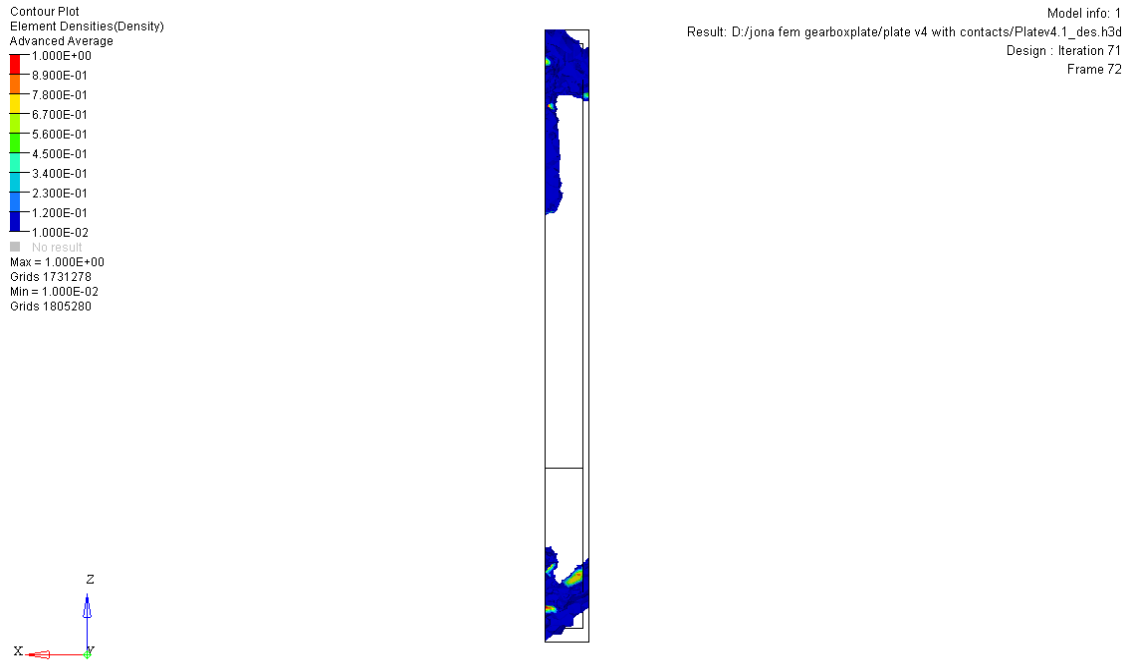


Plot 9.2-6: Motors plate and gear box plate at step I of optimization.

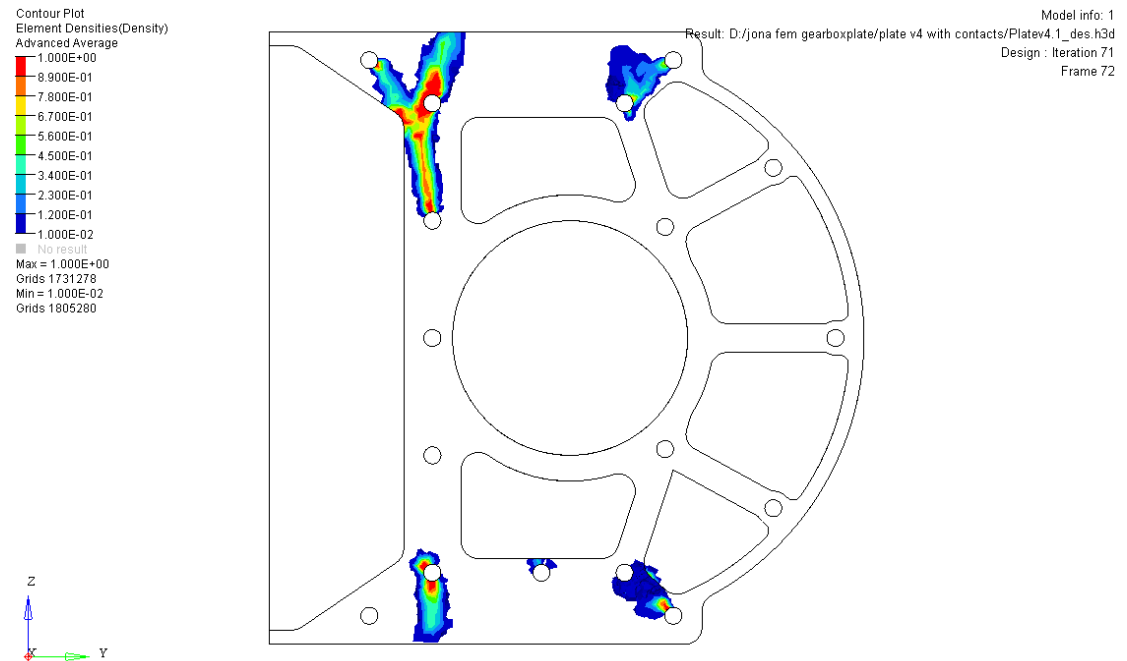


By virtue of that, It's necessary to refine raw model in order to obtain clearer results. First of all, It's necessary to split raw model into motors plate and gear-box plate. Then It's necessary to reduce design zone of both components, in order to bound development of coloured material into certain areas. Result of such process is displayed by Plot 9.2-6 and is defined as **"step I of optimization"**.

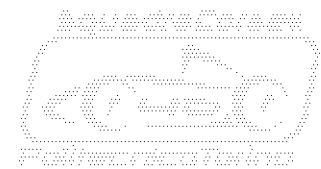
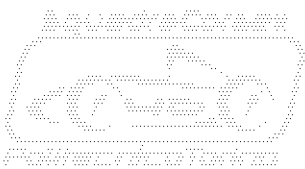
Following, It's possible to notice that simulation have been performed on an half of component only. Such solution hallows to reduce time of calculation without waste precious time to obtain a symmetric result. Simulation is now able to run, and results related to gear-box plate are displayed by following Plot 9.2-7, Plot 9.2-8 and Plot 9.2-9.



Plot 9.2-7: Topology optimization result on step I gear-box plate, lateral view.



Plot 9.2-8: Topology optimization result on step I gear-box plate, front view.

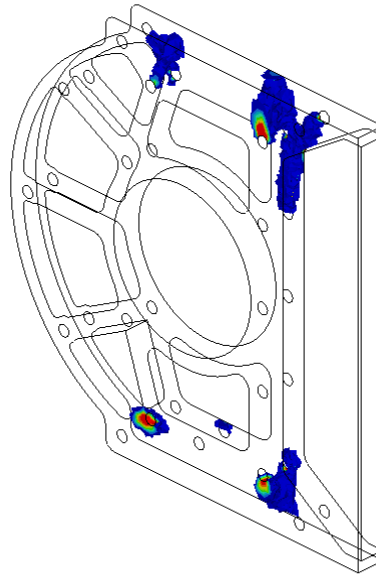
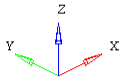


Contour Plot
 Element Densities(Density)
 Advanced Average

1.000E+00
8.900E-01
7.800E-01
6.700E-01
5.600E-01
4.500E-01
3.400E-01
2.300E-01
1.200E-01
1.000E-02
No result

Max = 1.000E+00
 Grids 1731278
 Min = 1.000E-02
 Grids 1805280

Model info: 1
 Result: D:\jona fem gearboxplate/plate v4 with contacts/Platev4.1_des.h3d
 Design : Iteration 71
 Frame 72



Plot 9.2-9: Topology optimization result on step I gear-box plate, isometric view.

By previous images It's useful to notice that geometry of material is more refined, in comparison with results provided by first optimization. Anyway, in order to obtain a well defined component, It's necessary perform some other steps of optimization.

Results of optimization related to motors plate are displayed by following Plot 9.2-10, Plot 9.2-11 and Plot 9.2-12.

Contour Plot
 Element Densities(Density)
 Advanced Average

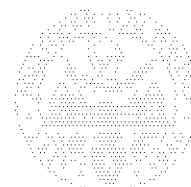
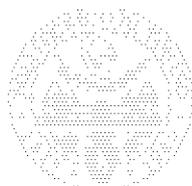
1.000E+00
8.900E-01
7.800E-01
6.700E-01
5.600E-01
4.500E-01
3.400E-01
2.300E-01
1.200E-01
1.000E-02
No result

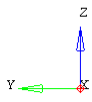
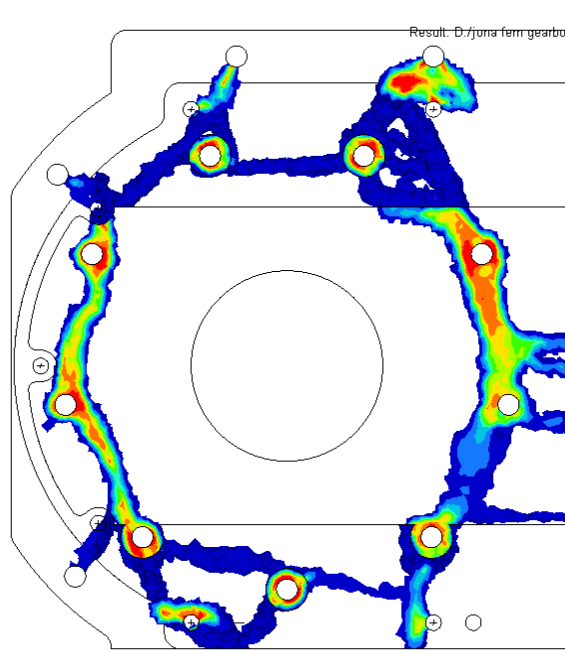
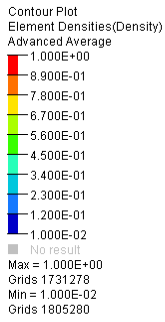
Max = 1.000E+00
 Grids 1731278
 Min = 1.000E-02
 Grids 1805280

Model info: 1
 Result: D:\jona fem gearboxplate/plate v4 with contacts/Platev4.1_des.h3d
 Design : Iteration 71
 Frame 72

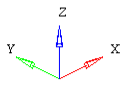
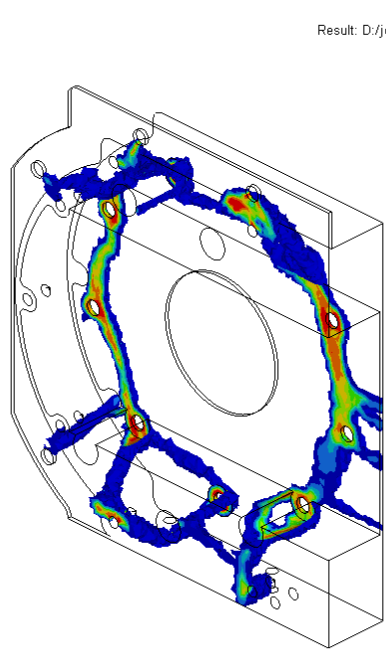
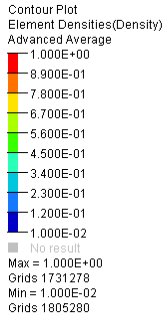


Plot 9.2-10: Topology optimization result on step I motors plate, lateral view.





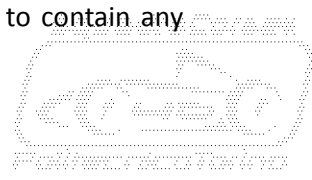
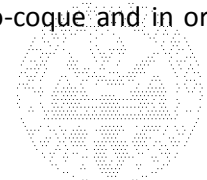
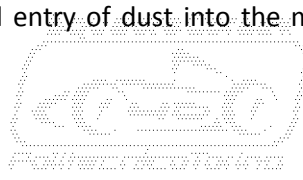
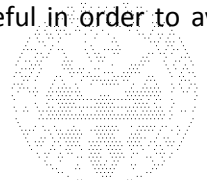
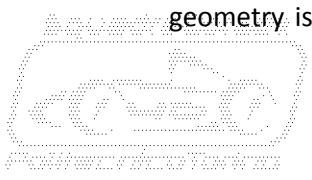
Plot 9.2-11: Topology optimization result on step I motors plate, front view.



Plot 9.2-12: Topology optimization result on step I motors plate, isometric view.

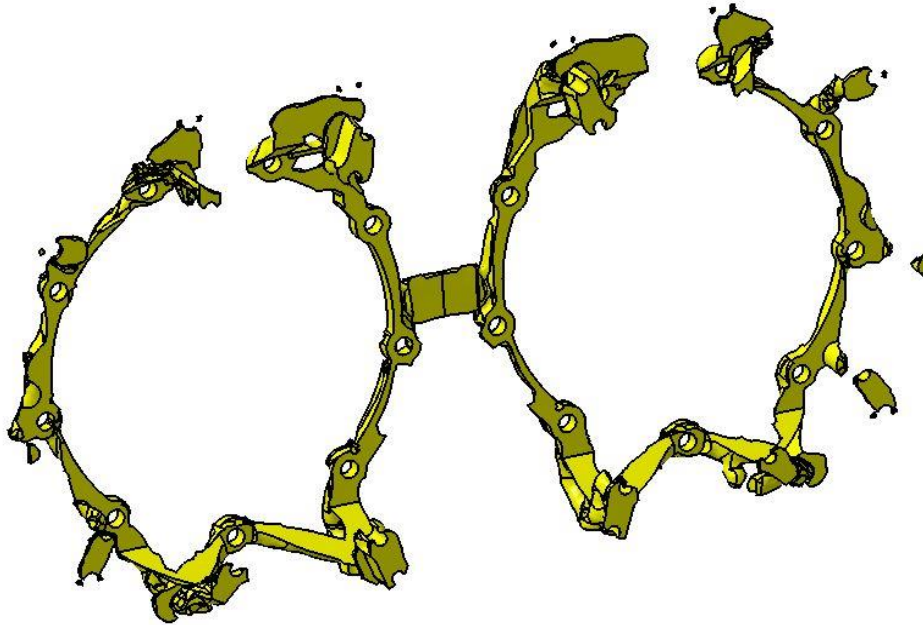
About results related to optimization of step I motors plate, It's necessary to notice that output of calculations is extremely refined. Indeed optimized material clearly joints holes where fixing screws are housed. In this way motors and gear-box plate are rigidly linked to the chassis.

Anyway so complex geometries, like those proposed by optimization process are so difficult an non convenient to be realized by mill machining. Best practice would be a metal 3D print of plates but such technology is so exotic and very expensive. In any case, two plates need to generate a closed box geometry which is the best solution to reach best weight-stiffness trade off. Furthermore, such geometry is useful in order to avoid entry of dust into the mono-coque and in order to contain any

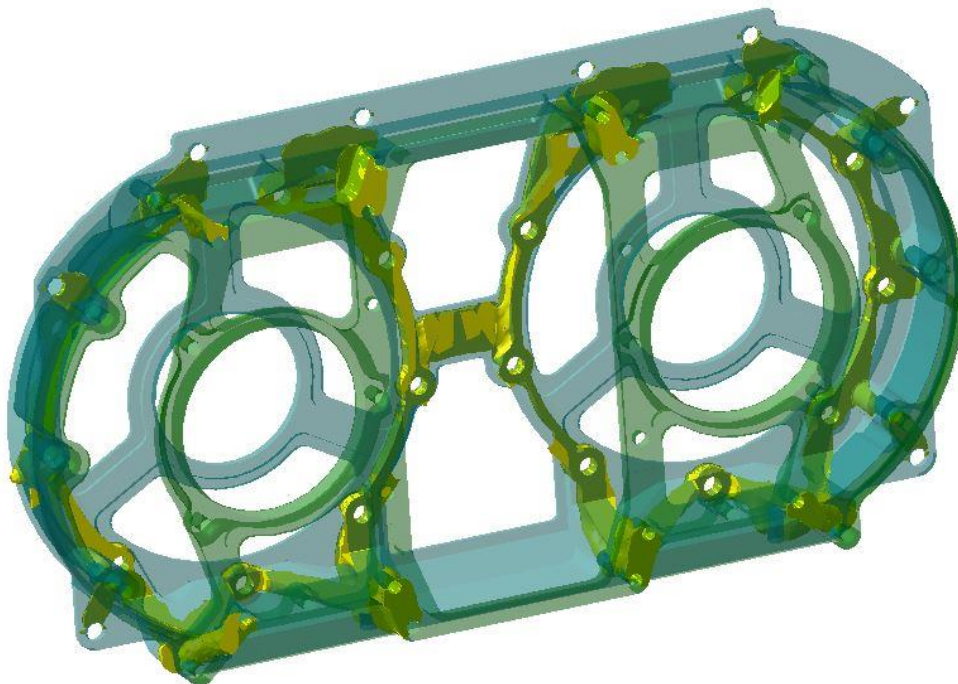


possible oil leakage due to complex geometry of gear-box joints. By virtue of that, a good compromise between optimization results and sealing duties have been found. Both studied components have been designed by a **skeleton aluminium machined plate** where holes are covered by bonded **carbon fibre sheets**.

To improve 3D design capabilities, another important feature of simulation software can be employed, the **export of 3D geometry**. How displayed by Plot 9.2-13, result of simulation can be converted into a 3D file and imported into C.A.D. software. Utility of such feature can be appreciated by Plot 9.2-14, where transparency of components is exploited to simplify the drawing process.

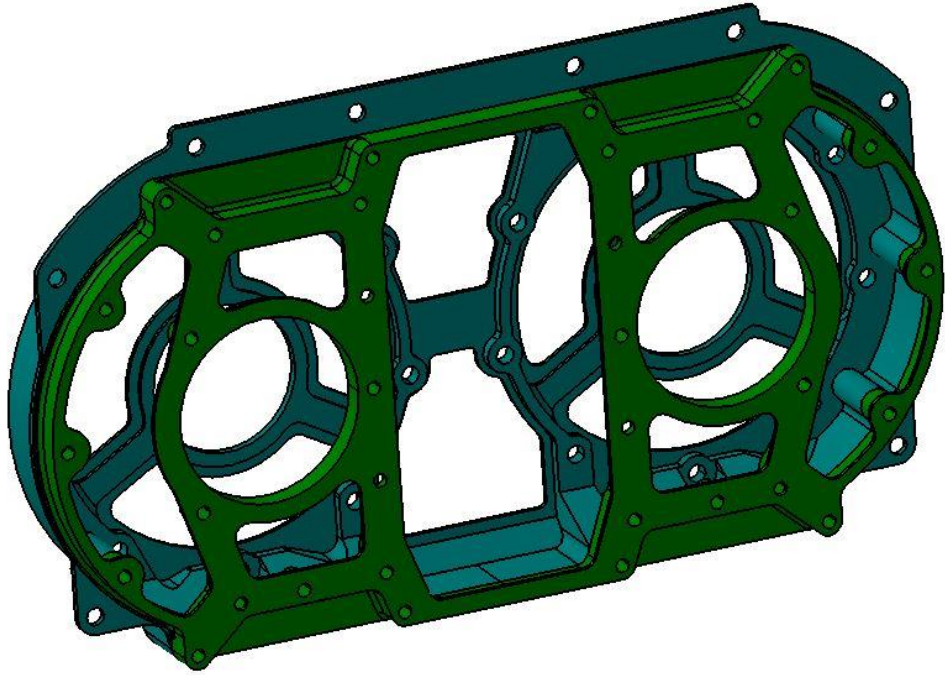


Plot 9.2-13: 3-Dimensional result of topologic optimization simulations.



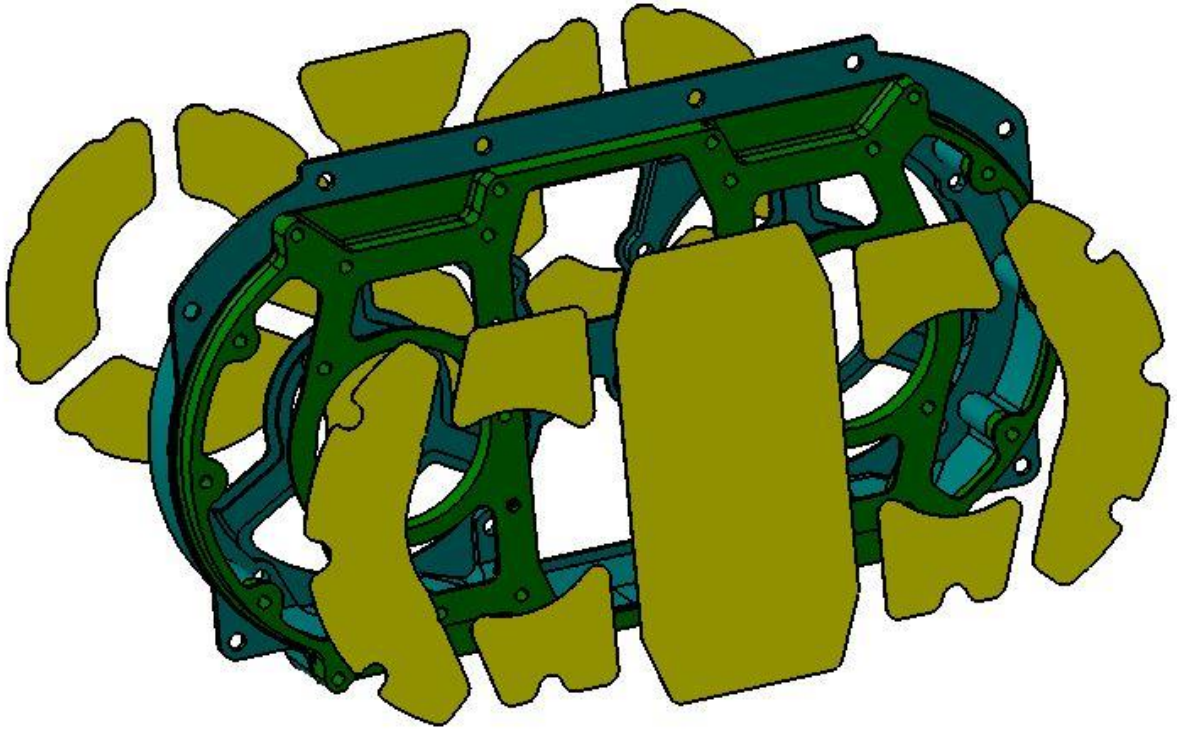
Plot 9.2-14: Comparison of calculation result and results of design process.



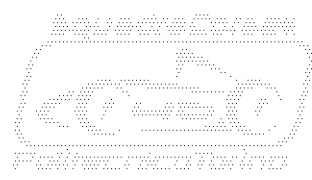
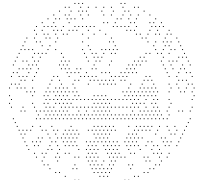
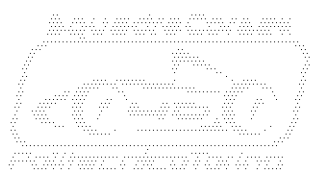
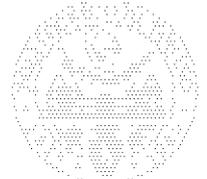
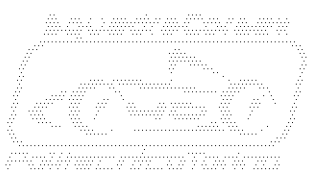


Plot 9.2-15: Motors plate and gear-box plate displayed in final step of optimization.

Final result of optimization iterations on motors plate and gear-box plate is displayed by Plot 9.2-15. How declared in advance, It's possible to appreciate skeleton geometry of components. Thin aluminium ribs connect each other fixing holes ensuring stiffness with an important save in terms of weight.



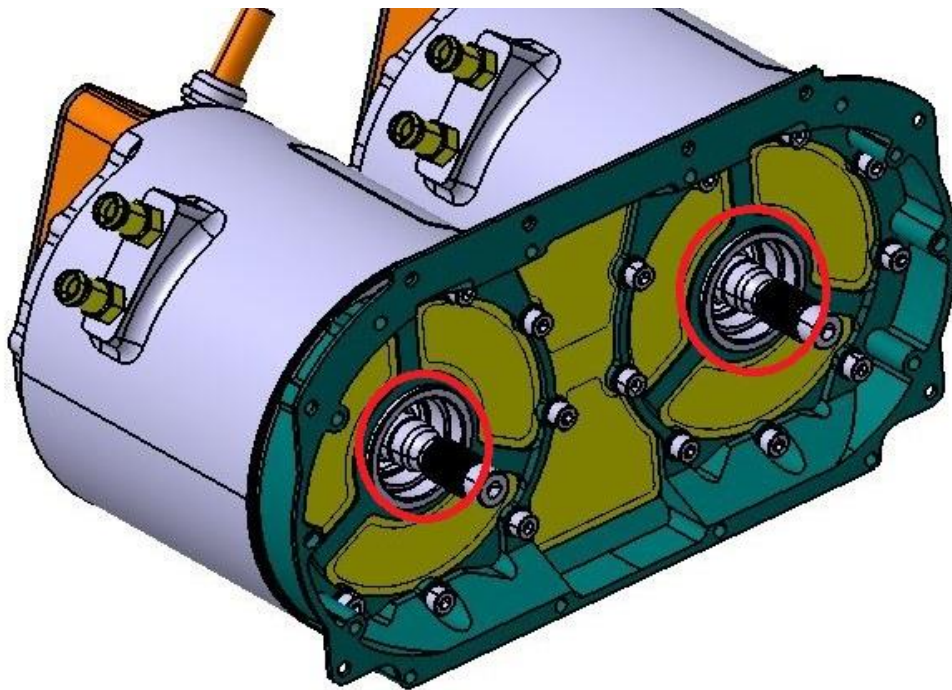
Plot 9.2-16: Carbon fibre panels of motors plate and gear-box plate.



Plot 9.2-16 shows cover panels made by two only layers of carbon fibre. Total weight of panels can be neglected and, by virtue of that, It's possible to write following dissertation about weight.

For what concerns motors plate, weight of step I geometry displayed by Plot 9.2-6 is around $3.300 [g]$. The same motors plate in its last step of optimization weighs around $1.150 [g]$. It's important to remark that optimization process allowed to save 50% of weight in only four cycles of calculation. It's the same for gear-box plate, weight of step I geometry displayed by Plot 9.2-6 is around $1380 [g]$. The same gear-box plate in its last step of optimization weighs around $550 [g]$. It's important to remark that optimization process allowed to save 60% of weight in only four cycles of calculation.

In order to conclude actual chapter, It's useful clarify how the right alignment of each component is obtained. Due to employ of a large number of components, It's not easy ensure alignment between motor and input shaft of transmission, by virtue of that, It's necessary recur to some manufacturing precautions. Starting from linkage between motors and relative plate, It's necessary to notice that 9 simple screws aren't enough to guarantee right position of motors. By virtue of that, a prominent centring diameter is realized on internal cooling jacket, axis of centring diameter coincides with axis of motor shaft.

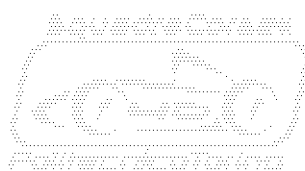
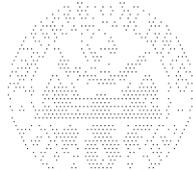


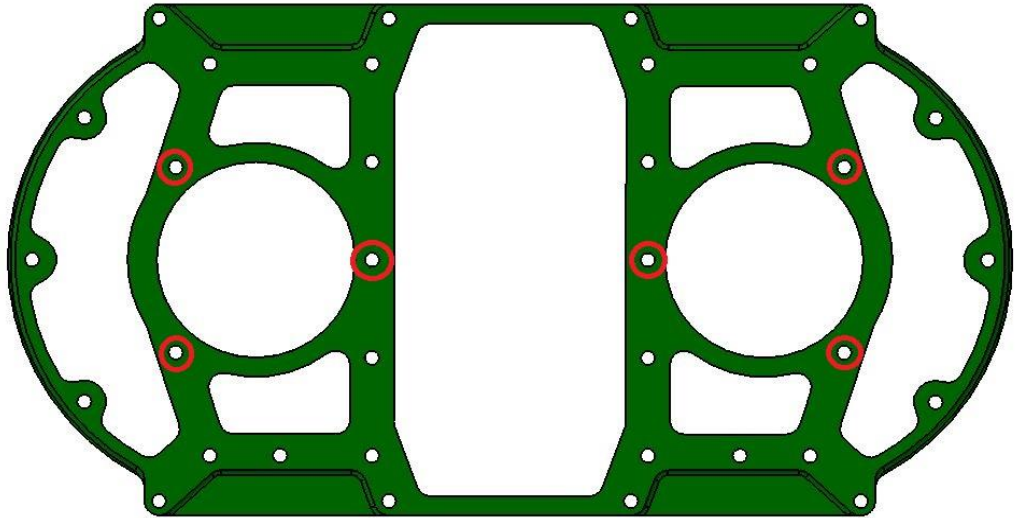
Plot 9.2-17: Centring diameters.

How It's highlighted by Plot 9.2-17, motors plate owns two housing realized by tight tolerance applied on dimension and in position. Here centring diameters of motors are coupled in order to ensure highest level of alignment.

How declared in advance, transmissions are fixed to gear-box plate. By virtue of that, such gear-box exploits three holes machined in H7 tolerance, displayed by Plot 9.2-18. Six I.S.O. 7379 precision rectified screws are inserted in such holes, in order to guarantee perfect alignment between gear-box plate and drive-train components of each sump.

In order to conclude actual dissertation It's necessary clarify how alignment between motors plate and gear-box plate is guaranteed. By Plot 9.2-19 It's possible to notice that two centring bushes are fixed with light interference into holes realized with tight tolerance on gear-box plate. Distance between bush and centring holes of gear-box highlighted on Plot 9.2-18 is ruled by a tight tolerance.

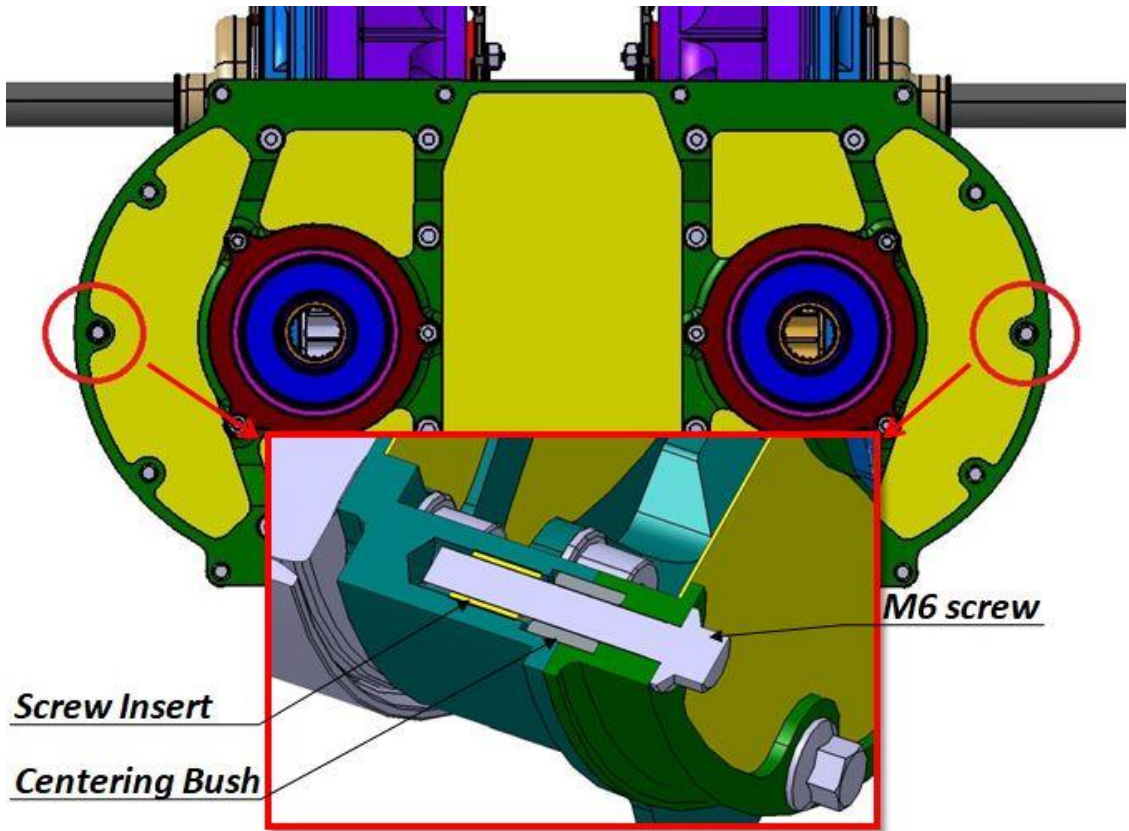




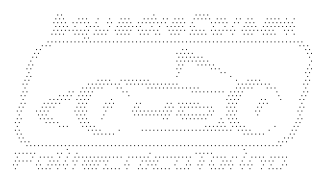
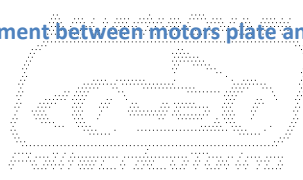
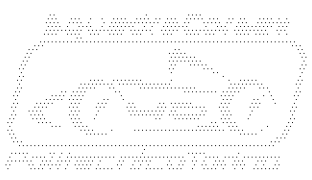
Plot 9.2-18: H7 alignment holes.

During assembly of transmission group to motors group, centring bushes inserts with light backlash into holes properly realized on motors plate. Such holes are accurately machined in order to guarantee a tight tolerance in position with centring diameter of motors. By virtue of that, centring between motor shaft and gear-box input shaft can be considered guarantee.

Before concluding dissertation, by Plot 9.2-19 It's useful notice presence of a screw insert. Due to scarce durability of aluminium female threads, in order to preserve endurance of threaded links between motors plate and gear-box plate, steel screw inserts have been installed on motors plate.

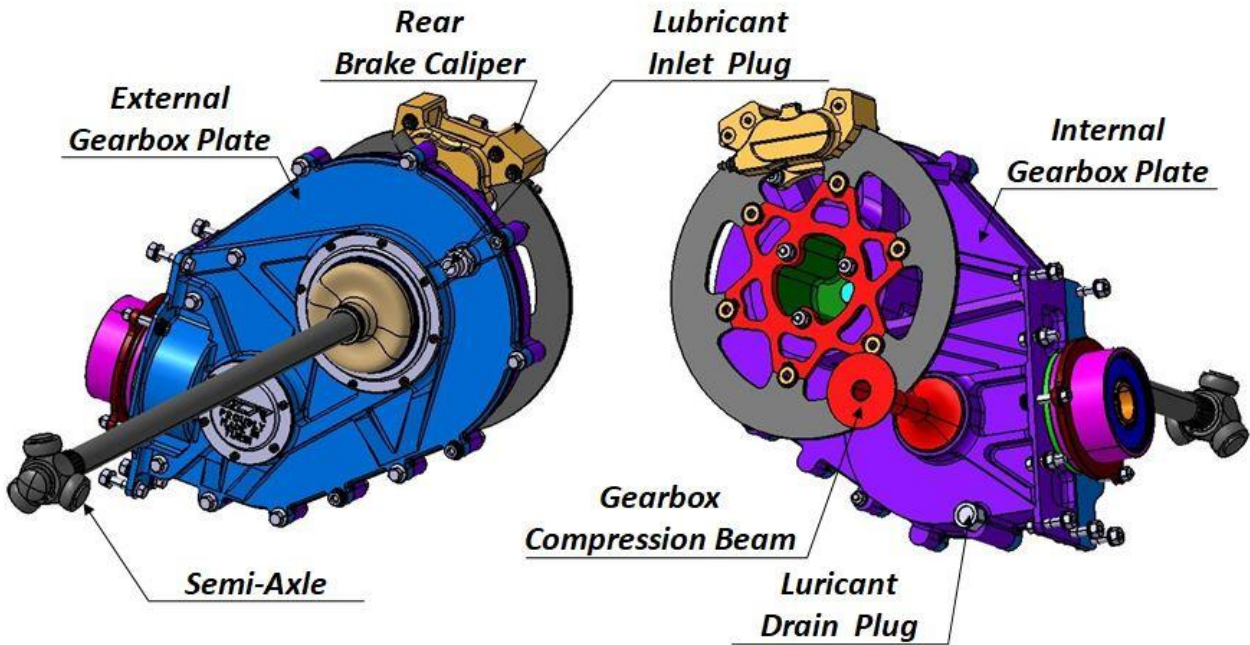


Plot 9.2-19: Alignment between motors plate and gear-box plate.



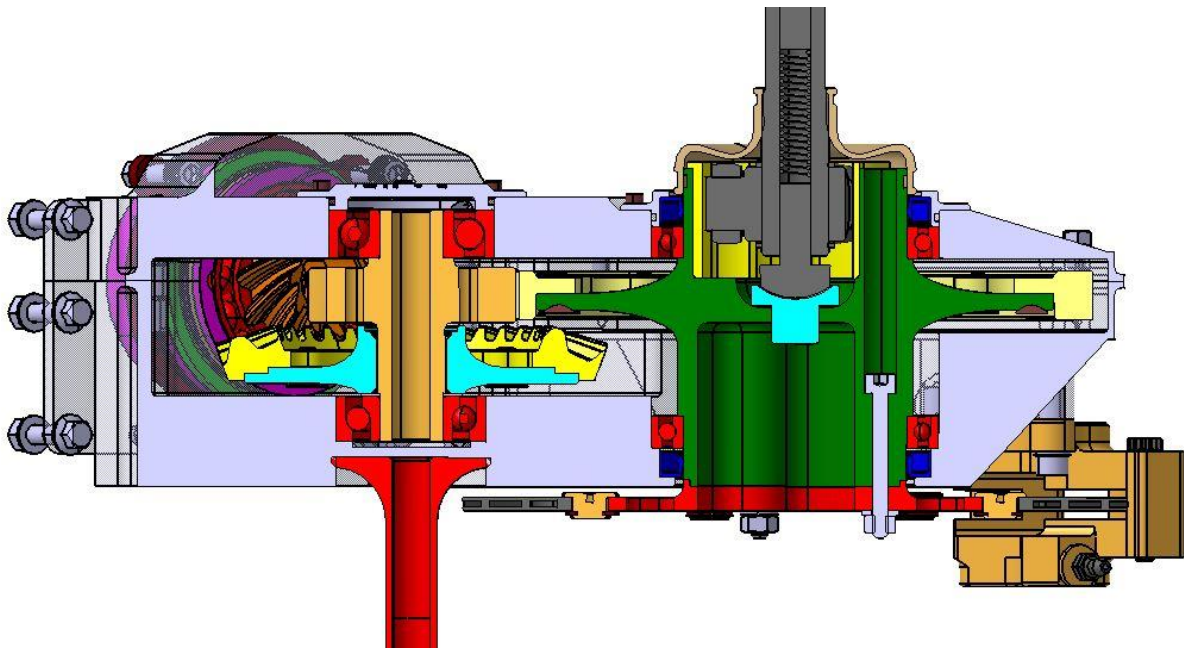
9.3. Interface with bearings and brakes.

Same techniques employed in design of motors plate and gear-box plate can be successfully employed in design of “external gear-box plate” and “internal gear-box plate”. Main components of the study are presented by Plot 9.3-1. It’s necessary notice that “gear-box compression beam”, mentioned by previous Chapter 9.1, have been designed and its effect will be considered in design optimization process of internal and external gear-box plate.

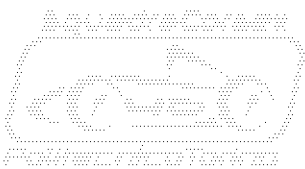


Plot 9.3-1: Details of assembled left gear-box.

With reference to Plot 9-1 It’s necessary start design from “nude shafts” condition in order to obtain raw models of internal and external gear-box plates. Differently from raw model depicted by Plot 9.2-2, presence of shafts, bearings and gaskets imposes an accurate definition of internal non design zones.



Plot 9.3-2: Detail of internal non design zones of left gear-box.

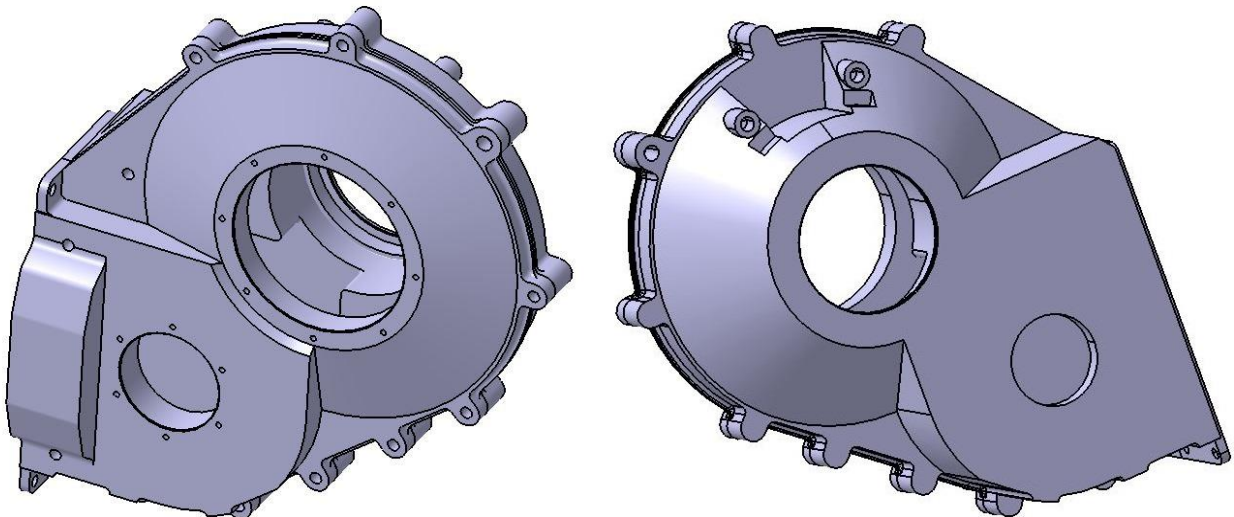


How It's possible to observe by Plot 9.3-2, internal non design zone is intended to guarantee minimum needed room to housed components. By virtue of that, walls of internal and external gear-box plate are 2 [mm] only far from gearwheels. In this way It's possible to obtain an high level of lubrication oil with introduction of a small quantity of it. Such kind of purpose is aided by screw housings set in cantilever position. Actual concept is going to be clarified in next Chapter 9.4. About screw housings, distance have been arbitrarily chosen observing solution adopted by production gear-boxes. In order to reduce risk of oil leakages, distance between screws have been reduced in lower part of the sump.

Once design of internal **non design zone** is defined, It's necessary determine position of junction plan between internal and external gear-box plane. Solution It's quite trivial because plan must coincide with axis of transmission input shaft, in order to simplify manufacturing and assembly of components.

In this case too, external non design zones must take into account about screws, shaft passages and, in addition, about brake calipers and relative fittings.

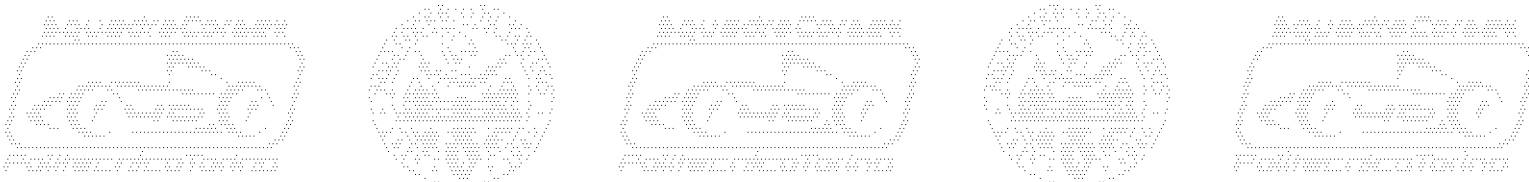
Raw models of internal and external gear-box plate are then defined and displayed by Plot 9.3-3.

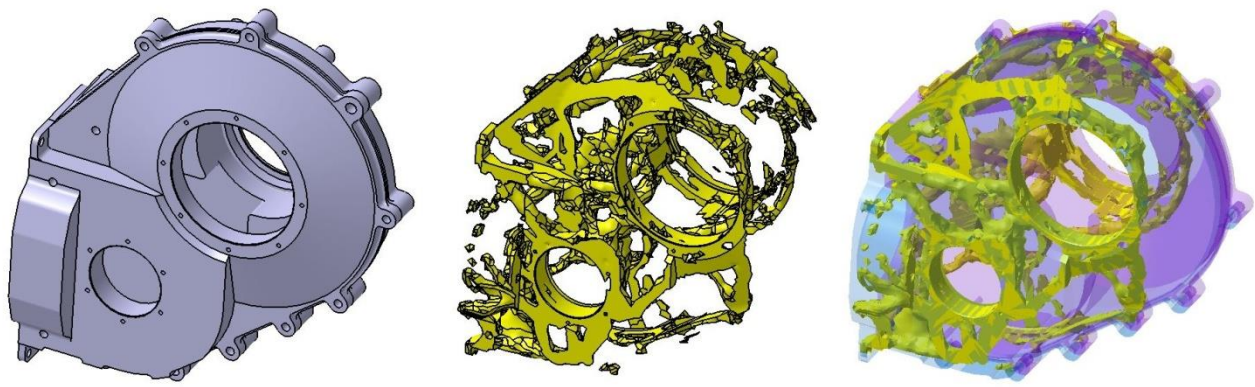


Plot 9.3-3: Raw model of external gear-box plate and internal gear-box plate.

Definition of material, loads and boundaries is completely identical to optimization of motors plate ad of gear-box plate. The only difference stands in the **criteria of stiffness**. While criteria of stiffness mustn't be so tight for previous case, criteria related to actual case must be fixed with great accuracy. Displacements caused by loads mentioned at Chapter 9.2 must not impair proper operation of gear stages and bearings. By virtue of that, elements simulating housing of bearings of shaft 2 and shaft 3 must not move more than 0,010 [mm] from their original position. That ensures the avoidance of dangerous misalignments and guarantees that offset between shaft 2 and shaft 3 axis remains in the prescribed value of tolerance. Such criteria, applied on shaft 2 bearing housings is strict enough to guarantee the proper operation of bevel stage too.

Once stiffness criteria are fixed, optimization process is able to run. Result of calculations is shown by Plot 9.3-4. It's possible to observe that geometry of optimized elements is much more complex respect to previous case displayed by Plot 9.2-13. By virtue of that, 3-Dimensional geometry is sudden exported and imported into C.A.D. software.



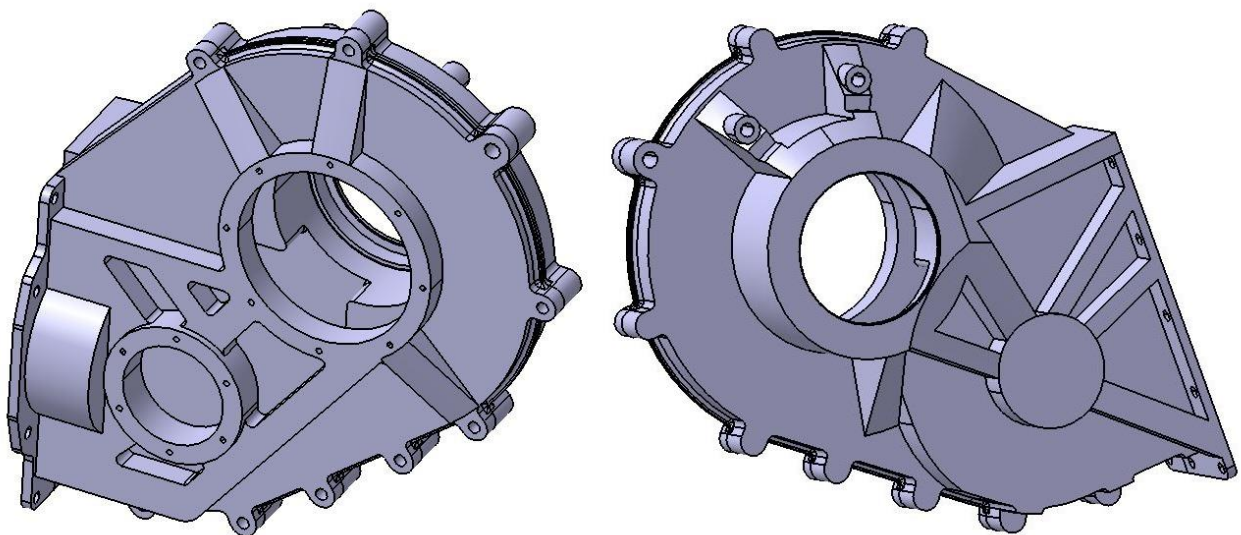


Plot 9.3-4: Optimization on raw model of internal gear-box plate and external gear-box plate.

Optimized geometry displayed by Plot 9.3-4, features a huge concentration of elements into “ribs” which connect bearing housings and fixing screws. Such result makes sense and proves the proper set-up of optimization process.

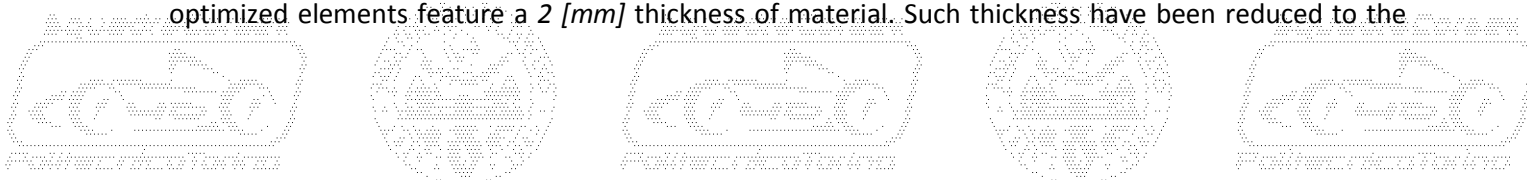
Anyway, obtained geometry concentrates large majority of elements in proximity of external surfaces of design zone. Indeed, It’s possible to notice that expected “tubular” elements, like those shown by Plot 9.2-13, have been replaced by very thin “skin” elements. Such condition contrasts with requirement of minimum internal room displayed by Plot 9.3-2 and with decision of machining ribs and lightening slots from external surface of components.

In any case, information provided by optimized elements displayed by Plot 9.3-4 is enough to modify raw models, in order to crate “**step I of optimization**” of internal gear-box plate and of external gear-box plate. Result is depicted by following Plot 9.3-5.



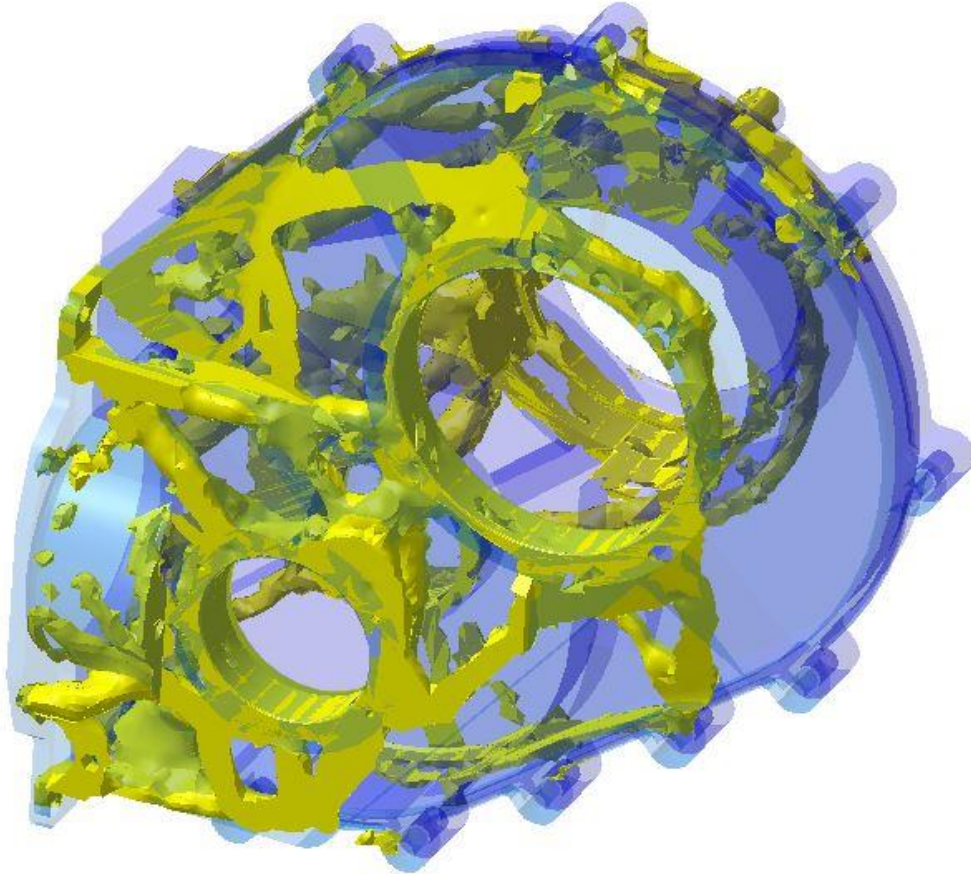
Plot 9.3-5: External gear-box plate and internal gear-box plate at step I of optimization.

Plot 9.3-5 shows two components provided of a geometry which looks easy to manufacture. Smooth external surfaces exploited by raw model of Plot 9.3-3 have been replaced by **reinforcement ribs** and **lightening slots**. In order to ensure containment of lubrication oil, skeleton geometries exploited by components illustrated at Chapter 9.2 aren’t impossible to realize. By virtue of that, zones excluded by optimized elements feature a 2 [mm] thickness of material. Such thickness have been reduced to the



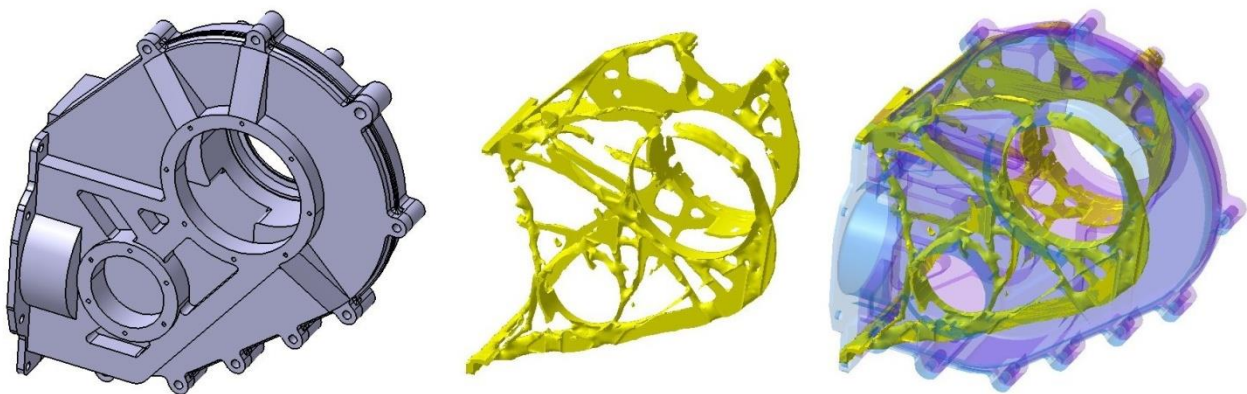
minimum and is large enough to avoid dangerous vibrations on the component during machining process.

By Plot 9.3-6, It's possible to notice that step I optimization geometries are a way to bound design zone into a shape which matches better with exposed design requirements.

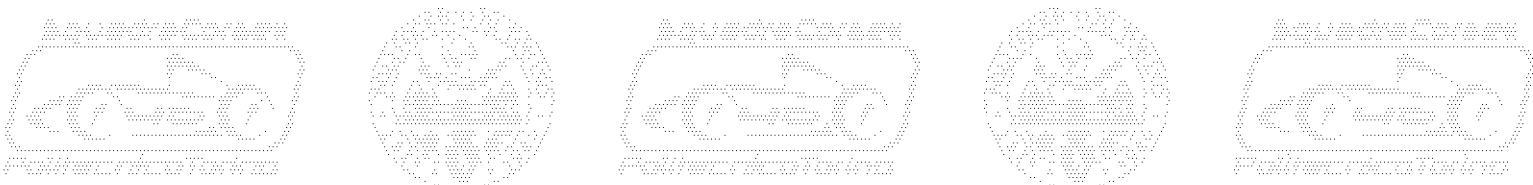


Plot 9.3-6: Superposition between step I optimization geometries and optimized elements.

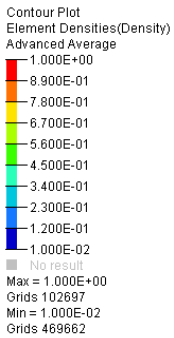
Once geometries obtained from step I if optimization are fully defined, It's possible run one more simulation. Result of calculation process is displayed by Plot 9.3-7, Plot 9.3-8 and Plot 9.3-9.



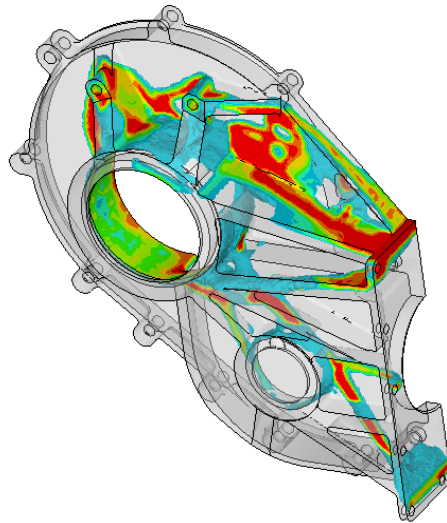
Plot 9.3-7: Results of step II of optimization.



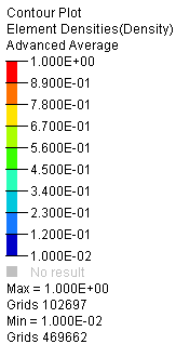
By analysis of Plot 9.3-7 It's possible to notice that elements of optimized geometry are more organized and easier to reproduce during manufacturing process. Large majority of elements is gathered around bearing housings and around brake caliper attachment. Then, It's necessary to notice some "ribs" which connect bearing housings each other and connect the same housings with screw holes which fix components to gear-box plate.



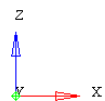
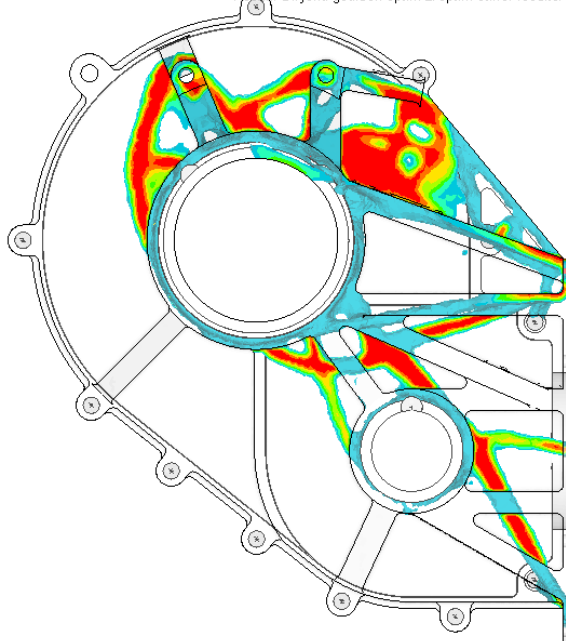
Result: D:/jona gearbox optim 2/optim stiffer results/Gearbox optim 1v2 drawdir 22may v4 optim finer_des.h3d
Model info: 1
Design : Iteration 48
Frame 49



Plot 9.3-8: Element density on gear-box internal plate, isometric view.

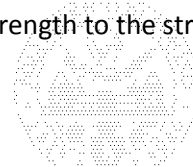
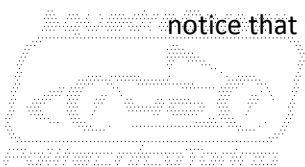


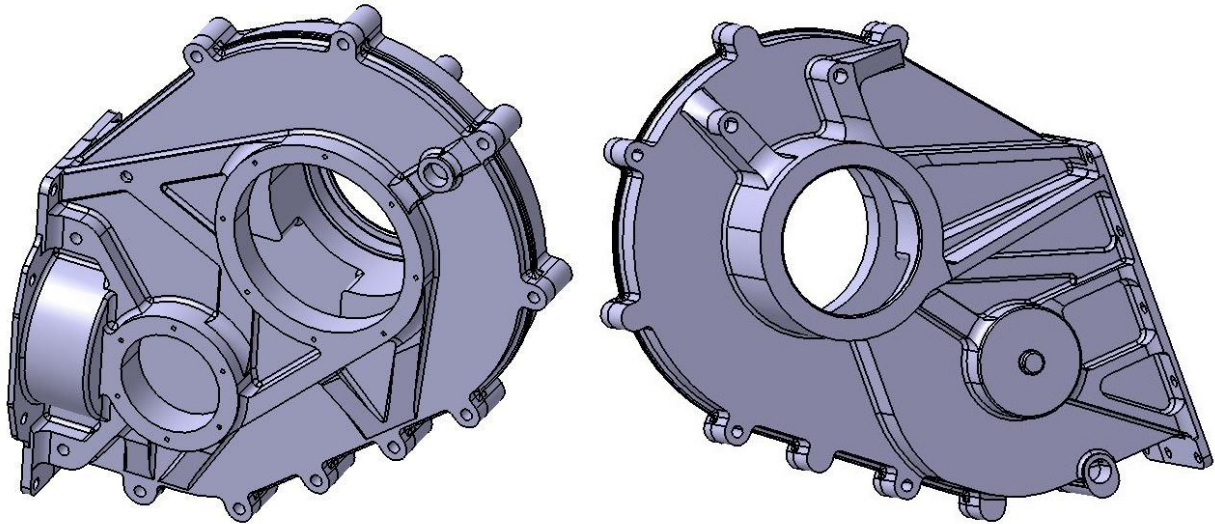
Result: D:/jona gearbox optim 2/optim stiffer results/Gearbox optim 1v2 drawdir 22may v4 optim finer_des.h3d
Model info: 1
Design : Iteration 48
Frame 49



Plot 9.3-9: : Element density on gear-box internal plate, lateral view.

Density of elements is represented by Plot 9.3-8 and Plot 9.3-9. By analysis of these, IT's possible to notice that some portions of 2 [mm] thick walls provide structural strength to the structure.

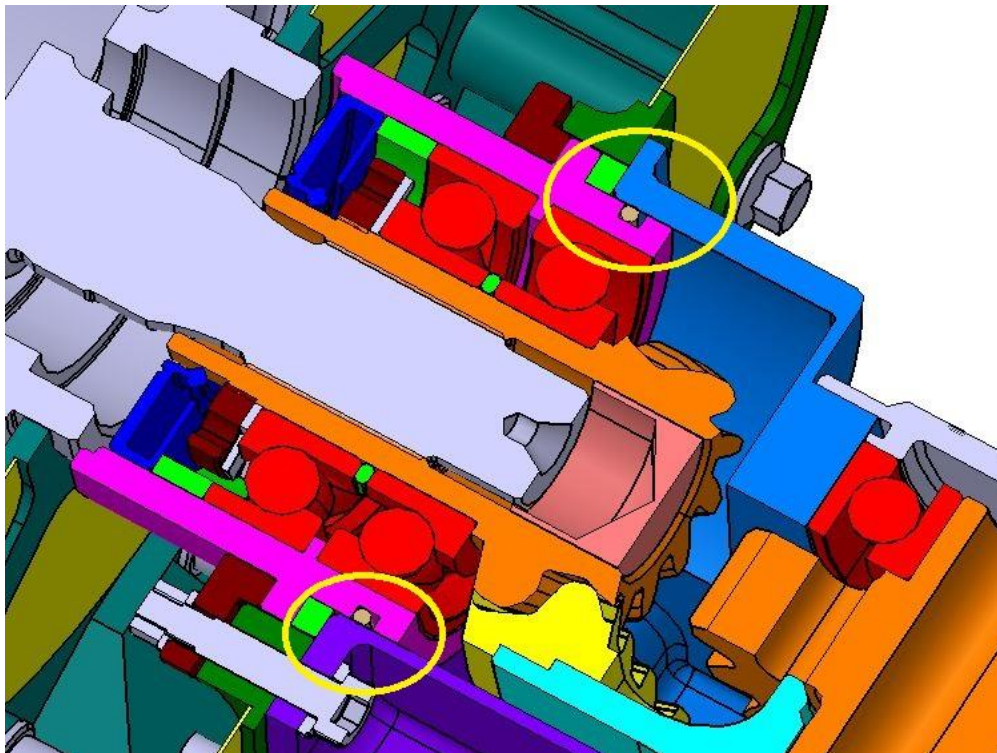




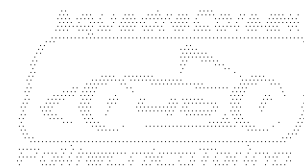
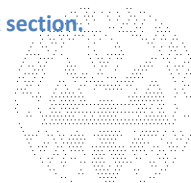
Plot 9.3-10: External gear-box plate and internal gear-box plate at step II of optimization.

Plot 9.3-10 displays components designed around geometry obtained by step II of optimization. By previous plot, it's possible to notice some details like inlet and outlet holes for lubrication oil, reinforced brake caliper attachment and centring diameter for gear-box compression beam. Geometry doesn't look so difficult to manufacture and production can be evaluated after a weight analysis.

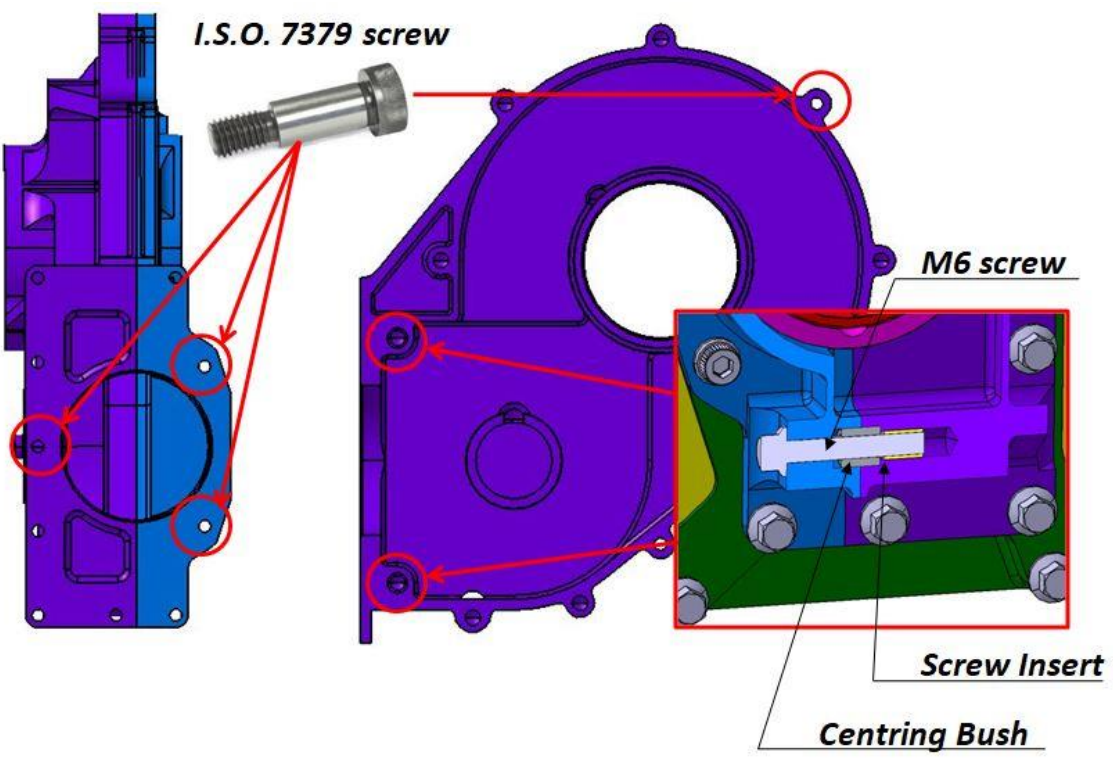
External gear-box plate after modifications suggested by step II optimization, weighs around 730 [g], saving of weight in comparison with step I of optimization is around 25%. Internal gear-box plate weighs around 1080 [g], saving of weight in comparison with step I of optimization is around 40%. By virtue of that, it's possible to state that both components reached a very good target of weight optimization and can be produced on the base of configuration displayed by Plot 9.3-10.



Plot 9.3-11: Alignment of shaft 1 on right gear-box section.



How It was done in previous Chapter 9.2, It's necessary to clarify how alignment of components is guaranteed. By observation of Plot 9.3-11, It's possible to notice that radial position of shaft 1 is guaranteed between a fine coupling between three different components: shaft 1 housing, internal gear-box plate and external gear-box plate. Use of coupling based on centring diameters make necessary that internal gear-box plate and external gear-box plate was machined together in order to realize slot for shaft 1 housing. In this case too, tolerances are fixed in the order of micron.

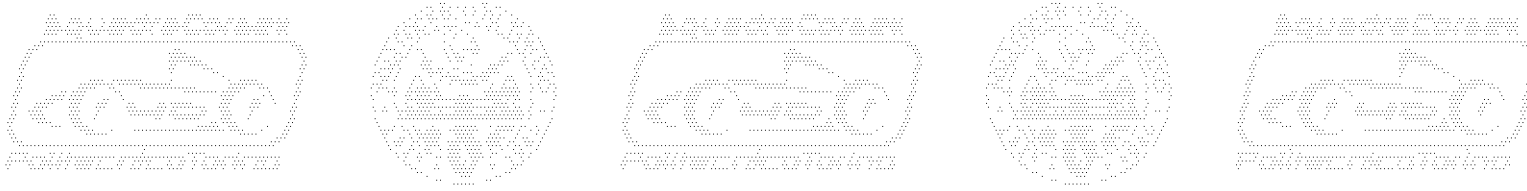


Plot 9.3-12: Solutions to overcome bearings alignment issue.

How It was revealed in advance, each transmission is fixed to gear-box plate by use of three I.S.O. 7379 screws housed in the precision holes displayed by left image of Plot 9.3-12. Corresponding holes are realized on gear-box plate too, how it was declared in advance.

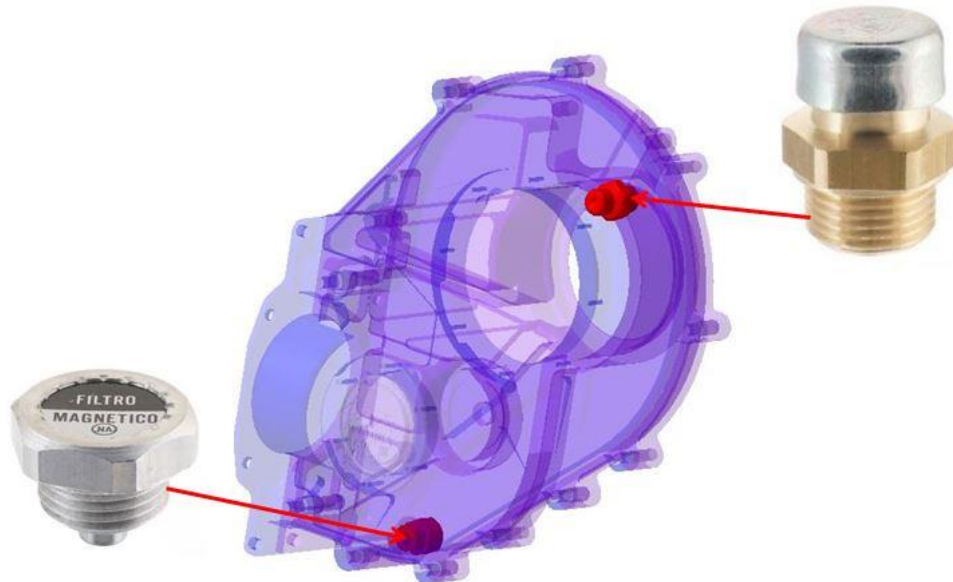
Dissertation treated by Chapter 9.1 declares that one of main issues relate to chosen design concept is alignment of shafts. Indeed bearings of the same shafts are housed on two different components. If these components aren't accurate enough, alignment of shaft 2 and shaft 3 is not guaranteed, impairing proper operation of bearings and shafts. By virtue of that, two centring bushes have been placed in the link between internal and external gear-box plate. In order to ensure right position of each bearing, there is a strict tolerance on distance between centring bush and bearing housing. In order to improve precision of manufacturing, a fourth I.S.O. 7379 screw have been placed on top screw housing, how It was shown by Plot 9.3-12.

Like in previous cases, It's necessary to overcome issues about endurance of female threads. By virtue of that, threaded steel inserts have been installed on internal gear-box plates.



9.4. Oil containment and lubrication.

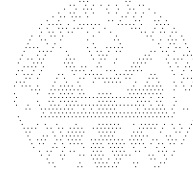
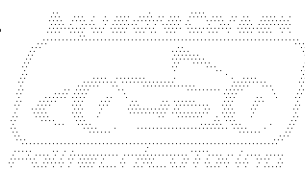
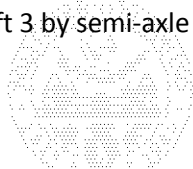
General information about lubrication method and chosen kind of lubrication oil have been widely displayed at Chapter 6.5. Purpose of actual chapter is describe how choices revealed in advance at Chapter 6.5 have been implemented during detailed design of gear-box components.

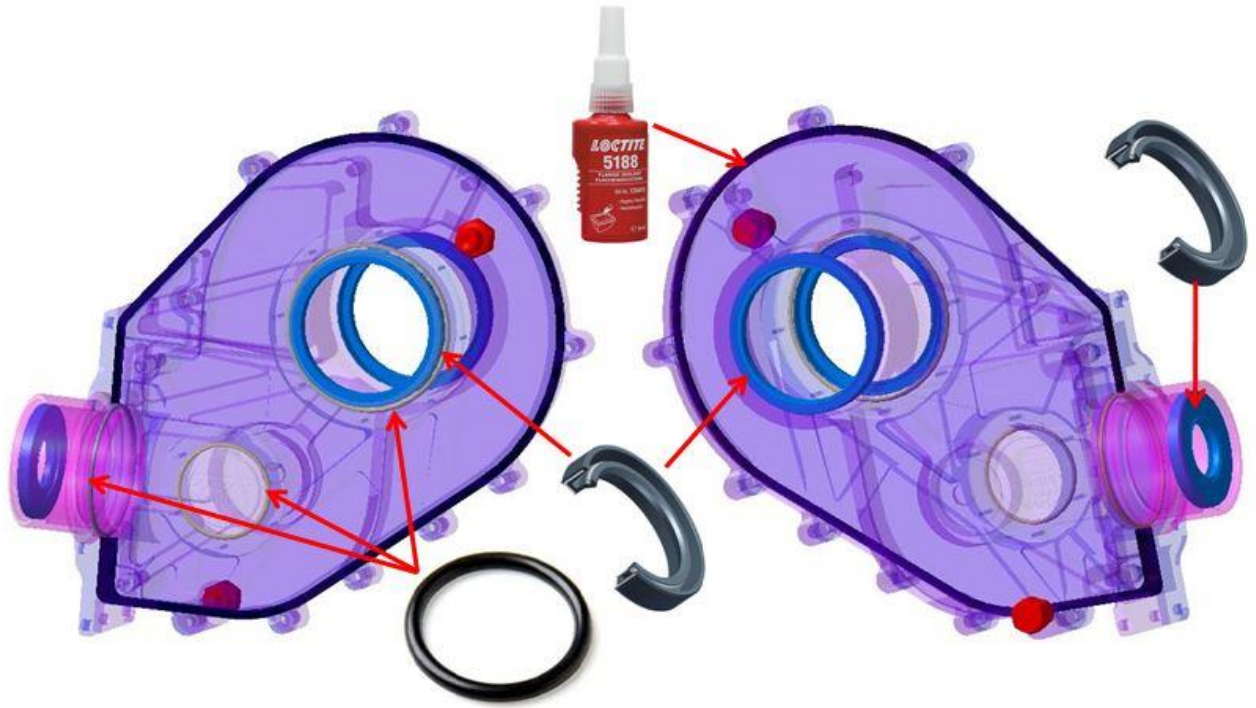


Plot 9.4-1: Lubrication oil plugs, drain and vent.

By analysis of Plot 9.4-1, It's possible to observe position of inlet and outlet lubrication oil plugs. Obviously, outlet oil plug must be housed in the lowest point of the sump. By virtue of that, a slot have been created on internal gear-box plate, just in the back of gearwheel 2. How it was declared in advance at Chapter 6.5.1, S.C.R. transmission is not provided of a forced lubrication system. That means absence of a conventional cylindrical paper filter, where lubricant is obliged to pass through. Despite absence of a obliged filter, a simple but less effective alternative solution can be adopted, the **magnetic plug**. Such plug attracts metal debris produced by gear meshing. Other particular that need s to be observed on Plot 9.4-1 is inlet oil plug. This item too exploits a two-fold effect because It operates as **vent valve**. Heat generated by operation of gearwheels causes expansion of air trapped into the upper part of the sump, causing slight increase of internal pressure. Such pressure is particularly dangerous for gaskets and seals, by virtue of that, a valve which maintains pressure to atmosphere level is needed. Obviously inlet, or vent plug, needs to be located in highest possible position, in order to rest far from oil bath. Proper position have been found on external gear-box plate, in correspondence with a reinforcement rib, how It's possible to notice by Plot 9.3-10.

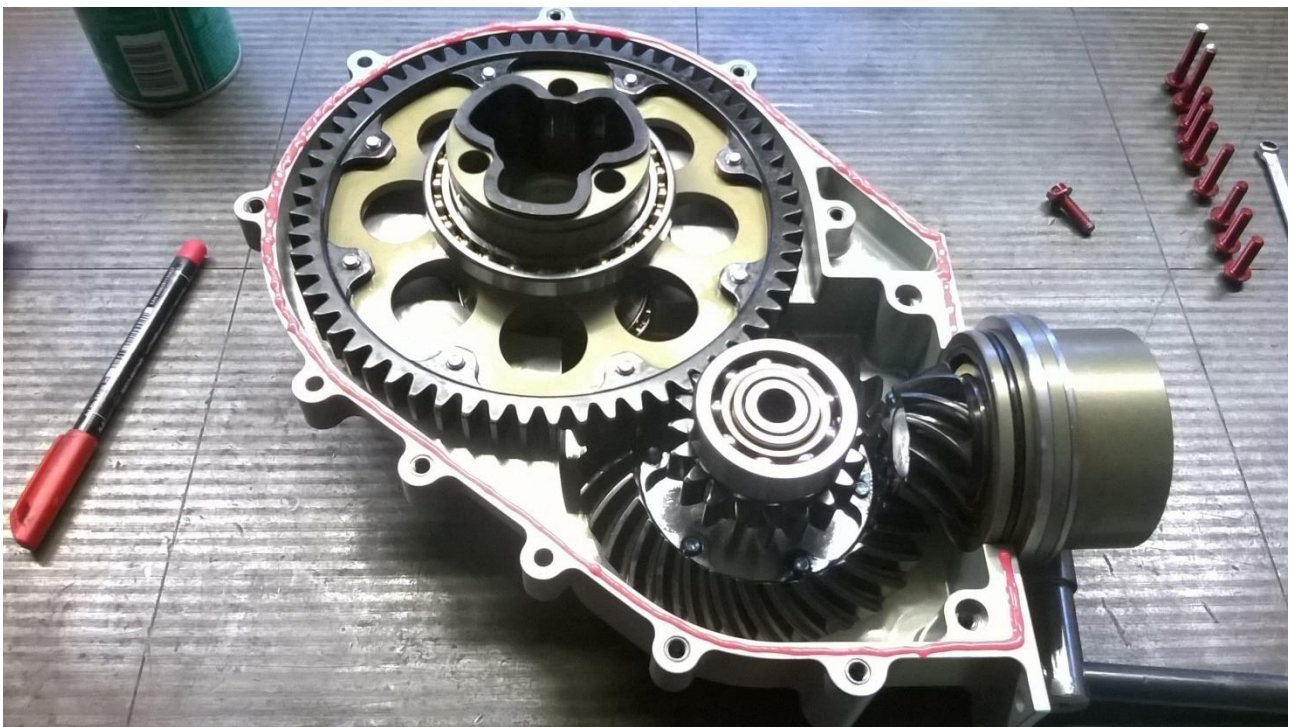
Next step of dissertation is description of system of **gaskets**, **rotary seals** and **o-rings** designed to contain lubrication oil into the sump, avoiding risk of leakages. By analysis of Plot 9.4-2, It's possible to observe that three rotary seals have been installed. Rotary seals are a particular type of dynamic gasket employed to prevent oil leakages between shaft and housing. Installation is typically operated by interference into housing. First rotary seal can be observed in detail on Plot 7.4-3, purpose of such seal is containment of lubricant between shaft 1 and its own housing. Second rotary seal have been installed on internal gear-box plate, in order to contain oil on shaft 3 by brake side. Third rotary seal have been installed into shaft 3 preload cap, how It's displayed by Plot 7.6-2, in order to prevent oil leakages on shaft 3 by semi-axle side.



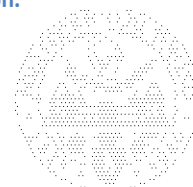
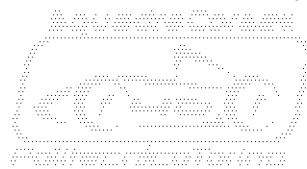
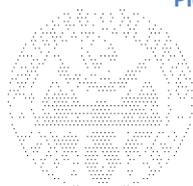
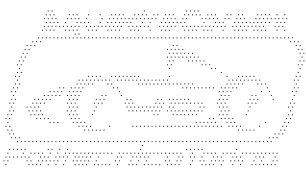


Plot 9.4-2: Gasket, O-Rings and Seals.

Continuing observation of Plot 9.4-2, It's possible to notice installation of three O-rings. O-rings are gaskets used to prevent oil passage between two static components. They are employed particularly to seal sumps or covers. First O-ring operates between three components: shaft 1 housing, internal gear-box plate and external gear-box plate. It can be observed on right side of Picture 9.4-1 and its purpose is prevent oil leakage from shaft housing 1 side.

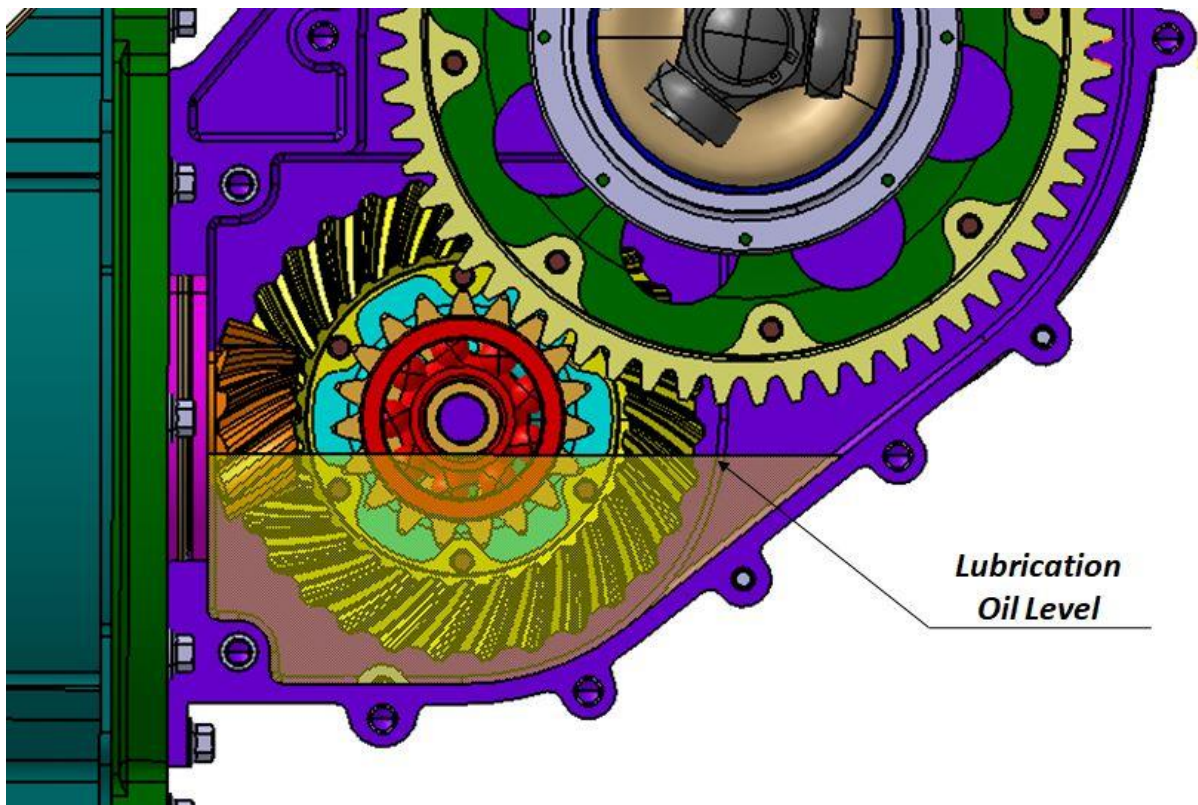


Picture 9.4-1: Loctite 5188 sealant deposition.



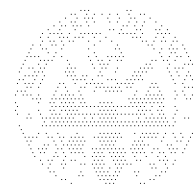
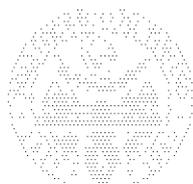
Finally, It's necessary to observe that oil containment system is completed by use of Loctite 5188 liquid gasket. Internal and external gear-box plate are provided by a peripheral flanged surface which features a thickness of 5 [mm]. Such flange represents interface between two plates, by virtue of that, It needs to be provided of gasket. Geometry of flange can be suitable for installation of a paper gasket, anyway non negligible thickness of paper sheet may impair work of internal components like gearwheels and bearings. On the other side, geometry is too complex to house an O-ring cord on the perimeter.

Most suitable solution is employ of liquid gasket which is applied on the flange at the moment of assembly. Such gasket features a negligible thickness and provides a sort of bonding effect between two parts at which is applied.



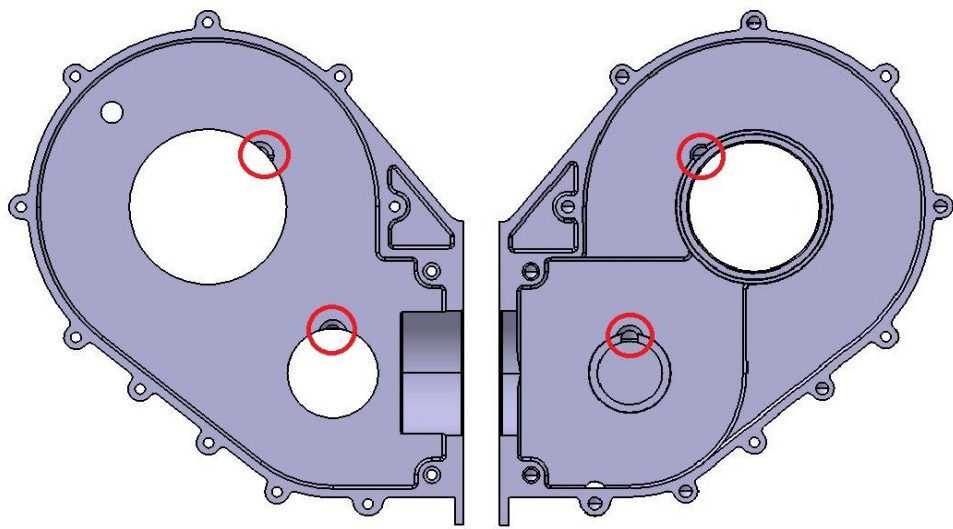
Plot 9.4-3: Level of lubrication oil in stationary conditions.

Next dissertation is about design choices regarding lubrication. How It was declared in advance at Chapter 6.5.1, lubrication of S.C.R. gear-box is realized by **oil splash in wet sump**. Efficacy of such solution depends largely by quantity of oil contained and, as consequence, depends by level of oil into the sump. Volume of chosen quantity of lubrication oil is about 400 [cc] per sump. How It's possible to observe on Plot 9.4-3, chosen quantity of lubrication oil ensures that, contact zone between gearwheel 1 and gearwheel 2 is very close to oil level, in static conditions. In this way, movement of oil in case of acceleration and braking events, wouldn't be able of compromise the proper lubrication. Indeed, viscosity is higher enough to keep oil adherent to gearwheel 2 and be dragged into teeth contact zone. That fact surely stands for contact area between gearwheel 3 and gearwheel 4 too, even if It's quite higher respect to contact zone of first stage. Therefore, chosen quantity of lubricant ensures that lower extremity of bearings installed on shaft 1 and shaft 2 lays into the wet zone during static conditions.



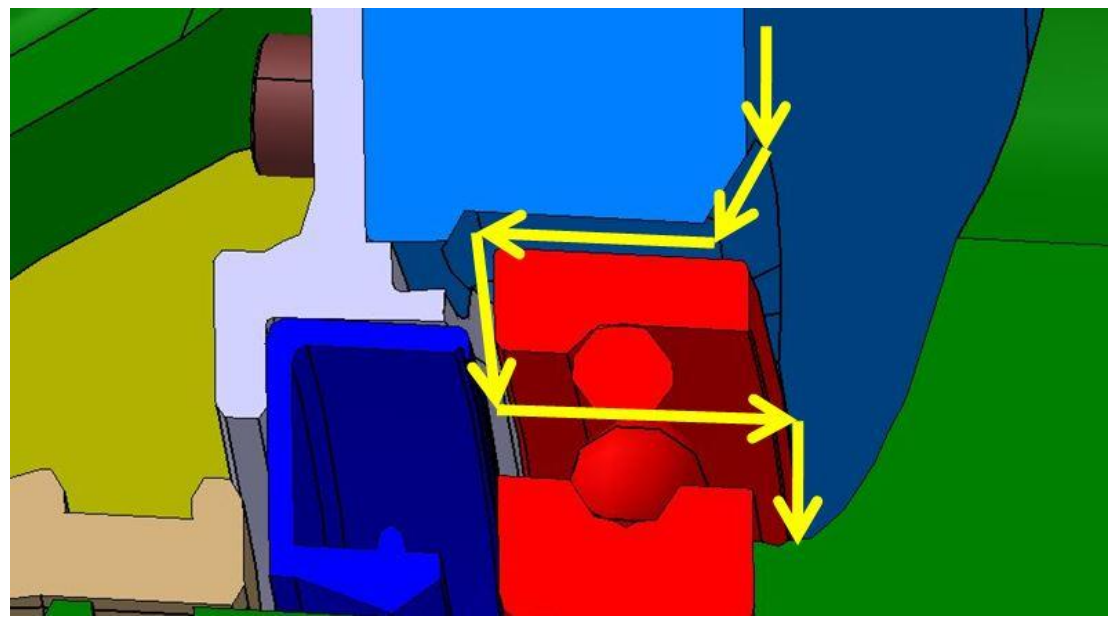
Most critical area, by lubrication point of view is represented by shaft 3 bearing housings. Lowest point of bearings is 60 [mm] higher than oil level in static condition. In addition, oil slam effect of large gearwheel 2 is stopped by wall of the gear-box laying upon it. Increase oil level into the sump is not a practicable solution because gearwheels of first stage, completely submerged, may suffer important loss of efficiency due to friction with lubrication oil. Moreover, excessive quantity of oil into a sump may cause emulsion of the fluid that leads to undesirable increase of temperature into the system.

Anyway, a slamming effect, tighter than those generated by gearwheel 2, is generated by gearwheel 3 and gearwheel 4. Indeed drops of lubricant are projected to the farthest periphery of the sump. Once drops hurt the walls of gear-box case, tend to adhere to surface and slowly return down to merge again with liquid in the sump. Tendency of lubricant to follow the surface on which is attached, can be taken in advantage to bring a small improvement to lubrication.

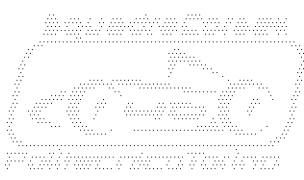
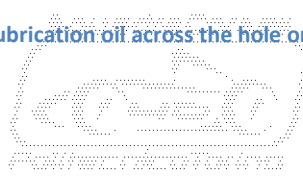
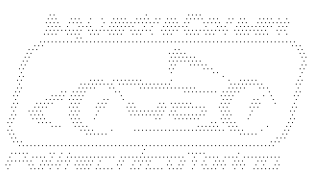


Plot 9.4-4: Lubrication drills on external gear-box plate (left) and internal gear-box plate (right).

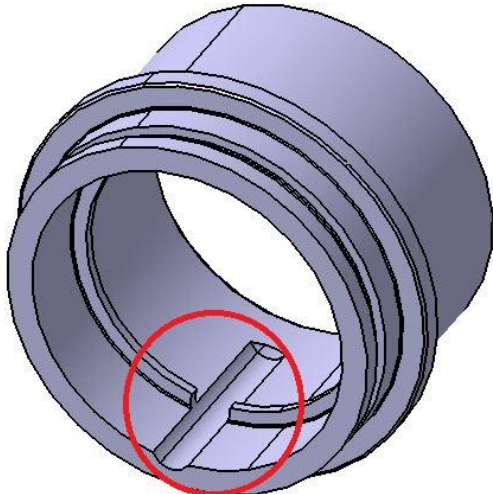
How It's possible to notice by Plot 9.4-4, some axial holes have been machined on bearing housings. Task of such holes is to guide oil, which is descending following gear-box walls, behind the bearing.



Plot 9.4-5: Path of lubrication oil across the hole on F bearing housing.



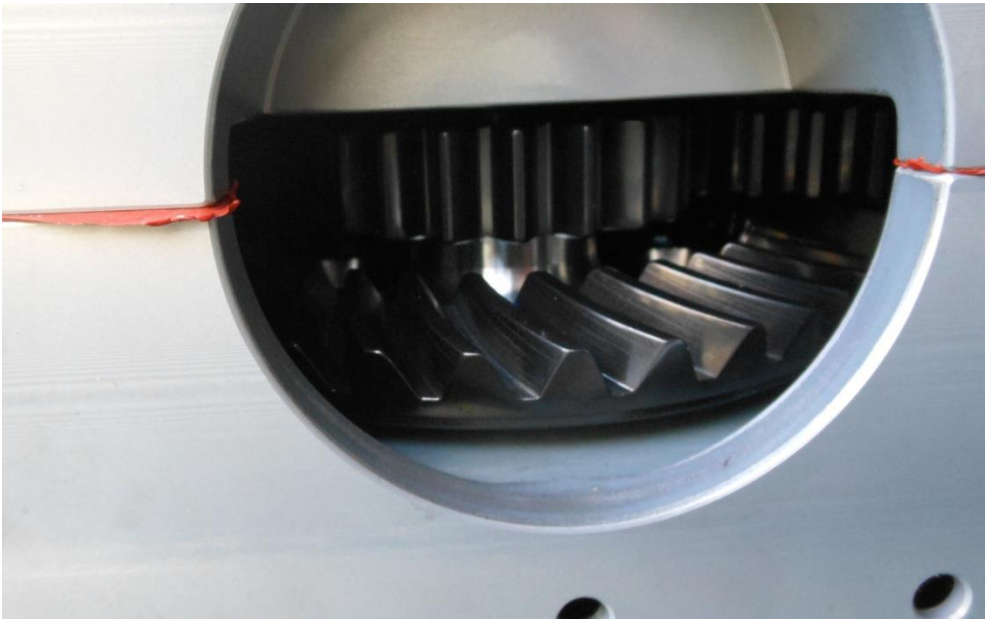
Path of descending lubrication oil is displayed by Plot 9.4-5, It's clear that goal is oil passing through bearing and being spread by spheres. How It's possible to notice, first part of the hole displays a conical surface which enlarges diameter of hole, working as collector surface.



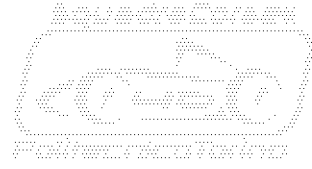
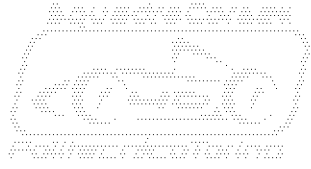
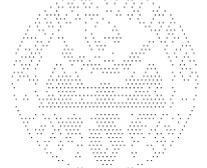
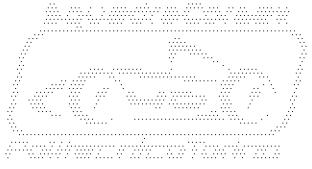
Plot 9.4-6: Lubrication drain hole on shaft 1 housing.

In order to conclude dissertation about lubrication, It's necessary to notice that shaft 1 housing displays something like a lubrication hole in Its lower part. Such hole have been machined in order to drain oil trapped between bearings of shaft 1. That fact helps to prevent dangerous rise of temperature and concentration of contaminants.

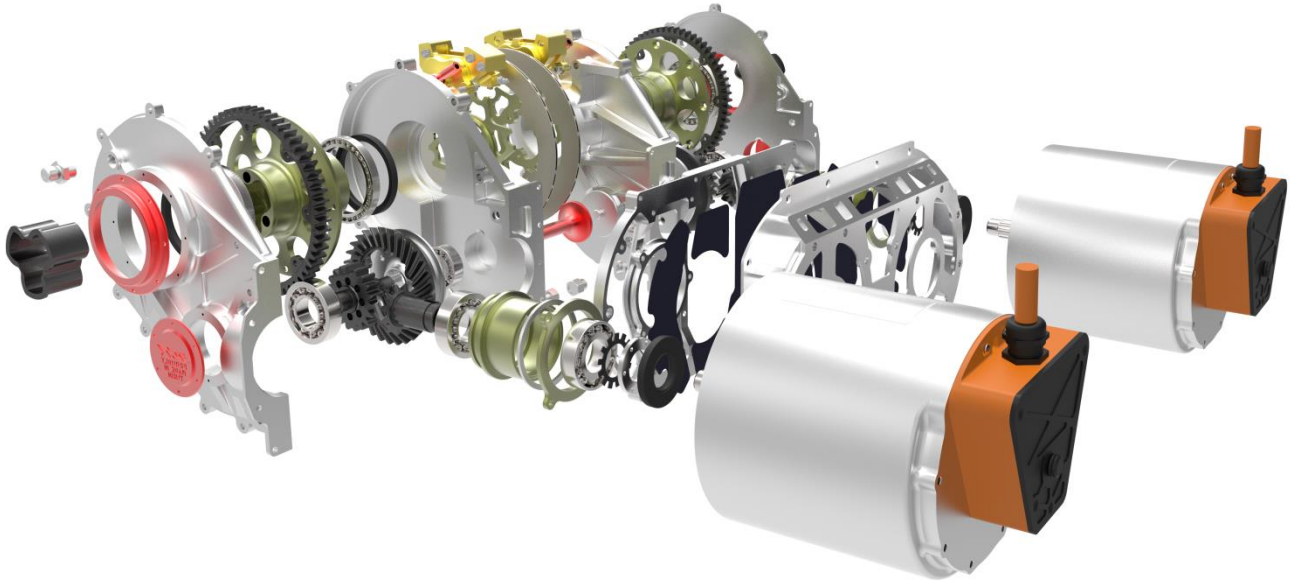
By general observation of gear-box layout, It's necessary underline that, once sump is drained from oil, shaft 1 complete of its housing can be removed by Its seat, in order to check wear on teeth of each single gearwheel. Such feature can be observed on Picture 9.4-2 and is going to be crucial during reliability checks of testing phase.



Picture 9.4-2: Shaft 1 housing seat operated as inspection window.



10. Manufacturing

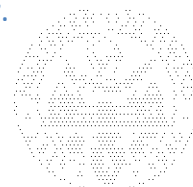
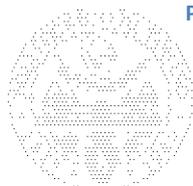


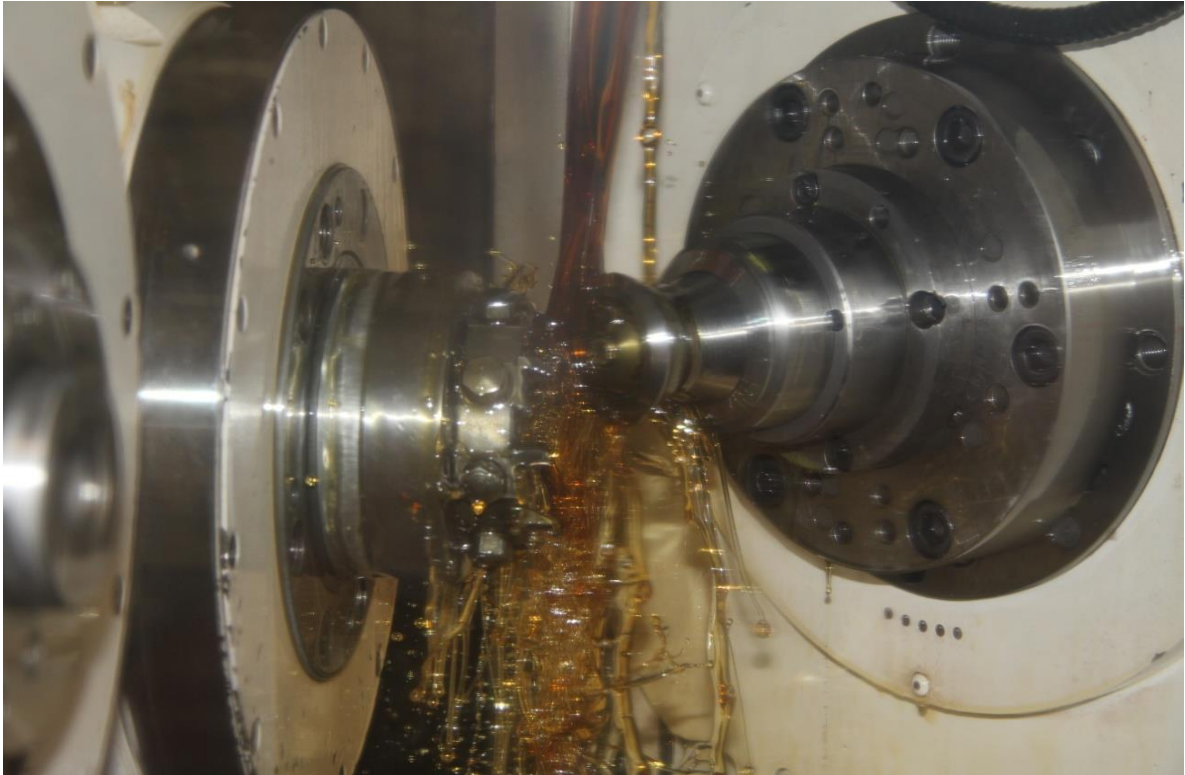
Plot 10-1: Exploded view of gear-box main components.

Once design phase is declared frozen, It's necessary to start with production of any single component and with purchase of few commercial normalized parts. How explained by previous chapters, large majority of S.C.R. gear-box components is custom, by virtue of that manufacturing phase is particularly consistent and delicate. Low production volume which consists of single component in most of cases, contrasts with production of moulds and specific harnesses. By virtue of that, entirety of components is realized by conventional machining processes like turning and milling of monolithic raw billets.



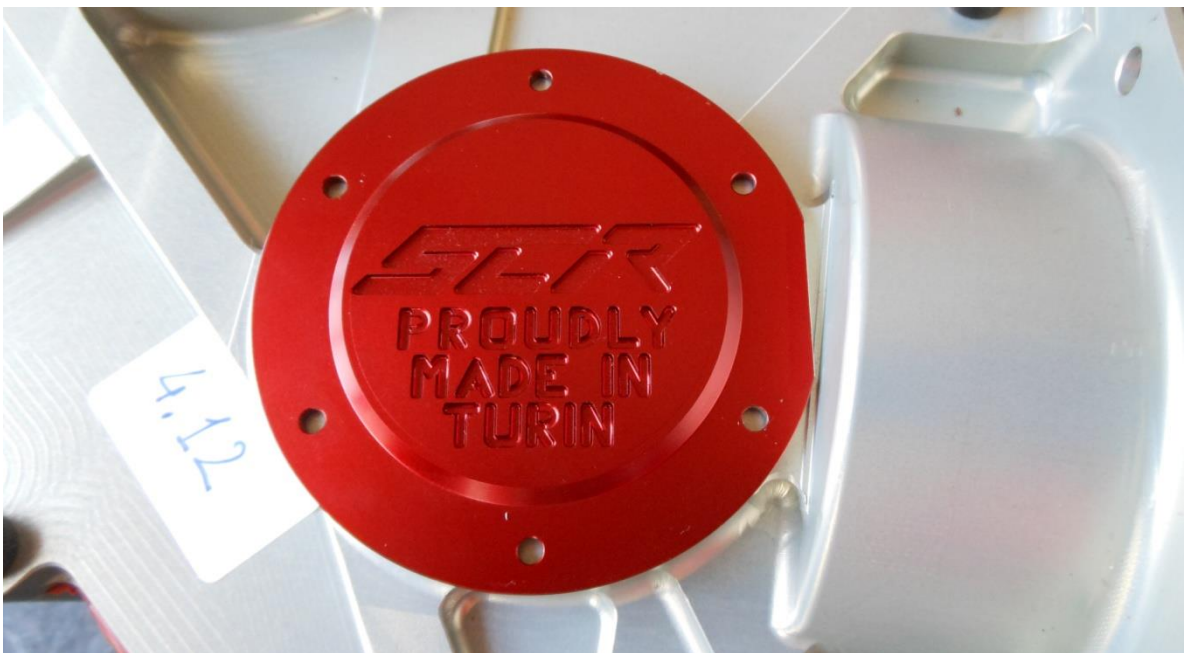
Picture 10-1: CNC milling of "motors plate".



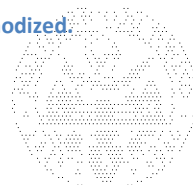
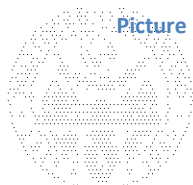


Picture 10-2: Manufacturing of a S.C.R. bevel gearwheel.

In particular, large aluminium plates that constitutes gear-box case are machined from monolithic billets of Al7075-T651 “Ergal” which is the high performances alloy introduced at Chapter 1.3. Pursuit of lightness made geometries of components quite complex to produce, and some needed to be realized by five axis computer numerical control, **C.N.C.**, milling machine. Squadra Corse doesn’t own machines and expertise to perform manufacturing of delicate transmission components. By virtue of that, team inquired to one of its best partners, Officine Meccaniche Giuseppe Massola. Components was realized and accurately checked in dimensions and geometrical tolerances, in order to guarantee an easy and accurate assembly of gear-box.



Picture 10-3: Shaft 2 preload cap engraved and anodized.

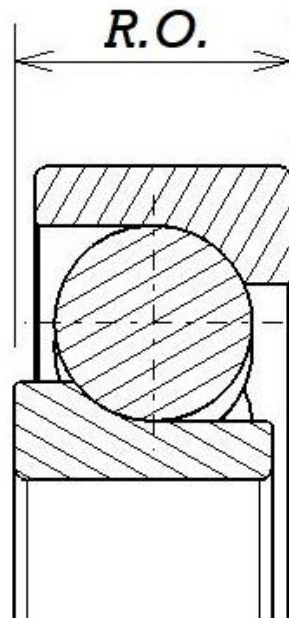


Large majority of aluminium parts where then finished by a particular surface treatment, the “*anodizing*”. It consists of an electrolytic passivation which protects metal by corrosion and improve aesthetical appearance of components with bright colours, as depicted by Picture 10-3.

Anodizing operates on the component as an oxide coating, by virtue of that, process of passivation needs to be managed in order to obtain the desired thickness of oxide layer. During process, components are submerged in a specific liquid solution, then current is applied for a well determined time, in order to determine the precise thickness. On some parts, thickness may lead to assembly problems, for this reason, bearing housings needs to be protected from liquid solution contact by special masks. That allows to maintain close dimensional tolerances which bearings require in order to exploit desired reliability and performances.

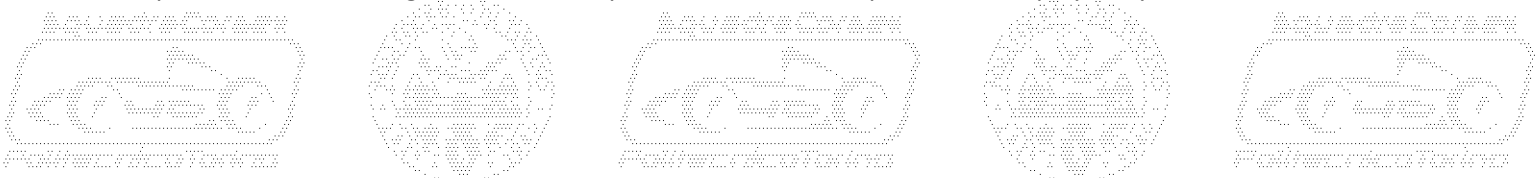
More detailed information about gearwheel manufacturing and related surface treatments have been deeply described at Chapter 6.

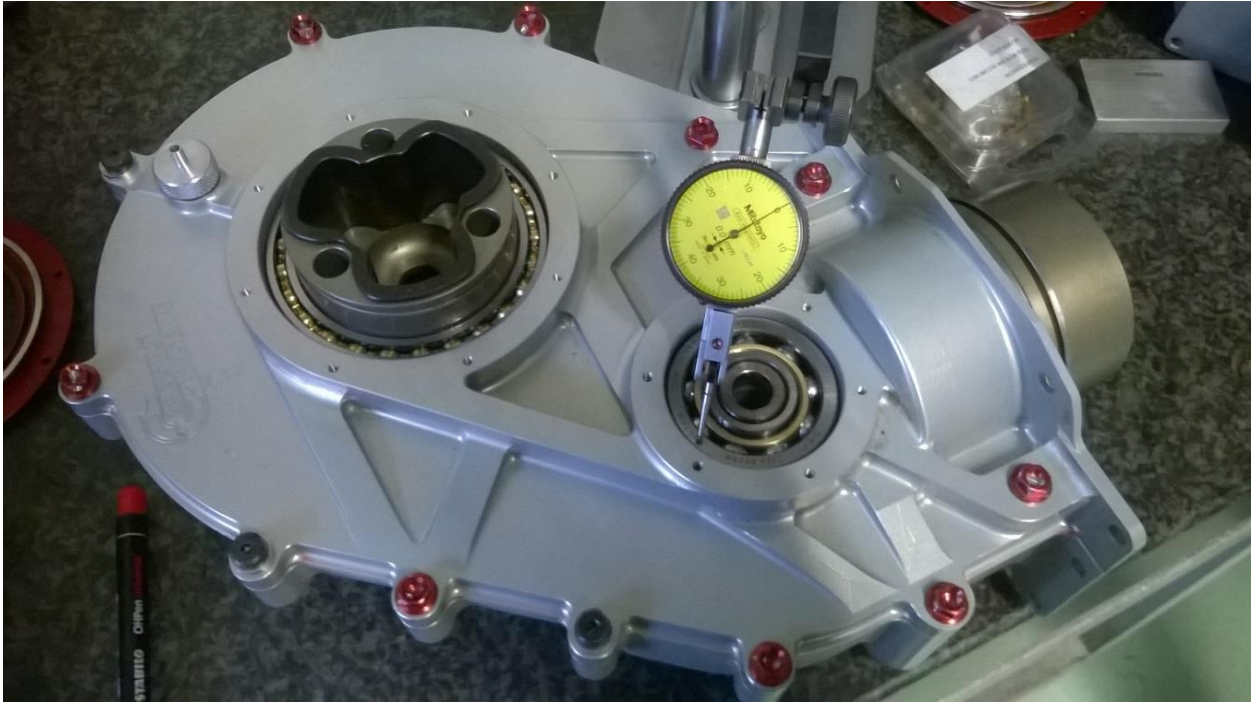
Next step in manufacturing of transmission is “*assembly*”. Such phase too is delicate requiring accurate measurement tools and many time to be performed. By virtue of previous dissertations about bevel gear axial touch and preload of bearings, It’s necessary to measure exactly all dimensions of components related with operation of spinning parts. In order to clarify actual dissertation, It’s necessary point out that often bearings, angular contact in particular, exploit some small differences from nominal dimensions. Such situation is displayed by Plot 10-2 where dimension of “*Raceways Offset*”, *R.O.*, is emphasized. How It’s possible to argue after deep study of Chapter 8, such dimension affects strongly the correct application of bearing preload, in “X” and “O” configuration both.



Plot 10-2: Cross section of angular contact bearing, offset between raceways is emphasized.

Anyway, It’s necessary to underline that difference between raceways offset and nominal thickness of the bearing is very tight and can be measured around few hundredths of millimetre. Such measure, to be consistent, needs to be performed with bearing under axial load condition. By virtue of that, in order to obtain best reliability and performances by mechanical system, an accurate measurement process needs to be performed on bearings, unassembled parts, and assembled parts, how displayed by Picture 10-4.



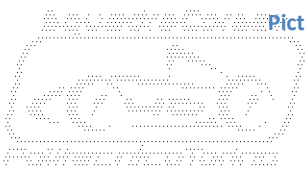


Picture 10-4: Measurement of bearing position in assembled configuration.

How It's possible to notice by Picture 10-5, precision of measurement needs to be very tight and value displayed correspond to a mean dimension calculated on three points around bearing circumference.



Picture 10.5: Mean distance between bearing external raceways and reference surface of housings.



Previous values are necessary to finally determine control dimension of preload caps of shaft 2 and shaft 3, how it was deeply explained in previous Chapter 7.5 and Chapter 7.6.



Picture 10-6: Daniele with components of S.C.R. gear-box, ready to final assembly, Danisi Engineering July 2013.



Picture 10-7: Complete gear-box assembled on S.C.R. gear-box during winter testing, Torino Aerialia Airfield, November 2013.



11. Conclusions.

In order to provide a complete description of S.C.R. gear-box project, It's necessary to spend some words to summarize crucial results of the work described by actual thesis. To better appreciate general results It's necessary take into mind targets declared at Chapter 3.

Gear-box of S.C.R., like any other component of the car, took roughly **eight months** to evolve from design concept phase to end of manufacturing phase. Such interval of time is absolutely surprising if compared with large majority of projects performed every day in all the automotive and motorsport engineering field. By virtue of that, total time elapsed can be considered the first achieved result.

Second result achieved is the **assembly**, correctly performed at first attempt. Often, in the field of accurate mechanical components, It's easy detect some undesired errors which compromise installation of the systems. Components of S.C.R. gear-box, proved to be accurately designed and machined with highest standards of quality. By virtue of that, none of gear-box components required to be modified or rebuilt. Such result is the proof of complete fulfilment of requirements described at Chapter 3.7.

With reference to Chapter 3.2, It's necessary underline that theoretical gear **efficiency**, calculated by software and declared at Chapter 6.7, may not be totally convergent to reality. Moreover, total efficiency of gear-box is strongly affected by friction of rotary seals, bearings and lubrication oil. By virtue of that, a test performed on the bench would be the best way to measure each of these loss of efficiency. Furthermore It would be possible to trace a map of efficiency through a wide range of loads and revolutions. Unfortunately tight times of the project and budget issues didn't allow to perform such important test.

Total **weight** of assembled gear-box is around **11,00 [kg]** including rear brakes. Such value can be quantified around **30%** higher than S.C.12e homologous system. Anyway, It's necessary to take into account that gear ratio and, torque discharged to the ground by consequence, have grown of about **50%**. That represents an important benefit for acceleration performances of the vehicle. Last observation about weight needs to be done noticing that total transmission weight and layout configuration hallowed to achieve desired car weight distribution of about **52%** to rear, as declared at Chapter 4.1.

Due to serious issues on high voltage components, the car never reached the maximum estimated operation of **4.000 [km]**, maximum mileage covered can be measured around **1.500 [km]**. Despite low mileage, general **reliability** of the gear-box system have been widely proved. No serious mechanical issue affected transmission operation. Moreover, none of gearwheel teeth displayed damages or traces of wear. Cleanliness of lubrication oil have been checked day by day, as explained at end of Chapter 9.4, and no alarming metal debris have been detected.

Previous dissertations about weight, reliability and recurring inspections are the proof of achievements declared at Chapter 3.6 and Chapter 3.8. A relative low weight and a good operation of gears are the proof of a good grade in achievement of **weight stiffness trade-off**. Instead, daily inspection on teeth are a proof of a good achievement in the matter of **assembly ease**.

Due to lack of propelling performance of high voltage components, S.C.R. could not exploit all of its potential on the track. By virtue of that, It wasn't possible to perform exhausting dynamic tests focused on achievement of performance results. It wasn't possible to "push" the car in a severe acceleration test and time estimated at Chapter 4.1 for **0-100 [km/h]** run, couldn't be achieved. On the other hand, It couldn't be



possible compare endurance performances of S.C.12e with those of S.C.R. Due to differences in partnerships, test tracks were changed between 2012 and 2013 season. That fact made a serious comparison between two projects impossible to realize. By virtue of that, dynamic superiority of S.C.R. is allocated in theory and simulations only. With reference to Chapter 3.5, It's possible to notice that effectiveness of specifications on gear ratio couldn't be proven.

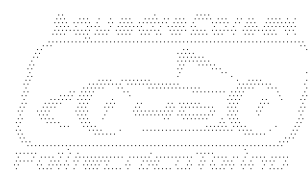
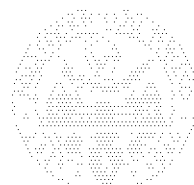
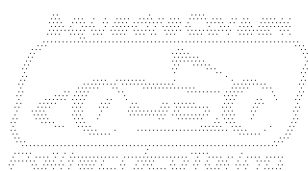
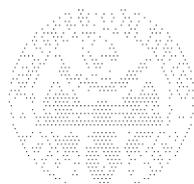
Even if, a real **temperature** sensor wasn't installed into the sump, some raw temperature measurements have been performed on gear-box case plates. By use of a basic infra red sensor, some temperatures have been measured on external surfaces of the sump. Collected values of temperatures never exceed $90^{\circ}[C]$ Such fact, combined with no detection of damage on teeth, represents the proof of the right choice on lubricant specifications.

Actual dissertation can be concluded with reference to Chapter 3.3. Entire S.C.R. project, despite its scarce sporting results, have been an ambitious experience which provided a strong base for design and development of any future Squadra Corse platform. Experience and awareness on errors, gained due to S.C.R. project in several fields, cannot be underestimated or forgotten. Knowledge on structural composite materials, gears and aerodynamic, derives almost entirely by actual project. By virtue of that, experience of S.C.R. can be considered the milestone for new design techniques employed by Squadra Corse PoliTo team.

12. References.

Such section contains complete references of books mentioned in previous chapters. Any of following texts have been scrupulously consulted during execution of execution of described work.

1. SAE – 2013 Formula SAE Rules 03-05-2013 revision – 2012, SAE International.
2. W.F. Milliken & D.L. Milliken – Race Cars Vehicle Dynamics – 1994, SAE International.
3. G. Genta – Meccanica dell'Autoveicolo – 2000, Levrotto & Bella.
4. J. Smith – Fundamentals of Motorsport Engineering – 2013, Nelson Thornes Ltd.
5. SAE – 2011 Formula SAE Rules – 2010, SAE International.
6. L. Morello – Progetto della Trasmissione Meccanica – 2005, Associazione Tecnica dell'Automobile.
7. G. Belforte – Meccanica Applicata alle Macchine – 2007, Levrotto & Bella.
8. Gear. In: Wikipedia [Internet]. <https://www.wikipedia.org/>.
9. L. Baldassini – Vademecum per Disegnatori e Tecnici 19°ed. – 2002, Hoepli.
10. R. G. Budynas, J. K. Nisbett – Shigley's Mechanical Engineering Design 9°ed. – 2011, Mc Graw-Hill.
11. U.N.I. – UNI SPERIMENTALE 8862-2:1987 – 1987, Ente Nazionale Italiano di Unificazione.
12. Bevel Gear. In: khkgears [Internet]. <https://khkgears.net/>.
13. Prodotti. In: Lafer [Internet]. <http://www.lafer.eu/>.
14. H. Naunheimer, B. Bertsche, J. Ryborz, W. Novak – Automotive Transmissions – 2010, Springer.
15. Rolling Bearings – 2012, SKF Group.
16. G. Curti F. a – Fondamenti di Meccanica Strutturale – 2006, CLUT Editrice.
17. Travi. In: hoepliscuola [Internet]. <http://www.hoepliscuola.it/>.



Appendix 1

----- KISSsoft - Release 03-2012 -----
KISSsoft evaluation

----- File -----
Nome : Bevel Stage 11 31
Modificato di: User Il: 24.03.2013 alle: 18:02:41

Indicazione importante: Nel calcolo sono intervenuti avvisi:

1-> Alcuni elementi del collettivo di carico sono insolitamente grandi. Controllare il collettivo di carico. (Elemento No. 6, Elemento No. 6)

2-> AGMA2003: I coefficienti del ciclo di sollecitazione CL(ZNT) sono documentati solo per gli acciai carbonitrurati. Il valore per l'acciaio carbonitrurato viene applicato anche in questo caso.

3-> I materiali del database KISSsoft rispecchiano le raccomandazioni AGMA2001 (ruote cilindriche). I dati per sat e sac secondo AGMA2003 (ruote cilindriche) sono in parte diversi.

Per correggere i valori, adattare i dati sui materiali con la funzione 'Inserimento dati personalizzati'.

CALCOLO RUOTA CONICA (INGR. CONICO)

Numero disegno/articolo:
Ruota 1: 0.000.0
Ruota 2: 0.000.0

Calcolo della resistenza con collettivo di carico

Durata vita nominale (h): 100.00

Collettivo di carico

Potenza nominale [P] 0.0010 W
Fattore d'applicazione [KA] 1.00

Collettivo di carico : Immissione propria
No. elementi collettivo di carico : 6
Ruota di riferimento: 1

1	[%]	[W]	[l/min]	[Nm]	KHb	Kgam	YM1	YM2
1	26.00000	-12.566.3706	6000.0000	-20.0000	1.2520	1.0000	0.7000	0.7000
2	18.00000	6283.1853	6000.0000	10.0000	1.2520	1.0000	0.7000	0.7000
3	25.00000	12566.3706	6000.0000	20.0000	1.2520	1.0000	0.7000	0.7000
4	14.00000	15707.9633	6000.0000	25.0000	1.2520	1.0000	0.7000	0.7000
5	9.00000	18849.5559	6000.0000	30.0000	1.2520	1.0000	0.7000	0.7000
6	8.00000	25132.7412	6000.0000	40.0000	1.2520	1.0000	0.7000	0.7000

Linea-Woehler nel settore limite di fatica secondo: secondo la norma

Indicazione:
Metodo di calcolo in base a:
- AGMA2001, Miners rule

Sicurezza piede: 3.73 4.01
Sicurezza fianco: 1.29 1.37

SOLO PER INFORMAZIONE: CALCOLO CON POTENZA DI RIFERIMENTO

Metodo di calcolo Ruote coniche AGMA 2003-C10
Calcolo geometria secondo ISO 23509:2006, metodo 1
Vano piede costante, figura 2 (Gleason duplex)
Metodo di fabbricazione: rodato
Dentatura ad arco



Procedura di fresatura singola
Raggio fresa a lame riportate (mm) [rc0] 100.00

----- RUOTA 1 ----- RUOTA 2 -----

Potenza (W) [P] 0.00
N. di giri (1/min) [n] 0.1 0.0
Senso di rotazione ruota 1 vista sulla sommità del cono: a destra
Momento torcente (Nmm) [T] 100.0 281.8
Ruota conduttrice (+) / condotta (-) + -
Overload factor [Ko] 1.00
Vita utile richiesta [H] 100.00

1. GEOMETRIA DENTE E MATERIALE

----- RUOTA 1 ----- RUOTA 2 -----

Offset dell'asse (mm) [a] 0.000
Angolo tra gli assi (°) [Sigma] 90.000
Modulo normale (nel mezzo) (mm) [mmn] 2.9284
Angolo di pressione normale (°) [alfn] 20.000
Angolo d'elica intermedio (°) [betm] 30.0000
Elica destro a sinistra
N. di denti [z] 11 31
Larghezza dente (mm) [b] 19.00 19.00
Larghezza impronta di contatto assunta o misurata (mm) [be] 19.00 19.00
Qualità della dentatura [Q-ISO17485] 3 3
Diametro interno corpo ruota (mm) [di] 0.00 0.00
Vertice del cono primitivo di rif. rispetto al lato interno del pezzo grezzo (mm) [yi] 0.00 0.00
Vertice del cono primitivo di rif. rispetto al lato esterno del pezzo grezzo (mm) [yo] 0.00 0.00
Materiale
Ruota 1: 42 CrMo 4 (3), Acciaio da bonifica, nitrurato
ISO 6336-5 Imagine 13a/14a (MQ)
Ruota 2: 42 CrMo 4 (3), Acciaio da bonifica, nitrurato
ISO 6336-5 Imagine 13a/14a (MQ)

----- RUOTA 1 ----- RUOTA 2 --

Durezza superficie HV 550 HV 550
Limite di snervamento (N/mm²) [sigs] 900.00 900.00
(lb/in²), (N/mm²) (lb/in²), (N/mm²)
Allowable bending stress number [sat] 53665, 370.01 53665, 370.01
Allowable contact stress number [sac] 145040,1000.02 145040,1000.02
Resistenza alla rottura (N/mm²) [Rm] 1100.00 1100.00
Limite di snervamento (N/mm²) [Rp] 900.00 900.00
Modulo di elasticità (N/mm²) [E] 206000 206000
Coefficiente di Poisson [ny] 0.300 0.300
Valore medio della rugosità Ra, fianco del dente (µm) [RAH] 3.00 3.00
Valore massimo della rugosità Rz, fianco (µm) [RZH] 20.00 20.00
Valore massimo della rugosità Rz, piede (µm) [RZF] 20.00 20.00

Utensile o profilo di riferimento della ruota 1 :
Profilo di riferimento (immissione propria) 1.25 / 0.30 / 1.0 ISO 53.2:1997 Profilo B
Fattore di addendum [haP*] 0.925
Fattore di dedendum [hfP*] 1.128
Fattore raggio testa [rhoaP*] 0.000
Fattore raggio piede [rhofP*] 0.250
Fattore addendum di forma [hFaP*] 0.000
Fattore altezza protuberanza [hprP*] 0.000
Angolo protuberanza [alfprP] 0.000
Angolo di semi-topping [alfKP] 0.000
non topping

Utensile o profilo di riferimento della ruota 2 :
Profilo di riferimento (immissione propria) 1.25 / 0.30 / 1.0 ISO 53.2:1997 Profilo B
Fattore di addendum [haP*] 0.925
Fattore di dedendum [hfP*] 1.128
Fattore raggio testa [rhoaP*] 0.000
Fattore raggio piede [rhofP*] 0.250
Fattore addendum di forma [hFaP*] 0.000
Fattore altezza protuberanza [hprP*] 0.000
Angolo protuberanza [alfprP] 0.000
Angolo di semi-topping [alfKP] 0.000
non topping

Riepilogo profilo di riferimento degli ingranaggi:
Altezza piede profilo di riferimento (per modulo) [hfP*] 1.128 1.128



Raggio piede profilo di riferimento (per modulo)	[roFP*]	0.250	0.250
Altezza testa profilo di riferimento (per modulo)	[haP*]	0.925	0.925
Fattore altezza protuberanza (per modulo)	[hprP*]	0.000	0.000
Angolo protuberanza (°)	[alfprP]	0.000	0.000
Fattore addendum di forma (per modulo)	[hFaP*]	0.000	0.000
Angolo di semi-topping (°)	[alfKP]	0.000	0.000
Dati per Rettificare / Levigatura (Honing):			
Profondita di immersione (per modulo)	[hgrind*]	1.029	1.029
Raggio alla testa utensile (per modulo)	[rgrind*]	0.100	0.100

Modifica del profilo: nessuno (soltanto valore rodagg
Spoglia di testa (µm) [Ca] 5.2 5.2

Nessuna variazione dell'addendum

Tipo di lubrificazione	lubrificazione a sbattimento d'olio		
Tipo olio	Olio: ISO-VG 46		
Base lubrificante	Base olio minerale		
Viscosità cinematica olio a 40 °C (mm²/s)	[nu40]	46.00	
Viscosità cinematica olio a 100 °C (mm²/s)	[nu100]	6.70	
FZG-Test A/8.3/90 passo	[FZGtestA]	12	
Densità spec. a 15 gradi (kg/dm³)	[rhoOil]	0.880	
Temperatura olio (°C)	[TS]	70.000	

		----- RUOTA 1 -----	RUOTA 2 -----
Rapporto trasmissione totale	[itot]		-2.818
Rapporto N. denti	[u]		2.818
Angolo d'elica esterno (°)	[bete]	31.006	31.006
Angolo d'elica intermedio (°)	[betm]	30.000	30.000
Angolo d'elica interno (°)	[beti]	29.882	29.882
Angolo di offset del pignone sul piano assiale (°)	[zetm]		0.000
Angolo di offset del pignone sul piano primitivo (°)	[zetmp]		0.000
Offset piano primitivo (mm)	[ap]		0.000
Modulo normale esterno (mm)	[men]		3.3934
Modulo frontale esterno (mm)	[met]	3.9590	3.9590
Modulo normale (nel mezzo) (mm)	[mmn]		2.9284
Modulo frontale centrale (mm)	[mnt]	3.3814	3.3814
Modulo normale interno (mm)	[min]		2.4310
Modulo frontale interno (mm)	[mit]	2.8038	2.8038
Somma dei coefficienti di spostamento del profilo			
Fattore di spostamento del profilo	[xhml+xhm2]		0.0000
Interferenza di taglio	[xhmin]	0.3927	-0.3927
Fattore modifica spessore dente	[xsmn]	0.0059	-7.0169
		0.0000	-0.0000
Diametro primitivo Esterno (mm)	[de]	43.549	122.730
Diametro testa esterno (mm)	[dae]	52.668	124.014
Diametro di piede Esterno (mm)	[dfe]	38.810	119.097
Diametro primitivo Metà (mm)	[dm]	37.196	104.824
Diametro primitivo Metà (mm)	[dam]	44.469	105.866
Diametro di piede Metà (mm)	[dfm]	33.137	101.845
Diametro primitivo Interno (mm)	[di]	30.842	86.918
Diametro di testa Interno (mm)	[dai]	36.270	87.719
Diametro di piede Interno (mm)	[dfi]	27.465	84.594
Addendum (mm)	[hae]	4.838	1.920
	[ham]	3.859	1.559
	[hai]	2.880	1.197
Dedendum (mm)	[hfe]	2.515	5.432
	[hfm]	2.153	4.453
	[hfi]	1.792	3.474
Altezza dente (mm)	[he]	7.352	7.352
	[hm]	6.012	6.012
	[hi]	4.672	4.672
Altezza utile totale	[whe]		6.758
	[whm]		5.418
	[whi]		4.077
Gioco di testa (mm)	[ce]	0.594	0.594
	[cm]	0.594	0.594
	[ci]	0.594	0.594
Lunghezza del cono di riferimento esterno (mm)	[Re]	65.114	65.114
Lunghezza del cono di riferimento intermedio (mm)	[Rm]	55.614	55.614
Lunghezza del cono di riferimento interno (mm)	[Ri]	46.114	46.114
Angolo del cono primitivo di riferimento (°)	[delta]	19.537	70.463



Altri angoli (°):	[dela]	25.419	72.642
	[thea=dela-delta]	5.883	2.179
	[delf]	17.358	64.581
	[thef=delta-delf]	2.179	5.883
Distanza sull'asse dal punto di incrocio degli assi (mm)	[txo]	59.747	19.965
	(mm)[txi]	42.496	14.293
Distanza dal vertice del cono primitivo al punto di incrocio degli assi (mm)	[tz]	0.000	-0.000
	(mm)[tzF]	-4.337	-0.583
	(mm)[tzR]	-0.125	1.406
Distanza in direzione dell'asse rispetto al vertice del cono (mm)	[ye]	61.365	21.775
	(mm)[yae]	59.747	19.965
	(mm)[yai]	42.496	14.293
Gioco di testa teorico (mm)	[c]	0.594	0.594
Gioco di testa effettivo (mm)	[c.e/i]	0.594 / 0.604	0.594 / 0.604
Parametri di dimensionamento	[Re2/b2]		3.427
	[b2/mm]		6.488

2. FATTORI D'INFLUSSO GENERALI

Larghezza dente determinante (mm)	[F,b]	19.00	
Forza periferica nominale sul cerchio di funzionamento (N)	[FTw]	5.4	
	[Ft]	5.4	
Forza periferica nel dia. di rif. (N)	[Fa]	3.7	1.1
Forza assiale (N)	[Fr]	1.1	3.7
Forza radiale (N)	[Fnorm]	6.6	
Forza normale (N)	[vm]	0.00	
Velocità periferica con dm (m/sec)	[ve]	0.00	
Velocità periferica con de (m/sec)	[Kmb]	1.250	
Modificatore distribuzione carico	[Km, Kmb]	1.252	
Load distribution factor	[Qv]	9	
Transmission accuracy grade number	[Kv]	1.001	
Dynamic factor	[NL]	0.001	0.000
Number of load cycles (in mio.)			

3. PORTATA PIEDE

	[KS, Yx]	----- RUOTA 1 -----	RUOTA 2 -----
Size factor		0.5200	0.5200
		(in), (mm)	(in), (mm)
Braccio leva flessione (mm)	[hN]	0.112, 2.84	0.109, 2.76
Tooth thickness at critical section	[2*sN]	0.239, 6.07	0.251, 6.38
Radius at curvature of fillet curve	[rfm]	0.032, 0.80	0.031, 0.80
Load angle (°)	[alfh]	24.48	19.00
Tooth form factor Y	[Y]	0.652	0.715
Stress correction factor	[Kf]	2.086	2.171
Raggio fresa a lame riportate (mm)	[rc0]	100.000	
Tooth lengthwise correction factor	[Kx, Ybet]	1.000	
Bending strength geometry factor J	[J]	0.258	0.255
		(lb/in ²), (N/mm ²)	(lb/in ²), (N/mm ²)
Bending stress number	[st]	22, 0.15	23, 0.16
Stress cycle factor	[KL, YNT]	2.000	2.000
(for general applications)			
Allowable bending stress number	[sat]	(lb/in ²), (N/mm ²)	(lb/in ²), (N/mm ²)
Temperature factor	[KT]	53665, 370.01	53665, 370.01
Reliability factor	[KR, YZ]	1.00	1.00
Reverse loading factor	[-]	1.00	1.00
Effective allow. b.s.n.	[sateff]	0.700	0.700
Bending strength power rating (hp)	[Pat]	107330, 740.01	107330, 740.01
Note: Pat calculated with Ko=1, KR=1, SFmin=1		0.01(0.01 kW)	0.01(0.00 kW)
Required safety factor	[SFmin]	1.00	1.00
Transmittable power	[Pat/SFmin]	0.01(0.01 kW)	0.01(0.00 kW)

AGMA2003, allegato C(M):
hfe1 = 2.51 mm hfe2 = 5.43 mm rhoa01= 0.73 mm rhoa02= 0.73 mm
s1 = 5.38 mm s2 = 3.72 mm thef1= 2.18 ° thef2= 5.88 °
Y1 = 0.65 Yf1 = 2.09 YK1 = 0.31 epsNJ= 1.00 Yi = 1.00
rmyo1= 20.59 mm rmp1= 19.73 mm b1' = 17.63 mm b1 = 19.00 mm
Y2 = 0.71 Yf2 = 2.17 YK2 = 0.33 epsNJ= 1.00 Yi = 1.00
rmyo2= 166.05 mm rmp2= 156.73 mm b2' = 16.27 mm b2 = 19.00 mm

4. SICUREZZA FIANCO



		----- RUOTA 1 -----	RUOTA 2 -----
Elastic coefficient	[Cp, ZE]	(lb ^{-.5} /in), (N ^{-.5} /mm)	
Size factor	[CS, Zs]	2285.3, 189.81	
Crowning factor	[Cxt, Zxt]	0.531	0.531
Geometry factor I	[I]	1.500	
		0.0891	
		(lb/in ²), (N/mm ²)	
Contact stress number	[sc, sigH]	6867, 47.34	
Stress cycle factor	[CL, ZNT]	2.000	2.000
(for general applications)			
Hardness ratio factor	[CH, ZW]	1.00	1.00
Temperature factor	[KT]	1.00	1.00
Reliability factor	[CR, ZZ]	1.00	1.00
		(lb/in ²), (N/mm ²)	(lb/in ²), (N/mm ²)
Allowable contact stress number	[sac]	145040, 1000.02	145040, 1000.02
Effective allow. c.s.n. (lb/in ²)	[saceff]	290080, 2000.03	290080, 2000.03
Pitting resistance power rating (hp)	[Pac]	0.00 (0.00 kW)	0.00 (0.00 kW)
Note: Pac calculated with Ko=1, KR=1, SHmin=1			
Safety factor (flanc)	[saceff/sc]	42.24	42.24
Required safety factor	[SHmin]	1.00	1.00
Transmittable power	[Pac/SHmin ²]	0.00 (0.00 kW)	0.00 (0.00 kW)
AGMA2003, allegato C(M):			
Re = 65.11 mm	hae1 = 4.84 mm	hae2 = 1.92 mm	del = 43.55 mm de2 = 122.73 mm
de1 = 19.54 °	del2 = 70.46 °	delal = 25.42 °	dela2 = 72.64 °
p2 = 11.09 mm	gan1 = 8.29 mm	gan2 = 4.44 mm	gc = 12.73 mm
rhoy0 = 8.74 mm	mmt = 3.38 mm	met = 3.96 mm	
Zi = 1.29 mm	epsNI = 0.96		

SERVICE FACTORS:

Service factor for tooth root	[KSF]	4805.62	4742.96
Service factor for pitting	[CSF]	1784.62	1784.62
Service factor for gear set	[SF]	1784.62	
Note: Service factors are calculated with Ko=1, KR=1			

Transmittable power including required service factors KSPmin, CSFmin (hp) 0.00 (0.00 kW)
KSPmin = 1.00, CSFmin = 1.00

6. SCARTI PER SPESSORE DENTE

		----- RUOTA 1 -----	RUOTA 2 -----
Tolleranza spessore dente	ISO 23509:2006 Q4-7 (Ta ISO 23509:2006 Q4-7 (Ta		
Scarto spessore dente in sezione normale (mm)	[As.e/i]	-0.035 / -0.052	-0.035 / -0.052
Le seguenti indicazioni valgono per l'asse della larghezza del dente:			
Spessore dente (cordale) sul cerchio primitivo (mm)	[smnc]	5.427	3.763
(mm)	[smnc.e/i]	5.392 / 5.375	3.728 / 3.711
Altezza sopra la corda a partire da dam (mm)	[hamc]	3.996	1.562
Gioco primitivo (mm)	[jmt]	0.120 / 0.081	
(mm)	[jet]	0.141 / 0.095	
Gioco normale sui fianchi (mm)	[jmn]	0.098 / 0.066	
(mm)	[jen]	0.113 / 0.076	

7. TOLLERANZE DENTATURA

		----- RUOTA 1 -----	RUOTA 2 -----
Secondo			
ISO 17485:2006:			
Qualità della dentatura	[Q-ISO17485]	8	8
(Diametro) (mm)	[dT]	40.13	103.78
Scostamento singolo del passo (µm)	[fpT]	24.00	25.00
Divergenza totale del modulo (µm)	[FpT]	84.00	90.00
Deviazione concentricità (µm)	[FrT]	67.00	72.00
Salto rotolamento fianco singolo (µm)	[fisTmax/fisTmin]	32.00/0.00	32.00/0.00
(fisTmax, fisTmin: ISO 17485:2006, Table B1, q=2)			
Deviazione rotolamento fianco singolo (µm)	[FisT]	115.00	122.00

9. DETERMINAZIONE DELLA FORMA DEL DENTE

10. DATI COMPLEMENTARI

Dati di immissione per il calcolo delle dimensioni ruota secondo



ISO 23509:2006

Dati tipo 1 (sec. tabella 3, ISO 23509:2006):
 xhm1= 0.3927 khap= 0.9250 khfp= 1.1280 xsmn= 0.0000
 Dati tipo 2 (sec. tabella 3, ISO 23509:2006):
 cham= 0.2877 kd= 1.8500 kc= 0.1097 kt= 0.0000

Coefficiente d'attrito medio (secondo Niemann)

	[mm]	0.151	
Striscamento d'usura secondo Niemann	[zetw]	0.633	
Potenza dissipata dalla dentatura (W)	[PVZ]	0.000	
(Rendimento dentatura (%))	[etaz]	97.347)	
Peso - calcolata con da (kg)	[Mass]	0.220	0.442

Fine Report

Righe: 402

----- KISSsoft - Release 03-2012 -----

KISSsoft evaluation

----- File -----
Nome : Spur Stage 19 6l
Modificato di: User Il: 24.03.2013 alle: 18:31:35

CALCOLO DI UNA COPPIA DI RUOTE CILINDRICHE A DENTATURA DIRITTA

Numero disegno/articolo:
Ruota 1: 0.000.0
Ruota 2: 0.000.0

Calcolo della resistenza con collettivo di carico

Durata vita nominale (h): 100.00

Collettivo di carico

Potenza nominale [P] 0.0010 W
Fattore d'applicazione [KA] 1.00

Collettivo di carico : Immissione propria
No. elementi collettivo di carico : 6
Ruota di riferimento: 1

i	[%]	[W]	[l/min]	[Nm]	KHb	Kgam	YM1	YM2
1	26.00000	-12.566.3706	2142.8571	-56.0000	1.5000	1.0000	0.7000	0.7000
2	18.00000	6283.1853	2142.8571	28.0000	1.5000	1.0000	0.7000	0.7000
3	25.00000	12566.3706	2142.8571	56.0000	1.5000	1.0000	0.7000	0.7000
4	14.00000	15707.9633	2142.8571	70.0000	1.5000	1.0000	0.7000	0.7000
5	9.00000	10149.5559	2142.8571	84.0000	1.5000	1.0000	0.7000	0.7000
6	8.00000	25132.7412	2142.8571	112.0000	1.5000	1.0000	0.7000	0.7000

Linea-Woehler nel settore limite di fatica secondo: secondo la norma

Indicazione:

Nei metodi ISO6336 e AGMA2001 risulta una diminuzione della resistenza nel settore della resistenza alla fatica (tra circa 10⁷ a 10¹⁰ cicli con una riduzione di circa 15 %). Questo viene tenuto in considerazione nel calcolo della durata, nonostante la scelta della curva Woehler secondo Miner!

Sicurezza piede: 2.05 1.70
Sicurezza fianco: 1.53 1.27

Sicurezza grippaggio (Integrale) 3.63
Sicurezza grippaggio (Flash) 4.82
(La sicurezza antigrippaggio/micropitting/EHT viene indicata per l'elemento più sfavorevole del collettivo.)

SOLO PER INFORMAZIONE: CALCOLO CON POTENZA DI RIFERIMENTO

Metodo di calcolo ISO 6336:2006 Metodo B

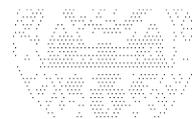
		----- RUOTA 1 -----	RUOTA 2 --
Potenza (W)	[P]		0.0010
N. di giri (l/min)	[n]	0.1	0.0
Momento torcente (Nm)	[T]	0.100	0.321
Fattore d'applicazione	[KA]		1.00
Vita utile richiesta	[H]		100.00
Ruota conduttrice (+) / condotta (-)		+	-

1. GEOMETRIA DENTE E MATERIALE

(Calcolo geometrico secondo
ISO 21771:2007)

Interasse (mm) [a] ----- RUOTA 1 ----- RUOTA 2 --
120.000

1/7



ISO 286:2010 Scarto js7

Tolleranza interasse			
Modulo normale (mm)	[mn]	3.0000	
Angolo di pressione normale (°)	[alfn]	20.0000	
Angolo d'elica sul diametro primitivo (°)	[beta]	0.0000	
N. di denti	[z]	19	61
Larghezza dente (mm)	[b]	17.00	15.00
Elica		Dentatura diritta	
Qualità della dentatura	[Q-ISO 1328:1995]	3	3
Diametro interno (mm)	[di]	0.00	0.00
Diametro interno della fasciatura (mm)	[dbi]	0.00	0.00

Materiale

Ruota 1: 42 CrMo 4 (3), Acciaio da bonifica, nitruato
ISO 6336-5 Imagine 13a/14a (MQ)

Ruota 2: 42 CrMo 4 (3), Acciaio da bonifica, nitruato
ISO 6336-5 Imagine 13a/14a (MQ)

		----- RUOTA 1 -----	RUOTA 2 --
Durezza superficie		HV 550	HV 550
Trattamento del materiale secondo ISO 6336:2006 Normale (Fattori durata di vita ZNT e YNT >=0.85)			
Limite di fatica piede del dente (N/mm²) [sigFlim]		370.00	370.00
Limite di fatica pressione di Hertz (N/mm²)			
	[sigHlim]	1000.00	1000.00
Resistenza alla rottura (N/mm²)	[Rm]	1100.00	1100.00
Limite di snervamento (N/mm²)	[Rp]	900.00	900.00
Modulo di elasticità (N/mm²)	[E]	206000	206000
Coefficiente di Poisson	[ny]	0.300	0.300
Valore medio della rugosità Ra, fianco del dente (µm)			
	[RAH]	3.00	3.00
Valore massimo della rugosità Rz, fianco (µm)			
	[RZH]	20.00	20.00
Valore massimo della rugosità Rz, piede (µm)			
	[RZF]	20.00	20.00

Utensile o profilo di riferimento della ruota 1 :

Profilo di riferimento 1.25 / 0.38 / 1.0 ISO 53.2:1997 Profilo A

Fattore di addendum	[haP*]	1.000
Fattore di dedendum	[hfP*]	1.250
Fattore raggio testa	[rhoaP*]	0.000
Fattore raggio piede	[rhofP*]	0.380
Fattore addendum di forma	[hFaP*]	0.000
Fattore altezza protuberanza	[hprP*]	0.000
Angolo protuberanza	[alfprP]	0.000
Angolo di semi-topping	[alfkp]	0.000

non topping

Utensile o profilo di riferimento della ruota 2 :

Profilo di riferimento 1.25 / 0.38 / 1.0 ISO 53.2:1997 Profilo A

Fattore di addendum	[haP*]	1.000
Fattore di dedendum	[hfP*]	1.250
Fattore raggio testa	[rhoaP*]	0.000
Fattore raggio piede	[rhofP*]	0.380
Fattore addendum di forma	[hFaP*]	0.000
Fattore altezza protuberanza	[hprP*]	0.000
Angolo protuberanza	[alfprP]	0.000
Angolo di semi-topping	[alfkp]	0.000

non topping

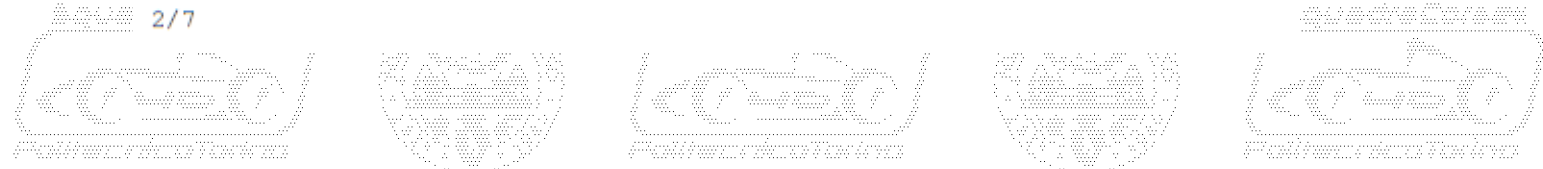
Riepilogo profilo di riferimento degli ingranaggi:

Altezza piede profilo di riferimento (per modulo)			
	[hfP*]	1.250	1.250
Raggio piede profilo di riferimento (per modulo)			
	[rofP*]	0.380	0.380
Altezza testa profilo di riferimento (per modulo)			
	[haP*]	1.000	1.000
Fattore altezza protuberanza (per modulo)			
	[hprP*]	0.000	0.000
Angolo protuberanza (°)	[alfprP]	0.000	0.000
Fattore addendum di forma (per modulo)	[hFaP*]	0.000	0.000
Angolo di semi-topping (°)	[alfkp]	0.000	0.000
Dati per Rettificare / Levigatura (Honing):			
Profondità di immersione (per modulo)	[hgrind*]	1.066	1.066
Raggio alla testa utensile (per modulo)	[rgrind*]	0.100	0.100

Modifica del profilo: nessuno (soltanto valore rodag)

Spoglia di testa (µm)	[Ca]	5.2	5.2
-----------------------	------	-----	-----

Tipo di lubrificazione	lubrificazione a sbattimento d'olio
Tipo olio	Olio: ISO-VG 46
Base lubrificante	Base olio minerale
Viscosità cinematica olio a 40 °C (mm²/s) [nu40]	46.00



Viscosità cinematica olio a 100 °C (mm ² /s)	[nu100]	6.70	
Test FZG A/8.3/90 (ISO 14635-1:2006)	[FZGtestA]	12	
Densità spec. a 15 gradi (kg/dm ³)	[roOil]	0.880	
Temperatura olio (°C)	[TS]	70.000	
			----- RUOTA 1 ----- RUOTA 2 --
Rapporto trasmissione totale	[itot]	-3.211	
Rapporto N. denti	[u]	3.211	
Modulo trasversale (mm)	[mt]	3.000	
Angolo di pressione sul dia. di riferimento (°)	[alf]		
Angolo di pressione di funzionamento (°)	[alfwt]	20.000	
Angolo di pressione normale in funzionamento (°)	[alfwt.e/i]	20.023 / 19.977	
Angolo d'elica del cerchio di funzionamento (°)	[alfwn]	20.000	
Angolo d'elica di base (°)	[betaw]	0.000	
Interasse di riferimento (mm)	[betab]	0.000	
Somma dei coefficienti di spostamento del profilo	[ad]	120.000	
Fattore di spostamento del profilo	[Summexi]	0.0000	
Spessore dente (arco) (per modulo)	[x]	0.3830	-0.3830
	[sn*]	1.8496	1.2920
Modifica addendum (mm)	[k*mn]	0.000	0.000
Diametro primitivo (mm)	[d]	57.000	183.000
Diametro di base (mm)	[db]	53.562	171.964
Diametro cerchio di testa (mm)	[da]	65.298	186.702
	[da.e/i]	65.298 / 65.288	186.702 / 186.692
Scarti cerchio di testa (mm)	[Ada.e/i]	0.000 / -0.010	0.000 / -0.010
Smusso di testa / arrotondamento di testa (mm)	[hK]	0.000	0.000
Diametro forma di testa (mm)	[dFa]	65.298	186.702
	[dFa.e/i]	65.298 / 65.288	186.702 / 186.692
Diametro di testa attivo (mm)	[dNa.e/i]	65.298 / 65.288	186.702 / 186.692
Diametro primitivo di funzionamento (mm)	[dW]	57.000	183.000
	[dW.e/i]	57.008 / 56.992	183.027 / 182.973
Diametro cerchio di fondo (mm)	[df]	51.798	173.202
Coefficienti di spostamento del profilo	[x.e/i]	0.3509 / 0.3326	-0.4265 / -0.4494
Cerchio di piede generato con xE (mm)	[df.e/i]	51.606 / 51.496	172.941 / 172.804
Gioco di testa teorico (mm)	[c]	0.750	0.750
Gioco di testa effettivo (mm)	[c.e/i]	0.972 / 0.863	0.924 / 0.829
Diametro di piede attivo (mm)	[dNf]	54.377	177.688
	[dNf.e/i]	54.400 / 54.360	177.718 / 177.662
Diametro cerchio di forma piede (mm)	[dFf]	54.260	176.183
	[dFf.e/i]	54.173 / 54.126	176.019 / 175.934
Reserve (dNf-dFf)/2 (mm)	[cF.e/i]	0.137 / 0.094	0.892 / 0.821
Addendum (mm)	[ha = mn * (haP*+x)]	4.149	1.851
	[ha.e/i]	4.149 / 4.144	1.851 / 1.846
Dedendum (mm)	[hf = mn * (hfP*-x)]	2.601	4.899
	[hf.e/i]	2.697 / 2.752	5.030 / 5.098
Angolo di rotolamento a dFa (°)	[xsi_dFa.e/i]	39.951 / 39.933	24.224 / 24.216
Angolo di rotolamento a dNa (°)	[xsi_dNa.e/i]	39.951 / 39.933	24.224 / 24.216
Angolo di rotolamento a dNf (°)	[xsi_dNf.e/i]	10.170 / 9.923	14.945 / 14.871
Angolo di rotolamento a dFf (°)	[xsi_dFf.e/i]	8.675 / 8.331	12.516 / 12.382
Altezza dente (mm)	[H]	6.750	6.750
No. denti di sostituzione	[zn]	19.000	61.000
Spessore dente normale sul cilindro di testa (mm)	[san]	1.559	2.481
	[san.e/i]	1.485 / 1.433	2.389 / 2.334
Vano normale sul cilindro del piede (mm)	[efn]	0.000	2.770
	[efn.e/i]	0.000 / 0.000	2.826 / 2.857
Velocità di striscamento massima sulla testa (m/s)	[vga]	0.000	0.000
Striscamento specifico alla testa	[zetaa]	0.627	0.586
Striscamento specifico al piede	[zetaf]	-1.414	-1.680
Coef. di scivolamento a la testa	[Kga]	0.411	0.233
Coef. di scivolamento al piede	[Kgf]	-0.233	-0.411
Passo (mm)	[pt]	9.425	
Passo base trasv. (mm)	[pbt]	8.856	
Passo base trasv. (mm)	[pet]	8.856	
Lunghezza di condotta (mm)	[ga, e/i]	13.984 (14.036 / 13.912)	
Lunghezza T1-A, T2-A (mm)	[T1A, T2A]	4.690 (4.638 / 4.754)	36.353 (36.353 / 36.340)
Lunghezza T1-B (mm)	[T1B, T2B]	9.818 (9.818 / 9.809)	31.225 (31.174 / 31.285)
Lunghezza T1-C (mm)	[T1C, T2C]	9.748 (9.735 / 9.760)	31.295 (31.256 / 31.334)
Lunghezza T1-D (mm)	[T1D, T2D]	13.546 (13.495 / 13.610)	27.496 (27.496 / 27.484)
Lunghezza T1-E (mm)	[T1E, T2E]	18.674 (18.674 / 18.665)	22.368 (22.317 / 22.428)
Lunghezza T1-T2 (mm)	[T1T2]	41.042 (40.991 / 41.094)	
Diametro punto di contatto singolo B (mm)	[d-B]	57.048 (57.048 / 57.042)	182.952 (182.917 / 182.993)



Diametro punto di contatto singolo D (mm)	[d-D]	60.024(59.978/60.082)	180.543(180.543/180.535)
Ricoprimento testa	[eps]	1.008(1.009/ 1.006)	0.571(0.576/ 0.565)
Lunghezza minima della linea di contatto (mm)	[Lmin]		15.000
Rapporto d'azione	[eps_a]		1.579
Ricoprimento di profilo con scarti	[eps_a.e/m/i]	1.585 / 1.578 / 1.571	
Rapporto di ricoprimento	[eps_b]		0.000
Ricoprimento totale	[eps_g]		1.579
Ricoprimento totale con scarti	[eps_g.e/m/i]	1.585 / 1.578 / 1.571	

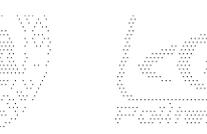
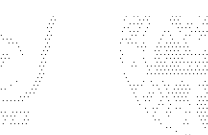
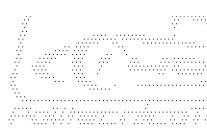
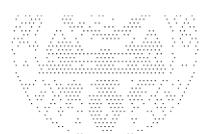
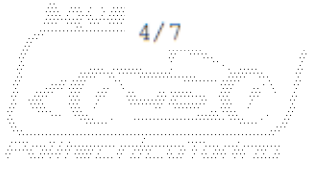
2. FATTORI D'INFLUSSO GENERALI

		----- RUOTA 1 -----	RUOTA 2 --
Forza periferica nel dia. di rif. (N)	[Ft]		3.5
Forza assiale (N)	[Fa]		0.0
Forza radiale (N)	[Fr]		1.3
Forza normale (N)	[Fnorm]		3.7
Forza periferica sul cerchio di riferimento per mm (N/mm)	[w]		0.23
Per informazione: Forze nel cerchio di funzionamento:			
Forza tangenziale nominale (N)	[Ftw]		3.5
Forza assiale (N)	[Faw]		0.0
Forza radiale (N)	[Frw]		1.3
Velocità periferica del cerchio primitivo di riferimento. (m/sec)	[v]		0.00
Valore rodaggio (µm)	[yp]		1.3
Valore rodaggio (µm)	[yf]		1.4
Fattore correzione	[CM]		0.800
Fattore corpo ruota	[CR]		1.000
Fattore profilo riferimento	[CBS]		0.975
Coefficiente materiale	[E/Est]		1.000
Rigidezza dente singola (N/mm/µm)	[c']		9.483
Rigidezza d'ingranamento (N/mm/µm)	[cgalf]		13.601
Rigidezza d'ingranamento (N/mm/µm)	[cgbet]		11.561
La formula per c' e cg con w*KA < 25 N/mm è troppo vaga!			
c', cg viene calcolato con w*KA = 25 N/mm.			
Massa ridotta (kg/mm)	[mRed]		0.01129
No. giri di risonanza (min-1)	[nEl]		17445
No. giri riferimento (-)	[N]		0.000
Zona acritica			
Coefficiente KV immesso:			
Fattore dinamico	[KV]		1.000
Coefficiente KHb immesso:			
Fattori larghezza - Fianco	[KHb]		1.500
- Piede dente	[KFb]		1.324
- Grippaggio	[KBb]		1.500
Coefficiente KHa immesso:			
Fattore trasv. - Fianco	[KHa]		1.000
- Piede dente	[KFa]		1.000
- Grippaggio	[KBa]		1.000
Fattore d'elica Grippaggio	[Kbg]		1.000
N. cicli di carico (in mio.)	[NL]	0.001	0.000

3. PORTATA PIEDE

Calcolo dei fattori forma dente secondo metodo: B
(Coeff. forma dente YF calcolati con spostamento del profilo x)

		----- RUOTA 1 -----	RUOTA 2 --
Fattore profilo dente	[YF]	1.21	1.64
Fattore correzione tensione	[YS]	2.21	1.78
Angolo di lavoro (°)	[alfFen]	22.55	18.74
Braccio leva flessione (mm)	[hF]	2.81	3.57
Spessore piede dente (mm)	[sFn]	6.42	6.29
Raggio piede dente (mm)	[roF]	1.36	1.82
(hF* = 0.936/1.190 sFn* = 2.140/2.097 roF* = 0.454/0.606 dsFn = 52.77/174.56 alfsFn = 30.00/30.00)			
Fattore rapporto condotta	[Yeps]		1.000
Fattore elica	[Ybet]		1.000
Fattore dentatura alta	[YDT]		1.000
Fattore di corona dentata	[YB]	1.000	1.000
Larghezza dente determinante (mm)	[beff]	17.00	15.00



Tensione nominale piede del dente (N/mm ²)			
	[sigF0]	0.18	0.23
Tensione piede del dente (N/mm ²)	[sigF]	0.24	0.30
Tensione piede dente consentita dalla ruota dentata di prova			
Fattore supporto	[YdrelT]	1.041	0.956
Fattore superficie	[YRrelT]	1.000	1.000
Fattore grandezza (piede dente)	[YX]	1.000	1.000
Fattore resistenza alla fatica limitata	[YNT]	1.600	1.600
	[YdrelT*YRrelT*YX*YNT]	1.666	1.529
Fattore di flessione alternata	[YM]	0.700	0.700
Fattore correzione tensione	[Yst]		2.00
Resistenza limite del piede del dente (N/mm ²)	[sigFG]	862.87	791.97
Tensione ammessa del piede del dente (N/mm ²)	[sigFP=sigFG/SFmin]	616.34	565.69
Sicurezza nominale	[SFmin]	1.40	1.40
Fattore di sicurezza per tensione di fondo dente	[SF=sigFG/sigF]	3563.40	2638.02
Potenza trasmissibile (W)	[kWRating]	2.67	1.97

4. SICUREZZA FIANCO

		----- RUOTA 1 -----	RUOTA 2 --
Fattore zona	[ZH]	2.495	
Fattore d'elasticità (N ^{0.5} /mm)	[ZE]	189.812	
Fattore rapporto condotta	[Zeps]	0.898	
Fattore inclinazione	[Zbet]	1.000	
Larghezza dente determinante (mm)	[beff]	15.00	
Pressione di contatto nominale (N/mm ²)	[sigH0]	31.21	
Pressione di contatto sul dia. primitivo di funz. (N/mm ²)	[sigHw]	38.22	
Fattore ingranamento singolo	[ZB, ZD]	1.00	1.00
Pressione di contatto (N/mm ²)	[sigH]	38.22	38.22
Fattore lubrificante	[ZL]	1.000	1.000
Fattore velocità	[ZV]	1.000	1.000
Fattore rugosità	[ZR]	1.000	1.000
Fattore accoppiamento materiale	[ZW]	1.000	1.000
Fattore resistenza alla fatica limitata	[ZNT]	1.300	1.300
	[ZL*ZV*ZR*ZW*ZNT]	1.300	1.300
Un limitato no. di alveoli è consentito (0=no, 1=si)		0	0
Coeff. di grandezza (fianco)	[ZX]	1.000	1.000
Resistenza limite al pitting (N/mm ²)	[sigHG]	1300.00	1300.00
Pressione di contatto consentita (N/mm ²)	[sigHP=sigHG/SHmin]	1300.00	1300.00
Sicurezza per pressione sul cerchio primitivo di funzionamento			
	[SHw]	34.01	34.01
Sicurezza nominale	[SHmin]	1.00	1.00
Potenza trasmissibile (W)	[kWRating]	1.21	1.21

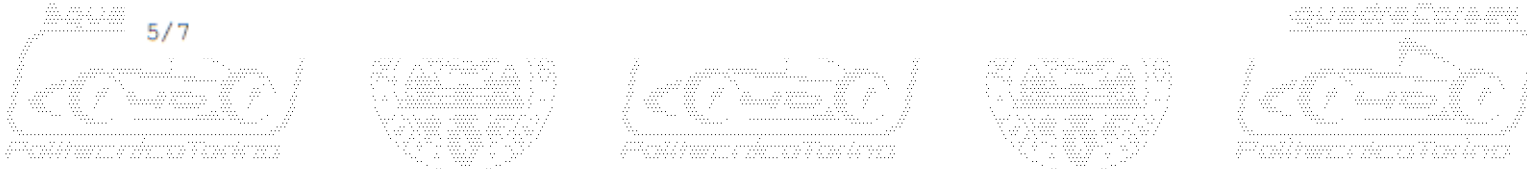
4b. MICROPITTING (pitting microscopico) SECONDO
ISO TR 15144-1:2010

Il calcolo non viene eseguito. (Lubrificante: Stadio di carico test di micropitting non è noto)

5. RESISTENZA AL GRIPPAGGIO

Metodo di calcolo secondo
ISO TR 13989:2000

Fattore del lubrificante (per il tipo di lubrificazione)	[XS]	1.000	
Fattore di ingranamento multiplo	[Xmp]	1.000	
Fattore struttura relativo (Grippaggio)	[XWrelT]	1.500	
Coefficiente di contatto termico (N/mm/s ^{0.5} /K)	[BM]	13.780	13.780
Spoglia di testa determinante (µm)	[Ca]	5.20	5.20
Spoglia di testa ottimale (µm)	[Ceff]	0.02	
Larghezza dente determinante (mm)	[beff]	15.000	
Forza tangenziale/larghezza dente determinante (N/mm)	[wBt]	0.351	
(Kbg = 1.000, wBt*Kbg = 0.351)			
Fattore angolo (eps1):			
1.008, eps2: 0.571) [Xalfbet]		0.978	



<p>Criterio temperatura lampo</p> <p>Fattore del lubrificante [XL] 0.882</p> <p>Temperatura massa (°C) [theMi] 70.00</p> <p>theM = theoil + XS*0.47*Xmp*theflm [theflm] 0.00</p> <p>Temperatura di grippaggio (°C) [theS] 454.68</p> <p>Coordinata Gamma (luogo temperatura più alta) [Gamma] 0.858</p> <p>[Gamma.A]= -0.519 [Gamma.E]= 0.916</p> <p>Temperatura di contatto più alta. (°C) [theB] 70.01</p> <p>Fattore temp. istantanea (°K*N^{-0.75}*s^{-0.5}*m^{-0.5}) [XM] 50.058</p> <p>Fattore di accesso [XJ] 1.000</p> <p>Fattore di distribuzione del carico [XGam] 0.437</p> <p>Viscosità dinamica (mPa*s) [etaM] 12.31</p> <p>Coefficiente attrito [mym] 0.182</p> <p>Criterio temperatura integrale</p> <p>Fattore del lubrificante [XL] 1.000</p> <p>Temperatura massa (°C) [theM-C] 70.00</p> <p>theM-C = theoil + XS*0.70*theflaint [theflaint] 0.00</p> <p>Temp. integrale di grippaggio (°C) [theSint] 447.22</p> <p>Fattore temp. istantanea (°K*N^{-0.75}*s^{-0.5}*m^{-0.5}) [XM] 50.058</p> <p>Fattore di rodaggio (rodaggio completato) [XE] 1.000</p> <p>Fattore rapporto condotta [Xeps] 0.241</p> <p>Viscosità dinamica (mPa*s) [etaOil] 12.31</p> <p>Coefficiente attrito medio [mym] 0.207</p> <p>Fattore geometria [XBE] 0.389</p> <p>Fattore ingranamento [XQ] 1.000</p> <p>Fattore spoglia testa [XCa] 1.963</p> <p>Temperatura fianco integrale (°C) [theint] 70.00</p>	
---	--

6. MISURE DI CONTROLLO PER SPESSORE DENTE

	----- RUOTA 1 -----	----- RUOTA 2 --
	DIN 3967:1978 cd2	DIN 3967:1978 cd2
Tolleranza spessore dente		
Scarto spessore dente in sezione normale (mm)	[As.e/i] -0.070 / -0.110	-0.095 / -0.145
N. denti di misura [k]	3.000	7.000
Quota Wildhaber senza gioco (mm) [Wk]	23.725	59.344
Quota Wildhaber effettiva (mm) [Wk.e/i]	23.659 / 23.622	59.254 / 59.207
Diametro di controllo (mm) [dMWk.m]	58.548	181.879
Diametro teorico del corpo di misura (mm) [DM]	5.804	4.976
Diametro effettivo del corpo di misura (mm) [DMeff]	6.000	5.000
Misura radiale con una sfera senza gioco (mm) [MrK]	34.198	93.683
Misura radiale con una sfera effettiva (mm) [MrK.e/i]	34.133 / 34.097	93.548 / 93.476
Diametro di controllo (mm) [dMMr.m]	59.400	180.447
Misura diametrale fra due sfere senza gioco (mm) [MdK]	68.182	187.305
Misura fra due sfere effettiva (mm) [MdK.e/i]	68.054 / 67.981	187.035 / 186.892
Misura fra due rulli senza gioco (mm) [MdR]	68.182	187.305
Misura fra due rulli effettiva (mm) [MdR.e/i]	68.054 / 67.981	187.035 / 186.892
Misura fra tre rulli senza gioco (mm) [Md3R]	67.970	187.245
Misura fra tre rulli effettiva (mm) [Md3R.e/i]	67.842 / 67.769	186.975 / 186.832
Spessore cordale senza gioco (mm) ['sn]	5.540	3.876
Spessore cordale effettivo del dente (mm) ['sn.e/i]	5.470 / 5.430	3.781 / 3.731
Altezza sopra la corda a partire da da.m (mm) [ha]	4.282	1.869
Spessore dente (arco) (mm) [sn]	5.549	3.876
(mm) [sn.e/i]	5.479 / 5.439	3.781 / 3.731
Interasse senza gioco (mm) [aControl.e/i]	119.772 / 119.646	
Interasse senza gioco, Tolleranze (mm) [jta]	-0.228 / -0.354	
Scostamento interasse (mm) [Aa.e/i]	0.018 / -0.018	
Gioco primitivo sui fianchi da Aa (mm) [jt_Aa.e/i]	0.013 / -0.013	
Gioco radiale (mm) [jr]	0.372 / 0.211	
Gioco primitivo (sezione trasversale) (mm) [jt]	0.268 / 0.152	
Angolo di torsione con ruota 1 tenuta ferma (°) [jn]	0.1677 / 0.0953	
Gioco normale sui fianchi (mm) [jn]	0.252 / 0.143	



7. TOLLERANZE DENTATURA

----- RUOTA 1 ----- RUOTA 2 --

Secondo

ISO 1328:1995:

	[Q-ISO1328]	8	8
Qualità della dentatura	[fpt]	17.00	18.00
Scostamento singolo del passo (µm)	[fpb]	16.00	17.00
Deviazione passo cerchio base (µm)	[Fpk/8]	24.00	36.00
Errore accumulato di passo su k/8 (µm)	[ffa]	17.00	19.00
Scostamento forma profilo (µm)	[fHa]	14.00	16.00
Deflessione angolo profilo (µm)	[Fa]	22.00	25.00
Deviazione totale profilo (µm)	[ffb]	15.00	16.00
Scostamento forma elica (µm)	[fHb]	15.00	16.00
Deflessione angolo elica (µm)	[Fb]	21.00	22.00
Deviazione totale elica (µm)	[Fp]	53.00	70.00
Divergenza totale del modulo (µm)	[Fr]	43.00	56.00
Deviazione concentricità (µm)	[Fi*]	72.00	86.00
Errore composto tangenziale su due fianchi (µm)	[fi*]	29.00	29.00
Rotolamento su due fianchi (µm)	[Fi']	89.00	110.00
Deviazione rotolamento fianco singolo (µm)	[fi']	36.00	39.00
Salto rotolamento fianco singolo (µm)			

Tolleranze posizione assi (raccomandazione sec. ISO TR 10064:1992, qualità

8)

Valore massimo disallineamento dell'asse (µm)	[fSigbet]	24.93 (Fb=22.00)
Valore massimo inclinazione dell'asse (µm)	[fSigdel]	49.87

8. DATI COMPLEMENTARI

Asse massimo possibile (eps_a=1.0)	[aMAX]	121.849	
Rigidzza contro torsione (MNm/rad)	[cr]	0.1	1.5
Coefficiente d'attrito medio (secondo Niemann)	[mum]	0.142	
Striscamento d'usura secondo Niemann	[zetw]	0.966	
Potenza dissipata dalla dentatura (W)	[FVZ]	0.000	
Peso - calcolata con da (kg)	[Mass]	0.446	3.215
Peso totale (kg)	[Mass]	3.661	
Momento d'inerzia (sistema riferito alla ruota 1): Calcolo non considerando la forma esatta del dente			
Ruote singolare ((da+df)/2...di) (kg*m ²)	[TraeghMom]	0.0001522	0.01205
System ((da+df)/2...di) (kg*m ²)	[TraeghMom]	0.001321	

9. DETERMINAZIONE DELLA FORMA DEL DENTE

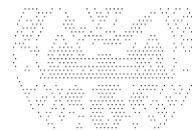
Dati per il calcolo della forma del dente:
Dati non a disposizione.

OSSERVAZIONI:

- I dati con [.e/i] significano: valore massimo [e] e valore minimo [i] tenendo conto di tutte le tolleranze
- I dati con [.m] significano: valore medio tolleranza
- Le tolleranze dell'interasse e gli scarti dello spessore del dente sono considerate nel gioco dei fianchi. Viene indicato il gioco massimo e minimo in funzione degli scarti maggiori o inferiori. Il calcolo è fatto per il cerchio di funzionamento..
- Dettagli relativi al metodo di calcolo:
cg secondo metodo B
KV secondo metodo B
KHb, Kfb secondo metodo C
fma sec. equazione (64), fsh sec. (57/58), Fbx sec. (52/53/54)
KHa, Kfa secondo metodo B

Fine Report

Righe: 554





GEAR 300 75W-90

Racing gearbox and differential lubricant

100% Synthetic – Ester based

TYPE OF USE

Specially designed for racing vehicle gearboxes : speed way, rally, raid...

All mechanical transmission, synchronized or not synchronized gearboxes, gearbox/differential, transfer gearboxes and hypoid differentials without limited slip system operating under shocks, heavy loads and low revolution speed or moderate loads and high revolution speed.

PERFORMANCES

STANDARDS API GL4 and GL5 / MIL-L-2105D

100% synthetic extreme pressure lubricant for an efficient anti-wear protection, a better resistance at high temperature and a longer life time.

0% shear loss : Unshearable oil film in extreme conditions.

Stays in 90 grade after KRL 20 hours shear test as requested by SAE J306 standard, July 1998 update.

Very high lubricating power which decreases friction and wear.

90 grade at hot temperature to provide outstanding oil film resistance at hot temperature and/or to reduce transmission noise.

Fluid at low temperature to allow easier gear shifting when the gearbox is cold.

Less effort required on the gear lever to shift the gears.

Suitable for any type of seal and yellow material used in gearboxes design.

Anti-corrosion, Anti-foam.

RECOMMENDATIONS

Oil change: According to manufacturers' requirements and adjust according to your own use.

PROPERTIES

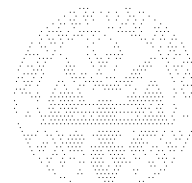
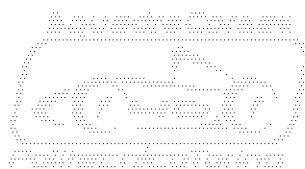
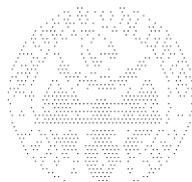
Viscosity grade	SAE J306	75W-90
Density at 20°C (68°F)	ASTM D1298	0.897
Viscosity at 40°C (104°F)	ASTM D445	72.6 mm ² /s
Viscosity at 100°C (212°F)	ASTM D445	15.2 mm ² /s
Viscosity index	ASTM D2270	222
Flash point	ASTM D92	200°C / 392°F
Pour point	ASTM D97	-60°C / -76°F

We retain the right to modify the general characteristics of our products in order to offer to our customers the latest technical development.

Product specifications are not definitive from the order which is subject to our general conditions of sale and warranty.

MOTUL - 119 Bd Félix Faure - 93303 AUBERVILLIERS CEDEX - BP 94 - Tel: 33 1 48 11 70 00 - Fax : 33 1 48 33 28 79 - Web Site : www.motul.fr

0910





GEAR Competition 75W-140

Racing lubricant for limited slip differential integrated in the gearbox or not.

100% Synthetic – Ester based

TYPE OF USE

Specially designed for racing vehicle gearboxes : speed way, rally, raid...
All hypoid differentials with limited slip system, gearbox with integrated limited slip differential, mechanical transmission, synchronized or not synchronized gearboxes, transfer gearboxes operating under shocks, heavy loads and low revolution speed or moderate loads and high revolution speed.

PERFORMANCES

STANDARDS Above Existing Standards
SPECIFICATIONS API GL5 – MUGEN Le Mans 24H – HEWLAND and X-TRAC Japanese GT

100% synthetic extreme pressure lubricant for an efficient anti-wear protection, a better resistance at high temperature and a longer life time.
Included friction modifier avoid noisy or dragging limited slip differential.
0% shear loss : Unshearable oil film in extreme conditions.
Stays in 140 grade after KRL 20 hours shear test as requested by SAE J306 Standard, July 1998 update
Very high lubricating power which decreases friction and wear.
140 grade at hot temperature to provide outstanding oil film resistance at hot temperature and/or to reduce transmission noise.
Fluid at low temperature to allow easier gear shifting when the gearbox is cold.
Less effort required on the gear lever to shift the gears.
Suitable for any type of seal and yellow material used in gearboxes design.
Anti-corrosion, Anti-foam.

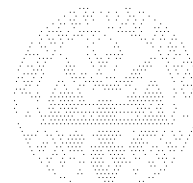
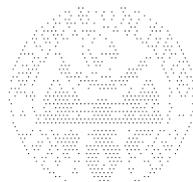
RECOMMENDATIONS

Oil change: According to manufacturers' requirements and adjust according to your own use.

PROPERTIES

Color	Visual	Blue
Viscosity grade	SAE J306	75W-140
Density at 20°C (68°F)	ASTM D1298	0.903
Viscosity at 40°C (104°F)	ASTM D445	170 mm ² /s
Viscosity at 100°C (212°F)	ASTM D445	24.7 mm ² /s
Viscosity index	ASTM D2270	178
Flash point	ASTM D92	212°C / 413°F
Pour point	ASTM D97	-36°C / -33°F

We retain the right to modify the general characteristics of our products in order to offer to our customers the latest technical development.
Product specifications are not definitive from the order which is subject to our general conditions of sale and warranty.
MOTUL - 119 Bd Félix Faure - 93303 AUBERVILLIERS CEDEX - BP 94 - Tel: 33 1 48 11 70 00 - Fax: 33 1 48 33 28 79 - Web Site: www.motul.fr





GEARBOX 80W-90

Gearbox and differential lubricant

Molybdenum bisulphide MOS₂ reinforced

Extreme pressure

TYPE OF USE

Specially recommended for noisy or/and loaded gearboxes.

All mechanical transmission, synchronised or not synchronised gearboxes, gearbox/differential, transfer gearboxes and hypoid differentials without limited slip system operating under shocks, heavy loads and low revolution speed or moderate loads and high revolution speed.

PERFORMANCES

STANDARDS API GL4 and GL5 / MIL-L-2105D

Extreme pressure lubricant for an efficient anti wear protection, reinforced with Molybdenum bisulphide to handle heavy loads.

Stays in 90 grade after KRL 20 hours shear test as requested by SAE J306 Standard, July 1998 update Very high lubricating power which decreases friction and wear.

90 grade at hot temperature to provide outstanding oil film resistance at hot temperature and/or to reduce transmission noise.

Suitable for any type of seal and yellow material used in gearboxes design.

Anti-corrosion, Anti-foam.

RECOMMENDATIONS

Oil change: According to manufacturers' requirements and adjust according to your own use.

PROPERTIES

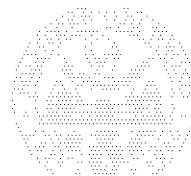
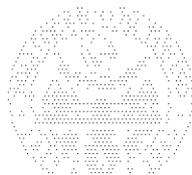
Viscosity grade	SAE J306	80W-90
Density at 20°C (59°F)	ASTM D1298	0.899
Viscosity at 40°C (104°F)	ASTM D445	164 mm ² /s
Viscosity at 100°C (212°F)	ASTM D445	21.7 mm ² /s
Viscosity index	ASTM D2270	157
Flash point	ASTM D92	198°C / 388°F
Pour point	ASTM D97	-24°C / -11°F

We retain the right to modify the general characteristics of our products in order to offer to our customers the latest technical development.

Product specifications are not definitive from the order which is subject to our general conditions of sale and warranty.

MOTUL - 119 Bd Félix Faure - 93303 AUBERVILLIERS CEDEX - BP 94 - Tel : 33 1 48 11 70 00 - Fax : 33 1 48 33 28 79 - Web Site : www.motul.fr

0910





HD 80W-90

Gearbox and differential lubricant

Extreme pressure

TYPE OF USE

All mechanical transmission synchronised or not synchronised gearboxes, gearbox/differential, transfer gearboxes and hypoid differentials without limited slip system operating under shocks, heavy loads and low revolution speed or moderate loads and high revolution speed.

PERFORMANCES

STANDARDS API GL4 and **GL5** / MIL-L-2105D

Extreme pressure lubricant for an efficient anti wears protection.
Stays in 90 grade after KRL 20 hours shear test as requested by SAE J306 Standard.
Very high lubricating power which decreases friction and wear.
90 grade at hot temperature to provide outstanding oil film resistance at hot temperature and/or to reduce transmission noise.
Suitable for any type of seal and yellow material used in gearboxes design.
Anti-corrosion, Anti-foam.

RECOMMENDATIONS

Oil change: According to manufacturers' requirements and adjust according to your own use.

PROPERTIES

Viscosity grade	SAE J 306	80W-90
Density at 20°C (68°F)	ASTM D1298	0.890
Viscosity at 40°C (104°F)	ASTM D445	144 mm ² /s
Viscosity at 100°C (212°F)	ASTM D445	15.0 mm ² /s
Viscosity index VIE	ASTM D2270	105
Flash point	ASTM D92	210°C / 410°F
Pour point	ASTM D97	-27°C / -16°F

We retain the right to modify the general characteristics of our products in order to offer to our customers the latest technical development.
Product specifications are not definitive from the order which is subject to our general conditions of sale and warranty.
MOTUL - 119 Bd Félix Faure - 93303 AUBERVILLIERS CEDEX - BP 94 - TEL : 33 1 48 11 70 00 - FAX : 33 1 48 33 28 79 - Web Site : www.motul.fr

